British Journal of Pharmacology

May 1995

Volume 115 Number 1 pages 1–216

British Journal of Pharmacology (1995) 115, 1-2

SPECIAL REPORT

Effect of a 5-HT_1 receptor agonist, CP-122,288, on oedema formation induced by stimulation of the rat saphenous nerve

Radhika Kajekar, *Paul Gupta, *Nicholas B. Shepperson & [1]Susan D. Brain

Pharmacology Group and Vascular Biology Research Centre, Division of Biomedical Sciences, King's College, Manresa Road, London SW3 6LX and *Department of Cardiovascular Biology, Pfizer Central Research, Sandwich, Kent, CT13 9NJ

Neurogenic oedema formation in the rat hind paw skin induced by electrical stimulation of the saphenous nerve and measured by extravasation of [^{125}I]-albumin, was inhibited by the 5-HT_{1B} receptor agonist, CP-93,129, and the novel tryptamine analogue, CP-122,288. Significant inhibition of up to 66% of control was observed with CP-122,288 (2×10^{-14}–2×10^{-7} mol kg^{-1}) and CP-93,129 (5×10^{-7}–5×10^{-6} mol kg^{-1}), with the minimum effective dose for CP-122,288 being about 10^7 fold less than that for CP-93,129. Oedema formation induced by the intradermal administration of exogenous mediators (substance P and histamine) in rat dorsal skin was not inhibited by CP-122,288 (2×10^{-10} mol kg^{-1}). These results suggest that CP-122,288 is a potent inhibitor of neurogenic inflammation in rat skin and that the effect may be due to a prejunctional inhibition of neuropeptide release.

Keywords: Neurogenic inflammation; 5-hydroxytryptamine; 5-HT_{1B}; CP-122,288; substance P; CGRP; sensory nerves

Introduction Electrical stimulation of the rat saphenous nerve leads to increased blood flow and oedema formation in skin of the hind paw (Lembeck & Holzer, 1979). Studies, using receptor antagonists, suggest that substance P and calcitonin gene-related peptide (CGRP) are major mediators of plasma protein extravasation and vasodilatation in this model (Garret *et al.*, 1991; Escott & Brain, 1993). Thus, attenuation of neurogenic inflammation may be achieved with selective receptor antagonists; however, this approach is limited to inhibiting postjunctional responses mediated *via* specific receptor types. An alternative approach is to inhibit neuropeptide release *via* a prejunctional mechanism. Sumatriptan, a 5-HT_{1D} receptor agonist and CP-93,129, a selective 5-HT_{1B} receptor agonist inhibit neurogenic plasma extravasation in the dura mater of rat and/or guinea-pig by inhibiting neuropeptide release (Buzzi & Moskowitz, 1990; Matsubara *et al.*, 1991). Furthermore, it has been suggested that the therapeutic efficacy of sumatriptan in migraine is related to this activity and that the inhibitory effects of sumatriptan-like agents have, to date, only been reported in selected tissues innervated by the trigeminal nerve. Recently, a C-3 conformationally restricted tryptamine analogue, CP-122,288 (Macor *et al.*, 1992), has been shown to be considerably more potent than sumatriptan in the guinea-pig dura mater (Lee & Moskowitz, 1993). In this study we provide evidence, for the first time, that CP-122,288 and CP-93,129 can also act to inhibit neurogenic inflammation induced after stimulation of non-trigeminal sensory nerves.

Methods Male Wistar rats (200–250 g), anaesthetized with sodium pentobarbitone (50 mg kg^{-1}, i.p.), were prepared to enable electrical stimulation (10 V, 1 ms, 2 Hz for 5 min) of the saphenous nerve of the test leg, while the contralateral leg served as a sham control (Escott & Brain, 1993). [^{125}I]-albumin (50 kBq), mixed with Evans Blue dye (25 mg kg^{-1}) and test ligand or saline (control) were given i.v. 5 min prior to stimulation. After stimulation, blood was taken and the rat killed. [^{125}I]-albumin was measured in a plasma sample and in the skin from the paws. Results are calculated as oedema (μl 100 mg^{-1} tissue) and expressed as a ratio of stimulated to unstimulated skin. The effect of test agents is shown as percentage (%) inhibition of the control response in saline-treated animals. Oedema responses (μl plasma per site) produced to intradermally-injected (i.d., 0.1 ml) agents were measured in rat dorsal skin (Brain & Williams, 1985). In separate experiments the haemodynamic effect of compounds following i.v. administration was studied in anaesthetized rats by measuring blood pressure *via* a carotid artery cannula.

Materials CP-122,288 ((R)-N-methyl-[3-(1-methyl-2-pyrrolidinylmethyl)-1*H*-indol-5-yl] methanesulphonamide) (Pfizer Central Research, Sandwich, U.K.), CP-93,129 (3-(1,2,5,6-tetrahydropyrid-4-yl)pyrrolo[3,2-b]pyrid-5-one) (Central Research Division, Pfizer Inc., Groton, U.S.A.), human α-CGRP (a gift from Dr U. Ney, Celltech, U.K.), substance P, histamine diphosphate salt and Evans Blue dye (Sigma Chemical Co., Dorset, U.K.), [^{125}I]-human serum albumin (Amersham International, U.K.) and sodium pentobarbitone (Sagatal, May and Baker, Essex, U.K.) were used.

Statistical analysis ANOVA followed by multiple comparisons test (Dunnett, Figure 1a and Bonferroni, Figure 1b).

Results In control studies (saline, 1 ml kg^{-1}, i.v.) plasma extravasation in the rat hind paw was 14.07 ± 0.96 μl in the stimulated, and 1.68 ± 0.08 μl in the sham paw, mean ± s.e.mean, $n = 29$. CP-93,129 and CP-122,288 inhibited oedema formation in the stimulated paw (Figure 1a), and the minimum effective doses for CP-93,129 and CP-122,288 were 5×10^{-7} mol kg^{-1} and 2×10^{-14} mol kg^{-1}, respectively. At the highest doses tested, both compounds produced a similar inhibitory effect (upto 66%). Thus, CP-122,288 was about 10^7 fold more potent than CP-93,129. Neither CP-122,288 nor CP-93,129 affected oedema formation in the sham paw (plasma extravasation in control 1.9 ± 0.3 μl, CP-122,288 (2×10^{-10} mol kg^{-1}) 2.07 ± 0.2 μl; CP-93,129 (5×10^{-6} mol kg^{-1}) 1.6 ± 0.1 μl; $n = 6$ for each group). Furthermore, no change in mean arterial pressure (MAP) was observed following i.v. administration of CP-122,288 (MAP: before CP-122,288 (2×10^{-10} mol kg^{-1}, i.v.), 82 ± 3, and 10 min after, 84 ± 3 mmHg; before saline (i.v.) 93 ± 12, and 10 min after, 98 ± 14 mmHg; $n = 5$ for both

[1] Author for correspondence.

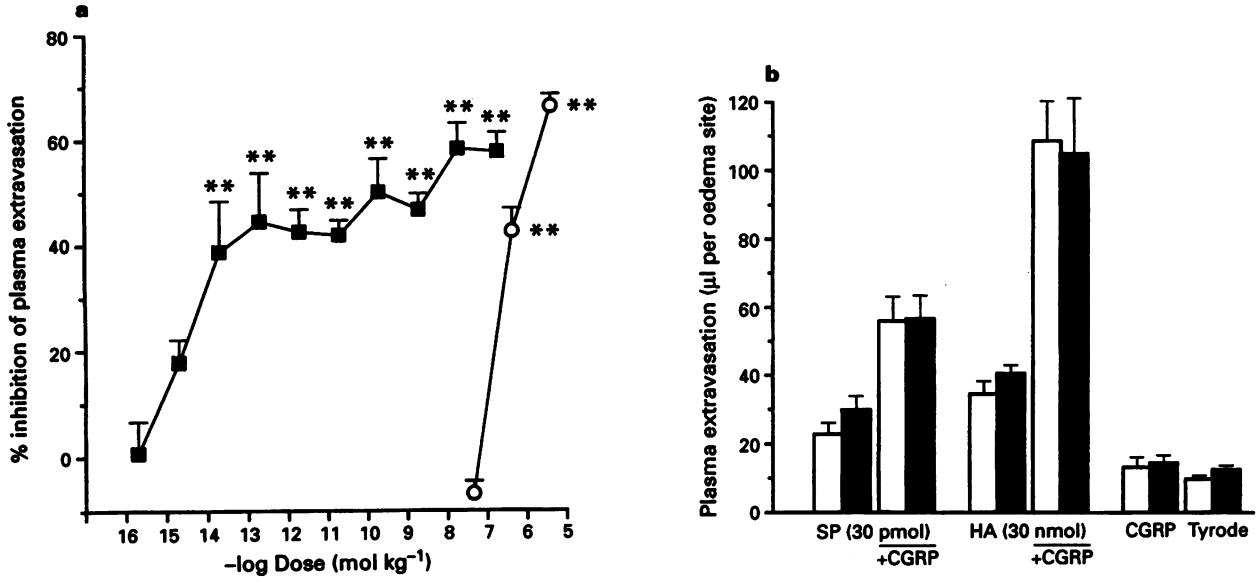

Figure 1 (a) Effect of CP-122,288 (■) and CP-93,129 (○) on plasma extravasation in rat skin after electrical stimulation (10 V, 1 ms, 2 Hz for 5 min) of the saphenous nerve. Results are expressed as % inhibition of oedema in test rats compared to control rats, mean ± s.e.mean, $n = 6$ in each group. $^{**}P < 0.01$, Dunnett multiple comparisons test. (b) Effect of i.v. CP-122,288 on oedema induced by substance P and histamine in rat skin. Mediators were injected i.d. 5 min after i.v. agent and oedema formation measured over 30 min. Responses to substance P (SP) and histamine (HA) ± calcitonin gene-related peptide (CGRP) are shown. Open columns represent control (saline) animals and solid columns represent CP-122,288 (2×10^{-10} mol kg^{-1})-treated animals. Results are expressed as the mean ± s.e.mean, $n = 6$. No significant difference of treatments was observed in CP-122,288 and saline-treated animals.

groups, $P > 0.05$). CP-122,288 (2×10^{-10} mol kg^{-1}, i.v.), as shown in Figure 1b, did not significantly inhibit oedema induced by i.d. administered substance P or histamine in either the presence or absence of a potentiating dose of the vasodilator CGRP (see Brain & Williams, 1985).

Discussion These results demonstrate that neurogenically-induced oedema formation in the rat paw is attenuated by CP-122,288 and CP-93,129. The inability of CP-122,288 to alter oedema formation induced by exogenously administered mediators of inflammation indicates that it does not act postjunctionally as a receptor antagonist. These findings lead us to suggest that CP-122,288 may inhibit neuropeptide release by acting *via* prejunctional receptors. It has been proposed that sumatriptan and CP-93,129 act selectively to inhibit neurogenic inflammation in the dura mater (Moskowitz, 1992) and our results indicate that CP-93,129 and sumatriptan (Escott & Brain, unpublished) possess only a weak activity in the rat paw. However, the inhibitory threshold level for CP-122,288 in the rat paw is comparable to that observed in the guinea-pig dura mater (Lee & Moskowitz, 1993). The receptor subtype at which CP-122,288 acts is not yet determined and the fact that a total inhibition of oedema formation was not observed will be the subject of further study. Nevertheless, the potent ability of CP-122,288 to inhibit neurogenic oedema in non-trigeminal sensory nerve-innervated tissue is clearly demonstrated. These results indicate that a drug such as CP-122,288 could be of use for the treatment of inflammatory disease states, in which neurogenic plasma extravasation occurs.

R.K. is funded by a Pfizer Ph.D studentship. We thank Dr P. Ellis and Mr P. Butler for their helpful discussions.

References

BRAIN, S.D. & WILLIAMS, T.J. (1985). Inflammatory oedema induced by synergism between calcitonin gene-related peptide (CGRP) and mediators of increased microvascular permeability. *Br. J. Pharmacol.*, **86**, 855–860.

BUZZI, M.G. & MOSKOWITZ, M.A. (1990). The antimigraine drug, sumatriptan (GR43175), selectively blocks neurogenic plasma extravasation from blood vessels in dura mater. *Br. J. Pharmacol.*, **99**, 202–206.

ESCOTT, K.J. & BRAIN, S.D. (1993). Effect of calcitonin gene-related peptide antagonist (CGRP8-37) on skin vasodilatation and oedema induced by stimulation of the rat saphenous nerve. *Br. J. Pharmacol.*, **110**, 772–776.

GARRET, C., CARRUETTE, A., FARDIN, V., MOUSSAOUI, S., PEYRONEL, J.-F., BLANCHARD, J.-C. & LADURON, P.M. (1991). Pharmacological properties of a potent and selective nonpeptide substance P antagonist. *Proc. Natl. Acad. Sci. U.S.A.*, **88**, 10208–10212.

LEE, W.S. & MOSKOWITZ, M.A. (1993). Conformationally restricted sumatriptan analogues, CP-122,288 and CP-122,638 exhibit enhanced potency against neurogenic inflammation in dura mater. *Brain Res.*, **626**, 303–305.

LEMBECK, F. & HOLZER, P. (1979). Substance P as neurogenic mediator of antidromic vasodilation and neurogenic plasma extravasation. *Naunyn Schmied. Arch. Pharmacol.*, **310**, 175–183.

MACOR, J.E., BLANK, D.H., POST, R.J. & RYAN, K. (1992). The synthesis of a conformationally restricted analog of the antimigraine drug sumatriptan. *Tetrahedron Lett.*, **33**, 8011–8014.

MATSUBARA, T., MOSKOWITZ, M.A. & BYUN, B. (1991). CP-93,129, a potent and selective 5-HT$_{1B}$ receptor agonist blocks neurogenic plasma extravasation within rat but not guinea-pig dura mater. *Br. J. Pharmacol.*, **104**, 3–4.

MOSKOWITZ, M.A. (1992). Neurogenic versus vascular mechanisms of sumatriptan and ergot alkaloids in migraine. *Trends Pharmacol. Sci.*, **13**, 307–311.

(Received January 26, 1995
Accepted February 14, 1995)

British Journal of Pharmacology (1995) 115, 3-10

Discrimination by benextramine between the NPY-Y_1 receptor subtypes present in rabbit isolated vas deferens and saphenous vein

[1]S. Palea, M. Corsi, J.M. Rimland & D.G. Trist

Glaxo Research Laboratories, Via Fleming 4, 37135, Verona, Italy

1 In order to characterize the neuropeptide Y (NPY) Y_1 receptors known to be present in rabbit isolated vas deferens and saphenous vein, the pharmacological activity of the selective NPY Y_1 receptor agonists, [Leu^{31},Pro^{34}] NPY and various other peptide agonists, together with the putative NPY antagonist, benextramine, were compared in the two tissues.

2 In rabbit isolated saphenous vein, cumulative dose-response curves to various NPY agonists were obtained. All the peptides tested caused contractions which developed quite slowly. The rank order of potency obtained was: PYY > NPY > [Leu^{31},Pro^{34}] NPY = NPY_{2-36} > hPP ≫ NPY_{13-36} = NPY_{18-36}. Incubation with benextramine (BXT) at 100 μM for 30 min irreversibly abolished the contractile response to [Leu^{31},Pro^{34}] NPY but was ineffective against NPY_{18-36}-induced contractions.

3 Cumulative dose-response curves to [Leu^{31},Pro^{34}] NPY were performed in the same preparation before and after incubation with 100 μM BXT for 20 min in order to inactivate NPY Y_1 receptors. The pK_A ($-\log K_A$) estimation for [Leu^{31},Pro^{34}] NPY was 7.60 ± 0.30 using the operational model and 7.20 ± 0.33 using the null method; the difference between the two methods was not statistically significant ($P = 0.36$).

4 Prostatic segments of rabbit vas deferens were electrically stimulated with single pulses. Immediately after stabilization of the contractile response, a cumulative dose-response curve to various NPY agonists was obtained in each tissue. The rank order of potency for twitch inhibition was: PYY > [Leu^{31},Pro^{34}] NPY ≥ NPY ≥ hPP > NPY_{2-36} ≫ NPY_{13-36} ≫ NPY_{18-36} which indicates the presence of a prejunctional NPY Y_1 receptor. BXT at 100 μM incubated for 10 or 60 min did not antagonize the response to [Leu^{31},Pro^{34}] NPY.

5 We conclude that rabbit isolated saphenous vein contains a population of post-junctional NPY Y_1 receptors irreversibly blocked by BXT, as well as a population of post-junctional NPY Y_2 receptors, which are insensitive to BXT. In contrast, the rabbit isolated vas deferens express a pre-junctional NPY Y_1 receptor subtype which is not blocked by BXT. Tetramine disulphides such as BXT could be useful tools in classifying NPY receptors.

Keywords: Rabbit isolated vas deferens and saphenous vein; [Leu^{31},Pro^{34}] NPY; NPY_{18-36}; benextramine; receptor inactivation methods; K_A

Introduction

Neuropeptide Y (NPY) is a 36 amino acid peptide belonging to the pancreatic polypeptide family, which also includes peptide YY (PYY) and the pancreatic polypeptide (PP). NPY is co-stored with noradrenaline (NA) and adenosine triphosphate (ATP) in noradrenergic sympathetic terminals of the mouse vas deferens (Stjärne *et al.*, 1986). In sympathetic nerves innervating most blood vessels NPY is co-released with NA and participates in the maintenance of smooth muscle tone (Ekblad *et al.*, 1984). It is generally accepted that NPY exerts its pharmacological effects via at least two distinct receptor subtypes, namely Y_1 and Y_2. Originally, it was proposed that Y_1 receptors are located exclusively post-junctionally and mediate vasoconstriction and potentiation of the NA response in many blood vessels, whereas Y_2 receptors are located exclusively pre-junctionally and are involved in the suppression of the electrically stimulated twitch contractile response of the isolated vas deferens (Wahlestedt *et al.*, 1986). However, this view has not been supported by some recent findings. For example, in the rat mesenteric arterial bed (McAuley & Westfall, 1992) and rat isolated caval vein (Grundemar *et al.*, 1992) the presence of post-junctional Y_2 and pre-junctional Y_1 receptors was suggested. Furthermore, from the rank order of potency exhibited by NPY and some truncated analogues, the presence of pre-junctional Y_1 receptors in rabbit isolated vas deferens was proposed (Doods & Krause, 1991).

Recently, the tetramine disulphide, benextramine, originally developed as an irreversible α-adrenoceptor blocking agent (Melchiorre, 1981; Plotek & Atlas, 1983), was claimed to be a selective Y_1 ligand in a rat brain binding assay (Doughty *et al.*, 1992), to bind to a Y_2 receptor in bovine hippocampus (Li *et al.*, 1991) and to be a non-competitive antagonist of post-junctional Y_1 and Y_2 receptors in the rat isolated femoral artery (Tessel *et al.*, 1993). The aim of this study was, therefore, to characterize the putative Y_1 receptor present in the rabbit isolated vas deferens and to compare it with the post-junctional Y_1 receptor present in rabbit isolated saphenous vein, a tissue recently found to express mainly or exclusively this receptor subtype (Cadieux *et al.*, 1993). The experiments were performed by using NPY, peptide YY (PYY), human pancreatic polypeptide (hPP) and some truncated analogues of NPY together with the selective Y_1 agonist, [Leu^{31},Pro^{34}]NPY (Fuhlendorf *et al.*, 1990). Furthermore, the antagonist activity of benextramine and its potential irreversible blocking properties on NPY receptors expressed in these tissues have been evaluated. A preliminary account of some of these results was presented to the British Pharmacological Society Meeting, Victoria University of Manchester, 13th-15th April, 1994 (Palea *et al.*, 1994).

[1] Author for correspondence.

Methods

Rabbit isolated vas deferens

Male New Zealand white rabbits weighing 2.5–2.8 kg were anaesthetized by intravenous administration of sodium pentobarbitone (60 mg kg^{-1}) and killed by exsanguination. Bilateral prostatic segments of vasa deferentia (cut as near as possible to the prostate) were removed and placed in a Petri dish containing cold, oxygenated Krebs solution. After dissection of connective tissue and blood vessels, the entire prostatic segment (2 cm long) was mounted vertically between two platinum electrodes (separated by 3 cm) and placed in a 2 ml sylanized organ bath filled with modified oxygenated (95% O_2 and 5% CO_2) Krebs solution of the following composition (mM): NaCl 133, $NaHCO_3$ 16.3, KCl 4.7, $MgCl_2$ 1.0, KH_2PO_4 1.4, $CaCl_2$ 2.0 and glucose 7.8. Experiments were performed at 33°C. Only two preparations were obtained from each animal and only one peptide was tested in each preparation.

The mechanical activity was recorded isometrically with a Grass FT 03 force displacement transducer connected to a Linseis model 7025 polygraph. Isolated vasa deferentia were allowed to equilibrate for 90 min with a tension of 1 g applied four times during the equilibration period and washed with fresh Krebs solution every 15 min. Electrical field stimulation (EFS) with single pulses (25 V, 1 ms, 0.15 Hz) was applied through a pair of platinum electrodes connected to a Grass S88 stimulator. As soon as a series of pulses gave identical responses (basal contractile response) a single cumulative concentration-response curve (CRC) to each peptide was obtained for each tissue. The resulting inhibition of the twitch response was expressed as the percentage of the basal contractile response.

Evaluation of benextramine antagonism

Benextramine tetrahydrochloride (BXT) was incubated at 100 μM for 10 or 60 min after the contractile response to EFS was stabilized. After 10 min EFS was stopped, tissues were washed out and allowed to recover for 15 min, then EFS was reapplied and tissues were challenged, as soon as the contractile response was stabilized, with [Leu^{31},Pro^{34}]NPY.

Rabbit isolated saphenous vein

Male New Zealand white rabbits weighing 2.0–2.4 kg were anaesthetized by intravenous administration of sodium pentobarbitone (60 mg kg^{-1}) and killed by exsanguination. A segment of 2 cm of the vena saphena lateralis was immediately dissected and placed in cold, oxygenated (95% O_2 and 5% CO_2) Krebs solution maintained at 37°C. The vein was cleaned of fat and connective tissue, cut into ring segments (3 mm of length) and mounted in 2 ml sylanized organ baths containing a modified Krebs solution of the following composition (mM): NaCl 118, $NaHCO_3$ 25.0, KCl 4.6, $MgCl_2$ 1.2, NaH_2PO_4 1.2, $CaCl_2$ 2.5 and glucose 11.1. The mechanical activity was recorded isometrically by a Grass FT 03 force displacement transducer connected to a Linseis model 7025 polygraph. Ring segments were allowed to equilibrate for 60 min with a tension of 1 g applied four times during the first 20 min of the equilibration period and washed with fresh Krebs solution every 10 min. Then, vein rings were challenged with KCl 80 mM twice every 20 min in order to establish tissue viability. The contractile response of NPY agonists was then referred to as % of the response to the second application of KCl. Thirty min after the second dose of KCl 80 mM, a single cumulative CRC to one agonist was performed on each tissue. For the experiments evaluating the antagonistic properties of BXT, two cumulative CRC to [Leu^{31},Pro^{34}]NPY or NPY_{18-36} were performed on each tissue with an interval of 60 min between them, during which tissues were washed-out with fresh Krebs solution. Benextramine (100 μM) was added before the second CRC when the tissues had reached the basal tone and was left in contact for 15, 20 or 30 min. Then, tissues were washed out three times every 10 min and the CRC to [Leu^{31},Pro^{34}]NPY was repeated. In some experiments benextramine was washed out for 2 h (washouts every 10 min) to ascertain the irreversibility of the antagonism.

Data analysis

Agonist potency was estimated by fitting the CRC data by the logistic equation:

$$Effect = \frac{E_{max} \times [A]^n}{[A]^n + [A_{50}]^n}$$

where, E_{max} is the maximal effect, [A] is the agonist concentration, and n is the slope parameter. For the experiments with the rabbit vas deferens A_{50} represents the concentration of the agonist that reduced by 50% the basal contractile response induced by electrical stimulation (IC_{50}), whereas in the rabbit saphenous vein A_{50} is the concentration of the agonist that induces 50% of the maximal effect (EC_{50}). Data are expressed as mean ± s.e.mean.

K_A estimation for [Leu^{31},Pro^{34}]NPY was performed as described in the operational method by Black *et al.* (1985) and in the null method by Furchgott (1966) and McKay (1966).

Operational method

Experimental data from control and BXT-treated CRC were simultaneously fitted to the equation:

$$Effect = \frac{Em \times \tau^n \times [A]^n}{(K_A + [A])^n + \tau^n \times [A]^n}$$

providing a common estimation of E_m (maximum possible effect), n (steepness of the occupancy-effect relation), and K_A (agonist dissociation constant) and a value of τ (efficacy of the agonist) for each curve in the pair. Mean values of the parameters estimated are quoted with s.e.mean.

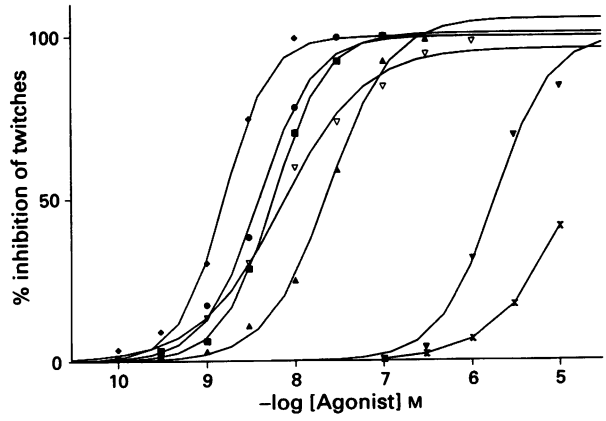

Figure 1 Effect of various agonists for neuropeptide Y (NPY) receptors on the twitch response of the rabbit isolated vas deferens. Data are expressed as % of the stabilized contractile response just before addition of agonists to the organ bath. Each curve is the mean of 6 experiments carried out in different tissues. The lines drawn through the data are derived from the fitting procedure using the logistic equation (see Methods). PYY (◆), [Leu^{31}-Pro^{34}]NPY (●), NPY (■), hPP (▽), NPY_{2-36} (▲), NPY_{13-36} (▼) and NPY_{18-36} (X).

Null methods (or double reciprocal method)

The agonist K_A value was calculated from the equation:

$$\frac{1}{[A]} = \frac{1}{[A']} \times \frac{1}{q} + \frac{1}{K_A} \times \frac{(1-q)}{q}$$

where [A] and [A'] are the equiactive concentrations of the agonist before and after treatment with BXT respectively, q is the fraction of functional receptor and K_A is the agonist dissociation constant. A straight line of slope 1/q and intercept $(1-q)/(q\ K_A)$, should be obtained on a plot 1/[A] against 1/[A']. The value of q can be calculated from 1/slope and K_A from (slope-1)/intercept.

Drugs

All peptides were obtained from Peninsula Laboratories Europe Ltd (St. Helens, Merseyside, U.K.). Benextramine tetrahydrochloride (approximately 90% pure) and tetrodotoxin were from Sigma. All peptides were dissolved, at a concentration of 100 μM, in twice distilled water containing bovine serum albumine (BSA) 0.5 mg ml^{-1} and stored in aliquotes frozen at −20°C. On the day of the experiment each peptide was diluted in a Krebs solution containing BSA 0.5 mg ml^{-1}.

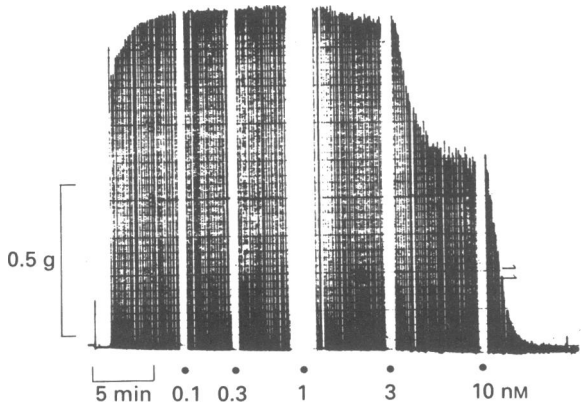

Figure 2 Experimental recording of a dose-response curve to [Leu^{31},Pro^{34}]NPY in the rabbit isolated vas deferens electrically stimulated with single pulses (25 V, 1 ms, 0.15 Hz).

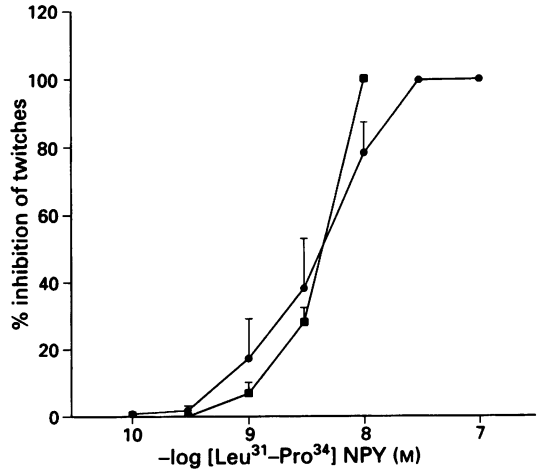

Figure 3 Lack of effect of benextramine incubation (100 μM for 30 min) on the dose-response curve to [Leu^{31},Pro^{34}]NPY in the rabbit isolated vas deferens electrically stimulated with single pulses (25 V, 1 ms, 0.15 Hz). Control curve (●), benextramine-treated curve (■).

Results

Agonist activity in rabbit vas deferens

Basal contractile responses to EFS were 1.22 ± 0.06 g ($n = 45$). These responses were completely abolished by 1 μM TTX, confirming their neurogenic origin (data not shown). The rank order of potency for twitch inhibition in rabbit vas deferens was: PYY > [Leu^{31}, Pro^{34}]NPY ⩾ NPY ⩾ hPP > $NPY_{2-36} \gg NPY_{13-36} \gg NPY_{18-36}$ (Figure 1).

PYY, the most potent agonist tested, was about 3 times more potent than NPY and [Leu^{31},Pro^{34}]NPY. hPP was equipotent to NPY and NPY_{2-36} was only 13.6 times less potent than PYY. All these peptides had a rather slow time course of inhibition of the twitches, with no sign of spontaneous recovery during prolonged contact of the agonists with the tissue (Figure 2). In Table 1, IC_{50} values (± s.e.mean) and equipotent molar ratios are given for all the peptides tested except NPY_{18-36}, for which the response obtained at 10 μM (the highest concentration that could be tested) was only 45% of the basal response.

Effect of benextramine in rabbit vas deferens

Preincubation with BXT at 100 μM for 10 min had a consistent inhibitory effect which partially recovered after 15 min of resting, during which tissues were washed twice. The basal contractile response after BXT treatment was reduced by 25.2 ± 1.3% compared with the response before BXT treatment ($n = 3$).

BXT treatment did not antagonize the [Leu^{31},Pro^{34}]NPY effect (Figure 3) but on the contrary, lowered the IC_{50} value (2.15 ± 0.07 nM versus 5.04 ± 0.63 nM for controls; $P = 0.008$ by the F-test). Increasing the concentration of BXT to 300 μM and the incubation time to 120 min resulted in an IC_{50} value for [Leu^{31},Pro^{34}]NPY (3.72 ± 0.52 nM) that was not significantly different from control value ($P = 0.086$ by the F-test).

BXT at 100 μM for 10 min was ineffective versus hPP ($n = 5$; data not shown).

Rabbit isolated saphenous vein

Mean magnitude of the KCl 80 mM-induced contraction for the rabbit isolated saphenous vein was 2.04 ± 0.08 g ($n = 57$).

[Leu^{31},Pro^{34}]NPY and all the NPY analogues tested induced strong contractions (responses at the highest concentration tested were normally greater than the KCl-induced contraction) which developed much more slowly at the lowest concentrations (Figure 4). TTX at 1 μM was without effect on the contractile effect of [Leu^{31},Pro^{34}] NPY, indicating that contraction was due to an interaction with an NPY receptor located on smooth muscle cells (data not shown).

The rank order of potency for the agonists tested was the

Table 1 IC_{50} and EC_{50} (nM, $n = 6$) and equipotent molar ratio (e.p.m.r.) (relative to peptide YY, PYY) exhibited by neuropeptide Y (NPY) and some analogues in rabbit isolated vas deferens and saphenous vein

	Vas deferens		*Saphenous vein*	
	IC_{50}	e.p.m.r.	EC_{50}	e.p.m.r.
PYY	1.76 ± 0.11	1	1.88 ± 0.05	1
[Leu^{31},Pro^{34}]NPY	5.04 ± 0.63	2.9	9.04 ± 0.27	4.8
NPY	5.72 ± 0.21	3.2	3.77 ± 0.30	2.0
hPP	6.41 ± 1.05	3.6	26.3 ± 3.8	14.0
NPY_{2-36}	24.0 ± 2.1	13.6	8.70 ± 0.75	4.6
NPY_{13-36}	1368 ± 20.4	777	188 ± 4.2	100
NPY_{18-36}	>10 μM	–	204 ± 13.1	108

Values are mean ± s.e.mean for IC_{50} and EC_{50}.

following: PYY > NPY > [Leu^{31},Pro^{34}]NPY = NPY_{2-36} > hPP >> NPY_{13-36} = NPY_{18-36} (Figure 5). EC_{50} values and equipotent molar ratios (e.p.m.r.) are presented in Table 1. Two consecutive CRC to [Leu^{31},Pro^{34}]NPY on the same tissue were reproducible after 60 min of wash-out (Figure 6a). The mean logistic parameters (± s.e.; $n = 6$) of these curves were as follows: first curve: $E_{max} = 116.9 \pm 6.3$; pA_{50} 7.88 ± 0.14; $n = 2.88 \pm 0.63$. Second curve: $E_{max} = 117.7 \pm 3.3$; $pA_{50} = 7.69 \pm 0.11$; $n = 2.91 \pm 0.62$.

BXT (100 μM) incubated either at 10, 20 or 30 min, depressed the maximal response to the selective NPY-Y_1 receptor agonist, [Leu^{31},Pro^{34}]NPY, in a time-dependent manner, 30 min of contact being sufficient to abolish completely the agonist's response (Figure 6b-c-d). Washout for 2 h did not modify the magnitude of BXT inhibition of the Y_1 receptor (Figure 6e).

BXT at 100 μM and 20 min of contact did not modify significantly the response to NPY_{18-36} ($n = 3$; Figure 7a–b).

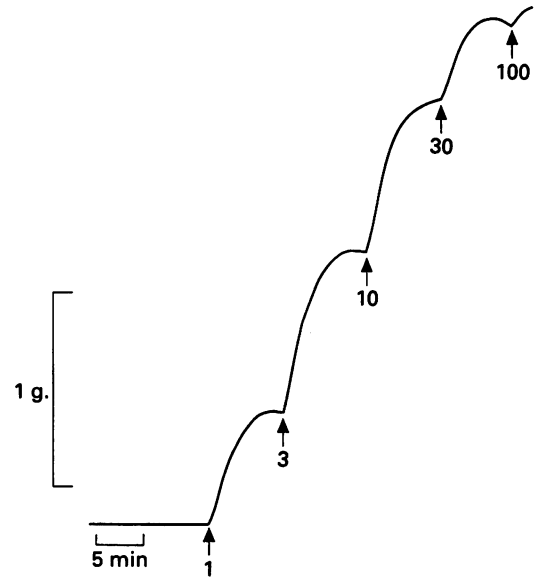

Figure 4 Experimental recording of a dose-response curve to [Leu^{31},Pro^{34}]NPY (1–100nM) in a ring segment of rabbit isolated saphenous vein.

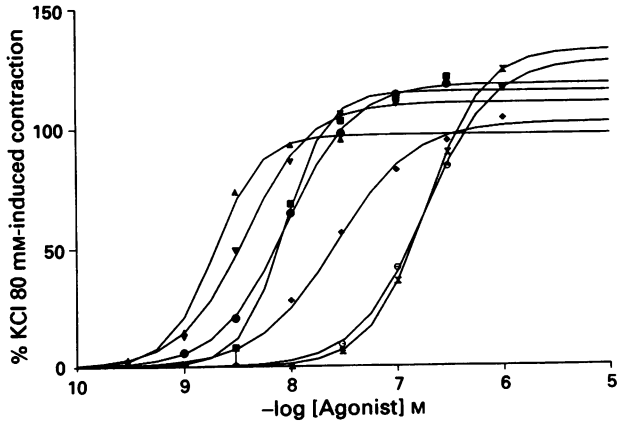

Figure 5 Effect of various neuropeptide Y (NPY) receptor agonists on ring segments of rabbit isolated saphenous vein. Data are expressed as % of the response induced by KCl 80 mM. Each curve is the mean of 6 experiments carried out in different tissues. The lines drawn through the data are derived from the fitting procedure using the logistic equation (see Methods). PYY (▲), NPY (▼), [Leu^{31},Pro^{34}]NPY (●), NPY_{2-36} (■), hPP (◆), NPY_{13-36} (○), NPY_{18-36} (X).

K_A estimation for [Leu^{31},Pro^{34}]NPY in rabbit saphenous vein

Assuming BXT to be an irreversible antagonist of the post-junctional Y_1 receptor, the K_A for [Leu^{31},Pro^{34}]NPY using both the operational method and the null method has been estimated (see Methods). Only pairs of CRC carried out in the same tissue in the absence and presence of BXT 100 μM (incubated for 20 min) were used in this analysis. BXT depressed the maximal response to the agonist to 20 ± 5.6% of the KCl 80 mM-induced contraction ($n = 8$). The estimated parameters by using the two methods are shown in Table 2. The estimated pK_A ($-\log K_A$) for the selective Y_1 agonist was 7.60 ± 0.30 using the operational method and 7.20 ± 0.33 for the null method, the difference not being statistically significant with the Student's t test ($P = 0.36$).

Discussion

Rabbit vas deferens

The current classification of NPY receptors is based upon the rank order of potency of the agonists, because no selective antagonists are available. A number of studies support the proposal that there are at least three receptor subtypes recognized by NPY (Y_1, Y_2 and Y_3) and a different receptor which binds selectively the pancreatic polypeptide (PP) (see Wahlestedt & Reis, 1993, for a review). In rabbit vas deferens several lines of evidence suggest the presence of a pre-junctional Y_1 receptor which seems to be somewhat different from the Y_1 post-junctional receptor characterized in vascular preparations. The selective Y_1 receptor agonist, [Leu^{31},Pro^{34}]NPY, was found to be equipotent to NPY and to abolish completely the twitch response at a concentration of 30 nM. In contrast, in the rat isolated vas deferens, a tissue known to functionally express the Y_2 receptor (Wahlestedt *et al.*, 1986) [Leu^{31},Pro^{34}]NPY at this concentration was completely ineffective (unpublished results).

The Y_3 receptor subtype has been recently postulated to be present both in the central nervous system (Grundemar *et al.*, 1991a,b; Foucart *et al.*, 1993) and in the periphery (Balasubramaniam *et al.*, 1990; Wahlestedt *et al.*, 1992). The rank order of agonist potency for this receptor in rat superior cervical ganglia neurones is rPP = NPY_{13-36} > NPY = [Leu^{31}, Pro^{34}]NPY whereas PYY is almost inactive, confirming previous reports that this peptide is ineffective on the Y_3 receptor type (Grundemar *et al.*, 1991a,b). So, our finding that PYY was the most potent agonist is clearly inconsistent with the involvement of a Y_3 receptor in the inhibition of electrically-induced contraction of the rabbit vas deferens.

The presence of the postulated PP receptor in rabbit isolated vas deferens is a matter of further discussion. In our paradigm we found an unusually high agonist activity of hPP, which was nearly equipotent to NPY, whereas in binding studies rPP was reported to be a very poor ligand of the Y_1 receptor expressed in PC12 cells (Schwartz *et al.*, 1987; 1990). To explain our results we advance the hypothesis that the contractile response to single pulse stimulation in rabbit vas deferens is controlled not only by the Y_1 receptor but also by a PP receptor, which is probably present also in the rat isolated vas deferens (Jorgensen *et al.*, 1990).

It has been reported that the NPY Y_1 receptor found in vascular tissues is stringent in its requirement for the N-terminal end of NPY since deletion of Tyr^1 results in a marked loss of potency (Wahlestedt & Reis, 1993). For example, it was shown that NPY_{2-36} was about 30 times less potent than NPY in increasing arterial blood pressure in anaesthetized rats (Grundemar & Hakanson, 1993) and was about 16 times less potent than NPY in eliciting increases in myocardial perfusion pressure in isolated heart of the guinea-pig (Rioux *et al.*, 1986). In rabbit vas deferens we found that NPY_{2-36} was only about 4 times less potent than NPY, itself

suggesting the possibility of a heterogeneity between Y_1 receptors expressed in vascular tissues (located postjunctionally) and Y_1 receptors found in our preparation, which are probably expressed at a pre-junctional level. To verify this hypothesis we decided to test the antagonistic activity of BXT, which was reported to block non-competitively the post-junctional Y_1 receptor mediating contraction of the rat isolated femoral artery (Tessel *et al.*, 1993). The tetramine

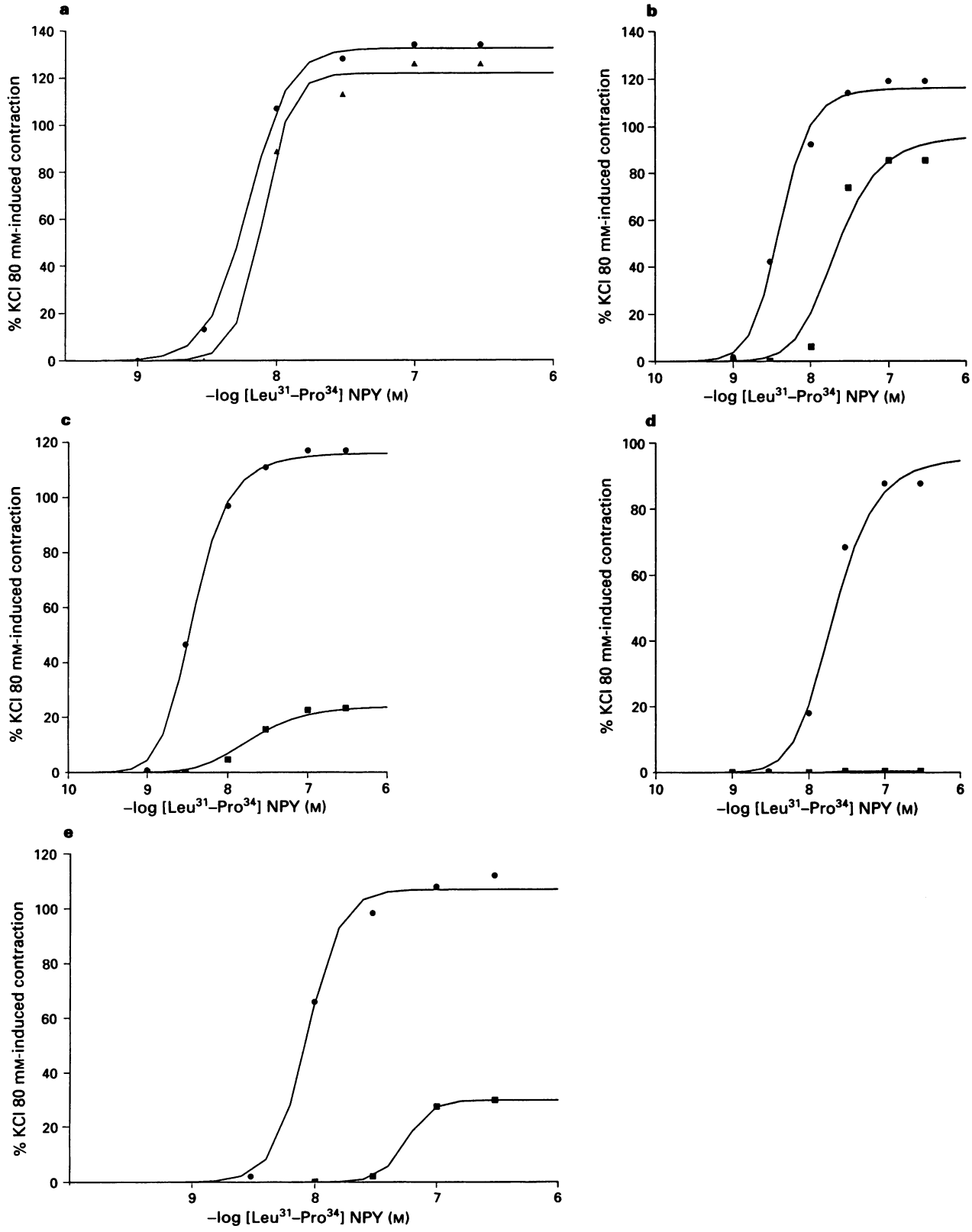

Figure 6 (a) Cumulative dose-response curves to [Leu^{31},Pro^{34}]NPY generated in the same tissue with an interval of 60 min. First curve (●) and second curve (▲). The response to the agonist appears to be quite reproducible. (b) Effect of incubation with a single dose of benextramine (100 μM) for 15 min; (c) for 20 min; (d) for 30 min; (e) for 20 min followed by 2 h of washout. Control curve (●), benextramine-treated curve (■). The lines through the data are the result of the operational model fitting using the receptor inactivation method.

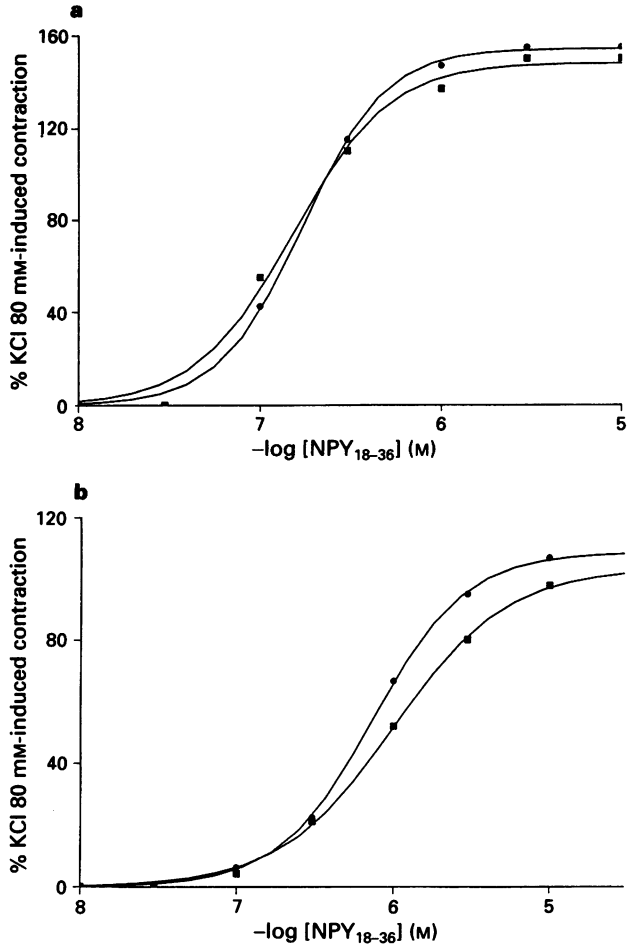

Figure 7 (a) Cumulative dose-response curves to NPY_{18-36} generated in the same tissue with an interval of 60 min. First curve (●) and second curve (■). (b) Effect of incubation with a single dose of benextramine (100 μM) for 20 min. Control curve (●), benextramine-treated curve (■).

disulphide BXT was originally described as an irreversible α-adrenoceptor antagonist. We found that an incubation time of 10 min at 100 μM partially inhibited the twitch response to electrical stimulation of the isolated vas deferens. However, after two washouts, to remove the excess of this compound from the organ bath, we found a partial recovery of the contractile response. So, the single pulse stimulation we used probably elicited the release of a purinergic neurotransmitter instead of an adrenergic one. In fact, we found that the P_2 antagonist, suramin, at 300 μM, completely abolished the contractile response to electrical stimulation (unpublished results). This seems to indicate that the inhibitory effect of BXT is not due to its α-adrenergic blocking properties but to other properties of this drug e.g. blockade of K^+ activated Ca^{2+} channels (Plotek & Atlas, 1983) which could be related to purinergic neurotransmission (Illes & Norenberg, 1993).

BXT (up to 300 μM) was completely ineffective in antagonizing [Leu^{31},Pro^{34}]NPY-induced suppression of the twitch response. This result is in contrast with both functional studies in rat isolated femoral artery (Tessel *et al.*, 1993) and ligand binding studies with rat brain membranes (Doughty *et al.*, 1992), both of which demonstrated an antagonism of BXT at 10 μM versus the putative NPY Y_1 receptor. The most plausible explanation is that rabbit vas deferens expresses a NPY Y_1 receptor subtype different from that mediating contraction of the rat femoral artery. Furthermore, it could be speculated that mammalian tissues can express two NPY Y_1 receptor subtypes, one pre-junctional and insensitive to BXT, the other post-junctional and sensitive to BXT. To confirm this hypothesis we decided to test

Table 2 pK_A estimation and related parameters obtained for [Leu^{31},Pro^{34}]NPY in the presence of benextramine 100 μM incubated for 20 min using both the operational method and the null method

	Operational method	*Null method*
pK_A	7.60 ± 0.30	7.20 ± 0.33
τ_1	7.4 ± 4.2	–
τ_2	0.81 ± 0.19	–
E_{max}	114 ± 13.9	–
n	4.78 ± 2.24	–
q	–	0.14 ± 0.04

Values are reported as mean ± s.e.mean ($n = 5$).

BXT antagonism in another rabbit tissue, the isolated saphenous vein, where NPY was reported to exert a direct post-junctional effect (Cadieux *et al.*, 1993).

Rabbit isolated saphenous vein

Isolated rings of the vena saphena lateralis were potently constricted by all the agonists tested. The agonist rank order of potency and the high efficacy exhibited by [Leu^{31}, Pro^{34}]NPY clearly indicates the presence of the NPY Y_1 receptor. However, comparing EC_{50} values with those obtained in the vas deferens, some differences can be noted. In the saphenous vein, NPY_{13-36} and NPY_{18-36} were nearly equipotent and only 100 times less potent than PYY itself, in contrast to the situation found in vas deferens where NPY_{13-36} was over 700 times less potent than PYY. These data seem to indicate the presence, in the saphenous vein, of a heterogeneous population of receptors, probably Y_1 and Y_2, both mediating direct smooth muscle contraction.

BXT depressed the maximal response to [Leu^{31},Pro^{34}]NPY in a time- and concentration-dependent manner, so we hypothesize that this compound irreversibly binds to the post-junctional, Y_1 receptor subtype. Nevertheless, BXT was without effect on the dose-response curve to NPY_{18-36} suggesting that this tissue expresses not only the 'classical' Y_1 receptor as described previously (Cadieux *et al.*, 1993) but also functional Y_2 receptors which are insensitive to BXT blockade.

The slow decline of the effect of BXT in this preparation allowed us to consider this antagonist irreversible and permitted a determination of the dissociation constant for [Leu^{31},Pro^{34}]NPY. The pK_A value is considered to be a drug-receptor-dependent parameter, therefore it may be used to classify receptors. Two different methods have been applied: the operational (Black & Leff, 1983) and the null method (Furchgott, 1966; MacKay, 1966), the difference occurring in the efficacy term that is introduced only in the former. The results obtained were comparable and not statistically different in terms of estimated pK_A ($-\log K_A$) value. However, the derived dissociation constants for [Leu^{31},Pro^{34}]NPY (7.20–7.60) were at least 30 fold lower than that obtained by binding experiments in a human cell line (SK-N-MC) thought to express naturally the NPY Y_1 receptor (Michel *et al.*, 1990). A similar result was obtained in our laboratories where a pK_i of 8.52 for [Leu^{31},Pro^{34}]NPY was found in displacement experiments using [^{3}H]-propionyl-NPY. Furthermore, BXT at 200 μM extensively decreased the binding of [^{3}H]-propionyl-NPY in these cells, thus confirming the presence of the NPY Y_1 receptor (unpublished results). The differences in [Leu^{31},Pro^{34}]NPY affinity for the NPY Y_1 receptor found between rabbit saphenous vein and SK-N-MC cells could be due to a real heterogeneity of receptors or to problems arising from the level of expression of the receptor in this cell line. In fact, it is known that the level of receptors expressed at different cell passages may vary considerably (McKinney *et al.*, 1984) generating different receptor/G-protein ratios that, in turn, can influence the measurements of agonist affinity (Kenakin, 1993).

Moreover, the utilization of the operational method allowed us to show that [Leu^{31},Pro^{34}]NPY behaves as a full agonist. In fact the efficacy term (τ_1) was 7.4, quite a large value. However, this result was expected from the fact that the pK_A estimated was 3–7 times lower than the potency for the same agonist, therefore representing the classical behaviour of a full agonist.

In conclusion, this work seems to support the hypothesis that pre-junctional (rabbit vas deferens) and post-junctional (rabbit saphenous vein) NPY Y_1 receptors are different and that BXT may be considered a tool to discriminate between them. Moreover, the rabbit saphenous vein probably also expresses a post-junctional NPY Y_2 receptor evoking smooth muscle contraction, which is insensitive to BXT. This fact and our observation that pre-junctional NPY Y_2 receptors located on rat vas deferens are also insensitive to BXT (Palea *et al.*, 1994) seem to indicate that this compound is a useful tool to discriminate also between NPY Y_1 and Y_2 receptors.

We would like to thank Dr Francesca Graziani for providing the binding data for NPY receptor in SK-N-MC cells.

References

BALASUBRAMANIAM, A., SHERIFF, S., RIGEL, D.F. & FISCHER, J.E. (1990). Characterization of neuropeptide Y binding site in rat cardiac ventricular membranes. *Peptides*, **11**, 545–550.

BLACK, J.W., LEFF, P., SHANKLEY, N.P. & WOOD, J. (1985). An operational model of agonism: the effect of E/[A] curve shape on agonist dissociation constant estimation. *Br. J. Pharmacol.*, **84**, 561–571.

CADIEUX, A., PHENG, L.H., St. PIERRE, S., FOURNIER, A. & BENCHEKROUN, M.T. (1993). The rabbit saphenous vein: a tissue preparation specifically enriched in NPY-Y1 receptor subtype. *Regul. Pept.*, **46**, 557–564.

DOODS, H.N. & KRAUSE, J. (1991). Different neuropeptide Y receptor subtypes in rat and rabbit vas deferens. *Eur. J. Pharmacol.*, **204**, 101–103.

DOUGHTY, M.B., LI, K., CHU, S.S. & TESSEL, R. (1992). Benextramine-neuropeptide Y (NPY) binding site interactions: characterization of ^{3}H-NPY binding site heterogeneity in rat brain. *Neuropeptides.*, **23**, 169–180.

EKBLAD, E., EDVINSSON, L., WAHLESTEDT, C., UDDMAN, R., HAKANSON, R. & SUNDLER, F. (1984). Neuropeptide Y co-exist and co-operates with noradrenaline in perivascular nerve fibers. *Regul. Pept.*, **8**, 225–235.

FOUCART, S., BLEAKMAN, D., BINDOKAS, V.P. & MILLER, R.J. (1993). Neuropeptide Y and Pancreatic Polypeptide reduce calcium currents in acutely dissociated neurons from adult rat superior cervical ganglia. *J. Pharmacol. Exp. Ther.*, **265**, 903–909.

FUHLENDORFF, J., GETHER, U., AAKERLUND, L., LANGELAND-JOHANSEN, N., THOGERSEN, H., MELBERG, S., OLSEN, U., THASTRUP, O. & SCHWARTZ, T. (1990). [Leu^{31}-Pro^{34}]Neuropeptide Y: a specific Y1 receptor agonist. *Proc. Natl. Acad. Sci. U.S.A.*, **87**, 182–186.

FURCHGOTT, R.F. (1966). The use of β-haloalkylamines in the differentiation of receptors and in the determination of dissociation constants of receptor-agonist complex. In *Advances in Drug Research*, vol. 3, ed. Harper, N. & Simmonds, A.B. pp. 21–55, New York: Academic Press.

GRUNDEMAR, L. & HAKANSON, R. (1993). Multiple neuropeptide Y receptors are involved in cardiovascular regulation. Peripheral and central mechanisms. *Gen. Pharmacol.*, **24**, 785–796.

GRUNDEMAR, L., JONAS, S.E., MÖRNER, N., HÖGESTÄTT, E.D., WAHLESTEDT, C. & HÅKANSON, R. (1992). Characterization of vascular neuropeptide Y receptors. *Br. J. Pharmacol.*, **105**, 45–50.

GRUNDEMAR, L., WAHLESTEDT, C. & REIS, D.J. (1991a). Long-lasting inhibition of the cardiovascular responses to glutamate and the baroreceptor reflex elicited by neuropeptide Y injected into the nucleus tractus solitarius. *Neurosci. Lett.*, **122**, 135–139.

GRUNDEMAR, L., WAHLESTEDT, C. & REIS, D.J. (1991b). Neuropeptide Y acts at an atypical receptor to evoke cardiovascular depression and to inhibit glutamate responsiveness in the brainstem. *J. Pharmacol. Exp. Ther.*, **258**, 633–638.

ILLES, P. & NORENBERG, W. (1993). Neuronal ATP receptors and their mechanism of action. *Trends Pharmacol. Sci.*, **14**, 50–54.

JORGENSEN, J.C., FUHLENDORFF, J. & SCHWARTZ, T.W. (1990). Structure-function studies on neuropeptide Y and pancreatic polypeptide-evidence for two PP-fold receptors in vas deferens. *Eur. J. Pharmacol.*, **186**, 105–114.

KENAKIN, T. (1993). Cell culture and the expression of receptors in surrogate systems. In *Pharmacologic Analysis of Drug-Receptor Interaction*. pp. 73–87. New York: Raven Press.

LI, W., MACDONALD, R.G. & HEXUM, T.D (1991). Benextramine irreversibly inhibits [^{125}I] neuropeptide Y affinity labeling of the Y_2 binding protein in bovine hippocampus. *Eur. J. Pharmacol. Mol. Section*, **207**, 89–91.

MACKAY, D. (1966). The use of β-haloalkylamines in the differentiation of receptors and in the determination of dissociation constants of receptor-agonist complex. In *Advances in Drug Research*, vol. 3, ed. Harper, N. & Simmonds, A.B. pp. 1–19, New York: Academic Press.

MCAULEY, M.A. & WESTFALL, T.C. (1992). Possible location and function of neuropeptide Y receptor subtypes in the rat mesenteric arterial bed. *J. Pharmacol. Exp. Ther.*, **261**, 863–868.

MCKINNEY, M., STENSTROM, S. & RICHELSON, E. (1984). Muscarinic response and binding in a murine neuroblastoma clone (N1E-115): selective loss with subculturing of the low-affinity agonist site mediating cyclic GMP formation. *Mol. Pharmacol.*, **26**, 156–163.

MELCHIORRE, C. (1981). Tetramine disulfides: a new tool in α-adrenergic pharmacology. *Trends Pharmacol. Sci.*, **2**, 209–211.

MICHEL, M.C., GAIDA, W., BECK-SICKINGER, A.G., WIELAND, H.A., DOODS, H., DURR, H., JUNG, G. & SCHNORRENBERG, G. (1992). Further characterization of Neuropeptide Y receptor subtypes using centrally truncated analogs of Neuropeptide Y: evidence for subtype-differentiating effects on affinity and intrinsic efficacy. *Mol. Pharmacol.*, **42**, 642–648.

PALEA, S., RIMLAND, J.M., CORSI, M. & TRIST, D.G. (1994). Evidence for the presence of an atypical prejunctional NPY Y_1 receptor in rabbit isolated vas deferens: comparison with the rat vas deferens. *Br. J. Pharmacol.*, **112**, 569P.

PLOTEK, Y. & ATLAS, D. (1983). Characterization of benextramine as an irreversible α-adrenergic blocker and as a blocker of potassium-activated calcium channels. *Eur. J. Biochem.*, **133**, 539–544.

RIOUX, F., BACHELARD, H., MARTEL, J.C. & ST-PIERRE, S. (1986). The vasoconstrictor effect of neuropeptide Y and related peptides in the guinea-pig isolated heart. *Peptides*, **7**, 27–31.

SCHWARTZ, T.W., FUHLENDORFF, J., KJEMS, L.L., KRISTENSEN, M.S., VERVELDE, M., O'HARE, M., KRSTENANSKY, J.L. & BJORNHOLM, B. (1990). Signal epitopes in the three-dimensional structure of Neuropeptide Y. *Ann. N.Y. Acad. Sci.*, **611**, 35–47.

SCHWARTZ, T.W., SHEIKH, S.P. & O'HARE, M.M.I. (1987). Receptors on pheocromocytoma cells for two members of the PP-fold family-NPY and PP. *FEBS Lett.*, **225**, 209–214.

STJÄRNE, L., LUNDBERG, J.M. & ÅSTRAND, P. (1986). Neuropeptide Y- a cotransmitter with noradrenaline and adenosine 5'-triphosphate in the sympathetic nerves of the mouse vas deferens? A biochemical, physiological and electropharmacological study. *Neuroscience*, **18**, 151–166.

TESSEL, R., MILLER, D.W., MISSE, G.A. DONG, X. & DOUGHTY, M.B. (1993). Characterization of vascular postsynaptic neuropeptide Y receptor function and regulation. 1. NPY-induced constriction in isolated rat femoral artery rings is mediated by both Y_1 and Y_2 receptors: evidence for benextramine protection studies. *J. Pharmacol. Exp. Ther.*, **265**, 172–177.

WAHLESTEDT, C., REGUNATHAN, S. & REIS, D.J. (1992). Identification of cultured cells selectively expressing Y1-, Y2-, or Y3-type receptors for neuropeptide Y/peptide YY. *Life Sci.*, **50**, PL7–12.

WAHLESTEDT, C. & REIS, D.J. (1993). Neuropeptide Y-related peptides and their receptors- are the receptors potential therapeutics drug targets? *Annu. Rev. Pharmacol. Toxicol.*, **32**, 309–352.

WAHLESTEDT, C., YANAIHARA, C. & HÅKANSON, R. (1986). Evidence for different pre- and post-junctional receptors for neuropeptide Y and related peptides. *Regul. Pept.*, **13**, 307–318.

(Received September 14, 1994
Revised December 20, 1994
Accepted December 22, 1994)

British Journal of Pharmacology (1995) 115, 11-14

Calcium homeostasis in mouse fibroblast cells: affected by U-73122, a putative phospholipase C_β blocker, via multiple mechanisms

Jeremy P Grierson & [1]Jacopo Meldolesi

Department of Pharmacology, DIBIT -S Raffaele Scientific Institute, via Olgettina 58, 20132 Milan, Italy

1 The inhibitory effects of the putative phospholipase C_β inhibitor, U-73122, on ligand-induced and thapsigargin-induced $[Ca^{2+}]_i$ transients were investigated in mouse fibroblast cells (the L line).

2 Ca^{2+} release from intracellular stores was stimulated either by ATP (and also by UTP or ADP) working through the activation of a P_{2U} receptor, or by lysophosphatidic acid, which elicited a more pronounced response.

3 U-73122 inhibited the Ca^{2+} mobilization produced by all the agonists in a dose-dependent manner, consistent with a mode of action involving phospholipase C inhibition.

4 In addition, however, U-73122 slowed the kinetics of intracellular Ca^{2+} release induced by the Ca^{2+}-ATPase inhibitor, thapsigargin, and reduced the influx of Ca^{2+} across the plasma membrane, following stimulation of store-dependent influx by the latter.

5 We conclude that U-73122 has multiple sites of action, all of which can lead to a change in Ca^{2+} homeostasis. Thus, particular caution is recommended when employing this agent and when interpreting the results obtained.

Keywords: U-73122; fibroblast; calcium homeostasis; phospholipase C; store-dependent Ca^{2+} influx; thapsigargin-induced Ca^{2+} release

Introduction

The release of intracellular Ca^{2+}, induced by the activation of many surface receptors, is a multistep process that includes, in sequence: (1) ligand binding and the activation of the receptor and its interaction with a G protein, (2) the dissociation of the G protein and guanine nucleotide exchange, (3) the activation of phospholipase C_β (PLC) by the alpha subunit, with hydrolysis of phosphatidylinositol 4,5-bisphosphate (PIP_2), (4) the release into the cytosol of the second messenger, inositol 1,4,5-trisphosphate (IP_3) and its binding to the intracellular receptors located on the rapidly exchanging Ca^{2+} stores, and (5) the release of stored Ca^{2+} (Berridge, 1993). Experimental investigation of the role of the various molecular components in this process has been greatly assisted by the existence of specific blockers and activators, effective at different stages of the signal transduction pathway. For example, aluminium fluoride can be used to stimulate IP_3 generation via an activation of the G proteins and, if there is access to the cell cytosol, heparin can be applied to block the IP_3 receptor. However, we are still limited by our inability to prevent the generation of IP_3 in intact cells. It was therefore of interest when the aminosteroid, U-73122, was reported to be an inhibitor of the PLC enzyme (Smith *et al.*, 1990; Bleasdale *et al.*, 1990). This membrane permeable compound was shown to inhibit the production of radiolabelled inositol phosphates (lithium blocked metabolism) in SK-N-SH neuroblastoma cells, when stimulated with oxotremorine, as well as to prevent the induced transients of cytosolic free Ca^{2+} ($[Ca^{2+}]_i$) (Thompson *et al.*, 1994). Furthermore, in rat pancreatic acinar cells, which exhibit cholecystokinin-evoked $[Ca^{2+}]_i$ oscillations, U-73122 was found to block the oscillatory activity (Yule & Williams, 1992). Thus, U-73122 was concluded to be a valuable tool with which to test the involvement of IP_3 generation in physiological processes.

In the course of our studies on Ca^{2+} homeostasis in mouse fibroblasts (L cells), we have found that U-73122 is indeed very effective in inhibiting the agonist-induced $[Ca^{2+}]_i$ transients sustained by release of the cation from intracellular stores. However, we also found that the compound can affect Ca^{2+} homeostasis in ways which appear to be unrelated to an interaction with PLC. In particular, the drug slowed the kinetics of intracellular Ca^{2+} release induced by the endoplasmic-sarcoplasmic reticulum Ca^{2+} ATPase (SERCA) inhibitor, thapsigargin (TG), and reduced the influx of Ca^{2+} that follows the emptying of intracellular stores (Clementi *et al.*, 1992). These additional effects of U-73122 can clearly complicate the interpretation of experiments in which the compound is used.

Methods

Cell culture

Mouse L fibroblasts (ATCC CCL 1, clone 929, a kind gift from Dr A. Mantovani, Mario Negri Inst. of Pharmacology, Milan) were plated in 10 cm plastic dishes and maintained in Dulbecco's modified Eagle's medium, supplemented with 10% foetal bovine serum, 2 mM glutamine and antibiotics, and at 37°C in a humidified, 5% CO_2 atmosphere. After culturing for 5-7 days, the cells were removed by light trypsinization and a stream of Ca^{2+}-free saline.

Determination of $[Ca^{2+}]_i$

Detached cells were loaded with fura-2 AM (2 μM from Calbiochem, San Diego, CA, U.S.A.) for 45 min in a HEPES-buffered saline (KRH): ($mmol^{-1}$) NaCl 125, KCl 5, KH_2PO_4 1.2, $MgSO_4$ 1.2, $CaCl_2$ 2, glucose 6, HEPES, 25 (pH 7.4), then centrifuged and resuspended in KRH containing 250 μM sulfinpyrazone. They were stored at room temperature, at a density of 2×10^6 ml^{-1} until use. For each experiment, the cells were diluted in 1:2 in KRH and transferred to a quartz cuvette of either 1.5 or 3 ml volume

[1] Author for correspondence.

(volume of cell suspension 0.75 or 1.5 ml, respectively). Fluorescence measurements were made with both LS-5 and LS-50 fluorimeters (Perkin-Elmer) and with both single- and dual-wavelength modes, at 37°C. The cells were constantly stirred at a moderately slow rate. Each trace was calibrated at the end with EGTA and Ca^{2+} after Triton X-100 permeabilization. Data from the LS-50 was transferred to a spreadsheet programme for offline analysis and plotting. $[Ca^{2+}]_i$ was estimated by the equation:

$$[Ca^{2+}]_i = K_d \times (F\text{-}F_{min})/(F_{max}\text{-}F)$$

Mn^{2+} quenching of fura-2 fluorescence

As described previously (Clementi *et al.*, 1992), cells loaded with fura-2 were resuspended in Ca^{2+}-free KRH with reduced phosphate (0.6 mM KH_2PO_4) and no sulphate ions. MnCl (50 μM) was added to the cells at the start of the experiment.

Materials

U-73122 and U-73343 (1-[6-[[17β-3-methoxyestra-1-3-5(10)-trien-17-yl]amino]hexyl]-1*H*-pyrrole-2,5-dione and 1-[6-[[17β-3-methoxyestra-1-3-5(10)-trien-17-yl] amino] hexyl]-2,5- pyrrolidine-dione, respectively) were purchased from Biomol Research Labs (Playmouth Meeting, PA, U.S.A.) and dissolved in dimethylsulphoxide (DMSO) at 2 mM. TG (Calbiochem) was 100 μM in DMSO. Unless stated otherwise, all additional chemicals were purchased from Sigma, St. Louis, MO, U.S.A.

Results

Suspensions of L fibroblast cells respond to ATP via a putative P_{2U} (or P_{2Y2}) type receptor (Cockcroft & Gomperts, 1979; Watson & Girdleston, 1993; Abbracchio & Burnstock, 1994; Grierson & Meldolesi, 1995) with a release of stored intracellular Ca^{2+} to produce a rapid elevation of $[Ca^{2+}]_i$. At maximal ATP concentration, 0.1 mM, the peak amplitude was 320 ± 23 nM ($n = 12$; see Figure 1). Results similar to those obtained with ATP were observed when UTP was employed at the same concentrations whereas ADP induced only minor responses even when used at 0.5 mM concentration (not shown). There appeared to be no major contribution from external Ca^{2+} to the ATP-induced rise, since the response was apparently unchanged in Ca^{2+}-free (1 mM Ca^{2+}/2 mM EGTA) saline. Furthermore, prior depletion of the internal Ca^{2+} stores by the SERCA-type Ca^{2+}-ATPase inhibitor, TG, prevented the ATP-induced Ca^{2+} transient (not shown). The cells also responded, with a release of intracellular Ca^{2+}, to low concentrations of lysophosphatidic acid (LPA) (Jalink *et al.*, 1990; Durieux & Lynch, 1993). This phospholipid was effective over the range 0.01 – 10 μM producing, at maximal concentrations, a Ca^{2+} transient of greater amplitude and duration than that produced by ATP (peak amplitude 435 ± 33 nM, $n = 5$; Figure 1).

Inhibition of Ca^{2+} transients by U-73122

When the aminosteroid, U-73122, was added to the cells prior to stimulation, a dose-dependent inhibition of agonist-induced $[Ca^{2+}]_i$ transients was produced, irrespective of which agonist was used. Figure 2a illustrates the inhibition by U-73122 of the $Ca^{2+}{}_i$ transients induced by 100 μM ATP, and similar families of curves were produced for other agonists, i.e. 100 μM UTP and 10 μM LPA. For LPA, an attenuation was observed over the range 1 to 8 μM, with an apparent EC_{50} around 3.5 μM (Figure 2b) and complete inhibition at the highest concentration. For ATP the inhibition curves were shifted further to the left and an apparent EC_{50}, for U-73122, of around 1.5 μM was obtained (Figure 2b). This difference could have been expected because of the stronger response induced by LPA with respect to ATP. In agreement

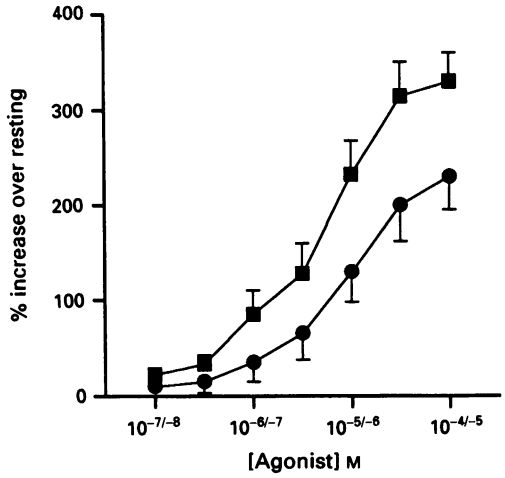

Figure 1 Concentration-dependence of the $[Ca^{2+}]_i$ responses by ATP and lysophosphatidic acid (LPA) in mouse L fibroblasts. Data shown are averages of results obtained in a total of 12 (ATP, ●) and 5 (LPA, ■) experiments. $[Ca^{2+}]_i$ of resting cells was 108 ± 25 nM. The concentration values in the abscissa scale run from 10^{-7} to 10^{-4} M for ATP and from 10^{-8} to 10^{-5} M for LPA.

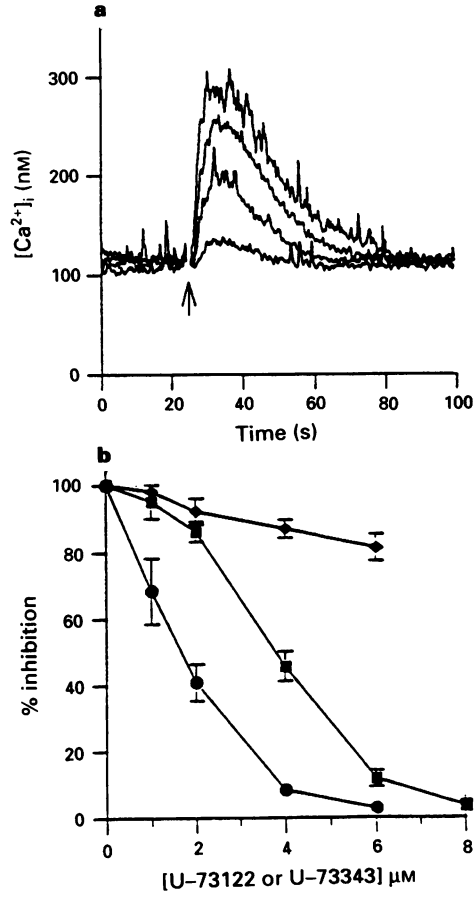

Figure 2 Inhibition by U-73122 of ATP and lysophosphatidic acid (LPA)-induced Ca^{2+} mobilization. (a) Inhibition by various concentrations of U-73122 of ATP-induced Ca^{2+} mobilization. The series of $[Ca^{2+}]_i$ transients were stimulated by the maximal concentration (100 μM) of ATP added at the arrow in the presence of 0, 2, 4 and 6 μM U-73122. The traces shown are representative of the results obtained in at least three experiments. (b) Inhibition curves for U-73122 and U-73343 on Ca^{2+} mobilization by 100 μM ATP (● and ◆, respectively) and for U-73122 on 10 μM LPA (■). Data are expressed as a percentage of the control response (vehicle alone) amounting to 310 and 415 nM for ATP and LPA, respectively. Values shown in (b) are means ± s.e. of three separate experiments.

with earlier reports (Thompson *et al.*, 1994), we found that U-73122 was very sensitive to the protein concentration and, therefore, the EC_{50} increased with cell density (a five fold increase of density induced an approximate doubling of the apparent EC_{50}, not shown). It has been suggested that the closely related compound U-73343, which has a succinimide side chain instead of the maleimide chain of U-73122, may provide a control for U-73122 (Yule & Williams, 1992). We found that this compound still attenuated the ATP-induced peak $[Ca^{2+}]_i$, however, to a maximum of only about 18% (Figure 2b). With LPA the attenuation was similar (maximum 15% not shown), while DMSO, the vehicle for both these compounds, had no inhibitory effect up to a maximal concentration of 0.4% (not shown).

Effect of U-73122 on TG-induced Ca^{2+} release

The release of stored intracellular Ca^{2+} by ionomycin was unaffected by treatment with U-73122 (not shown). In contrast, close examination of the kinetics of Ca^{2+} release after 0.1 μM TG addition revealed that, when compared with controls, release of Ca^{2+} in the presence of U-73122 was slowed. In control experiments, in a Ca^{2+}-free medium, TG induced an increase in $[Ca^{2+}]_i$ which peaked after 16 ± 4 (n = 5) s and then began to decline slowly (Figure 3). In the presence of 5 μM U-73122 on the other hand, the time required to attain the peak response was retarded by 10–20 s (mean 30 ± 8; n = 5) and the overall shape of the transient was also more rounded, although there was no significant change in peak height (Figure 3). In some preparations, the recovery of $Ca^{2+}{}_i$ to resting levels, after TG treatment, was retarded in the presence of U-73122. In contrast, U-73343 had no effect on the release kinetics of TG. Previous experiments have suggested that mouse L cells exhibit a constitutive activation of ATP P_{2U} receptors, from low levels of endogenous ATP released into the KRH, with a moderate stimulation of PIP_2 breakdown (Grierson & Meldolesi, 1995). We considered the possibility that the slowing effect of U-73122 on TG-induced release was caused by a decrease in the cytosolic concentration of IP_3, via the known effect of U-73122 on PLC. Indeed, when the activation of ATP receptors was prevented by adding the ATPase, apyrase, to the KRH, it was found that the rate of Ca^{2+} release was similarly retarded when compared with untreated control (not shown).

Effect of U-73122 on Ca^{2+} influx

When the intracellular Ca^{2+} pools were depleted by TG in the presence of EGTA, the re-introduction of Ca^{2+} to the medium resulted in an overshoot in the $[Ca^{2+}]_i$ rise which then declined to an elevated plateau (Figure 4a). These events are known to be due to the activation of a Ca^{2+} influx that is carefully related to the depletion of the stores (Clementi *et al.*, 1992). It was found that if U-73122 was administered prior to Ca^{2+} re-introduction, the Ca^{2+}-overshoot above the step rise in fluorescence, due to extracellular fura-2, became hardly appreciable (Figure 4a). This inhibition by U-73122 of Ca^{2+} influx across the plasma membrane was further investigated by using the manganese-quench technique. In these experiments, increased cationic influx was indicated by an increase in the rate of fluorescence quenching at the Ca^{2+}-insensitive wavelength of fura-2, 365 nm. Figure 4b shows that under control conditions, the Mn^{2+}-induced reduction in cellular fluorescence was 50% over 3 min. This value was halved in the presence of 5 μM U-73122, thus confirming that cationic influx was inhibited.

Discussion and Conclusions

In this investigation, we have shown that the putative PLC inhibitor, the aminosteroid, U-73122, has multiple effects on Ca^{2+} homeostasis. It appears not only to inhibit the effects that result from the generation of IP_3, i.e. the release of Ca^{2+} from intracellular stores, but also to affect the release that follows SERCA blockade, which is widely believed to be IP_3-independent and to involve a store-dependent Ca^{2+} influx across the plasma membrane.

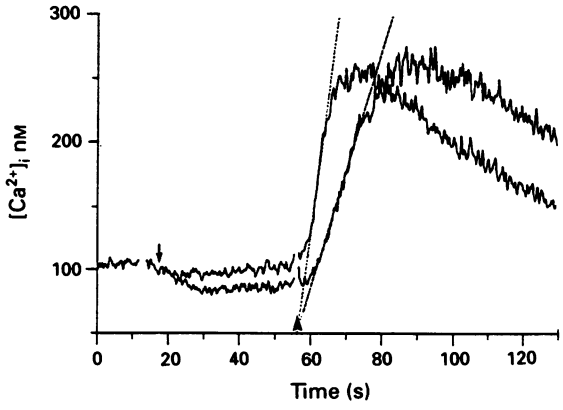

Figure 3 The effect of U-73122 on the thapsigargin (TG)-induced $[Ca^{2+}]_i$ transients. U-73122 or vehicle was administered at the arrow and this was followed by 100 nM TG (arrowhead). With vehicle alone (upper trace) TG induced a fairly rapid release of intracellular Ca^{2+} whereas in the presence of 5 μM U-73122 (lower trace), release was markedly slower. In this example, the rates of $[Ca^{2+}]_i$ rise are 21.6 and 9.2 nM s^{-1}, respectively, with the peak delayed in the U-73122-treated cells by approximately 14 s. Traces shown are representative of 5 separate experiments.

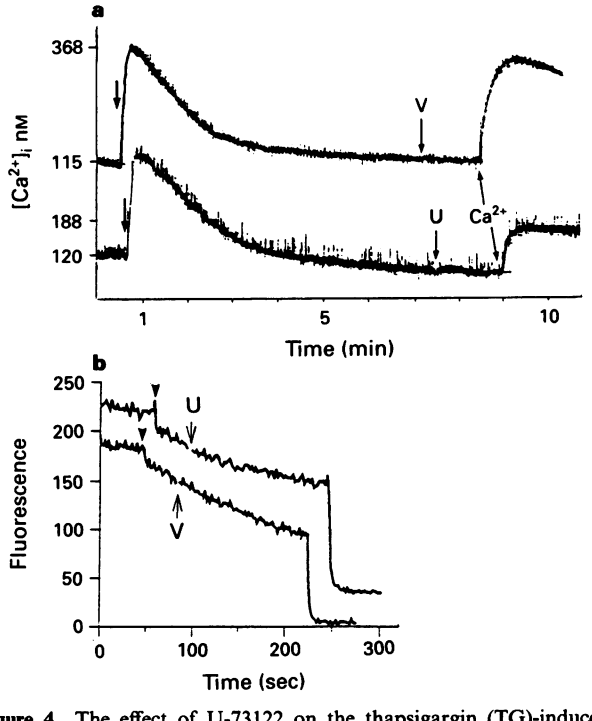

Figure 4 The effect of U-73122 on the thapsigargin (TG)-induced Ca^{2+} influx. (a) Following the depletion of internal Ca^{2+} pools by TG (0.1 μM, arrows) in the presence of 1 mM EGTA, the addition of vehicle (V) and the restitution of $[Ca^{2+}]_o$ (2 mM) induces an overshoot in the $[Ca^{2+}]_i$ transient (upper trace). In the lower trace U-73122 (5 μM) was added to the cuvette at 'U'. The cellular response when $[Ca^{2+}]_o$ was re-added shows that the Ca^{2+} overshoot was largely blocked inasmuch as the visible step rise in fluorescence is primarily due to extracellular fura-2. (b) Shows the effect of U-73122 on Mn^{2+} quenching of 365 nm fluorescence. The upper trace shows the addition of 50 μM Mn^{2+} at the arrowheads, followed by 5 μM U-73122 (U). The lower trace shows the effect of vehicle alone (V). Traces shown are representative of 5 (a) and 3 (b) separate experiments.

U-73122 was found to produce inhibition of $[Ca^{2+}]_i$ transients induced by ATP and LPA, and the active range of concentrations was similar to that reported for SK-N-SH neuroblastoma cells and rat pancreatic acinar cells (Thompson *et al.*, 1994; Yule & Williams, 1992). These effects appear to be consistent with the proposed mechanism of action of the aminosteroid, i.e., the disruption of the G-protein/phospholipase C_β coupling and inhibition of IP_3 synthesis (Thompson *et al.*, 1994). An additional effect of U-73122, namely disruption of the processing of phosphoinositides upstream of PIP_2 hydrolysis, could decrease PIP_2 availability (Vickers, 1993) and thus also contribute to the effect.

An explanation for the U-73122-induced slowing of Ca^{2+} release observed after SERCA blockade by TG is via a reduction in the intracellular concentration of IP_3. Indeed, our results with apyrase have revealed an at least partial disappearance of the aminosteroid effect when the autocrine stimulation by ATP was prevented. Moreover, other investigators (for example, Short *et al.*, 1993) have noted that the emptying of the Ca^{2+} store by TG is faster when combined with IP_3. However, it remains possible that U-73122 has a direct effect on the SERCA of these cells. Preliminary results (J. Grierson, unpublished observations) have shown that U-73122 can cause the emptying of the rapidly exchanging Ca^{2+} stores in a PC12 cell subclone (Clementi *et al.*, 1993).

TG-induced depletion of the rapidly exchanging Ca^{2+} pool has widely been employed to evoke the inward Ca^{2+} current which is used to replenish the store, known as 'capacitative entry' or 'store-dependent calcium influx' (SDCI) (Clementi *et al.*, 1992; Meldolesi, 1993). Many investigators believe that this current is initiated by a retrograde signal released from the pool, but the identity of such a message remains elusive (Meldolesi, 1993). The store dependent calcium influx of L cells appears to be relatively weak, in that there is no prolonged plateau of elevated $[Ca^{2+}]_i$, only a transient response when Ca^{2+} is re-introduced into the medium. This over-shoot was selectively eliminated by U-73122. An inhibition of IP_3 is not likely to be involved in this instance, since previous studies have shown that TG does not alter IP_3 synthesis or its metabolism (Thastrup *et al.*, 1990; Ely *et al.*, 1991). Possible sites of action could therefore be at the plasma membrane Ca^{2+} channel or at some stage of the retrograde signalling. It may be pertinent that recent evidence suggests that the retrograde messenger could be a small G protein (Fasolato *et al.*, 1993), i.e. a protein partially homologous to the α subunit of the trimeric G protein with which U-73122 is believe to react.

In conclusion, U-73122 seems not to act at just one site, as suggested previously, to provoke a change in Ca^{2+} homeostasis. Although the coupling of activated G protein to PLC_β appears to be the most important process disrupted by this compound, changes occur in Ca^{2+} flux across the membrane and probably also in the function of the SERCA Ca^{2+}-ATPase. These last two effects could contribute significantly to the overall effects of the aminosteroid. For example, $[Ca^{2+}]_i$ oscillations are known to involve the rhythmic uptake and release of Ca^{2+} from the IP_3-sensitive stores and to be sustained by the continuous supply of Ca^{2+} via trans-plasmalemmal influx (Harootunian, 1988; Berridge, 1993; Meldolesi, 1993). Thus, the blockade of Ca^{2+} oscillations by U-73122 could result not only from the disruption of IP_3 synthesis, but also from the two other coordinate effects revealed in the present study. Thus, the use of U-73122 as an experimental tool requires special caution and careful characterization of all of the effects of the drug in the cell type investigated.

The typing assistance of L. Di Giorgio is gratefully acknowledged. Supported in part by grants from the CNR Target Project on Biotechnology and Bioinstruments and EC, Copernicus Program. J.P.G. is an EMBO fellow.

References

ABBRACCHIO, M.P. & BURNSTOCK, G. (1994). Purinoceptors: are there families of P_{2X} and P_{2Y} purinoceptors? *Pharmacol Ther.*, **64**, 445–475.

BERRIDGE, M.J. (1993). Inositol trisphosphate and calcium signalling. *Nature*, **361**, 315–325.

BLEASDALE, J.E., THAKUR, N.R., GREMBAN, R.S., BUNDY, G.L., FITZPATRICK, F.A., SMITH, R.J. & BUNTING, S. (1990). Selective inhibition of receptor-coupled phospholipase C-dependent processes in human platelets and polymorphonuclear neutrophils. *J. Pharmacol. Exp. Ther.*, **255**, 756–768.

CLEMENTI, E., RACCHETTI, G., ZACCHETTI, D., PANZERI, M.C. & MELDOLESI, J. (1993). Differential expression of markers and activities in a group of PC12 nerve cell clones. *Eur. J. Neurosci.*, **4**, 944–953.

CLEMENTI, E., SCHEER, H., ZACCHETTI, D., FASOLATO, C., POZZAN, T. & MELDOLESI, J. (1992). Receptor-activated Ca^{2+} influx. *J. Biol. Chem.*, **267**, 2164–2172.

COCKCROFT, S. & GOMPERTS, B.D. (1979). Activation and inhibition of calcium-dependent histamine secretion by ATP ions applied to rat mast cells. *J. Physiol.*, **296**, 229–243.

DURIEUX, M.E. & LYNCH, K.R. (1993). Signalling properties of lysophosphatidic acid. *Trends Pharmacol. Sci.*, **14**, 249–254.

ELY, J.A., AMBROZ, C., BAUKAL, A.J., CHRISTENSEN, S.B., BALLA, T. & CATT, K.J. (1991). Relationship between agonist- and thapsigargin-sensitive calcium pools in adrenal glomerulosa cells. *J. Biol. Chem.*, **266**, 18635–18641.

FASOLATO, C., HOTH, M. & PENNER, R. (1993). A GTP-dependent step in the activation mechanism of capacitative calcium influx. *J. Biol. Chem.*, **268**, 20737–20740.

GRIERSON, J.P. & MELDOLESI, J. (1995). Shear stress-induced $[Ca^{2+}]_i$ transients and oscillations in mouse fibroblasts are mediated by endogenously released ATP. *J. Biol. Chem*, (in press).

HAROOTUNIAN, A.T., KAO, J.P.Y. & TSIEN, R.Y. (1988). Agonist-induced calcium oscillations in depolarized fibroblasts and their manipulation by photoreleased $Ins(1,4,5)P_3$, Ca^{++},and Ca^{++} buffer. *Cold Spring Harbour Symp. Quant. Biol.*, **53**, 935–943.

JALINK, K., VAN CORVEN, E.J. & MOOLENAAR, W.H. (1990). Lysophosphatidic acid, but not phosphatidic acid, is a potent Ca^{2+}-mobilizing stimulus in fibroblasts. *J. Biol. Chem.*, **265**, 12232–12239.

MELDOLESI, J. (1993). Keeping the stores full. *Curr. Biol.*, **3**, 910–912.

SHORT, A.D., KLEIN, M.G., SCHNEIDER, M.F. & GILL, D.L. (1993). Inositol 1,4,5-trisphosphate-mediated quantal Ca^{2+} release measured by high resolution imaging of Ca^{2+} within organelles. *J. Biol. Chem.*, **268**, 25887–25893.

SMITH, R.J., SAM, L.M., JUSTEN, J.M., BUNDY, G.L., BALA, G.A. & BLEASDALE, J.E. (1990). Receptor-coupled signal transduction in human polymorphonuclear neutrophils: effects of a novel inhibitor of phospholipase C-dependent processes on cell responsiveness. *J. Pharmacol. Exp. Ther.*, **253**, 688–697.

THASTRUP, O., CULLEN, P.J., DROBAK, B.K., HANLEY, M.R. & DAWSON, A.P. (1990). Thapsigargin, a tumor promoter, discharges intracellular Ca^{2+} stores by specific inhibition of the endoplasmic reticulum Ca^{2+}-ATPase. *Proc. Natl. Acad. Sci. USA*, **87**, 2466–2470.

THOMPSON, A.K., MOSTAFAPOUR, S.P.L., DENLINGER, C., BLEASDALE, J.E. & FISHER, S.K. (1994). The aminosteroid U-73122 inhibits muscarinic receptor sequestration and phosphoinositide hydrolysis in SK-N-SH neuroblastoma cells. *J. Biol. Chem.*, **266**, 23856–23862.

VICKERS, J.D. (1993). U73122 effects the equilibria between the phosphoinositides as well as phospholipase C activity in unstimulated and thrombin-stimulated human and rabbit platelets. *J. Pharmacol. Exp. Ther.*, **266**, 1156–1163.

WATSON, S. & GIRDLESTONE, D. (1993). Receptor Nomenclature Supplement. *Trends Pharmacol. Sci.*, **14**,

YULE, D.I. & WILLIAMS, J.A. (1992). U73122 inhibits Ca^{2+} oscillations in response to cholecystokinin and carbachol but not to JMV-180 in rat pancreatic acinar cells. *J. Biol. Chem.*, **267**, 13830–13835.

(Received September 22, 1994
Revised January 3, 1995
Accepted January 13, 1995)

British Journal of Pharmacology (1995) 115, 15-18

Ginsenosides-induced nitric oxide-mediated relaxation of the rabbit corpus cavernosum

[1]Xiu Chen & [2]Tony J.-F. Lee

Department of Pharmacology, SIU School of Medicine, Springfield, IL 62794-9230, U.S.A.

1 Ginsenosides, the active ingredients extracted from *Panax ginseng*, have been shown to promote nitric oxide (NO) release in bovine aortic endothelial cells. Since the endothelial cells and the perivascular nerves in penile corpus cavernosum contain NO synthase and an NO-like substance has been shown to be released from these cells which relaxes corpus cavernosum, the possibility that ginsenosides may relax corpus cavernosum by releasing endogenous NO was examined.

2 With an *in vitro* tissue superfusion technique, ginsenosides (250, 500 and 750 $\mu g\ ml^{-1}$) relaxed corpus cavernosum, concentration-dependently.

3 Using an *in vitro* tissue bath technique, acetylcholine (ACh)-induced relaxations were increased in the presence of ginsenosides (250 $\mu g\ ml^{-1}$).

4 Ginsenosides at 100 $\mu g\ ml^{-1}$ significantly enhanced the tetrodotoxin (TTX)-sensitive relaxation of corpus cavernosum elicited by transmural nerve stimulation.

5 The ginsenosides-induced, ACh-induced and ginsenosides-enhanced transmural nerve stimulation-elicited relaxations were significantly attenuated by N^G-nitro-L-arginine (100 μM) and oxyhaemoglobin (oxyHb; 5-10 μM), and were enhanced by superoxide dismutase (SOD; 50 u ml^{-1}).

6 The relaxations and their attenuation by N^G-nitro-L-arginine and TTX were associated with increase and decrease in tissue cyclic GMP levels, respectively.

7 It is concluded that ginsenosides may release NO from endothelial cells, and enhance NO release from endothelial cells elicited by other vasoactive substances and from perivascular nitrergic nerves in the corpus cavernosum. These endothelial and neurogenic effects of ginsenosides in inducing relaxation of the corpus cavernosum may account for the aphrodisiac effect of *Panax ginseng*.

Keywords: Ginsenosides; nitric oxide; rabbit corpus cavernosum; neurogenic vasodilatation; endothelium-dependent vasodilatation; aphrodisiac.

Introduction

It has been reported that ginsenosides, saponins extracted from *Panax ginseng*, relax pulmonary blood vessels (Chen *et al.*, 1984; Kim *et al.*, 1992) and that this relaxation is inhibited by N^G-nitro-L-arginine, a nitric oxide synthase (NOS) inhibitor (Chen *et al.*, 1993). Ginsenosides and one of its purified ingredients, Rg1, have also been shown to increase the conversion of L-arginine, a substrate for nitric oxide synthase (NOS), to citrulline, suggesting that ginsenosides enhance nitric oxide (NO) synthesis (Kim *et al.*, 1992). Since *Panax ginseng* is an essential constituent in traditional Chinese aphrodisiacs, and the relaxation of penile corpus cavernosum can be elicited by NO released from the endothelial cells and non-adrenergic, non-cholinergic (NANC) nerves innervating the corpus cavernosum (Ignarro, 1992; Bush *et al.*, 1992; Rajfer *et al.*, 1992), we examined the possibility that ginsenosides may relax the penile corpus cavernosum by modifying release of NO or a related substance from the endothelial cells and NANC nerves.

Methods

In vitro *techniques for recording tension changes*

Corpus cavernosum strips were prepared from penes of New Zealand white rabbits (3.5-4.4 kg) and mounted in tissue baths containing 10 ml Krebs bicarbonate solution at 37°C equilibrated with 95% O_2 and 5% CO_2 (Lee, 1982; Chen & Gillis, 1992). After 90 min equilibration, strips of corpus cavernosum were loaded with resting tensions of 2 g. Either a tissue superfusion technique or a tissue bath technique was used, with changes in isometric tension being measured by Grass FT03 transducers and recorded on a Grass Polygraph.

To detect the relaxation effect of ginsenosides and to avoid the potential foaming artifact generated by high concentrations of ginsenosides, a tissue superfusion technique (Chen & Gillis, 1992) was used. Krebs solution was superfused over strips of corpus cavernosum at 5 ml min^{-1} with a peristaltic pump. Experimental drugs were delivered with a second pump at 0.25 ml min^{-1} (1:10 dilution) for 2 min by direct application to the superfusate over the tissue. In the presence of active muscle tone induced by phenylephrine (3 μM), ACh (1 μM) was superfused for 2 min to verify the competency of the endothelial cells. At the end of each experiment, 1 μM 3-morpholino-sydnonimine (Sin-1), a NO-releaser, was superfused to induce a relaxation. The ginsenosides-induced relaxation was calculated as percentage of that induced by Sin-I.

To examine the effect of ginsenosides on ACh-induced relaxation, an *in vitro* tissue bath technique was used (Lee, 1982). After active muscle tone had been induced by phenylephrine (3 μM), ACh (0.3 μM-10 μM) was cumulatively applied to the bath. Thirty minutes after replacing the Krebs solution and in the presence of active muscle tone induced by phenylephrine (3 μM), ginsenosides (100, 250 or 500 $\mu g\ ml^{-1}$) were added 10 min before repeating the ACh concentration-response relationships. In some experiments, oxyhaemoglobin (oxyHb; 5-10 μM), prepared as described by Linnik & Lee (1989), was added to the tissue bath after the corpus cavernosum relaxation induced by ACh levelled off to detect the possibility of NO-mediated ACh-induced relaxation. The

[1] Present address: Department of Pharmacology, Hunan Medical University, Changsha 410078, People's Republic of China.
[2] Author for correspondence.

relaxations were calculated as percentage of active vessel tone induced by phenylephrine (3 μM).

To examine the effect of ginsenosides on the corpus cavernosum relaxation induced by transmural nerve stimulation, two parallel platinum electrodes, one on either side of the corpus cavernosum strips in the tissue bath were connected to a Grass 88 square wave pulse stimulator. This was coupled to a stimulus splitter (Med-Lab Stimu Splitter II) and two stimulus isolation units (Grass SIU5) to generate constant current biphasic square waves pulses (Lee, 1982). In the presence of active muscle tone induced by phenylephrine (3 μM) and with the current constantly monitored by an oscilloscope (BK Precision Model 1476), transmural nerve stimulation was delivered with a current of 200 mA and a pulse duration of 0.3 ms for 10 s at 2, 4, 8 and 16 Hz. Guanethidine (5 μM) and atropine (1 μM) were present (atropine was omitted when ACh was tested) throughout the entire experiment to eliminate the potential involvement of adrenergic and cholinergic components. Ginsenosides at different concentrations (100 μg ml^{-1} to 250 μg ml^{-1}) were added to the bath 10 min before repeating transmural nerve stimulation at the various frequencies. At the end of each experiment, TTX (0.3 μM), a sodium channel blocker, or N^G-nitro-L-arginine (50 μM), a NOS inhibitor, was added to the bath to verify the neurogenic origin or NO-mediated relaxation, respectively. Relaxation was calculated as a percentage of phenylephrine-induced active muscle tone.

Cyclic GMP assay

After maximum relaxation induced by various stimulants, corpus cavernosum strips were rapidly frozen in liquid nitrogen and stored at −70°C until assayed. Samples were pulverized by Wig-L-Bugamalgamator (Crescent Dental Manufacture Co. Lyons, IL, U.S.A.), homogenized, extracted in H_2O-saturated ether, and lyophilized to determine guanosine 3′:5′-cyclic monophosphate (cyclic GMP) levels by radioimmunoassay kits from Biochemical Technologies, Inc. (Stoughton, MA, U.S.A.) (Chen & Gillis, 1992).

Chemicals

Acetylcholine (ACh), atropine sulphate, guanethidine sulphate, phenylephrine, N^G-nitro-L-arginine, superoxide dismutase (SOD) and tetrodotoxin (TTX) were purchased from Sigma Chemical Co. (St. Louis, MO, U.S.A.). 3-Morpholinosydnonimine (Sin-1) was a gift from Hoechst AG (Frankfurt, Germany). Ginsenosides were extracted from *Panax ginseng* by C.A. Meyer as described by Shibata *et al.* (1965). Krebs bicarbonate solution consisted of (mM): NaCl 118.2, KCl 4.74, $CaCl_2$ 2.54, KH_2PO_4 1.19, $MgSO_4$ 1.19, $NaHCO_3$ 26.2, dextrose 11.1, indomethacin 0.006 and Na_2EDTA 0.023.

Statistics

Data were expressed as mean ± s.e.mean. Differences between the two groups were determined by Student's paired or unpaired *t* test and were considered significant if $P<0.05$.

Results

Ginsenosides-induced relaxation

Ginsenosides at 250, 500 and 750 μg ml^{-1} induced concentration-dependent relaxations. The induction of relaxation was immediate upon application of ginsenosides. These relaxations were significantly enhanced by SOD (50 u ml^{-1}) and were attenuated by N^G-nitro-L-arginine (50 μM) (Figure 1) and oxyHb (5 μM; $n=3$) (data not shown). N^G-nitro-L-arginine and oxyHb, but not SOD, significantly increased the resting muscle tone (data not shown). Ginsenosides at

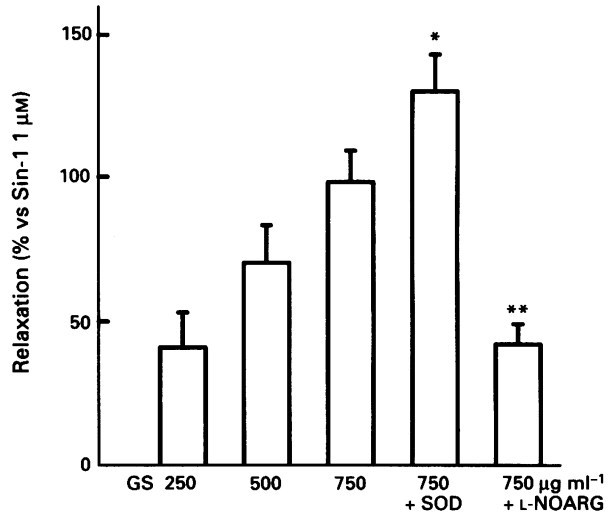

Figure 1 Ginsenosides (GS) induce relaxation of corpus cavernosum: GS (250, 500, 750 μg ml^{-1}) were superfused in Krebs solution over strips of corpus cavernosum for a period of 2 min each (for details, see methods). Superoxide dismutase (SOD) and N^G-nitro-L-arginine (L-NOARG) were superfused 3–5 min before superfusing GS. The relaxation induced by GS was concentration-dependent. The relaxation induced by GS at 750 μg ml^{-1} was equivalent to that induced by 1 μM Sin-1. This relaxation was significantly ($P<0.05$) enhanced by concomitant superfusion of SOD (50 u ml^{-1}), and was significantly attenuated by L-NOARG (50 μM). *$P<0.05$ and **$P<0.021$ indicate significant differences from GS 750 μg ml^{-1}, $n=6$ in each group.

750 μg ml^{-1} induced maximum relaxation which was equivalent to that induced by 1 μM Sin-1. Relaxation induced by Sin-1 (0.01–1 μM) was not affected by ginsenoside (250–500 μg ml^{-1}) (data not shown).

Ginsenosides-enhanced ACh-induced relaxation

In the presence of active muscle tone induced by phenylephrine (3 μM), the corpus cavernosum relaxed immediately upon application of ACh in a concentration-dependent manner (Figure 2). ACh-induced relaxation was blocked by atropine (1 μM), N^G-nitro-L-arginine (50 μM), and oxyHb (5 μM) (data not shown), and was enhanced in the presence of ginsenosides in a concentration-dependent manner.

Ginsenosides-enhanced transmural nerve stimulation-induced relaxation

Transmural nerve stimulation elicited relaxation of strips of corpus cavernosum in a frequency-dependent manner (Figure 3). The relaxation was significantly enhanced in the presence of 100 μg ml^{-1} ginsenosides. Higher concentrations of ginsenosides (250 μg ml^{-1}) did not further increase the relaxation elicited by transmural nerve stimulation at any frequency except 16 Hz. The enhanced-relaxation returned to normal after removing ginsenosides by washing with fresh Krebs solution. In the presence of TTX (0.3 μM), the relaxations elicited by transmural nerve stimulation at various frequencies were almost abolished while relaxations induced by ginsenosides and ACh persisted. The relaxations induced by transmural nerve stimulation at various frequencies were abolished by N^G-nitro-L-arginine (50 μM) (data not shown).

Effects of ginsenosides on cyclic GMP content

Relaxations of corpus cavernosum induced by ginsenosides (250 μg ml) and transmural nerve stimulation at 16 Hz were

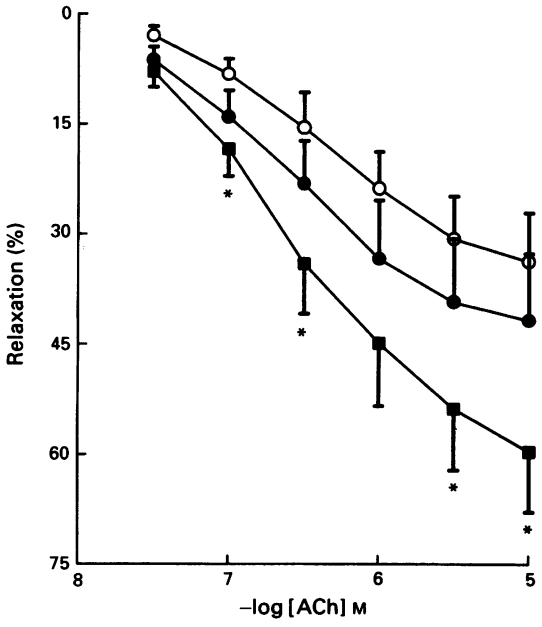

Figure 2 Ginsenosides (GS) concentration-dependently enhanced acetylcholine (ACh)-induced relaxation of corpus cavernosum. Ginsenosides at 250 μg ml^{-1} (■) but not at 100 μg ml (●) significantly enhanced the relaxation; (○) control. *$P<0.05$ indicates significant difference from the respective control, $n = 6$ in each group.

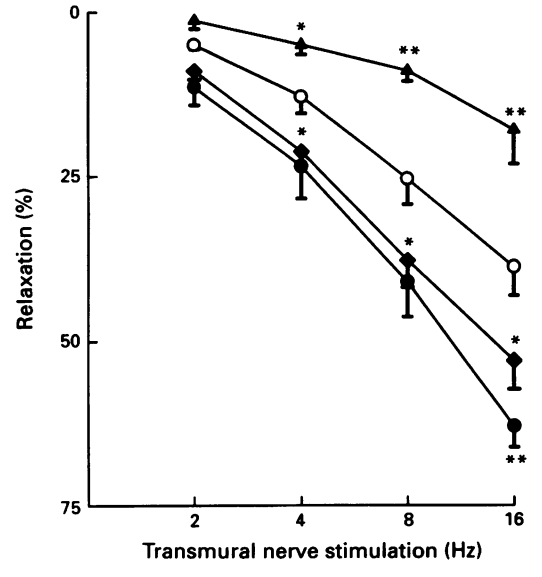

Figure 3 Ginsenosides (GS) enhanced transmural nerve stimulation-induced relaxation of the corpus cavernosum. Ginsenosides at 100 μg ml^{-1} (◆) enhanced transmural nerve stimulation-induced relaxation. At 250 μg ml^{-1}, (●) ginsenosides did not further enhance relaxation elicited by transmural nerve stimulation at various frequencies except 16 Hz. The relaxation was almost abolished by tetrodotoxin (TTX, 0.3 μM) (▲). Control (○). *$P<0.05$ indicate significant differences from the respective control, $n = 7$ in each group.

accompanied by significant increases in tissue cyclic GMP levels (Table 1). The increases were inhibited by N^G-nitro-L-arginine (50 μM) to a level significantly below the control values. In the presence of ginsenosides (250 μg ml^{-1}), transmural nerve stimulation at 16 Hz resulted in a greater increase in cyclic GMP content than that induced by ginsenosides or transmural nerve stimulation alone. This additive increase in cyclic GMP content was reversed by

Table 1 Effects of ginsenosides and transmural nerve stimulation (TNS) on cyclic GMP content in corpus cavernosum

	Cyclic GMP content (pmol g^{-1} wt)	n
Control	10.8 ± 1.2	4
Ginsenosides	18.4 ± 1.8*	4
TNS	18.6 ± 1.8*	4
Ginsenosides + TNS	29.3 ± 2.1**	4
Ginsenosides + TNS + TTX	16.0 ± 1.1*	4
Ginsenosides + N^G-nitro-L-arginine	4.7 ± 1.2*,†	4
Ginsenosides + TNS + N^G-nitro-L-arginine	4.8 ± 0.4*,†	4

Transmural nerve stimulation (16 Hz); ginsenosides (250 μg ml^{-1}); N^G-nitro-L-arginine (50 μM); tetrodotoxin (TTX, 0.3 μg ml^{-1}); n = number of experiments. *$P<0.01$ vs control, **$P<0.01$ vs ginsenosides or TNS, and †$P<0.01$ vs ginsenosides plus TNS indicate statistical significance (Student's unpaired t test).

TTX (0.03 μM) to the level equivalent to that induced by ginsenosides alone, while it was inhibited by N^G-nitro-L-arginine (50 μM) to a level significantly below the control values.

Discussion

In the present study, we have demonstrated that ginsenosides induce an endothelium-dependent relaxation, and enhance ACh-induced and transmural nerve stimulation-elicited relaxations in corpus cavernosum of the rabbits. These effects of ginsenosides appear to be mediated by release and/or the modification of release of NO from endothelial cells and perivascular nerves. This is based on the findings that both neurogenic and endothelium-mediated relaxations were enhanced by SOD, a scavenger of superoxide anion which is known to inactivate NO (Gryglewski *et al.*, 1986), and were blocked by N^G-nitro-L-arginine, a specific inhibitor of NOS (Rees *et al.*, 1990) and oxyHb which is known to trap NO (Martin *et al.*, 1985). Furthermore, relaxations of corpus cavernosum induced by transmural nerve stimulation, ginsenosides, or transmural nerve stimulation plus ginsenosides, and inhibition of these relaxations by N^G-nitro-L-arginine were associated respectively with increases and decreases in tissue cyclic GMP content.

It should be noted that the enhanced corpus cavernosum cyclic GMP content induced by ginsenosides and transmural nerve stimulation plus ginsenosides were decreased by N^G-nitro-L-arginine to a level significantly lower than that of the control, suggesting that there is a tonic release of endogenous NO in isolated corpus cavernosum. Furthermore, TTX, which almost abolished transmural nerve stimulation-elicited relaxation in the presence or absence of ginsenosides, decreased the tissue cyclic GMP content elicited by transmural nerve stimulation plus ginsenosides to a level equivalent to that induced by ginsenosides alone. These results provide further evidence that ginsenosides can modify the synthesis and release of NO in perivascular nerves and endothelial cells of the corpus cavernosum.

In the rabbit pulmonary and intrapulmonary arteries, ginsenosides have been shown to induce an endothelium-dependent, NO-mediated dilatation (Chen *et al.*, 1984; Kim *et al.*, 1992). It has also been shown that both ginsenosides (10 μg ml^{-1}) and Rgl (10 μM) significantly enhance the conversion of L-arginine to L-citrulline in bovine cultured aortic endothelial cells. This result suggests that ginsenosides can increase endothelial NOS activity and therefore NO production (Kim *et al.*, 1992). In the present study, although the ginsenosides-induced response in endothelium-denuded cor-

pus cavernosum was not examined due to difficulties in removing the endothelial cells, the corpus cavernosum vasodilator effect of ginsenosides qualitatively resembled that of ACh which is endothelium-dependent (Ignarro, 1992). Furthermore, ginsenosides enhance ACh-induced relaxation. These results suggest that the mechanism of ginsenosides-induced endothelium-dependent vasodilatation of corpus cavernosum is similar to that found in other vascular beds: both are mediated by activation of NOS and release of NO in the endothelium. Since the induction of relaxations by ginsenosides in corpus cavernosum and other vascular beds are immediate upon ginsenosides application (present study; Chen *et al.*, 1984; Kim *et al.*, 1992), it is most likely that ginsenosides activate an endothelial constitutive isoform of NOS.

In addition to the release of endothelial NO by ginsenosides, the present study, for the first time, demonstrated that ginsenosides enhanced neurogenic vasodilatation of the corpus cavernosum. It has been shown that electrical field stimulation of perivascular nerves of isolated corpus cavernosum of man and rabbits results in relaxation mediated by NO via activation of a constitutive isoform of NOS (Ignarro *et al.*, 1990; Moncada *et al.*, 1991; Bush *et al.*, 1992; Ignarro 1992). This NO-mediated neurogenic vasodilatation in the corpus cavernosum is supported by results of the present study. It is possible that ginsenosides may activate neuronal NOS activity similar to that observed in endothelial cells (Kim *et al.*, 1992). Thus, a given stimulation may increase synthesis and/or release of NO in the NANC nerves in ginsenosides-treated corpus cavernosum. This is supported by the finding of a greater increase in corpus cavernosum cyclic GMP content elicited by transmural nerve stimulation plus ginsenosides than the increase in cyclic GMP content induced by ginsenosides or transmural nerve stimulation alone. Ginsenosides enhancement of neurogenic vasodilatation is not due to modulation by ginsenosides of guanylate cyclase activity, since ginsenosides did not affect relaxation of the corpus cavernosum induced by Sin-1.

It is very likely that the enhanced neurogenic and endothelium-mediated vasodilatation in the corpus cavernosum induced by ginsenosides may contribute to the aphrodisiac effect of *Panax ginseng*, which is an essential constituent in the aphrodisiac prescription of traditional chinese medicine. It is interesting to note that the sensitivity of the corpus cavernosum to ginsenosides in inducing endothelium-dependent relaxation and enhancing transmural nerve stimulation-elicited relaxation appears to be different. The effective concentrations of ginsenosides ($250\,\mu g\,ml^{-1}$) in inducing relaxation and enhancing ACh-induced relaxation of corpus cavernosum is higher than that of ginsenosides ($100\,\mu g\,ml^{-1}$) in enhancing transmural nerve stimulation-elicited relaxation. These results suggest that ginsenosides have a preferential effect on neurogenic nitrergic vasodilatation in the corpus cavernosum. Although detailed pharmacokinetic data of ginsenosides in man remain to be determined, ginsenosides may exert a regional neurogenic vasodilatation in corpus cavernosum before inducing potential systemic hypotension through widespread endothelial mechanisms.

In summary, the results of the present study indicate that ginsenosides induce endothelium-dependent vasodilatation, enhance endothelium-dependent relaxation induced by ACh and increase neurogenic vasodilatation in the corpus cavernosum. The endothelial and neurogenic mechanism of ginsenosides in relaxing corpus cavernosum are predominantly mediated by NO and may, in part, account for the aphrodisiac effect of *Panax ginseng*.

This work was supported by Grants from NIH HL27763 and HL47574, American Heart Association (91010850), and SIU School of Medicine. We thank Ms Charlene Meents for preparing the manuscript and Mr Feng-Yuan Chen for valuable discussion.

References

BUSH, P.A., GONZALEZ, N.E. & IGNARRO, L.J. (1992). Biosynthesis of nitric oxide and citrulline from L-arginine by constitutive nitric oxide synthase present in rabbit corpus cavernosum. *Biochem. Biophys. Res. Commun.*, **186**, 308–314.

CHEN, X., CHEN, F.Y. & LEE, T.J.-F. (1993). Ginsenosides induce a NO-mediated relaxation of the corpus cavernosum of the rabbit. *FASEB J.*, **7**, A, 4446.

CHEN, X. & GILLIS, C.N. (1992). Enhanced photorelaxation in aorta, pulmonary artery and corpus cavernosum produced by BAY K 8644 or N-nitro-L-arginine. *Biochem. Biophys. Res. Commun.*, **186**, 1522–1527.

CHEN, X., GILLIS, C.N. & MAOLLI, R. (1984). Vascular effects of ginsenosides *in vitro*. *Br. J. Pharmacol.*, **82**, 485–491.

GRYGLEWSKI, R.J., PALMER, R.M.J. & MONCADA, S. (1986). Superoxide anion is involved in the breakdown of endothelium-derived vascular relaxing factor. *Nature*, **320**, 454–456.

IGNARRO, L.J. (1992). Nitric oxide as the physiological mediator of penile erection. *J. Natl. Inst. Health*, **4**, 59–62.

IGNARRO, L.J., BUSH, P.A., BUGA, G.M., WOODS, K.S., FUKUTO, J.M. & RAJEFER, J. (1990). Nitric oxide and cGMP formation upon electrical field stimulation cause relaxation of corpus cavernosum smooth muscle. *Biochem. Biophys. Res. Commun.*, **170**, 843–850.

KIM, (JUN) H., CHEN, X. & GILLIS, C.N. (1992). Ginsenosides protect pulmonary vascular endothelium against free radical-induced injury. *Biochem. Biophys. Res. Commun.*, **189**, 670–676.

LEE, T.J.-F. (1982). Cholinergic mechanism in the large cat cerebral artery. *Circ. Res.*, **50**, 870–879.

LINNIK, M.D. & LEE, T.J.-F. (1989). Effect of hemoglobin on neurogenic responses and cholinergic parameters in porcine cerebral arteries. *J. Cereb. Blood. Flow. Metab.*, **9**, 219–225.

MARTIN, W., VILLANI, G.M., JOTHIANANDAN, D. & FURCHGOTT, R.F. (1985). Selective blockade of endothelium-dependent and glyceryl trinitrate-induced relaxation by hemoglobin and by methylene blue in the rabbit aorta. *J. Pharmacol. Exp. Ther.*, **232**, 708–716.

MONCADA, S., PALMER, R.M.J. & HIGGS, E.A. (1991). Nitric oxide: physiology, pathophysyology and pharmacology. *Pharmacol. Rev.*, **43**, 109–142.

RAJFER, J., ARONSON, W.J., BUSH, P.A., DOREY, F.J. & IGNARRO, L.J. (1992). Nitric oxide as a mediator of relaxation of the corpus cavernosum in response to nonadrenergic, noncholinergic neurotransmission. *New Engl. J. Med.*, **326**, 90–94.

REES, D.D., SCHULZ, R., HODSON, H.F., PLAMER, R.M.J. & MONCADA, S. (1990). Identification of some novel inhibitors of the vascular nitric oxide synthase *in vivo* and *in vitro*. In *Nitric Oxide from L-arginine: A Bioregulatory System*. ed. Moncada, S. & Higgs, E.A., pp. 485–487, Elsevier: Amsterdam.

SHIBATA, S., TANAKA, O., SOMA, K., ILDA, Y. & NAMAMURA, H. (1965). Studies on saponins and sapogins of ginseng. *Tetrahedron Lett.*, **3**, 207–213.

(Received November 3, 1994
Revised December 21, 1994
Accepted January 17, 1995)

British Journal of Pharmacology (1995) 115, 19-24

Characterization of U-97775 as a $GABA_A$ receptor ligand of dual functionality in cloned rat $GABA_A$ receptor subtypes

Haesook K. Im, [1]Wha Bin Im, Jeff F. Pregenzer, Donald B. Carter, E. Jon Jacobsen & Beverly J. Hamilton

The Upjohn Company, CNS Diseases Research, 301 Henrietta St, Kalamazoo, Michigan 49001, U.S.A.

1 U-97775 (*tert*-butyl 7-chloro-4,5-dihydro-5-[(1-(3,4,5-trimethyl)piperazino)carbonyl]-imidazo[1,5-a])quinoxaline-3-carboxylate) is a novel $GABA_A$ receptor ligand of dual functionality and was characterized for its interactions with cloned rat $GABA_A$ receptors expressed in human embryonic kidney cells.

2 The drug produced a bell-shaped dose-response profile in the $\alpha 1\beta 2\gamma 2$ receptor subtype as monitored with GABA-induced Cl^- currents in the whole cell patch-clamp technique. At low concentrations ($<0.5\,\mu M$), U-97775 enhanced the currents with a maximal increase of 120% as normalized to $5\,\mu M$ GABA response (control). An agonist interaction of U-97775 with the benzodiazepine site is suggested, because Ro 15-1788 (an antagonist at the benzodiazepine site) abolished the current increase and [^{3}H]-flunitrazepam binding was inhibited by U-97775 with a K_i of 1.2 nM.

3 The enhancement of GABA currents progressively disappeared as the U-97775 concentration was raised above $1\,\mu M$, and the current amplitude was reduced to 40% below the control at $10\,\mu M$ U-97775. The current inhibition by U-97775 ($10\,\mu M$) was not affected by Ro 15-1788. It appears that U-97775 interacts with a second site on GABA receptors, distinct from the benzodiazepine site, to reverse its agonistic activity on the benzodiazepine site and also to inhibit GABA currents.

4 U-97775 at low concentrations reduced and at high concentrations enhanced [^{35}S]-TBPS binding. Ro 15-1788 selectively blocked the effect of U-97775 at low concentrations. Analysis of the binding data in the presence of Ro 15-1788 yielded a single low affinity site with an estimated K_d of 407 nM.

5 In other $\alpha\beta\gamma$ receptor subtypes, U-97775 at low concentrations enhanced Cl^- currents in the $\alpha 3\beta 2\gamma 2$, but not in the $\alpha 6\beta 2\gamma 2$ subtype. On the other hand, U-97775 at high concentrations reduced Cl^- currents in all the receptor subtypes we examined, including those of two subunits, $\alpha 1\beta 2$, $\beta 2\gamma 2$ and $\alpha 1\gamma 2$ subtypes.

6 Therapeutically, U-97775 could be unique among benzodiazepine ligands because of its ability to limit its own agonistic activity such that, at high doses the appearance of agonistic activity would be delayed until occupancy of its second site wanes. This property should make the total agonistic activity of U-97775 relatively constant over a wide range of drug doses, and may minimize its liability to abuse.

Keywords: U-97775; $GABA_A$ receptor subtypes; GABA-induced Cl^- current; biphasic effect

Introduction

$GABA_A$ receptors are supramolecular receptor-Cl^- channel complexes which are responsible for inhibitory neurotransmission in the brain, and appear to exist in combinations of various subunits (α, β, γ and δ), each of which consists of several isoforms in mammalian brains (Costa & Guidotti, 1979; Barnard *et al.*, 1987; Bormann, 1988; Schofield, 1989; Olsen & Tobin, 1990; Barnard *et al.*, 1993). Allosteric $GABA_A$ receptor ligands of diverse chemical structures have been widely used as therapeutic agents, i.e., numerous hypnotic and anxiolytic agents for the benzodiazepine site, barbiturates and progesterone metabolites (neurosteroids) (Sieghart, 1992). The benzodiazepine site modulators are functionally classified as agonists (positive modulators), inverse agonists (negative modulators), and neutral antagonists (binding, but without functional consequences). Recent studies with cloned rat $GABA_A$ receptors indicate that the allosteric modulation arises from interaction of drugs with distinct modulatory sites on the receptors including a few novel ones (Im *et al.*, 1993). Considering the presence of multiple binding sites for chemicals of diverse structure on $GABA_A$ receptors, it is not surprising to find drugs of dual functionality that interact with more than one modulatory site. In this study, we will describe such a drug, U-97775 (*tert*-butyl 7-chloro-4,5-dihydro-5-[(1-(3,4,5-trimethyl) piperazino) carbonyl]imidazo [1,5-a]) quinoxaline-3-carboxylate) (Figure 1).

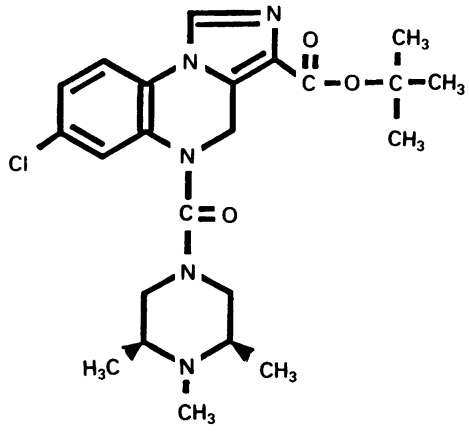

Figure 1 Chemical structure of U-97775.

[1] Author for correspondence.

Methods

Cloned cells

The stable human embryonic kidney cell lines (HEK-293) expressing the indicated combinations of α1, α3, α6, β2, and γ2 subunits of $GABA_A$ receptors were derived by transfection of plasmids containing cDNA and a plasmid encoding G418 resistance into the A293 cell as described elsewhere (Hamilton *et al.*, 1993). Preparation of baculovirus constructs (AcNPV) carrying rat cDNAs for $GABA_A$ receptor subunits and the growth of SF-9 cells in the presence of the recombinant baculovirus were carried out as described previously (Carter *et al.*, 1992).

Electrophysiology

The whole cell patch clamp technique (Hamill *et al.*, 1981) was used to record the GABA-mediated Cl^- currents in human embryonic kidney cells (A293) expressing various combinations of $GABA_A$ receptor subunits. Briefly, the pipette solution contained (mM): CsCl 140, EGTA 11, $MgCl_2$ 4, ATP 2 and HEPES 10, pH 7.3. Cells were bathed in an external solution containing (mM): NaCl 135, KCl 5, $MgCl_2$ 1, $CaCl_2$ 1.8 and HEPES 5, pH 7.2. GABA and drugs were dissolved in the external solution and were applied through a U-tube placed within 100 μm of the target cell. The concentration of GABA was varied according to the respective subtype, typically being near EC_{25} values or submaximal levels at which pentobarbitone and 5α-THDOC (3α,21-dihydroxy-5α-pregnan-20-one) produced robust enhancement of Cl^- currents. The current was recorded with an Axopatch 1D amplifier, a CV-4 headstage (Axon Instrument Co.), a Gould Recorder 220, and the holding potential of −60 mV at room temperature (21–24°C).

Binding studies

Binding of radioactive ligands was measured in membranes obtained from Sf-9 cells expressing recombinant receptors, using filtration techniques as described elsewhere (Pregenzer *et al.*, 1993). Briefly, displacement of [^{3}H]-flunitrazepam (α1β2γ2 and α3β2γ2) or [^{3}H]-Ro 15-4513 (ethyl 8-azido-6-dihydro-5-methyl-6-oxo-4H-imidazo [1,5-a]-[1,4] benzodiazepine-3-carboxylate) (α6β2γ2) by test compounds was measured in the medium containing (mM): NaCl 118, KCl 5, $CaCl_2$ 2, $MgCl_2$ 2, HEPES 20 (pH 7.3), the radioactive ligand (3 nM for flunitrazepam) and 30 μg membrane proteins in a total volume of 500 μl at 4°C for 60 min. The effects of test compounds on [^{35}S]-TBPS ([^{35}S]-t-butylbicyclophosphorothionate) binding were measured in the medium containing 1 M NaCl, and 10 mM Tris/HCl (pH 7.4), [^{35}S]-TBPS (3 nM), and 50 μg membrane proteins in a total volume of 500 μl at 24°C for 120 min. Non-specific binding was estimated and was subtracted to compute specific binding as described earlier (Pregenzer *et al.*, 1993).

Results

Dual effects of U-97775 on GABA-induced Cl^- currents in αβγ subtypes

We tested the effects of U-97775 at various concentrations on GABA-induced Cl^- currents in several subtypes of cloned rat $GABA_A$ receptors expressed in HEK 293 cells, using the whole cell patch clamp technique. Figure 2a shows Cl^- current traces induced by 5 μM GABA alone, with diazepam or U-97775 from 0.2 to 10 μM in the α1β2γ2, α3β2γ2 and α6β2γ2 subtypes of $GABA_A$ receptors. Figure 2b shows composite dose-response profiles obtained after normalization to standard GABA responses. In the α1β2γ2 subtype, U-97775 produced a bell-shaped response. The drug at low concentrations (<0.5 μM) increased GABA(5 μM)-induced Cl^- currents, maximally by 120 ± 22% as normalized to 5 μM GABA response (control), but as the drug concentration was raised, the amplitude of Cl^- currents was gradually decreased, by 39 ± 5% at 10 μM U-97775 from the control. A similar bell-shaped response was observed in the α3β2γ2 subtype. U-97775 enhanced Cl^- currents, maximally by 117 ± 33% at 0.2 μM, but reduced it to the control level at 10 μM. In the α6β2γ2 subtype, where classical benzodiazepines (i.e., diazepam) had no effect, U-97775 at low concentrations (<0.5 μM) produced no appreciable change, but at higher concentrations reduced the current amplitude by 45 ± 7% at 10 μM.

Selective block of the agonistic action of U-97775 by Ro 15-1788

We examined whether Ro 15-1788, a classical antagonist for the benzodiazepine site, influences U-97775 actions in the

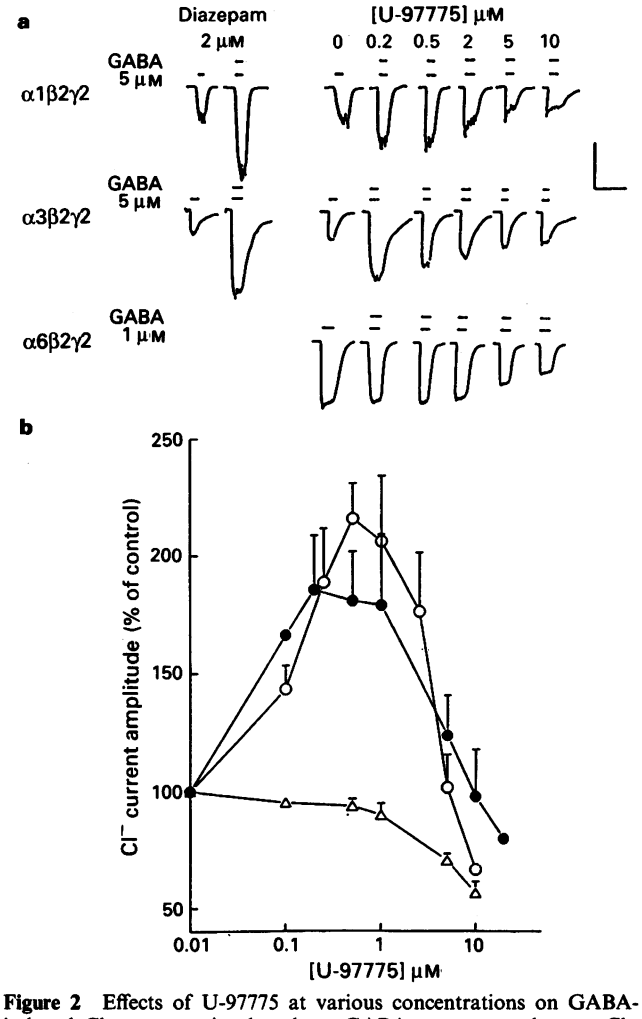

Figure 2 Effects of U-97775 at various concentrations on GABA-induced Cl^- currents in cloned rat $GABA_A$ receptor subtypes. Cl^- currents were measured by the whole-cell patch clamp technique in HEK293 cells expressing the α1β2γ2, α3β2γ2 or α6β2γ2 subtype. The holding potential was −60 mV under a symmetrical Cl^- gradient. GABA at 5 μM in the α1β2γ2 and α3β2γ2 subtypes or at 1 μM in the α6β2γ2 subtype was applied for 10 s with or without U-97775 at the indicated concentration. The GABA concentrations were about equivalent to the EC_{25} value in the respective subtype. Diazepam (2 μM) was used to monitor the ability of benzodiazepine site ligands to enhance Cl^- currents. In the α6β2γ2 subtype, diazepam had no effect on GABA-induced Cl^- currents. (a) Typical traces for GABA-induced Cl^- currents. (b) Plots showing changes in Cl^- current amplitude as a function of U-97775 concentrations: (○) α1β2γ2; (●) $\alpha_3\beta_2\gamma_2$ and (△) α6β2γ2. The currents were normalized to that observed with GABA alone. The data represent the mean ± s.e. from three experiments at least. The vertical calibration bar represents 500 pA and the horizontal bar represents 30 s.

α1β2γ2 subtype. Ro 15-1788 at 10 μM (alone, no effect on GABA-induced Cl^- currents) abolished the current increase by U-97775 at 0.25 μM (Figure 3a), but produced no appreciable effect on inhibition of the Cl^{-1} current by U-97775 at 10 μM (Figure 3b). The extent of inhibition by U-97775 (10 μM) was 35 ± 10% and 39 ± 5% in the presence or absence of Ro 15-1788 (10 μM), respectively. These results indicate that U-97775 interacts with at least two sites on $GABA_A$ receptors, the benzodiazepine site (high affinity, agonistic site) and a second site (low affinity, inverse agonistic site) distinct from the benzodiazepine site.

As shown in Figure 3b, the Cl^- current in the cell treated with U-97775 at 10 μM, upon washing with a drug-free solution, recovered well beyond the level of inhibition. Its amplitude became about double of the control (Figure 3b, washout). The increased current level was observed only with the receptors treated with U-97775 (10 μM) without preincubation with Ro 15-1788 (data not shown), and hardly changed during a 30 min washing period (only about 10% reduction). This could be interpreted to mean that the dissociation rate of U-97775 from the benzodiazepine site was much slower than from its second site, so that the benzodiazepine site remains occupied during washing and is responsible for the current enhancement. The prolonged occupancy of the benzodiazepine site by U-97775 was further supported by the observation that diazepam did not enhance GABA-induced Cl^- currents in the U-97775-treated cells during the washing out period (data not shown). Similar washout effects were observed with the α3β2γ2 subtype upon treatment with U-97775 at high concentrations (10 μM), but not with the α6β2γ2 subtype. This subtype selectivity for U-97775 resembles that for classical benzodiazepines (Luddens *et al.*, 1990).

Another interesting point was noted from the experiments with Ro 15-1788. The level of current inhibition by U-97775 (10 μM) was not appreciably altered in the presence or absence of Ro 15-1788 (see Figure 3b). If the two opposing effects of U-97775 were simply additive, one might expect a much greater degree of inhibition by U-97775 in the presence of Ro 15-1788, which eliminates its agonistic action. The failure to observe such a change here indicates independence of the two opposing effects of U-97775, and further suggests that certain allosteric interactions occur between the first and second sites, which lead to the abolition of its agonistic activity at the benzodiazepine site, in addition to the inhibition of Cl^- currents via the second site. Alternatively, the current inhibition by U-97775 at high concentrations could arise from a direct block of the chloride channel. If so, one would expect not only a voltage-dependence of the inhibition of Cl^- currents by U-97775, but also an ability to abolish the GABA potentiating actions of other allosteric ligands. Contrary to such expectations, the Cl^- current inhibition by U-97775 was not voltage-dependent and its ability to reverse GABA potentiation was restricted to benzodiazepine ligands (Figure 4). For instance, the current reduction by U-97775 at 10 μM was 33 ± 7% at −25 mV and 35 ± 8% at +25 mV (Figure 4a), which were not different from the level of inhibition at −60 mV, 39 ± 5%. Also U-97775 failed to antagonize the potentiating actions of pentobarbitone and 5α-THDOC (a neurosteroid) (Figure 4b and c). In the α1β2γ2 subtype, pentobarbitone at 20 μM and 5α-THDOC at 0.2 μM produced robust enhancements of GABA-induced Cl^- currents, a net increase of 230 and 290%, respectively, as normalized to the control (5 μM GABA response). In the presence of U-97775 at 10 μM, the amplitudes of GABA currents enhanced by pentobarbitone or 5α-THDOC were only partially reduced by the same amount as would be expected if their actions were additive with U-97775. It appears that U-97775 uncouples only the agonistic activity of benzodiazepine site ligands. These results favour the allosteric coupling between the low and the high affinity (benzodiazepine) sites for U-97775 over its direct blocking of Cl^- channels.

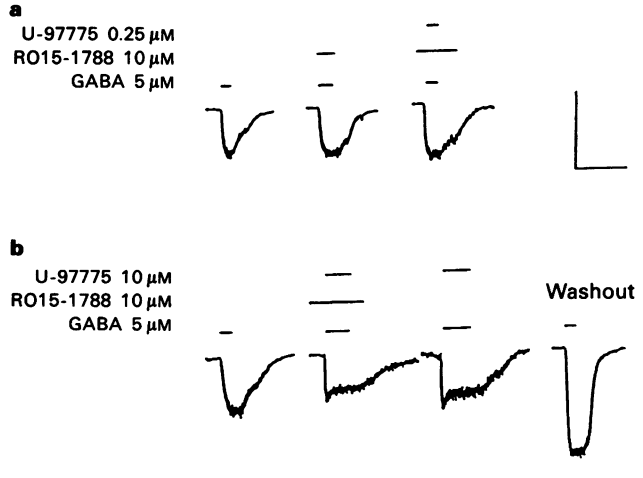

Figure 3 Differential sensitivity of U-97775 action on the Cl^- currents at low and high concentrations to Ro 15-1788. GABA-induced Cl^- currents in the whole cell configuration were measured with the α1β2γ2 subtype. Ro 15-1788 alone had no effect on Cl^- currents, but abolished the enhancement of Cl^- currents by U-97775 at 0.25 μM (a). In order to ensure occupancy of the benzodiazepine site with Ro 15-1788, the receptors were exposed to Ro 15-1788 for 5 min before the coapplication with U-97775. Ro 15-1788, on the other hand, had no effect on the current inhibition by U-97775 at 10 μM (35 ± 10%, the mean ± s.e. from three experiments) (b). Between drug applications, the patch was washed until the original GABA response was restored. It should be noted that the GABA response was restored to the initial value following application of the mixture of Ro 15-1788 and U-97775, but increased more than two fold following application of U-97775 at 10 μM due to the slow dissociation rate of the drug from the benzodiazepine site. The vertical calibration bar represents 500 pA and the horizonatal bar represents 30 s.

Monophasic inhibition of GABA-induced Cl^- currents by U-97775 in the α1β2, α1γ2 and β2γ2 subtypes

Receptor subtypes made of only two types of receptor subunits have often been useful to study the modes of interactions for novel ligands (Im *et al.*, 1993). Here we examined the effects of U-97775 on GABA-induced Cl^- currents on the α1β2, β2γ2 and α1γ2 subtypes (Figure 5). In all these subtypes, U-97775 at low concentrations (<0.5 μM) did not appreciably enhance GABA-mediated Cl^- currents, but at high concentrations (>0.5 μM) reversibly inhibited the currents in a concentration-dependent manner (Figure 5a). The U-97775 potency in blocking Cl^- currents was the highest in the β2γ2 subtype, followed by the α1γ2, α1β1 and α1β2γ2 subtypes (in the presence of Ro 15-1788); the IC_{50} values were 1.5 ± 0.3, 3.7 ± 0.2, 3.9 ± 0.3 and 5 ± 1 μM for the respective subtypes in the same order as above (Figure 5b). The variation in the IC_{50} values, albeit marginal, suggests the influence of quaternary interactions among subunits on the second site for U-97775.

Effect of U-97775 on benzodiazepine and TBPS binding

Interaction of U-97775 with the benzodiazepine site was further supported by equilibrium binding studies with the cloned α1β2γ2 receptor expressed in SF-9 insect cells which were infected with recombinant baculovirus carrying the $GABA_A$ receptor cDNAs. U-97775 displaced [^{3}H]-flunitrazepam with a K_i value of 1.2 ± 0.1 and 0.3 ± 0.04 nM for the α1β2γ2 and α3β2γ2 subtypes, respectively, but had no effect on [^{3}H]-Ro 15-4513 binding in the α6β2γ2 subtype (K_i> 10,000 nM), where classical benzodiazepines (i.e., diazepam) also failed to interact (Luddens *et al.*, 1990).

TBPS is another high affinity ligand specific for $GABA_A$ receptors and sensitive to allosteric modulators (Squires *et al.*, 1983; Gee *et al.*, 1986). Agonists and inverse agonists for $GABA_A$ receptors, for instance, have been shown to decrease

and increase TBPS binding, respectively, in the presence of 2 μM GABA (Im & Blakeman, 1991). In this study we tested the effect of U-97775 on TBPS binding in the membranes of SF-9 cells expressing the α1β2γ2 subtype of $GABA_A$ receptors (Figure 6). In the presence of GABA, U-97775 at low concentrations (<0.2 μM) reduced TBPS binding by 25 ± 7%, but at higher concentrations (>0.5 μM) reversed the early inhibition and increased TBPS binding by about 39% above the control. Ro 15-1788 (5 μM) abolished the inhibition of TBPS binding by U-97775 at low concentrations, but had no effect on the TBPS binding enhancement by the drug at high concentrations. Again, the maximal enhancement of TBPS binding by U-97775 at high concentrations (10 μM) was not appreciably changed by Ro 15-1788 (10 μM). In the absence of Ro 15-1788, U-97775 (10 μM) increased TBPS binding by 39 ± 6% above the control, a net shift of about 64%, including the 25% inhibition observed at low concentrations (0.02 μM). However, the maximal enhancement by U-97775 was still 35 ± 10% in the presence of Ro 15-1788, which abolished the inhibition of TBPS binding by U-97775 at low

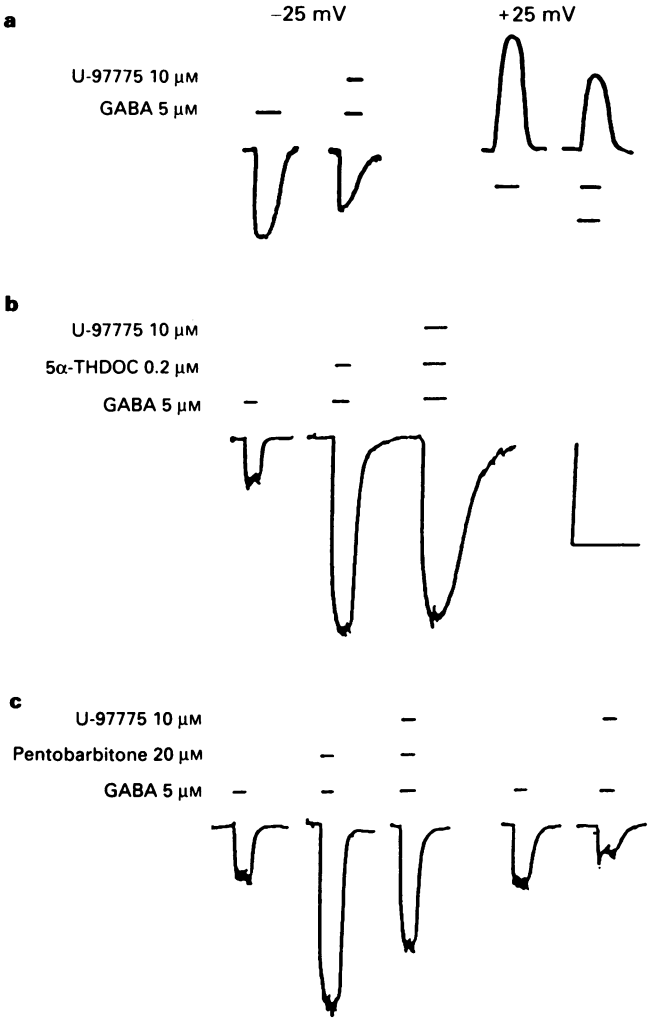

Figure 4 Voltage-independence of the Cl^- current inhibition by U-97775 at high concentrations and the absence of an interaction of U-97775 with binding sites for 5α-THDOC and barbiturates. GABA (5 μM)-induced Cl^- currents in the whole cell patch were measured with the α1β2γ2 subtype. U-97775 (10 μM) decreased Cl^- currents by 33 ± 7 and 35 ± 8% (the mean ± s.e. from six experiments) at the holding potential of −25 and +25 mV, respectively (a). The inhibition level was not different from that observed at −60 mV (39 ± 5%). Also we examined the effect of 0.2 μM 5α-THDOC or the mixture of 5α-THDOC and U-97775 on GABA(5 μM)-induced Cl^- currents (b); similarly the effect of 20 μM pentobarbitone alone or in combination with U-97775 was examined (c). Enhancement of GABA-induced Cl^- currents by 5α-THDOC or pentobarbitone was reduced in the presence of U-97775 (10 μM) by the same amount as the inhibition of GABA currents by U-97775 alone (about 30% as normalized to the 5 μM GABA response). This additiveness of the drug effects, which was consistently observed in three experiments, indicates no coupling between the binding sites for U-97775 and those for 5α-THDOC or pentobarbitone. The vertical calibration bar represents 500 pA and the horizontal bar represents 30 s.

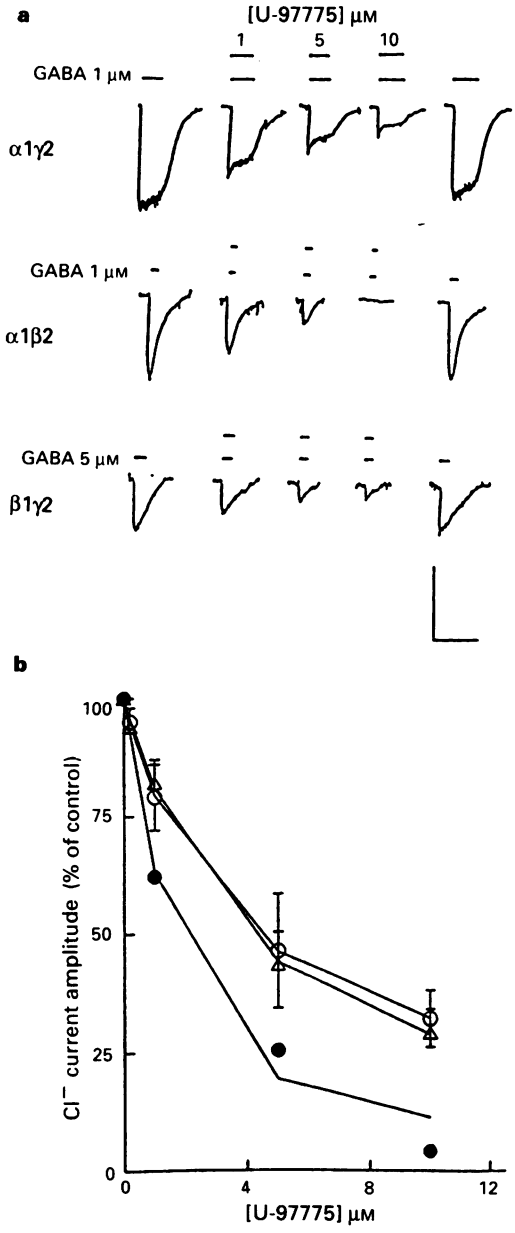

Figure 5 Concentration-dependent inhibition of GABA-induced Cl^- currents by U-97775 in the α1β2, β2γ2 and α1γ2 subtypes. Cl^- currents were induced with 1 μM GABA in the α1β2 subtype and with 5 μM in the β2γ2 and α1γ2 subtypes in the presence or absence of U-97775 at the indicated concentrations (a). The GABA concentrations represent submaximal levels at which pentobarbitone and 5α-THDOC produced robust enhancement of Cl^- currents. In these subtypes, the GABA response was immediately restored to the initial level following washout of U-97775 (10 μM), suggesting the absence of high affinity sites for the drug such as occur in the α1β2γ2 subtype. Changes in Cl^- current amplitude by U-97775 at various concentrations were normalized to the GABA response and plotted as a function of the drug concentration (b): (○) α1β2; (●) β2γ2; (△) α1γ2. The solid lines represent the data fitted with a logistic equation (see text). The currents were normalized to that observed with GABA alone. The data represent the mean from two or more experiments (with s.e.). The vertical calibration bar represents 500 pA and the horizontal bar represents 30 s.

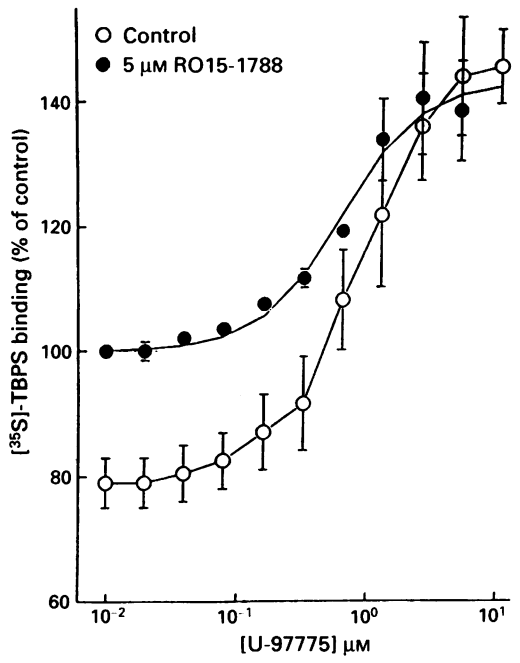

Figure 6 Effect of U-97775 on [^{35}S]-TBPS binding to the α1β2γ2 subtype of $GABA_A$ receptors. [^{35}S]-TBPS binding (3 nM) at equilibrium was measured in the membranes from Sf-9 cells expressing the α1β2γ2 subtype in the presence of 2 μM GABA, U-97775 at the indicated concentrations with (●) or without (O) 5 μM Ro 15-1788. U-97775-induced changes in TBPS binding were normalized to the level without the drug. The data representing changes in TBPS binding as a function of the U-97775 concentration in the presence of Ro 15-1788 were fitted with a logistic equation (see text). The data represent the mean ± s.e. from three experiments.

concentrations. This further supports the independence of the two opposing effects of U-97775, as noted above with electrophysiological data. The data in the presence of Ro 15-1788 was analyzed with a logistic equation, $E = E_{max} * [U\text{-}97775]/(K_{0.5} + [U\text{-}97775])$, which provided the half maximal concentration of U-97775 ($K_{0.5}$) of 407 ± 37 nM, and E_{max} of 39 ± 6%. Overall, the effects of U-97775 on TBPS binding are consistent with the functional characteristics observed in the electrophysiological studies described above, including its concentration-dependent dual action, sensitivity to Ro 15-1788, and independence of the two opposing effects.

Discussion

In this study we have shown that U-97775 is unique among $GABA_A$ receptor ligands in having two interaction sites of opposing functionality on the receptors. The drug produced a bell shaped dose-response profile as measured with GABA-induced whole cell currents in α1β2γ2 and α3β2γ2 $GABA_A$ receptors. The enhancement of the currents by U-97775 was attributed to the drug interaction with the benzodiazepine site as an agonist, because of its disappearance in the presence of Ro 15-1788 and its absence in the α6β2γ2 subtype where diazepam also failed to interact (Luddens *et al.*, 1990). Furthermore, U-97775 inhibited [^{3}H]-flunitrazepam binding with nanomolar affinity only in α1β2γ2 and α3β2γ2 subtypes, but not [^{3}H]-Ro 15-4513 binding in the α6β2γ2 subtype.

The second site (low affinity site) which was responsible for the descending limb of the bell shaped dose-response profile for U-97775, on the other hand, appeared to be distinct from the benzodiazepine site, judging from its insensitivity to Ro 15-1788 and its presence in all the subtypes tested, including α6β2γ2, α1β2, α1γ2 and β2γ2 subtypes. The interesting point, however, was that Ro 15-1788 neither abolished, nor enhanced the current inhibition by U-97775 (10 μM), although it eliminated the agonistic activity of U-97775 in the α1β2γ2 subtype. Thus, the disappearance of agonistic activity for U-97775 could not be explained by an algebraic sum of its positive and negative effects resulting from occupancy of its high and low affinity sites, respectively. Furthermore, the inhibition of Cl^- currents by U-97775 at high concentrations seems not to arise from a direct block of Cl^- channels, judging from the voltage-independence and the failure of U-97775 to antagonize the GABA potentiating action of pentobarbitone and 5α-THDOC (Figure 4). Also U-97775 blocked TBPS binding, which has been shown to be sensitive to modulation of Cl^- channels by allosteric ligands (Squires *et al.*, 1983; Gee *et al.*, 1986). Apparently, occupancy of the second site by U-97775 allosterically influences not only the GABA site (resulting in inhibition of GABA-induced Cl^- currents), but also the benzodiazepine site (leading to the abolition of its own agonistic action at this site). These two types of negative allosteric actions of U-97775 could conceivably arise from two distinct low affinity sites on the receptor, but that is highly unlikely since only one low affinity site with a K_d of 407 nM was detected from analysis of TBPS binding data at equilibrium in the presence of Ro 15-1788. At present, we cannot identify the location of the low affinity site, but it may not be localized at a selective subunit or subunit interface, because the drug effectively blocked GABA-induced Cl^- currents with an IC_{50} value ranging from 1 to 3 μM in α1β2, α1γ2 and β2γ2 subtypes. The low affinity site is likely to consist of common regions among the three subunits. This subunit nonselectivity has been observed with several $GABA_A$ receptor ligands, such as picrotoxin (also TBPS), barbiturates and neurosteroids (Im *et al.*, 1993), and may stem from 30 to 40% indentity in the amino acid sequence among $GABA_A$ receptor subunits (Olsen & Tobin, 1990).

The therapeutic potential of U-97775 deserves some consideration. At doses leading to occupancy of only the high affinity site, U-97775 would be expected to behave as a benzodiazepine site agonist (anxiolytic or hypnotic agent). However, at higher doses the drug should behave like a benzodiazepine site antagonist (or a weak inverse agonist at extremely high concentrations) because of its occupancy of the low affinity site. A delayed agonistic activity would then appear as drug occupancy of the second site wanes. These characteristics of U-97775 should result in an agonistic activity that is relatively constant over a wide range of the drug concentrations, unlike typical benzodiazepines. On the basis of the K_d for the low affinity site (407 nM as estimated from TBPS binding in the α1β2γ2 subtype), one would expect considerable occupancy of the low affinity site at the plasma concentration of 0.5 mg l^{-1} which is reachable under various clinical situations. Thus, the dual action of U-97775 on $GABA_A$ receptors may minimize its liability to abuse of the type associated with most of the benzodiazepines currently available on the market.

References

BARNARD, E.A., DARLISON, M.G. & SEEBURG, P. (1987). Molecular biology of the $GABA_A$ receptor: the receptor/channel superfamily. *Trends Neurosci.*, **10**, 502–509.

BARNARD, E.C., SUTHERLAND, M., ZAMAN, M., MATSUMOTO, M., NAYEEM, N., GREEN, T., DARLISSON, M.G. & BATESON, A.N. (1993). Multiplicity, structure and function in $GABA_A$ receptors. *Ann. N.Y. Acad. Sci.*, **707**, 117–125.

BORMANN, J. (1988). Electrophysiology of $GABA_A$ and $GABA_B$ receptor subtypes. *Trends Neurosci.*, **11**, 112–116.

CARTER, D.B., THOMSEN, D.R., IM, W.B., LENNON, D.J., NGO, D.M., GALE, W., IM, H.K., SEEBURG, P.H. & SMITH, M.W. (1992). Functional expression of $GABA_A$ Cl^- channels and benzodiazepine binding sites in Baculovirus infected insect cells. *Bio/Technology*, **10**, 679–681.

COSTA, E. & GUIDOTTI, A. (1979). Molecular mechanisms in the receptor action of benzodiazepines. *Annu. Rev. Pharmacol.*, **19,** 531–545.

GEE, K.W., LAWRENCE, L.J. & YAMAMURA, H.I. (1986). Modulation of the chloride ionophore by benzodiazepine receptor ligands: Influence of γ-aminobutyric acid and ligand efficacy. *Mol. Pharmacol.*, **30,** 218–225.

HAMILL, O.P., MARTY, A., NEHER, E., SAKMANN, B. & SIGWORTH, F.J. (1981). Improved patch-clamp techniques for high-resolution current recording from cells and cell-free membrane patches. *Pflügers Arch.*, **391,** 85–100.

HAMILTON, B.J., LENNON, D.J., IM, H.K., IM, W.B., SEEBURG, P.H. & CARTER, D.B. (1993). Stable expression of cloned rat $GABA_A$ receptor subunits in a human kidney cell line. *Neurosci. Lett.*, **153,** 206–209.

IM, W.B. & BLAKEMAN, D.P. (1991). Correlation between $GABA_A$ receptor ligand-induced changes in t-butylbicyclophosphorol [35S] thionate binding and 36Cl- uptake in rat cerebrocortical membranes. *Mol. Pharmacol.*, **39,** 394–398.

IM, H.K., IM, W.B., JUDGE, T.M., GAMMILL, R.B., HAMILTON, B.J., CARTER, D.B. & PREGENZER, J.F. (1993). Substituted pyrazinones, a new class of allosteric modulators for γ-aminobutyric $acid_A$ receptors. *Mol. Pharmacol.*, **44,** 468–472.

LUDDENS, H., PRICHETT, D.B., KOHLER, M., KILISCH, I., KEINANEN, K., MONYER, H., SPRENGEL, R. & SEEBURG, P.H. (1990). Cerebellar $GABA_A$ receptor selective for a behavioral alcohol antagonist. *Nature*, **346,** 648–651.

OLSEN, R.W. & TOBIN, A.J. (1990). Molecular biology of $GABA_A$ receptors. *FASEB J.*, **4,** 469–1480.

PREGENZER, J.F., IM, W.B., CARTER, D.B. & THOMSEN, D.R. (1993). Comparison of interactions of [^{3}H]muscimol, [^{35}S]t-butylbicyclophosphorothionate and [^{3}H]flunitrazepam with cloned γ-aminobutyric $acid_A$ receptors of the α1β2 and α1β2γ2 subtype. *Mol. Pharmacol.*, **43,** 801–806.

SCHOFIELD, P.R. (1989). The $GABA_A$ receptor: Molecular biology reveals a complex picture. *Trends Pharmacol. Sci.*, **10,** 476–478.

SIEGHART, W. (1992). $GABA_A$ receptors: ligand-gated Cl^- ion channels modulated by multiple drug-binding sites. *Trends Pharmacol. Sci.*, **13,** 446–450.

SQUIRES, R.F., CASIDA, J.E., RICHARDSON, M. & SAEDERAP, E. (1983). [^{35}S]t-butylbicyclophosphorothionate binds with high affinity to brain specific sites coupled to γ-aminobutyric acid-A and ion recognition sites. *Mol. Pharmacol.*, **23,** 326–336.

(Received November 10, 1994
Revised January 4, 1995
Accepted January 17, 1995)

British Journal of Pharmacology (1995) 115, 25-30

Subtypes of tachykinin receptors on tonic and phasic neurones in coeliac ganglion of the guinea-pig

F.-Y. Zhao, [1]K. Saito, [2]K. Yoshioka, J.-Z. Guo, T. Murakoshi, *S. Konishi & M. Otsuka

Department of Pharmacology, Faculty of Medicine, Tokyo Medical and Dental University, Bunkyo-ku, Tokyo 113 and *Mitsubishi Kasei Institute of Life Science, Machida, Tokyo 194, Japan

1 Intracellular recording techniques were used to investigate the characteristics of tachykinin receptors and their subtypes in tonic and phasic neurones, which constituted two major neuronal populations in the coeliac ganglion of the guinea-pig.

2 In 95% of phasic neurones a long-lasting after-hyperpolarization (LAH), 5–8 s in duration and 10–20 mV in amplitude, was observed following action potentials evoked by passing a train of depolarizing current pulses into the neurones. In contrast, LAH was observed in only 4% of tonic neurones.

3 In most tonic neurones, substance P (SP), neurokinin A (NKA) and senktide induced depolarizations, whereas in phasic neurones they usually inhibited LAH but rarely induced depolarization.

4 Tonic and phasic neurones were further classified into three groups based on their responses (depolarization for tonic neurones and LAH inhibition for phasic neurones) to these tachykinin receptor agonists: (1) neurones responsive to SP, NKA and senktide (71–78%); (2) those responsive to senktide but not to SP and NKA (12–23%) and (3) those not responsive to any of the three agonists (7–11%).

5 GR71251 (5 μM), an NK_1-selective tachykinin receptor antagonist, depressed the depolarization in tonic neurones and the LAH inhibition in phasic neurones induced by SP and NKA, but not those induced by senktide.

6 Selective NK_2 receptor agonists, [Nle^{10}]NKA_{4-10}, [β-Ala^8]NKA_{4-10} and GR64349, were without effect in both tonic and phasic neurones. Furthermore, an NK_2 receptor antagonist, L659,877, did not inhibit the depolarization induced by NKA, SP or senktide in tonic neurones.

7 It is suggested that NK_1 and NK_3 receptors are present on a large proportion of coeliac ganglion neurones. In tonic neurones both subtypes of tachykinin receptors are coupled to membrane depolarization, whereas in phasic neurones activation of these receptors leads to inhibition of LAH. The present study also suggests that NKA evokes the depolarization in tonic neurones and the LAH inhibition in phasic neurones via NK_1, but not NK_2 receptors.

Keywords: Tachykinin receptor; substance P; neurokinin A; senktide; GR71251; after-hyperpolarization; sympathetic ganglion

Introduction

Although information about subtypes of tachykinin receptors and responses mediated by these receptors in smooth muscle tissues is abundant, our knowledge about tachykinin receptors expressed in neurones is relatively limited. In mammalian prevertebral sympathetic ganglia of the guinea-pig, neurones are depolarized by tachykinins (Konishi & Otsuka, 1985; Saria *et al.*, 1985; Vanner *et al.*, 1993). There is evidence for the neurotransmitter role in generation of slow excitatory postsynaptic potentials (e.p.s.ps) of substance P (SP) and neurokinin A (NKA), which are released from axon collaterals of primary afferent fibres, in the prevertebral ganglia (Tsunoo *et al.*, 1982; Konishi & Otsuka, 1985; for review see Otsuka & Yoshioka, 1993). However, subtypes of tachykinin receptors present on these neurones were not fully clarified.

Neurones in sympathetic ganglia of the guinea-pig are inhomogeneous and have been classified into several types based on their discharge patterns to a depolarizing current pulse and the presence or absence of a long after-hyperpolarization (LAH) (e.g. Cassell & McLachlan, 1987; McLachlan & Meckler, 1989; Jänig & McLachlan, 1992). Recently, we examined the responses of neurones in the guinea-pig coeliac ganglion to stimulation of postganglionic nerves, in which tachykininergic primary afferent fibres are presumably contained, and found that two different non-cholinergic responses, i.e. slow e.p.s.p. and the inhibition of LAH, were observed depending upon the types of neurones (Saito & Konishi, 1993). We also provided evidence that tachykinins, SP and NKA, contribute to both types of responses.

In the present experiments, we examined tachykinin receptor subtypes involved in responses of neurones of the guinea-pig coeliac ganglion by using selective agonists and antagonists for NK_1, NK_2 and NK_3 receptors. Some of the results have been published in a preliminary form (Saito & Konishi, 1993; Zhao *et al.*, 1993a, b).

Methods

Guinea-pigs of either sex weighing 200–250 g were stunned and bled, and the coeliac ganglion with the attached mesenteric nerves (Macrae *et al.*, 1986; or coeliac nerves according to McLachlan & Meckler, 1989) was isolated under a stereomicroscope. The isolated preparation was placed in a recording chamber of 0.5 ml volume, which was perfused at 2 ml min^{-1} with a nutrient solution saturated by a mixed gas of 95% O_2 and 5% CO_2 and kept at 30°C. The composition of the solution was (mM): NaCl 138.6, KCl 3.35, NaH_2PO_4 0.58, $NaHCO_3$ 21.0, $MgCl_2$ 1.16, $CaCl_2$ 2.5, glucose 10.

[1]Present address: Biological Research Laboratory, Sankyo Co., Ltd., Shinagawa-ku, Tokyo 140, Japan.
[2]Author for correspondence.

Membrane potential changes were monitored through a glass microelectrode of 80–160 MΩ filled with 2 M potassium acetate on a storage oscilloscope, and recorded on a pen recorder and an X-Y plotter. Single depolarizing current pulses of 0.1–0.5 nA with 1.5 s duration were injected into neurones through the recording electrode to determine the cell types, and 10 successive depolarizing current pulses of 1 nA with 20 ms duration at 20 Hz were applied to examine whether the neurones produce an LAH. The magnitude of the LAH was expressed as the area under the resting potential level on the record.

To construct concentration-response curves to SP, NKA and senktide in tonic and phasic neurones (Figures 2 and 6), each agonist were applied for 1 min at intervals of 10–30 min to avoid tachyphylaxis. Responses to 2–7 concentrations of each agonist were examined on each neurone. Only the data from the neurones that were sensitive to all three agonists were used for the concentration-response curves.

Drugs

Drugs used were SP, [Sar^9, Met(O$_2$)^{11}]SP, SP methyl ester (SPOMe), NKA, [Nle^{10}]NKA$_{4-10}$, [β-Ala^8]NKA$_{4-10}$, [Trp^7, β-Ala^8]NKA$_{4-10}$ and [MePhe^7]neurokinin B ([MePhe^7]NKB) (purchased from Peninsular Laboratories, Inc.); L659,877 (*cyclo*[Gln-Trp-Phe-Gly-Leu-Met]) (purchased from Cambridge Research Biochemicals, Ltd.); senktide (succinyl-[Asp^6, MePhe^8]SP$_{6-11}$) (kindly supplied by Dr Z. Selinger of Hebrew University); GR71251 ([D-Pro^9]spiro-γ-lactam[Leu^{10},Trp^{11}]SP) and GR64349 ([Lys^3,Gly^8-(R)-γ-lactam-Leu^9] [NKA$_{3-10}$]) (kindly supplied by Dr R.M. Hagan of Glaxo Group Research Ltd.). All the drugs were dissolved in the perfusing solution and applied by perfusion. The tachykinin receptor antagonists were applied to the preparation for at least 20 min before examining their effects.

Statistical analysis

Results are expressed as mean ± s.e.mean. Statistical comparison was made by Student's *t* test. Probability of 0.05 or less was considered significant.

Results

Neurones in the guinea-pig coeliac ganglion were classified according to their discharge patterns in response to depolarizing current pulses and the presence or absence of LAH following repetitive action potentials (Cassell & McLachlan, 1987; McLachlan & Meckler, 1989; Jänig & McLachlan, 1992). Two major groups of neurones were identified (Zhao *et al.*, 1993b). The first group, tonic neurones, comprised 38% of the randomly sampled neurones, and exhibited maintained firing during the depolarizing pulse. Only a small portion (~4%) of tonic neurones showed obvious LAH following action potentials. The second group, phasic neurones, comprised 39% and exhibited an initial transient burst of discharges during the depolarizing pulse. Most of the phasic neurones (~95%) showed a typical LAH (5–8 s in duration and 10–20 mV in amplitude) following action potentials. A small percentage of neurones (23%) did not belong to either of the groups. In this study the responses to tachykinin receptor agonists and antagonists of 146 tonic neurones and 101 phasic neurones were analyzed.

Effects of SP, NKA, senktide and GR71251 on tonic neurones

The responses of tonic neurones to SP, NKA and senktide were examined. SP and NKA are endogenous tachykinins with preferential affinities for NK$_1$ and NK$_2$ receptors, respectively, and senktide is a water-soluble synthetic agonist with a high selectivity for the NK$_3$ receptor (Papir-Kricheli *et*

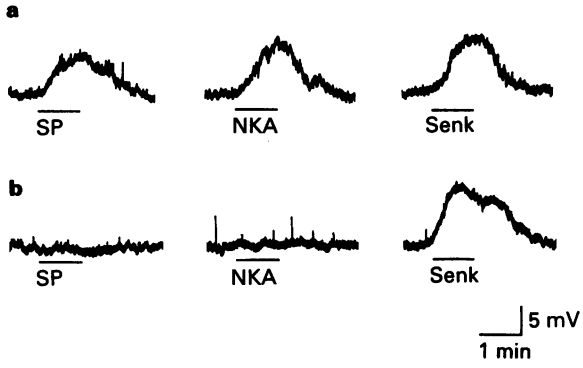

Figure 1 Responses of tonic neurones to substance P, neurokinin A and senktide. Substance P (SP), neurokinin A (NKA) and senktide (Senk) were applied for 1 min by perfusion during the periods indicated by the horizontal bars. The neurone shown in (a) was depolarized by SP (30 nM), NKA (30 nM) and senktide (30 nM), whereas the other neurone shown in (b) was depolarized by senktide (10 nM), but not by SP (300 nM) and NKA (300 nM). Resting potentials were −49 mV and −76 mV in neurones in (a) and (b), respectively.

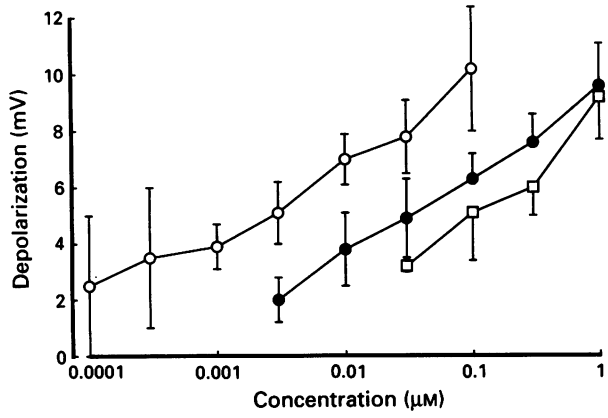

Figure 2 Concentration-response curves to tachykinin receptor agonists in tonic neurones. Ordinate scale: amplitude of depolarization in mV. Abscissa scale: concentration of tachykinin receptor agonists: (○) senktide; (●) substance P; and (□) neurokinin A. The data were obtained from tonic neurones that were sensitive to all the three agonists. Each point represents mean ± s.e.mean (n = 4–10).

Table 1 Responsiveness of tonic and phasic neurones to tachykinin receptor agonists

Neurone type: *Response to tachykinins:*	*Tonic* *Depolarization*	*Phasic* *LAH inhibition*
SP(+), NKA(+), Senk(+)	77.6%, (n = 59)	71.0%, (n = 22)
SP(−), NKA(−), Senk(+)	11.8%, (n = 9)	22.6%, (n = 7)
SP(−), NKA(−), Senk(−)	10.5%, (n = 8)	6.5%, (n = 2)

SP(+), SP(−), NKA(+), NKA(−), Senk(+) and Senk(−): presence (+) and absence (−) of responses to SP, NKA and senktide, respectively.

al., 1987). These tachykinin receptor agonists depolarized most of the tonic neurones. Neurones examined were regarded as responsive to an agonist, when a distinct depolarization of more than 3 mV amplitude was observed. The agonists were applied at concentrations of up to 1 μM for SP or NKA, and 100 nM for senktide. According to this criterion, tonic neurones were categorized into three groups (Table 1): neurones that were responsive to all three agonists (Figure 1a); neurones that were responsive only to senktide (Figure 1b), and neurones that were unresponsive to either of the three agonists. The neurones that were sensitive to SP invariably responded to NKA, and *vice versa*. These neurones were also responsive to senktide. Thus, there were no such neurones that responded to SP and NKA but not to senktide.

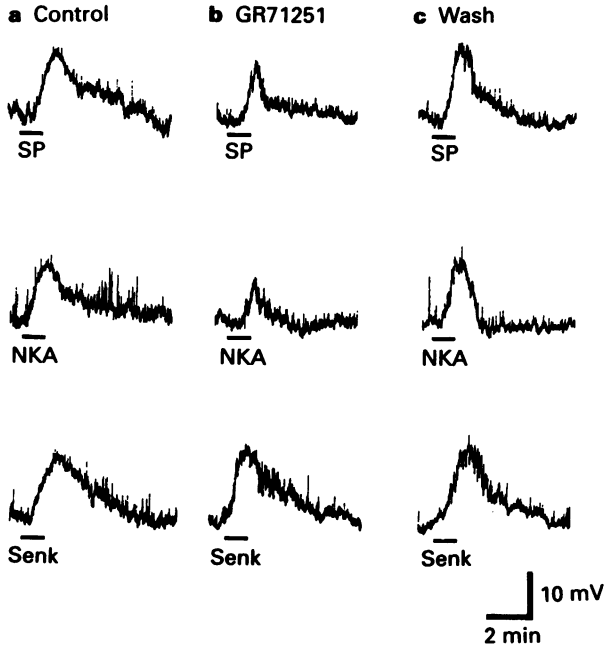

Figure 3 Depolarization induced by tachykinin receptor agonists in a tonic neurone and effects of GR71251. (a) Control responses to substance P (SP, 1 μM), neurokinin A (NKA, 1 μM) and senktide (Senk, 10 nM); (b) responses in the presence of GR71251 (5 μM); and (c) responses after washing out the antagonist. The agonists were applied for 1 min during the periods indicated by the horizontal bars. All records were obtained from a single tonic neurone.

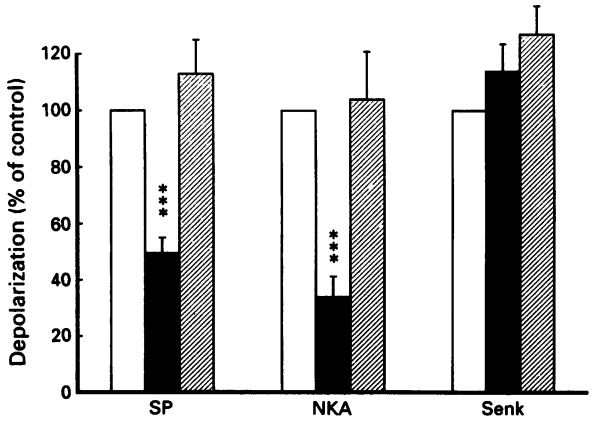

Figure 4 Effects of GR71251 on depolarization induced by tachykinin receptor agonists in tonic neurones. Ordinate scale: amplitude of depolarization expressed as percentage of the amplitude of the control response. Open columns, control; solid columns, depolarization in the presence of GR71251 (5 μM); and hatched columns, after washing out GR71251. Tachykinin receptor agonists were applied for 1 min at concentrations of 0.01~1 μM for substance P (SP), 0.1~1 μM for neurokinin A (NKA) and 10~100 nM for senktide (see Figure 2). $n = 8$ for SP; $n = 6$ for NKA; $n = 6$ for senktide. ***Significantly different from control ($P < 0.001$).

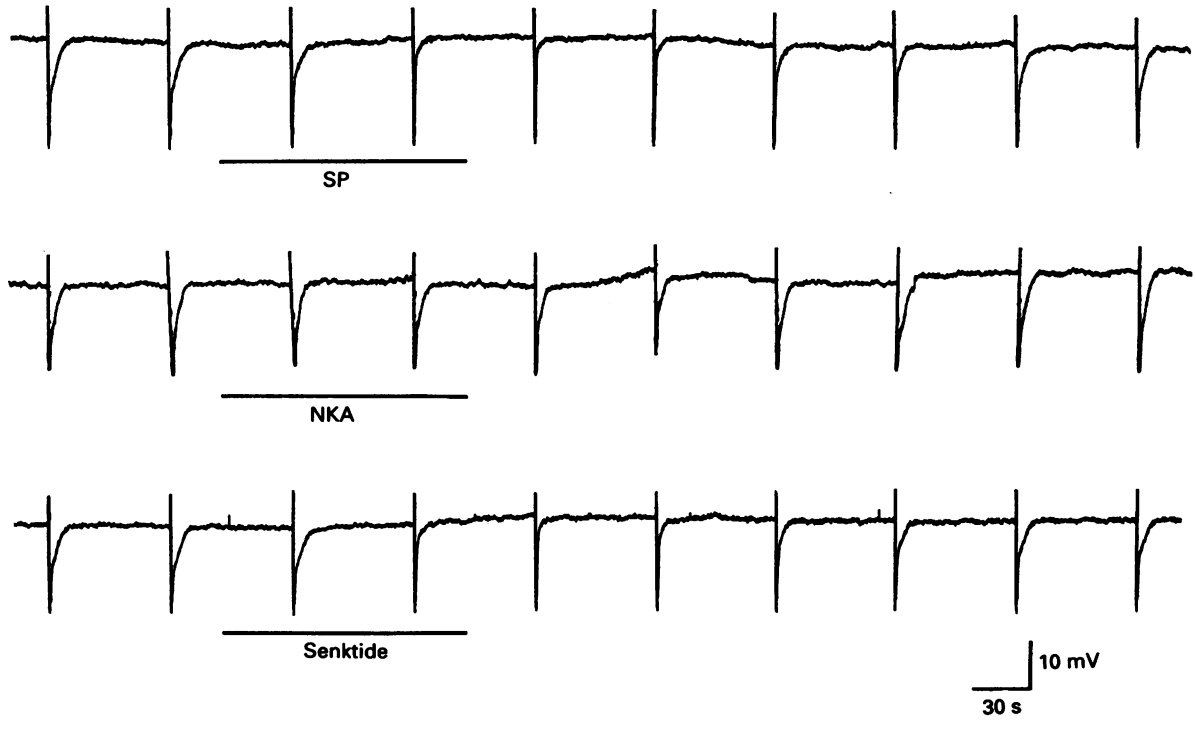

Figure 5 Responses of a phasic neurone to tachykinin receptor agonists. Long-lasting after-hyperpolarizations (LAHs) were evoked every 1 min following action potentials induced by 20 depolarizing current pulses of 20 ms duration and 0.5 nA intensity at 20 Hz. Substance P (SP, 30 nM), neurokinin (NKA, 30 nM) and senktide (3 nM) were applied during the periods indicated by the horizontal bars. LAH was inhibited by all the three agonists in this neurone. Resting potential was −53 mV.

The concentration-response curves for the three tachykinin receptor agonists in tonic neurones are shown in Figure 2. Senktide was the most potent among the three agonists and induced a depolarization of a few mV at the concentration as low as 0.1 nM. SP was effective at concentrations higher than 3 nM, and NKA was less potent than SP (Figure 2).

The NK_1 receptor antagonist GR71251 (Ward *et al.*, 1990), at 5 μM, inhibited both the SP-induced and NKA-induced depolarizations with similar effectiveness (Figures 3 and 4). In contrast, the depolarization induced by senktide was not affected by the antagonist.

Effects of SP, NKA, senktide and GR71251 on phasic neurones

SP, NKA and senktide did not obviously depolarize most of phasic neurones at concentrations up to 1 μM. A few cells were slightly depolarized (1–3 mV) by SP at a high concentration (10 μM). In many of the phasic neurones examined, LAH was inhibited by these agonists (Figure 5). Like tonic neurones, phasic neurones were classified into three groups based on the sensitivity to SP, NKA and senktide. In 22 neurones out of 31 (71%) LAH was inhibited by SP, NKA and senktide, whereas 2 neurones (7%) were insensitive to any of the three (Table 1). In the remaining 7 neurones (23%) LAH was inhibited by senktide but not by SP or NKA. The concentration-response curves for the three tachykinin receptor agonists in inhibiting LAH in phasic neurones are shown in Figure 6. Rank order of the potency was senktide >SP>NKA. The rank order was the same as in tonic neurones.

The SP- and NKA-induced inhibition of LAH was reduced by GR71251, whereas the senktide-induced LAH inhibition was not affected by the antagonist (Figures 7 and 8).

Effects of other tachykinin receptor agonists and antagonists on tonic and phasic neurones

The selective NK_1 receptor agonists, [Sar^9, $Met(O_2)$]SP ($n = 7$) and SPOMe ($n = 4$), evoked depolarizations at 1 μM in tonic neurones (not shown), whereas selective NK_2 receptor agonists, [Nle^{10}]NKA_{4-10}, [β-Ala^8]NKA_{4-10} and GR64349, did not depolarize tonic neurones at concentrations up to 1 μM ($n = 7$, Figure 9b). The latter finding suggests that NK_2 receptors do not exist on tonic neurones. In support of this, an NK_2 receptor antagonist, L659,877 (10 μM), did not inhibit the depolarizations induced by NKA ($n = 6$), SP ($n = 4$), and senktide ($n = 3$) in tonic neurones.

The NK_3-selective tachykinin receptor agonist, [$MePhe^7$] NKB, evoked a depolarization at 30–100 nM ($n = 3$) in tonic neurones. However, [Trp^7, β-Ala^8]NKA_{4-10} (1–3 μM), which was reported to be an NK_3 receptor antagonist in some preparations (Drapeau *et al.*, 1990), did not antagonize the depolarizing action of senktide ($n = 3$, data not shown).

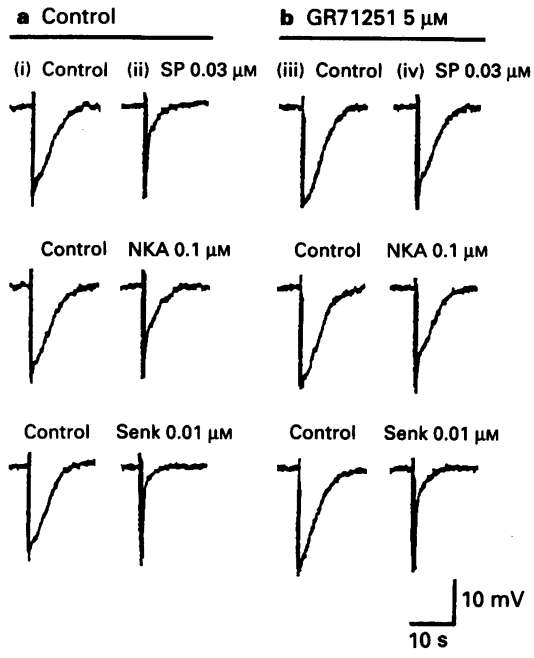

Figure 7 Long-lasting after-hyperpolarization (LAH) inhibition induced by tachykinin receptor agonists in a phasic neurone and effects of GR71251. (a) Responses to substance P (SP, 30 nM), neurokinin A (NKA, 0.1 μM) and senktide (Senk, 10 nM) before application of GR71251; and (b) responses in the presence of GR71251 (5 μM). (i) and (iii), LAHs before application of each tachykinin receptor agonist, and (ii) and (iv), LAHs at 90 s after the start of application of each agonist. Other details of experimental procedures are the same as in Figure 5.

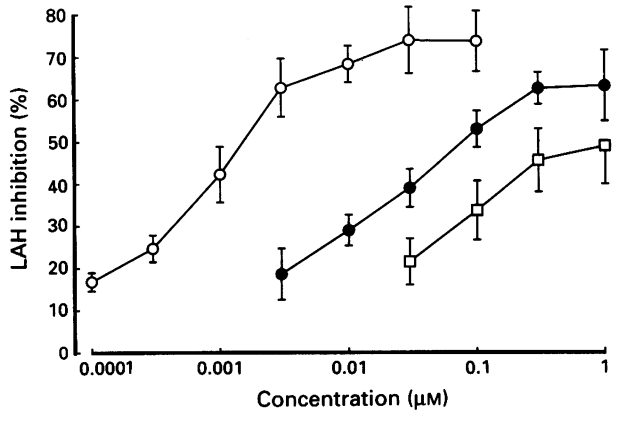

Figure 6 Concentration-response curves for long-lasting after-hyperpolarization (LAH) inhibition induced by tachykinin receptor agonists in phasic neurones. Ordinate scale: magnitude of LAH was measured as area under the resting potential level on the record, and the reduction of the magnitude of LAH induced by each tachykinin receptor agonist was determined 30–90 s after the start of the application and expressed as a percentage of the magnitude of control LAH. Abscissa scale: concentration of tachykinin receptor agonists, (○) senktide; (●) substance P; (□) neurokinin A. The data were obtained from phasic neurones that were sensitive to all the three agonists. Each point represents mean ± s.e.mean ($n = 4$–18).

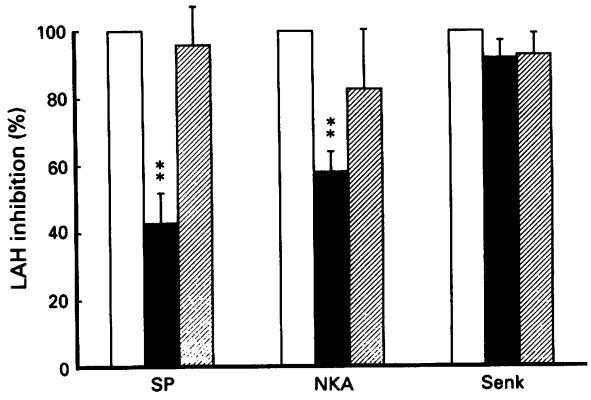

Figure 8 Effect of GR71251 on long-lasting after-hyperpolarization (LAH) inhibition induced by tachykinin receptor agonists in phasic neurones. Ordinate scale: the LAH inhibition induced by each agonist expressed as percentage of the control LAH inhibition. Open columns, control; solid columns, in the presence of GR71251 (5 μM); hatched columns, after washing out GR71251. The concentrations of the tachykinin receptor agonists were 10 nM~1 μM for substance P (SP, $n = 6$), 0.1~1 μM for neurokinin A (NKA, $n = 4$) and 10~100 nM for senktide (Senk, $n = 7$). **Significantly different from control ($P < 0.01$).

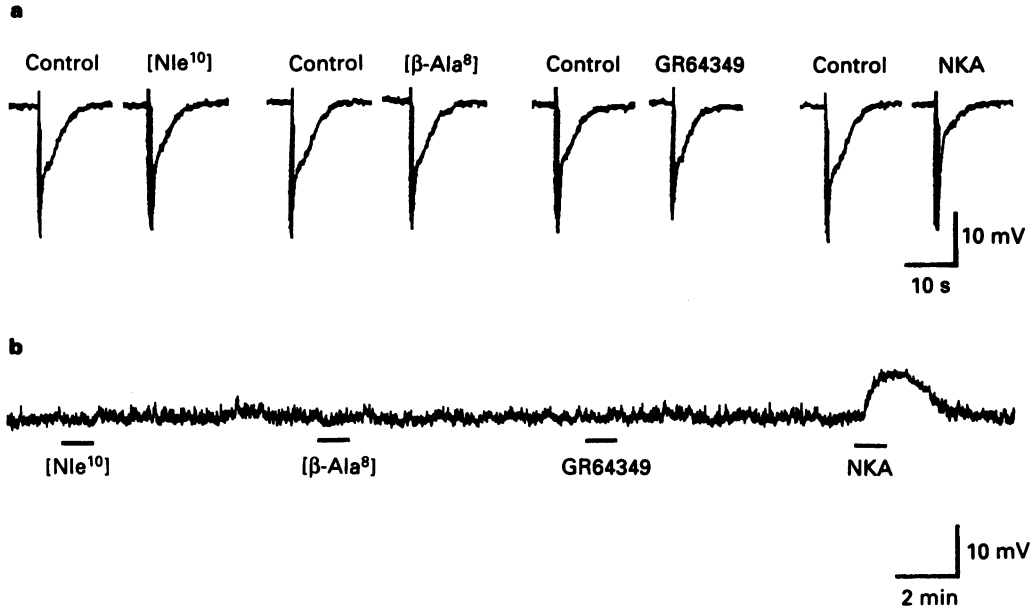

Figure 9 Effects of NK_2 receptor agonists on tonic and phasic neurones. (a) Effects of [Nle^{10}]NKA_{4-10} ([Nle^{10}]), [β-Ala^8]NKA_{4-10} ([β-Ala^8]), GR64349, and neurokinin A (NKA) on long lasting after-hyperpolarization (LAH) in a phasic neurone. Three synthetic agonists were applied at 1 μM whereas NKA was applied at 0.1 μM. (b) Effects of the NK_2 receptor agonists on a tonic neurone. All the agonists were applied at 1 μM. Other details are as in Figure 1 and Figure 5. Resting potentials were −72 mV and −82 mV for the neurones in (a) and (b), respectively.

In phasic neurones [Nle^{10}]NKA_{4-10}, [β-Ala^8]NKA_{4-10} and GR64349 did not inhibit LAH ($n = 4$, Figure 9a), whereas [Sar^9, $Met(O_2)$]SP ($n = 4$) and SPOMe ($n = 3$) evoked inhibition of LAH (data not shown).

Discussion

This study showed that SP induced a depolarization in a large proportion of tonic neurones and inhibition of LAH in most phasic neurones and that these actions were antagonized by the NK_1 receptor antagonist, GR71251. These findings suggest that both the depolarization in tonic neurones and LAH inhibition in phasic neurones induced by SP are mediated by NK_1 receptors. The effectiveness of the selective NK_1 receptor agonists, [Sar^9, $Met(O_2)$]SP and SPOMe in inducing a depolarization or LAH inhibition, also supports the presence of NK_1 receptors on these neurones. Although the types of response to SP were different between tonic and phasic neurones, the effective concentrations of SP needed to induce both types of responses were similar and both the actions of SP were antagonized by GR71251 with similar effectiveness. These results suggest that the subtype of tachykinin receptor activated by SP on tonic and phasic neurones is the same but that the receptor is coupled to different effector mechanisms in the two types of neurones.

Although NKA is known to have a preferential affinity for NK_2 receptors expressed in *Xenopus* oocytes or various smooth muscles, the peptide has also a weak affinity for NK_1 receptors (for review see Otsuka & Yoshioka, 1993). In the present study GR71251 antagonized the actions of NKA in inducing both depolarization and LAH inhibition at concentrations similar to those needed for antagonizing the action of SP, whereas the NK_2-selective antagonist, L659,877, was ineffective in antagonizing the actions of NKA. These results suggest that both the depolarization and the inhibition of LAH induced by NKA are mediated by NK_1 receptors but not NK_2 receptors. The results of studies in our laboratory on rat isolated neonatal spinal cord preparations also suggested that the depolarizing action of NKA on motoneurones is mediated by NK_1 receptors (Guo *et al.*, 1993; Hosoki *et al.*, 1994; Otsuka *et al.*, 1994). In the present study, whenever NKA showed either depolarizing or LAH inhibitory action on a neurone, SP had a greater effect on the same cell. This is consistent with the notion that SP and NKA act on a single subtype of NK_1 receptor in guinea-pig coeliac ganglion.

Senktide had potent actions on a large proportion of coeliac neurones. The NK_3-selective tachykinin receptor agonist, [$MePhe^7$]NKB, also showed depolarizing action on tonic neurones and LAH inhibition on phasic neurones. These results suggest the presence of NK_3 receptors on these neurones. Although the neurones responsive to SP and NKA were invariably responsive to senktide, there were some neurones that responded to senktide but not to SP and NKA. This suggests an extensive overlap of expression of NK_1 and NK_3 receptors in both the tonic and phasic neurones, with a slightly wider distribution of NK_3 receptor.

Recently we showed that in the coeliac ganglion of the guinea-pig, repetitive electrical stimulation of the mesenteric nerves evoked a slow e.p.s.p. in many tonic neurones (Zhao *et al.*, 1993a) and a prolonged inhibition of LAH in many phasic neurones (Zhao *et al.*, 1993b). Both effects of nerve stimulation were partly antagonized by GR71251, which suggests the involvement of NK_1 receptors in the generation of the nerve-evoked slow e.p.s.p. and the inhibition of LAH. Whether NK_3 receptors also play a role in synaptic transmission remains to be clarified.

This work was supported by grants-in aid for scientific research from Ministry of Education, Science and Culture, Japan (Nos. 04255101, 05557117 and 05454147).

References

CASSELL, J.F. & MCLACHLAN, E.M. (1987). Two calcium-activated potassium conductances in a subpopulation of coeliac neurones of guinea-pig and rabbit. *J. Physiol.*, **394**, 331–349.

DRAPEAU, G., ROUISSI, N., NANTEL, F., RHALEB, N.-E., TOUSIGNANT, C. & REGOLI, D. (1990). Antagonists for the neurokinin NK-3 receptor evaluated in selective receptor systems. *Regul. Pept.*, **31**, 125–135.

GUO, J.-Z., YOSHIOKA, K., YANAGISAWA, M., HOSOKI, R., HAGAN, R.M. & OTSUKA, M. (1993). Depression of primary afferent-evoked responses by GR71251 in the isolated spinal cord of the neonatal rat. *Br. J. Pharmacol.*, **110**, 1142–1148.

HOSOKI, R., YANAGISAWA, M., GUO, J.-Z., YOSHIOKA, K., MAEHARA, T. & OTSUKA, M. (1994). Effects of RP67580, a tachykinin receptor antagonist, on a primary afferent-evoked response of ventral roots in the neonatal rat spinal cord. *Br. J. Pharmacol.*, **113**, 1141–1146.

JÄNIG, W. & MCLACHLAN, E.M. (1992). Characteristics of function-specific pathways in the sympathetic nervous system. *Trends Neurosci.*, **15**, 475–481.

KONISHI, S. & OTSUKA, M. (1985). Blockade of slow excitatory post-synaptic potential by substance P antagonists in guinea-pig sympathetic ganglia. *J. Physiol.*, **361**, 115–130.

MACRAE, I.M., FURNESS, J.B. & COSTA, M. (1986). Distribution of subgroups of noradrenaline neurones in the coeliac ganglion of the guinea-pig. *Cell Tissue Res.*, **244**, 173–180.

MCLACHLAN, E.M. & MECKLER, R.L. (1989). Characteristics of synaptic input to three classes of sympathetic neurone in the coeliac ganglion of the guinea-pig. *J. Physiol.*, **415**, 109–129.

OTSUKA, M., SUZUKI, H., YANAGISAWA, M., HOSOKI, R., GUO, J-Z. & YOSHIOKA, K. (1994). Pharmacological characterization of receptors in the spinal cord of the newborn rat. In *Tachykinin Receptors*, ed. Buck, S.H. pp. 499–514. Totowa: Humana Press.

OTSUKA, M. & YOSHIOKA, K. (1993). Neurotransmitter functions of mammalian tachykinins. *Physiol. Rev.*, **73**, 229–308.

PAPIR-KRICHELI, D., FREY, J., LAUFER, R., GILON, C., CHOREV, M., SELINGER, Z. & DEVOR, M. (1987). Behavioral effects of receptor-specific substance P agonists. *Pain*, **31**, 263–276.

SAITO, K. & KONISHI, S. (1993). Different responses to tachykinins in tonic and phasic neurons of the guinea-pig coeliac ganglion. *Jpn J. Pharmacol.*, **61**, Suppl. I, 341P.

SARIA, A., MA, R.C. & DUN, N.J. (1985). Neurokinin A depolarizes neurones of the guinea pig inferior mesenteric ganglia. *Neurosci. Lett.*, **60**, 145–150.

TSUNOO, A., KONISH, S. & OTSUKA, M. (1982). Substance P as an excitatory transmitter of primary afferent neurons in guinea-pig sympathetic ganglia. *Neuroscience*, **7**, 2025–2037.

VANNER, S., EVANS, R.J., MATSUMOTO, S.G. & SURPRENANT, A. (1993). Potassium current and their modulation by muscarine and substance P in neuronal cultures from adult guinea-pig. *J. Neurophysiol.*, **69**, 1632–1644.

WARD, P., EWAN, G.B., JORDAN, C.C., IRELAND, S.J., HAGAN, R.M. & BROWN, J.R. (1990). Potent and highly selective neurokinin antagonists. *J. Med. Chem.*, **33**, 1848–1851.

ZHAO, F.-Y., SAITO, K., GUO, J.-Z., KONISHI, S., MURAKOSHI, T., YOSHIOKA, K. & OTSUKA, M. (1993a). Involvement of NK_1 receptors in synaptic transmission in the guinea pig coeliac ganglion. *Neurosci. Res.*, **18**, 245–248.

ZHAO, F.-Y., SAITO, K., GUO, J.-Z., MURAKOSHI, T., YOSHIOKA, K. & OTSUKA, M. (1993b). Involvement of NK_1 receptors in tachykininergic synaptic transmission in the coeliac ganglion of the guinea pig. *Neurosci. Res.*, Suppl. **18**, S40.

(Received December 2, 1994
Revised January 16, 1995
Accepted January 18, 1995)

British Journal of Pharmacology (1995) 115, 31-38

Multiple pathways underlying endothelium-dependent relaxation in the rabbit isolated femoral artery

[1]Frances Plane, Timothy Pearson & Christopher J. Garland

Department of Pharmacology, University of Bristol, University Walk, Bristol, BS8 1TD

1 In isolated segments of the rabbit femoral artery stimulated with noradrenaline, both acetylcholine (1nM–10 μM) and the calcium ionophore A23187 (1 nM–100 μM) evoked endothelium-dependent smooth muscle relaxation and hyperpolarization while bradykinin (0.01–100 nM) had no effect.

2 The nitric oxide synthase inhibitors, N^G-nitro-L-arginine (L-NOARG; 100 μM; 20 min) or N^G-nitro-L-arginine methyl ester (L-NAME; 100 μM; 20 min) each abolished the hyperpolarization and the majority of the relaxation to acetylcholine (maximal response reduced from 96.8 ± 2.3% to 2.0 ± 1.4%).

3 The potassium channel blocker, glibenclamide (10 μM; 10 min) also abolished the change in membrane potential to acetylcholine but did not modify the smooth muscle relaxation.

4 In contrast, neither L-NAME nor glibenclamide modified the comparable responses of the femoral artery to A23187, which were also unaffected by the cyclo-oxygenase inhibitor, indomethacin (10 μM).

5 In artery segments stimulated with potassium chloride (25 mM), the maximal change in tension and membrane potential evoked by A23187 (100 μM) was significantly reduced from 95.0 ± 4.5% and 23.0 ± 2.0 mV to 69.0 ± 10.1% and 12.0 ± 1.5 mV, respectively. Under these conditions L-NAME further reduced the relaxation but not the accompanying hyperpolarization to A23187.

6 Endothelium-denuded arterial segments sandwiched with endothelium-intact 'donor' segments gave qualitatively similar relaxant responses to those described above for acetylcholine and A23187.

7 Exogenous nitric oxide (0.5–10 μM) stimulated a transient relaxation in pre-contracted artery segments, which at concentrations above 5 μM was accompanied by smooth muscle hyperpolarization (maximum 8.5 ± 3.2 mV; $n = 4$). The hyperpolarization but not the relaxation to nitric oxide was abolished by either glibenclamide or 25 mM potassium.

8 These data indicate that in the femoral artery, acetylcholine-induced relaxation can be attributed solely to the release of nitric oxide from the endothelium, which then stimulates relaxation independently of a change in smooth muscle membrane potential. In contrast, both the relaxation and hyperpolarization evoked by A23187 appear to be mediated predominantly by nitric oxide-independent pathways which appear to involve a diffusible factor released from the endothelium. The results suggest that this diffusible hyperpolarizing factor can be released from endothelial cells in the femoral artery by A23187 but not by acetylcholine.

Keywords: Endothelium-dependent hyperpolarization, relaxation; rabbit isolated femoral artery; A23187; acetylcholine; nitric oxide

Introduction

Endothelium-derived relaxing factor (EDRF) has now been identified as nitric oxide, or a closely related molecule, which is synthesized from L-arginine by nitric oxide synthase (Palmer *et al.*, 1987). However, in many vessels endothelium-dependent relaxations, particularly to agents such as bradykinin and the calcium ionophore, A23187, are resistant to inhibitors of the nitric oxide transduction pathway. This indicates that other endothelium-derived factors may contribute to the local regulation of vascular smooth muscle tone (Chen & Suzuki, 1989; Cowan & Cohen, 1991; Nagao & Vanhoutte, 1992). Furthermore, direct measurements of smooth muscle guanosine 3':5'-cyclic monophosphate (cyclic GMP) have shown in isolated preparations such as the rat kidney, canine femoral vein and porcine coronary artery, that endothelium-dependent relaxations are unaffected when cyclic GMP formation is inhibited (Cacofeiro & Nasjletti, 1991; Cowan & Cohen, 1991; Vidal *et al.*, 1991).

Endothelium-dependent relaxation is usually accompanied by hyperpolarization of the vascular smooth muscle cell membrane and, although application of exogenous nitric oxide can elicit membrane hyperpolarization under certain conditions in some vessels, it has been suggested that the hyperpolarization may be mediated by a factor (EDHF) which is distinct from nitric oxide (Taylor *et al.*, 1988; Tare *et al.*, 1990). The release of EDHF may explain the resistance of some endothelium-dependent responses to inhibitors of nitric oxide synthase (Garland & McPherson, 1992; Nagao & Vanhoutte, 1992).

Preliminary experiments in the rabbit isolated femoral artery indicated that acetylcholine-evoked relaxations could be inhibited by L-NAME, but that relaxations elicited by the calcium ionophore A23187 were unaffected (Plane *et al.*, 1992). This suggested that acetylcholine and A23187 might have a differential influence on the release of nitric oxide and EDHF in this large artery. We have now investigated the contribution of smooth muscle hyperpolarization to endothelium-dependent relaxation in the femoral artery by making simultaneous measurements of changes in smooth muscle membrane potential and tension. In addition, we have also investigated the action of bradykinin, which may stimulate relaxation in arterial smooth muscle predominantly via the release of EDHF (Nagao & Vanhoutte, 1992; Nakashima *et al.*, 1993).

[1] Author for correspondence.

Methods

New Zealand white rabbits (2–3 kg) of either sex were anaesthetized with an intravenous injection of sodium pentobarbitone (60 mg kg^{-1}, i.v.) and killed by rapid exsanguination. The femoral arteries were carefully removed, cleaned of adhering fat and connective tissue and cut into cylindrical segments 2–3 mm in length. Segments were then mounted in a two-channel Mulvany-Halpern myograph (model 400A; J.P. Trading, Denmark) for simultaneous recording of changes in smooth muscle membrane potential and tension, as previously described (Garland, 1987). Briefly, two tungsten wires (each 40 μm diameter) were passed through the lumen of the segment and each wire attached to a metal foot in the myograph. The tissue segments were stretched between the two wires to a previously determined optimal preload of 1g, and superfused at 7–8 ml min^{-1} with Krebs buffer which had been bubbled with 95% O_2/5% CO_2. In some experiments, the endothelial cell layer was removed by gently rubbing the intimal surface with a human hair.

Drugs were equilibrated with the perfusate before it entered the tissue chamber. Nitric oxide solutions were injected from a gas-tight syringe close to the arterial segment, in volumes of not greater than 200 μl.

Electrophysiology

Measurement of smooth muscle membrane potential was made with a glass microelectrode advanced through the adventitial surface of the arterial segment. The electrodes were filled with 2 M KCl and had resistances of 60–120 MΩ. Membrane electrical events were recorded through a high impedance d.c. preamplifier (Neurolog 102G) and, together with data from the isometric force transducer, stored on disc (CVMS, McPherson Scientific).

Sandwich preparations

Endothelium-denuded segments of the femoral artery were mounted between stainless steel hooks in 10 ml organ baths under a resting tension of 1 g for isometric recording of tension changes. The tissues were maintained at 37°C in Krebs buffer bubbled with 95%O_2/5%CO_2. Removal of the endothelium was confirmed by the absence of any relaxation to acetylcholine or A23187 following pre-constriction with phenylephrine. To examine the transferable nature of the nitric oxide-independent relaxations, donor segments with an intact endothelium were wrapped round and attached with a small pin to a detector tissue denuded of endothelium. The tissues were then rechallenged with acetylcholine or A23187 in the absence and presence of L-NAME (100 μM).

Solutions and drugs

All experiments were carried out in Krebs buffer with the following composition (mM): NaCl 122, $NaHCO_3$ 25.5, KCl 5.2, $MgSO_4$ 1.2, $CaCl_2$ 1.6, disodium EDTA 0.027, ascorbate 0.114, and glucose 9.4. K^+ 25 mM Krebs solution was prepared by direct replacement of NaCl with KCl.

Drugs used were acetylcholine chloride (BDH), noradrenaline bitartrate (arterenol, Sigma), calcium ionophore A23187 (Sigma), phenylephrine (Sigma), N^G-nitro-L-arginine methyl ester (Sigma), N^G-nitro-L-arginine (Sigma) and glibenclamide (gift from Hoechst).

Preparation of nitric oxide solutions

Nitric oxide gas (research grade, BDH) was injected into Krebs solution which had been bubbled with helium (BOC) for 45–60 min. Nitric oxide solutions were injected from a gas-tight syringe close to the artery segments, in volumes of not greater than 200 μl. Control injections of helium-gassed Krebs solution were made to assess the extent of any potential injection artifacts.

Analysis of data

Relaxations are expressed as the percentage decrease in the tone induced by either noradrenaline (0.1–1.0 μM) or potassium chloride (25 mM). Data are expressed as mean ± s.e. mean. The significance of differences between mean values was calculated with the Wilcoxon test for paired samples.

Results

Membrane and tension responses to acetylcholine

Smooth muscle cells in the femoral artery were electrically quiescent and had a mean resting membrane potential of −64.3 ± 4.8 mV (51 cells from 29 preparations). The application of acetylcholine (1 nM–10 μM) to cells pre-contracted and depolarized with noradrenaline (0.1–1 μM; mean background contraction and depolarization of 14.9 ± 4.6 mN and 19.0 ± 2.3 mV, $n = 12$) evoked concentration-dependent smooth muscle repolarization and relaxation, both of which were endothelium-dependent. The maximal relaxation evoked by acetylcholine (10 μM) was 96.8 ± 2.3% ($n = 4$), and was accompanied by a maximal increase in membrane potential of 9.0 ± 2.7 mV ($n = 4$). The EC_{50} values for the relaxation and repolarization to acetylcholine were not significantly different (0.25 ± 0.05 μM and 0.29 ± 0.06 μM; $n = 4$; $P > 0.05$), although the concentration required to initiate membrane hyperpolarization was ten fold higher than for relaxation. A representative trace showing simultaneous measurements of changes in membrane potential and tension to acetylcholine is shown in Figure 1a.

Pre-incubation of femoral artery segments with either L-NOARG or L-NAME (100 μM; 20 min) caused an endothelium-dependent increase in basal tone of 4.41 ± 0.87 mN ($n = 12$) but had no significant effect on the resting membrane potential of the smooth muscle cells (mean resting membrane potential in the presence of L-NOARG or L-NAME was −63.0 ± 5.0 mV; $n = 5$; $P > 0.05$). After exposure to either of these inhibitors, acetylcholine-evoked repolarization was abolished and relaxation was dramatically reduced to only 2.0 ± 1.4% ($n = 4$; $P < 0.05$) in cells pre-stimulated with noradrenaline. Concentration-response curves for acetylcholine-evoked relaxation and hyperpolarization in the presence and absence of L-NAME are shown in Figure 2.

The application of the potassium channel blocker glibenclamide (10 μM; 10 min) did not affect either the basal tone or the resting membrane potential in smooth muscle of the femoral artery (mean resting membrane potential in the presence of glibenclamide was −64.5 ± 5.0 mV ($n = 3$)). However, after exposure to glibenclamide acetylcholine-evoked hyperpolarization was abolished although relaxation was not significantly altered (maximal response in the presence of glibenclamide; 94.6 ± 6.0%; $n = 4$; $P > 0.05$). Potassium chloride (25 mM) induced a similar contraction to noradrenaline (11.7 ± 4.7 mN; $n = 8$; $P > 0.05$), although the extent of smooth muscle depolarization was greater (29.5 ± 2.3 mV; $n = 4$; $P < 0.05$). In the presence of 25 mM potassium chloride, acetylcholine-evoked hyperpolarization was abolished, but as with glibenclamide, relaxation was not significantly altered (maximal response 89.9 ± 9.6%; $n = 4$; $P > 0.05$). Following exposure to L-NAME (100 μM), the relaxation to acetylcholine in segments contracted by potassium chloride was inhibited to a similar extent as in the segments contracted with noradrenaline. The maximal relaxation was reduced to only 10.3 ± 1.3% ($n = 4$; $P < 0.05$).

Indomethacin (10 μM) did not alter the relaxation to ace-

tylcholine in either noradrenaline- or potassium chloride-contracted tissues. In the presence of indomethacin, the maximal relaxation evoked by acetylcholine in noradrenaline- and potassium chloride-contracted arterial segments was 95.3 ± 4.0% ($n = 3$) and 90.5 ± 7.9% ($n = 3$), respectively.

Membrane and tension responses to A23187

The calcium ionophore, A23187 (1 nM–100 μM) evoked a concentration-dependent smooth muscle relaxation and repolarization in arterial segments stimulated with

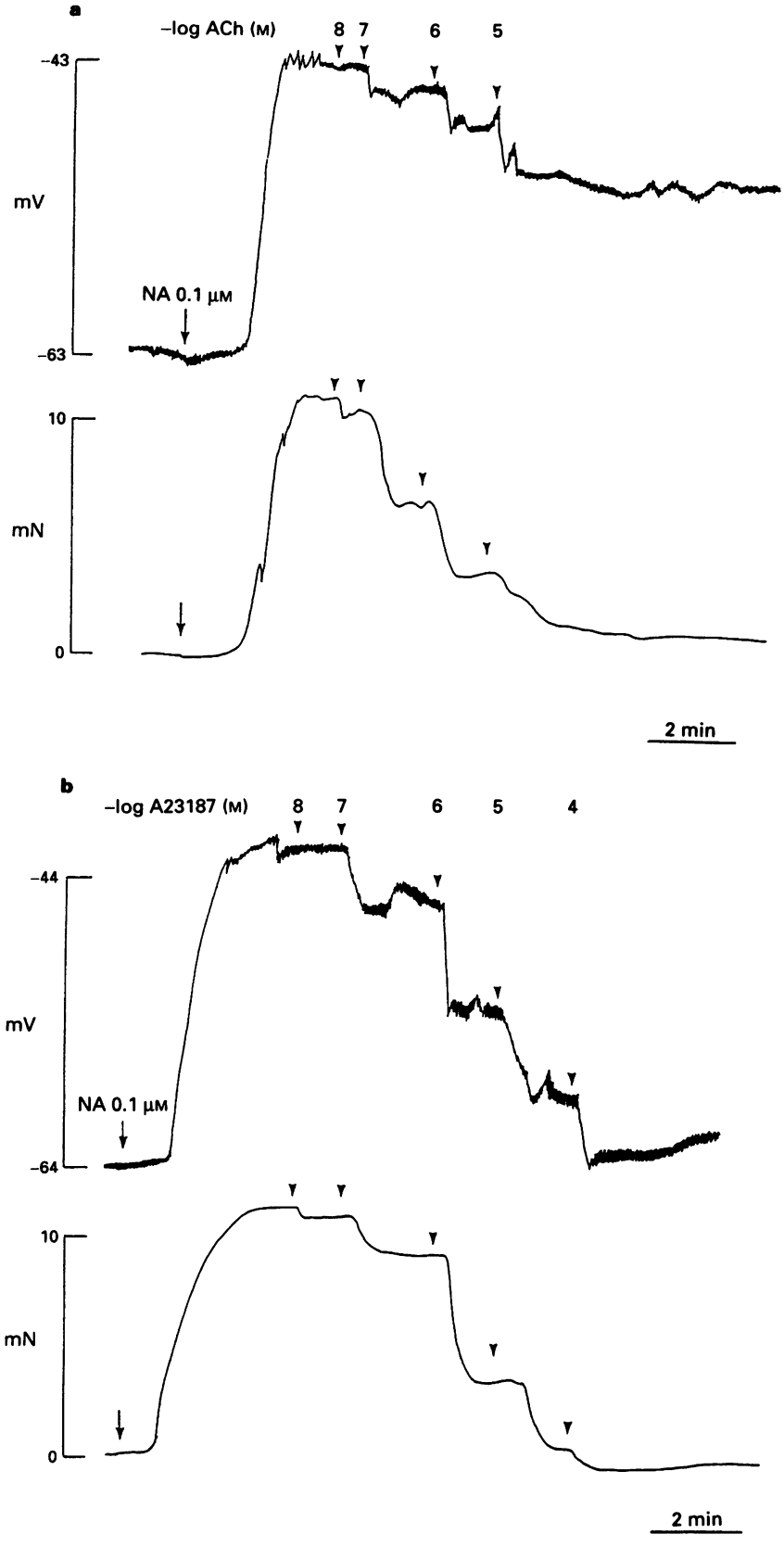

Figure 1 Representative traces showing simultaneous records of changes in membrane potential and tension elicited by acetylcholine (0.01–10 μM) and A23187 (0.01–100 μM) in noradrenaline (1.0 μM)-stimulated segments of the rabbit femoral artery: (**a**) acetylcholine (**b**) A23187.

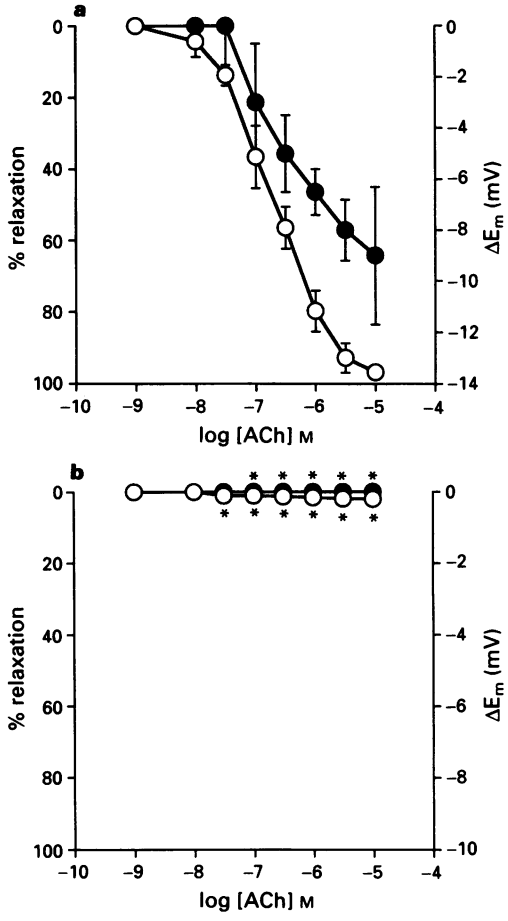

Figure 2 Mean concentration-response curves for acetylcholine in the rabbit femoral artery pre-contracted with noradrenaline (0.1–1.0 μM), in the presence and absence of N^G-nitro-L-arginine methyl ester (L-NAME, 100 μM; $n = 4$). Points show relaxation (○) and repolarization (●) and are the mean ± s.e. mean from 4 separate experiments. (a) Control responses; (b) in the presence of L-NAME. *$P < 0.05$.

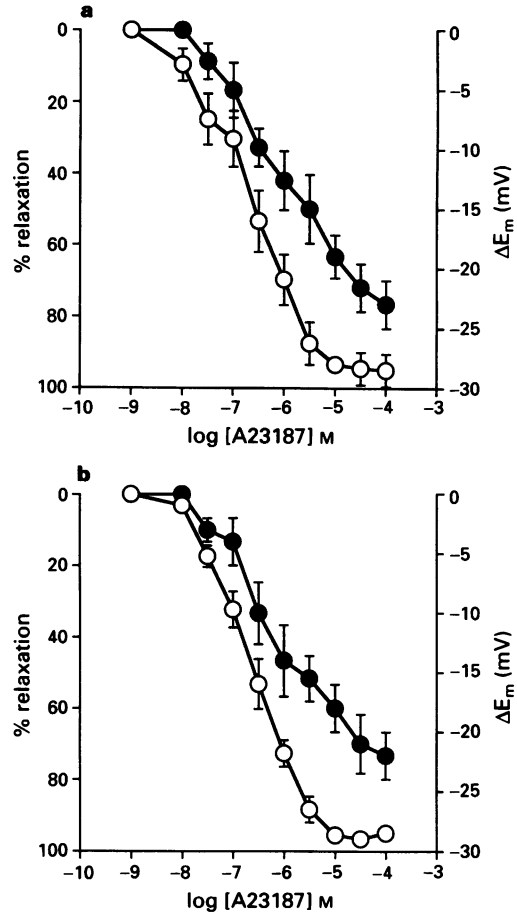

Figure 3 Mean concentration-response curves for A23187 in the rabbit femoral artery pre-contracted with noradrenaline (0.1–1.0 μM), in the presence and absence of N^G-nitro-L-arginine methyl ester (L-NAME, 100 μM; $n = 4$). Points show relaxation (○) and repolarization (●) and are the mean ± s.e. mean from 4 separate experiments. (a) Control responses; (b) in the presence of L-NAME. *$P < 0.05$.

noradrenaline (0.1–1 μM; mean background contraction and depolarization of 13.5 ± 3.0 mN and 17.5 ± 2.5 mV; $n = 12$). The maximal change in membrane potential and tension to A23187 (100 μM) was 23.0 ± 2.0 mV and 95.7 ± 2.5% ($n = 8$), respectively. As with acetylcholine, the concentration required to initiate repolarization was higher than for relaxation (0.01 μM and 0.03 μM, respectively). A representative trace of changes in membrane and tension to A23187 is shown in Figure 1b. Both the changes in membrane potential and tension were abolished by removal of the endothelium.

Unlike acetylcholine, both the relaxation and repolarization evoked by A23187 was unchanged by prior exposure to either L-NOARG or L-NAME (100 μM; 20 min) or to the potassium channel inhibitor glibenclamide (10 μM; 10 min). The maximal relaxation and change in membrane potential to A23187 in the presence of L-NAME was 95.5 ± 2.4% and 22.1 ± 3.5 mV, and in the presence of glibenclamide, 98.0 ± 1.5% and 21.5 ± 3.0 mV ($n = 4$; $P > 0.05$). Figure 3 shows the concentration-response curves for A23187-evoked relaxation and repolarization in noradrenaline-contracted tissues in the presence and absence of L-NAME.

In arterial segments pre-contracted with potassium chloride (mean background contraction and depolarization of 15.6 ± 3.5 mN and 26.8 ± 5.1 mV; $n = 6$), both the relaxation and repolarization to A23187 were significantly reduced compared to responses in noradrenaline-stimulated tissues. The maximal change in tension and membrane potential to A23187 was reduced to 69.0 ± 10.1% and 12.0 ± 1.5 mV ($n = 4$; $P < 0.05$), respectively. Subsequent exposure to L-NAME (100 μM) further attenuated the A23187-evoked relaxation in potassium chloride-contracted tissues, reducing the maximal relaxation to 42.0 ± 5.6% ($n = 4$) while the accompanying hyperpolarization was unaltered. Glibenclamide (10 μM) reduced the maximum relaxation in the presence of potassium to 57.7 ± 5.3% ($n = 4$; $P < 0.05$), and the repolarization to 6.1 ± 1.5 mV ($n = 4$; $P < 0.05$). Addition of L-NAME and glibenclamide together did not further depress relaxation. Figure 4 shows the concentration-response curves for A23187-evoked relaxation in potassium-contracted tissues in the presence and absence of L-NAME.

The cyclo-oxygenase inhibitor, indomethacin, did not affect relaxation to A23187 in either noradrenaline or potassium chloride-constricted artery segments. The maximal relaxation to A23187 in noradrenaline and potassium chloride contracted tissues in the presence of indomethacin was 97.3 ± 2.5% ($n = 3$) and 68 ± 8.3% ($n = 3$), respectively.

Transfer of tension changes in sandwich preparations

The use of sandwich preparations of femoral artery showed that the tension changes to acetylcholine and to A23187 could be transferred from one strip to another ($n = 8$). As shown in Figure 5 the application of either acetylcholine or A23187 to segments of femoral artery without an endothelium induced relaxation only if a donor tissue with a functional endothelium was wrapped round the denuded segment.

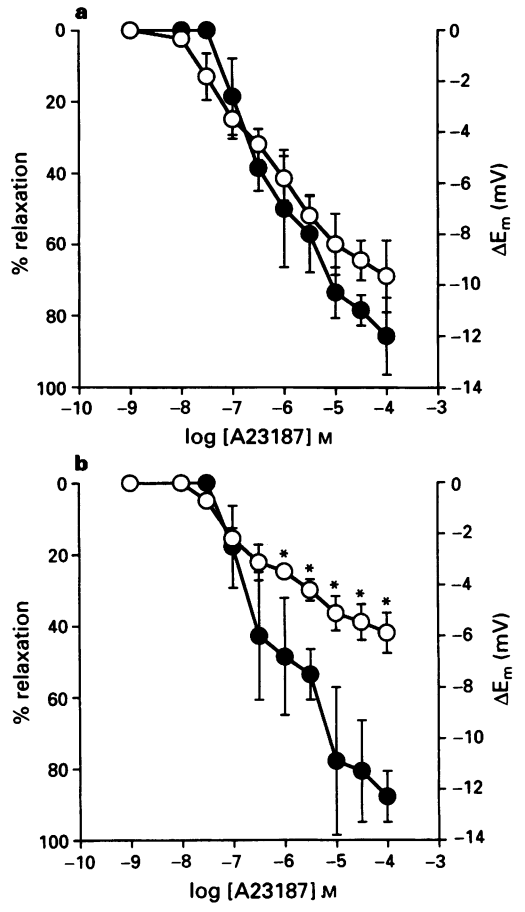

Figure 4 Mean concentration-response curves for A23187 in the rabbit femoral artery pre-contracted with potassium chloride (25 mM), in the presence and absence of N^G-nitro-L-arginine methyl ester (L-NAME, 100 μM; $n = 4$). Points show relaxation (○) and repolarization (●) and are the mean ± s.e. mean from 4 separate experiments. (a) Control responses; (b) in the presence of L-NAME. *$P < 0.05$.

The concentration-dependent relaxation to acetylcholine was almost totally abolished in the presence of L-NAME (100 μM; Figure 5c), whereas similar responses to A23187 were largely unaffected (Figure 5e). However, the relaxation to A23187 was reduced in the presence of L-NAME if the strips were initially contracted with 25 mM potassium, rather than phenylephrine (1 μM; Figure 5f).

Membrane and tension responses to bradykinin

The application of bradykinin (0.01–100 μM) to either resting or noradrenaline-stimulated tissues failed to evoke any change in smooth muscle tone or membrane potential ($n = 4$).

Membrane and tension responses to nitric oxide

Bolus doses of exogenous nitric oxide (0.5–10 μM), applied close to the arterial segment, initiated transient, concentration-dependent relaxation in tissues pre-contracted with noradrenaline (0.1–1 μM). At concentrations above 5 μM, smooth muscle relaxation was accompanied by a small, transient increase in membrane potential. The maximal change in membrane potential and tension evoked by 10 μM nitic oxide was 8.5 ± 3.2 mV and 86.5 ± 6.6% ($n = 4$), respectively. In the presence of glibenclamide (10 μM) or in tissues pre-contracted with 25 mM potassium chloride, the change in membrane potential to nitric oxide was abolished ($n = 4$), but the relaxation was unaffected. The maximal relaxation evoked by nitric oxide in the presence of either 25 mM potassium chloride or glibenclamide was 80.6 ± 7.9% ($n = 4$; $P > 0.05$) and 85.9 ± 7.4% ($n = 4$; $P > 0.05$), respectively.

Discussion

These data indicate that in the rabbit femoral artery, in common with other vessels, mechanisms which are both nitric oxide-dependent and -independent can contribute to endothelium-dependent smooth muscle relaxation. However, the relative importance of these mechanisms appears to vary, with nitric oxide-independent mechanisms apparently making a larger contribution to the responses evoked by A23187 than other agonists. Of particular interest is the finding that the endothelium-dependent hyperpolarization and relaxation to acetylcholine can be explained solely in terms of nitric oxide release, in spite of the fact that mechanisms independent of nitric oxide, but also capable of providing an important drive to relaxation, are functional in the same vessel. Simple contractile measurements in a variety of isolated arteries from the rat, have led to the suggestion that the relaxation to acetylcholine is mediated by nitric oxide in large, conducting vessels, while in smaller arteries voltage-sensitive mechanisms may predominate viz. EDHF (Nagao *et al.*, 1992). This suggestion was based mainly on the marked relaxation to acetylcholine which persisted in the presence of nitro-arginine in the smaller arteries, while a similar manoeuvre abolished the equivalent responses in larger vessels. Some studies are consistent with this suggestion, showing hyperpolarization in smooth muscle cells of large arteries which appears not to be of primary importance for relaxation and which, in some cases, is sensitive to glibenclamide (Chen *et al.*, 1988; Huang *et al.*, 1988; Brayden, 1990; Rand & Garland, 1992). However there are exceptions, as in large coronary arteries from the guinea-pig the smooth muscle cells developed an endothelium-dependent hyperpolarization to acetylcholine which was resistant to both L-NOARG and glibenclamide (Chen *et al.*, 1991).

The occurrence of more than one endothelium-dependent mechanism which can mediate relaxation in the same vessel has been demonstrated previously in a number of arteries. In the rabbit and bovine pulmonary arteries, bradykinin-evoked relaxation was partially antagonized by either methylene blue or indomethacin, and abolished by these two agents in combination (Chand *et al.*, 1987; Ignarro *et al.*, 1987). Furthermore, in rabbit coronary arteries prostacyclin appears also to contribute to bradykinin-evoked dilatation recorded in the presence of L-NOARG (Jackson *et al.*, 1993). However, in this as in other studies, a role for prostanoids in the nitric oxide-independent response to A23187 is unlikely, because indomethacin was without effect (Cowan & Cohen, 1991; Garland & McPherson, 1992; Adeagbo & Triggle, 1993).

Acetylcholine-evoked relaxation of the femoral artery was accompanied by repolarization of the smooth muscle cell membrane with both of the responses being inhibited by the nitric oxide synthase inhibitors, L-NAME or L-NOARG. This indicates that, as in the rabbit basilar and guinea-pig uterine arteries, the release of endothelium-derived nitric oxide has an important role to play in both the change in membrane potential and in tension to acetylcholine (Tare *et al.*, 1990; Rand & Garland, 1992). This proposal is supported by the finding that relaxation to exogenous nitric oxide was also accompanied by an increase in the membrane potential of the smooth muscle cells, with a maximum response of similar magnitude to that elicited by acetylcholine. In addition, both the acetylcholine and nitric oxide-evoked changes in membrane potential were totally blocked by the sulphonylurea compound, glibenclamide, and by an increased extracellular potassium concentration. The latter observations indicate that glibenclamide-sensitive potassium channels most probably underlie these membrane responses. Similar findings

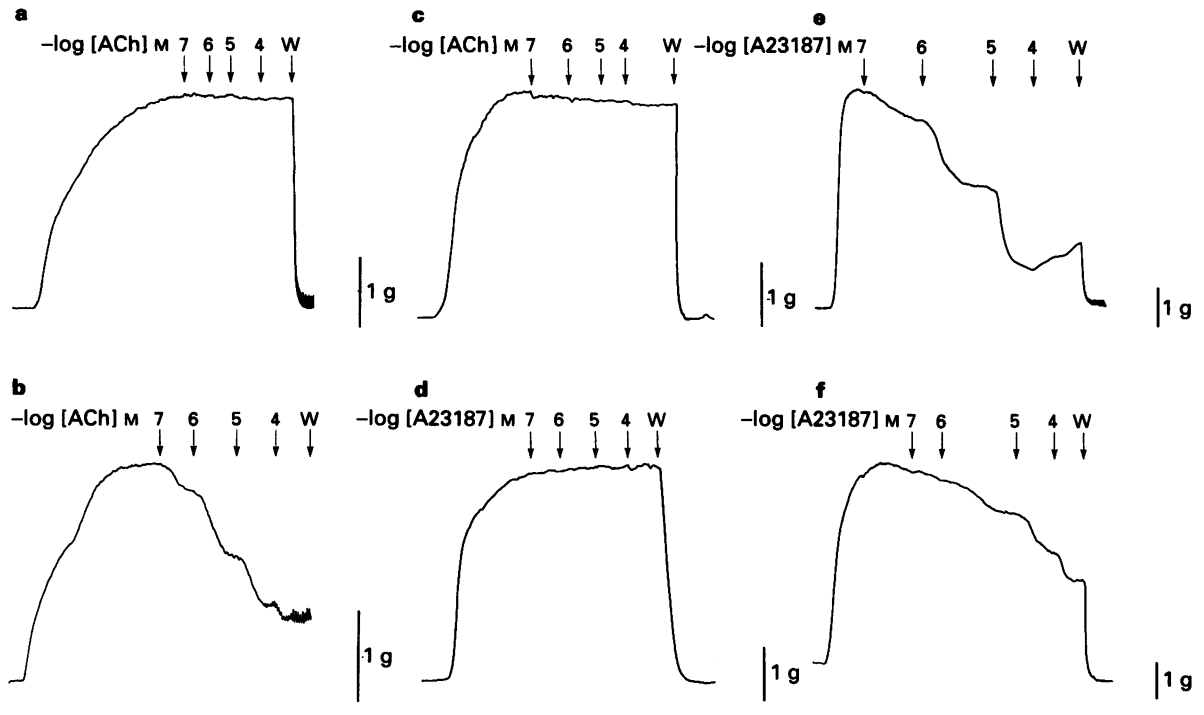

Figure 5 Representative traces, from eight experiments, showing tension change in the isolated femoral artery to either acetylcholine or A23187. Apart from (**f**), segments were precontracted by phenylephrine 1 μM. The artery segment was denuded of endothelium and exposed to acetylcholine in the absence (**a**) or presence of a donor segment containing functional endothelium (**b**) or a donor segment in the additional presence of N^G-nitro-L-arginine methyl ester (L-NAME) (**c**). Similar experiments using A23187 rather than acetylcholine are illustrated in (**d**). A23187 alone; (**e**) A23187 plus donor segment and L-NAME; (**f**) A23187 in an artery segment precontracted by 25 mM potassium.

have also been reported in other vessels, such as the rabbit middle cerebral artery, where nitric oxide- and acetylcholine-evoked changes in membrane potential were also inhibited by glibenclamide or raised extracellular potassium (Brayden, 1990). Our observations are in agreement with the studies of Huang *et al.* (1988) who suggested that the relaxation to acetylcholine in the femoral artery was mediated by nitric oxide. However, we were additionally able to block hyperpolarization to acetylcholine using specific nitric oxide-synthase inhibitors.

Inhibition of both the acetylcholine- and nitric oxide-induced hyperpolarization did not influence smooth muscle relaxation to either agent, indicating that the change in membrane potential is not normally important for reductions in tone. This contrasts with the rat mesenteric artery, where both nitric oxide, acting via cyclic GMP, and a nitric oxide-independent hyperpolarization stimulate significant relaxation in the response to acetylcholine, and where the nitric oxide-independent relaxations are markedly reduced under conditions which inhibit repolarization (Garland & McPherson, 1992; Waldron *et al.*, 1993). The potassium channel opener, levcromakalim, completely reversed the contraction to either noradrenaline or raised potassium in the femoral artery, so a link between an increase in membrane potential and smooth muscle relaxation is functional in these cells (Thirstrup & Nielson-Kidsk, 1992; Plane & Thomas, unpublished observations). Failure to reduce smooth muscle relaxation by blocking hyperpolarization presumably reflects a supramaximal action of nitric oxide via cyclic GMP.

The calcium inophore, A23187, also elicited both endothelium-dependent relaxation and repolarization in noradrenaline-stimulated segments of the rabbit femoral artery. However, in contrast to the acetylcholine-evoked responses, both the relaxation and the repolarization to A23187 were unaffected by pre-incubation with either of the nitric oxide synthase inhibitors L-NAME and L-NOARG, indicating that nitric oxide release does not make a significant contribution to these responses. This is consistent with an earlier study, where methylene blue, at a concentration which inhibited the relaxation evoked by sodium nitroprusside, did not modify A23187-evoked relaxation (Plane *et al.*, 1992). In addition to inhibiting the enzyme soluble guanylate cyclase, methylene blue also inactivates nitric oxide via the extracellular generation of superoxide anion. Therefore this observation suggests that the mediator of A23187-evoked responses, unlike nitric oxide, is not susceptable to oxygen-derived free radicals (Wolin *et al.*, 1990).

Although endothelium-dependent hyperpolarization is mediated by the opening of potassium channels, the type of channel involved has not been defined and may even vary between different vessels. Variation may also, at least in part, reflect the predominance of either EDHF or nitric oxide in the control of vessel tone. For example, in the rabbit basilar and middle cerebral arteries, endothelium-dependent hyperpolarization to acetylcholine is mediated by glibenclamide-sensitive potassium channels, whereas in the rat small mesenteric artery glibenclamide does not modify the increase in membrane potential to acetylcholine, even though glibenclamide-sensitive potassium channels are present in this vessel (Brayden, 1990; McPherson & Angus, 1990; Plane & Garland, 1993). In the rat perfused mesenteric bed, the component of smooth muscle relaxation to acetylcholine which is presumably mediated by this change in membrane potential, is in fact sensitive to the blocking action of apamin (Adeagbo & Triggle, 1993). Endothelium-dependent relaxation which is not mediated by nitric oxide has also been reported to be insensitive to glibenclamide in the porcine and guinea-pig coronary arteries (Chen *et al.*, 1991; Cowan & Cohen, 1992).

In the present study, nitric oxide- and acetylcholine-evoked hyperpolarization were each blocked by glibenclamide, while the A23187-evoked changes in smooth muscle membrane potential were not modified, except in the presence of raised extracellular potassium. This observation again indicates that A23187 operates through a different mechanism from acetyl-

choline, a mechanism which presumably involves potassium channels as both the repolarization and relaxation to A23187 were significantly reduced by raised extracellular potassium chloride concentrations. The glibenclamide sensitive component was only revealed once the predominant hyperpolarizing response to A23187 had been markedly reduced by lowering the potassium gradient. The glibenclamide-sensitive component may well reflect the release of nitric oxide, as under these conditions a similar sensitivity to L-NAME was also apparent. A direct effect of 25 mM potassium on the production or release of nitric oxide is unlikely, as in this and other studies, L-NAME-sensitive relaxations to acetylcholine were not significantly different in noradrenaline- or potassium chloride-contracted tissues (Parsons *et al.*, 1991; Plane & Garland, 1993). As both the amplitude of the repolarization and the nitric oxide-independent component of relaxation to A23187 were reduced by a similar amount, a casual link between the two events is indicated, supporting the possibility that smooth muscle hyperpolarization is responsible for nitric oxide-independent relaxation. Similar observations have recently been made with other agonists in vessels such as the porcine and canine coronary arteries and rat mesenteric arteries (Cowan & Cohen, 1991; 1992; Garland & McPherson, 1992; Nagao & Vanhoutte, 1992).

The fact that smooth muscle relaxation to acetylcholine and A23187 was recorded in the experiments with sandwich preparations of the femoral artery, which had a qualitatively similar sensitivity to L-NAME and raised extracellular potassium as in the individual segments, provides strong evidence that both nitric oxide and a transferable hyperpolarizing factor can be released by endothelial cells in this artery. Although it has been suggested that electrotonic spread of hyperpolarization from endothelial cells could underlie smooth muscle relaxation, the balance of available evidence favours the release of a diffusible hyperpolarizing factor. For example, acetylcholine induced smooth muscle hyperpolarization in smooth muscle cells of guinea-pig coronary artery denuded of endothelium, but only if sandwiched with a carotid artery with an intact endothelium. The hyperpolarization induced in this way was not sensitive to either nitroarginine or glibenclamide, but was blocked in the presence of TEA (Chen *et al.*, 1991). In the present study, relaxation was obtained in sandwiched preparations under conditions which would favour nitric oxide-independent hyperpolarization and associated smooth muscle relaxation, strongly supporting the suggestion that a diffusible hyperpolarizing factor is released from endothelial cells by A23187.

In contrast to acetylcholine, nitric oxide and A23187, bradykinin failed to evoke any measurable change in either smooth muscle membrane potential or tone in the femoral artery. Bradykinin has been shown to cause endothelium-dependent relaxation predominately by the release of EDHF in other vessels (Nagao & Vanhoutte, 1992). A similar effect of bradykinin has also been reported in human coronary arteries, an effect which is mimicked by A23187 (Nakashima *et al.*, 1993). As A23187 appeared to stimulate endothelium-dependent relaxation in the femoral artery predominately via EDHF, the lack of any response to bradykinin suggests an absence of receptors for this tachykinin on endothelial cells in the rabbit femoral artery.

In conclusion, these data indicate that in the rabbit femoral artery, which is a large condduit vessel, acetylcholine-evoked relaxations can be explained by the release of nitric oxide which then acts to stimulate relaxation by a voltage-independent mechanism. In contrast, in the femoral as in other arteries, A23187-evoked relaxations appear to be mediated predominantly by mechanisms independent of the release of nitric oxide and the activation of guanylate cyclase. A23187-evoked relaxations are mediated by a diffusible factor and are reduced together with accompanying smooth muscle hyperpolarization, indicating that the change in membrane potential provides a significant drive to relaxation.

This work was made possible by financial support from the Wellcome Trust. Glibenclamide was generously supplied by Hoechst.

References

ADEAGBO, A.S.O. & TRIGGLE, C.R. (1993). Varying extracellular [K^+]: A functional approach to separating EDHF- and EDNO-related mechanisms in perfused rat mesenteric arterial bed. *J. Cardiovasc. Pharmacol.*, **21**, 423–429.

BRAYDEN, J.E. (1990). Membrane hyperpolarization is a mechanism of endothelium-dependent cerebral vasodilation. *Am. J. Physiol.*, **259**, H668–H673.

CACOFEIRO, V. & NASJLETTI, A. (1991). Increased vascular responsiveness to bradykinin in kidneys of spontaneously hypertensive rats: effects of N^{ω}-nitro-L-arginine. *Hypertension*, **18**, 683–688.

CHAND, N., MAHONEY, T.P., DIAMANTIS, W. & SOFIA, R.D. (1987). Pharmacological modulation of bradykinin-, acetylcholine- and calcium ionophore A23187-induced relaxation of rabbit pulmonary arterial segments. *Eur. J. Pharmacol.*, **137**, 173–177.

CHEN, G. & SUZUKI, H. (1989). Some electrical properties of the endothelium-dependent hyperpolarization recorded from rat arterial smooth muscle cells. *J. Physiol.*, **410**, 521–534.

CHEN, G., SUZUKI, H. & WESTON, A.H. (1988). Acetylcholine releases endothelium-derived hyperpolarizing factor and EDRF from rat blood vessels. *Br. J. Pharmacol.*, **95**, 1165–1174.

CHEN, G., YOSHIMICHI, Y., MIWA, K. & SUZUKI, H. (1991). Hyperpolarization of arterial smooth muscle induced by endothelial humoral substances. *Am. J. Physiol.*, **260**, H1888–H1892.

COWAN, C.L. & COHEN, R.A. (1991). Two mechanisms mediate relaxation by bradykinin of pig coronary artery: NO-dependent and -independent responses. *Am. J. Physiol.*, **261**, H830–H835.

COWAN, C.L. & COHEN, R.A. (1992). Different mechanisms of relaxation of pig coronary artery to bradykinin and cromakalim are distinguished by potassium channel blockers. *J. Pharmacol. Exp. Ther.*, **260**, 248–253.

GARLAND, C.J. (1987). The role of membrane depolarization in the contractile response of the rabbit basilar artery to 5-hydroxytryptamine. *J. Physiol.*, **392**, 333–348.

GARLAND, C.J. & MCPHERSON, G.A. (1992). Evidence that nitric oxide does not mediate the hyperpolarization and relaxation to acetylcholine in the rat small mesenteric artery. *Br. J. Pharmacol.*, **105**, 429–435.

HUANG, A.H., BUSSE, R. & BASSENGE, E. (1988). Endothelium-dependent hyperpolarization of smooth muscle cells in rabbit femoral arteries is not mediated by EDRF (nitric oxide). *Naunyn-Schmied Arch. Pharmacol.*, **338**, 438–442.

IGNARRO, L.J., BYRNS, R.E., BUGA, G.M. & WOOD, K.S. (1987). Mechanisms of endothelium-dependent vascular smooth muscle relaxation elicited by bradykinin and VIP. *Am. J. Physiol.*, **253**, H1074–H1082.

JACKSON, W.F., KONIG, A.M., DAMBACHER, T. & BUSSE, R. (1993). Prostacyclin-induced vasodilation in the rabbit heart is mediated by ATP-sensitive potassium channels. *Am. J. Physiol.*, **264**, H238–H243.

MCPHERSON, G.A. & ANGUS, J.A. (1991). Evidence that acetylcholine mediated hyperpolarization of the rat small mesenteric artery does not involve the K^+ channel opened by cromakalim. *Br. J. Pharmacol.*, **103**, 1184–1190.

NAGAO, T., ILLIANO, S. & VANHOUTTE, P.M. (1992). Heterogeneous distribution of endothelium-dependent relaxations resistant to N^G-nitro-L-arginine in rats. *Am. J. Physiol.*, **263**, H1090–H1094.

NAGAO, T. & VANHOUTTE, P.M. (1992). Hyperpolarization as a mechanism for endothelium-dependent relaxations in the porcine coronary artery. *J. Physiol.*, **445**, 355–367.

NAKASHIMA, M., MOMBOULI, J.V., TAYLOR, A.A. & VANHOUTTE, P.M. (1993). Endothelium-dependent hyperpolarization caused by bradykinin in human coronary arteries. *J. Clin. Invest.*, **92**, 2867–2871.

PALMER, R.M.J., FERRIGE, A.G. & MONCADA, S. (1987). Nitric oxide release accounts for the biological activity of endothelium-derived relaxing factor. *Nature*, **327**, 524–526.

PARSONS, A.A., SCHILLING, L. & WAHL, M. (1991). Analysis of acetylcholine-induced relaxation of rabbit isolated middle cerebral artery: Effects of inhibitors of nitric oxide synthesis, Na,K-ATPase and ATP-sensitive K channels. *J. Cereb. Blood Flow Metab.*, **11**, 700–704.

PLANE, F. & GARLAND, C.J. (1993). Differential effects of acetylcholine, nitric oxide and levcromakalim on smooth muscle membrane potential and tone in the rabbit basilar artery. *Br. J. Pharmacol.*, **110**, 651–656.

PLANE, F., PEARSON, T. & GARLAND, C.J. (1992). Differences between endothelium-dependent relaxation to acetylcholine and A23187 in the rabbit isolated femoral artery. *Br. J. Pharmacol.*, **107**, 201P.

RAND, V.E. & GARLAND, C.J. (1992). Endothelium-dependent relaxation to acetylcholine in the rabbit basilar artery: importance of membrane hyperpolarization. *Br. J. Pharmacol.*, **106**, 143–150.

TARE, M., PARKINGTON, H.C., COLEMAN, H.A., NEILD, T.O. & DUSTING, G.J. (1990). Hyperpolarization and relaxation of arterial smooth muscle caused by nitric oxide derived from the endothelium. *Nature*, **346**, 69–71.

TAYLOR, S.G., SOUTHERTON, J.S., WESTON, A.H. & BAKER, J.R.L. (1988). Endothelium-dependent effects of acetylcholine in rat aorta: a comparison with sodium nitroprusside and cromakalim. *Br. J. Pharmacol.*, **64**, 853–863.

THIRSTRUP, S. & NIELSON-KUDSK, J.E. (1992). Effects of K^+ channel blockers on the relaxant action of dihydralazine, cromakalim and nitroprusside in isolated rabbit femoral arteries. *Eur. J. Pharmacol.*, **215**, 177–183.

VIDAL, M., VANHOUTTE, P.M. & MILLER, V.M. (1991). Dissociation between endothelium-dependent relaxation and increases in cGMP in systemic veins. *Am. J. Physiol.*, **260**, H1531–H1537.

WALDRON, G.J., MCPHERSON, G.A. & GARLAND, C.J. (1993). Acetylcholine-induced relaxation in the rat isolated mesenteric artery: relative importance of smooth muscle hyperpolarization. *Br. J. Pharmacol.*, **108**, 3P.

WOLIN, M.S., CHERRY, P.D., RODENBURG, J.M., MESSINA, E.J. & KALEY, G. (1990). Methylene blue inhibits vasodilation of skeletal muscle arterioles to Acetylcholine and nitric oxide via the generation of superoxide anion. *J. Pharmacol. Exp. Ther.*, **254**, 872–876.

(Received November 15, 1994
Accepted January 20, 1995)

British Journal of Pharmacology (1995) 115, 39-46

Suppression of eosinophil function by RP 73401, a potent and selective inhibitor of cyclic AMP-specific phosphodiesterase: comparison with rolipram

[1]John E. Souness, Christopher Maslen, Stephen Webber, Martyn Foster, David Raeburn, Malcolm N. Palfreyman, Michael J. Ashton & Jan-Anders Karlsson

Rhône-Poulenc Rorer Central Research, Dagenham Research Centre, Rainham Road South, Dagenham, Essex RM10 7XS

1 We have investigated the inhibitory potency of RP 73401, a novel, highly selective and potent inhibitor of cyclic AMP-specific phosphodiesterase (PDE IV), against partially-purified PDE isoenzymes from smooth muscle and the particulate PDE IV from guinea-pig eosinophils. The inhibitory effects of RP 73401 on the generation of superoxide ($.O_2^-$), major basic protein (MBP) and eosinophil cationic protein (ECP) from guinea-pig eosinophils have also been studied.

2 RP 73401 potently inhibited partially-purified cyclic AMP-specific phosphodiesterase (PDE IV) from pig aortic smooth muscle (IC_{50} = 1.2 nM); it was similarly potent against the particulate PDE IV from guinea-pig peritoneal eosinophils (IC_{50} = 0.7 nM). It displayed at least a 19000 fold selectivity for PDE IV compared to its potencies against other PDE isoenzymes. Rolipram was approximately 2600 fold less potent than RP 73401 against pig aortic smooth muscle PDE IV (IC_{50} = 3162 nM) and about 250 times less potent against eosinophil PDE IV (IC_{50} = 186 nM).

3 Solubilization of the eosinophil particulate PDE IV increased the potency of rolipram 10 fold but did not markedly affect the potency of RP 73401. A similar (10 fold) increase in the PDE IV inhibitory potency of rolipram, but not RP 73401, was observed when eosinophil membranes were exposed to vanadate/glutathione complex (V/GSH).

4 Reverse transcription polymerase chain reaction (RT-PCR), using primer pairs designed against specific sequences in four distinct rat PDE IV subtype cDNA clones (PDE IV_{A-D}), showed only mRNA for PDE IV_D in guinea-pig eosinophils. PDE IV_D was also the predominant subtype expressed in pig aortic smooth muscle cells.

5 RP 73401 ($K_{i\,app}$ = 0.4 nM) was 4 fold more potent than (±)-rolipram ($K_{i\,app}$ = 1.7 nM) in displacing [^{3}H]-(±)-rolipram from guinea-pig brain membranes.

6 In intact eosinophils, RP 73401 potentiated isoprenaline-induced cyclic AMP accumulation (EC_{50} = 79 nM). RP 73401 also inhibited leukotriene B_4-induced generation of $.O_2^-$ (IC_{50} = 25 nM), and the release of major basic protein (IC_{50} = 115 nM) and eosinophil cationic protein (IC_{50} = 7 nM). Rolipram was 3-14 times less potent than RP 73401.

7 Thus RP 73401 is a very potent and selective PDE IV inhibitor which suppresses eosinophil function suggesting that it may be a useful agent for the treatment of inflammatory diseases such as asthma. The greatly different inhibitory potencies of rolipram against PDE IV from smooth muscle and eosinophils (in contrast to the invariable effects of RP 73401) are unlikely to be attributable to diverse PDE IV subtypes but suggest distinct interactions of the two inhibitors with the enzyme.

Keywords: Cyclic AMP-phosphodiesterase; RP 73401; rolipram; eosinophil; superoxide; major basic protein; eosinophil cationic protein

Introduction

Much attention has recently focused on the therapeutic potential of adenosine 3':5'-cyclic monophosphate (cyclic AMP)-specific phosphodiesterase (PDE IV) inhibitors for the treatment of asthma (Torphy & Undem, 1991; Giembycz, 1992; Raeburn *et al.*, 1993). This stems primarily from the wide-ranging anti-inflammatory properties of PDE IV inhibitors *in vitro* and *in vivo*. For example, the archetypal PDE IV inhibitor, rolipram, suppresses functional responses (e.g. generation of reactive oxygen species, cytokines, mediators and cytotoxic proteins) in mast cells (Torphy *et al.*, 1992a), basophils (Peachell *et al.*, 1992), monocytes (Semmler *et al.*, 1993), macrophages (Schade & Schudt, 1993), neutrophils (Fonteh *et al.*, 1993; Wright *et al.*, 1990), lymphocytes (Epstein *et al.*, 1984; Robicsek *et al.*, 1991) and eosinophils (Dent *et al.*, 1991; Souness *et al.*, 1991). *In vivo*, PDE IV inhibitors suppress microvascular leakage (Raeburn & Karlsson, 1993), eosinophil accumulation (Underwood *et al.*, 1993), passive cutaneous anaphylaxis (Davies & Evans, 1973) and anaphylactic bronchospasm (Underwood *et al.*, 1993). As well as their anti-inflammatory effects, PDE IV inhibitors relax airways smooth muscle and exhibit bronchodilator activity *in vivo* (Harris *et al.*, 1989). Furthermore, PAF-induced bronchial hyperresponsiveness in guinea-pigs is attenuated by rolipram (Raeburn & Lewis, 1991).

Asthma is a disease characterized by variable airways obstruction and bronchial hyperresponsiveness which has been linked to mucosal inflammation and, in particular, the influx and activation of eosinophils (Barnes *et al.*, 1988; Kay, 1985). PDE IV inhibitors, with their dual anti-inflammatory and bronchodilator activities, may be useful for treating both the symptoms and the underlying causes of the disease. We have synthesized a PDE IV inhibitor, RP 73401 (3-cyclopentyloxy-*N*-[3,5-dichloro-4-pyridyl]-4-methoxybenzamide) (Figure 1) (Ashton *et al.*, 1994) and compared its inhibitory activities against PDE IV preparations from smooth muscle

[1] Author for correspondence.

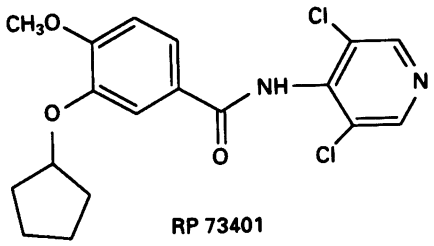

RP 73401

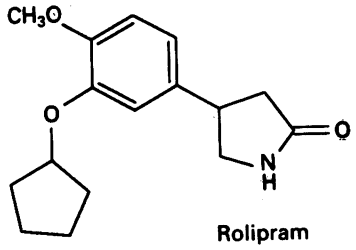

Rolipram

Figure 1 Structures of RP 73401 and rolipram.

and eosinophils with those of the standard PDE IV inhibitor, rolipram. We have also investigated the effects of these compounds on the physiological responses of eosinophils to exogenously applied stimuli.

Methods

Preparation of guinea-pig peritoneal eosinophils

Male, Dunkin-Hartley guinea-pigs (250–400 g) were injected (i.p.) with 0.5 ml of donor horse serum twice weekly for 4 weeks. At least 5 days after the final injection, the guinea-pigs were killed by CO_2 asphyxiation. A ventral incision was made into the peritoneum and 30 ml of Hank's buffered salts solution (HBSS) without Ca^{2+} (Gibco, U.K. Ltd) were poured into the abdominal cavity. The abdomen was gently massaged for approximately 1 min and the peritoneal exudate aspirated and centrifuged (250 *g*, 10 min, 4°C). The supernatant was discarded and the pellet washed once (HBSS, 10 ml) and resuspended in HBSS containing 5% (v/v) foetal calf serum (FCS). Aliquots (1 ml) of the cell suspension were layered onto a discontinuous (55%, 65%, 70%, v/v) Percoll gradient prepared in resuspension buffer. The gradients were centrifuged (250 *g*, 20 min, 20°C) and the normo-dense and hypo-dense eosinophils, which accumulated at the 65%/70% and 55%/65% Percoll gradient interfaces, respectively, were resuspended in HBSS (10 ml). Total cell counts were determined with a Coulter counter (Z1) and differential cell counts were obtained from cytospin slides fixed in methanol and stained with Wright-Giemsa. Cell viability was greater than 95% and eosinophil purity greater than 97%.

Preparation of eosinophil subcellular fractions

Cells ($100–200 \times 10^6$), suspended in HBSS, were centrifuged (250 *g*, 10 min, 4°C), the supernatant removed and the resulting pellet resuspended in 5 ml of homogenization buffer (Tris/HCl, 20 mM [pH 7.5]; $MgCl_2$, 2 mM; dithiothreitol, 1 mM; ethylenediaminetetraacetic acid (EDTA), 5 mM; sucrose, 0.25 M; *p*-tosyl-L-lysine-chloromethylketone (TLCK), 20 μM; leupeptin, 10 μg ml^{-1}; aprotinin, 2000 u ml^{-1}). Cells were homogenized with a Dounce homogenizer (10 strokes). The homogenate was centrifuged (105,000 *g*, 60 min), the supernatant collected and the pellet resuspended in an equal volume of homogenization buffer.

Solubilization of membrane-associated cyclic AMP PDE from eosinophils

The membrane-bound cyclic AMP PDE was solubilized by homogenizing freshly prepared membranes with a Dounce homogenizer (10 strokes) in homogenization buffer containing deoxycholate (0.5%) and NaCl (100 mM). The homogenate was centrifuged (100,000 *g*, 30 min) and the supernatant containing the solubilized activity removed.

Partial purification of smooth muscle PDE isoenzymes

Ca^{2+}/calmodulin-dependent PDE (PDE I), cyclic GMP-inhibited PDE (PDE III), cyclic AMP-specific PDE (PDE IV) and cyclic GMP-specific PDE (PDE V) were isolated from pig aortic smooth muscle. Isoenzymes were partially purified by DEAE-trisacryl anion exchange chromatography (IBF, Villeneuve La Garenne, France) from the 100,000 *g* supernatant fraction of aortic smooth muscle strips which were prepared and processed as previously described (Souness & Scott, 1993). Cyclic GMP-stimulated PDE (PDE II) was partially purified by the same homogenization and chromatography procedure except that the source of the isoenzyme was fresh bovine cervical trachealis isolated according to Giembycz & Barnes (1991).

Measurement of PDE activity

PDE activity was determined by the two-step radioisotope method of Thompson *et al.* (1979). The reaction mixture contained (mM): Tris-HCl 20 (pH 8.0), $MgCl_2$ 10, 2-mercaptoethanol 4, ethyleneglycol-*bis*-(β-aminoethyl ether) N,N,N',N'-tetraacetic acid (EGTA) 0.2, bovine serum albumin 0.05 mg ml^{-1}. Unless otherwise stated, the substrate concentration was 1 μM.

The IC_{50} values (concentration which produced 50% inhibition of substrate hydrolysis) for the compounds were determined from concentration (0.1 nM to 40 μM)-response curves. At least three concentration-response curves were generated for each agent.

For kinetic studies, the concentration of cyclic AMP was varied while the amount of ^3H-labelled cyclic AMP remained constant.

Categorisation of PDE isoenzymes

The nomenclature adopted in this paper for the different cyclic nucleotide PDEs is based on that of Beavo & Reifsnyder (1990). PDE IV subtypes referred to in this paper are based on four rat cDNA nucleotide sequences (PDE IV_{A-D}/rpdes 1-4) as reported by Swinnen *et al.* (1989).

Preparation of Na_3VO_4/GSH complex (V/GSH)

The V/GSH complex was prepared according to Souness *et al.* (1985). Briefly, reduced glutathione (GSH – 224 mM) and Na_3VO_4 (112 mM) were mixed together to form a green complex; 10 μl of this solution was added to the 400 μl assay mix, immediately prior to addition of enzyme. The final concentration of GSH and Na_3VO_4 were 2.8 mM and 1.4 mM, respectively.

Measurement of eosinophil cyclic AMP accumulation

For measurement of cyclic AMP, freshly prepared eosinophils (1×10^6 cells ml^{-1}) were preincubated in HBSS containing Ca^{2+} and Mg^{2+}. To test the effects of PDE IV inhibitors, compounds (0.0064 μM–100 μM) were routinely added to cell suspensions for 10 min, after which incubations were continued for a further 2 min, either in the absence or presence of isoprenaline (10 μM). Incubations were terminated with 50 μl of 100% trichloroacetic acid (TCA).

The TCA extract was briefly sonicated (10 s), centrifuged

(3000 g) for 15 min and the supernatant removed to a clean tube. TCA was removed with 3 washes of water saturated diethyl ether (5 vols). The last traces of ether were removed by gassing with nitrogen, and sodium acetate (pH 6.2) was added to a final concentration of 50 mM. Samples were acetylated and cyclic AMP quantified by radioimmunoassay (RIA, NEN Chemicals GmbH).

Measurement of eosinophil superoxide generation

Superoxide anion ($.O_2^-$) generation was determined as the superoxide dismutase (SOD) inhibitable reduction of *p*-iodonitrotetrazolium violet (INTV) as previously described (Souness *et al.*, 1991). Briefly, cells (1×10^6/well) were incubated for 15 min (37°C) in 96-well microtitre plates in HBSS (0.225 ml) containing INTV (0.5 mg ml^{-1}) with either vehicle control (0.1% dimethyl sulphoxide) or PDE inhibitors (0.001–10 μM). SOD (1 mg ml^{-1}) was added to some incubations to determine what proportion of dye reduction was attributable to $.O_2^-$ generation. Following the initial 15 min incubation, leukotriene B_4 (LTB_4) (10 nM) was added and incubations continued for a further 10 min. The cells were then centrifuged (500 g, 10 min) and the supernatant aspirated. The pellet was solubilized by incubation overnight at room temperature in DMSO containing 0.6 M HCl and the absorbance of the reduced dye measured at 492 nm (Titertek Multiskan MCC/340). The results are expressed as % inhibition of the SOD inhibitable $.O_2^-$ release.

Measurement of major basic protein (MBP) and eosinophil cationic protein (ECP)

Cells (1×10^6/ml) were incubated for 15 min (37°C) in 96-well microtitre plates in HBSS (0.225 ml) containing cytochalasin B (5 μg ml^{-1}) with vehicle control (0.1%) or PDE IV inhibitors (0.001–1 μM). Leukotriene B_4 (LTB_4, 10 nM) was then added and the incubation was continued for a further 10 min; 200 μl of the supernatant was removed from each well and stored at −20°C prior to quantification of MBP and ECP.

MBP was measured by a modification of the antigen capture ELISA previously described (Hunt *et al.*, 1993). Briefly, microtitre plates (Falcon Pro-Bind) were coated with monoclonal antibodies for MBP (BMK13, Sera-Lab, 3 μg ml^{-1}) in sodium carbonate (15 mM)/sodium bicarbonate (35 mM) coating buffer. After overnight incubation (4°C), the plates were washed with phosphate buffered saline (PBS) containing Tween-20 (0.05%, v/v). The remaining free binding sites were blocked with BSA (1%). Eosinophil supernatants (100 μl undiluted), or eosinophil MBP (0–800 μg ml^{-1}, prepared and stabilized as previously described (Gleich *et al.*, 1973; Wassom *et al.*, 1979)), were then added to the plates and incubated for 2 h (with shaking). Plates were washed three times with PBS/Tween-20. Detection antibody (alkaline phosphatase labelled IgG diluted 1:400 in PBS) was added to the wells and incubated for 90 min at room temperature. Following second antibody incubation, the plates were washed three times with PBS/Tween-20 and the detection substrate bromochloroindophenol (BCIP) was added and incubated for 60 min at 37°C. Plates were then read at 590 nm.

ECP was measured by a similar antigen capture ELISA using polyclonal anti-human ECP antibodies (DA178, Kabi Pharmacia Diagnostics, Milton Keynes, U.K.). The assay was identical to that described above for MBP except that primary antibody was coated onto 96-well plates at a concentration of 5 μg ml^{-1}, calibration curves for standard human ECP (Kabi Pharmacia Diagnostics) were in the range 0–3.2 μg ml^{-1} and the alkaline phosphatase detection antibody was used at a 1:500 dilution. Results are expressed as % inhibition of LTB_4-induced MBP or ECP release.

Measurement of [^{3}H]-(±)-rolipram binding to brain membranes

(±)-Rolipram was brominated in CCl_4 and dispatched to Amersham International where it was tritiated by catalytic reduction with palladium and charcoal. The specific radioactivity of the [^{3}H]-(±)-rolipram was 24.7 Ci $mmol^{-1}$.

Guinea-pig brain membranes were prepared and the binding assay was performed as described by Schneider *et al.* (1986) with [^{3}H]-rolipram (2 nM) and membrane samples corresponding to 500 μg of brain tissue.

Expression of mRNA for PDE IV subtypes

Total RNA was prepared with a Total RNA Separator kit from Clontech. Briefly, 1×10^5–1×10^6 cells were homogenized in denaturing solution: guanidinium thiocyanate, 4 M; Na^+ citrate, 25 mM [pH 7.0]; sarcosyl, 0.5%; 2-mercaptoethanol, 0.1 M, followed by phenol/chloroform/isoamyl alcohol extraction and isopropanol precipitation according to the manufacturers protocol. First strand cDNA synthesis and cDNA amplification were performed using a GeneAMP RNA PCR kit (Perkin Elmer Cetus). Primers specific for the different rat PDE IV subtypes were designed by Mr I. Giddings (Molecular Medicine Unit, King's College, London) based on reported sequences (Swinnen *et al.*, 1989) from the Genbank data-base (Table 1). PCR amplification was performed with a DNA Thermal Cycler 480 (Perkin Elmer Cetus) set for 35–55 cycles. The temperatures set for PCR were: denature 95°C, 30 s; primer anneal 55°C, 120 s; primer extension 72°C, 180 s. Primer fragments were analysed by electrophoresis on 2% agarose gels, and DNA was visualized by ethidium bromide staining. Each set of primers was first tested using rat brain and rat lung poly (A^+) mRNA (Clontech). Agarose gel electrophoresis of ethidium bromide-stained DNA fragments generated after 55 cycles of amplification showed that there

Table 1 Primers used in RT-PCR experiments

Oligonucleotide	*	*Sequences* (position 1-5′)	*Fragment size* (bases)
5 pde 1	5 PDE IV_C	CYYAYGTGGCYTAYCACAACA	535
3 pde 1	3 PDE IV_C	GTCCACTGGCGGTAGAGGGGT	
5 pde 2	5 PDE IV_A	CYYAYGTGGCYTAYCACAACA	174
3 pde 2	3 PDE IV_A	TTAGGAACTGGTTGGAGAGCG	
5 pde 3	5 PDE IV_D	CYYAYGTGGCYTAYCACAACA	331
3 pde 3	3 PDE IV_D	ATGGCCATTTTCCTTAAAGAT	
5 pde 4	5 PDE IV_B	CYYAYGTGGCYTAYCACAACA	593
3 pde 4	3 PDE IV_B	CATTCCCCTCTCCCGTTCTTT	

Y = Inosine.
*Nomenclature of Beavo & Reifsnyder (1990).

was one DNA fragment in each reaction corresponding to the size of the expected PDE IV subtype fragment as defined by the primers used in the PCR. To verify their identity, PCR products were sequenced with Sequenase DNA sequencing kits (Amersham, Bucks, U.K.).

Inhibition of methacholine-induced contraction of guinea-pig trachealis

Guinea-pig trachealis was prepared and organ bath studies performed as described previously (Souness *et al.*, 1994). The relaxant effects of RP 73401 and rolipram were determined in tissue contracted with a concentration of methacholine which produced a 30% of maximal contraction (EC_{30}) as determined by computerised linear regression analysis. The mean EC_{30} value for methacholine was 0.09 ± 0.01 μM ($n = 10$). IC_{50} values (means ± s.e.mean, $n = 6$) were taken as the concentration of relaxant producing 50% relaxation of methacholine-induced contraction.

Materials

RP 73401 and rolipram [4-(3-cyclopentyloxy-4-methoxyphenyl)-2-pyrrolidinone] were synthesized by the department of Discovery Chemistry, Rhône-Poulenc Rorer Ltd (Dagenham, Essex, U.K.). Cyclic [2,8-^{3}H]-AMP (41 Ci mmol^{-1}) and cyclic [8-^{3}H]-GMP (13.8 Ci mmol^{-1}) were from Amersham International (Amersham, Bucks., U.K.). The cyclic AMP radioimmunoassay kit was purchased from NEN Chemicals GmbH. Cell culture reagents were from Gibco BRL (Paisley, Scotland). Donor horse serum was purchased from Flow Laboratories Ltd. (Irvine, Scotland). The monoclonal antibody for major basic protein (BMK10) was from Sera-Lab (Crawley Down, Sussex, U.K.) and the monoclonal antibody for eosinophil cationic protein (DA178) was from Pharmacia (Milton Keynes, U.K.). The Clontech total RNA Separator kit was purchased from Cambridge BioScience (Cambridge, U.K.) and the GeneAMP RNA PCR kit was from Perkin Elmer Cetus (Vaterstetten, Germany). All other chemicals were obtained from Sigma Chemical Co. or BDH Chemicals (both of Poole, Dorset, U.K.) and Rhône-Poulenc Ltd. (Eccles, Manchester, U.K.). Male Dunkin-Hartley guinea-pigs were purchased from a local supplier.

Results

Inhibition of partially-purified PDEs from pig aortic and bovine tracheal smooth muscle

RP 73401 potently and selectively inhibited PDE IV from pig aortic smooth muscle (Table 2). It was at least 19,000 times less potent aginst PDEs I, II (bovine trachea), III and V. In comparison, rolipram was a relatively weak, though still selective (>70 fold), inhibitor of PDE IV (Table 2). A similar inhibitory potency difference between the two compounds was observed against partially-purified PDE IV from bovine tracheal smooth muscle ($-\log IC_{50}$ [M]: RP 73401 = 9.00 ± 0.06, $n = 4$; $-\log IC_{50}$ [M]: rolipram = 5.71 ± 0.05, $n = 3$).

Inhibition of eosinophil PDE IV by RP 73401 and rolipram – effects of solubilization and V/GSH

RP 73401 displayed similar potencies against the eosinophil and pig aortic PDE IV (Tables 2 and 3). In contrast, and as reported previously (Souness & Scott, 1993), rolipram was over 10 times more potent as an inhibitor of membrane-bound PDE IV from eosinophils than of the partially-purified PDE IV from pig aorta (Table 3). Solubilization with deoxycholate plus NaCl or treatment of membranes with V/GSH increased the potency of rolipram by a further 10 fold (Table 3). Neither solubilization nor V/GSH had any significant effect on the inhibitory potency of RP 73401 (Table 3). The potency of rolipram ($-\log IC_{50}$ [M] = 6.18 ± 0.08, $n = 4$) decreased when tested against membrane-bound PDE IV from eosinophils which had been stored at −80°C; however, the potency of RP 73401 ($-\log IC_{50}$ [M] = 9.00 ± 0.06, $n = 4$) was unaffected by these storage conditions.

The inhibitory effects of RP 73401 and rolipram against the solubilized, eosinophil PDE IV are not competitive (Figure 2). Indeed, the nature of the inhibition is difficult to interpret in view of the marked non-linearity of the Lineweaver-Burk plots, especially in the presence of inhibitor.

Table 2 Inhibition of smooth muscle phosphodiesterases (PDEs) by RP 73401 and rolipram

PDE type	$-\log IC_{50}$ [M] ± s.e.mean RP 73401	Rolipram
I	4.36 ± 0.01 ($n = 5$)	<3 ($n = 4$)
II	4.14 ± 0.02 ($n = 3$)	3.70 ± 0.01 ($n = 3$)
III	3.83 ± 0.26 ($n = 5$)	3.18 ± 0.15 ($n = 4$)
IV	8.93 ± 0.02 ($n = 4$)	5.50 ± 0.08 ($n = 5$)
V	4.66 ± 0.10 ($n = 5$)	3.05 ± 0.10 ($n = 3$)

PDEs I and V were measured with 1 μM cyclic GMP substrate, the former in the presence of 2 mM $CaCl_2$ + 10 u ml^{-1} calmodulin. PDEs III and IV were measured using 1 μM cyclic AMP substrate. PDE II was measured with 1 μM cyclic AMP substrate in the presence of 10 μM cyclic GMP.

Table 3 Effects of solubilization and vanadate/glutathione complex (V/GSH) on the inhibitory potencies of RP 73401 and rolipram against eosinophil PDE IV

Treatment	$-\log IC_{50}$ [M] ± s.e.mean RP 73401	Rolipram
None	9.15 ± 0.20 ($n = 3$)	6.73 ± 0.09 ($n = 8$)
Solubilization	9.07 ± 0.18 ($n = 4$)	7.55 ± 0.09 ($n = 7$)
V/GSH	8.68 ± 0.06 ($n = 4$)	7.94 ± 0.11 ($n = 7$)

Cyclic AMP PDE activity in the bound, particulate (−/+V/GSH) and deoxycholate/NaCl-solubilized preparations was measured with 1 μM substrate.

Stimulation of eosinophil cyclic AMP accumulation

Both RP 73401 and rolipram potently enhanced the accumulation of cyclic AMP in intact eosinophils elicited by isoprenaline (Figure 3). RP 73401 ($-\log EC_{50}$ [M] = 7.11 ± 0.13, $n = 3$) was approximately 4 fold more potent than rolipram ($-\log EC_{50}$ [M] = 6.66 ± 0.02, $n = 3$). Little or no effect of either PDE inhibitor was observed in the absence of isoprenaline (data not shown), nor was an increase in cyclic AMP accumulation observed after a 10 min incubation with isoprenaline alone.

Inhibition of LTB_4-induced release of $.O_2^-$, MBP and ECP from eosinophils

RP 73401 was approximately 6 fold more potent than rolipram in inhibiting LTB_4-stimulated superoxide generation from eosinophils (Figure 4a). The $-\log IC_{50}$ [M] values were 7.60 ± 0.08, ($n = 4$) and 6.73 ± 0.04 ($n = 4$) for RP 73401 and rolipram, respectively. RP 73401 was also a very potent inhibitor of LTB_4-induced ECP ($-\log IC_{50}$ [M]: 8.16 ± 0.10, $n = 4$) generation but was less potent in suppressing MBP ($-\log IC_{50}$ [M]: 6.94 ± 0.04, $n = 4$) release (Figure 4b,c). Rolipram was less potent than RP 73401 against both cationic proteins, exhibiting inhibitory potencies ($-\log IC_{50}$ [M]) of 6.99 ± 0.07, ($n = 4$) and 6.22 ± 0.02 ($n = 4$) on ECP and MBP generation, respectively (Figure 4b,c).

Displacement of rolipram binding from brain membranes

RP 73401 was a very potent inhibitor of [^{3}H]-(±)-rolipram binding to membranes prepared from guinea-pig brains ($-\log K_{i\,app}$ [M] = 9.42 ± 0.11, $n = 3$) (Figure 5). (±)-Rolipram was about 4 fold less potent in displacing the tritiated ligand ($-\log K_{i\,app}$ [M] = 8.77 ± 0.07, $n = 3$).

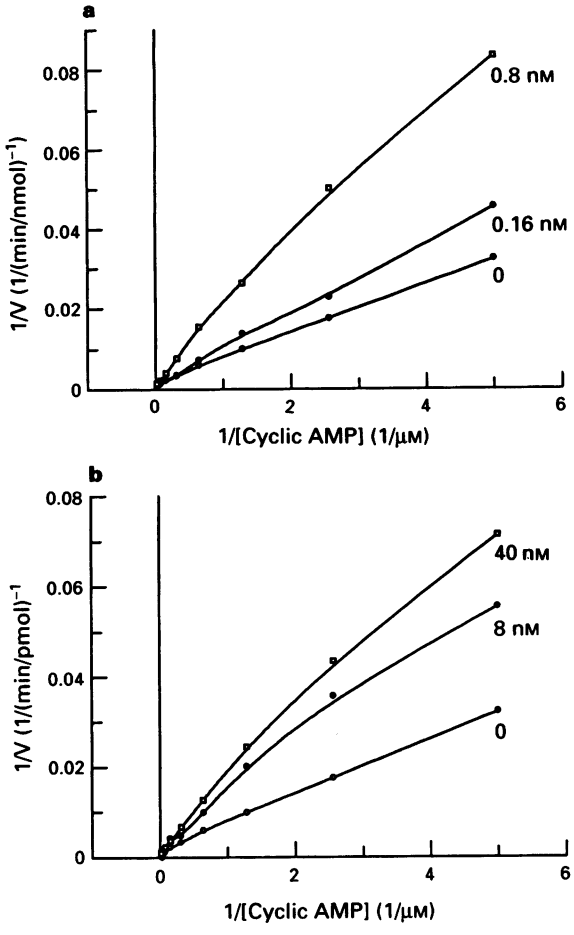

Figure 2 Kinetic analysis of RP 73401 (a) and rolipram (b) inhibition of solubilized eosinophil PDE IV. The data represent Lineweaver-Burk plots in the presence of increasing concentrations of RP 73401 (a) or rolipram (b).

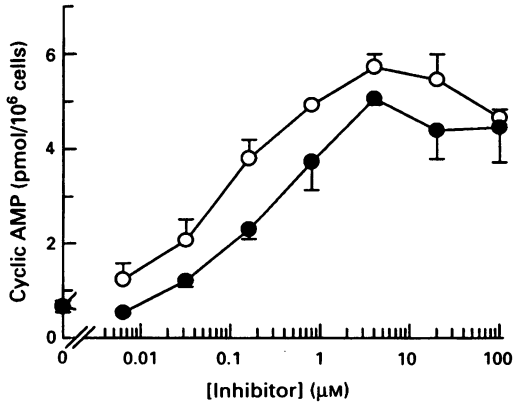

Figure 3 Enhancement of isoprenaline-induced cyclic AMP accumulation in intact eosinophils by RP 73401 and rolipram. Cells were preincubated for 10 min in the presence of the indicated concentrations of RP 73401 (○) and rolipram (●) before exposure to isoprenaline (10 μM) for a further 2 min. Control cells contained 0.91 ± 0.25 pmol of cyclic AMP/10^6 cells ($n = 5$). The results represent the means ± s.e.mean ($n = 3$).

Expression of PDE IV subtypes in eosinophils and smooth muscle

RT-PCR was used to determine the PDE IV subtypes expressed in eosinophils and smooth muscle. Primers designed to recognize sequences in the genes of 4 different rat PDE IV subtypes (PDE IV_{A-D}/rpdes 1–4) (Swinnen *et al.*, 1989) were employed in these studies (Table 1). Each set of primers was first tested employing reverse transcribed rat brain-, guinea-pig brain- and rat lung-poly (A^+) mRNA (Clontech) from which PCR amplified cDNA fragments of the correct size

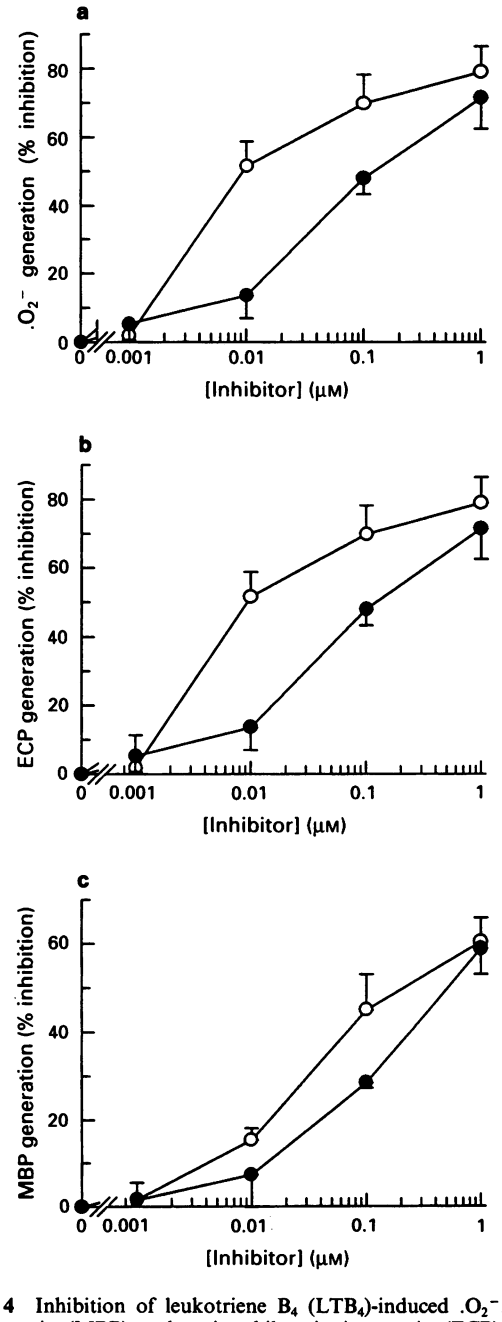

Figure 4 Inhibition of leukotriene B_4 (LTB_4)-induced $.O_2^-$, major basic protein (MBP) and eosinophil cationic protein (ECP) release from eosinophils by RP 73401 and rolipram. Cells were preincubated with the indicated concentrations of RP 73401 (○) and rolipram (●) for 15 min. LTB_4 (10 nM) was then added and the incubations were continued for a further 10 min before cells were pelleted and the medium was assayed for $.O_2^-$ (a), ECP (b) and MBP (c). Resting cells released 285 ± 42 ng ECP/10^6 cells and 38 ± 6 ng MBP/10^6 cells. After stimulation with LTB_4, media contained 1460 ± 120 ng ECP/10^6 cells and 268 ± 31 ng MBP/10^6 cells. The results, expressed as % inhibition of LTB_4-alone values, represent means ± s.e.mean of 4 separate incubations.

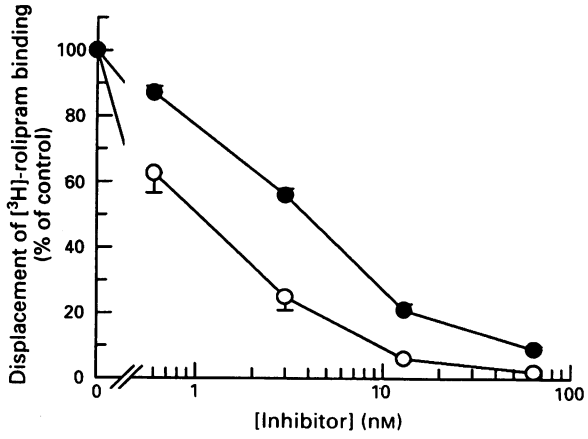

Figure 5 Displacement of [^{3}H]-(±)-rolipram from brain membranes by RP 73401 and rolipram. [^{3}H]-(±)-rolipram binding to brain membranes was measured in the presence of the indicated concentrations of RP 73401 (○) and rolipram (●). The results represent means ± s.e.means ($n = 3$).

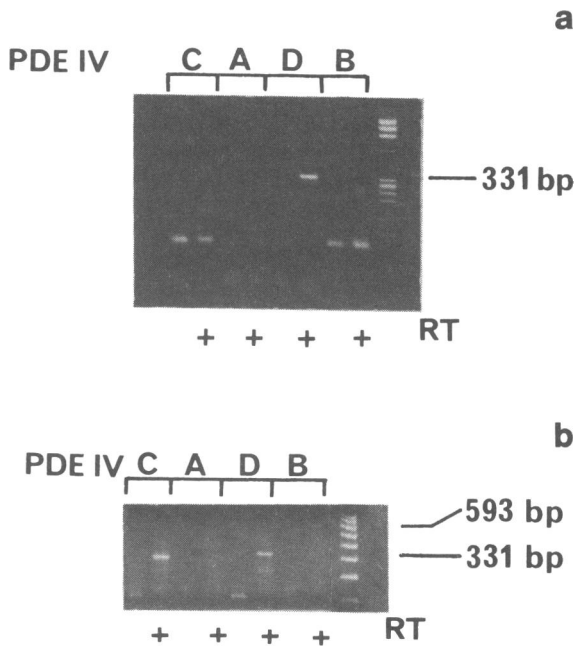

Figure 6 PDE IV message amplification phenotyping in eosinophils and smooth muscle. RNA from guinea-pig eosinophils (a) and pig aortic smooth muscle cells (Souness *et al.*, 1992a) (b) was extracted from 10^6 cells. First strand cDNA synthesis and PCR amplification (55 cycles) (using primers recognizing unique sequences in PDE IV_{A-D} (rpdes 1-4)) of total RNA from eosinophils and pig aortic smooth muscle cells were performed as described in the Methods section.

corresponding to PDE IVs_{A-D} were detected. Ethidium bromide staining of gels of RT-PCR products of guinea-pig eosinophil total RNA revealed an amplified cDNA fragment corresponding to that predicted for PDE IV_D (predicted fragment size: 331 bases) (Figure 6a). Sequencing confirmed that this PCR product corresponded to PDE IV_D. No RT-PCR-amplified products of the correct molecular sizes were detected employing primers recognizing sequences in PDE IV_A, PDE IV_B or PDE IV_C. RT-PCR of total RNA from pig aortic smooth muscle cells (using rat primers) demonstrated PDE IV_D to be the major subtype expressed (Figure 6b). A faint band corresponding to PDE IV_B was also detected. The PCR fragment detected in lane 2 of Figure 6b did not correspond to the predicted size for PDE IV_C. The only RT-PCR fragment detected employing poly (A^+) mRNA from rat smooth muscle (Clontech) corresponded to PDE IV_D (data not shown).

Inhibition of methacholine-induced contraction of guinea-pig trachealis

RP 73401 ($-\log IC_{50}$ [M] = 7.53 ± 0.12, $n = 6$) was about 3 fold more potent than rolipram ($-\log IC_{50}$ [M] = 7.01 ± 0.04, $n = 6$) in reversing methacholine-induced contractions of guinea-pig trachealis.

Discussion

RP 73401 is a very potent and selective inhibitor of cyclic AMP hydrolysis. It inhibits PDE IV with a very high potency and displays great selectivity over PDEs I, II, III and V. Rolipram was considerably less selective. PDE IV is the predominant isoenzyme regulating cyclic AMP levels and (consequently) function in a wide-range of inflammatory cells (Torphy & Undem, 1991) including eosinophils (Dent *et al.*, 1991; Souness *et al.*, 1991). RP 73401 suppresses eosinophil function *in vitro* and exhibits anti-inflammatory activity *in vivo* (Raeburn *et al.*, 1994), effects that can be attributed to elevation of cyclic AMP through inhibition of PDE IV.

Blood and lung eosinophil numbers are elevated in asthma and may correlate with the severity of the disease (Kay, 1985; Barnes *et al.*, 1988). The cytotoxic potential of the eosinophil is due to its ability to generate reactive oxygen species and cationic proteins which can induce epithelial damage and increase airways reactivity as demonstrated in experimental animals *in vivo* (Kay, 1985; Barnes *et al.*, 1988). We and others (Dent *et al.*, 1991; Souness *et al.*, 1991) have previously shown that PDE IV inhibitors, such as rolipram, suppress oxygen radical formation. We now show that RP 73401 was 7 fold more potent than rolipram in blocking this parameter of the eosinophil's cytotoxic armoury. More importantly, however, RP 73401 potently inhibited ECP and MBP release from eosinophils further indicating the anti-inflammatory potential of this compound. These cytotoxic proteins are associated with eosinophil-mediated damage of the respiratory mucosa, in particular epithelial disruption and shedding (Barnes *et al.*, 1988). The potent dampening effects of RP 73401 on eosinophil function may be one explanation for the potent anti-inflammatory properties of RP 73401 in guinea-pigs and rats (Raeburn *et al.*, 1994). Furthermore, the inhibition of platelet-activating factor-induced airway hyperresponsiveness in guinea-pigs by RP 73401 (Raeburn *et al.*, 1994) may also be related to suppression of MBP and ECP release.

Interesting differences were observed between the inhibitory actions of RP 73401 and rolipram against eosinophil PDE IV; in particular, solubilization or V/GSH-treatment of membrane-bound eosinophil PDE IV increases (10 fold) the potency of rolipram but leaves that of RP 73401 unaffected. The basis for this disparity is uncertain, although the demonstration by molecular biology studies (Swinnen *et al.*, 1989; Torphy *et al.*, 1992b; McLaughlin *et al.*, 1993) of four PDE IV genes may offer one possible explanation. If multiple PDE IV subtypes exist in eosinophils against which rolipram displays different affinities, the effects of solubilization and V/GSH treatment could be rationalized if these treatments selectively activated a subtype for which rolipram is more potent. If this assertion is correct, RP 73401, in contrast to rolipram, would not discriminate between the two subtypes. Our RT-PCR data do not support this hypothesis since only mRNA for PDE IV_D was detected in these cells.

An alternative hypothesis (Souness & Scott, 1993), proposes that solubilization or V/GSH treatment induces a conformational change in PDE IV which increases the potency

of rolipram. Under these conditions, there is a very strong correlation between the potency order of compounds in inhibiting catalytic activity and displacing high-affinity [^{3}H]-rolipram from brain membranes (Souness & Scott, 1993). Although high-affinity rolipram binding is known to be localized on PDE IV (Torphy *et al.*, 1992b; McLaughlin *et al.*, 1993), its nature and relevance is at present unclear. Solubilization and V/GSH-treatment induces marked potency shifts only in the compounds (rolipram, denbufylline, Ro 20-1724) with IC_{50} values in displacing [^{3}H]-(±)-rolipram from PDE IV lower than those for inhibition of cyclic AMP hydrolysis (Souness *et al.*, 1992b; Souness & Scott, 1993). Conversely, no potency shifts occur with compounds (dipyridamole, trequinsin) that are more potent inhibitors of PDE IV activity than of [^{3}H]-(±)-rolipram binding (Torphy *et al.*, 1992b; Souness *et al.*, 1992b). RP 73401 exhibited similar potencies on cyclic AMP hydrolysis (smooth muscle or inflammatory cell PDE IVs) and rolipram binding and its activity on eosinophil PDE IV was, predictably, not influenced by solubilization or V/GSH treatment.

The reason why rolipram was greater than 100 fold more potent against eosinophil PDE IV (solubilized or +V/GSH) than partially-purified PDE IV from smooth muscle, whereas RP 73401 does not discriminate between the enzymes from the two sources, is again unclear. Our finding that the predominant subtype in smooth muscle is, as in eosinophils, PDE IV_D indicates that subtype selectivity does not offer a satisfactory explanation for the disparity. Whether the alternative splicing of PDE IV_D (Sette *et al.*, 1994), which may influence subcellular localization (Shakur *et al.*, 1993), differentially affects the potency of inhibitors is an issue which has not been addressed. It should be noted, however, that in spite of the great potency difference between the two compounds against partially-purified PDE IV from smooth muscle, RP 73401 was only 2–3 fold more potent than rolipram in relaxing airways smooth muscle. This demonstrates that the functional effects of compounds are not mirrored in their inhibition of partially-purified smooth muscle PDE IV. A similar observation was made previously by Harris *et al.* (1989).

Tissue disruption, by releasing proteases which clip an amino acid sequence necessary for high-affinity binding, or chromatography procedures, by altering the conformational state of the enzyme (see Souness & Scott, 1993), may both influence the nature of the interaction of rolipram with partially-purified PDE IV and change its potency. If the native smooth muscle PDE IV is essentially similar to its counterpart in eosinophils, it is clear that, in contrast to rolipram, preparative procedures do not influence the potency of RP 73401, supporting the view that the two compounds exert their inhibitory effects through distinct interactions with the enzyme. Kinetic analysis of the data is not helpful in further elucidating this possibility. For both RP 73401 (Souness *et al.*, unpublished data) and rolipram (Torphy & Cieslinski, 1990), the kinetics of inhibition against partially, purified smooth muscle PDE IV are competitive whereas this is clearly not the case for either compound against the solubilized eosinophil PDE IV.

RP 73401 is 3 to 14 fold more potent than rolipram in increasing cyclic AMP accumulation and inhibiting eosinophil function ($.O_2^-$, MBP, ECP). These whole cell responses reflect better the relative potency differences of the two compounds against the solubilized or V/GSH-stimulated enzyme (10 fold) than the untreated, eosinophil particulate PDE IV (200 fold) or the smooth muscle PDE IV (3000 fold). It seems probable, therefore, that the native eosinophil (and smooth muscle) PDE IV exists in a form similar to the solubilized or V/GSH-treated enzyme.

In conclusion, RP 73401 is a potent and selective inhibitor of PDE IV and will be a useful investigative tool for elucidating the intracellular regulatory roles of PDE IV. RP 73401 increases cyclic AMP levels and potently inhibits eosinophil functions *in vitro*. Because of the importance of eosinophils in airway inflammation, our findings suggest that RP 73401 may be a promising new drug for the treatment of airway disease such as asthma. Based on the pharmacological data presented in this paper, it is likely that RP 73401 and rolipram exert their effects on cyclic AMP hydrolysis through distinct interactions with PDE IV.

The authors wish to acknowledge the technical assistance of Ms L.C. Scott, Ms L. Wood and Ms C. McCarthy.

References

ASHTON, M., COOK, D.C., FENTON, G., KARLSSON, J.-A., PALFREYMAN, M.N., RAEBURN, D., RATCLIFFE, A.J., SOUNESS, J.E., THURAIRATNAM, S. & VICKER, N. (1994). Selective type IV phosphodiesterase inhibitors as anti-asthmatic agents. The synthesis and biological activities of 3-cyclopentyloxy-4-methoxybenzamides and analogues. *J. Med. Chem.*, **37**, 1696–1703.

BARNES, P.J., CHUNG, K.F. & PAGE, C.P. (1988). Inflammatory mediators and asthma. *Pharmacol. Rev.*, **40**, 49–84.

BEAVO, J.A. & REIFSNYDER, D.H. (1990). Primary sequence of cyclic nucleotide phosphodiesterase isozymes and the design of selective inhibitors. *Trends Pharmacol. Sci.*, **11**, 150–155.

DAVIES, G.E. & EVANS, D.P. (1973). Studies with two new phosphodiesterase inhibitors (ICI 58,301 and ICI 63,197) on anaphylaxis in guinea-pigs, mice and rats. *Int. Arch. Allergy Appl. Immunol.*, **45**, 467–478.

DENT, G., GIEMBYCZ, M.A., RABE, K.F. & BARNES, P.J. (1991). Inhibition of eosinophil cyclic nucleotide PDE activity and opsonised zymosan-stimulated respiratory burst by 'type-IV'-selective PDE inhibitors. *Br. J. Pharmacol.*, **103**, 1339–1346.

EPSTEIN, P.M. & HACHISU, R. (1984). Cyclic nucleotide phosphodiesterase in normal and leukemic human lymphocytes and lymphoblasts. *Adv. Cyclic Nucleotide Protein Phosphorylation Res.*, **16**, 303–324.

FONTEH, A.N., WINKLER, J.D., TORPHY, T.J., HERAVI, J., UNDEM, B.J. & CHILTON, F.H. (1993). Influence of isoproterenol and phosphodiesterase inhibitors on platelet-activating factor biosynthesis in the human neutrophil. *J. Immunol.*, **151**, 339–350.

GIEMBYCZ, M.A. (1992). Could isoenzyme-selective phosphodiesterase inhibitors render bronchodilator therapy redundant in the treatment of bronchial asthma? *Biochem. Pharmacol.*, **43**, 2041–2051.

GIEMBYCZ, M.A. & BARNES, P.J. (1991). Selective inhibition of high-affinity Type IV cyclic AMP phosphodiesterase in bovine trachealis by AH-21-132: relevance to the spasmolytic and anti-spasmogenic actions of AH-21-132 in the intact tissue. *Biochem. Pharmacol.*, **42**, 663–677.

GLEICH, G.J., LOEGERING, D.A. & MALDONADO, J.E. (1973). Identification of a major basic protein in guinea-pig eosinophil granules. *J. Exp. Med.*, **137**, 1459–1471.

HARRIS, A.L., CONNELL, M.J., FERGUSON, E.W., WALLACE, A.M., GORDON, R.J., PAGANI, E.D. & SILVER, P.J. (1989). Role of low Km cyclic AMP phosphodiesterase inhibition in tracheal relaxation and bronchodilation in the guinea-pig. *J. Pharmacol. Exp. Ther.*, **251**, 199–206.

HUNT, T.C., SUMMERS, J.A., CAMPOS, M.G., RIMMER, S.J., STURTON, G., PALFAI, S. & CHURCH, M.K. (1993). Monoclonal antibodies specific for guinea-pig eosinophil major basic protein: their use in an ELISA, immunocytochemistry and flow cytometry. *Clin. Exp. Allergy*, **23**, 425–434.

KAY, A.B. (1985). Eosinophils as effector cells in immunity and hypersensitivity disorders. *Clin. Exp. Immunol.*, **62**, 1–12.

McLAUGHLIN, M.M., CIESLINSKI, L.B., BURMAN, M., TORPHY, T.J. & LIVI, G.P. (1993). A low-Km, rolipram-sensitive, cAMP-specific phosphodiesterase from human brain. Cloning and expression of cDNA, biochemical characterisation of recombinant protein, and tissue distribution of mRNA. *J. Biol. Chem.*, **268**, 6470–6476.

PEACHELL, P.T., UNDEM, B.J., SCHLEIMER, R.P., MACGLASHAN, D.W. Jr., LICHTENSTEIN, L.M., CIESLINSKI, L.B. & TORPHY, T.J. (1992). Preliminary identification and role of phosphodiesterase isozymes in human basophils. *J. Immunol.*, **148**, 2503–2510.

RAEBURN, D. & KARLSSON, J.-A. (1993). Effects of isoenzyme-selective inhibitors of cyclic nucleotide phosphodiesterase on microvascular leak in guinea pig airways *in vivo*. *J. Pharmacol. Exp. Ther.*, **267**, 1147–1152.

RAEBURN, D. & LEWIS, S. (1991). Rolipram inhibits PAF-induced bronchial hyperreactivity (BHR) in the guinea-pig in vivo: comparison with theophylline and salbutamol. *Eur. Resp. J.*, **4** (suppl. 14), 307S.

RAEBURN, D., SOUNESS, J.E., TOMKINSON, A. & KARLSSON, J.-A. (1993). Isozyme-selective cyclic nucleotide phosphodiesterase inhibitors: biochemistry, pharmacology and therapeutic potential in asthma. *Prog. Drug Res.*, **40**, 9–32.

RAEBURN, D., UNDERWOOD, S.L., LEWIS, S.A., WOODMAN, V.R., BATTRAM, C.H., TOMKINSON, A., SHARMA, S., JORDAN, R., SOUNESS, J.E., WEBBER, S.E. & KARLSSON, J.-A. (1994). Anti-inflammatory and bronchodilator properties of RP 73401, a novel and selective phosphodiesterase type IV inhibitor. *Br. J. Pharmacol.*, **113**, 1423–1431.

ROBICSEK, S.A., BLANCHARD, D.K., DJEU, J.Y., KRZANOWSKI, J.J., SZENTIVANYI, A. & POLSON, J.B. (1991). Multiple high-affinity cAMP-phosphodiesterases in human T-lymphocytes. *Biochem. Pharmacol.*, **42**, 869–877.

SCHADE, F.U. & SCHUDT, C. (1993). The specific type III and IV phosphodiesterase inhibitor zardavarine suppresses formation of tumor necrosis factor by macrophages. *Eur. J. Pharmacol.*, **230**, 9–14.

SCHNEIDER, H.H., SCHMIECHEN, R., BREZINSKI, M. & SEIDLER, J. (1986). Stereospecific binding of the antidepressant rolipram to brain protein structures. *Eur. J. Pharmacol.*, **127**, 105–115.

SEMMLER, J., WACHTEL, H. & ENDRES, S. (1993). The specific type IV phosphodiesterase inhibitor rolipram suppresses tumor necrosis factor-α production by human mononuclear cells. *Int. J. Immunopharmacol.*, **15**, 409–413.

SETTE, C., VICINI, E. & CONTI, M. (1994). The rat PDE3/IVd phosphodiesterase gene codes for multiple proteins differentially activated by cAMP-dependent protein kinase. *J. Biol. Chem.*, **269**, 18271–18274.

SHAKUR, Y., PRYDE, J.G. & HOUSLAY, M.D. (1993). Engineered deletion of the unique N-terminal domain of the cyclic AMP-specific phosphodiesterase RD1 prevents plasma membrane association and the attainment of enhanced thermostability without altering its sensitivity to inhibition by rolipram. *Biochem. J.*, **292**, 677–686.

SOUNESS, J.E., CARTER, C.M., DIOCEE, B.K., HASSALL, G.A., WOOD, L.J. & TURNER, N.C. (1991). Characterization of guinea-pig eosinophil phosphodiesterase activity. Assessment of its involvement in regulating superoxide generation. *Biochem. Pharmacol.*, **42**, 937–945.

SOUNESS, J.E., HASSALL, G.A. & PARROTT, D.P. (1992a). Inhibition of pig aortic smooth muscle cell DNA synthesis by selective type III and type IV cyclic AMP phosphodiesterase inhibitors. *Biochem. Pharmacol.*, **44**, 857–866.

SOUNESS, J.E., MASLEN, C. & SCOTT, L.C. (1992b). Effects of solubilization and vanadate/glutathione complex on inhibitor potencies against eosinophil cyclic AMP-specific phosphodiesterase. *FEBS Lett.*, **302**, 181–184.

SOUNESS, J.E. & SCOTT, L.C. (1993). Stereospecificity of rolipram actions on eosinophil cyclic AMP-specific phosphodiesterase. *Biochem. J.*, **291**, 389–395.

SOUNESS, J.E., THOMPSON, W.J. & STRADA, S.J. (1985). Adipocyte cyclic nucleotide phosphodiesterase activation by vanadate. *J. Cyclic Nucleotide Protein Phosphorylation Res.*, **10**, 383–396.

SOUNESS, J.E., VILLAMIL, M.E., SCOTT, L.C., TOMKINSON, A., GIEMBYCZ, M.A. & RAEBURN, D. (1994). Possible role of cyclic AMP phosphodiesterase in the actions of ibudilast on eosinophil thromboxane generation and airways smooth muscle tone. *Br. J. Pharmacol.*, **111**, 1081–1088.

SWINNEN, J.V., JOSEPH, D.R. & CONTI, M. (1989). Molecular cloning of rat homologues of the Drosophilia melanogaster dunce cAMP phosphodiesterase: evidence for a family of genes. *Proc. Natl. Acad. Sci. U.S.A.*, **86**, 5325–5329.

THOMPSON, W.J., TERASAKI, W., EPSTEIN, P.M. & STRADA, S.J. (1979). Assay of cyclic nucleotide phosphodiesterase and resolution of multiple molecular forms of the enzyme. *Adv. Cyclic Nucleotide Res.*, **10**, 69–92.

TORPHY, T.J. & CIESLINSKI, L.B. (1990). Characterization and selective inhibition of cyclic nucleotide phosphodiesterase isozymes in canine tracheal smooth muscle. *Mol. Pharmacol.*, **37**, 206–214.

TORPHY, T.J., LIVI, G.P., BALCAREK, J.M., WHITE, J.R., CHILTERN, F.H. & UNDEM, B.J. (1992a). Therapeutic potential of isozyme-selective phosphodiesterase inhibitors in the treatment of asthma. *Adv. Second Messenger Phosphoprotein Res.*, **25**, 289–305.

TORPHY, T.J., STADEL, J.M., BURMAN, M., CIESLINSKI, L.B., McLAUGHLIN, M.M., WHITE, J.R. & LIVI, G.P. (1992b). Co-expression of human cAMP-specific phosphodiesterase activity and high-affinity rolipram binding in yeast. *J. Biol. Chem.*, **267**, 1798–1804.

TORPHY, T.J. & UNDEM, B.J. (1991). Phosphodiesterase inhibitors: new opportunities for the treatment of asthma. *Thorax*, **46**, 512–523.

UNDERWOOD, D., OSBORN, R.R., NOVAK, L.B., MATTHEWS, J.K., NEWSHOLME, S.J., UNDEM, B.J., HAND, J.M. & TORPHY, T.J. (1993). Inhibition of antigen-induced bronchoconstriction and eosinophil infiltration in the guinea-pig by the cyclic AMP-specific phosphodiesterase inhibitor, rolipram. *J. Pharmacol. Exp. Ther.*, **266**, 306–313.

WASSOM, D.L. LOEGERING, D.A. & GLEICH, G.J. (1979). Measurement of guinea-pig eosinophil major basic protein by radioimmunoassay. *Mol. Immunol.*, **16**, 711–719.

WRIGHT, C.D., KUIPERS, P.J., KOBYLARZ-SINGER, D., DEVALL, L.J., KLINKEFUS, B.A. & WEISHAR, R.E. (1990). Differential inhibition of human neutrophil functions. Role of cyclic AMP-specific, cyclic GMP-insensitive phosphodiesterase. *Biochem. Pharmacol.*, **40**, 699–707.

(Received November 23, 1994
Revised December 23, 1994
Accepted January 20, 1995)

British Journal of Pharmacology (1995) 115, 47-56

A comparative study of functional 5-HT$_4$ receptors in human colon, rat oesophagus and rat ileum

Peter G. McLean, [1]Ian M. Coupar & *Peter Molenaar

School of Pharmaceutical Pharmacology, Victorian College of Pharmacy, Monash University, Parkville, Victoria 3052, Australia and *Department of Pharmacology, University of Melbourne, Parkville, Victoria 3052, Australia

1 The pharmacological properties of 5-hydroxytryptamine (5-HT), the 5-HT$_4$ receptor agonists, DAU 6236 and SC 53116 and the 5-HT$_4$ receptor antagonist, GR 113808, were studied in the rat oesophagus, rat ileum and human colon.

2 5-HT relaxed the longitudinal muscle of the rat oesophagus and rat ileum and the circular muscle of the human colon. Absolute values of relaxation were measured and showed the order of the maximum responses, rat oesophagus>>human colon>rat ileum with EC_{50} values of 189 ± 15 nM, 157 ± 4 nM, 306 ± 72 nM, respectively. 5-HT also inhibited the spontaneous contractions of the human colon with an EC_{50} value of 119 ± 1 nM. The effect of 5-HT on the human colon was not affected by methysergide (10 μM) or ondansetron (1 μM).

3 The use of the uptake and metabolism inhibitors, cocaine (30 μM) and pargyline (100 μM), did not increase the potency of 5-HT in the rat oesophagus or human colon. In the rat oesophagus, cocaine (30 μM) produced a reduction in carbachol-induced tone of 22.2 ± 0.6% and reduced the 5-HT maximum effect by 52.0 ± 0.4%.

4 The compounds, DAU 6236 and SC 53116, showed a different pattern of potencies and efficacies in the rat oesophagus, rat ileum and human colon compared to 5-HT. DAU 6236 relaxed the human colonic circular muscle with an EC_{50} value of 129 ± 16 nM but its efficacy was less than that of 5-HT. DAU 6236 (1 μM) also antagonized the 5-HT-induced relaxation of the human colon with a dose-ratio of 9.9. In the rat oesophagus and rat ileum, DAU 6236 was inactive in the majority of tissues. In the minority of oesophagus tissues that did respond the EC_{50} value was 1.2 ± 0.7 μM. DAU 6236 also antagonized the effect of 5-HT in the rat oesophagus in a non-surmountable fashion. SC 53116 relaxed the rat oesophagus with an EC_{50} value of 91 ± 4 nM, with an efficacy less than that observed to 5-HT; however, at 200 nM it did not antagonize the 5-HT-induced relaxation of the rat oesophagus. SC 53116 showed no agonist activity in the rat ileum and human colon, but at 1 μM it did antagonize the effect of 5-HT in the human colon with a dose-ratio of 11.3 ± 0.3.

5 GR 113808 competitively antagonized the 5-HT$_4$ receptor-mediated relaxation of the rat oesophagus with a pA_2 value of 8.59 (8.18-9.00) against 5-HT and 9.05 (8.79-9.31) against SC 53116. GR 113808 (0.01 μM) also antagonized the 5-HT-induced relaxation of human colonic circular muscle with an apparent pA_2 value of 9.02 ± 0.12. However at 1 μM the apparent pA_2 value was significantly lower than that measured at 0.01 and 0.1 μM. GR 113808 (0.01 μM) antagonized the 5-HT$_4$ receptor-mediated relaxation of the rat ileum with an apparent pA_2 value of 9.30 ± 0.21.

6 In conclusion, these studies have shown that the human colon, rat oesophagus and rat ileum contain functional 5-HT$_4$ receptors. However, the 5-HT$_4$ receptor agonists displayed differences in these tissues making it necessary to be cautious when extrapolating from animal to human tissue. This emphasizes the importance of the use of human tissue in the development of therapeutic drugs.

Keywords: 5-Hydroxytryptamine; 5-HT$_4$ receptors; DAU 6236; SC 53116; GR 113808; rat oesophagus; rat ileum; human colon

Introduction

The neurones of the enteric nervous system contain many neurotransmitters including 5-hydroxytryptamine (5-HT). Indeed, almost all of the 5-HT in the body is found in the alimentary tract (Thompson, 1971), where it is located in the interneurones that terminate in the myenteric and submucosal plexus (Branchek & Gershon, 1987), and to a greater extent in the enterochromaffin cells of the mucosa (Erspamer, 1954). Once released, 5-HT can act as a local hormone, or a neurotransmitter (Costall & Naylor, 1990) acting on a number of different 5-HT receptors.

In the alimentary tract stimulation of 5-HT$_4$ receptors leads to neuronally-mediated contraction of the guinea-pig ileum (Eglen *et al.*, 1990) and colon (Elswood *et al.*, 1991), enhancement of the 'twitch' response in transmurally stimulated guinea-pig ileum (Craig & Clarke, 1990), facilitation of the peristaltic reflex in the guinea-pig ileum (Craig & Clarke, 1991; Costall *et al.*, 1993), relaxation of the smooth muscle of the rat oesophagus (Baxter *et al.*, 1991; Reeves *et al.*, 1991) which occurs via adenylyl cyclase activation (Ford *et al.*, 1992), induction of chloride secretion by the mucosa of the rat distal colon (Bunce *et al.*, 1991) and an increase of the short circuit current response across the human small intestine mucosa (Borman & Burleigh, 1993).

5-HT has been shown to cause relaxation or contraction of the longitudinal muscle and to decrease the spontaneous activity of the circular muscle of the human colon (Fishlock & Parks, 1963; Fishlock, 1964; Misiewicz *et al.*, 1966; Wright & Sheppard, 1966). Recent studies have also shown that 5-HT mediates inhibition of the spontaneous contractions of human colonic circular smooth muscle via a 5-HT$_4$ receptor (Tam *et al.*, 1994; Hillier *et al.*, 1994). There is also some evidence that 5-HT mediates relaxation of the rat terminal ileum via a 5-HT$_4$ receptor (Tuladhar *et al.*, 1991).

The 5-HT$_4$ receptor is currently characterized on the basis of both agonist and antagonist activities. 5-HT$_4$ receptor agonists include 5-HT, and a series of indoleamine derivatives such as 5-methoxytryptamine (5-MeOT) and 5-

[1] Author for correspondence.

carboxamidotryptamine (5-CT); the substituted benzamide derivatives such as cisapride, renzapride and zacopride; the benzimidazolone derivatives, BIMU 1, BIMU 8 and DAU 6236 (Tonini *et al.*, 1991; Rizzi *et al.*, 1992) and the substituted pyrrolizidine, SC 53116 (Flynn *et al.*, 1992). 5-HT$_4$ receptor antagonists include GR 113808 (pA$_2$ value of 9.2 in the guinea-pig distal colon and 9.5 in the rat oesophagus, Grossman *et al.*, 1993a,b; Gale *et al.*, 1994), SDZ 205-557 (pA$_2$ = 7.4 in the guinea-pig ileum, Buchheit *et al.*, 1992), and DAU 6285 (pA$_2$ 6.9 and 7.0 in the rat tunica muscularis mucosae and guinea-pig ileum respectively, Waikar *et al.*, 1992). However, variations in agonist potency between CNS and peripheral tissues have led some authors to suggest the possibility of 5-HT$_4$ receptor subtypes (Kaumann *et al.*, 1991; Waikar *et al.*, 1994).

The present study aims to compare three previously defined preparations as assay tissues for drugs acting at the 5-HT$_4$ receptor, the longitudinal muscle of the rat oesophagus and rat ileum and the circular muscle of the human colon. In addition, the study aims to investigate the pharmacological properties of SC 53116 and DAU 6236, two novel compounds which are reportedly selective 5-HT$_4$ receptor agonists, and GR 113808 a reportedly selective 5-HT$_4$ receptor antagonist. These compounds are used to compare the effects of 5-HT$_4$ receptor activation and blockade in the rat models to the human colon.

Shortened versions of this paper have been published in the Medical Journal of Australia (McLean *et al.*, 1993a) and presented in part at the Australasian Society of Clinical and Experimental Pharmacologists and Toxicologists meeting, Brisbane, Australia, December 1993 (McLean *et al.*, 1993b) and at the XIIth International Congress of Pharmacology, Montreal, Canada (McLean *et al.*, 1994).

Methods

Rat oesophagus

The method of Reeves *et al.* (1991) was used as follows: Segments of distal oesophagus (2 cm) from female hooded Wistar rats (200–250 g) with muscle layers and mucosa intact were suspended in the longitudinal plane under a tension of 0.75 g at 37°C in Krebs-Henseleit solution containing indomethacin (3 μM) to prevent the relaxant effects of prostanoids (see Craig & Clarke, 1990) and ketanserin (1 μM) to prevent possible 5-HT$_2$ receptor-mediated contraction of the oesophagus (Akbarali *et al.*, 1987). Previous studies have estbalished that pargyline does not affect the response to 5-HT in the rat oesophagus (Reeves *et al.*, 1991; Baxter *et al.*, 1991), so it was not included in the bathing solution in the present series of experiments. Reeves *et al.* (1991) reported that cocaine does not increase the potency of 5-HT in the rat oesophagus, but it was shown by Baxter *et al.* (1991) to cause a leftward shift of the 5-HT-induced relaxant concentration-effect curve in this preparation. Consequently, the effect of cocaine (30 μM) was investigated. Since cocaine did not increase the potency of 5-HT it was not included in subsequent experiments.

Effects of agonists and antagonists The oesophageal preparations were contracted by addition of a submaximal concentration of carbachol (1 μM) to the bathing solution. On establishing a stable contractile response, usually within 20 min, cumulative concentrations of 5-HT were added every 3 min and the resultant relaxations recorded.

Following the construction of the control concentration-effect curve to 5-HT, the preparations were washed with fresh Krebs-Henseleit solution containing indomethacin and ketanserin and allowed to recover for at least 1 h, with further washes, before re-contracting with carbachol prior to the construction of the concentration-effect curve to the test agonist.

In antagonist studies, a control concentration-effect curve to 5-HT was constructed. Following washout, the tissue was contracted with carbachol (1 μM), a stable contraction obtained and the tissue equilibrated with antagonist (30 min) before another agonist concentration-effect curve.

Only two concentration-effect curves were constructed to 5-HT per tissue since the third curve is not reproducible (Reeves *et al.*, 1991; this study). The first curve was constructed to 5-HT followed by washout. A second curve was then obtained to either DAU 6236, SC 53116 or alternatively to 5-HT in the presence of GR 113808. Multiple concentration-effect curves to SC 53116 were not reproducible in any of the tissues studied, therefore only one concentration effect curve was constructed per tissue. Subsequently paired tissues were used, one serving as a control and the other to compare the response in the presence of the antagonist.

Rat ileum

The method of Tuladhar *et al.* (1991, 1993, personal communication) was used as follows: 5 cm of the terminal ileum was removed from female hooded Wistar rats (200–250 g) and transferred to warm oxygenated Krebs-Henseleit solution. The mesentery was cut away, without touching the ileum itself; the lumen was flushed carefully and the tissues mounted in an organ bath and bathed with Krebs-Henseleit solution containing methysergide (1 μM) and atropine (0.1 μM) and maintained at 37°C. The tissues were equilibrated for 1 h with washes every 15 min. No tension was applied initially but was gradually applied to a maximum tension of 0.75 g over a period of 15 min. As noted by Tuladhar (1993, personal communication), any deviation from these methods results in tissues which display a high degree of spontaneous activity making interpretation of the effects of the agonists and antagonists difficult. Tuladhar *et al.* (1992) have also shown that pargyline did not effect the response to 5-HT and hence it was not included in these experiments.

Effects of agonists and antagonist Once the ileal preparations were quiescent (i.e. displayed minimal spontaneous activity) and a reasonably stable baseline was achieved, 5-HT was added cumulatively with a 2 min contact time at each concentration. In agonist studies, paired tissues were used to compare the response to 5-HT with other agonists or in the presence of an antagonist. The antagonist was incubated for a period of 30 min before the addition of the agonist. A submaximal concentration of carbachol (1 μM) was used in experiments designed to investigate the effect of pre-contracting the rat ileum.

Human colon

Specimens of ascending, transverse or sigmoid colon were obtained from male and female patients undergoing surgical resection for colonic or rectal cancer. The specimens were placed in cold Krebs-Henseleit solution as soon as possible after surgical resection. The mucosa was cut away from the muscle layers which were cut along the circular axis to give 3 to 4 strips of 3–5 cm in length and 3–5 mm in width. These were mounted in Krebs-Henseleit solution, warmed at 37°C and equilibrated under a tension of 0.75 g for 45 min. The Krebs-Henseleit solution used in this study as in that of Tam *et al.* (1994) was free of 5-HT$_1$, 5-HT$_2$, and 5-HT$_3$ receptor antagonists, since methysergide (10 μM) and ondansetron (1 μM) did not affect the 5-HT-induced responses. Cocaine (30 μM) and pargyline (100 μM) also did not increase the potency of 5-HT, therefore they were not included in subsequent experiments.

Effects of agonists and antagonists Within 30 min most tissues showed regular spontaneous contractions with a relatively stable baseline. A cumulative concentration-effect

curve to the agonists was determined on each strip after 45 min using a 2 min exposure time. The effect of 5-HT on the muscle strips was two fold consisting of a reduction in the basal tone in the majority of tissues and often decrease in the amplitude of the contractions. The method of analysis employed in quantifying these effects primarily involved measuring the extent of the reduction of the resting basal tone following the addition of 5-HT. The reduction of the amplitude of the spontaneous contractions was also measured in the analyses. In experiments designed to investigate the effect of pre-contracting the human colon, a submaximal concentration of carbachol (1 μM) was used prior to the addition of 5-HT.

Four separate pieces of colon were used to study the effects of the antagonist, GR 113808. One was used to determine the control EC_{50} value to the agonist while the other 3 tissues were incubated with 3 separate concentrations of GR 113808 for 30 min before determination of the agonist concentration-effect curve. The relative effect of the agonists in the presence or absence of antagonists were compared using the absolute responses measured.

General methods

In all experiments, tissues were mounted in 30 ml jacketed organ baths containing Krebs-Henseleit solution of the following composition (mM): NaCl 118, KCl 4.7, $NaHCO_3$ 25, KH_2PO_4 1.2, $CaCl_2$ 2.5, $MgSO_4$ 1.2, D-(±)-glucose 11, oxygenated with 95% O_2 and 5% CO_2 and maintained at 37°C. Ugo Basile isotonic transducers connected to a Grass model 79D polygraph which amplified the responses 5–20 fold, were used to measure isotonic changes in length of the tissues.

Drugs

5-Hydroxytryptamine creatanine sulphate (Sigma, Australia), atropine sulphate (Sigma, Australia), carbachol (Sigma, Australia), ketanserin (Janssen-Cilag, Sydney, Australia), SC 53116 (1-S,8-S)-4-amino-5-chloro-*N*-[(hexahydro-1*H*-pyrrolizin-1-yl)methyl]-2-methoxy-benzamide, hydrochloride, Searle, Skokie, Illinois, U.S.A.), DAU 6236 (endo-8-methyl-8-azabicyclo [3.2.1] oct-3-yl 2,3-dihydro-3-ethyl-2-oxo-1*H*-benzimidazole-1-carboxylate hydrochloride, Dr Carlo Rizzi, Boehringer-Ingelheim, Milan, Italy) and GR 113808 ({1-[2-(methyl-sulphonylamino)ethyl]-4-piperidinyl}methyl 1-methyl-1*H*-indole-3-carboxylate, Glaxo, Melbourne, Australia) were dissolved in distilled water. Methysergide hydrogen maleate (Sandoz, Basle, Switzerland) was dissolved in ethanol 90% and diluted with (+)-tartaric acid 0.1% in distilled water. Indomethacin (Merk Sharp & Dohme, Sydney, Australia) was dissolved in 0.5% w/v sodium bicarbonate and diluted with distilled water.

Data analysis

The relaxations induced by 5-HT and 5-HT$_4$ receptor agonists were expressed in absolute terms, as mm cm^{-1} of tissue to enable direct comparison of the responses between the three tissues. The resting length of tissue was measured at the end of the equilibration period. Length changes in response to the test drugs were recorded with calibrated isotonic transducers which enabled an accurate measure of the length change of the tissues. The responses were also recorded and expressed in terms of their potency as EC_{50} values relative to individual maxima. EC_{50} values were calculated by linear regression analysis for each preparation from the 50% response level and expressed as arithmetic means ± s.e.mean. The potency of the antagonist was expressed as the pA_2 value with 95% confidence limits (Arunlakshana & Schild, 1959) which was computed using the 3 point method of Tallarida & Murray (1987), or as an apparent pA_2 value which was calculated using single point analysis from

$$pA_2 = \log (DR\text{-}1) - \log [B]$$

where DR is the dose-ratio of agonist used in the presence and absence of antagonist (B) and is expressed as pA_2 ± s.e.mean. The assumption of simple competition (i.e. slope of unity) between antagonist and agonist for 5-HT$_4$ receptors was checked with a Schild plot (Arunlakshana & Schild, 1959). The dose-ratios required for the above analysis were determined from EC_{50} values in the presence and absence of antagonist. The number of observations is indicated by *n*.

The significance of differences between the values was determined by use of Student's unpaired two tail *t* test. The criterion for statistical significance was set at $P<0.05$.

Results

Comparison of the responses to 5-HT in each tissue

In the rat oesophagus, a submaximal concentration of carbachol (1 μM) produced a well-maintained contraction (of between 4–6 mm cm^{-1} of oesophagus) for at least 60 min. 5-HT produced concentration-dependent relaxations of the precontracted oesophagus preparations (Figure 1) with a mean EC_{50} value of 189 ± 15 nM and a mean maximum reduction of carbachol-induced tone of 61.6 ± 5.5% ($n = 19$). The mean maximum relaxation (E_{max}) caused by the maximum concentration of 5-HT (< 100 μM) was 2.49 ± 0.43 mm cm^{-1} of tissue ($n = 19$). These results are summarised in Table 1.

The responses to 5-HT were reproducible in the rat oesophagus and two similar consecutive concentration-effect curves could be obtained in each preparation. In experiments designed to test this, the EC_{50} values were 227.3 ± 1.3 and 225.7 ± 1.4 nM ($n = 4$) for the first and second curves respectively. The E_{max} of the second curve was 98.5 ± 0.7% of the

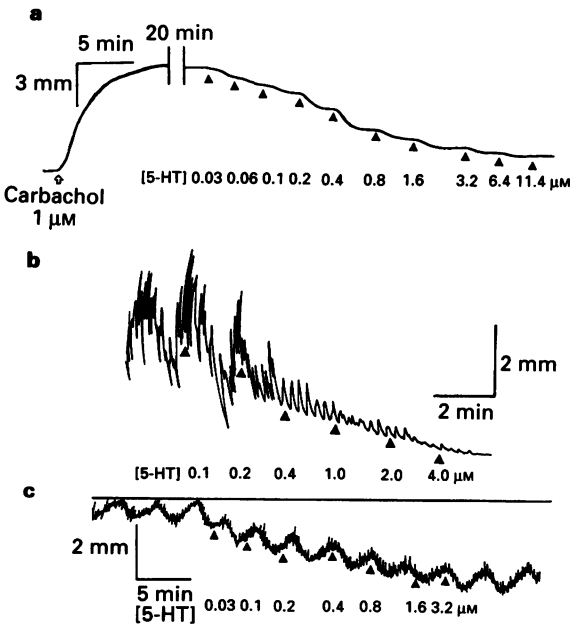

Figure 1 Relaxant effect of 5-hydroxytryptamine (5-HT) on the (a) longitudinal muscle of the rat isolated oesophagus contracted with carbachol (1 μM) in the presence of indomethacin (3 μM) and ketanserin (1 μM); (b) circular muscle of the human colon (spontaneous contractions returned after washing) and (c) longitudinal muscle of the rat isolated ileum in the presence of methysergide (1 μM) and atropine (0.1 μM).

Table 1 Summary of comparative agonist potency and maximum effect values in the rat oesophagus and human colon[a]

Tissue	*Agonist*	EC_{50} (nM)	E_{max} (mm cm^{-1})	n^b
Rat oesophagus	5-HT	189 ± 15	2.49 ± 0.43	19/19
	SC 53116	91 ± 4	1.27 ± 0.17	15/15
	DAU 6236	1200 ± 700	1.21 ± 0.11	4/14
Human colon	5-HT	157 ± 4	0.81 ± 0.02	19/19
	SC 53116	–	–	0/3
	DAU 6236	130 ± 2	0.23 ± 0.09	5/5

[a]See text for a summary of data obtained with the rat ileum
[b]Indicates the proportion of tissues responding over the total number of tissues.

first curve. The control curves were reproducible provided that at least 1 h with washes was allowed between curves. Concentrations of 5-HT up to 10 μM had no measurable effect on the oesophagus preparation not pre-contracted with carbachol. Cocaine (30 μM) incubated in the organ bath for 30 min did not increase the potency of 5-HT but produced a reduction in carbachol-induced tone of 22.2 ± 0.6% and reduced the 5-HT (> 10 μM) maximum effect by 52.0 ± 0.4% ($n = 6$).

In the human colon, 5-HT usually induced three effects; direct relaxation of the tissue, inhibition of the amplitude of the spontaneous contractions, and a decrease in the frequency of the spontaneous contractions (Figure 1). Only relaxation and decrease in amplitude were used in quantifying drug effects. The relaxant effect of 5-HT was concentration-dependent with an EC_{50} value of 157 ± 4 nM and E_{max} of 0.81 ± 0.02 mm cm^{-1} of tissue ($n = 19$, Table 1). 5-HT also caused a marked and concentration-dependent inhibition of the amplitude of the spontaneous contractions with an EC_{50} value of 119 ± 1 nM ($n = 6$). The potency values obtained for these two different effects of 5-HT were not significantly different ($P > 0.05$). The amplitude of the spontaneous contractions before the addition of 5-HT was 0.25 ± 0.10 mm cm^{-1} of tissue and this was inhibited to 0.08 ± 0.01 mm cm^{-1} of tissue ($n = 6$) by the maximum concentration of 5-HT (2 μM). However, concentration-dependent effects of 5-HT on the amplitude of the spontaneous contractions were variable as they were either inhibited in a concentration-dependent fashion ($n = 4$) or in an all-or-none fashion ($n = 2$). In most cases spontaneous contractions were inhibited completely by high concentrations of 5-HT (approx. 4 μM) but spontaneous contractions often returned at even higher concentrations. Consequently direct relaxation was the parameter most often used to quantify the response to 5-HT. The relaxant effect of 5-HT was not antagonized by the combination of methysergide (10 μM) and ondansetron (1 μM) (dose-ratio = 0.87 ± 0.30, $P > 0.05$, $n = 3$). Likewise, cocaine (30 μM) and pargyline (100 μM) did not affect the sensitivities of the tissues to 5-HT (dose-ratio = 1.33 ± 0.23, $P > 0.05$, $n = 3$). Concentrations of 5-HT up to 10 μM had no measurable effect on the colon preparation pre-contracted with carbachol (1 μM).

The responses of the rat ileum were inconsistent to 5-HT which relaxed only 10 of 18 tissues tested. It was also difficult to distinguish clear concentration-related relaxations in some tissues tested due to a high degree of spontaneous activity (Figure 1). The maximum absolute relaxant effect of 5-HT (6.4 μM) was relatively small (E_{max} = 0.37 ± 0.06 mm cm^{-1}, $n = 10$). However, the tissues in which the response was quantified an EC_{50} value of 306 ± 72 nM ($n = 10$) was calculated. The effects of 5-HT above 6.4 μM (< 100 μM) were variable. In most tissues no further relaxation occurred ($n = 6$); however, further relaxation occurred in a biphasic fashion in 3 tissues and the relaxation was reduced by higher concentrations of 5-HT in one tissue (as reported by Tuladhar *et al.*, 1991). The within tissue responses to 5-HT were not reproducible in that two similar consecutive concentration-effect curves could not be obtained. Concentrations of 5-HT up to 10 μM had no measurable effect on the ileum preparation pre-contracted with carbachol (1 μM).

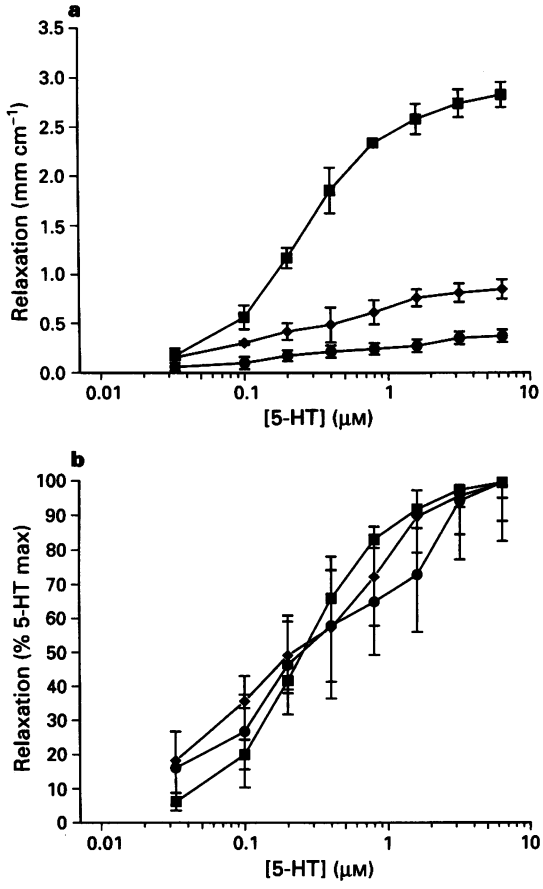

Figure 2 Concentration-effect curves to 5-hydroxytryptamine (5-HT) in the rat oesophagus (■), human colon (◆), and rat ileum (●). Data are means ± s.e.mean ($n = 5$). Relaxant effects are expressed as (a) mm relaxation per cm of tissue and (b) as the percentage of the maximum response elicited by 5-HT.

The responses to 5-HT measured in each tissue under the above conditions are compared (Figure 2) both in absolute terms to enable direct comparison of the responses between the three tissues and as a percentage of the individual maxima from which EC_{50} values were derived (see Table 1). The order of E_{max} values in the three tissues was rat oesophagus (pre-contracted, E_{max} = 2.49 ± 0.43 mm cm^{-1}) >> human colon (not pre-contracted, E_{max} = 0.81 ± 0.02 mm cm^{-1}) > rat ileum (not pre-contracted, E_{max} = 0.37 ± 0.06 mm cm^{-1}). Although the efficacies of 5-HT as measured by the E_{max} values were significantly different ($P < 0.05$) in each of the three tissues, the potency of 5-HT in the rat oesophagus (EC_{50} = 189 ± 15 nM), human colon (EC_{50} = 157 ± 4 nM), and rat ileum (EC_{50} = 306 ± 72 nM) were not significantly different ($P > 0.05$, Figure 2).

Effects of 5-HT$_4$ receptor agonists

SC 53116, a substituted pyrrolizidine which is selective for the 5-HT$_4$ receptor in the tunica muscularis mucosae of the rat oesophagus (Flynn *et al.*, 1992) caused concentration-dependent relaxations of the rat oesophagus with a mean EC_{50} value of 91 ± 4 nM ($n = 15$). This potency value was around 2 fold higher than 5-HT. SC 53116 caused a maximum reduction of carbachol-induced tone of 48.0 ± 6.1% and a maximum relaxation of 1.27 ± 0.17 mm cm^{-1} of tissue

in the rat oesophagus ($n = 15$, Table 1). This value was 51 ± 1% of the response relative to 5-HT indicating that SC 53116 might be a partial agonist. However, at a concentration of 200 nM (20 min incubation time) SC 53116 did not act as an antagonist of 5-HT ($n = 3$). In contrast to 5-HT the responses to SC 53116 were not reproducible in that a second concentration-effect curve produced a smaller response in each preparation. The comparative agonist effects of 5-HT and SC 53116 in the rat oesophagus are shown in Figure 3 and summarised in Table 1. SC 53116 (< 10 μM), in contrast to 5-HT, possessed no intrinsic activity in the human colon causing neither relaxation, nor inhibition of spontaneous contractions ($n = 3$). SC 53116 did, however, act as an antagonist in the human colon. At 1 μM, it caused a rightward shift in the concentration-effect curve to 5-HT with a dose-ratio of 11.3 ± 0.3 ($n = 4$). Like 5-HT, the responses caused by SC 53116 were inconsistent in rat ileum. SC 53116 (< 10 μM) relaxed only 1 of 5 tissues studied in a non-concentration-dependent fashion.

DAU 6236, a selective 5-HT$_4$ receptor agonist in the guinea-pig ileum (Rizzi *et al.*, 1992), was inconsistent in its activity in the rat oesophagus. Whereas 5-HT relaxed all strips tested, DAU 6236 (< 10 μM) relaxed only 4 of 14 preparations. Of these, DAU 6236 ($E_{max} = 1.2 \pm 0.1$ mm cm^{-1}) had a lower intrinsic activity relative to 5-HT ($E_{max} = 2.5 \pm 0.4$ mm cm^{-1}). DAU 6236 ($EC_{50} = 1.2 \pm 0.7$ μM) was also less potent than 5-HT ($EC_{50} = 189 \pm 15$ nM, Table 1). DAU 6236 did not only produce a response in well coupled tissues as there was no relationhip between the potency of the individual tissues to 5-HT and the ability of DAU 6236 to evoke a response. DAU 6236 at a similar concentration to its EC_{50} in the rat oesophagus (1 μM) was shown to inhibit 5-HT-induced relaxations of the rat oesophagus where it produced a rightward shift of the 5-HT concentration-effect curve with a dose-ratio of around 7. This antagonism was not completely surmountable in that the E_{max} in the absence of DAU 6236 (76.7 ± 0.5% reduction of carbachol-induced tone) was significantly reduced in its presence (61.7 ± 0.7% reduction of carbachol-induced tone, $P < 0.05$, $n = 4$). DAU 6236 did not significantly reduce the response to carbachol. The dose-ratios for carbachol in the presence of DAU 6236 at 2 and 10 μM were 1.2 ± 0.8 and 2.0 ± 1.1 respectively ($P > 0.05$, $n = 4$).

The responses caused by DAU 6236 in the rat ileum were also inconsistent. DAU 6236 (< 10 μM) caused relaxation in only 1 of 5 preparations, and in this DAU 6236 possessed a similar intrinsic activity to 5-HT but a clear concentration-related effect was not observed in this tissue.

In contrast to the above tissues, DAU 6236 inhibited both the amplitude of spontaneous contractions as well as causing direct relaxation of all strips of human colonic circular muscle. The relaxant effect of DAU 6236 was concentration-dependent with a mean EC_{50} value of 130 ± 2 nM ($n = 5$). This inhibition usually occurred with concentrations below 1 μM. However, at higher concentrations (1–10 μM) spontaneous contractions returned or were increased. The potency of DAU 6236 in producing relaxation was similar to 5-HT itself (Figure 4). However, DAU 6236 ($E_{max} = 0.23 \pm 0.09$) was not a full agonist having an intrinsic activity less than that of 5-HT ($E_{max} = 0.81 \pm 0.02$, Figure 4, Table 1) indicating that, as with its action in the rat oesophagus, it might be a partial agonist. In this respect, DAU 6236 (1 μM) was shown to be a surmountable antagonist in the human colon, shifting the 5-HT-induced concentration-effect curve to the right with a dose-ratio of 9.86 ± 0.55 ($n = 4$).

Effects of the 5-HT$_4$ receptor antagonist, GR 113808

GR 113808 (0.01, 0.1, 1 μM) caused parallel, dextral shifts of the concentration-effect curves to 5-HT in the rat oesophagus ($n = 9$, Figure 5a). The maximum response to 5-HT (> 3 μM) was not significantly affected ($P > 0.05$) by GR 113808. The slope of the Schild regression was 0.98 (95% CL, 0.55–1.41) which was not significantly different from 1 and yielded a pA_2 estimate of 8.59 (95% CL, 8.18–9.00, Table 2). GR 113808 (0.01, 0.1, 0.5 μM) also caused parallel, dextral shifts of the concentration-effect curves to the 5-HT$_4$ receptor agonists, SC 53116 ($n = 9$, Figure 5b). The maximum response to SC 53116 (> 2 μM) was not significantly altered ($P > 0.05$) in the presence of GR 113808 and the slope of the Schild regression was 0.72 (95% CL, 0.39–1.04) which was not significantly different from 1 (Table 2). Affinity estimates for GR 113808 against SC 53116 gave a pA_2 value of 9.05 (95% CL, 8.79–9.31) with the slope constrained to 1 (Table 2). The pA_2 values obtained for GR 113808 against SC 53116 and 5-HT were not significantly different ($P > 0.05$).

GR 113808 caused rightward shifts of the concentration-effect curves to the relaxant effect of 5-HT in the human colon ($n = 11$, Figure 6). At 0.01 μM GR 113808 antagonized the 5-HT-induced relaxations with an apparent pA_2 value of 9.02 ± 0.12 ($n = 5$). Higher concentrations of GR 113808 (0.1, 1 μM) shifted the concentration-effect curve to 5-HT to the right but the magnitude of the shift was not as great as that predicted for simple competitive antagonism (Table 3, Figure 6). The slope of the 3 point Schild regression was 0.58 (95% CL, 0.34–0.83) which is significantly different from 1 (Table 2). GR 113808 (0.01 μM) also antagonized the inhibition of spontaneous activity caused by 5-HT with an apparent pA_2 of 9.26 ± 0.14 which is not significantly different ($P > 0.05$) from the value obtained against the 5-HT-induced relaxation of the circular muscle. This antagonism of 5-HT-induced inhibition of spontaneous activity was also not com-

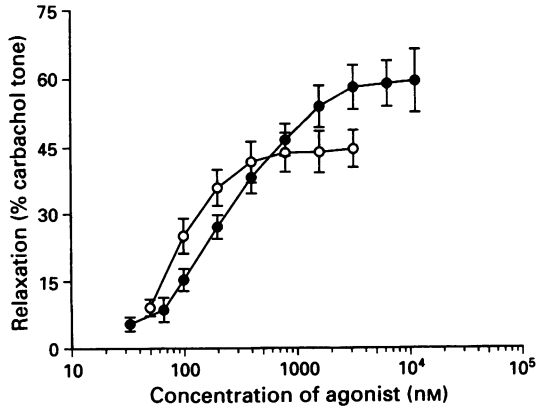

Figure 3 The effect of (●) 5-hydroxytryptamine ($n = 19$) and (○) the 5-HT$_4$ receptor agonist SC 53116 ($n = 15$) in the rat oesophagus. Each point is the mean ± s.e.mean calculated as a percentage of the carbachol-induced tone.

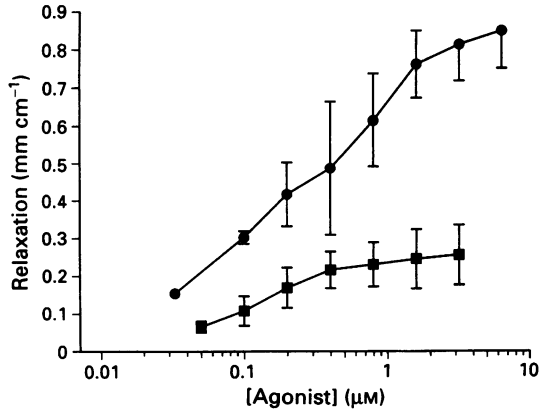

Figure 4 The effects of (●) 5-hydroxytryptamine ($n = 19$) and (■) the 5-HT$_4$ receptor agonist DAU 6236 ($n = 5$) in the human colonic circular muscle. Each point is the mean ± s.e.mean expressed as the absolute relaxant effect in mm cm^{-1}.

petitive as higher concentrations of GR 113808 did not cause the predicted increases in dose-ratios.

GR 113808 (0.01, 0.1, 1 μM) caused rightward shifts of the concentration-effect curves to 5-HT in the rat ileum ($n = 7$). At 0.01 μM GR 113808 antagonized the 5-HT induced relaxations with an apparent pA_2 value of 9.30 ± 0.21 ($n = 3$, Table 2). Higher concentrations of GR 113808 (0.1, 1 μM) shifted the concentration-effect curve to 5-HT to the right but this antagonism was not of a simple competitive nature. The maximum response to 5-HT was increased in the presence of GR 113808 in 4 of 7 tissues. The slope of the Schild regression was significantly different from unity and hence a meaningful estimate of a pA_2 value could not be made (Table 2).

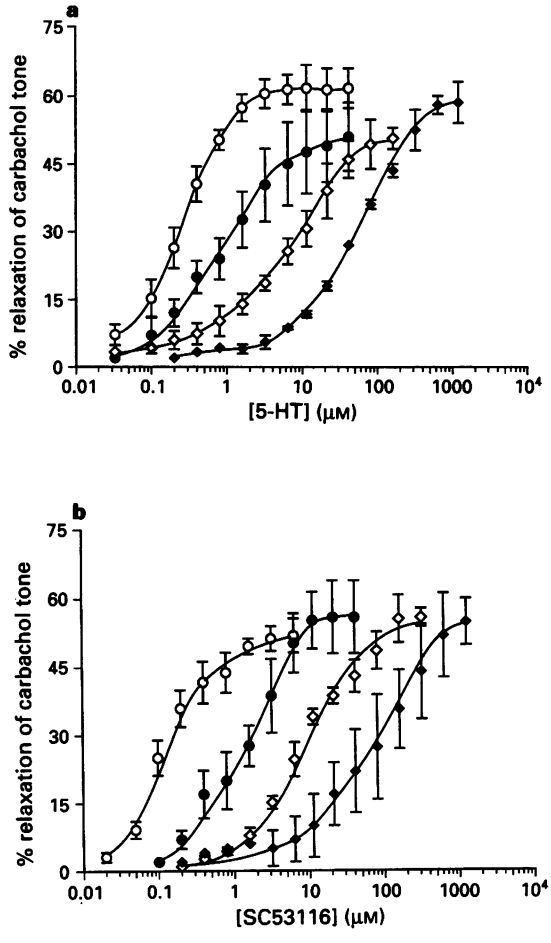

Figure 5 Antagonism of the concentration-effect curve to (a) 5-hydroxytryptamine (5-HT) and (b) SC 53116 by GR 113808 in the rat oesophagus pre-contracted with carbachol. Data obtained in the absence (○), or presence of GR 113808 0.01 μM (●), 0.1 μM (◇), and (a) 1 μM, (b) 0.5 μM (◆). The slope of Schild regression was (a) 0.98 (95% CL, 0.55–1.41) and (b) 0.7 (95% CL, 0.3–1.1). The pA_2 estimates were (a) 8.59 ($n = 8$) and (b) 9.1 ($n = 9$).

Discussion

This study extends the pharmacological profiles of the 5-HT_4 receptor agonists, DAU 6236 and SC 53116 and the antagonist GR 113808. This was achieved by comparing their activities in the longitudinal muscle of the rat isolated oesophagus and ileum and the circular muscle of the human colon. These tissues have been shown to contain functional 5-HT_4 receptors in earlier studies in which some 5-HT_4 receptor agonists and antagonists were screened (Reeves *et al.*, 1991; Tuladhar *et al.*, 1991; Tam *et al.*, 1994). However, the present study is the only one to date that compares the three tissues, giving an indication of their relative usefulness as assays for drugs acting at the 5-HT_4 receptor. To date there is no published data on the effects of SC 53116 and DAU 6236 on the human colon or the effects of SC 53116, DAU 6236 and GR 113808 on the rat ileum, nor is there data available on the effects of DAU 6236 and the effects of GR 113808 against SC 53116 on the rat oesophagus. An independent study (Hillier *et al.*, 1994) has shown that GR 113808 is active as an antagonist at the 5-HT_4 receptor in the human

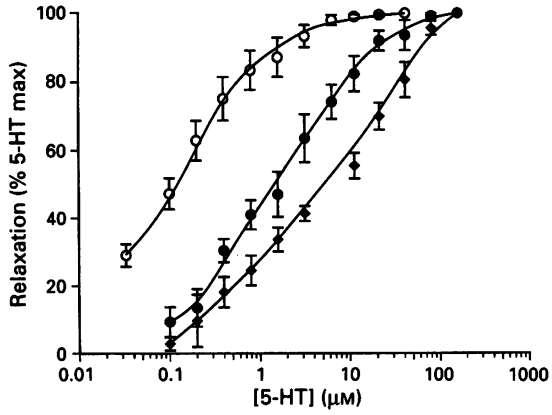

Figure 6 Antagonism of the concentration-effect curve to 5-hydroxytryptamine (5-HT) by GR 113808 in human colonic circular muscle. Data obtained in the absence (○), or presence of GR 113808 0.01 μM (●), 0.1 μM (◆); 1 μM not shown for clarity. The slope of Schild regression was 0.58 (95% CL, 0.34–0.83). The apparent pA_2 estimate at 0.01 μM was 9.0 ($n = 5$).

Table 3 Apparent pA_2 values of GR 113808 in the human colon

[GR 113808]	*Dose-ratio*	*pA_2*	n
0.01 μM	14 ± 0.6	9.02 ± 0.12	5
0.1 μM	56 ± 0.8	8.72 ± 0.07	6
1 μM	145 ± 3.7	8.06 ± 0.20[a]	3

[a]Indicates a significant difference from the apparent pA_2 values at 0.01 and 0.1 μM ($P < 0.05$, Student's t test).

Table 2 pA_2 estimates for GR 113808 in the rat oesophagus, rat ileum and human colon

Agonist	*Tissue*	*pA_2*	*Schild slope*	n
5HT	Human colon	9.02 ± 0.12[a]	0.51 (0.34–0.83)[b]	5
	Rat oesophagus	8.59 (8.18–9.00)	0.98 (0.55–1.41)	9
	Rat ileum	9.30 ± 0.21[a]	0.59[c]	4
SC 53116	Rat oesophagus	9.05 (8.79–9.31)	0.72 (0.39–1.04)	9

[a]Single point analysis at 0.01 μM GR 113808.
[b]The slope of the three point Schild plot was different from one.
[c]The slope of the two point Schild plot was different from one.

colon. The present study aims to extend the pharmacological profile of GR 113808 in the human colon.

Tissue comparison

The three *in vitro* methods used in this study differed in the composition of the Krebs-Henseleit solution. The antagonists which were used routinely in the bathing solution in experiments on the rat oesophagus and rat ileum were present to confine the responses to those of the 5-HT$_4$ receptor. This study used the same concentrations of the same antagonists as used in the previous studies (Reeves *et al.*, 1991; Tuladhar *et al.*, 1991) to ensure that the results were directly comparable. Antagonists were not used routinely in experiments on the human colon because we established that the inhibitory effect of 5-HT on the spontaneous contractions of human colonic circular muscle as previously reported (Fishlock & Parks, 1963; Fishlock, 1964; Misiewicz *et al.*, 1966; Wright & Sheppard, 1966) were not altered by methysergide and ondansetron. This has also been confirmed independently in other studies (Tam *et al.*, 1994; Borman & Burleigh, 1994). Another difference in the composition of the Krebs-Henseleit solution was the inclusion of carbachol to precontract the rat oesophagus preparations (see Reeves *et al.*, 1991). The rat ileum and human colon preparations were not pre-contracted since it has been established that these tissues have sufficient intrinsic tone to reveal 5-HT$_4$ receptor-mediated responses (Tuladhar *et al.*, 1991; Tam *et al.*, 1994).

In an attempt to improve these established methods, however, the rat ileum and human colon were pre-contracted with carbachol. Pre-contracting these tissues did not significantly improve the responses and conversely, no response was observed to 5-HT in the rat oesophagus preparation if the tissue was not pre-contracted.

To date there is no published data with regard to absolute values for 5-HT$_4$ receptor-mediated relaxation in these tissues. This study provides a detailed analysis of the responses to 5-HT and 5-HT$_4$ receptor agonists in absolute terms which allows direct comparison of the responses displayed by each tissue and provides a convenient method for comparing the suitability of the *in vitro* methods as assay tissues for drugs acting at 5-HT$_4$ receptors. The order of magnitude of the 5-HT-induced relaxations in each preparation was shown to be: rat oesophagus$>>$human colon$>$rat ileum. Therefore, drug effects were relatively easy to quantify in the rat oesophagus and human colon but not in the rat ileum.

The study also compared the methods as judged by their ability to respond reproducibly. The rat oesophagus and human colon responded to 5-HT with relatively large and consistent responses and small variations between tissues. However, the rat ileum was not a reliable preparation in that not all tissues tested were relaxed by 5-HT. This is in contrast to the study by Tuladhar *et al.* (1991; 1993, personal communication) who claim that all tissues they tested were relaxed by 5-HT. The inconsistencies between the two studies can be explained by the high degree of fast and slow wave intrinsic spontaneous activity seen in this study. This highly variable basal tone masks the small effect of 5-HT$_4$ receptor activation making it hard or impossible to distinguish clear concentration-related responses. This problem is compounded with the drugs which are not full agonists in other preparations, such as SC 53116 and DAU 6236. In light of these findings we question the usefulness of this model as a reliable quantitative tool for drugs which act at the 5-HT$_4$ receptor.

Interestingly, the use of the uptake and metabolism inhibitors cocaine and pargyline did not increase the potency of 5-HT in the rat oesophagus or human colon. The results in the rat oesophagus, where cocaine was shown to reduce the efficacy of both carbachol and 5-HT, parallel the results obtained by Reeves *et al.* (1991). However, they are not in accordance with those of Baxter *et al.* (1991) who reported that cocaine increased the potency of 5-HT. A possible explanation for this discrepancy is in the composition of the Krebs-Henseleit bathing solution. The present study, as in Reeves *et al.* (1991), used indomethacin and ketanserin routinely in the bathing solution whereas Baxter *et al.* (1991) used only methysergide when testing the effect of cocaine. Cocaine and pargyline also did not increase the potency of 5-HT in the human colon. This result is confirmed by the study of Tam *et al.* (1994).

5-HT$_4$ receptor agonists

Ideally animal models which are used for receptor characterization should show similarities to human tissue. However, this study showed marked differences in responses to the agonists SC 53116 and DAU 6236.

It has been suggested recently that the substituted pyrrolizidine, SC 53116, acts as an agonist at the 5-HT$_4$ receptor in the rat oesophagus tunica muscularis mucosae, causing relaxation (Flynn *et al.*, 1992). In the present study, SC 53116 was shown to relax the rat isolated whole oesophagus preparation via stimulation of 5-HT$_4$ receptors, since the pA$_2$ of GR 113808 against SC 53116 (pA$_2$ = 9.1) was characteristic of antagonism at 5-HT$_4$ receptors (pA$_2$ value of 9.2 in the guinea-pig distal colon and 9.5 in the rat oesophagus, Grossman *et al.*, 1993a). However, the intrinsic activity of SC 53116 was significantly less than that observed to 5-HT indicating that it may act as a partial agonist. Further experiments discounted such an action of SC 53116 which displayed no antagonism of 5-HT in the rat oesophagus. SC 53116 displayed tissue selectivity in that it was a relatively potent agonist in the rat oesophagus but it displayed virtually no measurable intrinsic activity in the human colon and rat ileum. Although SC 53116 was not an agonist in the human colon it did act as a weak antagonist of the 5-HT-mediated relaxation. The lack of agonist activity of SC 53116 in the human colon is possibly due to a different efficiency of the receptor coupling mechanism in that it has the properties of a silent antagonist without agonist activity. Similarly, in the rat ileum SC 53116 was variable in its action. This can be explained, as mentioned earlier, by the inherently small and variable response observed with this tissue, which would mask the effect of a weak agonist such as SC 53116.

Recently it has been suggested that DAU 6236, which is a member of a new class of compounds having a benzimidazolone structure, may act as an agonist at central 5-HT$_4$ receptors. This class of compound was found to stimulate adenylyl cyclase activity in mouse embryo colliculi (Dumuis *et al.*, 1991) and guinea-pig hippocampal neurones (Monferini *et al.*, 1991). DAU 6236 has also been reported to act as a 5-HT$_4$ receptor agonist facilitating cholinergic transmission and peristalsis in the guinea-pig ileum (Rizzi *et al.*, 1992). The present study extends the available pharmacological data on DAU 6236 to agonist activity at 5-HT$_4$ receptors in the human colon. This was shown by the findings that DAU 6236 inhibits spontaneous contractions and relaxes human colonic circular muscle with a similar potency to 5-HT. However, the efficacy of DAU 6236 was significantly less than that observed to 5-HT indicating that it may act as a partial agonist. Further experiments confirmed such an action of DAU 6236 in which it antagonized 5-HT-induced relaxation in the human colon.

This study revealed unexpected observations in tissue selectivity to DAU 6236. DAU 6236 was a reasonably potent agonist in the human colon but in marked contrast both the efficacy and potency of DAU 6236 were both highly variable and small compared to 5-HT in the rat oesophagus. This was a surprising result since the rat oesophagus has been used widely to assay compounds with potential activity at the 5-HT$_4$ receptor. A possible explanation for the variable response to DAU 6236 in the rat oesophagus (only 4 of 14 tissues responded) is that it may have only been active in tissues which were well coupled. However, this does not seem to be the case since the potency of 5-HT was no greater in

the tissues in which DAU 6236 was active. The relaxant action of DAU 6236 in the small number of oesophagus preparations may also be due to an anticholinoceptor effect. This possibility was discounted since DAU 6236 (2 μM and 10 μM) did not antagonize the effect of carbachol. DAU 6236 was, however, a weak antagonist of 5-HT in the rat oesophagus indicating that its action in this tissue is that of a partial agonist with only weak agonist activity. DAU 6236 also displayed a lower potency and efficacy compared to 5-HT in the rat ileum which is explained by the inherently small and variable responses observed with this tissue. A previous study has established that DAU 6236 is also less potent than 5-HT in the guinea-pig ileum (Rizzi *et al.*, 1992). The relatively high agonist potency of DAU 6236 in the human colon (7–9 times higher than in the rat oesophagus and rat ileum) and its similar potency relative to 5-HT in the human colon is an important aspect of the currently described pharmacological profile.

The overall results of the present study show that SC 53116 and DAU 6236 have varying activities according to the tissue in which they are tested. This may indicate the existence of heterogeneity among 5-HT$_4$ receptors as has been suggested elsewhere (Kaumann *et al.*, 1990; Rizzi, 1993, personal communication; Waikar *et al.*, 1994). These differences in agonist activities may be used to explore further the possibilities that different 5-HT$_4$ receptors exist which can be differentiated by the order of agonist potency. However, these results may also be explained by other factors such as differences in the efficiency of the receptor coupling mechanisms between the tissues or differences in the molecular structure of the 5-HT$_4$ receptor. Further studies are required to examine these possibilities.

The 5-HT$_4$ receptor antagonist, GR 113808

GR 113808 was recently established as a novel 5-HT$_4$ receptor antagonist with a pA_2 of 9.2 and 9.3 in guinea-pig colon and rat oesophagus respectively (Gale *et al.*, 1994; Grossman *et al.*, 1993a). Its pA_2 values were 6.0 or less at other 5-HT receptors indicating about 1000 fold selectivity for the 5-HT$_4$ receptor. It has also been suggested that it antagonizes human and porcine atrial 5-HT$_4$ receptors (Kaumann, 1993; Medhurst & Kaumann, 1993; Gale *et al.*, 1994). The present study confirms that GR 113808 is a competitive antagonist of 5-HT in the rat oesophagus with the same pA_2 value as has been reported previously in the tunica muscularis mucosae of the rat oesophagus. Further, it was shown that GR 113808 behaved as a competitive antagonist against a 5-HT$_4$ receptor agonist of a different chemical class, namely SC 53116. The pA_2 value was not significantly different from that obtained against 5-HT. This indicates that GR 113808 acts as an agonist-independent antagonist and provides evidence that both 5-HT and SC 53116 act at the same receptor in the rat oesophagus.

Other workers have found that GR 113808 does not always behave as a competitive antagonist. For example Medhurst & Kaumann (1993) have shown that GR 113808 does not display competitive antagonism of 5-HT in the piglet isolated right atrium. Similarly, in the present study GR 113808 did not act competitively in the rat ileum. Although GR 113808 at the low concentration of 0.01 μM caused a rightward displacement of 5-HT, higher concentrations (0.1 μM, 1 μM) produced little or no further rightward shift. This deviation from competitive antagonism may result from either the high degree of experimental error associated with the rat ileum, as discussed earlier, or a true tissue-dependent form of non-competitive antagonism. Whereas it has not been possible to establish the latter possibility in the rat ileum, the present study shows that GR 113808 apparently does act non-competitively in human colon. In this tissue GR 113808 produced rightward shifts of the 5-HT curves, however the Schild plot slope was non linear at concentrations of GR 113808 above 0.1 μM. This property of GR 113808 was observed previously by Hillier *et al.* (1994), who reported a pK_B value of 8.89 for GR 113808 when used at a concentration of 0.003 μM, which is similar to the value obtained in the present study (apparent $pA_2 = 9.0$ at 0.01 μM). These values are also similar to the values obtained in the rat oesophagus ($pA_2 = 8.6$) where GR 113808 was shown to behave competitively. However, higher concentrations of GR 113808 (0.01–0.1 μM) in the study performed by Hillier *et al.* (1994) and in the present study (1 μM) produced little or no further shift to the right of the 5-HT concentration-effect curve giving rise to a Schild slope which was significantly different from unity. This suggests that another receptor, in addition to the 5-HT$_4$ receptor, may mediate the 5-HT-induced effects in the human colon. However, the use of antagonists of 5-HT$_1$, 5-HT$_2$ and 5-HT$_3$ receptors, at least at the concentrations used, indicated a lack of involvement of other previously characterized 5-HT receptors in this tissue.

The results obtained in this study have highlighted no differences, with regard to the apparent affinity values of GR 113808, between the 5-HT$_4$ receptors mediating the relaxation response in the rat oesophagus, rat ileum and human colon. These findings are consistent with the findings in other peripheral tissues, e.g. human atrial 5-HT$_4$ receptors ($pK_B = 8.8$, Kaumann, 1993), and brain tissues from guinea-pig and rat ($pK_i = 9.5$ and 9.6 respectively, Grossman *et al.*, 1993a,b). Thus if differences exist between central nervous system and peripheral 5-HT$_4$ receptors (as was interpreted by Kaumann *et al.*, 1990; Bockaert *et al.*, 1992), the present studies in rat oesophagus and ileum and human colon suggest that they are not discriminated by GR 113808.

The apparent affinity value of GR 113808 in the human colon where direct relaxation was the parameter quantified to measure agonist potency was not significantly different from the value obtained using inhibition of spontaneous activity as the measure of agonist potency. In addition the potency of 5-HT causing direct relaxation is not significantly different from the potency causing inhibition of spontaneous activity. These results suggest that 5-HT$_4$ receptor activation causes both relaxation and inhibition of spontaneous activity in human colonic circular muscle. These findings extend the known pharmacology of 5-HT in the human colon as reported earlier (Fishlock & Parks, 1963; Fishlock, 1964; Misiewicz *et al.*, 1966; Wright & Sheppard, 1966) and more recently (Tam *et al.*, 1994).

In conclusion, the present study provides information on the relative usefulness of the rat oesophagus, rat ileum and human colon as assay tissues for drugs acting at 5-HT$_4$ receptors. The study has revealed novel data on the action of the 5-HT$_4$ receptor agonists, DAU 6236 and SC 53116 and the antagonist GR 113808 on these tissues. The differences between the rat tissues and the human colon has demonstrated the value of using human material in developing therapeutic drugs. Given the activity of GR 113808 and DAU 6236 in the human colon we suggest that clinical evaluation of these compounds may be worthwhile in helping to determine whether they have specific therapeutic value in treating conditions of the alimentary tract.

We thank Prof. P. Bhathal and colleagues of the Anatomical Pathology Department, Royal Melbourne Hospital, and Prof. P. Desmond and colleagues of the Gastroenterology Department, St. Vincent's Hospital, Melbourne for the specimens of human colon. We also thank Dr C. Rizzi of Boerhinger-Ingelheim, Milan for DAU 6236, Glaxo Group Research for GR 113808 and Searle for SC 53116. P.M. is an NH & MRC Research Fellow.

References

AKBARALI, H.I., BEIGER, D. & TRIGGLE, C.R. (1987). Effects of cold storage on relaxation responses in the rat oesophageal tunica muscularis mucosae. *Can. J. Physiol. Pharmacol.*, **65**, 23–29.

ARUNLAKSHANA, O. & SCHILD, H.O. (1959). Some quantitative uses of drug antagonism. *Br. J. Pharmacol. Chemother.*, **14**, 48–58.

BAXTER, G.S., CRAIG, D.A. & CLARKE, D.E. (1991). 5-Hydroxytryptamine$_4$ receptors mediate relaxation of the rat oesophageal tunica muscularis mucosae. *Naunyn-Schmied. Arch. Pharmacol.*, **343**, 439–446.

BOCKAERT, J., FOZARD, J.R., DUMUIS, A. & CLARKE, D.E. (1992). The 5-HT$_4$ receptor: a place in the sun. *Trends Pharmacol. Sci.*, **13**, 141–145.

BORMAN, R.A. & BURLEIGH, D.E. (1993). Evidence for the involvement of a 5-HT$_4$ receptor in the secretory response of human small intestine to 5-HT. *Br. J. Pharmacol.*, **110**, 927–928.

BORMAN, R.A. & BURLEIGH, D.E. (1994). Heterogeneity of 5-HT receptors in human sigmoid colon. *Br. J. Pharmacol.*, **112**, 558P.

BRANCHECK, T.A. & GERSHON, M.D. (1987). Development of neural receptors for serotonin in the murine bowel. *J. Comp. Neurology*, **258**, 597–610.

BUCHHEIT, K.H., GAMSE, R. & PFANNKUCHE, H.J. (1992). SDZ 205-557, a selective, surmountable antagonist for 5-HT$_4$ receptors in the isolated guinea-pig ileum. *Naunyn-Schmied. Arch. Pharmacol.*, **345**, 387–393.

BUNCE, K.T., ELSWOOD, C.J. & BALL, T.T. (1991). Investigation of the 5-HT receptor mechanism mediating the short circuit current response in rat colon. *Br. J. Pharmacol.*, **102**, 811–816.

COSTALL, B. & NAYLOR, R.J. (1990). 5-Hydroxytryptamine: new receptors and novel drugs for gastrointestinal motor disorders. *Scand. J. Gastroenterol.*, **25**, 769–787.

COSTALL, B., NAYLOR, R.J. & TULADHAR, B.R. (1993). 5-HT$_4$ receptor mediated facilitation of the emptying phase of the peristaltic reflex in guinea-pig isolated ileum. *Br. J. Pharmacol.*, **110**, 1572–1578.

CRAIG, D.A. & CLARKE, D.E. (1990). Pharmacological characterisation for a neuronal receptor for 5-hydroxytryptamine in guinea-pig ileum with properties similar to the 5-HT$_4$ receptor. *J. Pharmacol. Exp. Ther.*, **252**, 1378–1386.

CRAIG, D.A. & CLARKE, D.E. (1991). Peristalsis evoked by 5-HT and renzapride: evidence for a putative 5-HT$_4$ receptor activation. *Br. J. Pharmacol.*, **102**, 563–564.

CRAIG, D.A., EGLEN, R.M., WALSH, L.K.M., PERKINS, L.A., WHITING, R.L. & CLARKE, D.E. (1995). 5-Methoxytryptamine and 2-methyl-5-hydroxytryptamine-induced desensitisation as a discriminative tool for the 5-HT$_3$ and putative 5-HT$_4$ receptors in the guinea-pig ileum. *Naunyn-Schmied. Arch. Pharmacol.*, **345**, 264–269.

DUMUIS, A., SEBBEN, M., MONFERINI, E., NICOLA, M., TURCONI, M., LADINSKY, H. & BOCKAERT, J. (1991). Azabicycloalkyl benzimidazolone derivatives as a novel class of potent agonists at the 5-HT$_4$ receptor positively coupled to adenylate cyclase in brain. *Naunyn-Schmied. Arch. Pharmacol.*, **343**, 245–251.

EGLEN, R.M., SWANK, S.R., WALSH, L.K.M. & WHITING, R.L. (1990). Characterisation of 5-HT$_3$ and 'atypical' 5-HT receptors mediating guinea-pig ileal contractions *in vitro*. *Br. J. Pharmacol.*, **101**, 513–520.

ELSWOOD, C.J., BUNCE, K.T. & HUMPHREY, P.P.A. (1991). Identification of putative 5-HT$_4$ receptors in guinea-pig ascending colon. *Eur. J. Pharmacol.*, **196**, 149–155.

ERSPAMER, V. (1954). Pharmacology of indolealkylamines. *Pharmacol. Rev.*, **6**, 425–487.

FISHLOCK, D.J. (1964). The action of 5-HT on the circular muscle of human ileum and colon *in vitro*. *J. Physiol.*, **170**, 11P.

FISHLOCK, D.J. & PARKS, A.G. (1963). A study of human colonic muscle *in vitro*. *Br. Med. J.*, **2**, 666.

FLYNN, D.L., ZABRAWSKI, D.L., BECKER, D.P., NOSAL, R., VILLAMIL, C.I., GULLIKSON, G.W., MOUMMI, C. & YANG, D. (1992). SC-53116: the first selective agonist at the newly identified serotonin 5-HT$_4$ receptor subtype. *J. Med. Chem.*, **35**, 1486–1489.

FORD, A.P.D.W., BAXTER, G.S., EGLEN, R.M. & CLARKE, D.E. (1992). 5-Hydroxytryptamine stimulates cyclic AMP formation in the tunica muscularis mucosae of the rat oesophagus via 5-HT$_4$ receptors. *Eur. J. Pharmacol.*, **211**, 117–120.

GALE, J.D., GROSSMAN, C.J., WHITEHEAD, J.W.F., OXFORD, A.W., BUNCE, K.T. & HUMPHREY, P.P.A. (1994). GR 113808: a novel, selective antagonist with high affinity at the 5-HT$_4$ receptor. *Br. J. Pharmacol.*, **111**, 332–338.

GROSSMAN, C.J., GALE, J.D., BUNCE, K.T., KILPATRICK, G.J., WHITEHEAD, J.W.F., OXFORD, A.W. & HUMPHREY, P.P.A. (1993a). Development of a radioligand binding assay for the 5-HT$_4$ receptor: use of a novel antagonist. *Br. J. Pharmacol.*, **108**, 106P.

GROSSMAN, C.J., KILPATRICK, G.J. & BUNCE, K.T. (1993b). Development of a radioligand binding assay for 5-HT$_4$ receptors in guinea-pig and rat brain. *Br. J. Pharmacol.*, **109**, 618–624.

HILLIER, K., TAM, F.S-F., BUNCE, K.T. & GROSSMAN, C. (1994). Inhibition of motility induced by the activation of 5-HT$_1$ and 5-HT$_4$ receptor types in isolated human colon smooth muscle. *Br. J. Pharmacol.*, **112**, 102P.

KAUMANN, A.J. (1993). Blockade of human atrial 5-HT$_4$ receptors by GR 113808. *Br. J. Pharmacol.*, **110**, 1172–1174.

KAUMANN, A.J., SANDERS, L., BROWN, A.M., MURRAY, K.J. & BROWN, M.J. (1990). A 5-hydroxytryptamine receptor in human atrium. *Br. J. Pharmacol.*, **110**, 879–885.

KAUMANN, A.J., SANDERS, L., BROWN, A.M., MURRAY, K.J. & BROWN, M.J. (1991). A 5-HT$_4$-like receptor in human right atrium. *Naunyn-Schmied. Arch. Pharmacol.*, **344**, 150–159.

MCLEAN, P.G., COUPAR, I.M. & MOLENAAR, P. (1993a). Effect of the novel 5-HT$_4$ receptor agonists DAU 6236 in human colon. *Med. J. Aus.*, **159**, 834.

MCLEAN, P.G., COUPAR, I.M. & MOLENAAR, P. (1993b). the 5-HT$_4$ receptor in the alimentary tract. *Clin. Exp. Pharmacol. Physiol.*, **Suppl. 1**, 47.

MCLEAN, P.G., COUPAR, I.M. & MOLENAAR, P. (1994). Characterisation of the 5-HT$_4$ receptor in the rat and human alimentary tract. *Can. J. Physiol. Pharmacol.*, **72** Suppl. 1, 242.

MEDHURST, A.D. & KAUMANN, A.J. (1993). Characterization of the 5-HT$_4$ receptor mediating tachycardia in piglet isolated right atrium. *Br. J. Pharmacol.*, **110**, 1023–1030.

MISIEWICZ, J.J., WALLER, S.L. & EISNER, M. (1966). Motor responses of human gastrointestinal tract to 5-hydroxytryptamine in vivo and in vitro. *Gut*, **7**, 208.

MONFERINI, E., PARENTI, M., DONIN, L., ZOCCHETTI, A., RIZZI, C.A. & GIRALDO, E. (1991). A new class of 5-HT$_4$ receptor agonists positively coupled to adenylate cyclase in guinea-pig hippocampus. *Serotonin 1991* Conference: Birmingham, U.K. July 14–17, p. 68.

REEVES, J.J., BUNCE, K.T. & HUMPHREY, P.P.A. (1991). Investigation into the 5-hydroxytryptamine receptor mediating smooth muscle relaxation in the rat oesophagus. *Br. J. Pharmacol.*, **103**, 1067–1072.

RIZZI, C.A., COCCINI, T., ONORI, L., MANZO, L. & TONINI, M. (1992). Benzimidazone derivatives: a new class of 5-hydroxytryptamine$_4$ receptor agonists with prokinetic and acetylcholine releasing properties in the guinea-pig ileum. *J. Pharmacol. Exp. Ther.*, **261**, 412–419.

TALLARIDA, R.J. & MURRAY, R.B. (1987). *Manual of Pharmacologic Calculations with Computer Programs*. Berlin: Springer-Verlag.

TAM, F.S.-F., HILLIER, K. & BUNCE, K.T. (1994). Characterization of the 5-hydroxytryptamine receptor type involved in inhibition of spontaneous activity of human isolated colonic circular muscle. *Br. J. Pharmacol.*, **113**, 143–150.

THOMPSON, J.H. (1971). Serotonin and the alimentary tract. *Res. Commun. Chem. Pathol. Pharmacol.*, **2**, 687–781.

TONINI, M., RIZZI, C.A., MANZO, L. & ONORI, L. (1991). Novel enteric 5-HT$_4$ receptors and gastrointestinal prokinetic action. *Pharmacol. Res.*, **24**, 5–14.

TULADHAR, B.R., COSTALL, B. & NAYLOR, R.J. (1991). Putative 5-HT$_4$ receptor involvement in the relaxations induced by 5-HT in the rat ileum. *Br. J. Pharmacol.*, **104**, 151P.

TULADHAR, B.R., COSTALL, B. & NAYLOR, R.J. (1992). Potentiation of the relaxation response to 5-methoxytryptamine in the rat ileum with mono amine oxidase inhibitors. *Br. J. Pharmacol.*, **107**, 122P.

WAIKAR, M.V., FORD, A.P.D.W. & CLARKE, D.E. (1994). Evidence for an inhibitory 5-HT$_4$ receptor in urinary bladder of *Rhesus* and *Cynomolgus* monkeys. *Br. J. Pharmacol.*, **111**, 213–218.

WAIKAR, M.V., HEDGE, S.S., FORD, A.P.D.W. & CLARKE, D.E. (1992). Pharmacological analyses of Endo-6-methoxy-8-methyl-8-azabicyclo[3.2.1]oct-3-yl-2,3-dihydro-2-oxo-1H-benzimidazolone-1-carboxylate hydrochloride (DAU 6285) at the 5-hydroxytryptamine$_4$ receptor in the tunica muscularis mucosae of rat oesophagus and ileum of guinea-pig: role of endogenous 5-hydroxytryptamine. *J. Pharmacol. Exp. Ther.*, **264**, 654–661.

WRIGHT, P.G. & SHEPPARD, J.J. (1966). Some observations on the response of normal human sigmoid colon to drugs *in vitro*. *Gut*, **7**, 41.

(Received November 24, 1994
Accepted January 23, 1995)

British Journal of Pharmacology (1995) 115, 57-66

JB-9322, a new selective histamine H_2-receptor antagonist with potent gastric mucosal protective properties

Beatriz Palacios, [1]Mª José Montero, Mª Angeles Sevilla & Luis San Román

Laboratorio de Farmacognosia y Farmacodinamia, Departamento de Fisiología y Farmacología, Facultad de Farmacia, Universidad de Salamanca, Avda, Campo Charro s/n, 37007 Salamanca, Spain

1 JB-9322 is a selective histamine H_2-receptor antagonist with gastric antisecretory activity and mucosal protective properties.

2 The affinity of JB-9322 for the guinea-pig atria histamine H_2-receptor was approximately 2 times greater than that of ranitidine.

3 *In vivo*, the ID_{50} value for the inhibition of gastric acid secretion in pylorus-ligated rats was 5.28 mg kg^{-1} intraperitoneally. JB-9322 also dose-dependently inhibited gastric juice volume and pepsin secretion. In gastric lumen-perfused rats, intravenous injection of JB-9322 dose-dependently reduced histamine-, pentagastrin- and carbachol-stimulated gastric acid secretion.

4 JB-9322 showed antiulcer activity against aspirin and indomethacin-induced gastric lesions and was more potent than ranitidine.

5 JB-9322 effectively inhibited macroscopic gastric haemorrhagic lesions induced by ethanol. Intraperitoneal injection was effective in preventing the lesions as well as oral treatment. The oral ID_{50} value for these lesions was 1.33 mg kg^{-1}. By contrast, ranitidine (50 mg kg^{-1}) failed to reduce these lesions. In addition, the protective effect of JB-9322 was independent of prostaglandin synthesis.

6 These results indicate that JB-9322 is a new antiulcer drug that exerts a potent cytoprotective effect in addition to its gastric antisecretory activity.

Keywords: JB-9322; ranitidine; histamine H_2-receptor antagonist; gastric acid secretion; mucosal protection; cytoprotection

Introduction

Since Black *et al.* (1972) first defined the H_2-receptor and characterized a number of H_2-antagonists, various types of these compounds have been developed and used clinically. The introduction of H_2-antagonists has revolutionized the treatment of peptic ulcers and it has been proved that ulcer healing effects of these drugs are due mainly to the inhibition of gastric acid secretion through blockade of histamine H_2-receptors by competitive antagonism at the receptor (Angus *et al.*, 1980; Takana *et al.*, 1987). However, it has been demonstrated that the recurrence ratio of peptic ulcer is relatively high after healing by long-term H_2-antagonist therapy (Grant *et al.*, 1989; Debongnie, 1992; Shamburek & Schubert, 1993). In the clinical stage, patients are treated with H_2-antagonists in combination with defensive factors potentiating-agents to prevent the ulcer relapse. On the other hand, interest has grown in discovering therapeutic agents that prevent ulcer formation or relapse by increasing defensive factors in the gut. The property of a drug that protects the gastric mucosa against necrotizing agents such as acid and ethanol has been coined cytoprotection (Robert *et al.*, 1979). Although these cytoprotective mechanisms are unknown, the protective effect by an agent is mainly considered to be due to the increase of gastric mucosal defensive integrity.

From this point of view, in our search for an H_2-receptor antagonist which exerts antisecretory and cytoprotective activities, we have found JB-9322 (Figure 1). In the present study we describe the pharmacological profile of JB-9322, a potent antisecretory H_2-antagonist which has inherent mucosal protective properties that are independent of endogenous prostaglandin synthesis, at doses similar to its antisecretory ID_{50} value. Ranitidine has been utilized as reference H_2-receptor antagonist (Bradshaw *et al.*, 1979).

[1] Author for correspondence.

Methods

In vitro *assay techniques*

H_2-receptor antagonism in guinea-pig isolated atria Antagonism at the histamine H_2-receptor was determined in guinea-pig isolated right atria. Male Dunkin-Hartley guinea pigs weighing 350-600 g were killed by cervical dislocation and exsanguination. The hearts were excised from animals and placed in a Petri dish containing oxygenated (95% O_2 + 5% CO_2) Krebs-Henseleit solution (composition, mM: NaCl 118.0, KCl 4.7, $CaCl_2$ 2.5, KH_2PO_4 1.3, $MgSO_4.7H_2O$ 1.2, $NaHCO_3$ 30.0 and glucose 12.0). The right spontaneously beating atrium was dissected free carefully and suspended in 10-ml tissue bath with oxygenated Krebs-Henseleit solution and kept at 37°C. The tissue was attached with an initial load of 1 g to an isometric force-displacement transducer and recorded on a polygraph. After a 30-min stabilization period, three histamine concentration-response curves were established at 20-min intervals by measuring the chronotropic effect of increasing concentrations of histamine given in a cumulative fashion until the maximal response was consistent. The histamine-induced increase in atrial rate was allowed to plateau before the next successive concentration was added. Between each curve the tissues were washed out several times and the heart rate allowed to return to basal level. The second curve served as control and the third was

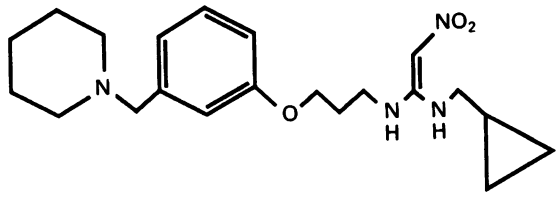

Figure 1 Chemical structure of JB-9322 (N-[3-[3-(piperidin-1-ylmethyl)phenoxy]propyl]-*N'*-cyclopropylmethyl-2-nitro-1,1-ethenediamine).

repeated either 5 or 30 min after the tissue was incubated with various concentrations of JB-9322 or reference H_2-antagonist, ranitidine, adding higher concentrations of histamine as needed.

H_1-receptor antagonism in guinea-pig isolated ileum A 2- to 3-cm piece of ileum was removed from the animal and suspended in 20 ml tissue muscle bath containing atropinized Tyrode solution of the following composition (mM): NaCl 136.9, KCl 2.7, $MgSO_4.7H_2O$ 1.0, NaH_2PO_4 0.3, glucose 5.5, $CaCl_2$ 1.8, $NaHCO_3$ 11.9 and atropine 2.0×10^{-4}. The solution was maintained at 37°C and bubbled with air. The recordings were made as above. The tissue was attached to an isometric force-displacement transducer with an initial load of 1 g, and it was allowed to stabilize for 30 min. After the stabilization period, cumulative concentration-response curves to histamine were established in 15-min periods until obtaining a reproducible contraction. After 5-min incubation with 10^{-6} M of JB-9322 or ranitidine, the histamine concentration-response curve was repeated.

Muscarinic-receptor antagonism in rat isolated duodenum Male Wistar rats weighing 250 to 300 g fed *ad libitum* were used. Immediately after the rats had been killed by decapitation, the duodenum was surgically removed. A 2-cm length of duodenum was suspended in 10-ml tissue bath filled with Tyrode solution with the composition given above. The solution was maintained at 35°C and bubbled continuously with air. The tissue was attached to an isometric force-displacement transducer with an initial load of 1 g. After a 30-min stabilization period, concentration-response curves to acetylcholine in 10-min periods were carried out in a cumulative form until the maximal response was consistent. When a reproducible contraction was obtained, a new concentration-response curve was repeated after 5-min incubation with 10^{-6} M of JB-9322 or ranitidine.

Calculation and statistical analysis

Data were expressed as a percentage of the maximal agonist response established in the absence of the antagonist for each preparation in the control curve. Concentration-response curves in the above *in vitro* preparations were obtained by plotting the percentage of the maximal control response against log concentration of histamine or acetylcholine. Each point shows the mean and s.e.mean of at least 5 experiments. The cumulative concentration-response curves, with and without the antagonists were analysed using the Tallarida & Murray computer programme (1984). This programme subjects to linear regression the data between 20% and 80% of the maximum control response to obtain the EC_{50} values and the extreme values are not used.

In the atrium assay, the pA_2 values and slopes of the Schild regression were calculated according to the method of Arunlakshana & Schild (1959). The dose-ratios for this analysis have been calculated for each curve pair. Statistical comparisons between groups were performed by Student's *t* test for paired data, and values of *P* of 0.05 or less were regarded as significant from controls.

In vivo *assay techniques*

Wistar rats kept in cages with raised mesh bottoms were deprived of solid diet 24 h before experiments began but received a nutritive solution of 8 g 100 ml^{-1} sucrose in 0.2 g 100 ml^{-1} NaCl to avoid excessive dehydration. This solution was removed 2 h before starting experiments.

Effects on gastric acid secretion

Measurement of acid secretion in the lumen-perfused stomach of the anaesthetized rat The procedure followed for the measurement of gastric acid secretion was described by Ghosh & Schild (1958). Male Wistar rats weighing 200–250 g were used. In brief animals were anaesthetized with urethane (1.25 g kg^{-1}, i.p.) and the trachea intubated. A soft catheter was passed down the oesophagus through an incision in the cervical side so that the opening was just proximal to the cardiac sphincter and secured in this position by a ligature. After a laparotomy, a second polyethylene cannula was inserted into the stomach via an incision in the duodenum, held in place by two ligatures and let outside the abdominal wall for collection of gastric secretion. In studies in which secretion was stimulated, the jugular vein was cannulated for administration of the secretagogues. The penile vein was cannulated for i.v. administration of saline or drugs. At the beginning of the experiment, the stomach was flushed with 20–40 ml of saline at 37°C to remove any solid content.

Once the surgical preparation had been completed, the gastric lumen was perfused continuously with warm saline (NaCl 0.9% w/v, 37°C) at a rate of 1 ml min^{-1} by the use of a peristaltic pump via the oesophageal cannula. After a period of 45 min for stabilization, the perfusate flowing from the stomach was collected at 15-min intervals and H^+ output determined by automatic titration (Crison titrator, micro TT 2050, Barcelona, Spain) of aliquots (10 ml) of the perfusate with 0.01 N NaOH to pH 7.0. Gastric acid secretion was stimulated by the i.v. infusion at the rate of 1 ml h^{-1} of histamine (5 mg kg^{-1} h^{-1}) or pentagastrin (10 μg kg^{-1} h^{-1}) during a 4.5 h period or during a 5 h period for carbachol (10 μg kg^{-1} h^{-1}), starting 45 min after determination of three basal values of acid secretion. In the case of the stimulation with histamine and pentagastrin, the acid secretion reached a steady state 60 min after the beginning of infusion of the secretagogues. To reach the steady state in the carbachol-induced gastric acid secretion at 90 min, carbachol (5 μg kg^{-1}) was injected as a bolus through the cannulated penile vein when the infusion started.

H_2-antagonists or vehicle (0.9% saline) were administered i.v. in a volume of 1 ml kg^{-1} 60 min (histamine- and pentagastrin-stimulation) or 90 min (carbachol-stimulation) after the start of the secretagogue stimulation. Data were expressed as a percentage of the value of acid secretion 60 min (histamine and pentagastrin stimulation) or 90 min (carbachol stimulation) after the initiation of secretagogue infusion. The dose-response relationship was established using the area under the dose-response curve from 60 to 270 min (histamine and pentagastrin) or from 90 to 300 min (carbachol) after the start of secretagogue infusion.

In the experiments to determine the influence of JB-9322 and ranitidine on basal acid secretion, after stabilization (45 min) drugs or saline were infused continuously via the penile vein at 5 mg kg^{-1} h^{-1}, 1 ml h^{-1} for 150 min. The concentration of H^+ was estimated every 10 min.

Gastric secretion in pylorus-ligated rat The pylorus-ligated rat model first described by Shay *et al.* (1945) was used. Male Wistar rats weighing 180–200 g were used: 2 h before and throughout the collection periods no access to the nutritive solution was allowed. The surgical manipulation was carried out under light ether anaesthesia. A small abdominal incision was made and the pylorus was ligated. Care was taken to avoid trauma to the surrounding vasculature. The incision was closed with silk sutures and test substances or vehicle (0.9% saline) were administered i.p. in a volume of 1 ml kg^{-1} immediately after surgery. The animals were killed 4 h after ligation of the pylorus, the abdomen re-opened and the stomach was excised carefully keeping the oesophagus closed, opened along the greater curvature and the luminal contents were collected and centrifuged for 15 min at 4500 r.p.m. to remove residual debris. The volume was measured and aliquots were taken for determination of the acidity by automatic titration, using the titration system mentioned above, with 0.1 N NaOH to the endpoint of pH 7.0. Total acid output was expressed as microequivalents of H^+ per 4 h. Pepsin concentration was determined by a modification of

the colorimetric method of Anson (1938) involving haemoglobin digestion (2%, pH 2.0, 37°C, 15 min) followed by alkaline condensation with Folin-Ciocalteu reagent and spectrophotometric measurement of the absorption at 578 nm.

For assessment of duration of antisecretory action in the Shay rat, in a separate series of experiments compounds 30 mg kg^{-1} or saline were administered i.p. 7 h before the pylorus was ligated.

Experimentally induced gastric lesion studies

Aspirin and indomethacin-induced gastric lesions Male Wistar rats weighing 170–190 g were used. The selection of the ulcerogenic agent was the result of preliminary studies. Gastric lesions were induced by administration of aspirin (200 mg kg^{-1}, orally, suspended in 1% carboximethylcellulose in water) plus indomethacin (40 mg kg^{-1}, s.c., dissolved in 0.9% saline) at the same time. The indomethacin solution was freshly prepared and the aspirin suspension homogenized immediately before use. JB-9322, ranitidine or vehicle (0.9% saline) were given orally (10 ml kg^{-1}) 30 min before the ulcerogenic drugs. Five hours after the aspirin plus indomethacin administration, rats were decapitated, their stomachs removed, opened along the greater curvature, gently rinsed under tap water and pinned on a paraffin and plastic polimer plate. The stomachs were then photographed, the photograph amplified and the area of each macroscopic lesion (mm^2) in the glandular portion was measured by computerized planimetry (Ibas Interactive Image Analysis System, Kontron). The total area of the lesions was regarded as the lesion index. The lesion index was expressed as the mean lesion area for each group of rats.

The possible inaccuracy inherent in this assessment was minimized by ensuring that the lesions were measured by the same person.

Gastric protective activity in rats: ethanol-induced lesions Gastric protection activity studies were conducted in female Wistar rats weighing 170–200 g using the method of Robert *et al.* (1979). Rats were pretreated with drugs or vehicle (0.9% saline), administered either orally (10 ml kg^{-1}) or intraperitoneally (2 ml kg^{-1}); 30 min later the rats were given 1 ml of absolute ethanol orally. After another 30 min the animals were killed and the stomachs excised. The remaining procedure was the same as described above for aspirin and indomethacin-induced gastric lesions.

In experiments designed to determine whether mucosal protection by JB-9322 is dependent on the synthesis of prostaglandins, rats were given indomethacin (10 mg kg^{-1}) subcutaneously 90 min before the oral drug or vehicle pretreatment. This dose of indomethacin has been shown previously to eliminate the production of prostaglandins in the gastric mucosa (Ligumsky *et al.*, 1982). Protection was then determined as described.

The results were expressed as the percentage of the total glandular mucosal area occupied by necrotic lesions.

Calculations and statistical analysis

Data are presented as the mean ± s.e.mean. The inhibitory ratio (%) was obtained by comparing the values in the treated animals with that of the control group. The doses causing 50% inhibition (ID_{50}) were calculated from the dose-inhibition relationships by least squares regression: 95% confidence limits of the ID_{50} values were determined by Simfit programme (University of Manchester, U.K.). The significance of differences was assessed by Student's unpaired *t* test and a *P* value of less than 0.05 was considered to be significant.

Drugs

The following drugs were used: JB-9322 (synthesized in the Department of Organic Chemistry, Faculty of Chemistry, University of Salamanca), ranitidine hydrochloride, acetylcholine chloride, carbachol and aspirin (Sigma), histamine dihydrochloride (Merck), carboximethylcellulose (Panreac). Indomethacin (Inacid, Merck Sharp & Dohme) and pentagastrin (Peptavlon, ICI) were used as the preparations available for clinical use. The compounds were dissolved in isotonic saline immediately before use. Doses of JB-9322 and ranitidine are expressed as free base.

Results

In vitro *studies*

The histamine H_2-receptor antagonist properties of the test compounds were determined by their inhibition of the chronotropic effects of histamine on guinea-pig isolated atria (Black *et al.*, 1972). In our preliminary experiments, JB-9322 and ranitidine showed the same antagonism on the response to histamine in atria with 5 min and 30 min incubations. Thus, for the assessment of the inhibitory effect of these drugs a 5 min incubation was used. JB-9322 and ranitidine did not affect the resting atrial rate (201.7 ± 4.2 contractions min^{-1}) during the period of incubation. JB-9322 (10^{-8}–3×10^{-7} M) and ranitidine (10^{-7}–3×10^{-6} M) produced a concentration-related parallel shift of histamine concentration-response curve to the right without affecting ($P > 0.05$) the maximal response (297.7 ± 6.9 contractions min^{-1}) (Figure 2). The Schild regressions of log (dose ratio-1) vs log molar concentration of these compounds were linear with slopes and 95% confidence limits of 0.94 (0.85–1.02) and 0.76 (0.55–1.04) for JB-9322 and ranitidine, respectively which were not significantly different from unity (Figure 2). JB-9322 and ranitidine showed a competitive antagonistic activity and their pA_2 values and 95% confidence limits were 7.76 (7.70–7.83) and 7.36 (7.01–7.71), respectively. The dose-ratios for the Schild analysis have been calculated for each curve pair and due to differences in the location of the control curve, the mean concentration-effect curves in Figure 2 do not accurately represent the information generated from an individual tissue. For this reason, the Schild plots for each compound are shown. Thus, JB-9322 has an affinity for the histamine H_2-receptor which is approximately 2 times greater than that of ranitidine.

JB-9322 and ranitidine 10^{-6} M did not cause any significant displacement of the histamine or acetylcholine concentration-response curve in ileal and duodenal preparations, respectively.

In vivo *studies*

Effect on gastric acid secretion

Effect on acid secretion in the gastric lumen-perfused rats Basal acid secretion was 3.57 ± 0.20 (μEq H^+ 15 min^{-1}) in the gastric lumen-perfused rats. A stable secretion (24.76 ± 1.25 μEq H^+ 15 min^{-1}) was seen 60 min after the infusion of histamine (submaximal dose: 5 mg kg^{-1} h^{-1}). The histamine-induced acid secretion decreased gradually, but significant secretion was observed for at least 4.5 h after the beginning of the infusion. JB-9322 and ranitidine administered i.v. inhibited the histamine-stimulated acid secretion with a clear dose-response relationship. As shown in Figure 3, the maximum inhibitory effect obtained with JB-9322 and ranitidine was observed 30 min after the i.v. administration in both cases. However, the recovery from the antisecretory activity of JB-9322 was appreciably faster than the recovery from this of ranitidine. The values of ID_{50} at each time interval are listed in Table 1.

On the pentragastrin- and carbachol-stimulated acid secretion, JB-9322 and ranitidine also inhibited the secretion dose-dependently and the maximum inhibitory effect was observed between 30–60 min after the i.v. administration of com-

pounds in both cases. But as in the case of histamine-stimulated acid secretion, the recovery from the inhibitory activity was faster with JB-9322 (Figure 3). The values of ID_{50} for pentagastrin and carbachol at each time interval are listed in Tables 2 and 3, respectively.

JB-9322 (5 mg kg^{-1} h^{-1}, i.v.) decreased the acid concentration of the unstimulated stomach but was less potent than ranitidine at the same dose (Figure 4).

Gastric secretion in pylorus-ligated rats Gastric secretion was evaluated as gastric juice volume, acid output and pepsin output for 4 h after ligation of the pylorus. These values in control rats given vehicle were 5.13 ± 0.54 ml 4 h^{-1}, 383.70 ± 57.51 μEq H^+ 4 h^{-1} and 26.75 ± 3.86 mg 4 h^{-1}, respectively. When administered immediately after ligation, JB-9322 (3, 10 and 30 mg kg^{-1}, i.p.) dose-dependently inhibited the gastric acid secretion, gastric juice volume as well as pepsin secretion. Ranitidine (1, 3, 10 and 30 mg kg^{-1}, i.p.) also caused a marked decrease in each secretory parameter. The decrease of pepsin output was due largely to a reduction in gastric volume inasmuch as concentration was not greatly changed. However at higher doses of these compounds, the acid output was inhibited to a greater extent than the volume of secretion (Figure 5).

The intraperitoneal ID_{50} values and 95% confidence limits for reduction in gastric acid secretion for JB-9322 and ranitidine were 5.28 mg kg^{-1} (3.69–7.64) and 3.72 mg kg^{-1} (1.23–7.30), respectively. JB-9322 inhibited to a greater extent the gastric juice volume and pepsin secretion.

When injected i.p. 7 h before ligation, an equipotent dose in terms of the immediate effect (30 mg kg^{-1}) of JB-9322 and ranitidine, ranitidine significantly inhibited both gastric juice volume and acid output; however, this potency was weaker in comparison with that observed when ranitidine was administered immediately after ligation. The effect of JB-9322 on gastric juice volume and acid output was not significant (Figure 6).

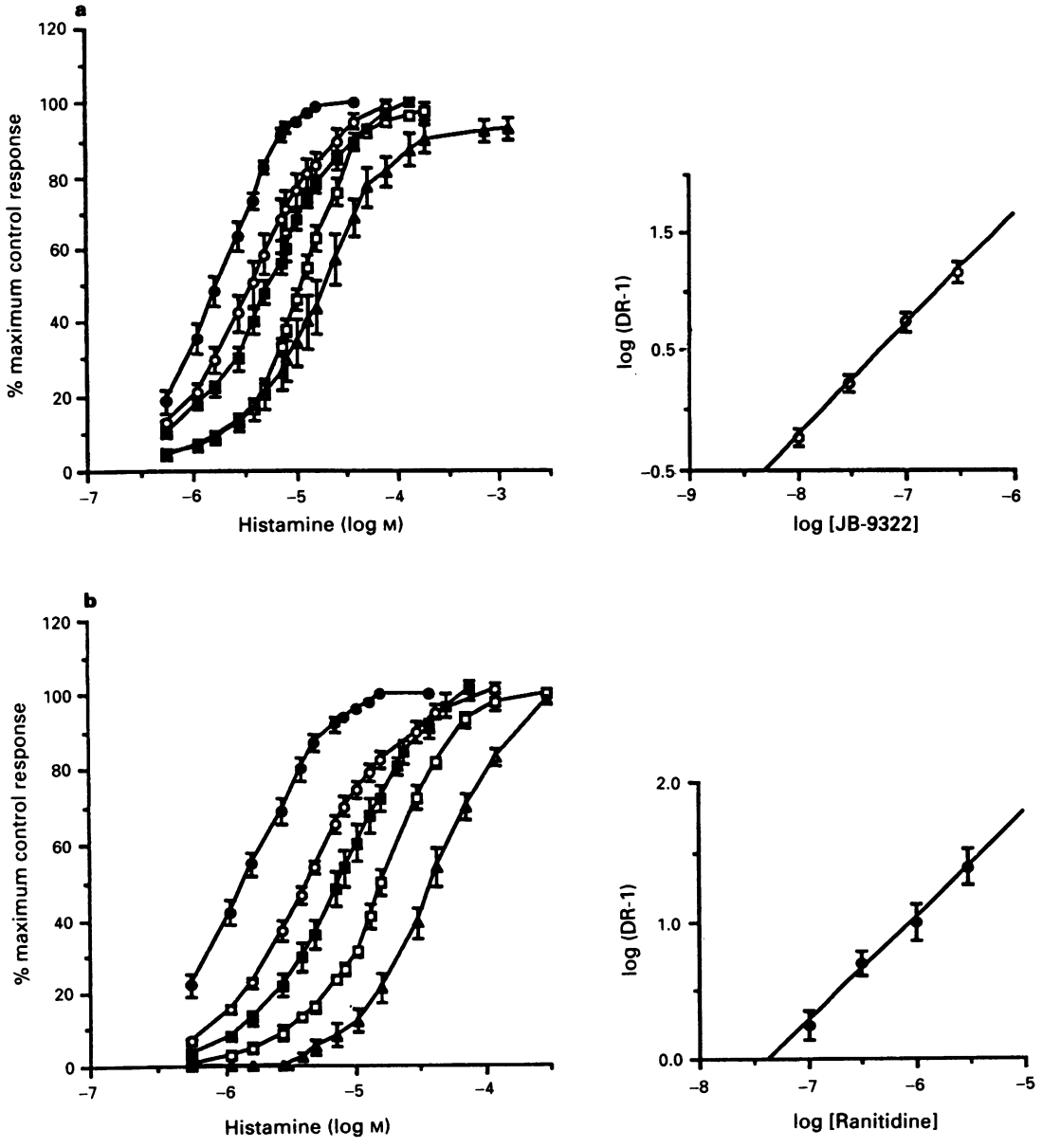

Figure 2 Effect of a 5-min incubation with JB-9322 (a) and ranitidine (b) on the positive chronotropic concentration-response curve to histamine in guinea-pig isolated right atrium. Control (●); JB-9322: 3×10^{-7} M (△), 10^{-7} M (□), 3×10^{-8} M (■), 10^{-8} M (○); ranitidine: 3×10^{-6} M (△), 10^{-6} M (□), 3×10^{-7} M (■), 10^{-7} M (○). Each curve represents the mean ± s.e.mean response obtained in at least 5 tissues. Beside these curves, Schild plots for JB-9322 and ranitidine are shown. DR = histamine dose-ratio.

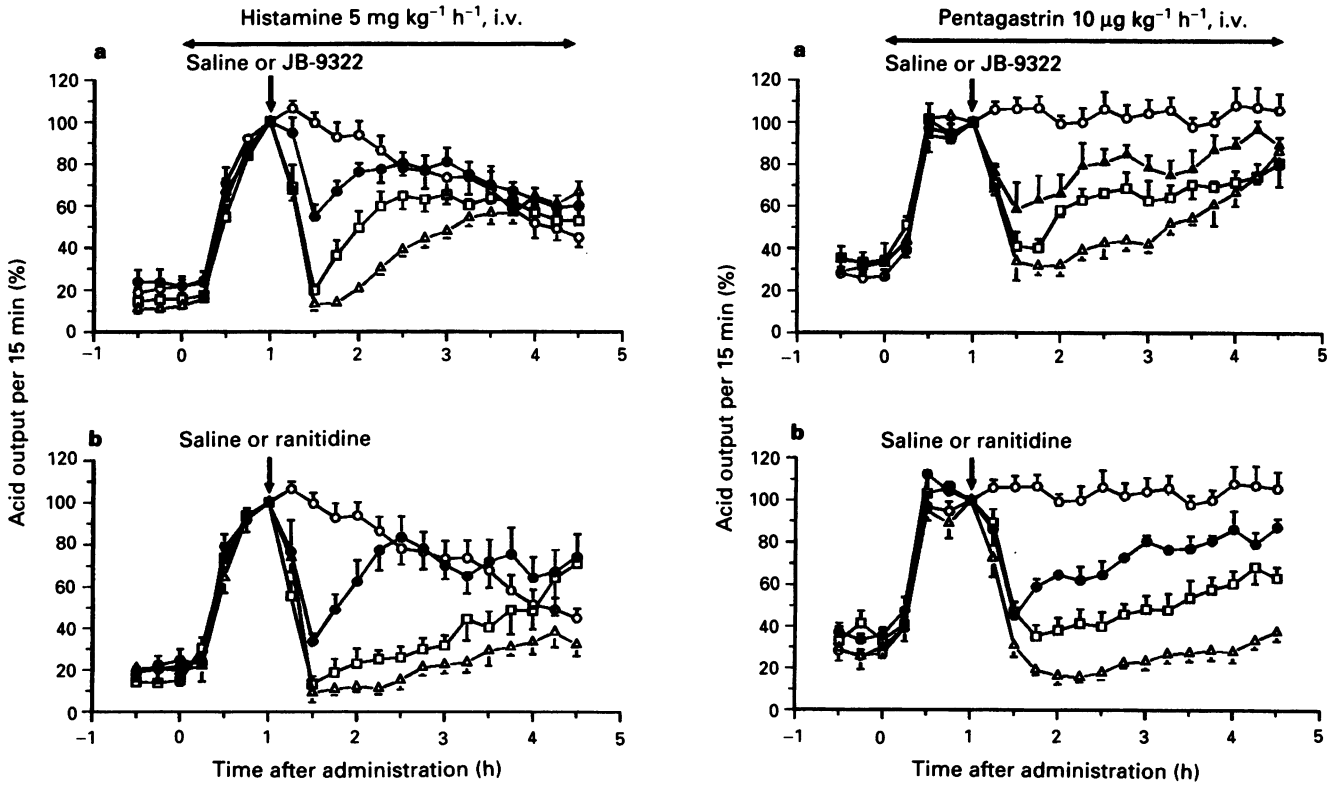

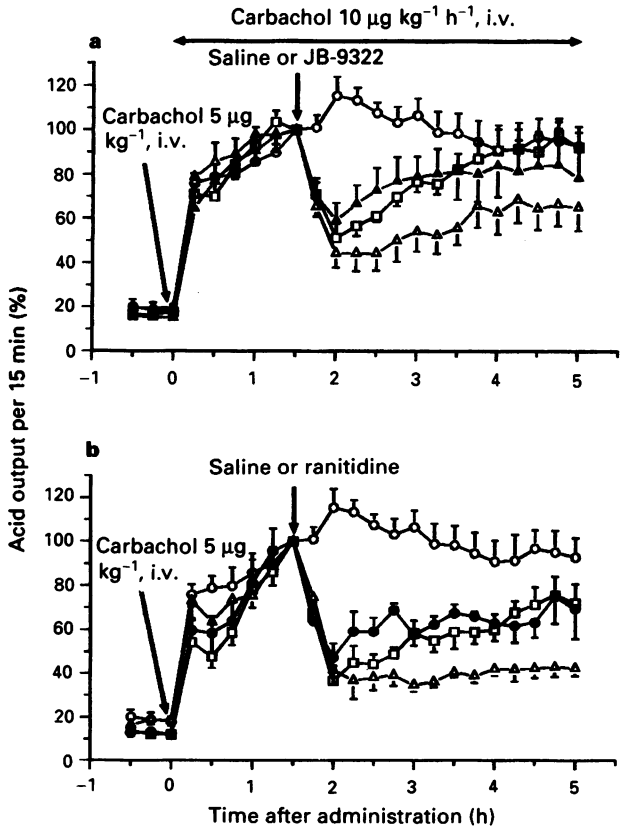

Figure 3 Antisecretory effect of JB-9322 (a) and ranitidine (b) on the histamine-, pentagastrin- and carbachol-stimulated gastric acid secretion in lumen-perfused rats. Data were expressed as a percentage of value of acid secretion 60 min (histamine- and pentagastrin-stimulation) or 90 min (carbachol-stimulation) after the initiation of secretagogue infusion. Each point indicates the mean ± s.e.mean obtained from 5 to 9 rats. Control (○); JB-9322 (mg kg^{-1}; i.v.): 0.3 (●), 0.6 (▲), 1 (□), 3 (△). Ranitidine (mg kg^{-1}, i.v.): 0.3 (●), 1 (□), 3 (△).

Table 1 ID_{50} of JB-9322 and ranitidine for inhibition of histamine-stimulated gastric acid secretion in lumen perfused rats

Treatment (i.v.)	ID_{50} (mg kg^{-1}) Time after drug administration (min) 60–120	60–180	60–210	60–240	60–270
Ranitidine	0.34 (0.12–0.81)	0.65 (0.33–1.15)	0.77 (0.44–1.31)	0.96 (0.60–1.52)	1.20 (0.87–1.73)
JB-9322	0.89 (0.56–1.44)	1.31 (1.16–1.49)	1.79 (1.60–2.03)	2.56 (2.23–2.98)	4.25 (3.41–5.46)

Each value represents ID_{50} with the 95% confidence limits in parentheses.

Table 2 ID_{50} of JB-9322 and ranitidine for inhibition of pentagastrin-stimulated gastric acid secretion in lumen-perfused rats

Treatment (i.v.)	ID_{50} (mg kg^{-1}) Time after drug administration (min) 60–120	60–180	60–210	60–240	60–270
Ranitidine	1.24 (0.78–2.02)	0.73 (0.67–0.82)	0.79 (0.72–0.86)	0.82 (0.74–0.91)	0.89 (0.80–0.99)
JB-9322	1.96 (1.12–3.69)	1.54 (1.29–1.88)	1.66 (1.40–2.00)	1.86 (1.52–2.32)	2.30 (1.80–3.04)

Each value represents ID_{50} with the 95% confidence limits in parentheses.

Table 3 ID_{50} of JB-9322 and ranitidine for inhibition of carbachol-stimulated gastric acid secretion in lumen-perfused rats

Treatment (i.v.)	ID_{50} (mg kg^{-1}) Time after drug administration (min) 90–150	90–210	90–240	90–270	90–300
Ranitidine	2.36 (0.98–5.73)	0.88 (0.87–0.90)	1.00 (1.00–1.15)	1.16 (0.85–1.59)	1.36 (0.85–2.21)
JB-9322	2.78 (2.43–3.25)	2.30 (2.08–2.54)	2.83 (2.40–3.37)	4.19 (2.62–6.78)	4.27 (2.95–6.68)

Each value represents ID_{50} with the 95% confidence limits in parentheses.

Experimentally induced gastric lesion studies

Aspirin and indomethacin-induced gastric lesions The selection of the ulcerogenic drugs was determined from preliminary studies. Administration of indomethacin at doses between 10 and 60 mg kg^{-1} orally or subcutaneously caused slight gastric ulceration. No gastric lesions were observed in animals treated with aspirin orally at a dose of 250 mg kg^{-1}. In our experience, the most suitable conditions for evaluation of JB-9322 and ranitidine were the combined effect of administration of indomethacin (40 mg kg^{-1}, s.c.) plus aspirin (200 mg kg^{-1}, oral).

No gastric lesions were observed in animals treated with aspirin vehicle (1% carboximethylcellulose). Administration of aspirin plus indomethacin resulted in the production of gastric lesions in the glandular segment of the stomach, primarily the corpus, but occasionally the antrum also, in 100% of the control animals. Pretreatment with JB-9322 and ranitidine 30 min before the NSAIDs gavage produced a significant and dose-dependent reduction in the severity and incidence of these lesions (Figure 7). Some of the animals that received the highest dose of JB-9322 (20 mg kg^{-1}) were completely protected from ulcer formation. The estimated oral ID_{50} values and 95% confidence limits were 2.63 mg kg^{-1} (1.82–3.74) and 4.93 mg kg^{-1} (4.13–5.76) for JB-9322 and ranitidine, respectively.

Therefore, in this model the inhibitory activity of JB-9322 was higher than that of ranitidine.

Ethanol-induced gastric lesions Oral administration of absolute ethanol produced severe gastric haemorrhagic lesions visible from the outside of the stomach as thick black or red lines. After opening the stomach, lesions were found in the glandular mucosa and consisted of elongated bands, 2–12 mm long by 2–4 mm wide, usually parallel to the long axis of the stomach. They were located mostly in the corpus, the antrum was less affected. The control rats with vehicle had gastric lesions of 159.2 ± 29.8 mm^2. When rats were orally pretreated with JB-9322, 30 min before the ethanol treatment, the formation of these haemorrhagic lesions was inhibited in a dose-dependent manner and the ID_{50} and 95% confidence limits were 1.33 mg kg^{-1} (1.06–1.68). In the group

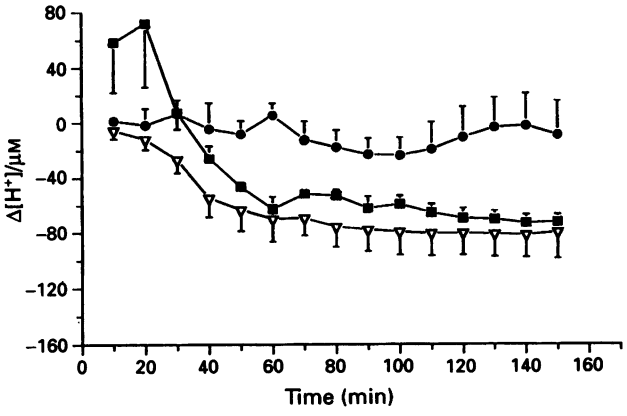

Figure 4 Effect of 5 mg kg^{-1} h^{-1} of JB-9322 (■) and ranitidine (▽) on basal acid secretion in lumen-perfused rats. Control (●). Data were expressed as the difference between the [H$^+$] at each 10-min interval during drug infusion and the [H$^+$] just before the initiation of infusion. Each point indicates the mean ± s.e.mean obtained from 5 to 7 rats.

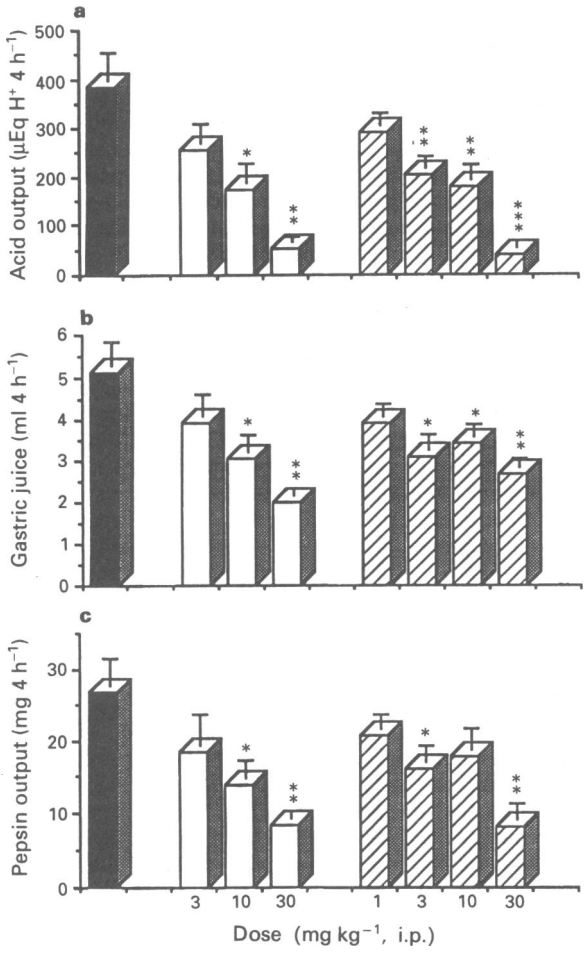

Figure 5 Effect of saline (solid columns), JB-9322 (open columns) and ranitidine (hatched columns) on basal gastric secretion in pylorus-ligated rats. (a) Gastric acid secretion; (b) gastric juice volume; (c) pepsin secretion. Each drug was given intraperitoneally immediately after surgery. Animals were killed 4 h after pylorus ligation. Each column represents the mean ± s.e.mean of 8 animals. Significantly different from control: $*P<0.05$; $**P<0.01$; $***P<0.001$.

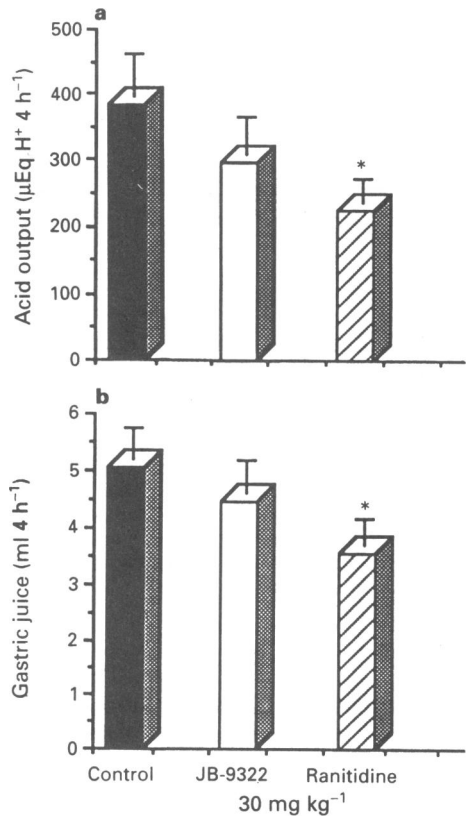

Figure 6 Duration of antisecretory effect of JB-9322 (open columns) and ranitidine (hatched columns) in pylorus-ligated rats. Rats were intraperitoneally dosed with saline (solid columns) or drugs 7 h before the pylorus ligation. Four hours after ligation the rats were killed and gastric acid output (a) and gastric juice volume (b) determined as described. Each column represents the means ± s.e.mean of 6 animals. $*P<0.05$ compared to control.

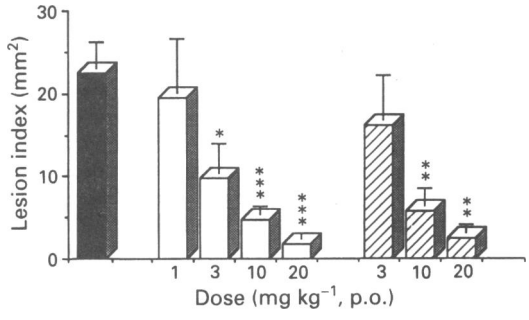

Figure 7 Inhibition by JB-9322 and ranitidine of aspirin and indomethacin-induced gastric lesions. Rats were orally dosed with saline (solid columns), JB-9322 (open columns) or ranitidine (hatched columns) 30 min before each rat received 200 mg kg^{-1} of aspirin orally plus 40 mg kg^{-1} of indomethacin subcutaneously. Each column represents the mean ± s.e.mean of at least 6 animals. Significantly different from control $*P<0.05$; $**P<0.01$; $***P<0.001$.

receiving JB-9322 (50 mg kg^{-1}), the pinpoint round and linear lesions were only partly found in the glandular portion.

In similar experiments, no reduction in ethanol-induced haemorrhagic lesions was seen following the oral administration of ranitidine (50 mg kg^{-1}) (Figure 8).

In order to determine whether JB-9322 acted locally or systemically, its cytoprotective activity against ethanol-induced gastric lesions was tested by i.p. administration. In comparison to the control value of 18.6 ± 2.6%, ethanol lesions were reduced to 16.4 ± 3.5% (not significant) and 1.6 ± 0.5% ($P<0.001$) of lesioned corpus in the groups ($n = 8$ each) pretreated with JB-9322, 3 and 10 mg kg^{-1} i.p., respectively.

Effect of indomethacin on the protective activity of JB-9322

The role of endogenous prostaglandins on the protective effect of JB-9322 was examined in rats that were subcutaneously pretreated with 10 mg kg^{-1} of the cyclo-oxygenase inhibitor, indomethacin. Indomethacin itself significantly increased the amount of lesioning approximately 2 times. The protective effect of JB-9322, however, was not diminished when prostaglandin biosynthesis had been inhibited beforehand by indomethacin. In the placebo-pretreated groups, JB-9322 (10 mg kg^{-1}) reduced ethanol-induced lesions from 14.7 ± 1.3 to 5.5 ± 1.9% of lesioned corpus. In the indomethacin-pretreated groups, the gastric lesions due to ethanol were 30.9 ± 2.3 and 4.8 ± 1.5% of lesioned corpus for vehicle control and JB-9322-treated groups, respectively. The inhibition of mucosal lesion formation by JB-9322 compared to the respective control group, was highly significant in each case ($P<0.001$).

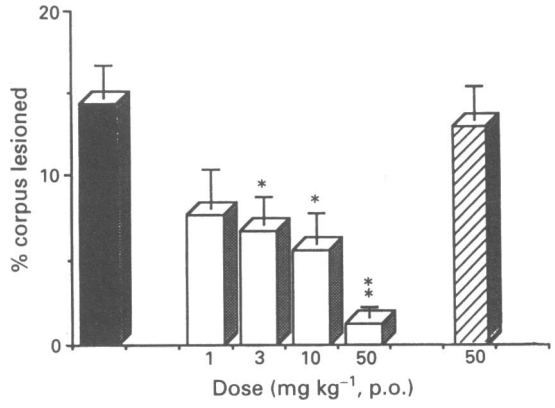

Figure 8 Effect of JB-9322 and ranitidine on ethanol-induced gastric haemorrhagic lesions in the rats. Rats were orally given saline (solid column); JB-9322 (open columns) or ranitidine (hatched column) 30 min before receiving an oral gavage of 1 ml of absolute ethanol. Each column represents the mean ± s.e.mean of at least 7 animals. Significantly different from control: $*P<0.05$; $**P<0.01$.

Discussion

JB-9322 is a histamine H_2-receptor antagonist possessing mucosal protective properties as well as gastric antisecretory activity.

In guinea-pig atrium assay, ranitidine produced parallel shifts and surmountable antagonism. The pA_2 value determined by us for ranitidine agrees with values reported by previous authors (Daly *et al.*, 1981; Lumma *et al.*, 1982; Katz *et al.*, 1986a). JB-9322, like ranitidine, shifted the histamine concentration-response curve in a parallel, surmountable manner after either a 5 or 30 min period of incubation. Our results are not consistent with the findings of other investigators that have observed noncompetitive kinetics in the guinea-pig isolated atrial assay with certain H_2-receptor antagonists having, as a part of their substructure, a [(piperidinylmethyl)phenoxy] propylamine moiety (Brittain & Jack, 1983; Torchiana *et al.*, 1983; Katz *et al.*, 1986b; Santilli *et al.*, 1988) as does JB-9322. In those papers, the initial concentration-response curve shifts elicited at low concentrations of antagonists were rightward and parallel, but as the antagonist concentration was increased, the concentration-response curve shifts became increasingly nonparallel, accompanied by diminished maxima, that were decreased in a time-dependent manner. A recent paper (Sekiguchi *et al.*, 1993a), as in our study, has demonstrated that using a similar phenoxy derivative H_2-blocker, the positive chronotropic response of guinea-pig right atrium to histamine was shifted to the higher concentrations with the increase of H_2-antagonist concentration without changing the maximum response as shown in Figure 2 and showing the same antagonism with 5- and 30-min incubations. These differences might be due to the effects of other structural changes in each molecule.

Selectivity of JB-9322 for the H_2-receptor was demonstrated by a lack of significant inhibition against histamine in guinea-pig isolated ileum and acetylcholine in rat isolated duodenum.

The antagonism of the histamine H_2-receptor by JB-9322 is reflected *in vivo* by gastric antisecretory activity. In submaximally histamine-stimulated rats, the maximum intravenous antisecretory activity of JB-9322 and ranitidine was reached 30 min after the administration but as shown in Figure 3, the recovery from the inhibitory effect was faster with JB-9322 than with ranitidine. On the pentagastrin- and carbachol-stimulated acid secretion, the potency of the inhibitory effect of ranitidine was slightly greater than that of JB-9322 and the duration of the antisecretory action of JB-9322 was also shorter than that of ranitidine. These results agree well with the higher gastric acid antisecretory activity and longer duration of action of ranitidine in pylorus-ligated rats, as evidenced by the suppression of gastric acid output for 7 h after i.p. administration of ranitidine, compared with the lack of antisecretory action by JB-9322 in this paradigm.

Despite JB-9322 having an affinity for the histamine H_2-receptor which was approximately 2 times greater than that of ranitidine, its gastric acid antisecretory effect was weaker in lumen-perfused and pylorus-ligated rats. This means that JB-9322 might be rapidly metabolized *in vivo* and lose its activity due to its pharmacokinetic characteristics.

The inhibitory effect of histamine H_2-receptor antagonists on experimental lesion formation has been reported (Okabe *et al.*, 1977; Takeda *et al.*, 1982; Isobe *et al.*, 1990; Shibata *et al.*, 1990; Hakkinen *et al.*, 1991; Sekiguchi *et al.*, 1993b), showing that these drugs can be very useful for peptic ulcer patients. Aspirin and other non-steroidal anti-inflammatory drugs (NSAIDs) are associated with gastrointestinal damage in man and animals (Rainsford, 1975; Kuwayama *et al.*, 1990). Measures such as vagotomy and pretreatment with anticholinoceptors, histamine H_2-receptor antagonists and H^+/K^+-ATPase inhibitors that are known to decrease gastric acidity, all cause a marked amelioration in gastric damage by NSAIDs (Kasuya *et al.*, 1979; Long *et al.*, 1983; Shibata *et al.*, 1990; Sekiguchi *et al.*, 1993b). Therefore, our findings that both JB-9322 and ranitidine could prevent the development of aspirin plus indomethacin-induced gastric lesions were expected from their antisecretory action, which might improve gastric tolerance to nonsteroidal anti-inflammatory drugs as indicated by Grassi *et al.* (1991). Furthermore, some work shows that the presence of HCl throughout the experiment removes the inhibitory effect of histamine H_2-receptor antagonists on the NSAIDs-induced erosions that was demonstrated when HCl was not present (Carmichael *et al.*, 1978; Katsura *et al.*, 1994). That the prevention of this ulcer formation by ranitidine is ascribed to the suppression of acid secretion is also based on the results that its effective doses in the inhibition of these ulcers are sufficient to decrease the acid secretion in pylorus-ligated rats. Our results clearly demonstrate that JB-9322 has a higher potency than ranitidine in this model, as in the cold stress plus indomethacin-induced lesion model (Palacios *et al.*, 1993).

Cytoprotection was first demonstrated in rats by Robert *et al.* (1979), who showed that many prostaglandins protected the mucosa of the stomach against the haemorrhagic and erosive effects of intragastric administration of absolute ethanol and other necrotizing agents. This pharmacological property is independent of inhibition of gastric secretion. Possible mechanisms include stimulation of mucus and bicarbonate secretion, stimulation of the sodium pump, strengthening of the gastric mucosal barrier, etc. (Guth, 1982). In the present study, we showed that JB-9322 prevented the development of gastric lesions provoked by intragastric ethanol in a dose-related manner, indicating presence of cytoprotective activity. The antisecretory and cytoprotective activities are exhibited in the same dose-range. Ranitidine at 50 mg kg^{-1} orally was inactive, in agreement with the prevailing view that ranitidine is not cytoprotective (Del Soldato *et al.*, 1985; Hakkinen *et al.*, 1991).

Two lines of evidence indicate that the mucosal protective effect of JB-9322 is a direct action of the compound and not the result of adaptive cytoprotection, which occurs following the application of mild irritants to the gastric mucosa and which may be mediated by increased levels of tissue prostaglandins (Robert *et al.*, 1983). First, the protective effect of JB-9322 is not only present when administered orally but also intraperitoneally, thus the protective effect is not dependent on contact of the drug with the gastric mucosa. Second, in a separate series of experiments, rats were pretreated subcutaneously with indomethacin prior to drug treatment and the ethanol challenge, which eliminates the production of prostaglandins in the gastric mucosa and inhibits the protective effect of mild irritants (Robert *et al.*, 1983). Treatment

1983). Treatment with indomethacin alone significantly increased the injury after the ethanol gavage, probably due to the removal of the protective endogenous prostaglandins. Despite the indomethacin pretreatment, the full protective effect of JB-9322 on the gastric mucosa remained, indicating that the presence of endogenous prostaglandins is not essential to the expression of mucosal protective activity of JB-9322.

Ranitidine, having a more potent antisecretory effect than JB-9322, revealed weaker activity than JB-9322 on NSAIDs and cold stress plus indomethacin-induced gastric lesion models. This might indicate that the gastroprotective effect of JB-9322 against these induced injuries is not completely dependent on the ability of gastric antisecretion, but also it depends on its potent cytoprotective effect, since JB-9322 prevented the ulcer formation at doses less than the ID_{50} for reduction in the acid output in pylorus-ligated rats.

In summary, JB-9322 is a specific, competitive histamine H_2-receptor antagonist with strong antiulcer and gastroprotective properties. Advantages of JB-9322 over ranitidine include mucosal protective activity and this activity is at doses similar to its antisecretory ID_{50} value. Thus, JB-9322 may prove to be a useful agent in the treatment of peptic ulcer disease.

The authors would like to thank C. Caballero, M. Grande and J.J. Navarro for the synthesis of JB-9322 and J.C. Villoria for technical assistance. Our thanks to the Junta de Castilla y León for a fellowship to B.P.

References

ANGUS, J.A., BLACK, J.W. & STONE, M. (1980). Estimation of pK_B values for histamine H_2-receptor antagonists using an *in vitro* acid secretion assay. *Br. J. Pharmacol.*, **68**, 413–423.

ANSON, M.L. (1938). The estimation of pepsin, trypsin, papain and cathepsin with haemoglobin. *J. Gen. Physiol.*, **22**, 79–89.

ARUNLAKSHANA, O. & SCHILD, H.O. (1959). Some quantitative uses of drug antagonists. *Br. J. Pharmacol. Chemother.*, **14**, 48–58.

BLACK, J.W., DUNCAN, W.A.M., DURANT, C.J., GANELLIN, C.R. & PARSONS, E.M. (1972). Definition and antagonism of histamine H_2-receptors. *Nature*, **236**, 385–388.

BRADSHAW, J., BRITTAIN, R.T., CLITHEROW, J.W., DALY, M.J., JACK, D., PRICE, B.J. & STABLES, R. (1979). Ranitidine (AH 19065): a new potent, selective histamine H_2-receptor antagonist. *Br. J. Pharmacol.*, **66**, 464P.

BRITTAIN, R.T. & JACK, D. (1983). Histamine H_2-antagonists past, present and future. *J. Clin. Gastroenterol.*, **5** (Suppl. 1), 71–79.

CARMICHAEL, H.A., NELSON, L.M. & RUSSELL, R.I. (1978). Cimetidine and prostaglandin: evidence for different modes of action on the rat gastric mucosa. *Gastroenterology*, **74**, 1229–1232.

DALY, M.J., HUMPHRAY, J.M. & STABLES, R. (1981). Some *in vitro* and *in vivo* actions of the new histamine H_2-receptor antagonist, ranitidine. *Br. J. Pharmacol.*, **72**, 49–54.

DEBONGNIE, J.C. (1992). Actualité des antagonistes des récepteurs H_2 dans le traitement de l'ulcère. *Acta Gastroenterol. Belg.*, **55**, 415–422.

DEL SOLDATO, P., FOSCHI, D., VARIN, L. & DANIOTTI, S. (1985). Comparison of the gastric cytoprotective properties of atropine, ranitidine and PGE_2 in rats. *Eur. J. Pharmacol.*, **106**, 53–58.

GHOSH, M.N. & SCHILD, H.O. (1958). Continuous recording of acid gastric secretion in the rats. *Br. J. Pharmacol. Chemother.*, **13**, 54–61.

GRANT, S.M., LANGTRY, H.D. & BROGDEN, R.N. (1989). Ranitidine. An updated review of its pharmacodynamic and pharmacokinetic properties and therapeutic use in peptic ulcer disease and other allied diseases. *Drugs*, **37**, 801–870.

GRASSI, A., IPPEN, J., BRUNO, M. & THOMAS, G. (1991). BAY P 1455, a thiazolylaminobenzimidazole derivative with gastroprotective properties in the rat. *Eur. J. Pharmacol.*, **195**, 251–259.

GUTH, P.H. (1982). Pathogenesis of gastric mucosal injury. *Annu. Rev. Med.*, **33**, 183–194.

HAKKINEN, J.P., HOLT, W.F., GODDARD, C.J., OATES, P.J., MURPHY, W.R., MACIEJKO, J.J. & REITER, L.A. (1991). CP-66,948: an antisecretory histamine H_2-receptor antagonist with mucosal protective properties. *Dig. Dis. Sci.*, **36**, 1721–1727.

ISOBE, Y., NAGAI, H., MURAMATSU, M., AIHARA, H. & OTOMO, S. (1990). Antisecretory and antilesional effect of a new histamine H_2-receptor antagonist, IT-066, in rats. *J. Pharmacol. Exp. Ther.*, **255**, 1078–1082.

KASUYA, Y., URUSHIDANI, T. & OKABE, S. (1979). Effect of various drugs and vagotomy on indomethacin-induced gastric ulcers in the rat. *Jpn. J. Pharmacol.*, **29**, 670–673.

KATSURA, Y., INOUE, Y., TOMISHI, T., ISHIKAWA, H. & TAKASUGI, H. (1994). Studies on antiulcer drugs. 7. 2-Guanidino-4-pyridylthiazoles as histamine H_2-receptor antagonists with potent gastroprotective effects against nonsteroidal anti-inflammatory drug-induced injury. *J. Med. Chem.*, **37**, 57–66.

KATZ, L.B., SCOTT, C.K. & SHRIVER, D.A. (1986a). Pharmacology of ORF 17578, a new histamine H_2-receptor antagonist: comparison with cimetidine and ranitidine. *J. Pharmacol. Exp. Ther.*, **237**, 404–410.

KATZ, L.B., SCOTT, C.K. & SHRIVER, D.A. (1986b). Pharmacological comparison of ORF 17910, a potent, long-acting histamine H_2-receptor antagonist, to cimetidine and ranitidine. *J. Pharmacol. Exp. Ther.*, **238**, 587–593.

KUWAYAMA, H., MATSUO, Y. & EASTWOOD, G.L. (1990). Gastroduodenal mucosal injury by nonsteroidal anti-inflammatory drugs. *Drug Invest.*, **2** (Suppl. 1), 22–26.

LIGUMSKY, M., HANSEN, D.G. & KAUFFMAN, G.L. J.R. (1982). Salicilic acid blocks indomethacin- and aspirin-induced cyclooxigenase inhibition in rat gastric mucosa. *Gastroenterology*, **83**, 1043–1046.

LONG, J.F., CHIU, P.J.S., DERELANKO, M.J. & STEINVERG, M. (1983). Gastric antisecretory and cytoprotective activities of SCH 28080. *J. Pharmacol. Exp. Ther.*, **226**, 114–120.

LUMMA, W.C., ANDERSON, P.S., BALDWIN, J.J., BOLHOFER, W.A., HABECKER, C.N., HIRSHFIELD, J.M., PIETRUSZKIEWICZ, A.M., RANDALL, W.C., TORCHIANA, M.L., BRITCHER, S.F., CLINES-CHMIDT, B.V., DENNY, G.H., HIRSCHMANN, R., HOFFMAN, J.M., PHILLIPS, B.T. & STREETER, K.B. (1982). Inhibitors of gastric acid secretion: 3,4-diamino-1,2,5-thiadiazole 1-oxides and 1,1-dioxides as urea equivalents in a series of H_2-receptor antagonist. *J. Med. Chem.*, **25**, 207–210.

OKABE, S., TAKEUCHI, K., URUSHIDANI, T. & TAKAGI, K. (1977). Effects of cimetidine, a histamine H_2-receptor antagonist, on various experimental gastric and duodenal ulcers. *Dig. Dis. Sci.*, **22**, 677–684.

PALACIOS, B., MONTERO, M.J., SEVILLA, M.A., SAN ROMAN, L., NAVARRO, J.J., CABALLERO, C. & GRANDE, M. (1993). JB-9322, un piperidino-metilfenoxipropilamino derivado, con propiedades gastroprotectoras. *Abstract Book of the VIII Congress of the Spanish Society of Therapeutic Chemistry*, 41P.

RAINSFORD, K.D. (1975). The biochemical pathology of aspirin-induced gastric damage. *Agents Actions*, **5**, 326–344.

ROBERT, A., NEZAMIS, J.E., LANCASTER, C., DAVIS, J.P., FIELD, S.O. & HANCHAR, A.J. (1983). Mild irritants prevent gastric necrosis through adaptive cytoprotection mediated by prostaglandins. *Am. J. Physiol.*, **245**, G113–G121.

ROBERT, A., NEZAMIS, J.E., LANCASTER, C. & HANCHAR, A.J. (1979). Cytoprotection by prostaglandins in rats. Prevention of gastric necrosis produced by alcohol, HCl, NaOH, hypertonic NaCl and thermal injury. *Gastroenterology*, **77**, 433–443.

SANTILLI, A., SCOTESE, A.C., MORRIS, R.L., SCHIEHSER, G.A., TELLER, D.M., NIELSEN, S.T. & STRIKE, D.P. (1988). Syntheses and gastric acid antisecretory properties of the H_2-receptor antagonist N-[3-[3-(1-piperidinyl-methyl)phenoxy]propyl]thieno[3,4-d]isothiazol-3-amine-1,1-dioxide and related derivatives. *J. Med. Chem.*, **31**, 1479–1486.

SEKIGUCHI, H., HAMADA, K., KOBAYASHI, F., TAGA, F. & UCHIDA, H. (1993a). Pharmacological profiles of the new histamine H_2-receptor antagonist N-ethyl-N'-[3-[3-(piperidinomethyl)-phenoxy]propyl]urea. *Arzneim. Forsch.*, **43**, 129–133.

SEKIGUCHI, H., HAMADA, K., TAGA, F. & NISHINO, K. (1993b). Effects of the new histamine H_2-receptor antagonist N-ethyl-N'-[3-[3-(piperidino-methyl)phenoxy]propyl]urea with potent gastric mucosal protective activity on acute gastric lesions and duodenal ulcers in rats. *Arzneim. Forsch.*, **43**, 134–138.

SHAMBUREK, R.D. & SCHUBERT, M.L. (1993). Pharmacology of gastric acid inhibition. *Baill. Clin. Gastroenterol.*, **7**, 23–54.

SHAY, H., KOMAROU, S.A., FEELS, S.S., MERANZE, D., GRUESTEIN, M. & SIPLET, H.A. (1945). A simple method for the uniform production of gastric ulceration in the rat. *Gastroenterology*, **5**, 43–61.

SHIBATA, M., YAMAURA, T., SEKINE, A., NISHIKAWA, M., CHIDA, Y. & OHNISHI, H. (1990). Effects of FRG-8701 on gastric acid secretion, gastric mucosal lesions by necrotizing agents and experimental gastric or duodenal ulcer in rats. *Jpn. J. Pharmacol.*, **54**, 277–285.

TAKANA, A., NISHIHARA, S., MISAWA, T. & IBAYASHI, H. (1987). Effects of H_2-receptor antagonists on ^{3}H-cimetidine binding and histamine cellular cAMP in isolated guinea pig gastric glands. *Jpn. J. Pharmacol.*, **45**, 97–105.

TAKEDA, M., TAKAGI, T., YASHIMA, Y. & MAENO, H. (1982). Effect of a new H_2-blocker, 3-[[[2-[(diaminomethylene)amino]-4-thiazolyl]methyl]thio]-N^2-sulfamoyl propionamide (YM-11170), on gastric secretion, ulcer formation and weight of male accessory sex organs in rats. *Arzneim. Forsch.*, **32**, 734–737.

TALLARIDA, R.J. & MURRAY, R.B. (1984). *Manual of Pharmacologic Calculations with Computer Programs*. New York: Springer-Verlag.

TORCHIANA, M.L., PENDLETON, R.G., COOK, P.G., HANSON, C.A. & CLINESCHMIDT, B.V. (1983). Apparent irreversible H_2-receptor blocking and prolonged gastric antisecretory activities of 3-N-{3-[3-(1-piperidino-methyl) phenoxy]propyl] amino-4-amino-1, 2, 5-thia-diazole-1-oxide (L-643,441). *J. Pharmacol. Exp. Ther.*, **224**, 514–519.

(Received May 23, 1994
Revised January 3, 1995
Accepted January 23, 1995)

British Journal of Pharmacology (1995) 115, 67-72

Electrophysiological actions of phenytoin on *N*-methyl-D-aspartate receptor-mediated responses in rat hippocampus *in vitro*

[1]Alison J. Laffling, [2]Patrick Scherr, Joseph G. McGivern, Leslie Patmore & [3]Robert D. Sheridan

Department of Pharmacology, Syntex Research Centre, Research Avenue South, Edinburgh EH14 4AP

1 The effects of the anticonvulsant, phenytoin, have been examined on *N*-methyl-D-aspartate (NMDA) receptor-mediated population spikes in the CA1 region of the rat hippocampus *in vitro*.

2 The 'conventional' (AMPA receptor-mediated) CA1 population spike, evoked by electrical stimulation of the Schaffer collateral/commissural pathway, was abolished by 5 min treatment with 5×10^{-6} M 6-cyano-7-nitroquinoxaline-2,3-dione (CNQX), after which superfusion with a nominally Mg^{2+}-free Krebs solution (containing 5×10^{-6} M CNQX) led to the appearance of an epileptiform population spike which was fully developed by 30–40 min.

3 The epileptiform population spike was abolished by the non-competitive NMDA antagonist, dizocilpine (1×10^{-6} M, 20–30 min) and inhibited by the competitive NMDA receptor antagonist, D-CPP (IC_{50} for reducing the amplitude of the first spike in the train = 8.3×10^{-7} M), demonstrating that the response was mediated by activation of NMDA receptors and validating its use as an assay for antagonists acting at the NMDA receptor/channel complex.

4 Phenytoin (0.1, 0.3 and 1×10^{-4} M applied cumulatively for 30 min at each concentration) failed to inhibit the NMDA receptor-mediated epileptiform population response ($n = 7$ slices).

5 Phenytoin (3×10^{-6} M to 1×10^{-4} M) attenuated the effects of the sodium channel activator, veratridine (2×10^{-6} M), on the CA1 population spike amplitude (recorded in normal Krebs solution), indicating that the previously observed lack of effect of phenytoin on the NMDA receptor-mediated response was not due to impaired access of phenytoin to the biophase.

6 These data support the conclusion that antagonism of NMDA receptor-mediated events is not a pharmacological property of phenytoin and that such an action is therefore unlikely to contribute to the anticonvulsant activity of this drug.

Keywords: Hippocampus; anticonvulsants; phenytoin; NMDA receptors; epilepsy; glutamate receptors; D-CPP; CNQX; dizocilpine; veratridine

Introduction

It is widely believed that the therapeutic action of the well-established anticonvulsant agent, phenytoin, depends on the voltage-dependent inhibition of Na^+ and/or Ca^{2+} channels in the central nervous system, although other equally plausible mechanisms have been proposed (reviewed by Rogawski & Porter, 1990). Thus, at therapeutically relevant concentrations, phenytoin inhibits Na^+ currents both in neuroblastoma cells (Matsuki *et al.*, 1984; Willow *et al.*, 1985) and in voltage-clamped *Xenopus* oocytes expressing human brain Na^+ channels (Tomaselli *et al.*, 1989). A similar inhibitory action of phenytoin on T-type Ca^{2+} currents in neuroblastoma cells has been described (Twombly *et al.*, 1988). An inhibitory action of phenytoin on calmodulin-dependent kinase has been demonstrated and this may also contribute to the anticonvulsant properties of the drug by down-regulating the phosphorylation state of ion channels involved in the epileptiform firing behaviour of neurones (DeLorenzo, 1986). Finally, an inhibition of neurotransmitter release as a result of one or more of the aforementioned actions may play a role in the anticonvulsant activity of phenytoin (Rogawski & Porter, 1990). However, while each of the above effects could potentially explain the therapeutic efficacy of phenytoin, it is clear that despite many years of research the mechanism of action of the drug is not known with certainty.

Recently, an additional pharmacological action of phenytoin has been described in primary cultures of embryonic mouse spinal cord neurones (Wamil & McLean, 1993). These authors found that phenytoin, in therapeutically relevant low micromolar concentrations, inhibited depolarizing responses to *N*-methyl-D-aspartate (NMDA), and suggested that this action may contribute to the therapeutic profile of phenytoin. If this novel action of phenytoin could be demonstrated in a clinically more relevant central tissue then it may have important implications for the design of new anticonvulsant agents.

Therefore, in the present experiments we have examined the effects of phenytoin on NMDA receptor-mediated responses generated synaptically in the rat hippocampus *in vitro*. Some of this work has appeared in abstract form (Sheridan *et al.*, 1994).

Methods

Slice preparation

Transverse hippocampal slices (500 μm thickness) from adult male Sprague-Dawley rats (weighing 180–250 g) were prepared as described previously (Sheridan & Sutor, 1990). Slices were placed in a holding chamber containing standard composition Krebs solution (see below) gassed continuously

[1] Present address: Division of Biosciences, University of Hertfordshire, College Lane, Hatfield, Herts AL10 9AB.
[2] Present address: Hochfeldweg 34, CH-4106 Therwil, Switzerland.
[3] Author for correspondence.

with a mixture of 95% O_2/5% CO_2 (at 18–21°C). The slices were left undisturbed for at least 1 h, after which one slice was transferred to the recording chamber and superfused with standard composition Krebs solution (at 30°C). Stimulation and recording electrodes were positioned in the slice (see below) and the slice left for 30 min to recover from the above procedure. The superfusant temperature was then raised to 35°C for the remainder of the experiment.

Electrical stimulation and recording

A concentric stainless steel electrical stimulation electrode was placed in *stratum radiatum* in the apical dendritic region of area CA2 (to enable stimulation of the Schaffer collateral/commissural pathway). The extracellular recording electrode (containing 4 M NaCl; 1–2 MΩ resistance) was positioned in the CA1 pyramidal cell layer for recording of population spikes. The signal from the recording electrode was amplified (Axoclamp 2A, Axon Instruments, CA, U.S.A.), displayed on an oscilloscope and simultaneously digitized (CED 1401, Cambridge Electronic Design, Cambridge, U.K.), and stored on hard disc on computer (Tandon 286) for subsequent analysis.

Drug application

Drugs were applied from concentrated stock solutions to give the appropriate final concentrations in the superfusate. Concentration-response curves to drugs were obtained by cumulative addition, allowing sufficient time for effects to achieve apparent equilibrium (for details see Results).

Drugs and solutions

Standard composition Krebs solution contained (in mM): NaCl 118, KCl 3, $CaCl_2$ 2, $MgCl_2$ 1.3, NaH_2PO_4 1.25, $NaHCO_3$ 25, D-glucose 10 (pH 7.4 when gassed with 95% O_2/5% CO_2). Nominally Mg^{2+}-free Krebs solution contained the same constituents as standard Krebs except that no $MgCl_2$ was added. The following drugs were used (all from RBI): D-CPP (R-3-(2-carboxypiperazin-4-yl)-propyl-1-phosphonic acid), dizocilpine ((+)-MK-801), phenytoin, and CNQX (6-cyano-7-nitroquinoxaline-2,3-dione). All drug stock solutions were dissolved in deionized water with the exception of CNQX, which was dissolved in dimethyl sulphoxide (DMSO) to give a 10^{-2} M stock, and veratridine, which was dissolved in absolute ethanol to give a 10^{-1} M stock. The final concentrations of DMSO (0.05%) and ethanol (0.002%) were found in pilot experiments to have no detectable effects on slice electrophysiology.

Results

Establishment of a putative NMDA receptor-mediated response in CA1

Having obtained a conventional CA1 population spike in standard composition Krebs solution (Figure 1a), addition of the competitive AMPA receptor antagonist, CNQX (5×10^{-6} M, 5 min), led to the disappearance of the population spike with only the afferent volley remaining (representing activation of the Schaffer collateral/commissural fibres) (Figure 1b). Subsequent superfusion with Mg^{2+}-free Krebs solution (containing 5×10^{-6} M CNQX) led to the appearance of an epileptiform population spike (Figure 1c). The epileptiform response was fully developed by 20 to 30 min and had a duration of 40 to 50 ms.

Effect of dizocilpine on the epileptiform response

The non-competitive NMDA channel blocker, dizocilpine, was applied to 3 hippocampal slices. Figure 2 shows the effect of dizocilpine (10^{-6} M, 30 min) on the epileptiform population spike in one slice. The epileptiform response was all but abolished by this concentration of dizocilpine and the effect was not reversed by up to 60 min washout of the drug. Dizocilpine, tested at a single concentration of 3×10^{-7} M in one slice, induced an approximate 50% decrease in the amplitude of the first spike of the epileptiform response. The effects of dizocilpine in all slices are summarized in Table 1.

Effect of D-CPP on the epileptiform response

The competitive NMDA receptor antagonist, D-CPP, applied to 4 slices in cumulative concentrations ranging from

Table 1 Summary of the effects of dizocilpine, D-CPP and phenytoin on the amplitude of the first spike of the epileptiform population response (number of experiments shown in parentheses)

Concentration (M)	*Amplitude of first spike* (mV) *Dizocilpine*	*D-CPP*	*Phenytoin*
0	3.02 ± 0.69 (3)	3.24 ± 0.41 (4)	2.14 ± 0.19 (7)
3×10^{-7}	1.39 (1)	2.28 ± 0.39 (4)	–
1×10^{-6}	0 (3)	1.22 ± 0.27 (4)	–
3×10^{-6}	–	0.69 ± 0.43 (4)	–
1×10^{-5}	–	0 (4)	2.03 ± 0.15 (7)
3×10^{-5}	–	–	2.03 ± 0.18 (7)
1×10^{-4}	–	–	2.42 ± 0.20 (7)

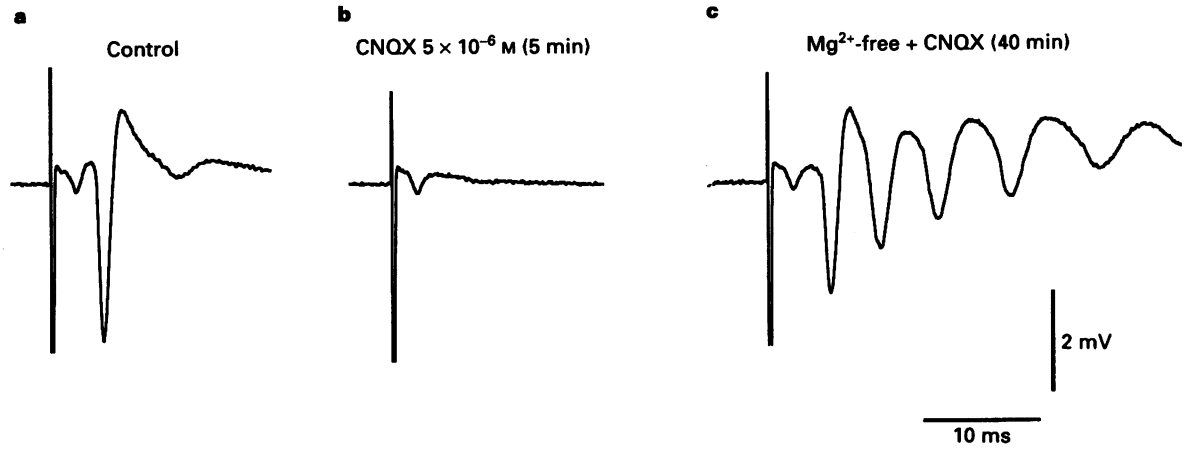

Figure 1 Establishment of the NMDA receptor-mediated epileptiform response. The conventional CA1 population spike (a) was abolished by 5×10^{-6} M CNQX (b). Following superfusion with Mg^{2+}-free Krebs solution (containing 5×10^{-6} M CNQX) an epileptiform response developed (c).

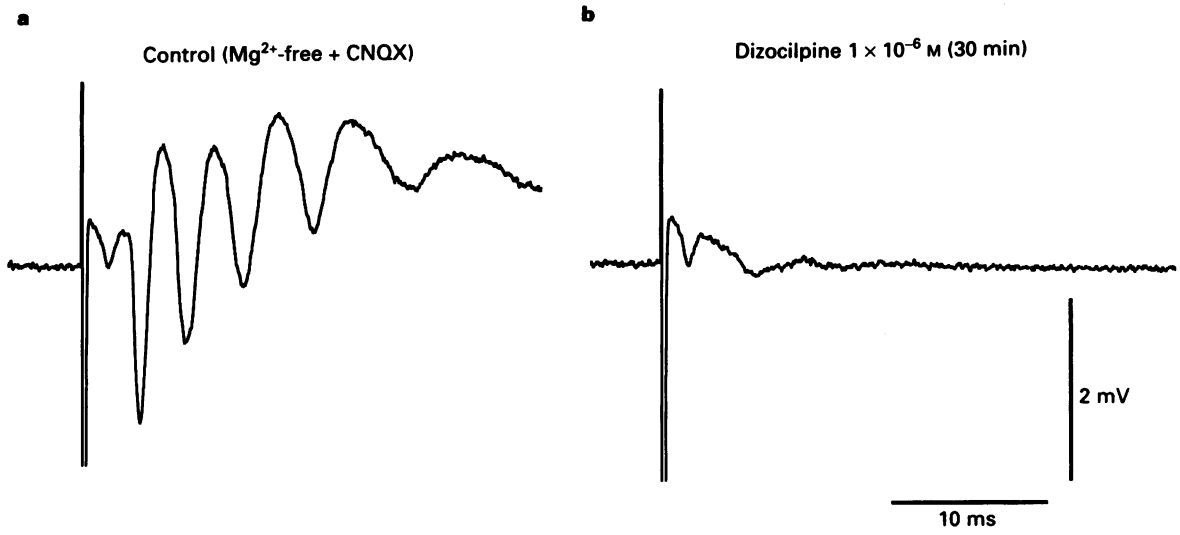

Figure 2 (a) Epileptiform response recorded in Mg^{2+}-free Krebs solution containing 5×10^{-6} M CNQX. (b) Superfusion with dizocilpine (10^{-6} M, 30 min) led to the disappearance of the epileptiform response.

3×10^{-7} M to 1×10^{-5} M, produced a concentration-dependent decrease in the amplitude of the first spike of the epileptiform response (Table 1 and Figure 3b) which readily reversed upon washout of the antagonist. The IC_{50} for this inhibition by D-CPP was 8.3×10^{-7} M. Figure 3a illustrates the effect of D-CPP on the epileptiform response in a single slice.

Validity of the epileptiform response as an assay for NMDA receptor/channel antagonists

Taken together, the antagonistic effects of the NMDA channel blocker, dizocilpine, and the competitive NMDA receptor antagonist, D-CPP, provide firm evidence that the epileptiform response is mediated exclusively by activation of NMDA receptors, thus validating the response as a suitable assay for antagonists at the NMDA receptor/channel complex.

Effect of phenytoin on the NMDA receptor-mediated epileptiform response

Phenytoin (0.1, 0.3 and 1×10^{-4} M, allowing 30 min equilibration at each concentration) was applied to a total of 7 hippocampal slices. The effect of phenytoin in one slice is shown in Figure 4 and a summary of its effects in all slices studied is shown in Table 1. Phenytoin had no statistically significant action on the amplitude of the first spike of the epileptiform response.

Effect of phenytoin on veratridine-induced loss of synaptic responsiveness

To confirm that the lack of effect of phenytoin against the NMDA receptor-mediated response was not due simply to a failure of phenytoin to achieve sufficient concentrations in the slice, we examined the effect of phenytoin on the loss of the CA1 population spike (recorded in normal Krebs solution) induced by the sodium channel activator, veratridine. In the absence of phenytoin, veratridine (2×10^{-6} M) induced a progressive decline of the population spike (90% reduction after 30 min perfusion with veratridine; $n = 3$ slices). However, following 30 min pretreatment with phenytoin (3×10^{-6} to 1×10^{-4} M) the effect of veratridine was attenuated in a concentration-dependent manner. The results from these experiments are summarized in Figure 5.

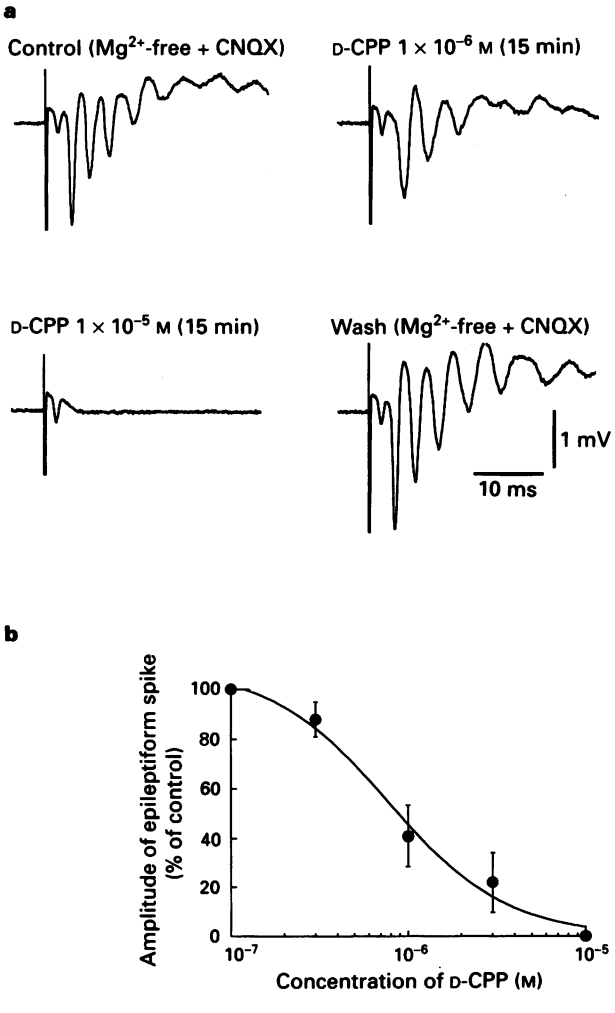

Figure 3 (a) Effect of D-CPP on the epileptiform responses recorded in a single slice superfused with Mg^{2+}-free Krebs solution containing 5×10^{-6} M CNQX. The response was concentration-dependently reduced by D-CPP and readily reversed on washout. (b) Effect of D-CPP on the amplitude of the first spike of the epileptiform response (each data point shows the mean ± s.e.mean from 4 slices). The smooth line was obtained from a fit to the Hill equation and yielded an IC_{50} of 8.3×10^{-7} M.

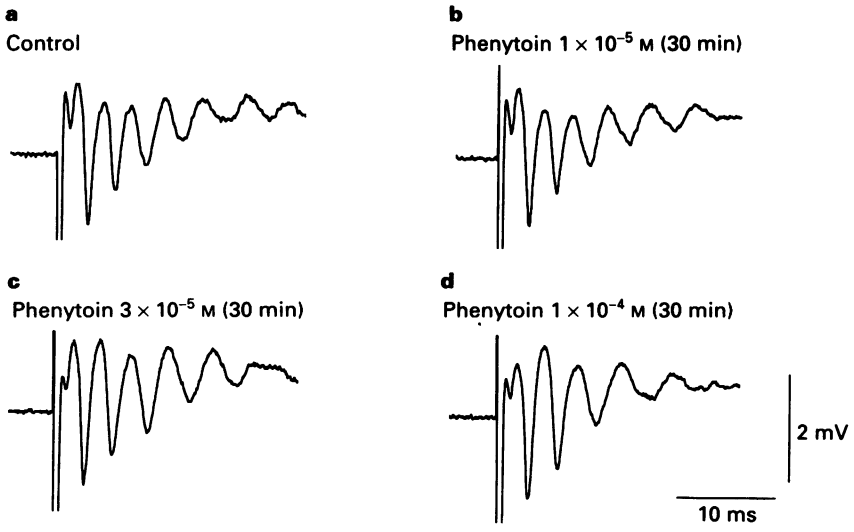

Figure 4 The effect of phenytoin (1×10^{-5} M, 3×10^{-5} M and 1×10^{-4} M) on the epileptiform response recorded in a single slice superfused with Mg^{2+}-free Krebs solution containing 5×10^{-6} M CNQX. Phenytoin was applied cumulatively, allowing 30 min at each of the 3 concentrations. In this slice phenytoin had no effect on the amplitude of the first spike of the epileptiform response. A summary of the effects of phenytoin in all slices studied is shown in Table 1.

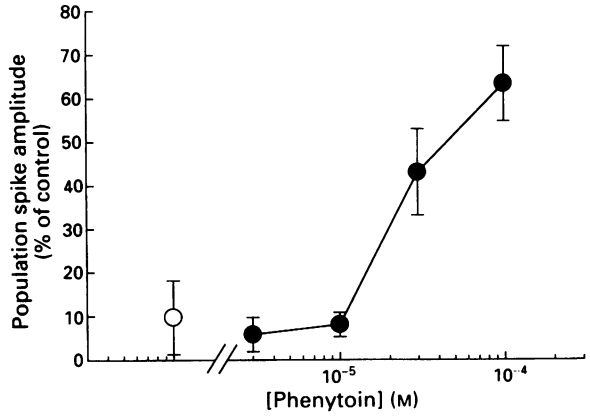

Figure 5 Effect of veratridine (2×10^{-6} M, 30 min) on the amplitude of the CA1 population spike in the absence (○) and in the presence (●) of phenytoin (3×10^{-6} M to 1×10^{-4} M). Phenytoin was present for 30 min before veratridine was applied and was present throughout the veratridine application. Each point represents the mean (± s.e.mean) effect recorded from 3 or 4 slices. These experiments were performed in standard Krebs solution.

Discussion

The anticonvulsant agent, phenytoin, has been used for over 50 years in the clinical management of partial and generalized tonic-clonic seizures. However, despite intensive research its mechanism of action is not definitively known (*see* Introduction). The present study was designed to establish whether a recently described inhibitory action of phenytoin on depolarizing responses of mouse spinal cord neurones to NMDA (Wamil & McLean, 1993) could be observed in a more relevant central nervous system tissue, the hippocampus.

Electrical stimulation of the Schaffer collateral/commissural pathway in hippocampal slices taken from a variety of species leads to the generation of the well-documented CA1 population spike. This response, which represents the extracellularly recorded synchronous depolarization of many CA1 neurones, is generated synaptically and results from liberation of excitatory amino acid neurotransmitter (glutamate and aspartate) from the presynaptic terminals of the Schaffer collateral fibres (Collingridge *et al.*, 1983; Fleck *et al.*, 1993). Under conventional recording conditions (normal Krebs solution and infrequent electrical stimulation of the Schaffer collateral fibres) the population spike is generated exclusively by activation of the AMPA glutamate receptor subtype, and the spike may be abolished by the selective AMPA receptor antagonist, CNQX (Andreasen *et al.*, 1989; Blake *et al.*, 1989). However, under certain experimental conditions it is possible to unmask a component of the postsynaptic response which is mediated by activation of NMDA receptors. Thus, high frequency stimulation of the Schaffer collateral/commissural pathway (Collingridge *et al.*, 1983) or removal of extracellular magnesium (Coan & Collingridge, 1985) leads to the appearance of a component of the response which is sensitive to inhibition by selective NMDA receptor antagonists. Under suitable conditions, therefore, it should be possible to record the NMDA receptor-mediated component in isolation, and thereby examine the effects of putative NMDA receptor/channel antagonists on the NMDA receptor-mediated postsynaptic CA1 response.

Previous attempts to establish an action of phenytoin on NMDA receptor-mediated responses in hippocampus have produced negative results. Both Stringer & Lothman (1988) and Birnstiel & Haas (1991) failed to observe an inhibition by phenytoin of long-term potentiation (LTP) in the CA1 region of the rat hippocampus *in vitro* (LTP is readily blocked by NMDA receptor/channel antagonists; Collingridge *et al.*, 1983). Furthermore, Psarropoulou & Haas (1989), also using the rat hippocampus *in vitro*, failed to find an effect of phenytoin on the CA1 population spike recorded in Mg^{2+}-free medium which they could attribute to an inhibition of NMDA-mediated responses. However, under the experimental conditions employed in the latter study the population spike was generated by a mixed synaptic activation of both AMPA and NMDA receptors, thereby possibly obscuring any potential antagonistic action of phenytoin on the NMDA receptor-mediated component.

In the present study, therefore, we reassessed the findings of Psarropoulou & Haas (1989) by examining the effects of phenytoin on a pure NMDA receptor-mediated synaptically-generated response in the rat hippocampus *in vitro*. To achieve this we used firstly the competitive AMPA antagonist, CNQX, to abolish the conventional AMPA

receptor-mediated CA1 population spike. Following this, superfusion with Mg^{2+}-free solution (combined with CNQX treatment) led to the unmasking of an epileptiform population response in CA1. Previous experiments have shown that the epileptiform spike is inhibited by Mg^{2+} with an IC_{50} of about 1×10^{-4} M (Sheridan, 1991). In the present study the first series of experiments was designed to characterize the epileptiform population spike in terms of its NMDA receptor pharmacology in order to validate the response as an assay for antagonists at the NMDA receptor/channel complex. This was achieved by demonstrating that both the NMDA channel blocker, dizocilpine (Wong *et al.*, 1986) and the competitive NMDA receptor antagonist, D-CPP (Lehmann *et al.*, 1987), could completely inhibit the epileptiform response, and that this action occurred at concentrations consistent with the known potencies of these compounds as NMDA antagonists. The inhibition by D-CPP reached a rapid equilibrium (within 5 min) and readily reversed upon washout. The effect of dizocilpine, however, took much longer to achieve equilibrium (20–30 min) and was not reversible within the time-course of the experiment (up to 60 min washout). The slow onset and lack of reversibility of the effect of dizocilpine are both consistent with the known use-dependent blocking and unblocking kinetics of the compound at the NMDA channel and are in agreement with the findings of others (Huettner & Bean, 1988; Halliwell *et al.*, 1989).

Having established the suitability of the epileptiform response as an NMDA antagonist assay, we next looked at the effects of phenytoin. The results obtained with dizocilpine and D-CPP in the present experiments suggested that quantification of the actions of potential NMDA antagonists would be best achieved by measuring drug-induced changes in the amplitude of the first spike in the epileptiform response. When looked at in this way, phenytoin, applied in concentrations ranging from 1×10^{-5} M to 1×10^{-4} M, failed to inhibit the epileptiform response. This lack of effect of phenytoin on NMDA receptor-mediated events is in good agreement with the findings of Stringer & Lothman (1988), Birnstiel & Haas (1991) and Psarropoulou & Haas (1989), but fail to support the conclusions of Wamil & McLean (1993). There are at least two potential reasons why the latter authors' findings conflict with those obtained in the present study. Firstly, the possibility exists that the receptor/channel complex mediating the effects of NMDA in mouse spinal cord neurones is different from that in rat hippocampus. There is growing evidence for the existence of several distinct molecular species of NMDA receptor (see review by Stone, 1993) and it is not inconceivable that these putative subtypes may be differentially affected by ion channel modulators like phenytoin. However, there is as yet no direct experimental evidence to support the contention that spinal and hippocampal NMDA receptors are different or that they are differentially affected by phenytoin. Secondly, the inhibitory effects of phenytoin on the response of spinal neurones to exogenously applied NMDA observed by Wamil & McLean (1993) may reflect a non-specific action of the anticonvulsant: the experiments were performed on 'current clamped' neurones and it is likely that the depolarizing responses to NMDA were mediated by a combination of cationic current flow through both the NMDA channel and voltage-dependent sodium and calcium channels. Block of sodium and calcium currents by phenytoin is well-established (*see* Introduction) and indeed an effect attributable to an action on sodium channels in 'current clamped' mouse spinal cord neurones *in vitro* has been described (McLean & Macdonald, 1983). Although Wamil & McLean (1993) still observed an inhibitory action of phenytoin in the presence of tetrodotoxin it remains likely that at least part of the depolarizing response to NMDA is mediated by current carried through voltage-dependent calcium channels, and that these channels may be sensitive to phenytoin. Resolution of the above issues will have to await examination of the effects of phenytoin on NMDA-induced currents in voltage clamped spinal neurones.

It is also conceivable that the lack of effect of phenytoin on the NMDA receptor-mediated response observed in the present study was due to physicochemical rather than to biological factors, and that phenytoin failed to penetrate the slice in sufficient concentrations. However, this possibility was discounted in experiments in which the effects of phenytoin on veratridine-induced failure of synaptic transmission were examined. In these experiments phenytoin (3×10^{-6} M to 1×10^{-4} M) markedly attenuated the effects of veratridine. Veratridine is an alkaloid neurotoxin that exerts its effects by shifting the current/voltage relation for sodium channel activation to more negative potentials, thereby inducing a persistent activation of the channel at membrane potentials where, in the absence of veratridine, the channel would normally be in a non-conducting state (Catterall, 1980). The protective effect of phenytoin against veratridine-induced loss of the CA1 population spike is therefore consistent with the sodium channel blocking property of the anticonvulsant. This finding also provides evidence that phenytoin is available to the tissue and that its failure to inhibit the NMDA receptor-mediated response represents a genuine absence of pharmacological effect.

In addition to its lack of effect on the amplitude of the first spike of the NMDA receptor-mediated response, phenytoin also failed to modify either the number or the amplitude of the subsequent spikes in the epileptiform event. Why this should be the case is not entirely clear. Phenytoin is known to exert its sodium channel blocking actions by selectively interacting with (and stabilizing) the inactivated state of the channel (Matsuki *et al.*, 1984; Willow *et al.*, 1985). Since the proportion of sodium channels in the inactivated state is dependent on the membrane potential, one consequence of this interaction is that the potency of phenytoin (in voltage-clamp studies) is directly related to the holding potential at which the experiments are performed. Thus, in voltage-clamped rat hippocampal CA1 neurones the concentration of phenytoin required to inhibit by 50% the sodium current evoked by a 15 ms depolarizing step to −10 mV is 2.6×10^{-4} M at a holding potential of −80 mV, whereas only 7×10^{-5} M is required at a holding potential of −70 mV (Kuo & Bean, 1994). It follows then that in a non-voltage clamped preparation (such as that used in the present study) the ability of phenytoin to inhibit sodium channel-dependent events will depend on the membrane potential of the neurones in that preparation. Given that the resting membrane potential of the neurones responsible for generating the hippocampal CA1 population spike is likely to be around −70 mV, one might expect phenytoin to exert an inhibitory effect both on the conventional population spike and on the NMDA receptor-mediated epileptiform response. Although we did not examine the effects of phenytoin on the conventional CA1 population spike in the present study, results from other workers have produced contrasting data. Stringer & Lothman (1988) failed to observe an effect of phenytoin (applied at a concentration of about 7×10^{-5} M) on the rat hippocampal CA1 population spike, whereas Griffith & Taylor (1988) found a small decrease in the slope of the rising phase of the rat hippocampal CA1 field e.p.s.p. produced by phenytoin (3×10^{-6}, and 1×10^{-4} M). Since the action of phenytoin is related to the neuronal resting membrane potential, it may be that whether or not an effect of phenytoin is seen is dependent on such factors as the metabolic state of the preparation and the extracellular potassium concentration. The failure in the present experiments to observe an effect of phenytoin on the epileptiform response may be explained by the possibility that CA1 neurones in our preparation have a resting membrane potential of, say, −80 mV, and that in order to see an effect we would have needed to use much higher concentrations of phenytoin (see earlier discussion). Although the resting membrane potential would determine the degree

of steady-state inactivation of the neuronal sodium channels in our preparation (and therefore the potency of phenytoin), there is clearly additional channel inactivation occurring during the neuronal activity underlying the epileptiform burst. However, it is likely that the duration (about 50 ms) and number of spikes (about 6) constituting the epileptiform event were not sufficient to allow the neuronal sodium channels to be in the inactivated state long enough for phenytoin to bind. This latter possibility is supported by the requirement in voltage clamp studies to depolarize the membrane for at least 1000 ms to detect phenytoin-induced shifts in the steady-state inactivation curve (see, for example, Kuo & Bean, 1994), whereas during the epileptiform response the sodium channels are likely to be inactivated (over-and-above the resting membrane potential-dependent inactivation) for less than 10 ms.

In conclusion, the failure in the present study to identify an antagonistic effect of phenytoin on NMDA receptor-mediated responses in rat hippocampus confirms and extends the findings of a number of previous studies. On the basis of these results it would be premature to attribute a component of the anticonvulsant activity of phenytoin to such an action at NMDA receptors.

References

ANDREASEN, M., LAMBERT, J.D. & JENSEN, M.S. (1989). Effects of new non-N-methyl-D-aspartate antagonists on synaptic transmission in the *in vitro* rat hippocampus. *J. Physiol.*, **414**, 317–336.

BIRNSTIEL, S. & HAAS, H.L. (1991). Anticonvulsants do not suppress long-term potentiation (LTP) in the rat hippocampus. *Neurosci. Lett.*, **122**, 61–63.

BLAKE, J.F., YATES, R.G., BROWN, M.W. & COLLINGRIDGE, G.L. (1989). 6-Cyano-7-nitroquinoxaline-2,3-dione as an excitatory amino acid antagonist in area CA1 of rat hippocampus. *Br. J. Pharmacol.*, **97**, 71–76.

CATTERALL, W.A. (1980). Neurotoxins that act on voltage-sensitive sodium channels in excitable membranes. *Annu. Rev. Pharmacol. Toxicol.*, **20**, 15–43.

COAN, E.J. & COLLINGRIDGE, G.L. (1985). Magnesium ions block an N-methyl-D-aspartate receptor-mediated component of synaptic transmission in rat hippocampus. *Neurosci. Lett.*, **53**, 21–26.

COLLINGRIDGE, G.L., KEHL, S.J. & MCLENNAN, H. (1983). Excitatory amino acids in synaptic transmission in the Schaffer collateral-commissural pathway of the rat hippocampus. *J. Physiol.*, **334**, 33–46.

DELORENZO, R.J. (1986). A molecular approach to the calcium signal in brain: relationship to synaptic modulation and seizure discharge. *Adv. Neurol.*, **44**, 435–464.

FLECK, M.W., HENZE, D.A., BARRIONUEVO, G. & PALMER, A.M. (1993). Aspartate and glutamate mediate excitatory synaptic transmission in area CA1 of the hippocampus. *J. Neurosci.*, **13**, 3944–3955.

GRIFFITH, W.H. & TAYLOR, L. (1988). Phenytoin reduces excitatory synaptic transmission and post-tetanic potentiation in the *in vitro* hippocampus. *J. Pharmacol. Exp. Ther.*, **246**, 851–858.

HALLIWELL, R.F., PETERS, J.A. & LAMBERT, J.J. (1989). The mechanism of action and pharmacological specificity of the anticonvulsant NMDA antagonist MK-801: a voltage clamp study on neuronal cells in culture. *Br. J. Pharmacol.*, **96**, 480–494.

HUETTNER, J.E. & BEAN, B.P. (1988). Block of N-methyl-D-aspartate-activated current by the anticonvulsant MK-801: selective binding to open channels. *Proc. Natl. Acad. Sci. U.S.A.*, **85**, 1307–1311.

KUO, C.-C. & BEAN, B.P. (1994). Slow binding of phenytoin to inactivated sodium channels in rat hippocampal neurones. *Mol. Pharmacol.*, **46**, 716–725.

LEHMANN, J., SCHNEIDER, J., MCPHERSON, S., MURPHY, D.E., BERNARD, P., TSAI, C., BENNETT, D.A., PASTOR, G., STEEL, D.J., BOEHM, C., CHENEY, D.L., LIEBMAN, J.M., WILLIAMS, M. & WOOD, P.L. (1987). CPP, a selective N-methyl-D-aspartate (NMDA)-type receptor antagonist: characterization *in vitro* and *in vivo*. *J. Pharmacol. Exp. Ther.*, **240**, 737–746.

MATSUKI, N., QUANDT, F.N., TEN EICK, R.E. & YEH, J.Z. (1984). Characterization of the block of sodium channels by phenytoin in mouse neuroblastoma cells. *J. Pharmacol. Exp. Ther.*, **228**, 523–530.

MCLEAN, M.J. & MACDONALD, R.L. (1985). Multiple actions of phenytoin on mouse spinal cord neurones in cell culture. *J. Pharmacol. Exp. Ther.*, **227**, 779–789.

PSARROPOULOU, C. & HAAS, H.L. (1989). Action of anticonvulsants on hippocampal slices in Mg-free medium. *Naunyn-Schmied. Arch. Pharmacol.*, **339**, 613–616.

ROGAWSKI, M.A. & PORTER, R.J. (1990). Antiepileptic drugs: pharmacological mechanisms and clinical efficacy with consideration of promising developmental stage compounds. *Pharmacol. Rev.*, **42**, 223–285.

SHERIDAN, R.D. (1991). Antagonism by magnesium of N-methyl-D-aspartate (NMDA) receptor-mediated responses in rat hippocampus *in vitro*. *Fund. Clin. Pharmacol.*, **5**, 445.

SHERIDAN, R.D. & SUTOR, B. (1990). Presynaptic M_1 muscarinic cholinoceptors mediate inhibition of excitatory synaptic transmission in the hippocampus *in vitro*. *Neurosci. Lett.*, **108**, 273–278.

SHERIDAN, R.D., LAFFLING, A.J., MCGIVERN, J.G. & PATMORE, L. (1994). Does inhibition of N-methyl-D-aspartate (NMDA) receptor-mediated responses contribute to the anticonvulsant action of phenytoin? *Br. J. Pharmacol.*, **113**, 32P.

STONE, T.W. (1993). Subtypes of NMDA receptors. *Gen. Pharmacol.*, **24**, 825–832.

STRINGER, J.L. & LOTHMAN, E.W. (1988). Phenytoin does not block hippocampal long-term potentiation or frequency potentiation. *Ann. Neurol.*, **23**, 281–286.

TOMASELLI, G.F., MARBAN, E. & YELLEN, G. (1989). Sodium channels from human brain RNA expressed in Xenopus oocytes. Basic electrophysiologic characteristics and their modification by diphenylhydantoin. *J. Clin. Invest.*, **83**, 1724–1732.

TWOMBLY, D.A., YOSHII, M. & NARAHASHI, T. (1988). Mechanisms of calcium channel block of phenytoin. *J. Pharmacol. Exp. Ther.*, **246**, 189–195.

WAMIL, A.J. & MCLEAN, M.J. (1993). Phenytoin blocks N-methyl-D-aspartate responses of mouse central neurons. *J. Pharmacol. Exp. Ther.*, **267**, 218–227.

WILLOW, M., GONOI, T. & CATTERALL, W.A. (1985). Voltage-clamp analysis of the inhibitory actions of diphenylhydantoin and carbamazepine on voltage-sensitive sodium channels in neuroblastoma cells. *Mol. Pharmacol.*, **27**, 549–558.

WONG, E.H.F., KEMP, J.A., PRIESTLEY, T., KNIGHT, A.R., WOODRUFF, G.N. & IVERSEN, L.L. (1986). The anticonvulsant MK-801 is a potent N-methyl-D-aspartate antagonist. *Proc. Natl. Acad. Sci. U.S.A.*, **83**, 7104–7108.

(Received September 26, 1994
Revised January 11, 1995
Accepted January 24, 1995)

British Journal of Pharmacology (1995) 115, 73-76

Blockade by ONO-NT-012, a unique prostanoid analogue, of prostaglandin E_2-induced allodynia in conscious mice

*†Toshiaki Minami, *†Isao Nishihara, †Kazuichi Sakamoto, [1]†‡Seiji Ito, *Masayoshi Hyodo & †Osamu Hayaishi

*Department of Anaesthesiology, Osaka Medical College, Takatsuki 569; †Department of Cell Biology, Osaka Bioscience Institute, Suita 565 and ‡Department of Medical Chemistry, Kansai Medical University, Moriguchi 570, Japan

1 Intrathecal (*i.t.*) administration of prostaglandin E_2 (PGE_2) to conscious mice was reported to induce allodynia, a state of discomfort and pain evoked by innocuous tactile stimuli through prostaglandin E receptor subtype EP_1 and hyperalgesia through prostaglandin E receptor subtypes EP_2 and/or EP_3. In the present study, we investigated the effects of an EP_1 antagonist on these sensory disorders by use of ONO-NT-012 or AH6809.

2 ONO-NT-012 dose-dependently antagonized the PGE_2-induced allodynia but had no effect on the PGE_2-induced hyperalgesia by the hot plate test. On the other hand, AH6809 blocked the PGE_2-induced hyperalgesia at the highest dose examined (50 $\mu g\ kg^{-1}$) but had no effect on the PGE_2-induced allodynia. The *i.t.* injection of AH6809 or ONO-NT-012 alone did not have any effect on the response to noxious or innocuous stimuli.

3 Increasing doses (5 $pg\ kg^{-1}$-500 $ng\ kg^{-1}$) of ONO-NT-012 produced parallel shifts to the right of the dose-response curves to PGE_2. The Schild plot regression line was linear and the slope was close to unity. The pA_2 value against PGE_2 was calculated to be 9.96.

4 The present study demonstrates that *i.t.* administration of PGE_2 exerts allodynia through EP_1 in the mouse spinal cord and that ONO-NT-012 is a highly potent, simple competitive antagonist for the PGE_2-induced allodynia.

Keywords: ONO-NT-012; EP_1 antagonist; allodynia; hyperalgesia; spinal cord

Introduction

We recently reported that intrathecal (*i.t.*) administration of prostaglandin E_2 (PGE_2) to conscious mice induced allodynia, a state of discomfort and pain evoked by innocuous tactile stimuli: the mice showed squeaking, biting, and scratching movements in response to low-threshold stimuli, and hyperalgesia by the hot plate test (Minami *et al.*, 1994c).

PGE_2 produces a broad range of biological actions in diverse tissues through its binding to specific receptors on plasma membranes (Coleman *et al.*, 1987; 1989; Campbell, 1990). EP-receptors are pharmacologically divided into at least three subtypes, EP_1, EP_2, and EP_3; and are considered to be coupled to Ca^{2+} mobilization and stimulation and inhibition of adenylate cyclase, respectively. The diversity of PGE_2 actions could be ascribed to EP-receptor subtypes coupled to different signal transduction pathways. We have demonstrated, on the basis of data obtained with 7 synthetic prostanoid analogues, that PGE_2 might exert allodynia through EP_1-receptors and hyperalgesia through EP_2- and/or EP_3-receptors in the mouse spinal cord (Minami *et al.*, 1994b). Confirmation of this conclusion has however been hampered by the lack of selective EP-receptor subtype antagonists. Previously, EP-receptors in isolated tissues that are susceptible to blockade by SC19220 and AH6809 were designated as EP_1-receptors (Coleman *et al.*, 1985). AH6809 was also a prostaglandin D_2-receptor specific blocking agent in human platelets and some cultured cells (Keery & Lumley, 1988; Ito *et al.*, 1990). ONO-NT-012 has recently been reported to be a unique compound with both EP_1/thromboxane A_2-receptor antagonist activity and EP_3-receptor agonist activity (Maruyama *et al.*, 1994). In the present study, we investigated the effects of ONO-NT-012 or AH6809 on the PGE_2-induced allodynia and hyperalgesia.

[1] Author for correspondence.

Methods

Intrathecal administration

Male ddY-mice weighing 22 ± 2 g were used in this study. The animals were housed under conditions of a 12-h light-dark cycle and a constant temperature of 22 ± 2°C and 60 ± 10% humidity. In order to insert a needle quickly and accurately, we incised the skin on the back (1 cm circumference) and inserted a 27-gauge stainless-steel needled (0.35 mm, o.d.) attached to a microsyringe between L_5 and L_6 vertebrae by the method of Hylden & Wilcox (1980). Drugs in vehicle were injected slowly into the subarachnoid space of conscious mice at 22 ± 2°C. The volume of the *i.t.* injection was 5 µl. It was previously confirmed by use of Commassie brilliant blue and [^{3}H]-PGE_2 that the injected solution does not extend to the cervical segments (Uda *et al.*, 1990).

Studies on allodynia

Studies on allodynia were carried out essentially according to the method of Yaksh & Harty (1988). The mice were divided into various groups ($n = 6-8$ per group). Control mice were given physiological saline (5 µl). Drug-treatment groups were injected with 5 µl of vehicle containing various doses of test agents. After the *i.t.* injection, each mouse was placed in an individual 13 × 8.5 × 13 cm Plexiglas enclosure with wood chips on the floor and observed. Allodynia was assessed once every 5 min over a 50-min period by light stroking of the flank of the mice with a paintbrush. The allodynia response was ranked as follows: (0) no response; (1) mild squeaking with attempts to move away from the stroking probe; (2) vigorous squeaking evoked by the stroking probe, biting at the probe, and strong efforts to escape.

To evaluate the effects of the agents on allodynia, the values obtained over the 50-min test period were cumulated and expressed as a percentage of the maximum possible

score. Thus, the maximum possible score for allodynia per animal was 20.

Hot plate test

Mice were placed on a hot plate maintained at 55°C, and the elapsed time until the mice showed the first avoidance responses (licking the feet, jumping, or rapidly stamping the paws) was recorded as described by Woolfe & MacDonald (1944). The response time of the mice to the hot plate was measured at 30 min after *i.t.* injection.

The animals were used only for one measurement in each experiment. This study was conducted in accordance with the guidelines of the Ethics Committee of the International Association for the Study of Pain (Zimmermann, 1983).

Drugs

PGE_2 and ONO-NT-012 (5(Z)-7-[(1S, 2S, 3S, 5R)-3-(*trans*-β-styren) sulphonamido-6,6-dimethylbicyclo (3.1.1) hept-2-yl]-5-heptenoic acid) were generous gifts from Ono Central Research Institute (Osaka, Japan). PGE_2 and ONO-NT-012 were stored in ethanol solution at −20°C. For injection, an aliquot of the desired stock PGE_2 or ONO-NT-012 solution was placed in a borosilicate tube and the ethanol was removed by evaporation to dryness under nitrogen gas. Sterile saline was then added to dissolve the PGE_2 or ONO-NT-012. AH6809 (6-isopropoxy-9-oxoxanthene-2-carboxylic acid) was kindly provided by Glaxo Group Research Ltd. (Hertfordshire, U.K.). AH6809 was dissolved and diluted in 1% $NaHCO_3$ in 0.9% NaCl (saline). All solutions were kept on ice until used. All drugs, including saline, were coded to assure 'blind' testing.

Statistics

The statistical analyses were carried out by analysis of variance (ANOVA). Statistical significance ($P<0.05$) was further examined with Duncan's test for multiple comparison. IC_{50} values with 95% confidence limits (95% CL) were calculated by use of a computerized Probit test.

Results

Effect of AH6809 or ONO-NT-012 on PGE_2-evoked allodynia

In order to examine the effect of EP_1-receptor antagonists on the PGE_2-induced allodynia, we used AH6809 and ONO-NT-012. When assessed by a cumulative score during the 50 min period, the allodynia caused by PGE_2, 0.5 μg kg^{-1}, was dose-dependently blocked by ONO-NT-012 with IC_{50} values (95% CL) of 1.04 ng kg^{-1} (477 pg kg^{-1}–2.03 ng kg^{-1}). On the other hand, AH6809 had little effect on the PGE_2-induced allodynia at doses up to 50 μg kg^{-1} (Figure 1). ONO-NT-012 produced parallel and dose-dependent rightward shifts in the dose-response curve to PGE_2 (Figure 2a). A Schild plot analysis was carried out based on these data, by which dose-ratios were calculated at a response intersecting all curves obtained with 5 pg kg^{-1}–0.5 μg kg^{-1} ONO-NT-012 (representing 20% of the maximum possible cumulative score over the 50-min period). As shown in Figure 2b, a Schild plot regression line revealed a linear relationship and the slope was close to unity. The pA_2 value against PGE_2 was 9.96.

These results indicate that ONO-NT-012 is a simple and competitive antagonist of PGE_2-induced allodynia in the spinal cord.

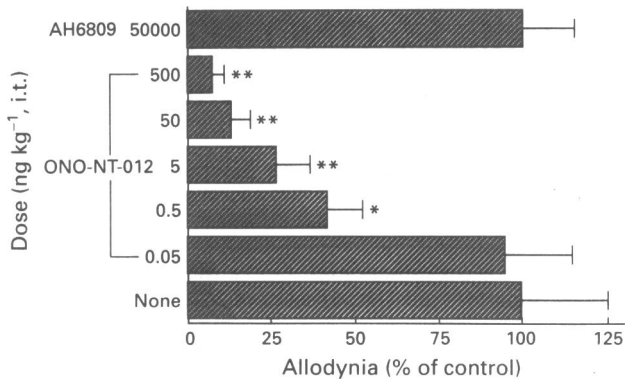

Figure 1 Effect of AH6809 or ONO-NT-012 on prostaglandin E_2 (PGE_2)-induced allodynia. PGE_2 (0.5 μg kg^{-1}) was injected simultaneously with various doses of AH6809 or ONO-NT-012 into the subarachnoid space. Assessment of allodynia was made as described under Methods. The score of PGE_2 alone was taken as 100%. The values shown are the mean ± s.e.mean ($n = 6$). Statistical analyses were carried out by Duncan's test. *$0.01 \leq P < 0.05$, **$P < 0.01$, as compared with PGE_2-injected group.

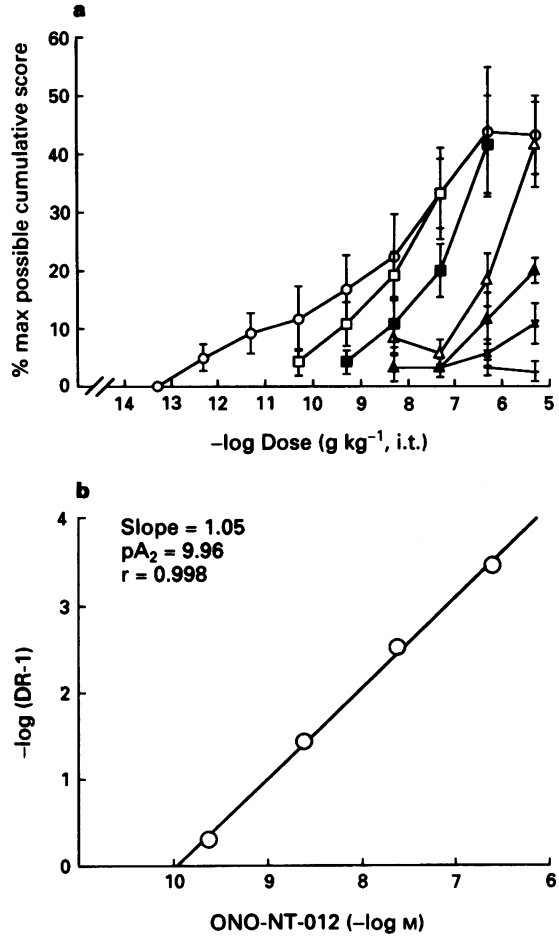

Figure 2 Effect of ONO-NT-012 on prostaglandin E_2 (PGE_2)-induced allodynia. (a) Dose-response curves of ONO-NT-012 for the PGE_2-induced allodynia. PGE_2 was injected simultaneously without (○) or with 0.5 μg kg^{-1} (+), 50 ng kg^{-1} (×), 5 ng kg^{-1} (▲), 0.5 ng kg^{-1} (△), 50 pg kg^{-1} (■), or 5 pg kg^{-1} (□) ONO-NT-012 into the subarachnoid space. Assessment of allodynia was made as described under Methods. The values shown are the mean ± s.e. mean ($n = 6$–8). (b) Schild plot analysis for the antagonism of response to PGE_2 by ONO-NT-012. DR, dose-ratio, i.e., the ratio of the dose of the PGE_2 required to produce 20% of the maximum possible cumulative score over the 50-min period of the PGE_2-induced allodynia in the presence of a given dose of ONO-NT-012 to that without ONO-NT-012. The best fit to the line and the correlation coefficient (r) were calculated by linear least squares regression.

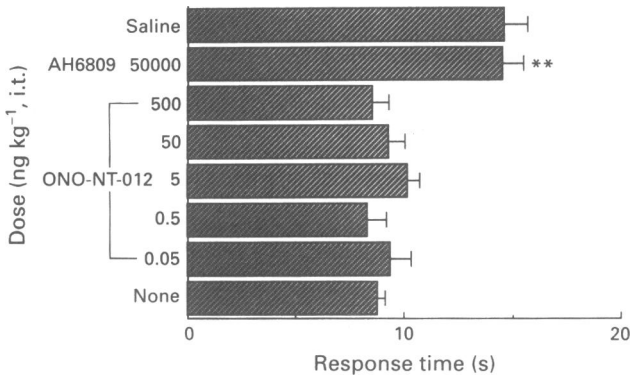

Figure 3 Effect of AH6809 or ONO-NT-012 on prostaglandin E_2 (PGE_2)-induced hyperalgesia. PGE_2 (0.5 μg kg^{-1}) was injected simultaneously with various doses of AH6809 or ONO-NT-012 into the subarachnoid space. The time until the mice showed the first avoidance response to the hot plate test (55°C) was measured at 30 min after *i.t.* injection. Each column represents the mean ± s.e. mean of responses in 10 mice. Statistical analyses were carried out by Duncan's test. $^{**}P < 0.01$, as compared with the PGE_2-injected group.

Effect of AH6809 or ONO-NT-012 on PGE_2-evoked hyperalgesia

As reported previously (Uda *et al.*, 1990), PGE_2-induced hyperalgesia was observed between 3 and 30 min after *i.t.* injection of PGE_2. In the present study, the response time of mice to the hot plate (55°C) was measured at 30 min after *i.t.* injection of PGE_2 or vehicle so that the effect of PGE_2-induced allodynia would be minimized. There was no significant difference in the latency period between the saline control (14.7 ± 1.1 s, mean ± s.e.mean) and the untreated control (15.4 ± 0.9 s). As reported previously (Minami *et al.*, 1994c), PGE_2 produced its hyperalgesic action over a wide range of doses from 50 pg kg^{-1} to 0.5 μg kg^{-1} with two apparent hyperalgesic peaks at 0.5 ng kg^{-1} (11.0 ± 0.7 s) and 0.5 μg kg^{-1} (8.8 ± 0.4 s). The hyperalgesia caused by 0.5 μg kg^{-1} of PGE_2 was not blocked by ONO-NT-012 at all. On the other hand, the hyperalgesia caused by 0.5 μg kg^{-1} of PGE_2 was blocked by AH6809 at the highest dose examined (50 μg kg^{-1}) (Figure 3).

The *i.t.* injection of ONO-NT-012 or AH6809 alone did not have any effects on the response to noxious or innocuous stimuli.

Discussion

We recently reported that the *i.t.* administration of PGE_2 to conscious mice induced allodynia and hyperalgesia (Uda *et al.*, 1990; Minami *et al.*, 1994a, c) and that PGE_2 might exert allodynia through the EP_1-receptor and hyperalgesia through EP_2- and/or EP_3-receptors in the mouse spinal cord (Minami *et al.*, 1994b). In the present study, the effects of ONO-NT-012 (a novel EP_1/thromboxane A_2-receptor antagonist and EP_3-receptor agonist) on two pain models of PGE_2-induced allodynia and hyperalgesia were tested and compared with those of AH6809. The PGE_2-induced allodynia was dose-dependently blocked by ONO-NT-012, but not by AH6809 (Figure 1). On the other hand, the PGE_2-induced hyperalgesia assessed by the hot plate test was blocked by AH6809, but not by ONO-NT-012 (Figure 3). The pA_2 value of ONO-NT-012 against PGE_2 was 9.96 (Figure 2b) *i.e.* much smaller than that reported previously with longitudinal smooth muscle of guinea-pig ileum ($pA_2 = 5.7$) (Maruyama *et al.*, 1994). EP-receptors in isolated tissues that are susceptible to blockade by SC19220 and AH6809 were designated as EP_1-receptors (Coleman *et al.*, 1985). Recently the EP_1-receptor was cloned from the mouse lung cDNA library but AH6809 showed only weak inhibition of binding of [^{3}H]-PGE_2 to membranes prepared from EP_1-receptor cDNA-transfected CHO cells (Watabe *et al.*, 1993). Therefore it was suggested that there may be another form of EP_1-receptor besides one sensitive to AH6809 or that the action of AH6809 is species-specific with little effect on the mouse receptor.

In conclusion, the present study demonstrates that ONO-NT-012 is a potent, competitive, and selective antagonist for PGE_2-induced allodynia. In addition to conventional nociceptive tests such as the tail-flick test, formalin test, and hot plate test, allodynia induced by *i.t.* injection of prostaglandins provides a new model of pain when testing the efficacy of analgesic agents in animals.

We would like to thank Dr Toru Oku for statistical analysis. This work was supported in part by Grant-in-Aid for Scientific Research on Priority Areas, for Scientific Research (B) (06454171) and (C) (06670177), and for Encouragement of Young Scientists (06671243) from the Ministry of Education, Science, and Culture of Japan, and by grants from the Ono Medical Research Foundation, Yamanouchi Foundation for Research on Metabolic Disorders, the Naito Foundation, and Takeda Science Foundation.

References

CAMPBELL, W.B. (1990). Lipid-derived autacoids: eicosanoids and platelet-activating factor. In *The Pharmacological Basis of Therapeutics*, 8th Ed., ed. Gilman, A.G., Rall, T.W., Nies, A.S. & Taylor, P. pp. 600–617. New York: Pergamon Press.

COLEMAN, R.A., KENNEDY, I., HUMPHREY, P.P.A., BUNCE, K. & LUMLEY, P. (1989). Prostanoids and their receptors. In *Comprehensive Medical Chemistry. The Rational Design, Mechanistic Study and Therapeutic Application of Chemical Compounds*. Vol. 3. ed. Hansch, C., Sammes, P.G., Taylor, J.B. & Emmett, J.C. pp. 643–714. Oxford: Pergamon Press.

COLEMAN, R.A., KENNEDY, I. & SHELDRICK, R.L.G. (1985). AH6809, a prostanoid EP_1-receptor blocking drug. *Br. J. Pharmacol.*, **85**, 273P.

COLEMAN, R.A., KENNEDY, I. & SHELDRICK, R.L.G. (1987). Evidence for the existence of three subtypes of PGE_2 (EP) sensitive receptors in smooth muscle. *Br. J. Pharmacol.*, **91**, 323P.

HYLDEN, J.L.K. & WILCOX, G.L. (1980). Intrathecal morphine in mice: a new technique. *Eur. J. Pharmacol.*, **67**, 313–316.

ITO, S., OKUDA, E., SUGAMA, K., NEGISHI, M. & HAYAISHI, O. (1990). Evaluation of ZK110841 and AH6809, an agonist and an antagonist of prostaglandin DP-receptors on human platelets, with a PGD_2-responsive cell line from bovine embryonic trachea. *Br. J. Pharmacol.*, **99**, 13–14.

KEERY, R.J. & LUMLEY, P. (1988). AH6809, a prostaglandin DP-receptor blocking drug on human platelets. *Br. J. Pharmacol.*, **94**, 745–754.

MARUYAMA, T., KOUKETU, M., TOKUMOTO, H., KONDO, K. & HAMANAKA, N. (1994). ONO-NT-012, an unique prostanoid receptor agonist (EP_3) & antagonist (EP_1, TP), *Abstract for the 9th International. Conference on Prostaglandins and Related Compounds*, 88p.

MINAMI, T., NISHIHARA, I., UDA, R., ITO, S., HYODO, M. & HAYAISHI, O. (1994a). Involvement of glutamate receptors in allodynia induced by prostaglandins E_2 and $F_{2\alpha}$ injected into conscious mice. *Pain*, **57**, 225–231.

MINAMI, T., NISHIHARA, I., UDA, R., ITO, S., HYODO, M. & HAYAISHI, O. (1994b). Characterization of EP-receptor subtypes involved in allodynia and hyperalgesia induced by intrathecal administration of prostaglandin E_2 to mice. *Br. J. Pharmacol.*, **112**, 735–740.

MINAMI, T., UDA, R., HORIGUCHI, S., ITO, S., HYODO, M. & HAYAISHI, O. (1994c). Allodynia evoked by intrathecal administration of prostaglandin E_2 to conscious mice. *Pain*, **57**, 217–223.

UDA, R., HORIGUCHI, S., ITO, S., HYODO, M. & HAYAISHI, O. (1990). Nociceptive effects induced by intrathecal administration of prostaglandin D_2, E_2 or $F_{2\alpha}$ to conscious mice. *Brain Res.*, **510**, 26–32.

WATABE, A., SUGIMOTO, Y., HONDA, A., IRIE, A., NAMBA, T., NEGISHI, M., ITO, S., NARUMIYA, S. & ICHIKAWA, A. (1993). Cloning and expression of cDNA for a mouse prostaglandin E receptor EP_1 subtype. *J. Biol. Chem.*, **268**, 20715–20718.

WOOLFE, G. & MACDONALD, A.D. (1944). The evaluation of the analgesic action of pethidine hydrochloride (Demerol). *J. Pharmacol. Exp. Ther.*, **80**, 300–307.

YAKSH, T.L. & HARTY, G.J. (1988). Pharmacology of the allodynia in rats evoked by high dose intrathecal morphine. *J. Pharmacol. Exp. Ther.*, **244**, 501–507.

ZIMMERMANN, M. (1983). Ethical guidelines for investigations of experimental pain in conscious animals. *Pain*, **16**, 109–110.

(Received November 16, 1994
Revised January 18, 1995
Accepted January 24, 1995)

British Journal of Pharmacology (1995) 115, 77-80

Modulation of epidermal growth factor effects on epithelial ion transport by intestinal trefoil factor

R. Chinery & [1]H.M. Cox

Department of Pharmacology, The Royal College of Surgeons of England, 35-43, Lincoln's Inn Fields, London WC2A 3PN

1 The direct epithelial effects of epidermal growth factor (EGF) and its modulation by intestinal trefoil factor (ITF) have been studied in a human colonic adenocarcinoma cell line called Colony-29 (Col-29).

2 When grown in culture as confluent monolayers and voltage-clamped in Ussing chambers, these epithelia responded with an increase in short circuit current (SCC) to basolateral as well as to apically applied EGF although the latter responses (at 10 nM) were only 25% of those observed following basolateral peptide.

3 Recombinant rat ITF (added to the basolateral surface) did not alter basal SCC levels, but it did enhance the electrogenic effects of basolateral EGF. The EC_{50} values for EGF-induced ion transport were 0.25 nM in control, and 0.26 nM in ITF pretreated Col-29 epithelia. A significant increase in the size of EGF responses (0.1 nM-10 nM) was observed in the presence of 10 nM ITF and the half-maximal concentration for this modulatory effect of ITF was 7.6 nM.

4 The EGF-induced increases in SCC were partially inhibited (50%) by piretanide pretreatment, indicating that Cl^- secretion is involved. EGF responses either in the presence or absence of ITF were also significantly reduced (84% and 66% respectively) by the cyclo-oxygenase inhibitor, piroxicam, therefore implicating prostaglandins as mediators of EGF-stimulated anion secretion.

5 We conclude that in confluent Col-29 epithelia, basolateral EGF stimulates a predominantly prostaglandin-dependent increase in Cl^- secretion that is enhanced by basolateral ITF, and that these two peptides may interact in normal and damaged mucosa to alter the local apical solute and fluid environment.

Keywords: Epidermal growth factor; intestinal trefoil factor; electrogenic ion transport

Introduction

Epidermal growth factor (EGF) has been observed to exert acute effects upon intestinal solute and fluid secretion, for example, increasing glucose-stimulated Na^+ absorption in the rabbit jejunum (Opleta-Madsen *et al.*, 1991). Specific receptors for EGF have been identified along the length of the intestine in basolateral as well as microvillar membranes (Thompson, 1988). Autoradiographic studies with rat small intestine have shown that [^{125}I]-EGF labels columnar and goblet cells of villi and crypts (Chabot *et al.*, 1982) and a quantitative analysis of the crypt-villus axis in the mouse jejunum has identified three times the level of EGF binding in crypt versus villus cells (Gallo-Payet & Hugon, 1985). Activation of the EGF receptor results in tyrosine autophosphorylation (for review see Hernandez-Sotomayor & Carpenter, 1992) and this mechanism is pivotal in the mitogenic effects of EGF.

Another group of structurally distinct proteins are the trefoil peptides whose regional expression along the gastrointestinal tract and up-regulation at sites of ulceration (Poulsom & Wright, 1993) implicates them as important factors involved in restitutive mucosal mechanisms. Recent studies of one of these peptides, namely intestinal trefoil factor (ITF) have shown that it stimulates motogenic rather than mitogenic effects in gastrointestinal epithelia (Dignass *et al.*, 1994; Chinery & Playford, 1995). The aim of the present study was to investigate epithelial interactions between these two mucosal peptides in an adenocarcinoma cell line, Colony-29, which when grown as a monolayer (devoid of other mucosal cell types) exhibits characteristic changes in ion transport when stimulated by different selective agonists (MacVinish *et al.*, 1993; Cox & Tough, 1994). The sidedness of EGF responses in this cell line and the mediators involved in EGF effects upon ion transport both alone and following pretreatment with ITF were also studied.

Methods

Colony-29 (Col-29) epithelia were grown and maintained in Dulbecco's modified Eagles medium supplemented with foetal calf serum (10%), kanamycin (100 $\mu g\,ml^{-1}$) and amphotericin B (1.2 $\mu g\,ml^{-1}$) as described in detail previously (Cuthbert *et al.*, 1987). For voltage-clamp studies cells were seeded onto 0.2 cm^2 areas of collagen-coated Millipore filters (0.45 μm) and formed confluent monolayers within 7-10 days. Each filter with epithelia was placed between two halves of an Ussing chamber, bathed in oxygenated (95% O_2/5% CO_2) Krebs-Henseleit solution at 37°C and short-circuited with a W-P dual-voltage clamp. The resulting short circuit current (SCC, quoted as $\mu A\,cm^{-2}$) was monitored continuously and peak changes in SCC occurring within 7 min of peptide addition to either the basolateral or apical reservoir were recorded. The Krebs-Henseleit buffer had the following composition (in mM): NaCl 118, KCl 4.7, $CaCl_2$ 2.5, $MgSO_4$ 1.2, KH_2PO_4 1.2, $NaHCO_3$ 25.0 and glucose 11.1. The means ± 1 s.e.mean of peak changes in SCC from different data groups were analysed statistically by Student's unpaired *t* tests. Concentration-response curves were constructed from single additions of peptide made to the basolateral surface of each monolayer, and EC_{50} values were obtained by applying pooled data to the iterative curve-fitting programme, Graphpad.

All chemicals were of reagent grade and drugs were obtained from the following sources: recombinant human EGF, piroxicam and acetazolamide were purchased from

[1] Author for correspondence.

Sigma Chemical Company Ltd (Poole, Dorset) and piretanide was a generous gift from Hoechst Pharmaceuticals (Hounslow, Middx). Recombinant rat ITF was produced using the expression vector, pGEX-3X and maintained in *E. coli*. Purification of rat ITF was achieved by conventional techniques (Gearing *et al.*, 1989) with the exception of the cleavage of fusion protein, which utilised blood coagulation factor Xa.

Results

Col-29 epithelia exhibited a basal SCC of $4.1 \pm 0.8\ \mu A\ cm^{-2}$ ($n = 59$) and resistance of $61.1 \pm 5.3\ \Omega cm^2$ ($n = 59$). Addition of EGF (10 nM, a maximal concentration) to the basolateral surface resulted in a relatively slow rise in SCC reaching a peak ($2.1 \pm 0.3\ \mu A\ cm^{-2}$ above baseline, $n = 11$) within 7 min (Figure 1) and remaining elevated for at least 30 min. The sidedness of EGF responses was investigated by comparing EGF-induced increases in SCC following addition of the peptide to both or to one surface, either apical or basolateral (Figure 2). There was no significant difference between the size of EGF (10 nM) responses following peptide addition to both sides simultaneously, compared with those following basolateral EGF either alone or after pretreatment with apical EGF. Peak apical EGF responses (10 nM) were 25% of control basolateral responses ($P<0.01$) and the former were abolished by prior exposure to basolateral peptide ($P<0.01$, Figure 2).

Pretreatment of monolayers with ITF (10 nM, basolateral) did not significantly alter basal SCC levels *per se* (Figure 3) but the trefoil did significantly ($P<0.03-0.001$) enhance responses to EGF at concentrations from 0.1 nM to 10 nM (Figures 1 and 3). The control EGF concentration-response profile (Figure 3) exhibited an EC_{50} of 0.25 nM with a maximal effect (at 1 nM EGF) of $2.2 \pm 0.2\ \mu A\ cm^{-2}$ ($n = 8$). In the presence of 10 nM ITF the EC_{50} for EGF was unchanged at 0.26 nM but the maximum (at 1 nM) was increased significantly ($3.3 \pm 0.1\ \mu A\ cm^{-2}$, $n = 4$, $P<0.01$). The potency with which ITF modulated basolateral EGF responses was assessed by using the maximally effective EGF concentration (1 nM) and varying that of ITF (Figure 4). An EC_{50} value of 7.6 nM was obtained for ITF, with a maximal modulatory effect at 30 nM ITF (following which EGF responses were $3.7 \pm 0.4\ \mu A\ cm^{-2}$, $n = 4$, $P<0.01$ compared with 1 nM EGF responses in the absence of ITF).

The Na,K,2Cl cotransport inhibitor, piretanide (200 μM, basolateral) reduced basal SCC levels (by $-1.1 \pm 0.1\ \mu A\ cm^{-2}$, $n = 23$) and significantly inhibited EGF responses whether in the presence or absence of ITF. Pretreatment with the cyclo-oxygenase inhibitor, piroxicam (5 μM, added to both sides, which reduced basal SCC by $-2.0 \pm 0.2\ \mu A\ cm^{-2}$, $n = 12$) also significantly reduced EGF responses ($P<0.01$). The combination of piretanide and piroxicam virtually abolished EGF responses in the presence of 10 nM ITF ($P<0.01$, compared with controls) while in monolayers exposed to EGF alone this same combination of inhibitors reversed the polarity of EGF responses (Figures 1, 5a and b). There was no significant difference between these EGF responses (plus piretanide and piroxicam, either with or without ITF) and those observed following co-administration of the carbonic anhydrase inhibitor, acetazolamide (450 μM to both sides, and which alone attenuated basal SCC by $-0.4 \pm 0.1\ \mu A\ cm^{-2}$, $n = 6$).

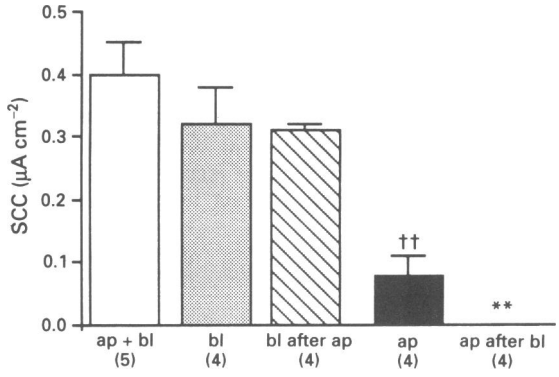

Figure 2 The sidedness of epidermal growth factor (EGF) responses in Col-29 epithelia. The peak increases in SCC to EGF (10 nM) applied to either the basolateral (bl) or apical (ap) surface or to ap + bl, were recorded within 7 min of peptide addition. Each column represents the mean + 1 s.e.mean from 4 observations in all columns except EGF ap + bl which was $n = 5$. Significant differences were observed between apical EGF alone and apical following basolateral EGF (**$P<0.01$) and comparing the means of apical EGF versus basolateral EGF alone (††$P<0.01$).

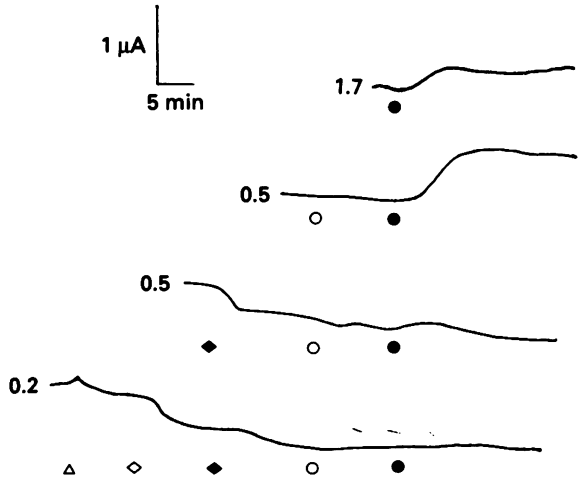

Figure 1 Representative traces of responses to epidermal growth factor (EGF) alone (10 nM, basolateral, ●) and following pretreatment with intestinal trefoil factor (ITF, 10 nM, basolateral, ○) and other transport inhibitors. Piroxicam (5 μM, ◆), and acetazolamide (450 μM, △) were added to both sides. Piretanide (200 μM, ◇) was added to only the basolateral surface. The baseline SCC values for each monolayer are shown in μA to the left of each trace.

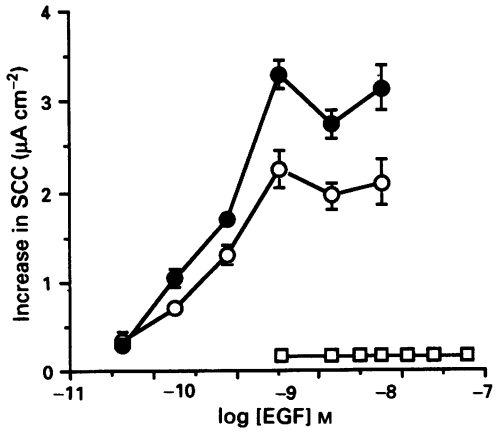

Figure 3 Concentration-response curves for epidermal growth factor (EGF) in the presence (●) or absence (○) of 10 nM intestinal trefoil factor (ITF). Single concentrations of EGF were added to the basolateral surface of Col-29 monolayers, some of which had previously been exposed to 10 nM basolateral ITF (for 10 min, □). Each point represents the mean ± 1 s.e.mean of 3–13 observations with the exception of control 50 nM EGF responses where $n = 2$.

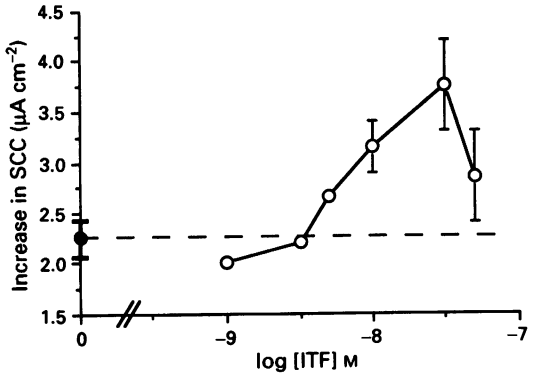

Figure 4 The modulatory effect of increasing concentrations of intestinal trefoil factor (ITF) (basolateral) upon epidermal growth factor (EGF, 1 nM, basolateral, O) responses. Control EGF responses (●) in the absence of ITF increased SCC by $2.2 \pm 0.2\ \mu A\ cm^{-2}$ ($n = 8$) and all points are the mean ± 1 s.e.mean from 3–4 observations.

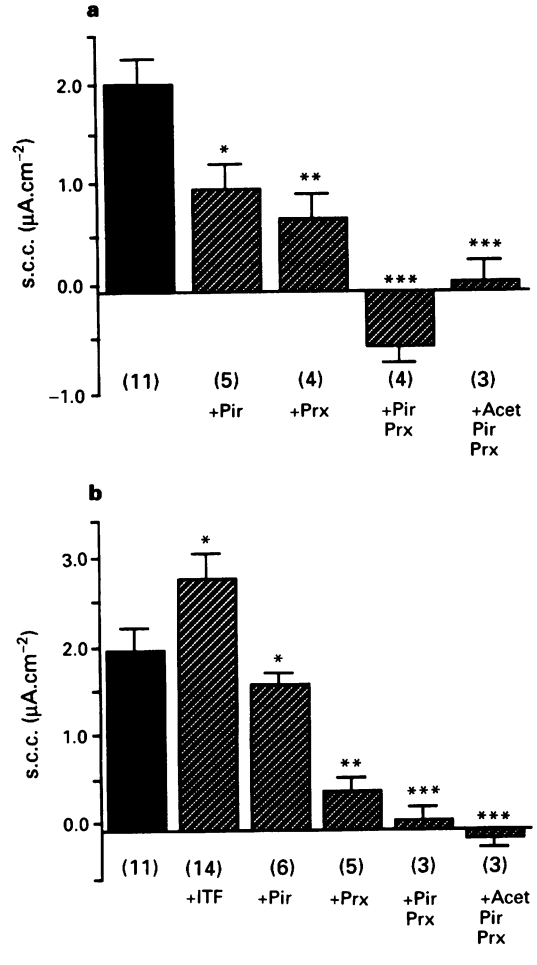

Figure 5 Sensitivity of epidermal growth factor (EGF, 10 nM, basolateral) responses in the absence (a) or presence (b) of intestinal trefoil factor (ITF, 10 nM, basolateral) to various specific transport inhibitors. Control responses to EGF alone are represented by the solid columns. Monolayers were treated with either piretanide alone (200 μM, basolateral, + Pir), piroxicam alone (5 μM to both sides, + Prx) or, a combination of the two (+ Pir Prx). Additionally acetazolamide (450 μM, to both sides, Acet) was also added in combination with piretanide and piroxicam. Each column represents the mean ± 1 s.e.mean and the number of observations in each group are shown in parentheses. Significant differences between data groups and their respective EGF (a) or EGF plus ITF controls (b) were; $*P<0.05$; $**P<0.01$; $***P<0.001$.

Discussion

EGF-induced responses in Col-29 monolayers appear to be mediated via receptors predominantly located on the basolateral surface, since (i) apical peptide produced increases in SCC that were significantly lower than basolateral controls and, (ii) pretreatment with basolateral EGF abolished responses to apically applied peptide. There has been some recent controversy concerning the location of EGF receptors in particular cell systems. Ultrastructural studies in rat jejunum show that EGF receptors are located within the basolateral and microvillar domains (Thompson, 1988; Scheving *et al.*, 1989). It is clear from our own studies that in Col-29 epithelia, EGF receptors are targeted to the basolateral domain, and that stimulation of these receptors results in a change in electrogenic ion transport.

The potency with which EGF stimulated epithelial ion transport was not altered by basolateral ITF pretreatment (EC_{50} values were 0.25 nM and 0.26 nM respectively in the absence and presence of 10 nM ITF), however, the maximum response achieved by EGF (at 1 nM–10 nM) was significantly increased. ITF alone (1 nM–50 nM) did not alter basal SCC levels in Col-29 epithelia, in contrast with observations obtained in *in vitro* preparations of rat jejunum (but not descending colon) where electrogenic responses were stimulated by nM concentrations of basolateral ITF (Cox *et al.*, 1993). Col-29 epithelia are derived from a human colonic adenocarcinoma cell line, HCA-7 (Marsh *et al.*, 1993) and both lines exhibit electrogenic responses to a range of secretory and antisecretory stimuli (MacVinish *et al.*, 1993; Cox & Tough, 1994) the size of which exceed those elicited by EGF. The EC_{50} concentration (7.6 nM) for the modulatory effect of ITF upon EGF responses is well within the peptide concentration range extrapolated from ITF levels found in the intestinal mucosa (Taupin & Giraud, 1994). Equally, the half-maximally effective EGF concentrations observed with Col-29 epithelial layers are not dissimilar from the higher affinity EGF receptors described by Blay & Brown (1985) in the rat intestinal epithelial cell line, RIE-1.

The predominant ionic species responsible for EGF-induced changes in electrogenic ion transport (measured as increased SCC) is Cl^- moving in a basolateral to apical direction. Piretanide attenuated EGF responses (alone, and following ITF) by 50%, by blocking the basolateral Na,K,2Cl co-transporter and therefore reducing intracellular Cl^- available for secretion through apical Cl^- channels. Although some inhibitory effects were observed with acetazolamide these were not significant, and we conclude that HCO_3^- transport is not therefore of major importance in EGF responses in these cells. Cyclo-oxygenase inhibition by piroxicam pretreatment reduced EGF responses by 66%, while in the presence of ITF a 84% reduction of EGF responses was observed. This indicates that eicosanoids are generated by Col-29 cells in response to EGF and this mechanism is potentiated by the presence of ITF. Prostaglandin E_2 (PGE_2) stimulates Cl^- secretion in Col-29 epithelia (MacVinish *et al.*, 1993) most probably via a cyclic AMP-dependent pathway. Therefore prostaglandins (and possibly also thromboxane A_2) are providing a component of the Cl^- secretory response to EGF in these cells. PGE_2 production is increased by EGF in gastric parietal cells (Shaw *et al.*, 1987) and EGF increases PGE_2 release in perfused rat stomach (Chiba *et al.*, 1982) although this eicosanoid does not appear to be involved in EGF-induced inhibition of acid secretion (Shaw *et al.*, 1987).

The modulation of EGF responses by ITF has been observed previously in preliminary studies with Col-29 epithelia (Chinery & Playford, 1995) where EGF was added to both epithelial surfaces. The enhancement of EGF-stimulated, prostaglandin-mediated Cl^- secretion in these epithelial monolayers by ITF, provides evidence for an interaction between two prominent mucosal peptides that may facilitate their restitutive potential. In addition to having

direct motogenic effects (Dignass *et al.*, 1994; Chinery & Playford, 1995) ITF also sensitizes Col-29 epithelia to EGF, augmenting the latter peptide's ability to stimulate Cl^- secretion, thereby increasing local solute and fluid secretion. This could in turn result in an alteration of the viscosity of the overlying mucus layer but the exact consequences of such anion secretion and how this may relate to each factor's role in mucosal restitution remains to be determined.

This work was supported by the Wellcome Trust.

References

BLAY, J. & BROWN, K.D. (1985). Functional receptors for epidermal growth factor in an epithelial-cell line derived from the rat small intestine. *Biochem.*, **225**, 85–94.

CHABOT, J.G., GUY, J. ST ARNAUD, R., WALKER, P. & PELLETIER, G. (1982). Autoradiographic localisation of epidermal growth factor receptors in different tissues of the rat. *J. Cell Biol.*, **95**, 179a.

CHIBA, T., HIRATA, Y., TAMINATO, T., KADOWAKI, S., MATSUKURA, S. & FUJITA, T. (1982). Epidermal growth factor stimulates prostaglandin E release from isolated perfused rat stomach. *Biochem. Biophys. Res. Commun.*, **105**, 370–374.

CHINERY, R. & PLAYFORD, R.J. (1995). Combined intestinal trefoil factor and epidermal growth factor is prophylactic against indomethacin-induced gastric damage in the rat. *Clin. Sci.*, (in press).

COX, H.M., CHINERY, R. & WRIGHT, N.A. (1993). An epithelial ion transport role for intestinal trefoil factor but not for pancreatic spasmolytic polypeptide. *Regul. Pept.*, **47**, 90.

COX, H.M. & TOUGH, I.R. (1994). Calcitonin gene-related peptide receptors in human gastrointestinal epithelia. *Br. J. Pharmacol.*, **113**, 1243–1248.

CUTHBERT, A.W., EGLEME, C., GREENWOOD, H., HICKMAN, M., KIRKLAND, S.C. & MACVINISH, L.J. (1987). Calcium- and cyclic AMP-dependent chloride secretion in human colonic epithelia. *Br. J. Pharmacol.*, **91**, 503–515.

DIGNASS, A., LYNCH-DEVANEY, K., KINDON, H., THIM, L. & PODOLSKY, D.K. (1994). Trefoil peptides promote epithelial migration through a transforming growth factor independent pathway. *J. Clin. Invest.*, **94**, 376–383.

GALLO-PAYET, N. & HUGON, J.S. (1985). Epidermal growth factor receptors in isolated adult mouse intestinal cells: studies *in vivo* and in organ culture. *Endocrinology*, **116**, 194–201.

GEARING, D.P., NICOS, A.N., METCALF, D., FOOTE, S., WILLSON, T.A., GOUGH, N.M. & WILLIAMS, R.L. (1989). Production of leukemia inhibitory factor in *Escherichia coli* by a novel procedure and its use in maintaining embryonic stem cells in culture. *Biotechnology*, **7**, 1157–1161.

HERNANDEZ-SOTOMAYOR, S.M.T. & CARPENTER, G. (1992). Epidermal growth factor receptor: elements of intracellular communication. *J. Membrane Biol.*, **128**, 81–89.

MACVINISH, L.J., PICKLES, R.J. & CUTHBERT, A.W. (1993). Cyclic AMP and Ca^{2+} interactions affecting epithelial chloride secretion in human cultured colonic epithelia. *Br. J. Pharmacol.*, **108**, 462–468.

MARSH, K.A., STAMP, G.W.H. & KIRKLAND, S.C. (1993). Isolation and characterisation of multiple cell types from a single human colonic carcinoma: tumourigenicity of these cell types in a xenograft system. *J. Pathol.*, **170**, 441–450.

OPLETA-MADSEN, K., HARDIN, J. & GALL, D.G. (1991). Epidermal growth factor upregulates intestinal electrolyte and nutrient transport. *Am. J. Physiol.*, **260**, G807–G818.

POULSOM, R. & WRIGHT, N.A. (1993). Trefoil peptides: a newly recognised family of epithelial mucin-associated molecules. *Am. J. Physiol.*, **265**, G205–G213.

SHAW, G.P., HATT, J.F., ANDERSON, N.G. & HANSON, P.J. (1987). Action of epidermal growth factor on acid secretion by rat isolated parietal cells. *Biochem. J.*, **244**, 699–704.

SCHEVING, L.A., SHIURBA, R.A., NGUYEN, T.D. & GRAY, G.M. (1989). Epidermal growth factor receptor in the intestinal enterocyte. Localisation to laterobasal but not brush border membranes. *J. Biol. Chem.*, **264**, 1735–1747.

TAUPIN, D.R. & GIRAUD, A.S. (1994). Distribution of the trefoil peptides spasmolytic polypeptide and intestinal trefoil factor in the rat gut. *Gastroenterol.*, **106**, A635.

THOMPSON, J.F. (1988). Specific receptors for epidermal growth factor in rat intestinal microvillus membranes. *Am. J. Physiol.*, **254**, G429–G435.

(Received September 12, 1994
Revised December 15, 1994
Accepted January 27, 1995)

British Journal of Pharmacology (1995) 115, 81-83

Inhibitory actions of GABA on rabbit urinary bladder muscle strips: mediation by potassium channels

[1]D.R. Ferguson & J.S. Marchant

Department of Pharmacology, University of Cambridge, Tennis Court Road, Cambridge, CB2 1QJ

1 The actions of γ-aminobutyric acid (GABA) upon rabbit urinary bladder muscle were investigated to determine whether they were mediated through potassium channels.

2 *In vitro* experiments were undertaken in which bladder muscle strips were caused to contract with carbachol. Addition of GABA or baclofen reduced the size of such evoked contractions in the case of GABA by 20.7 ± 3.2%, in the case of baclofen by 22.4 ± 2.2%.

3 Electrical stimulation of autonomic nerves in bladder wall strips also evoked contractions which were significantly smaller in potassium-free Krebs solution. The size of contractions produced by carbachol on the other hand were unaffected by the absence of potassium in the Krebs solution.

4 The inhibitory actions of GABA and baclofen on carbachol-induced contractions of bladder muscle were detected at much lower concentrations in potassium-free compared with potassium containing solutions.

5 The inhibitory effects of baclofen were completely reversed by tetraethyl ammonium chloride between 1 and 5 mM, caesium chloride between 0.5 and 3 mM and barium chloride between 0.5 and 2.5 mM. The actions of baclofen were only partially reversed by 4-amino-pyridine between 1 and 5 mM.

6 It was concluded that the $GABA_B$ receptor-mediated inhibitory actions on rabbit urinary bladder smooth muscle cells were produced by activation of potassium channels.

Keywords: Urinary bladder; $GABA_B$ receptor; potassium channels; smooth muscle function

Introduction

Although it has been known for some time that γ-aminobutyric acid (GABA) inhibits the contractile activity of urinary bladder by its actions on autonomic nerves (Kusunoki *et al.*, 1984; Maggi *et al.*, 1985), its capacity to inhibit the contractile activity of the bladder smooth muscle itself has only recently been demonstrated (Chen *et al.*, 1992). This action is mediated through $GABA_B$ receptors as it is produced by baclofen and inhibited by 2-hydroxy-saclofen. $GABA_B$ receptor-mediated effects of this type appear to be produced either through blockade of calcium channels (Dunlap & Fischbach, 1981) or by activation of potassium channels (Inoue *et al.*, 1985).

This present work presents results of experiments designed to test the hypothesis that the $GABA_B$ actions on urinary bladder smooth muscle cells are effected by activation of potassium channels.

Methods

Male Dutch rabbits (600–1000 g) were killed by cervical dislocation, their urinary bladders rapidly removed, washed and the detrusor muscle cut into strips with scissors. No attempt was made to remove the urothelium. The muscle strips were suspended in 0.2 ml capacity superfusion chambers (Brading & Sibley, 1983), and oxygenated Krebs solution at 37°C was pumped over them at 2 ml min^{-1}. A loading tension of 0.5 g was applied and the muscle strips allowed to equilibrate for 1 h. Isometric muscle contractions were produced by the addition of carbachol (1×10^{-5} M) to the superfusion solution for 5 s, (this approximated to the EC_{50} for carbachol on this preparation) and the contractions obtained were demonstrated to be submaximal. It was found possible to repeat carbachol doses at 15 min intervals and still to produce consistent responses. Evoked contractions were recorded with Grass FTO3 transducers, an amplifier, and a Kipp & Zonen BD 112 pen recorder.

Either GABA or baclofen dissolved in Krebs solution was perfused over the muscle strips until the contractile responses to carbachol reached a new consistent level. Results were calculated from at least 4 consecutive responses. Administration of potassium channel antagonists was undertaken for 2 min prior to repeated administration of carbachol. Composition of Krebs solution was (mM): NaCl 124, KCl 5, $MgCl_2$ 1.3, $NaHCO_3$ 26, $CaCl_2$ 0.8, KH_2PO_4 1.4 and glucose 10. Potassium-free Krebs solution contained (mM): NaCl 129, $MgCl_2$ 1.3, $NaHCO_3$ 26, $CaCl_2$ 0.8, NaH_2PO_4 1.4 and glucose 10. Carbachol, (±)-baclofen, 4-aminopyridine, and tetraethyl ammonium chloride were obtained from Sigma, Poole, Dorset, U.K. Barium chloride and caesium chloride from BDH Ltd., Poole, Dorset, U.K. Remaining reagents were of Analar grade.

Data are presented as mean values ± standard error of the mean and significance of differences calculated with Student's *t* test. Differences were regarded as significant when $P<0.05$.

Results

Detrusor muscle strips were stimulated to contract by the superfusion of carbachol (1×10^{-5} M) for 5 s. Doses were repeated at 15 min intervals until consistent responses were obtained. When the detrusor strips were similarly challenged with carbachol, but in the presence of various concentrations of GABA (between 1×10^{-7} M and 3×10^{-4} M) GABA caused a dose-dependent reduction in the magnitude of the contractile responses (Figure 1). Addition of tetrodotoxin (1×10^{-7} M) abolished neither the contractions due to carbachol nor the inhibition due to GABA ($n = 6$). This concentration of tetrodotoxin has previously been shown to abolish

[1] Author for correspondence.

bladder muscle contractions induced by electrical field stimulation of intrinsic autonomic nerves (Chen *et al.*, 1992). The superfusion of increasing concentrations of baclofen (between 1×10^{-7} M and 1×10^{-4} M) produced a similar sized inhibition of carbachol-induced contraction.

The inhibition produced by both GABA and baclofen was not demonstrable in all detrusor muscle strips tested; approximately 60% of the detrusor strips from any one animal responded in this way. Intramural nerve stimulation (30 V, 0.2 ms duration, 3 s trains at 1 to 50 Hz) evoked contractions in potassium-free Kerbs solution which were smaller in amplitude than those in normal Krebs solution. In contrast, superfusion with potassium-free Krebs solution had an insignificant effect on the amplitude of carbachol-induced contractions (data not shown). Whereas potassium-free Krebs solution does not affect the magnitude of the contractile responses induced by carbachol alone, the inhibitory actions of both GABA and baclofen (Figure 2a and b) were demonstrated to occur at much lower concentrations than in control experiments. In the absence of potassium in the bathing solution, the concentrations of GABA or baclofen required to produce maximal inhibition are at least three orders of magnitude lower than in its presence.

Four compounds, tetraethyl ammonium chloride (TEA), caesium chloride (Cs^{2+}), barium chloride (Ba^{2+}) and 4-aminopyridine (4-AP), all known to be potassium channel blockers, were used to determine their effects on the GABA or baclofen-mediated inhibition of carbachol-induced contractions. Prior application of TEA (1–5 mM), Cs^{2+} (0.5–3 mM) or Ba^{2+} (0.2–2.5 mM) to individual strips was able to block, in a dose-dependent manner, the $GABA_B$ receptor-mediated inhibition previously demonstrated in each strip with 10^{-4} M baclofen. The highest concentration of each potassium channel blocker used was able to reverse fully the maximal demonstrable inhibition (Table 1). However, although increasing concentrations of 4-AP were able to attenuate the inhibitory effects of baclofen in a similar manner to the other antagonists, complete reversal of the inhibition was unattainable even at 5 mM 4-AP (Table 1).

Discussion

In cultured chick sensory neurones, $GABA_B$ receptor stimulation was reported by Dunlap & Fischbach (1981) to decrease conductance to calcium ions. However, in guinea-pig hippocampal slices Inoue *et al.* (1985) demonstrated that the $GABA_B$ receptor action was mediated by an increase in potassium conductance. These experiments were complicated by the presence in the experimental preparation of both $GABA_A$ and $GABA_B$ receptor types. In rat cultured dorsal root ganglion cells, Dolphin & Scott (1986) using a whole cell patch-clamp technique, demonstrated the inhibition by baclofen of voltage-dependent inward calcium currents, of the calcium-dependent slow outward potassium current and of a calcium-independent, voltage-dependent outward potassium current. Evidence from patch-clamp experiments (Premkumar *et al.*, 1990) in which potassium channels isolated from GABA or baclofen in the surrounding medium by the recording pipette still opened when the inhibitors were present, indicated the presence of a second messenger system rather than directly coupled ion channels. The fact that these ion channels did not open in membranes treated with pertussis toxin demonstrated the requirement for a pertussis toxin-sensitive G-protein in the second messenger system.

The present experiments investigate the direct inhibitory action of GABA on detrusor smooth muscle contraction, with particular reference to the nature of the downstream effector targets directly coupled to $GABA_B$ receptor activa-

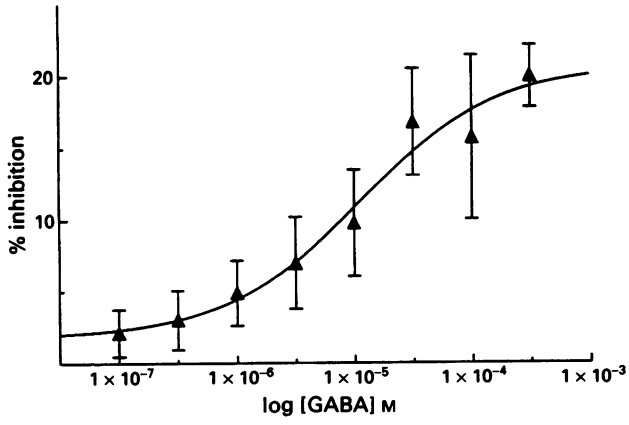

Figure 1 Inhibitory action of GABA on carbachol-induced contractions of urinary bladder muscle strips. Carbachol (1×10^{-5} M) was superfused for 5 s, whereas GABA was continuously perfused at the concentrations shown. Results are expressed as a percentage of the muscle contraction elicited by carbachol alone. Means of at least 6 observations ± s.e.mean. The data were fitted to a hyperbolic function. The inhibition obtained at 5×10^{-4} M GABA was significantly different from control $P<0.001$, by t test.

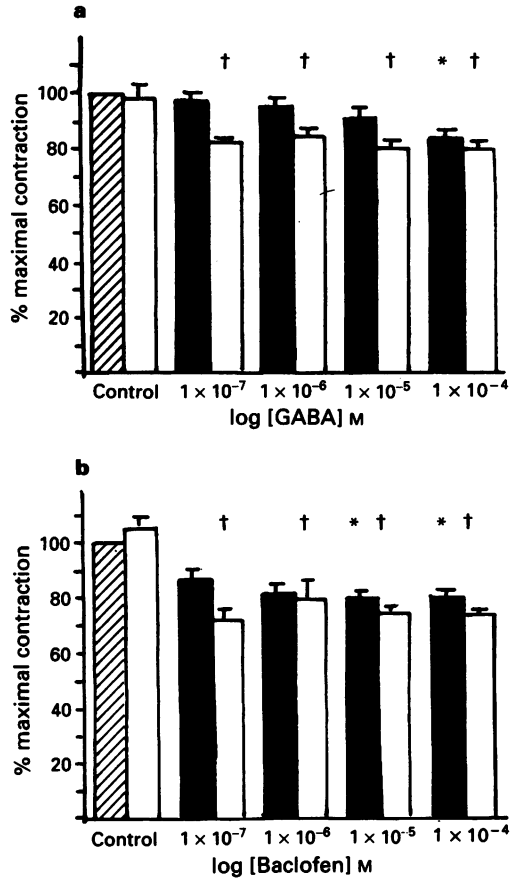

Figure 2 Comparison of the actions of GABA (a) and baclofen (b) on carbachol-induced bladder muscle strip contractions in the presence (solid and hatched columns) and absence (open columns) of potassium in the Krebs solution. Contractions were produced by a 5 s application of 1×10^{-5} M carbachol in each case. These contractions were taken as 100% and shown by the hatched column, and responses in the presence of GABA or baclofen were expressed as a percentage of these values, means ± s.e.means of at least 6 observations were calculated. Responses to GABA or baclofen which are significantly different from control values in the presence of potassium are indicated by *, responses significantly different from control in the absence of potassium are indicated by †. It is clear that while neither 1×10^{-7} M GABA nor 1×10^{-7} M baclofen produce significant inhibition of the response to carbachol in normal Krebs solution, they both produce maximal inhibitory actions in the absence of potassium.

Table 1 Reversal of inhibitory actions of baclofen by potassium channel blockers

Antagonist	*Effect of baclofen expressed as % of control contraction*	*Contraction size as % of control in the presence of both baclofen and potassium channel blocker, concentration of latter given as mM*							
		0.5	*1.0*	*1.5*	*2.0*	*2.5*	*3.0*	*4.0*	*5.0*
Ba^{2+}	81.3 ± 4.4	84.3 ± 1.6	90.3 ± 2.4		99.6 ± 2.3	99.1 ± 0.9			
	NA	NS	NS		✓ (4)	✓ (4)			
	✓ (4)	✓ (4)	✓ (2)		NS	NS			
Cs^{2+}	76.4 ± 4.6	89.3 ± 2.7	84.5 ± 1.6	92.5 ± 3.0	97.9 ± 2.8	101.1 ± 4.4	99.2 ± 1.3		
	NA	NS	NS	✓ (2)	✓ (4)	✓ (4)	✓ (4)		
	✓ (4)	✓ (5)	✓ (4)	NS	NS	NS	NS		
TEA	76.4 ± 4.6		84.5 ± 1.4		87.3 ± 3.2		89.8 ± 5	94.8 ± 3.2	98.1 ± 3.5
	NA		NS		✓ (1)		✓ (1)	✓ (3)	✓ (3)
	✓ (3)		✓ (3)		✓ (2)		NS	NS	NS
4-AP	76.4 ± 4.6		79.1 ± 4.0		82.2 ± 4.3		87.6 ± 1.2	91.5 ± 0.6	90.6 ± 1.7
	NA		NS		NS		✓ (2)	✓ (3)	✓ (2)
	✓ (4)		✓ (4)		✓ (3)		✓ (4)	✓ (3)	✓ (2)

Results are expressed as % of control contraction to carbachol in the presence of baclofen with or without potassium channel blockers. Values are ± s.e.mean, $n = 4$. The first row beneath the experimental data shows the statistical significance of differences between the responses to carbachol in the presence of K^+ channel antagonists and those to baclofen alone. The second row shows the statistical significance of differences between the responses to carbachol in the presence both of baclofen and K^+ channel antagonists and the responses of control muscle strips to carbachol alone. Probability levels are: (1) $P<0.05$, (2) $P<0.025$, (3) $P<0.01$, (4) $P<0.005$; NS, not significant.

tion. The results of the protocol employing potassium-free Krebs solution and those using potassium channel antagonists provide complementary data consistent with potassium channel activation following $GABA_B$ receptor stimulation. It might be anticipated that the absence of potassium from the bathing solution might affect the function of bladder muscle stips, for example by reducing the activity of the sodium-potassium activated ATP-ase in cell membranes; our findings show that although electrical stimulation of the autonomic nerves in the strips show reduced responses, the responses to added carbachol were unaffected at least over a relatively short time. Activation of potassium channels has been demonstrated in neurones by a wide variety of inhibitory neurotransmitters in addition to GABA including adenosine, noradrenaline, dopamine and 5-hydroxytryptamine. The characteristics of such potassium channels have been found to be similar to those of voltage-sensitive, inward-rectifying potassium channels designated I_{K1} (Halliwell, 1990). Although we have identified the presence of GABA-operated potassium channels in smooth muscle cells our experimental evidence does not allow us to identify them more closely.

References

BRADING, A.F. & SIBLEY, G.N.A. (1983). A superfusion apparatus to study field stimulation of 'smooth muscle from mammalian urinary bladder. *J. Physiol.*, **334**, 11–12.

CHEN, T.F., DOYLE, P.T. & FERGUSON, D.R. (1992). Inhibitory role of gamma-amino-butyric acid in the rabbit urinary bladder. *Br. J. Urol.*, **69**, 12–16.

DOLPHIN, A.C. & SCOTT, R.H. (1986). Inhibition of calcium currents in cultured rat dorsal root ganglion neurones by (−)-baclofen. *Br. J. Pharmacol.*, **88**, 213–220.

DUNLAP, K. & FISCHBACH, G.D. (1981). Neurotransmitters decrease the calcium conductance activated by depolarization of embryonic chick sensory neurones. *J. Physiol.*, **317**, 519–535.

HALLIWELL, J.V. (1990). K^+ channels in the central nervous system. In *Potassium Channels, Structure, Classification, Function and Therapeutic Potential.* ed Cook, N.S. pp. 348–381. Chichester: Ellis Horwood.

INOUE, M., MATSUO, T. & OGATA, N. (1985). Baclofen activates voltage dependent and 4-aminopyridine sensitive potassium conductance in guinea-pig hippocampal pyramidal cells maintained *in vitro*. *Br. J. Pharmacol.*, **84**, 833–841.

KUSUNOKI, M., TANIYAMA, K. & TANAKA, C. (1984). Neuronal GABA release and GABA inhibition of ACh release in guinea-pig urinary bladder. *Am. J. Physiol.*, **246**, R502–R509.

MAGGI, C.A., SANTICIOLI, P. & MELI, A. (1985). $GABA_A$ and $GABA_B$ receptors in detrusor strips from guinea-pig bladder dome. *J. Auton. Pharmacol.*, **5**, 55–64.

PREMKUMAR, L.S., CHUNG, S-H, & GAGE, P.W. (1990). GABA-induced potassium channels in cultured neurons. *Proc. R. Soc. B.*, **241**, 153–158.

(Received May 6, 1994
Revised December 23, 1994
Accepted January 26, 1995)

British Journal of Pharmacology (1995) 115, 84-94

The anti-emetic effects of CP-99,994 in the ferret and the dog: role of the NK_1 receptor

[1]J.W. Watson, S.F. Gonsalves, A.A. Fossa, S. McLean, T. Seeger, S. Obach & *P.L.R. Andrews

Departments of Immunology, General Pharmacology, Neuroscience and Drug Metabolism, Central Research Division, Pfizer Inc, Groton, CT 06340, U.S.A. and *Department of Physiology, St. George's Hospital Medical School, London

1 The selective NK_1 receptor antagonist, CP-99,994, produced dose-related (0.1-1.0 mg kg^{-1}, s.c.) inhibition of vomiting and retching in ferrets challenged with central (loperamide and apomorphine), peripheral ($CuSO_4$) and mixed central and peripheral (ipecac, cisplatin) emetic stimuli.

2 Parallel studies with the enantiomer, CP-100,263 (1 mg kg^{-1}, s.c.), which is > 1 000 fold less potent as a NK_1 antagonist, indicated that it was without significant effect against $CuSO_4$, loperamide, cisplatin and apomorphine-induced emesis. Against ipecac, it inhibited both retching and vomiting, expressing approximately 1/10th the potency of CP-99,994.

3 The $5\text{-}HT_3$ receptor antagonist, tropisetron (1 mg kg^{-1}, s.c.) inhibited retching and vomiting to cisplatin and ipecac, but not $CuSO_4$ or loperamide.

4 CP-99,994 (1 mg kg^{-1}, i.v.) blocked retching induced by electrical stimulation of the ventral abdominal vagus without affecting the cardiovascular response, the apnoeic response to central vagal stimulation or the guarding and hypertensive response to stimulation of the greater splanchnic nerves. CP-99,994 (1 mg kg^{-1}, i.v.) did not alter baseline cardiovascular and respiratory parameters and it failed to block the characteristic heart rate, blood pressure and respiratory rate/depth changes in response to i.v. 2-methyl-5-HT challenge (von Bezold-Jarisch reflex).

5 Using *in vitro* autoradiography, [^{3}H]-substance P was shown to bind to several regions of the ferret brainstem with the density of binding in the nucleus tractus solitarius being much greater than in the area postrema. This binding was displaced by CP-99,994 in a concentration-related manner.

6 In dogs, CP-99,994 (40 $\mu g\ kg^{-1}$ bolus and 300 $\mu g\ kg^{-1}\ h^{-1}$, i.v.) produced statistically significant reductions in vomiting to $CuSO_4$ and apomorphine as well as retching to $CuSO_4$.

7 Together, these studies support the hypothesis that the NK_1 receptor antagonist properties of CP-99,994 are responsible for its broad spectrum anti-emetic effects. They also suggest that CP-99,994 acts within the brainstem, most probably within the nucleus tractus solitarius although the involvement of the area postrema could not be excluded.

Keywords: Substance P; NK_1 antagonist; CP-99,994; vagal stimulation; emesis in dog; emesis in ferret; area postrema; nucleus tractus solitarius

Introduction

Identification of the anti-emetic effects of the 5-hydroxytryptamine$_3$ ($5\text{-}HT_3$) receptor antagonists (e.g. granisetron, ondansetron and troprisetron) has transformed the clinical management of nausea and vomiting induced by cytostatic anti-cancer therapy (Aapro, 1991). However, the anti-emetic effects of the $5\text{-}HT_3$ receptor antagonists are relatively circumscribed, with major effects being confined to the acute phase of emesis induced by cytotoxic drugs (e.g. cisplatin, cyclophosphamide, doxorubicin, see Aapro, 1991; Andrews, 1994 for reviews) and radiation (Priestman, 1989; Andrews *et al.*, 1992a; Rabin & King, 1992). Some anti-emetic effects have been reported for some $5\text{-}HT_3$ receptor antagonists against post-operative emesis, muscarinic receptor agonists and erythromycin (for review see Andrews, 1994), but to date the efficacy appears much less than against the cytostatic stimuli.

Identification of the site and mechanism of the anti-emetic effects of the $5\text{-}HT_3$ receptor antagonists has stimulated research into the area of emesis. At present it appears that the induction of emesis by cytostatic drugs is mediated predominantly through activation of abdominal visceral afferents (mainly vagal) by 5-HT released from enterochromaffin cells in the mucosa of the upper gut. Because the vagus appears to play a critical role in emesis induced by cytostatic drugs in a range of species (ferret, *Suncus*, dog, and monkey) (Andrews & Davis, 1993, for review) the possibility that drugs targeted at other vagal afferent transmitter systems (e.g. substance P, acetylcholine, CCK-8) could have anti-emetic actions has been considered (Leslie, 1985; Dockray & Sharkey, 1986; Dockray *et al.*, 1989). In addition, as $5\text{-}HT_3$ receptor antagonists do not block all components of the emesis induced by cytotoxic drugs (Aapro, 1991) or all vagally-dependent emesis, e.g. copper sulphate and hypertonic saline (Bhandari & Andrews, 1991) or emesis induced by centrally acting emetic stimuli, e.g. motion, loperamide, morphine or apomorphine (Stott *et al.*, 1989; Bermudez *et al.*, 1989; Bhandari *et al.*, 1992; Thompson *et al.*, 1992) other transmitters were implicated in these responses.

A number of pieces of evidence, including the location of substance P and the induction of emesis by substance P (reviewed in the discussion) suggested that investigation of the anti-emetic potential of a substance P receptor antagonist would be worthwhile. Because substance P was the most likely endogenous ligand and in view of the relative neuronal versus non-neuronal distributions of neurokinin$_1$ (NK_1) and neurokinin$_2$ (NK_2) receptors, an NK_1 receptor antagonist was selected as the candidate test agent. The highly selective and potent NK_1 receptor antagonist, CP-99,994 (McLean *et al.*, 1992) and its > 1 000 times less potent optical enantiomer, CP-100,263, provided the opportunity to test directly the

[1] Author for correspondence at: Pfizer Central Research, Groton, CT 06340, U.S.A.

degree of involvement of the NK_1 receptor in emesis. The usefulness of CP-99,994 for investigation of the possible involvement of NK_1 receptors in emesis has also been recognized by others (Bountra *et al.*, 1993; Tattersall *et al.*, 1993; 1994).

The results of this extensive investigation into the anti-emetic and related effects of CP-99,994 suggest that this compound may provide a novel approach to the blockade of emesis provoked by a wide variety of stimuli. The potential sites of drug action are discussed in the context of the insights they provide into the neuropharmacology of central emetic pathways.

Methods

Emesis in the ferret

Adult male ferrets (Marshall Farms, 750 to 1445 g) were housed individually in a temperature, light and humidity controlled environment for one to two weeks before experiments. They were given a standard pelleted diet and water *ad libitum*. They were fasted overnight prior to administration of intra-gastric copper sulphate and ipecac.

The prototype NK_1 selective, substance P receptor antagonist, CP-99,994 (0.1, 0.3 or 1.0 mg kg^{-1}), or its >1 000 times less active (2R,3R) enantiomer, CP-100,263 (1 mg kg^{-1}) was administered subcutaneously at 30 min and 5 min prior to intra-gastric administration of copper sulphate (0.5 mg ml^{-1}, 12.5 mg kg^{-1}), ipecac syrup (1 mg kg^{-1} of ether soluble alkaloids of ipecac) or subcutaneous administration of apomorphine (200 $\mu g\ kg^{-1}$) or 30 min prior to subcutaneous injection of loperamide (250 $\mu g\ kg^{-1}$). The latency to emesis after cisplatin (10 mg kg^{-1}, i.p.), is about 75 min in the ferret. Therefore, CP-99,994 or its enantiomer was given subcutaneously 45 min after the cisplatin. For each emetogen the doses used had previously been reported to induce emetic responses in this species. For comparison to the NK_1 receptor antagonist, the $5\text{-}HT_3$ receptor antagonist, tropisetron (ICS 205-930) (1 mg kg^{-1}, s.c.), was also tested for its ability to block each of the emetogens (apomorphine excepted) using a 30 min pretreatment time.

Following administration of the emetic substance, ferrets were observed continuously in individual polycarbonate cages for 60–120 min. Previous studies have demonstrated that these intervals are adequate for characterization of the response to the above emetic stimuli. The timing and number of retches and vomits observed were recorded for each animal. As in previous studies (e.g. Bhandari & Andrews, 1991) retching was quantified by counting rhythmic abdominal contractions. Vomits were scored for each oral expulsion of liquid or solid upper gastrointestinal tract contents. An individual animal was tested no more than three times with at least 7 days between experiments.

In order to establish drug exposure, blood samples were taken via cardiac puncture in some animals anaesthetized (6 mg kg^{-1} Rompun and 20 mg kg^{-1} Ketamine, s.c.) at the end of a 1 h emesis observation period. The samples were spun to obtain plasma then stored at −20°C until the day of assay. Analysis of CP-99,994 and CP-100,263 was by gas chromatography with electron capture detection.

Emesis in the dog

Six mongrel dogs, which had been trained to stand in a sling, were fasted overnight and cannulated percutaneously in the cephalic vein for drug administration and external jugular vein for sampling of blood. Dogs to be given apomorphine, but not copper sulphate, were fed 450 g of canned meat just prior to the start of the experiment. CP-99,994 or saline vehicle at an equal volume was infused as a slow push to deliver 40 $\mu g\ kg^{-1}$ over 6 min, followed immediately by an infusion of 300 $\mu g\ kg^{-1}\ h^{-1}$ for 54 min. The dogs were then given either apomorphine HCl (10 $\mu g\ kg^{-1}$) i.v. or copper sulphate (6 mg kg^{-1}) p.o. The infusion of CP-99,994 or vehicle continued for an additional 30 min. Using a complete cross-over design, the same six dogs received, in random order, CP-99,994 or vehicle with both emetics. A minimum three-day washout period was provided between studies with dogs that received CP-99,994. The frequency and latency of responses were noted for vomiting and retching. Although most responses occurred within the first 5 min, observations were continued for 2 h after emetic challenge.

Site of anti-emetic effect

As it was likely that any anti-emetic effects of an NK_1 receptor antagonist involved the nucleus tractus solitarius, it was decided to study the effect of CP-99,994 on a number of reflexes mediated via this nucleus to gain an insight into the selectivity of the antagonist for the emetic reflex.

The von Bezold-Jarisch reflex Ferrets were anaesthetized with urethane (1.5 g kg^{-1}, i.p.). Arterial blood pressure was monitored with a Gould fluid-filled pressure transducer connected to a cannula inserted into the common carotid artery. Respiration was monitored from a catheter inserted orally into the mid-thoracic portion of the oesophagus. After a stable heart rate and blood pressure were established, 30 $\mu g\ kg^{-1}$ of 2-methyl-5-HT was rapidly injected through a cannula in the external jugular vein. The prompt, profound decreases in heart rate and blood pressure evoked by this procedure in the ferret, are blocked by $5\text{-}HT_3$ receptor antagonists or cervical vagotomy (Andrews & Bhandari, 1992b; Andrews *et al.*, 1992). After evoking the response twice by injection of 2-methyl-5-HT at 15 min intervals, 1 mg kg^{-1} CP-99,994 was given as a slow bolus i.v. injection and 5 min later (15 min after previous 2-methyl-5-HT challenge) the response to 2-methyl-5-HT was redetermined. The results from this study were quantified by measuring the fall in heart rate and change in rate and depth of respiration following 2-methyl-5-HT. In addition, arterial blood pressure was measured prior to injection and after the initial bradycardia when pressure rises due to reflex cardiovascular effects.

Gag reflex The gag reflex is mediated by mechanoreceptors in the superior laryngeal nerve, which projects to the NTS (Mifflin, 1993). In these experiments the gag reflex was evoked in conscious ferrets by gentle tactile stimulation of the pharynx and larynx and was recorded as an all or none event before and after s.c. injection of CP-99,994, 1 mg kg^{-1}, given at 30 and again 5 min before testing the reflex.

Vagal afferent stimulation In the ferret, retching can be induced under urethane anaesthesia by electrical stimulation of abdominal vagal afferents (Andrews *et al.*, 1990). This response provides a convenient method for directly investigating the effect of CP-99,994 on centrally (AP and NTS)-mediated responses to vagal afferent drive. Ferrets were anaesthetized with urethane (1.5 g kg^{-1}, i.p.) and cannulae placed in the external jugular vein (drug administration), common carotid artery (blood pressure) and the mid-thoracic oesophagus (intra-thoracic pressure). The dorsal or ventral abdominal vagus was isolated and ligated and the central cut-end stimulated before and 15 min after administration of CP-99,994 (1 mg kg^{-1}, i.v.) using parameters (25 V, 0.5 ms, 40 Hz, 30 s) that have previously been shown to reliably evoke retching (Andrews *et al.*, 1990). In two animals the response to vagal stimulation was retested 90 min after CP-99,994, a time at which, based on other *in vivo* experiments, it was expected that the drug would have lost its effect. The cervical vagus was also stimulated (5 s, 40 Hz, 25 V, 0.5 ms) to evoke a reflex apnoea, a component of the Hering-Breuer inflation reflex that is mediated via the nucleus tractus solitarius. In addition the central cut end of the left greater

splanchnic was stimulated (5 s, 40 Hz, 25 V, 0.5 ms) to evoke a reflex increase in blood pressure and a 'guarding' response characterized by contraction of the skeletal muscle of the ipsilateral anterior abdominal wall. Both the cervical vagus and the greater splanchnic nerve were stimulated before and after CP-99,994. These stimuli were performed after stimulation of the abdominal vagus.

Autoradiographic evaluation of [^{3}H]-substance P binding in ferret brainstem

Ferret brains were frozen in isopentane (−20°C) and stored at −65°C. The brains were sectioned at 20 μm thickness, thaw mounted on gelatin-coated slides, and dried under vacuum. The resulting sections were pre-incubated for 15 min at room temperature in 50 mM Tris-HCl, 5 mM $MgCl_2$, 0.02% bovine serum albumin, 20 μg ml^{-1} bacitracin, 4 μg ml^{-1} leupeptin, and 2 μg ml^{-1} chymostatin, adjusted to pH 7.3. They were then incubated for 30 min at room temperature in the above buffer containing 2 nM [^{3}H]-substance P, with or without various concentrations of CP-99,994. Nonspecific binding was defined by the addition of 2 μM CP-96,345, a well characterized potent and selective NK_1 antagonist (Snider *et al.*, 1991). Sections were selected based on reference to previously published accounts of ferret brainstem histology (Reynolds *et al.*, 1991; Strominger *et al.*, 1994). All sections were washed twice in ice-cold buffer for 5 min each, dipped briefly in distilled water to remove salts and dried under a stream of compressed air. The sections were placed in standard X-ray cassettes, and apposed to tritium-sensitive film (Amersham Hyuperfilm) for 3–4 months. Quantitative determination of binding levels was done on the resulting films with a MCID M1 image analysis system (Imaging Research Inc.). The data are reported as mean optical density values.

Receptor binding assays

NK_1 receptor binding NK_1 receptor binding was assessed using human lymphoblasts (IM-9 cells), and various tissue homogenates. IM-9 cells were obtained from American Tissue Culture Corporation (Rockville, MD). The IM-9 cells were cultured according to previously described methods (Payan *et al.*, 1984). The IM-9 cells were harvested by centrifugation, washed twice in buffer (50 mM Tris-HCl, pH 7.4 at 4°C, 1 mM $MnCl_2$) and resuspended in binding buffer (50 mM Tris-HCl, pH 7.4 at 22°C, 50 μg ml^{-1} chymostatin, 10 μg ml^{-1} bacitracin, 20 μg ml^{-1} phosphoramidon, 40 μg ml^{-1} leupeptin, 1 mM $MnCl_2$, 1 mM $MgCl_2$ and 0.02% BSA). Assays were initiated by adding 3×10^5 IM-9 cells to 250 μl of buffer containing 0.1 nM ^{125}I-labelled Bolton Hunter conjugate of substance P ([^{125}I]-BH-SP, specific activity = 2200 Ci mmol^{-1}, New England Nuclear) and various concentrations of CP-99,994 or other inhibitors and allowed to incubate for 30 min at 22°C. Nonspecific binding was defined as the radioactivity remaining in the presence of 1 μM substance P.

Ferret brain membrane substance P binding assay Ferret forebrains were homogenized with 10 strokes of a teflon homogenizer in 0.32 M sucrose and spun 8 min at 3 200 r.p.m. The supernatant was decanted and centrifuged at 17,000 r.p.m. for 25 min. The resulting pellet was lysed in 5 mM Tris HCl, pH 7.4 for 10 min at 4°C, then spun at 17,000 r.p.m. for 20 min. The pellet was washed twice and resuspended in 5 mM Tris HCl, pH 7.4 and stored at −80°C for later use. Frozen membranes were diluted with an equal volume of 5 mM Tris HCl pH 7.4 (100 μg final protein concentration) and added to an incubation mixture containing 1.4 nM [^{3}H]-substance P (New England Nuclear, 29.7 Ci mmol^{-1}) in 50 mM Tris HCl, pH 7.4, 1 mM $MnCl_2$, 1 mM $MgCl_2$, 50 μg ml^{-1} chymostatin, 10 μg ml^{-1} bacitracin, 40 μg ml^{-1} leupeptin, 20 μg ml^{-1} phosphoramidon, and 0.02% BSA. CP-99,994 at 1 μM was used to determine nonspecific binding. Following incubation at 22°C for 30 min, the reaction was terminated by cold wash with 50 mM Tris HCl pH 7.4, 1 mM $MnCl_2$ through a Skatron cell harvester (setting 555) and harvested onto 0.3% PEI-soaked Schleicher & Scheul No. 30 filters. Filterdiscs were soaked in 4 ml of liquid scintillation cocktail, and the radioactivity allowed to extract overnight. The samples were counted on a Wallac 1410 liquid scintillation counter, and data analysed with Lundon1 or Lundon2 software.

Statistics

Results are expressed as mean ± s.e.mean, n = number of animals. ANOVA followed by Dunnett's multiple comparison test was used to test statistical significance. In cases where a data set did not exhibit a normal distribution, the Wilcoxon sign rank test was used to determine statistical significance. A $P < 0.05$ value was considered statistically significant.

Reagents

Ipecac syrup was obtained from Barre-National Inc., Baltimore, MD, U.S.A. Note that this syrup contains 1.4 mg ml^{-1} of ether-soluble alkaloids of ipecac, 1.5% alcohol, and unspecified concentrations of de-ionized water, glycerin, sucrose syrup and the preservatives, methylparaben and propylparaben. Copper sulphate pentahydrate (copper sulphate), apomorphine, loperamide HCl (loperamide), 2-methyl-5-HT and *cis*-platinum(II) diamine dichloride (cisplatin) were purchased from Sigma Chemical Company, St. Louis, MO, U.S.A. Loperamide was dissolved in distilled water containing 7% propylene glycol. Apomorphine and cisplatin were dissolved in 154 mM NaCl. The following compounds were synthesized by the Medicinal Chemistry Department at Pfizer Inc: ICS 205-930 (troprisetron), CP-99,994 (dihydrochloride salt) ((+)-(2S,3S)-3-(2-methoxybenzylamino)-2-phenylpiperidine) and CP-100,263 (dihydrochloride salt) the **2R,3R** enantiomer of CP-99,994.

Results

Binding data

CP-99,994 displaced [^{125}I]-Bolton Hunter-substance P from ferret brain membranes with an IC_{50} of 1.97 ± 1.2 nM (n = 4). Using the same compound lot used in the *in vivo* experiments, CP-100,263 failed to displace [^{125}I]-Bolton Hunter-substance P from IM-9 cell membranes (IC_{50} > 10 μM, n = 4), a preparation in which CP-99,994 expressed an IC_{50} of 0.45 nM (n = 24).

Behavioural effects of CP-99,994

No overt changes in behaviour were observed in ferrets following administration of CP-99,994 or its enantiomer (CP-100,263) even at the highest doses (1 mg kg^{-1}, s.c.). In addition, no overt changes in behaviour were observed in dogs receiving an infusion of CP-99,994 (total dose of 310 μg kg^{-1} over 60 min). Most importantly, neither the ferrets nor dogs showed signs of sedation.

Anti-emetic effects of CP-99,994 in conscious ferrets

In ferrets, CP-99,994 decreased the frequency of copper sulphate (Table 1), loperamide (Table 2), cisplatin (Table 3), and ipecac-induced (Table 4) retching and vomiting in a dose-dependent manner. CP-99,994 also completely blocked apomorphine-induced retching and vomiting at a dose of 1 mg kg^{-1} (Table 5). Administration of CP-99,994 at doses that did not completely block the emetic responses was with-

Table 1 Effects of CP-99,994, CP-100,263 and ICS 205-930 (tropisetron) on copper sulphate-induced (12.5 mg kg^{-1}, p.o.) emesis in the ferret

Emetogen	*Treatment*	*Dose* (mg kg^{-1})	*R/T*	*V/T*	*Retches*	*Vomits*
Copper sulphate	Saline		20/21	20/21	24.9 ± 3.7 (0–69)	4.4 ± 0.5 (0–8)
	CP-99,994	0.1	3/5	4/5	7.4 ± 3.7 (0–19)	2.6 ± 1.0 (0–6)
		0.3	2/5	3/5	1.4 ± 1.0*** (0–5)	1.0 ± 0.5** (0–2)
		1.0	0/8	0/8	0***	0***
	CP-100,263	1.0	5/5	5/5	21.4 ± 6.0 (9–40)	3.4 ± 0.6 (2–5)
	Tropisetron	1.0	5/5	5/5	38.6 ± 6.4 (26–58)	5.4 ± 1.0 (2–8)

CP-99,994 and CP-100,263 were injected s.c. 30 min and 5 min prior to intragastric administration of the emetogen. ICS-205,930 was administered as a single s.c. injection 30 min prior to copper sulphate. Animals were observed for 60 min. R/T = number of animals that showed retching compared to the number of animals tested. V/T = number of animals that showed vomiting compared to the number of animals tested. Mean values were based on all animals tested. Statistically significant difference from control indicated by ***$P<0.0001$, **$P<0.001$. Values are mean ± s.e.mean; range in parentheses.

Table 2 Effects of CP-99,994, CP-100,263 and ICS 205-930 (tropisetron) on loperamide-induced (250 μg kg^{-1}, s.c.) emesis in the ferret

Emetogen	*Treatment*	*Dose* (mg kg^{-1})	*R/T*	*V/T*	*Retches*	*Vomits*
Loperamide	Saline		24/25	22/25	51.9 ± 5.2 (0–96)	4.4 ± 0.6 (0–12)
	CP-99,994	0.1	7/7	6/7	36.1 ± 7.1 (18–57)	2.7 ± 0.7 (0–5)
		0.3	6/7	2/7	13.9 ± 2.9** (0–22)	0.7 ± 0.5*** (0–3)
		1.0	3/10	2/10	2.60 ± 1.4*** (0–11)	0.2 ± 0.1*** (0–1)
	CP-100,263	1.0	7/7	5/7	50.1 ± 11.6 (9–93)	3.0 ± 0.8 (0–5)
	Tropisetron	1.0	9/10	9/10	37.4 ± 7.8 (0–83)	5.4 ± 1.2 (0–12)

All compounds were administered as a single s.c. injection 30 min prior to administration of the emetogen. Animals were observed for 90 min. R/T = number of animals that showed retching compared to the number of animals tested. V/T = number of animals that showed vomiting compared to the number of animals tested. Mean values were based on all animals tested. Statistically significant difference from control indicated by ***$P<0.0001$, **$P<0.001$. Values are mean ± s.e.mean; range in parentheses.

Table 3 Effects of CP-99,994, CP-100,263 and ICS 205-930 (tropisetron) on cisplatin-induced (10 mg kg^{-1}, i.p.) emesis in the ferret

Emetogen	*Treatment*	*Dose* (mg kg^{-1})	*R/T*	*V/T*	*Retches*	*Vomits*
Cisplatin	Saline		4/5	4/5	31.6 ± 10.4 (0–58)	4.6 ± 1.4 (0–7)
	CP-99,994	0.1	5/5	5/5	17.4 ± 4.7 (7–33)	3.0 ± 0.3 (2–4)
		0.3	2/5	2/5	9.0 ± 6.8* (0–35)	1.6 ± 0.3* (0–6)
		1.0	0/5	1/5	0 ± 0* (0–0)	0.6 ± 0.6* (0–3)
	CP-100,263	1.0	8/10	8/10	31.5 ± 8.4 (0–73)	4.3 ± 1.2 (0–11)
	Tropisetron	1.0	0/5	0/5	0 ± 0* (0–0)	0 ± 0* (0–0)

Both CP-99,994 and CP-100,263 were dosed once s.c. 45 min after cisplatin challenge. ICS 205-930 was injected once s.c. 30 min before cisplatin challenge. Animals were observed for 120 min. Mean values were based on all animals tested. Statistically different from control group indicated by *$P<0.05$. Values are mean ± s.e.mean; range in parentheses.

Table 4 Effects of CP-99,994, CP-100,263 and ICS 205-930 (tropisetron) on ipecac syrup-induced (1 mg kg^{-1}, p.o.) emesis in the ferret

Emetogen	*Treatment*	*Dose* (mg kg^{-1})	*R/T*	*V/T*	*Retches*	*Vomits*
Ipecac syrup	Vehicle		10/10	10/10	31.7 ± 3.4 (18–51)	4.1 ± 0.4 (2–6)
	CP-99,994	0.03	4/5	4/5	19 ± 7.8 (2–40)	2.6 ± 0.9 (0–5)
		0.1	3/5	3/5	8.4 ± 3.6*** (0–18)	1.6 ± 0.68*** (0–3)
		0.3	3/5	3/5	4.0 ± 2.0*** (0–10)	0.8 ± 0.37*** (0–2)
		1.0	0/5	0/5	0 ± 0*** (0–0)	0 ± 0*** (0–0)
	CP-100,263	0.3	5/5	5/5	20 ± 7.8 (5–47)	2.4 ± 0.6 (1–4)
		1.0	3/5	3/5	10.8 ± 5.6*** (0–32)	1.2 ± 0.73*** (0–4)
	Tropisetron	1.0	0/5	0/5	0 ± 0*** (0–0)	0 ± 0*** (0–0)

Both CP-99,994 and CP-100,263 were given 30 min and 5 min prior to ipecac. ICS 205-930 was injected once s.c. 30 min before ipecac. Animals were observed for 60 min. Mean values were based on all animals tested. Statistically significant difference from control indicated by ***$P<0.0001$. Values are mean ± s.e.mean; range in parentheses.

Table 5 Effects of CP-99,994 and CP-100,263 on apomorphine-induced (200 μg kg^{-1}, s.c.) emesis in the ferret

Emetogen	*Treatment*	*Dose* (mg kg^{-1})	*R/T*	*V/T*	*Retches*	*Vomits*
Apomorphine	Vehicle		20/25	16/25	11.5 ± 2.0 (0–33)	1.4 ± 0.3 (0–5)
	CP-99,994	1	0/25	0/25	0 ± 0*** (0–0)	0 ± 0*** (0–0)
	CP-100,263	1	13/25	11/25	8.3 ± 2.6 (0–39)	0.92 ± 0.27*** (0–5)

Both CP-99,994 and CP-100,263 were given 30 min and 5 min prior to apomorphine. Animals were observed for 60 min. Mean values were based on all animals tested. Statistically significant difference from control indicated by ***$P<0.0001$. Values are mean ± s.e.mean; range in parentheses.

out significant effect on the latency of the retching response to cisplatin and copper sulphate. Both ipecac and loperamide showed a trend towards increased latency with increasing doses of the CP-99,994 (ipecac control: 23.3 ± 1.5 min [$n = 10$], 0.03 mg kg^{-1}: 26.0 ± 7.7 min [$n = 4$], 0.1 mg kg^{-1}: 30.3 ± 1.4 min [$n = 3$], 0.3 mg kg^{-1}: 33.0 ± 3.8 min [$n = 3$]; loperamide control: 12.7 ± 1.4 min [$n = 24$], 0.1 mg kg^{-1}: 11.9 ± 1.4 min [$n = 7$], 0.3 mg kg^{-1}: 14.7 ± 2.5 min [$n = 6$], 1.0 mg kg^{-1}: 31.7 ± 4.3 min [$n = 3$]).

CP-99,994 produced a 50% reduction in retches at doses between 0.03 and 0.1 mg kg^{-1} for both ipecac and copper sulphate. In contrast both cisplatin and loperamide were slightly less sensitive to the effects of CP-99,994, which produced a 50% reduction in retching at doses between 0.1 and 0.3 mg kg^{-1}. At a dose of 1 mg kg^{-1}, CP-99,994 blocked apomorphine, ipecac and copper sulphate-induced vomiting and retching completely; reduced retching and vomiting in loperamide-treated animals by 96% and reduced cisplatin-induced retching by 100% and vomiting by 87%.

CP-100,263, the (2**R**,3**R**) enantiomer of CP-99,994, given at 1 mg kg^{-1}, did not significantly reduce the frequency of retching or vomiting in response to loperamide, cisplatin, apomorphine or copper sulphate. In contrast, both retching and vomiting were significantly reduced by CP-100,263 in animals challenged with ipecac with the magnitude of the effect being similar to that of 0.1 mg kg^{-1} of its enantiomer, CP-99,994. In addition, there was a trend towards increased latency to retch from the control values of 23.3 ± 1.5 min ($n = 10$) to 30.4 ± 3.9 min at 0.3 mg kg^{-1} ($n = 5$) and to 37.0 ± 6 min ($n = 3$) at 1 mg kg^{-1}. Although the magnitude of the emetic response to apomorphine was not affected by CP-100,263 the latency to retch increased ($P<0.0001$) from 9.5 ± 1.0 min ($n = 25$) in vehicle-treated animals to 39.0 ± 1.2 min ($n = 13$) after 1 mg kg^{-1} CP-100,263. The latency to the onset of retching was unaffected by CP-100,263 (1 mg kg^{-1}, s.c.) in animals which had received copper sulphate (3.9 ± 0.2 min, $n = 20$ vs 5.0 ± 0.8 min, $n = 5$) or loperamide (12.7 ± 1.4 min, $n = 24$ vs 11.9 ± 2.3 min, $n = 7$).

Plasma drug levels

Plasma samples collected from animals dosed s.c. 90 and again 65 min before blood sampling with either 1 mg kg^{-1} CP-99,994 or 1 mg kg^{-1} CP-100,263 contained 119 ± 30 ($n = 5$) or 142 ± 20 ($n = 5$) ng drug ml^{-1} plasma, respectively.

Anti-emetic effects of tropisetron in ferrets

The 5-HT$_3$ receptor antagonist, tropisetron, given at 1 mg kg^{-1} s.c., totally blocked vomiting and retching in response to cisplatin and ipecac while it produced no significant changes in the incidence, latency or frequency of the emetic responses to copper sulphate or loperamide (Tables 1, 2, 3, 4).

Anti-emetic effects of CP-99,994 in the dog

In the dog, CP-99,994 significantly ($P<0.05$) reduced the vomiting response to both copper sulphate and apomorphine (Table 6). Complete protection was obtained against copper

Table 6 Effects of CP-99,994 on apomorphine (10 μg kg^{-1}, i.v.) and $CuSO_4$ (6 mg kg^{-1}, p.o.)-induced emesis in the dog

Emetogen	*Treatment*	*Dose* (mg kg^{-1})	*R/T*	*V/T*	*Retches*	*Vomits*
Apomorphine	Saline		4/6	6/6	4.2 ± 2.3 (0–15)	1.8 ± 0.3 (1–3)
	CP-99,994	40 μg kg^{-1} + 5 μg kg^{-1} min^{-1}	2/6	2/6	0.7 ± 0.5 (0–3)	0.3 ± 0.2* (0–10)
$CuSO_4$	Saline		6/6	6/6	10.6 ± 3.6 (3–27)	2.5 ± 0.6 (1–5)
	CP-99,994	40 μg kg^{-1} + 5 μg kg^{-1} min^{-1}	2/6	0/6	0.5 ± 0.3* (0–2)	0* 0

CP-99,994 was injected i.v. as a 40 μg kg^{-1} dose over 6 min followed by an infusion of 300 μg kg^{-1} for 54 min. Animals were observed for 120 min. Mean values were based on all animals tested. Statistically significant difference from control indicated by *$P<0.05$. Values are mean ± s.e.mean; range in parentheses.

sulphate-induced vomiting in all 6 animals and in 4 out of 6 animals receiving apomorphine. In the remaining two animals only a single vomit occurred. Retching was also completely blocked for copper sulphate. Although CP-99,994 produced a reduction in apomorphine-induced retching, it failed to reach statistical significance because of the highly variable frequency of the control response.

Effects of CP-99,994 on the von Bezold-Jarisch reflex

At a dose of 1 mg kg^{-1}, CP-99,994 had no significant effect on the resting blood pressure, respiration rate or depth or the modulation of blood pressure by respiration. It was without effect on the resting heart rate (basal 1: 32 ± 0.2 beats 5 s^{-1}, basal 2: 32 ± 0.3 beats 5 s^{-1}, after CP-99,994: 32 ± 0.6 beats 5 s^{-1}) or on the reflex bradycardia induced by bolus intravenous injection of 30 μg kg^{-1} of 2-methyl-5-HT (Figure 1). The transient reflex increase in blood pressure which follows the bradycardia was not significantly affected by CP-99,994 (Figure 1). In addition, the stimulation of respiratory frequency and depth which is an additional characteristic of the response to 2-methyl-5-HT in the ferret (Andrews *et al.*, 1992b) was not significantly affected by CP-99,994 (Figure 2).

The gag reflex and retching response to abdominal vagal afferent stimulation.

In the conscious ferret, the gag reflex was unaffected by CP-99,994 at a dose (1 mg kg^{-1}, s.c.) that had pronounced anti-emetic effects in the above studies ($n = 4$). In the anaesthetized ferret, the retching response evoked by electrical stimulation of the abdominal vagal afferents was blocked after administration of 1 mg kg^{-1} CP-99,994 i.v. ($n = 4$) (Figure 3). The retching response to abdominal vagal afferent stimulation is usually preceded by licking and swallowing (Andrews *et al.*, 1990), but these epiphenomena were not seen in animals which had been treated with CP-99,994. However, the increase in blood pressure, which also precedes retching, appeared unaffected by CP-99,994. In the same animals, the apnoeic response to cervical vagal stimulation was unaffected as were the guarding and hypertensive responses to central greater splanchnic nerve stimulation. In 2 animals, retesting the response to abdominal vagal afferent stimulation 90 min after administration of CP-99,994 showed that the retching response had returned. An additional animal retested 45 min after CP-99,994 showed a partial recovery with a delayed response starting 30 s after the start of stimulation in contrast to the usual latency of ~15 s. In an additional animal, the initial 1 mg kg^{-1} dose of CP-99,994 delayed but failed to block the response; however, increasing the dose to 3 mg kg^{-1} did block the response. At this higher dose, the reflex responses to cervical vagal and greater splanchnic stimulation were not blocked.

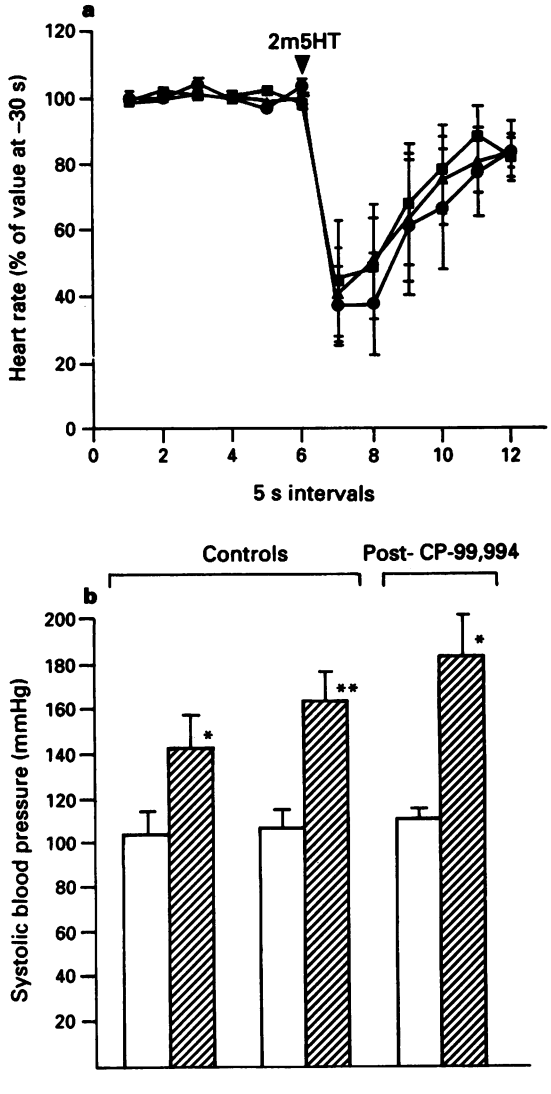

Figure 1 The heart rate and systolic blood pressure response to CP-99,994 and to 2-methyl-5-HT with and without CP-99,994 is shown. 2-Methyl-5-HT (30 μg kg^{-1}) was administered i.v., 3 times to ferrets anaesthetized with urethane. CP-99,994 (1 mg kg^{-1}, i.v.) was administered between the second and third 2-methyl-5-HT challenge. In (a): (■) 1st control; (●) 2nd control and (▲) post-CP-99,994. CP-99,994 did not alter baseline heart rate (a) or systolic blood pressure (b) nor did it alter the statistically significant reduction in heart rate or subsequent compensatory increase in systolic blood pressure following 2-methyl-5-HT (*$P<0.05$, **$P<0.01$). In (b), open columns represent values before 2-methyl-5-HT challenge; hatched columns represent values after 2-methyl-5-HT. Data are mean ± s.e.mean, $n = 5$.

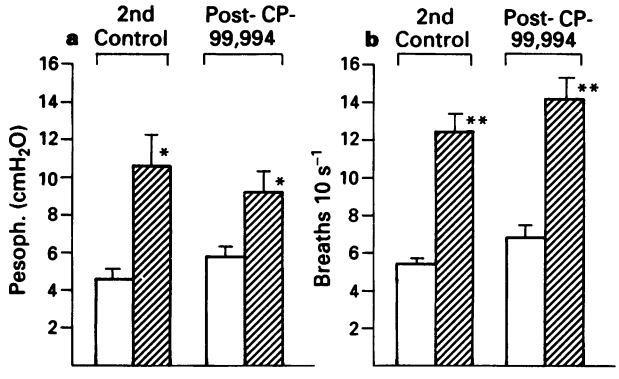

Figure 2 The pulmonary response to CP-99,994 and to 2-methyl-5-HT with and without CP-99,994 is shown. 2-Methyl-5-HT (30 $\mu g\,kg^{-1}$) was administered i.v. 3 times to ferrets anaesthetized with urethane, only the second and third challenges are shown. CP-99,994 (1 $mg\,kg^{-1}$, i.v.) was administered between the second and third 2-methyl-5-HT challenge. While 2-methyl-5-HT challenge produced statistically significant elevations in Pesoph (a) and respiratory rate (b), CP-99,994 did not alter baseline values for either, nor did it alter elevations produced by 2-methyl-5-HT challenge ($^*P<0.05$, $^{**}P<0.005$). Open columns represent values before 2-methyl-5-HT challenge; hatched columns represent values after 2-methyl-5-HT. Data are mean ± s.e.mean, $n = 5$.

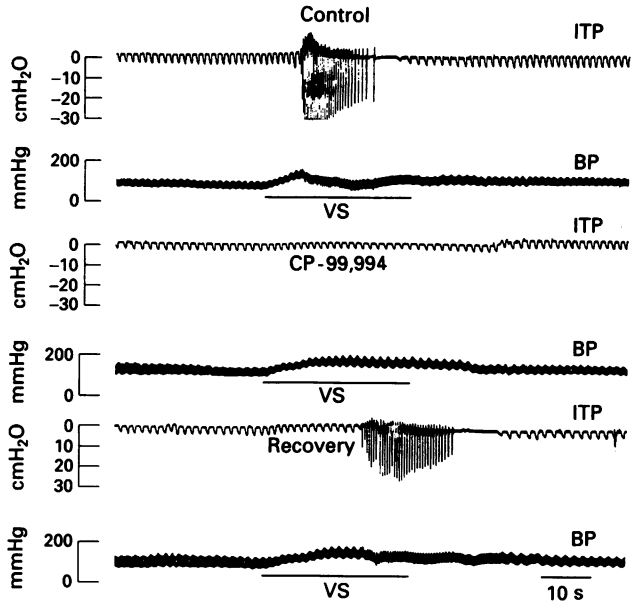

Figure 3 A representative strip chart recording of intra-thoracic pressure (ITP) and blood pressure (BP) responses to ventral abdominal vagus stimulation (vs) before (upper, Control), 15 min following (middle, CP-99,994) and 90 min after (lower, Recovery) administration of 1 $mg\,kg^{-1}$ CP-99,994, i.v.

Autoradiographic studies of the brainstem distribution of [^{3}H]-substance P and the displacement by CP-99,994

Visual inspection and densitometric analysis of representative sections of the dorsal brainstem including the area postrema and the nucleus tractus solitarius revealed the following distribution of [^{3}H]-substance P binding (Figure 4 and Table 7). Dense binding was present in the dorsal motor nucleus of the vagus, along the dorsal edge of the hypoglossal nucleus and in a band along the ventromedial aspect of the fourth ventricle (NTS). The binding along the edge of the ventricle may be associated with ventricular ependymal cells; however, in several sections the binding was clearly associated with a band of cells corresponding to the subnucleus gelatinosus. A lower binding density was present in the rest of the nucleus of the solitory tract and the area postrema. No specific binding was detected in the medial lemniscus. The binding of [^{3}H]-substance P was displaced by incubation with CP-99,994 in a concentration-dependent manner over the range of 0.1 nM to 100 nM (Figure 4b, c and d). CP-99,994 at 100 nM displaced [^{3}H]-substance P binding to levels of nonspecific binding as defined by 2 μM of the specific NK_1 antagonist CP-96,345 (Snider *et al.*, 1991) (Figure 4e).

Discussion

For convenience the results from this study will be discussed firstly in terms of the spectrum of anti-emetic activity and secondly the possible site(s) of the anti-emetic effect of CP-99,994.

Spectrum of anti-emetic activity

This study is the first to demonstrate that the selective NK_1 receptor antagonist, CP-99,994, is a potent, broad spectrum anti-emetic in both the dog and the ferret. It blocked or significantly reduced vomiting and retching in ferrets given loperamide, copper sulphate, cisplatin, syrup of ipecac and apomorphine. It also blocked retching in anaesthetized ferrets following electrical stimulation of abdominal vagal afferents. Similarly, we have shown it to be a potent inhibitor of the retching and vomiting response to copper sulphate and apomorphine in dogs. In a previous preliminary study Bountra *et al.* (1993) demonstrated that CP-99,994 reduced retching in ferrets challenged with cisplatin, copper sulphate, cyclophosphamide, ipecac, morphine, and radiation. In contrast to the present study, Bountra *et al.* (1993) investigated only one dose of a racemic mix containing CP-99,994 administered intraperitoneally or subcutaneously. Also in the ferret, Tattersall *et al.* (1993, 1994) demonstrated a dose-related (0.3–3 $mg\,kg^{-1}$, i.v. or i.p.) reduction in emesis induced by cisplatin and apomorphine. Together the data from all these studies indicate that CP-99,994 is a broad spectrum anti-emetic which is active when given by subcutaneous, intravenous or intraperitoneal routes.

This broad spectrum of anti-emetic activity is unique among selective receptor antagonists, although agonists at $5\text{-}HT_{1A}$, μ-opioid and perhaps vanilloid receptors have been shown to have similar broad spectrum anti-emetic effects in the ferret (Lucot & Crampton, 1989; Barnes *et al.*, 1991; Rudd *et al.*, 1992; 1993; Andrews & Bhandari, 1993). Previous studies have indicated, and we have in part confirmed using tropisetron (ICS 205-930), that $5\text{-}HT_3$ receptor antagonists can block emesis triggered by cisplatin (Miner & Sanger, 1986; Costall *et al.*, 1986; Fitzpatrick *et al.*, 1990; Bhandari *et al.*, 1989; Yoshida *et al.*, 1992) and ipecac (Costall *et al.*, 1990) but not emesis triggered by apomorphine (Bermudez *et al.*, 1989; Costall *et al.*, 1990; Fitzpatrick *et al.*, 1990; Yoshida *et al.*, 1992), loperamide (Bhandari *et al.*, 1992), or copper sulphate (Costall *et al.*, 1990; Fitzpatrick *et al.*, 1990; Bhandari & Andrews, 1991). Similarly, dopamine receptor antagonists block emesis triggered by apomorphine (Costall *et al.*, 1990), but are much weaker inhibitors of cisplatin and ipecac-induced emesis (Costall *et al.*, 1990) while having no effect on the emetic response to loperamide (Bhandari *et al.*, 1992), copper sulphate (Costall *et al.*, 1990) and X-ray or gamma radiation (Andrews *et al.*, 1992a; Cordts *et al.*, 1987). Similarly limited, the muscarinic receptor antagonists reduce emesis induced by emetine, one of the main emetic constituents of ipecac (Roylance *et al.*, 1989), but have no significant effects on the emetic responses to apomorphine (Lang & Marvig, 1989), copper sulphate (Roylance *et al.*, 1989; Lang & Marvig, 1989; Makale & King, 1992), cyclophosphamide (Roylance *et al.*, 1989) or radiation (Roylance *et al.*, 1989).

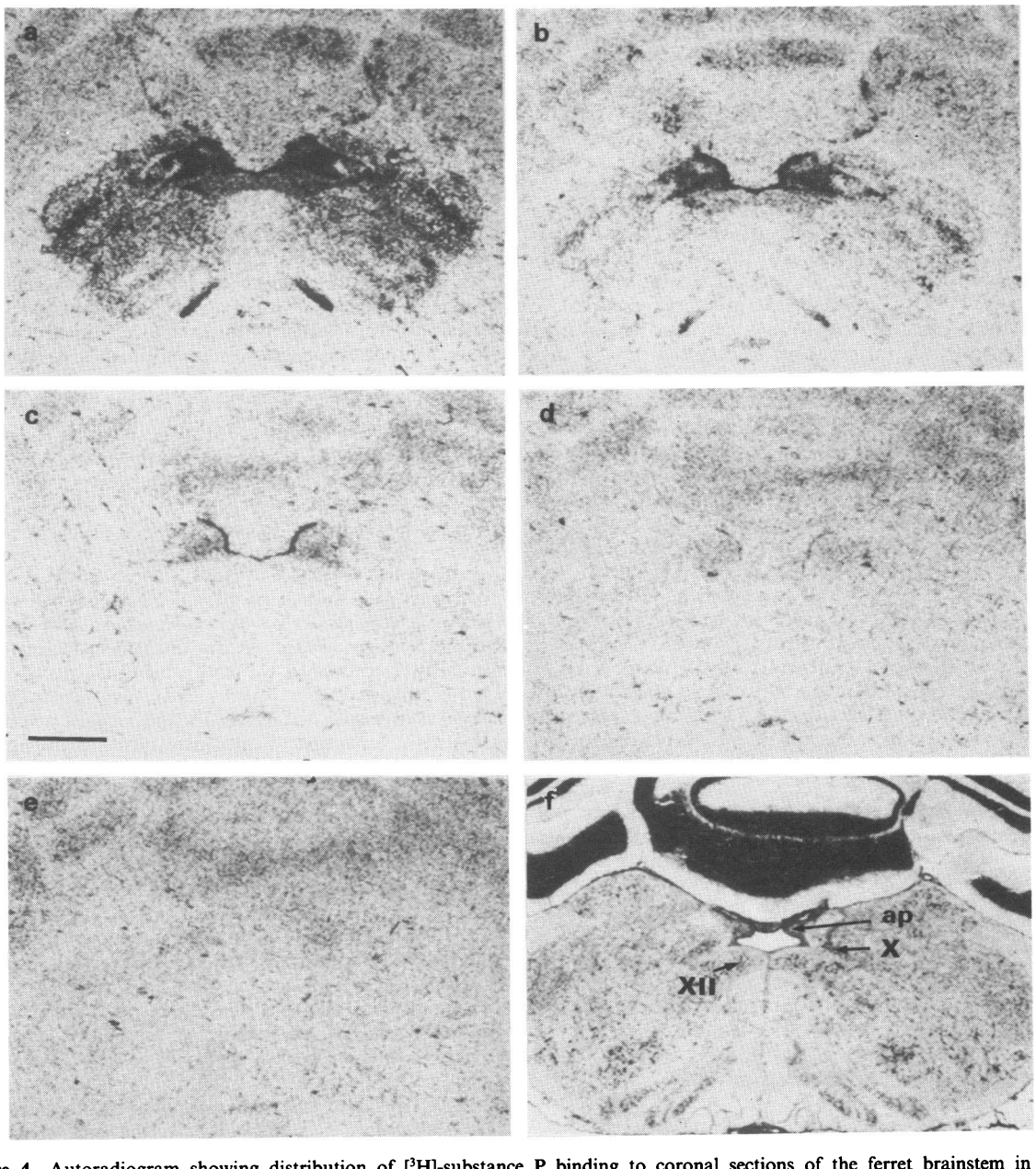

Figure 4 Autoradiogram showing distribution of [^{3}H]-substance P binding to coronal sections of the ferret brainstem in the absence (a) and presence of CP-99,994 at 0.1 nM (b), 10 nM (c), and 100 nM (d). Dark areas correspond to regions of dense binding. Nonspecific binding was determined in the presence of 2 μM CP-96,345 (e). The corresponding cresyl-violet-stained section is shown in (f). Abbreviations are as follows: ap – area postrema, X – dorsal motor nucleus of vagus, XII – hypoglossal nucleus.

The broad anti-emetic profile of CP-99,994 does not appear to be explained by nonspecific actions or a combination of 5-HT$_3$, dopamine or muscarinic receptor antagonist activity. The data indicate both *in vitro* and *in vivo* receptor specificity of this compound. *In vitro*, CP-99,994 has no appreciable affinity ($IC_{50} > 1$ μM) for NK_2, NK_3, dopamine (D_1 and D_2), 5-hydroxytryptamine (5-HT_{1A}, 5-HT_{1B}, 5-HT_{1C}, 5-HT_{1D}, 5-HT_2, 5-HT_3), opiate (μ), noradrenaline (α_1, α_2, and β), histamine (H_1), acetylcholine (muscarinic and nicotinic), glutamate (AMPA, kainate, glycine), benzodiazepine, GABA, cholecystokinin (A and B), calcitonin-gene related peptide or corticotropin releasing hormone receptors (McLean *et al.*, 1993). However, CP-99,994 is a potent antagonist at the ferret and human NK_1 receptor. CP-99,994 displaced ^{125}I-labelled Bolton Hunter conjugate of substance P from ferret brain membranes and human fibroblast (IM9) membranes with IC_{50}s of 1.97 nM and 0.45 nM, respectively. *In vivo*, CP-99,994 had no effect on the von Bezold-Jarisch reflex in anaesthetized ferrets, a model sensitive to the pharmacological actions of 5-HT$_3$ receptor antagonists and an observation which supports the above result from the binding study.

Table 7 Relative optical density units read from film autoradiograms of [^{3}H]-substance P binding to coronal sections of ferret brainstem

Brain area	*Relative optical density*
Area postrema	0.033 ± 0.01
Nucleus tractus solitarius	0.125 ± 0.032
Dorsal motor nucleus of vagus	0.181 ± 0.036
Hypoglossal nucleus	0.155 ± 0.033

The data representing specific binding are derived from 4–5 sections per brain from 3 animals. Non specific binding ranging from 0.08 to 0.11 optical density units has been subtracted.

Enantiospecificity is demonstrated by CP-99,994 at the NK_1 receptor. The (2R,3R) enantiomer of CP-99,994, CP-100,263 is >1 000 times less potent than CP-99,994 at displacing [^{125}I]-Bolton Hunter-substance P binding to ferret brain membranes and IM-9 cells (IC_{50}> 10 μM). CP-100,263, at doses and blood exposures equal to or exceeding those observed in animals dosed with CP-99,994, did not significantly reduce vomiting or retching in response to apomorphine, cisplatin, copper sulphate or loperamide. These results are consistent with those presented by Tattersall *et al.* (1993, 1994) who studied cisplatin and apomorphine-induced emesis and with the anecdotal comments made by Bountra *et al.* (1993) who studied a wider range of emetic stimuli. In the present study however, there was a significant dose-related reduction in ipecac-induced emesis with a concomitant increase in latency. The potency of CP-100,263 in this test was estimated to be about 10 times lower than CP-99,994. The activity of CP-100,263 in this assay was not due to contamination with CP-99,994 as binding studies on IM-9 membranes confirmed the inactivity (IC_{50}> 10 μM) of this lot of compound. The only other significant effect of CP-100,263 was a 4 fold increase in the latency of apomorphine-induced emesis in the ferret, although the number of emetic episodes was unaffected. This result was consistent with previous work (Tattersall *et al.*, 1994) showing a small nonsignificant increase in the latency of apomorphine-induced emesis when CP-100,263 was given intraperitoneally. Further, the recent study of Gardner *et al.* (1994) showed that the anti-emetic effect of 10 μg CP-100,263 was similar to that of 1 μg CP-99,994 when both were injected into the dorsal brainstem of ferrets receiving cisplatin. These observations on the enantiomer suggest that it may have some anti-emetic activity; however, it is far less potent than CP-99,994 and of greater interest, does not appear to have a wide spectrum of activity. Although, under limited conditions CP-100,263 expresses anti-emetic activity that would not be predicted by its potency as an NK_1 antagonist, taken together, both the present and previous studies (Tattersall *et al.*, 1993; 1994; Bountra *et al.*, 1993) support the hypothesis that the broad spectrum anti-emetic activity of CP-99,994 is mediated through the specific blockade of NK_1 receptors. The pharmacological properties of the enantiomer merit further investigation.

Involvement of substance P in emesis

Prior to this and the other preliminary studies it was suggested that substance P neurotransmission was a promising target for the development of new anti-emetics.

(i) Substance P or substance P-like immunoreactivity (SP-li) has been demonstrated in significant levels in two areas of the brainstem intimately involved in emesis namely, the nucleus tractus solitarius and the area postrema (Gillis *et al.*, 1980; Armstrong *et al.*, 1981; 1982; Newton *et al.*, 1985; Leslie, 1985; Baude *et al.*, 1989). In addition SP-li has been demonstrated in axons and varicosities making synaptic contact with neurones in the NTS and area postrema. The cell bodies of some vagal afferents located in the nodose ganglion contain substance P immunoreactivity (Dockray & Sharkey, 1986; Baude *et al.*, 1989) although it is thought that the majority of these cell bodies are the nuclei of thoracic rather than abdominal vagal afferents. In man, substance P-li has been demonstrated in the abdominal vagus and it was presumed to be present in the afferent axons (Lundberg *et al.*, 1976). More recent studies in the cat have demonstrated that the majority of vagal fibres in the brainstem containing substance P were unmyelinated, an observation of potential significance as the majority of unmyelinated afferent fibres in the vagus supply the abdominal viscera (Andrews, 1986; Martini *et al.*, 1992).

(ii) Studies initially performed in the dog and more recently in the ferret, have shown that systemic administration of substance P can induce emesis (Carpenter *et al.*, 1984; Knox *et al.*, 1993). In the urethane-anaesthetized ferret, topical application of substance P to the region of the area postrema induced retching after a latency of about 30 s (Andrews, 1994). Recordings from neurones of the area postrema in the anaesthetized dog have demonstrated that iontophoretic application of substance P, induced firing in about 48% of neurones tested (Carpenter *et al.*, 1983).

(iii) A study of the ultrapotent capsaicin analogue, resiniferatoxin, demonstrated that this agent, when given subcutaneously to ferrets, markedly reduced or abolished the emetic response to both peripherally (vagally dependent: copper sulphate, 'low' dose X-radiation) and centrally (area postrema-dependent: loperamide) acting stimuli in the ferret (Andrews & Bhandari, 1993). Based on several pieces of circumstantial evidence, these authors suggested that the most likely mechanism was a 'depletion of a neurotransmitter, possibly substance P or CGRP, at a central site in the emetic pathway'.

Site of action of CP-99,994

The emetic agents were selected to typify emetic stimuli acting through predominantly central (area postrema) or peripheral (abdominal visceral, predominantly vagal afferent) pathways (see Andrews & Davis, 1993, for review). Apomorphine, a dopamine (D_2) receptor agonist, and loperamide (a μ-opioid receptor agonist), are thought to trigger emesis centrally at the level of the area postrema (Borison & Wang, 1953; Bhandari *et al.*, 1992). In contrast, it has previously been established that cisplatin and copper sulphate trigger emesis by activation of abdominal visceral afferents with the vagi making the predominant contribution (Andrews *et al.*, 1990). Ipecac appears to act acutely at both central and peripheral sites in the ferret (Leslie & Reynolds, 1992).

While the site of anti-emetic action of CP-99,994 has not been completely elucidated, a central site of action is presumed from its ability to block emesis induced by both centrally and peripherally acting agents and an agent such as ipecac, which it is thought, acts at both sites. In addition, CP-99,994 blocked the retching response to abdominal vagal afferent stimulation. As the first synapse in this pathway is within the brainstem, a central site of action has been proposed. The NK_1 receptor antagonist thus differs from 5-HT_3 receptor antagonists that appear to block emesis mediated by vagal afferent pathways activated by the local release of 5-HT in the gut wall (see Andrews, 1994, for review). The contribution of a central site to the anti-emetic effect of 5-HT_3 receptor antagonists is unclear, as for example, they do not affect emesis induced by central stimuli such as apomorphine (Bhandari *et al.*, 1989; Bermudez *et al.*, 1989; Costall *et al.*, 1990) or motion (Stott *et al.*, 1989) and do not block the emetic response to electrical stimulation of abdominal vagal afferents (Milano *et al.*, 1990). However, cisplatin induced emesis can be reduced by central administration of some but not all 5-HT_3 receptor antagonists (Higgins *et al.*, 1989; Fukui *et al.*, 1992). Within the CNS, there are two possible sites for CP-99,994's anti-emetic action.

(i) *The 'vomiting centre'* Because CP-99,994 can affect emesis from a variety of causes it is possible that it affects the region of the brainstem that has been termed the 'vomiting centre'. Although no anatomical correlate has been identified, this region is regarded as the area that integrates all the disparate emetic inputs and coordinates them to generate the sensory, visceral and somatic outputs that comprise nausea and emesis. Both parallel and sequential models have been proposed (Davis *et al.*, 1986) and the NK_1 receptor antagonist could work equally well in either. As there is no anatomical site yet identified, this site cannot be formally investigated; however, if any emetic agent (e.g. motion) were to induce emesis in the presence of a fully potent NK_1 receptor antagonist then it would suggest that this is not the main site of action. It is of interest that a recent paper examining the connectivity of the dorsal vagal complex in the

ferret suggested that the motor emetic centre was located in the nucleus tractus solitarius (Strominger *et al.*, 1994).

(ii) *The nucleus tractus solitarius* From the present study it appears that the NTS is the most likely site of action of CP-99,994 because, this region of the dorsal brainstem is the major site of termination of abdominal vagal afferents and efferents from the area postrema. Thus, it appears to be the first convergence point of the two inputs known to be activated by the various emetic stimuli used in this study. In addition, the dorsal vagal complex, NTS, and in particular the subnucleus gelatinosus were shown to exhibit dense binding of [^{3}H]-substance P, which is displaceable by CP-99,994 in the nmolar to μmolar range. This conclusion is supported by the results in a recent abstract by Gardner *et al.* (1994) showing a dose-related blockade of cisplatin-induced emesis by CP-99,994 injected into the region of the nucleus tractus solitarius in the ferret.

It must be emphasized that the selective nature of CP-99,994's *in vivo* effects rules out a dominant role of NK_1 receptors in a number of other homeostatic neural pathways known to be mediated through the NTS. The reason for this conclusion is that other reflexes which involve the NTS are unaffected by CP-99,994. These include the von Bezold-Jarisch reflex, vago-vagal bradycardia, the subsequent reflex increase in blood pressure and the stimulation of respiration, which involves sympathetic afferents (Andrews *et al.*, 1992b); the swallowing and gag reflexes evoked by pharyngeal stimulation, involving glossopharyngeal, laryngeal and vagal afferents and efferents to the diaphragm (phrenic nerve), abdominal muscles, pharyngeal (hypoglossal, glossopharyngeal) and oesophageal muscles (vagus); and the transient apnoea involving vagal pulmonary afferent inhibition of the phrenic nerve. In contrast, the retching and associated licking and swallowing induced by electrical stimulation of abdominal vagal afferents were blocked by CP-99,994 as were the emetic responses evoked by cisplatin, copper sulphate and ipecac, all of which have been shown to be affected by abdominal vagotomy (Andrews *et al.*, 1988).

Further studies using electrophysiological techniques are required to define more precisely the site of action of NK_1 receptor antagonists and in particular the effects of the antagonists on transmission in the nucleus tractus solitarius and the area postrema.

In conclusion, this study is the first full description of the anti-emetic properties of an NK_1 receptor antagonist (CP-99,994) in two species. In addition a body of evidence is presented from physiological studies of visceral reflexes and autoradiography of the medullary distribution of [^{3}H]-SP which, taken together with the broad spectrum of the anti-emetic activity of CP-99,994, suggests that the main site of action is in the nucleus tractus solitarius although this does not exclude an involvement of a peripheral site (e.g. vagal afferents responding to mucosally released SP, Andrews *et al.*, 1988) for some stimuli (e.g. copper sulphate).

We gratefully acknowledge the technical contributions of D.K. Bryce, M.J. DePasquale, L. Ringer, R.L. Winslow, M. Monroe, G. Antognoli, Ruani Beck and C.A. Ashton.

References

AAPRO, M.S. (1991). 5-HT_3 receptor antagonists. An overview of their present status and future potential in cancer therapy-induced emesis. *Drugs*, **42**, 551–568.

ANDREWS, P.L.R. (1986). Vagal afferent innervation of the gastrointestinal tract. In *Prog. Brain Res.*, Vol. 67, pp. 65–86. ed. Cervero, F. & Morrison, J.F.B. Amsterdam: Elsevier Sci. Publ.

ANDREWS, P.L.R. (1994). 5-HT_3 receptor antagonists and anti-emesis. In *5-HT_3 Receptor Antagonists*. pp. 255-317. ed. King, F.D., Jones, B. & Sanger, G.J. Boca Raton, U.S.A.: CRC Press.

ANDREWS, P.L.R. & BHANDARI, P. (1992). The 5-HT_3 receptor antagonists as anti-emetics: preclinical evaluation and mechanism of action. *Eur. J. Cancer*, **29A**, 511–516.

ANDREWS, P.L.R. & BHANDARI, P. (1993). Resiniferatoxin, an ultrapotent capsaicin analogue, has anti-emetic properties in the ferret. *Eur. J. Pharmacol.*, **32**, 799–806.

ANDREWS, P.L.R., BHANDARI, P. & DAVIS, C.J. (1992a). Plasticity and modulation of the emetic reflex. In *Mechanisms and Control of Emesis*. ed. Bianch, A.L., Grelot, L., Miller, A.D. & King, G.L. Vol. 233, pp. 275–284. INSERM, John Libbey Eurotext.

ANDREWS, P.L.R., BHANDARI, P., GUPTA, A. & WELLS, U. (1992b). The von Bezold-Jarisch reflex in the ferret: evidence for the involvment of non-vagal 5-HT_3 receptors. *Lorenzini Foundation Symposium*, **223**, A48.

ANDREWS, P.L.R. & DAVIS, C.J. (1993). The mechanism of emesis induced by anti-cancer therapies. In *Emesis of Anti-Cancer Therapy: Mechanisms and Treatment*. ed. Andrews, P.L.R. & Sanger, G.J. pp. 113–161. London, U.K.: Chapman & Hall.

ANDREWS, P.L.R., DAVIS, C.J., BINGHAM, S., DAVIDSON, H.I.M., HAWTHORN, J. & MASKELL, L. (1990). The abdominal visceral innervation and the emetic reflex: pathways, pharmacology and plasticity. *Can. J. Physiol. Pharmacol.*, **68**, 325–345.

ANDREWS, P.L.R., RAPEPORT, W.G. & SANGER, G.J. (1988). Neuropharmacology of emesis induced by anti-cancer therapy. *Trends Pharmacol. Sci.*, **9**, 334–341.

ARMSTRONG, D.M., PICKEL, V.M., JOH, T.H., REIS, D.J. & MILLER, R.J. (1981). Immunocytochemical localization of catecholamine synthesizing enzymes and neuropeptides in the area postrema and medial nucleus tractus solitarius of rat brain. *J. Comp. Neurol.*, **196**, 505–517.

ARMSTRONG, D.M., PICKEL, V.M. & REIS, D.J. (1982). Electron microscopic immunocytochemical localization of substance P in the area postrema. *Brain Res.*, **243**, 141–146.

BARNES, N.M., BUNCE, K.T., NAYLOR, R.J. & RUDD, J.A. (1991). The action of fentanyl to inhibit drug induced emesis. *Neuropharmacol.*, **30**, 1073–1083.

BAUDE, A., LANOIR, J., VERNIER, P. & PUIZILLOUT, J.J. (1989). Substance P-immunoreactivity in the dorsal medial region of the medulla in the cat: the effects of nodosectomy. *J. Chem. Neuroanat.*, **2**, 67–81.

BERMUDEZ, J., BOYLE, E.A., MINER, W.D. & SANGER, G.J. (1989). The anti-emetic potential of the 5-hydroxytryptamine-3 receptor antagonist BRL 43694. *Br. J. Cancer*, **58**, 644–651.

BHANDARI, P. & ANDREWS, P.L.R. (1991). Preliminary evidence for the involvement of the putative 5HT-4 receptor in zacopride and copper sulfate-induced vomiting in the ferret. *Eur. J. Pharmacol.*, **204**, 273–280.

BHANDARI, P., BINGHAM, S. & ANDREWS, P.L.R. (1992). The neuropharmacology of loperamide-induced emesis in the ferret: The role of the area postrema, vagus, opiate and 5-HT_3 receptors. *Neuropharmacol.*, **31**, 735–742.

BHANDARI, P., GUPTA, Y.K. & SETH, S.D. (1989). BRL 43694, a new 5-HT_3 receptor antagonist, prevents cisplatin-induced emesis in dogs. *Exp. Clin. Pharmacol.*, **11**, 361–363.

BORISON, H.L. & WANG, S.C. (1953). Physiology and pharmacology of vomiting. *Pharmacol. Rev.*, **5**, 193–230.

BOUNTRA, C., BUNCE, K., DALE, T., GARDNER, C., JORDAN, C., TWISSELL, D. & WARD, P. (1993). Anti-emetic profile of a non-peptide neurokinin NK-1 receptor antagonist, CP-99,994, in ferrets. *Eur. J. Pharmacol.*, **249**, R3–R4.

CARPENTER, D.O., BRIGGS, D.B. & STROMINGER, N.L. (1983). Response of neurons of canine area postrema to neurotransmitters and peptides. *Cell. Mol. Neurobiol.*, **3**, 113–126.

CARPENTER, D.O., BRIGGS, D.B. & STROMINGER, N. (1984). Peptide induced emesis in dogs. *Behav. Brain Res.*, **11**, 277–281.

CORDTS, R.F., YOCHMOWITZ, M.G. & HARDY, K.A. (1987). Evaluation of domperidone as a modifier of gamma-radiation induced emesis. *Int. J. Rad. Oncol. Biol. Phys.*, **13**, 1333–1337.

COSTALL, B., DOMENEY, A.M., NAYLOR, R.J. & TATTERSALL, F.D. (1986). 5-hydroxytryptamine M receptor antagonism to prevent cisplatin-induced emesis. *Neuropharmacol.*, **26**, 669–677.

COSTALL, B., DOMENEY, A.M., NAYLOR, R.J., OWERA-ATEPO, J.B., RUDD, J.A. & TATTERSALL, F.D. (1990). Fluphenazine, ICS 205,930 and dl-fenfluramine differentially antagonize drug-induced emesis in the ferret. *Neuropharmacol.*, **29**, 453–462.

DAVIS, C.J., HARDING, R.K., LESLIE, R.A. & ANDREWS, P.L.R. (1986). The organization of the vomiting reflex as a protective reflex. In *Nausea and Vomiting: Mechanisms and Treatment*. ed. Davis, C.J., Lake-Bakaar, G.V. & Grahame-Smith, D.G. pp. 65–75. Berlin: Springer Verlag.

DOCKRAY, G.J., GREEN, T. & VARO, A. (1989). The afferent peptidergic innervation of the upper gastrointestinal tract. In *Nerves and the GI Tract*. ed. Singer, M.V. & Goebell, H. Falck Symposium 50, pp. 105–122. GDR: Kluver Academic.

DOCKRAY, G.J. & SHARKEY, K.A. (1986). Neurochemistry of visceral afferent neurones. *Prog. Brain Res.*, **67,** 133–148.

FITZPATRICK, L.R., PENDLEY, C.E., LAMBERT, R., BOSTWICK, J., DAVIS, M.A. & CHASE, B.J. (1990). Preclinical pharmacology of RG-12915, an extremely potent serotonin-3 receptor antagonist and blocker of antineoplastic induced emesis. *Gastroenterology*, **98,** A494.

FUKUI, H., YAMAMOTO, M. & SATO, S. (1992). Vagal afferent fibers and peripheral 5-HT_3 receptors mediate cisplatin-induced emesis in dogs. *Jpn. J. Pharmacol.*, **59,** 221–222.

GARDNER, C.J., BOUNTRA, C., BUNCE, K.T., DALE, T.J., JORDAN, C.C., TWISSEL, D.J. & WARD, P. (1994). Anti-emetic activity of neurokinin NK-1 receptor antagonist is mediated centrally in the ferret. *Br. J. Pharmacol.*, (in press).

GILLIS, R.A., HELKE, C.J., HAMILTON, B.L., NORMAN, W.P. & JACOBWITZ, D.W. (1980). Evidence that substance P is a neurotransmitter of baro- and chemoreceptor afferents in nucleus tractus solitarius. *J. Brain Res.*, **181,** 476–481.

HIGGINS, G.A., KILPATRICK, G.J., BUNCE, K.T., JONES, B.J. & TYERS, M.B. (1989). 5-HT_3 receptor antagonists injected into the area postrema inhibit cisplatin induced emesis in the ferret. *Br. J. Pharmacol.*, **97,** 247–255.

KNOX, A.P., STROMINGER, N.L., BATTLES, A.H. & CARPENTER, D.O. (1993). Behavioural studies of emetic sensitivity in the ferret. *Brain Res. Bull.*, **31,** 477–484.

LANG, I.M. & MARVIG, J. (1989). Functional localization of specific receptors mediating gastrointestinal motor correlates of vomiting. *Am. J. Physiol.*, **256,** G92–G99.

LESLIE, R.A. (1985). Neuroactive substances in the dorsal vagal complex of the medulla oblongata: nucleus of the tractus solitarius, area postrema, and dorsal motor vagal nucleus. *Neurochem. Int.*, **7,** 191–211.

LESLIE, R.A. & REYNOLDS, J.A. (1992). Functional anatomy of the emetic circuitry in the brainstem. In *Mechanisms and Control of Emesis*. ed. Bianch, A.L., Grelot, L., Miller, A.D. & King, G.L. Vol. 233, pp.19–27. Colloque INSERM, John Libbey Eurotext.

LUCOT, J.B. & CRAMPTON, G.H. (1989). 8-OH-DPAT suppresses vomiting in the cat elicited by motion, cisplatin or xylazine. *Pharmacol. Biochem. Behav.*, **33,** 627–631.

LUNDBERG, J., AHLMAN, H., DAHLSTROM, A. & KEWENTER, J. (1976). Catecholamine containing nerves in the human abdominal vagus. *Scand. J. Gastroenterol.*, **70,** 472–475.

MAKALE, M.T. & KING, G.L. (1992). Surgical and pharmacological dissociation of cardiovascular and emetic responses to intragastric CuSO4. *Am. J. Physiol.*, **263,** R284–291.

MARTINI, F., BAUDE, A. & PUIZILLOUT, J.J. (1992). Substance P in the dorsal vagal nucleus: are preganglionnar cells directly connected by substance P containing afferents. In *Mechanisms and Control of Emesis*. ed. Bianch, A.L., Grelot, L., Miller, A.D. & King, G.L. Vol. 233, pp. 89–90. Colloque INSERM, John Libbey Eurotext.

MCLEAN, S., GANONG, A., SEYMOUR, P.A., SNIDER, R.M., DESAI, M.C., ROSEN, T., BRYCE, D.K., LONGO, K.P., REYNOLDS, L.S., ROBINSON, G., SCHMIDT, A.W., SIOK, C. & HEYM, J. (1993). Pharmacology of CP-99,994: a non-peptide antagonist of the tachykinin NK-1 receptor. *J. Pharmacol. Exp. Ther.*, **267,** 472–479.

MIFFLIN, S.W. (1993). Laryngeal afferent inputs to the nucleus of the solitary tract. *Am. J. Physiol.*, **265,** R269–276.

MILANO, GRELOT, L., CHEN, Z. & BIANCHI, A.L. (1990). Vagal-induced vomiting in decerebrate cat is not suppressed by specific 5-HT_3 receptor antagonists. *J. Auton. Nerv. Syst.*, **31,** 109–118.

MINER, W.D. & SANGER, G.J. (1986). Inhibition of cisplatin induced vomiting by selective 5HT-M receptor antagonism. *Br. J. Pharmacol.*, **88,** 497–499.

NEWTON, B.W., MALEY, B. & TRAURIG, H. (1985). The distribution of substance P, enkephalin and serotonin immunoreactivities in the area postrema of the rat and cat. *J. Comp. Neurol.*, **234,** 87–104.

PAYAN, D.G., BREWSTER, D.R. & GOETZL, E.S. (1984). Stereospecific receptors for substance P on cultured IM-9 lymphoblasts. *J. Immunol.*, **133,** 3260–3265.

PRIESTMAN, T.J. (1989). Clinical studies with ondansetron in control of radiation-induced emesis. *J. Cancer Clin. Oncol.*, **25** (suppl. 1), S29–S33.

RABIN, B.M. & KING, G.L. (1992). Is all radiation-induced emesis ameliorated by 5-HT_3 receptor antagonists? In *Mechanisms and Control of Emesis*. ed. Bianch, A.L., Grelot, L., Miller, A.D. & King, G.L. Vol. 233, pp. 147–155. Colloque INSERM: John Libbey Eurotext.

REYNOLDS, D.J.M., BARBER, N.A., GRAHAME-SMITH, D.G. & LESLIE, R.A. (1991). Cisplatin-evoked induction of c-fos protein in the brainstem of the ferret: the effect of cervical vagotomy and the anti-emetic 5-HT_3 receptor antagonist granisetron (BRL 43694). *Brain Res.*, **565,** 231–236.

ROYLANCE, R.R., ANDREWS, R.L.R., HAWTHORN, J., BINGHAM, S. & DAVIDSON, H.I. (1989). The anti-emetic effects of atropine sulfate in the ferret. *Br. J. Pharmacol.*, **96,** 330P.

RUDD, J.A., BUNCE, K.T. & NAYLOR, R.J. (1992). The effect of 8-OH-DPAT on drug-induced emesis in the ferret. *Br. J. Pharmacol.*, **106,** 101P.

RUDD, J.A., BUNCE, K.T. & NAYLOR, R.J. (1993). The effect of 5-HT_{1A} receptor ligands on copper sulphate-induced emesis in the ferret. *Br. J. Pharmacol.*, **110,** 99P.

SNIDER, R.M., CONSTANTINE, J.W., LOWE, J.A., LONO, D.P., LEBEL, W.S., WOODY, H.A., DROZA, S.E., DESAI, M.C., VINICK, F.J., SPENCER, R.W. & HESS, H.-J. (1991). A potent non peptide antagonist of the substance P (NK-1 receptor). *Science*, **251,** 435–439.

STOTT, J.R.R., BARNES, G.R., WRIGHT, R.J. & RUDDOCK, C.J.S. (1989). The effect on motion sickness and oculomotor function of GR 38032F, a 5-HT_3 receptor antagonist with anti-emetic properties. *Br. J. Clin. Pharmacol.*, **27,** 1–11.

STROMINGER, N.L., KNOX, A.P. & CARPENTER, D.O. (1994). The connectivity of the area postrema in the ferret. *Brain Res. Bull.*, **33,** 33–47.

TATTERSALL, F.D., RYCROFT, W., HARGREAVES, J. & HILL, R.G. (1993). The tachykinin NK-1 receptor antagonist CP-99,994 attenuates cisplatin induced emesis in the ferret. *Eur. J. Pharmacol.*, **250,** R5–R6.

TATTERSALL, F.D., RYCROFT, W., HILL, R.G. & HARGREAVES, R.J. (1994). Enantioselective inhibition of apomorphine-induced emesis in the ferret by the neurokinin-1 receptor antagonist CP-99,994. *Neuropharmacol.*, **33,** 259–260.

THOMPSON, P.I., BINGHAM, S., ANDREWS, P.L.R., PATEL, N., JOEL, S.P. & SLEVIN, M.L. (1992). Morphine 6-glucuronide: a metabolite of morphine with greater emetic potency than morphine in the ferret. *Br. J. Pharmacol.*, **106,** 3–8.

YOSHIDA, N., OMOYA, H. & ITO, T. (1992). DAT-582 a novel serotonin 3 receptor antagonist is a potent and long lasting anti-emetic agent in the ferret and dog. *J. Pharmacol. Exp. Ther.*, **260,** 1151–1165.

(Received August 15, 1994
Revised November 14, 1994
Accepted November 16, 1994)

British Journal of Pharmacology (1995) 115, 95-100

Effect of 5-hydroxytryptamine on the membrane potential of endothelial and smooth muscle cells in the pig coronary artery

M. Frieden & [1]J.-L. Bény

Department of Zoology and Animal Biology, University of Geneva, Sciences III, 30 quai Ernest-Ansermet, 1211 Geneva 4, Switzerland

1 Many endothelium-dependent vasodilators hyperpolarize the endothelial cells in blood vessels. It is not known whether these hyperpolarizations are linked to nitric oxide synthesis or to an endothelium-derived hyperpolarizing phenomenon, since most of the vasodilators release both factors. In this context, we first verified that the endothelium-dependent relaxations induced by 5-hydroxytryptamine (5-HT) on pig coronary arteries are due only to the activation of the nitric oxide pathway. Then we studied the effects of 5-HT on membrane potential of endothelial and smooth muscle cells.

2 In the absence of endothelium, 5-HT caused a concentration-dependent contraction of coronary artery strips. No change of the smooth muscle cell membrane potential was observed during contraction to 1 μM 5-HT.

3 In the presence of 1 μM ketanserin to suppress the contractile effect of 5-HT, 5-HT induced concentration-dependent relaxation of endothelium-intact strips precontracted by 10 μM prostaglandin $F_{2\alpha}$ ($PGF_{2\alpha}$). These relaxations were suppressed by 1 μM N^G-nitro-L-arginine, an inhibitor of nitric oxide synthesis, showing that they were produced predominantly by nitric oxide.

4 In the presence of 1 μM ketanserin, 1 μM 5-HT did not change the smooth muscle cell membrane potential of strips precontracted by either 10 μM $PGF_{2\alpha}$ or by 10 μM acetylcholine (ACh). In the same conditions, 1 μM 5-HT caused a weak 2.6 ± 0.4 mV hyperpolarization, of the endothelial cells.

5 In conclusion, the fact that 5-HT did not change the membrane potential of smooth muscle cells and only weakly hyperpolarized the endothelial cells during relaxations, suggests that in both cell types no electrical events accompany activation of the nitric oxide pathway. This is in contrast to the hyperpolarizations observed in endothelial and smooth muscle cells when the endothelium-derived hyperpolarization factor (EDHF) pathway is activated.

Keywords: Electrophysiology; endothelial cells; 5-HT; nitric oxide; pig coronary artery; membrane potential

Introduction

Many endothelium-dependent vasodilators relax vascular smooth muscles by inducing the release of endothelial agents such as nitric oxide, prostacyclin and the putative endothelium-dependent hyperpolarizing factor (EDHF) (Rubanyi & Vanhoutte, 1990). These agents are produced in different proportions by the endothelial cells, depending on the blood vessel and the vasodilator inducing their release.

In pig coronary arteries, the two kinins substance P (SP) and bradykinin (BK), relax the smooth muscle in an endothelium-dependent manner by releasing nitric oxide from the endothelium, and by triggering the phenomenon known as EDHF (Pacicca *et al.*, 1992). During these endothelium-dependent relaxations caused by kinins, the membrane potential of endothelial and of underlying smooth muscle cells simultaneously hyperpolarizes in the same manner, even when the synthesis of nitric oxide is inhibited (Bény *et al.*, 1986; 1987; Brunet & Bény, 1989; Bény, 1990a,b; Pacicca *et al.*, 1992). However, it is not known whether the two hyperpolarizations are cause-effect related. In addition, exogenous nitric oxide does not hyperpolarize the smooth muscle cells of pig coronary artery (Bény & Brunet, 1988), or of canine mesenteric artery (Komori *et al.*, 1988). Unlike the kinins, which stimulate nitric oxide synthesis and EDHF phenomenon, 5-hydroxytryptamine (5-HT) releases only nitric oxide from the pig coronary artery endothelium and probably no or very little EDHF (Vanhoutte, 1987; Richard *et al.*, 1990; Bruning *et al.*, 1993). Our purpose in the present study was to determine the role of membrane potential changes in endothelium and smooth muscle cells when nitric oxide, but not the EDHF pathway, is activated.

In pig coronary arteries, at least two types of 5-HT receptors are present. The 5-HT_1, characterized as 5-HT_{1D}-subtype by Schoeffter & Hoyer (1990), is located on the endothelial cells. Its activation leads to vascular relaxation (Cocks & Angus, 1983; Cohen *et al.*, 1983) via the release of nitric oxide (Richard *et al.*, 1990). The 5-HT_2 receptor is located on smooth muscle cells and produces vasoconstriction when activated by 5-HT (for review see Vanhoutte *et al.*, 1984). This effect is inhibited by the selective 5-HT_2 receptor antagonist, ketanserin (R 41468) (Van Neuten *et al.*, 1981; Leysen *et al.*, 1981).

We first verified that, with our methodology, 5-HT relaxes pig coronary arteries in an endothelium-dependent manner only via the nitric oxide pathway. Then we observed the membrane potential changes in endothelial or smooth muscle cells during contraction or relaxation of coronary artery strips induced by 5-HT.

Methods

Preparation of tissues

Anterior descending branches of pig coronary arteries were obtained at the slaughterhouse. The coronary lumen were rinsed by injection of cold, oxygenated (95% O_2, 5% CO_2) Krebs solution (mM: NaCl 118.7, KCl 4.7, $CaCl_2$ 2.5, KH_2PO_4 1.2, $NaHCO_3$ 24.8, $MgSO_4$ 1.2, glucose 10.1; pH 7.3-7.4). Segments of the coronary artery were cleaned out of adherent tissue, and cut into rings of about 2 mm width. These rings were cut longitudinally to give strips about 5 mm in length. In some experiments, the endothelium was removed by rubbing the luminal face of the strip with a cotton-tip.

[1] Author for correspondence.

The lack of response to SP or BK was taken as evidence for the complete removal of the endothelium (Bény *et al.*, 1986; 1987).

Electrophysiology of endothelial and smooth muscle cells

Mechanical isometric tension and transmembrane potential of the smooth muscle or the endothelial cells were simultaneously recorded as previously described (Bény *et al.*, 1986). The strip was incubated in a 200 µl Perspex bath continuously perfused with oxygenated Krebs (3.7 ml min^{-1}) at 36°C with a peristaltic pump. Peptides and drugs were delivered to the preparations by diluting them directly in the plastic beaker containing the perfusion solution. This avoided any perturbation in the perfusion flow rate.

One extremity of the strip was pinned on a silicon rubber surface with the intimal surface facing up. The other extremity was fixed horizontally to a force transducer. Changes in tension were measured isometrically with a transducer (Grass FT03C, USA), amplified (Lectromed) and recorded on a polygraph (W&W Electronics, USA). A force of about 10 mN was first applied to the strip by pulling the transducer with a micromanipulator. The tension stabilized to about 5 mN. In experiments studying relaxation to 5-HT, 10 µM prostaglandin $F_{2\alpha}$ ($PGF_{2\alpha}$) or 10 µM acetylcholine (ACh) were then added throughout the experiment to the perfusion fluid to produce a reproducible state of initial tension of the strip.

The membrane potential was measured with a conventional glass microelectrode (60–80 MΩ) filled with 3 M KCl. Cells were impaled near the fixed points of the tissue in order to reduce problems due to muscle movements. The criteria for accepting a record were a stable membrane potential and a sharp rise to 0 mV when the electrode was withdrawn from the recorded cell.

The technique for determining which cell type is impaled was the following. We slowly advanced the microelectrode to the intimal face of the strip. It first penetrated an endothelial cell, and then touched the internal elastic lamina which presented a mechanical resistance, visible as an erratic change in the potential measured by the electrode. After crossing the internal elastic lamina the electrode penetrated smooth muscle cells. The efficiency of this technique was proved by microiontophoretic injection of the lucifer yellow dye through the recording electrode, followed by examination with a fluorescence microscope.

Lucifer yellow injection

By injection of lucifer yellow we verified that the experimentally selected cells were actually endothelial cells. This identification was performed in approximately 50% of the cases. The method has already been described in detail (Bény & Gribi, 1989; Bény & Connat, 1991). Briefly, the cell membrane potential was measured with a glass microelectrode with its tip filled with a lucifer yellow solution (5% in water), back-filled with 150 mM LiCl. The microiontophoretic injection of the fluorescent dye was achieved by passing a direct current of 0.35 nA through the electrode for 0.5–5 min. To identify the injected cells, the tissue was fixed with 4% paraformaldehyde. The luminal face of the strip was examined with a fluorescence microscope (Nikon diaphot; excitation wavelength, 450–490 nm). The injected endothelial cells appeared as a cluster of fluorescent, ellipsoidal cells, whereas the smooth muscle cells appeared as a bundle of fluorescent, fusiform cells (Bény & Connat, 1991).

Establishment of concentration-response curve

When only mechanical tension was measured to obtain concentration-response curves, ligatures were attached to both ends of the strips, which were mounted with a resting isometric tension of about 10 mN in a 85 µl tissue bath as previously described (Bény *et al.*, 1986; 1987). To establish concentration-response curves for 5-HT, strips, contracted by 10 µM $PGF_{2\alpha}$, were superfused with a Krebs solution containing each concentration of 5-HT in an ascending, non-cumulative manner, with sufficient time between each challenge to allow full relaxation (a 20–40 min wash-out period was performed between successive concentration). 5-HT was administered to the preparations by diluting it directly in the plastic beaker that contained the perfusion solution. Where indicated in the results section, different inhibitors were used: 10 µM indomethacin to block cyclo-oxygenase, 1 µM ketanserin to suppress the contracting effect of 5-HT_2 receptors, and 1 µM N^G-nitro-L-arginine (L-NOARG) for inhibiting nitric oxide synthase. These inhibitors were administered to the strips in the perfusion fluid for at least 25 min before the first application of 5-HT.

Preparation of peptides and chemicals

The peptides, BK and SP, were prepared at a concentration of 1 mg ml^{-1} in 0.25% acetic acid. They were stored in 50 µl aliquots and kept frozen at −20°C until use. The $PGF_{2\alpha}$ was prepared at a concentration of 1 mg ml^{-1} in 75% ethanol. L-NOARG was prepared at a concentration of 10 mg ml^{-1} in 0.02% HCl, and indomethacin at a concentration of 2 mg ml^{-1} in >99.8% ethanol. Ketanserin was prepared at a concentration of 3.95 mg ml^{-1} in N-N dimethyl formamide (DMF) and aliquots of 200 µl were kept frozen at −20°C until use. 5-HT was prepared at a concentration of 0.4 mg ml^{-1} in water. $PGF_{2\alpha}$, peptides and inhibitors were diluted subsequently to the desired concentrations with Krebs solution.

Drugs

$PGF_{2\alpha}$, ACh, indomethacin and lucifer yellow were obtained from Sigma (St. Louis, MO, U.S.A.). SP and BK were obtained from Bachem Feinchemikalien (AG, Budendorf, Switzerland). L-NOARG was obtained from Aldrich (Steinheim, Germany). 5-HT and ketanserin were obtained from Fluka (Buchs, Switzerland).

Statistical analysis

For electrophysiological experiments, *n* corresponds to the number of impalements. The number of coronary arteries used to obtain this value of *n* is specified in the results section. For the other experiments, *n* corresponds to the number of coronary arteries, each of which originates from a different pig heart. Data were calculated as the mean ± standard error of the mean (s.e.mean). Student's test was used to compare results. A P value <0.05 was taken as significant. The effective concentrations of 5-HT that provoked 50% of maximal effect (inhibitory concentration 50; IC_{50} or excitatory concentration 50; EC_{50}) was calculated for each concentration-response curve by interpolation between two points on either side of the half maximal response and followed by reading the corresponding concentration on the logarithmic scale. The mean ± s.e.mean of these readings was calculated.

Results

Dual effects of 5-HT on coronary strip isometric tension

These experiments were performed with an intact endothelium. Strips were continuously, tonically contracted by 10 µM $PGF_{2\alpha}$ in the presence of 10 µM indomethacin to suppress prostacyclin synthesis. 5-HT relaxed strips from a concentration of 10 nM up to a maximal relaxation that occurred at 30 nM. At higher concentrations of 5-HT, the relaxation diminished. Starting at a concentration of 1 µM, 5-HT con-

tracted strips, thus producing a biphasic concentration-response curve. The contraction reached a maximum at 3 μM 5-HT. This maximum represents an additional contraction of about 45% above the tonic contraction caused by $PGF_{2\alpha}$ ($n = 4$, Figure 1).

Contractile effect of 5-HT on strips without endothelium

Strips without endothelium were concentration-dependently contracted by 5-HT. We observed this effect when 5-HT was applied to strips already contracted by 10 μM $PGF_{2\alpha}$ as well as on non-precontracted strips. The two concentration-response curves so obtained were superimposable. The contraction began in response to a concentration of about 20 nM 5-HT, and reached a maximum at about 20 μM. The excitatory concentration giving half maximal contraction was 680 ± 72 nM ($n = 4$) when strips were precontracted, and 795 ± 270 nM ($n = 4$) when not precontracted (Figure 1). In contrast, to the ACh provoked contractions, which begin with a phasic contraction followed by a weaker tonic contraction (Ito *et al.*, 1979), the 5-HT contractions are sustained as long as the agonist is present.

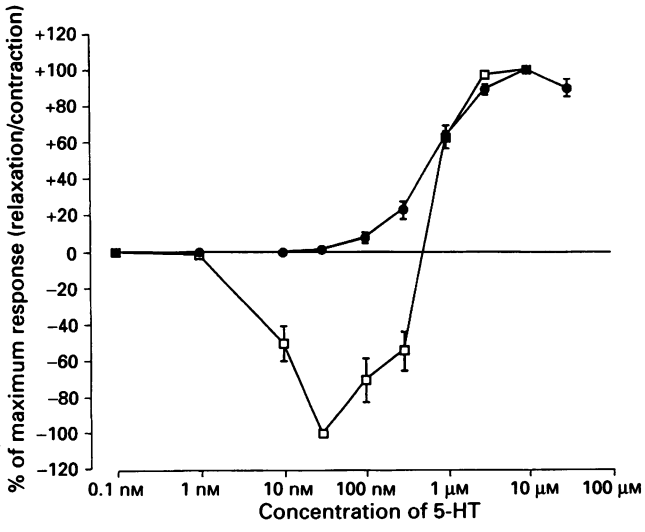

Figure 1 Concentration-response curves to 5-hydroxytryptamine (5-HT): (□) strip with an intact endothelium and tonically contracted by 10 μM prostaglandin $F_{2\alpha}$ ($PGF_{2\alpha}$), in the presence of 10 μM indomethacin and without ketanserin ($n = 4$); (●) strip without endothelium and tonically contracted by 10 μM $PGF_{2\alpha}$ ($n = 4$). Values are mean ± s.e.mean.

Endothelium-dependent relaxant effect of 5-HT

In the presence of 10 μM indomethacin to inhibit cyclooxygenase activity, and 1 μM ketanserin to suppress the contractile effect mediated by $5\text{-}HT_2$ receptors, 5-HT relaxed precontracted strips (10 μM $PGF_{2\alpha}$) with an intact endothelium. The relaxation began at 3 nM 5-HT and reached a maximum at 0.3 μM (corresponding to an inhibition of about 70% of the contraction caused by $PGF_{2\alpha}$), with an IC_{50} of 21.3 ± 2.7 nM ($n = 5$, Figures 2a, b). Endothelium-dependent relaxation was suppressed by inhibition of nitric oxide synthase with 1 μM L-NOARG ($n = 6$, Figure 2b).

Effect of 5-HT on smooth muscle cell membrane potential in strips without endothelium

In the absence of endothelium and ketanserin, the smooth muscle cell membrane potential was −47 ± 2 mV ($n = 11$; 9 arteries). 5-HT (1 μM) contracted the strip without any effect on smooth muscle cell membrane potential, which remained at −46.4 ± 2.4 mV ($n = 11$; $P > 0.4$) during the onset of contraction (Figure 3). Because of the strong strip contraction, the microelectrode was generally dislodged after the contraction had reached approximately 20% of its maximal value. Consequently, membrane potential was also measured in cells

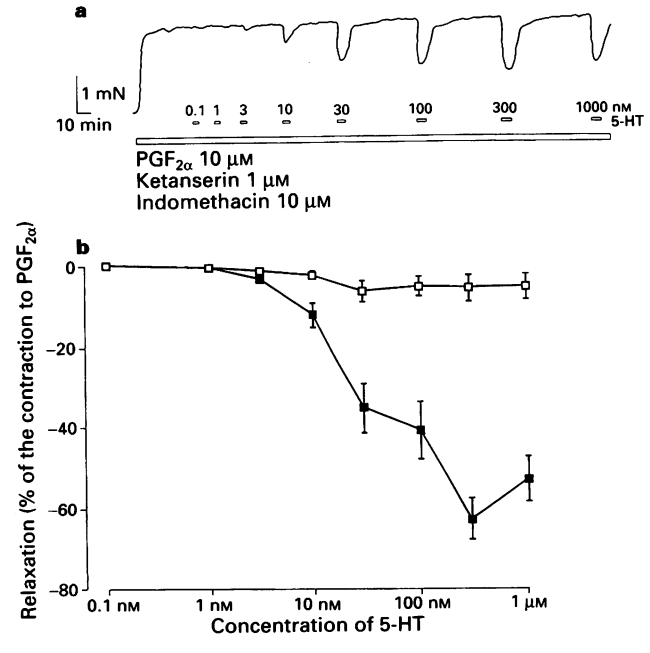

Figure 2 (a) Original recording of mechanical activity of a strip tonically contracted by 10 μM prostaglandin $F_{2\alpha}$ ($PGF_{2\alpha}$) in the presence of 1 μM ketanserin and 10 μM indomethacin. Relaxations produced by graded concentrations of 5-hydroxytryptamine (5-HT) are shown. (b) Concentration-response curve for 5-HT applied to strips tonically contracted by 10 μM $PGF_{2\alpha}$ in the presence of 1 μM ketanserin and 10 μM indomethacin; with (□; $n = 6$) and without (■; $n = 5$) N^G-nitro-L-arginine (L-NOARG), an inhibitor of nitric oxide synthase. Values are mean ± s.e.mean.

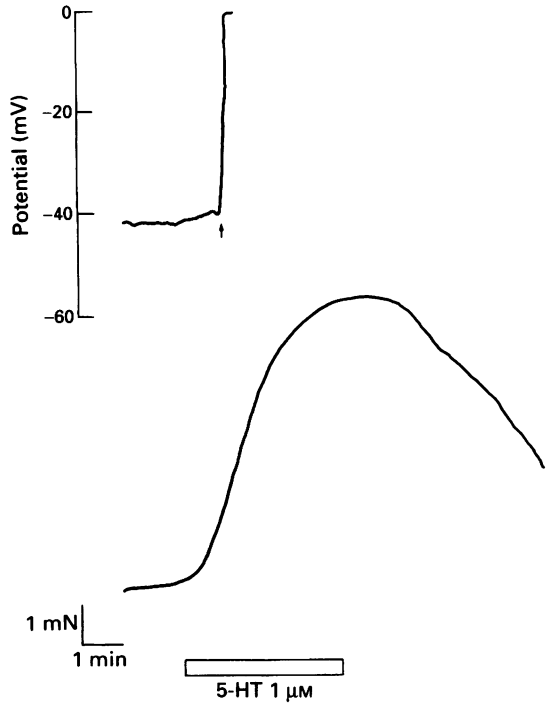

Figure 3 Simultaneous recording of smooth muscle cell membrane potential (upper trace) and isometric tension of the strip (lower trace) without endothelium. The strip was not precontracted. 5-Hydroxytryptamine (5-HT) 1 μM, did not change the membrane potential during the onset of the contraction. The arrow indicates when the microelectrode was withdrawn from the cell.

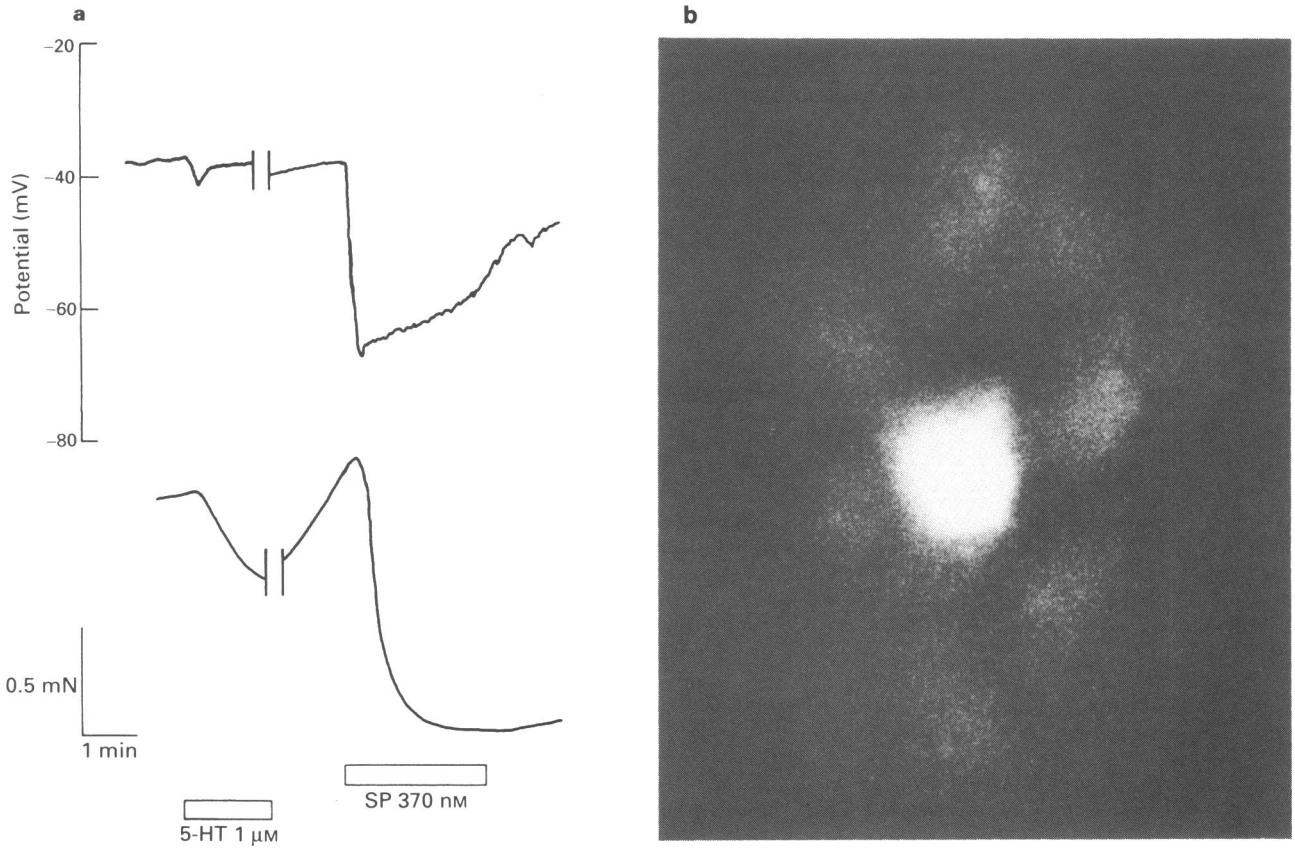

Figure 4 (a) Simultaneous recording of endothelial cell membrane potential (upper trace) and isometric tension of the strip (lower trace). The strip was tonically contracted by 10 μM prostaglandin $F_{2\alpha}$ ($PGF_{2\alpha}$) in the presence of 10 μM indomethacin and 1 μM ketanserin. 5-Hydroxytryptamine (5-HT) 1 μM, had no significant effect on the membrane potential; by comparison, the effect of substance P (SP) 370 nM proved that the recorded cell and the strip were functional. For technical reasons, recording was interrupted during the lucifer yellow injection. (b) Fluorescent microscope image of the intimal face of the pig coronary artery strip. The endothelial cell in the middle of the photograph was injected with the fluorescent dye lucifer yellow during the membrane potential recording (a). The photograph shows clearly that the endothelial cells were dye coupled.

impaled after contraction reached a stable maximal value. In this condition, membrane potential was -43.9 ± 1.6 ($n = 12$; 4 arteries), which was not significantly different from the membrane potential ($P > 0.15$) measured before the application of 5-HT.

Effect of 5-HT on the membrane potential of endothelial cells

These experiments were achieved in strips contracted by 10 μM $PGF_{2\alpha}$, in the presence of 10 μM indomethacin and 1 μM ketanserin. The endothelial cell membrane potential was -42.4 ± 2 mV ($n = 10$; 7 arteries). 5-HT (1 μM) caused a weak change in the membrane potential of endothelial cells to -45 ± 2 mV, which corresponds to a hyperpolarization of 2.6 ± 0.4 mV. In comparison, SP (370 nM) hyperpolarized these cells by 28.8 ± 2.1 mV ($n = 5$, Figure 4a). The impaled cells were identified as endothelial cells by injection of lucifer yellow after application of 5-HT ($n = 4$, Figure 4b).

Endothelium-dependent effect of 5-HT on smooth muscle cell membrane potential

The membrane potential was recorded in strips with an intact endothelium, tonically contracted by 10 μM $PGF_{2\alpha}$, in the presence of 10 μM indomethacin and 1 μM ketanserin. The smooth muscle cell membrane potential was -45.2 ± 2.9 mV ($n = 9$; 8 arteries). 5-HT (1 μM) had no significant effect ($P > 0.4$) on this potential, -46.1 ± 3.2 mV ($n = 9$), (for up to 90 s following the application of 5-HT). These results were obtained by continuous recording of the membrane potential

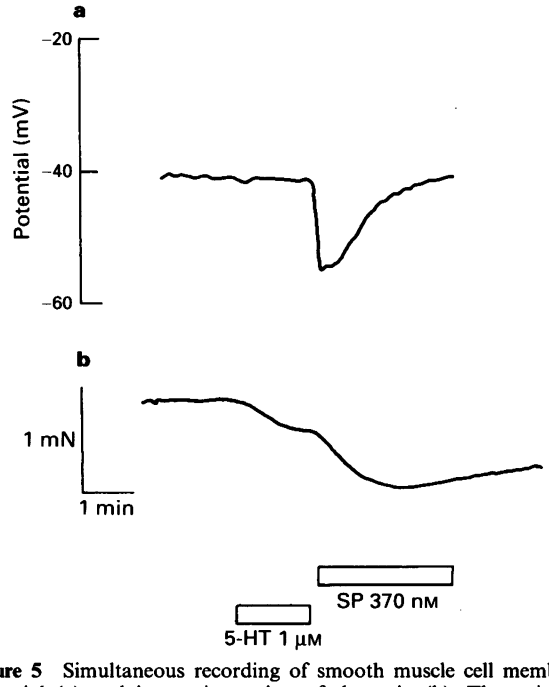

Figure 5 Simultaneous recording of smooth muscle cell membrane potential (a) and isometric tension of the strip (b). The strip was continuously contracted by acetylcholine (10 μM) in presence of 1 μM ketanserin and 10 μM indomethacin. 5-Hydroxytryptamine (5-HT) 1 μM, had no effect on the membrane potential; by comparison, the effect of substance P (SP) 370 nM proved that the recorded cell and the strip were functional.

before and during the application of 5-HT. We verified the responsiveness of these cells by applying 370 nM SP, which hyperpolarized the cells by 15.3 ± 1 mV ($n = 7$) in an endothelium-dependent manner. The relaxation caused by the application of 5-HT, recorded simultaneously with the membrane potential, proved that the strip was physiologically functional.

In our past publications, ACh was used as the contracting agent. To be able to compare the present results with those already obtained on this tissue, we also studied the effect of 5-HT on a strip continuously contracted by 10 μM ACh instead of $PGF_{2\alpha}$. The smooth muscle cell membrane potential was then −44.8 ± 1 mV ($n = 6$; 3 arteries). 5-HT (1 μM) did not change the membrane potential, which remained at −45.1 ± 0.9 mV ($n = 6$; $P > 0.4$). SP (370 nM) induced a transient hyperpolarization of 13.4 ± 1.8 mV ($n = 5$, Figure 5).

Discussion

The biphasic aspect of the concentration-response curve for 5-HT reflects the existence of two receptor types in this tissue (Cocks & Angus, 1983; Cohen *et al.*, 1983; Vanhoutte *et al.*, 1984; Houston & Vanhoutte, 1986; Angus, 1989). The biphasic curve results from the algebraic sum of the contractile effect of 5-HT (as displayed by the concentration-response curve obtained without endothelium), and the endothelium-dependent relaxant effect (in the presence of ketanserin that inhibits the $5\text{-}HT_2$ receptors). The IC_{50} (about 20 nM) and EC_{50} (about 700 nM) of dual 5-HT effects are compatible with those already determined for pig coronary arteries (Molderings *et al.*, 1989; Richard *et al.*, 1990; Schoeffter & Hoyer, 1990), and for human or bovine coronary arteries (Ratz & Flaim, 1985; Bax *et al.*, 1993).

The fact that L-NOARG suppressed the relaxation indicates that the only endothelium-dependent relaxant factor released by 5-HT is nitric oxide. The effect of L-NOARG on the endothelium-dependent relaxation induced by SP or BK is rather different, since L-NOARG inhibits relaxation by only 30% (Pacicca *et al.*, 1992).

All the smooth muscle cell membrane potentials measured were of the same order of magnitude (range −38 to −62 mV) as those already published for the pig coronary arteries (Ito *et al.*, 1979; Bény *et al.*, 1986; Bény & Pacicca, 1994). This relatively depolarized state set the membrane potential far from the K^+ equilibrium potential, and thus would favour hyperpolarization and then vasodilatation.

In the basilar artery, Garland (1987) showed that contraction of smooth muscle cells caused by 5-HT is accompanied by a synchronized depolarization, even if contraction seems mainly due to other mechanisms. In our model, we did not observe any depolarization during the onset of contraction nor during the plateau of the tonic contraction. The fact that 5-HT can contract the smooth muscle cells without changing their membrane potential is not so surprising in this tissue. These cells are silent and usually never exibit action potentials. They fire only when their potassium channels are inhibited by a blocker such as tetrabutylammonium (Von der Weid & Bény, 1993). Moreover Ito *et al.* (1979) demonstrated that ACh causes a phasic contraction followed by a smaller tonic plateau without any change in the membrane potential of the smooth muscle cells. The phasic contraction is caused by the release of sarcoplasmic reticulum into the cytosol, whereas the entry of extracellular calcium into the cells is responsible for the weak tonic phase that follows (for review see Itoh, 1991). Interestingly, the 5-HT induced contraction is not biphasic and the force developed by the muscle lasts as long as 5-HT is applied. The mechanisms responsible for these distinct contractions remain to be established.

BK causes a hyperpolarization in the endothelial cells. It has been proposed that this hyperpolarization is necessary to maintain the electrochemical gradient that ensures the entry of extracellular calcium (Schilling, 1989; Lückhoff & Busse, 1990). This imported calcium allows the calcium-calmodulin-dependent synthesis of nitric oxide. But BK not only releases nitric oxide, it also triggers the phenomenon described by the acronym EDHF. Consequently, the exact role played by the hyperpolarization is difficult to assess. Our results using a pure nitric oxide releaser do not confirm the above-mentioned theory, at least in our model, since 5-HT induces nitric oxide production without hyperpolarizing the endothelial cells. In addition, use of a high potassium solution to separate nitric oxide-induced relaxations from EDHF-induced relaxations already indirectly showed that hyperpolarization is not necessary for nitric oxide synthesis (Kilpatrick & Cocks, 1994). Indeed, in a high potassium solution, endothelial cells cannot hyperpolarize, but are nevertheless able to release nitric oxide that relaxes smooth muscle cells (Kilpatrick & Cocks, 1994). This could indicate that an endothelial cell hyperpolarization induced by an agonist is the marker for the EDHF phenomenon and not for nitric oxide synthesis. However, this remains to be confirmed by other studies involving EDHF versus nitric oxide release in distinct tissues. In conclusion, the present study constitutes first observations of the effect on membrane potential of a pure nitric oxide releaser compared to substances like BK or SP that release both nitric oxide and EDHF. The difference we observed is that 5-HT, which releases only nitric oxide, does not markedly hyperpolarize the endothelial cells, whereas releasers of EDHF do. The observation that the endothelium-dependent relaxation of the smooth muscle cell is not accompanied by a hyperpolarization confirms previous findings showing that nitric oxide released by endothelial cells (in pig coronary and canine mesenteric arteries) is not responsible for endothelium-dependent smooth muscle cells hyperpolarization observed in these tissues during relaxation caused by SP or BK (Bény & Brunet, 1988; Komori *et al.*, 1988).

We thank Michèle Bény for typing the manuscript and Robert Peck for reviewing the manuscript.

This work was supported by the Swiss National Science Foundation Grant No. 31-29972.90.

References

ANGUS, J.A. (1989). 5-HT receptors in the coronary circulation. *Trends Pharmacol. Sci.*, **10**, 89–90.

BAX, W.A., RENZENBRINK, G.J., VAN HEUVEN-NOLSEN, D., THIJSSEN, E.J.M., BOS, E. & SAXENA, P.R. (1993). 5-HT receptors mediating contractions of the isolated human coronary artery. *Eur. J. Pharmacol.*, **239**, 203–210.

BÉNY, J.-L. (1990a). Effect of substance P on the membrane potential of coronary arterial endothelial cells *in situ*. *Agents Actions*, **31**, 317–320.

BÉNY, J.-L. (1990b). Endothelial and smooth muscle cells hyperpolarized by bradykinin are not dye coupled. *Am. J. Physiol.*, **258**, H836–H841.

BÉNY, J.-L. & BRUNET, P.C. (1988). Neither nitric oxide nor nitroglycerine accounts for all the characteristics of endothelially mediated vasodilatation of pig coronary arteries. *Blood Vessels*, **25**, 308–311.

BÉNY, J.-L., BRUNET, P.C. & HUGGEL, H. (1986). Effect of mechanical stimulation, substance P and vasoactive intestinal polypeptide on the electrical and mechanical activities of circular smooth muscles from pig coronary arteries contracted with acetylcholine: role of endothelium. *Pharmacology*, **33**, 61–68.

BÉNY, J.-L., BRUNET, P.C. & HUGGEL, H. (1987). Interaction of bradykinin and des-Arg^9-bradykinin with isolated pig coronary arteries: mechanical and electrophysiological events. *Regulat. Pept.*, **17**, 181–190.

BÉNY, J.-L. & CONNAT, J.-L. (1991). An electron-microscopic study of smooth muscle cell dye coupling in the pig coronary arteries. *Circ. Res.*, **70**, 49–55.

BÉNY, J.-L. & GRIBI, F. (1989). Dye and electrical coupling of endothelial cells *in situ*. *Tissue Cell*, **21**, 797–802.

BÉNY, J.-L. & PACICCA, C. (1994). Bidirectional electrical communication between smooth muscle and endothelial cells in the pig coronary artery. *Am. J. Physiol.*, **266**, H1465–H1472.

BRUNET, P.C. & BÉNY, J.-L. (1989). Substance P and bradykinin hyperpolarize pig coronary artery endothelial cells in primary culture. *Blood Vessels*, **26**, 228–234.

BRUNING, T.A., CHANG, P.C., BLAUW, G.J., VERMEIJ, P. & VAN ZWIETEN, P.A. (1993). Serotonin-induced vasodilatation in the forearm is mediated by the 'nitric oxide-pathway': no evidence for involvement of the 5-HT$_3$-receptor. *J. Cardiovasc. Pharmacol.*, **22**, 44–51.

COCKS, T.M. & ANGUS, J.A. (1983). Endothelium-dependent relaxation of coronary arteries by noradrenaline and serotonin. *Nature*, **305**, 627–630.

COHEN, R.A., SHEPHERD, J.T. & VANHOUTTE, P.M. (1983). 5-Hydroxytryptamine can mediate endothelium-dependent relaxation of coronary arteries. *Am. J. Physiol.*, **245**, H1077–H1080.

GARLAND, C.J. (1987). The role of membrane depolarization in the contractile response of the rabbit basilar artery to 5-hydroxytryptamine. *J. Physiol.*, **392**, 333–348.

HOUSTON, D.S. & VANHOUTTE, P.M. (1986). Serotonin and the vascular system. *Drugs*, **31**, 149–163.

ITO, Y., KITAMURA, K. & KURIYAMA, H. (1979). Effects of acetylcholine and catecholamines on the smooth muscle cell of the porcine coronary artery. *J. Physiol.*, **294**, 595–611.

ITOH, T. (1991). Pharmacomechanical coupling in vascular smooth muscle cells. *Jpn. J. Pharmacol.*, **55**, 1–9.

KILPATRICK, E.V. & COCKS, T.M. (1994). Evidence for differential roles of nitric oxide (NO) and hyperpolarization in endothelium-dependent relaxation of pig isolated coronary artery. *Br. J. Pharmacol.*, **112**, 557–565.

KOMORI, K., LORENZ, R.R. & VANHOUTTE, P.M. (1988). Nitric oxide, ACh, and electrical and mechanical properties of canine arterial smooth muscle. *Am. J. Physiol.*, **255**, H207–H212.

LEYSEN, J.E., AWOUTERS, F., KENNIS, L., LADURON, P.M., VANDENBERK, J. & JANSSEN, P.A.J. (1981). Receptor binding profile of R41 468, a novel antagonist at 5-HT$_2$ receptors. *Life Sci.*, **28**, 1015–1022.

LÜCKHOFF, A. & BUSSE, R. (1990). Calcium influx into endothelial cells and formation of endothelium-derived relaxing factor is controlled by the membrane potential. *Pflügers Arch.*, **416**, 305–311.

MOLDERINGS, G.J., ENGEL, G., ROTH, E. & GÖTHERT, M. (1989). Characterization of an endothelial 5-hydroxytryptamine (5-HT) receptor mediating relaxation of the porcine coronary artery. *Naunyn-Schmied. Arch. Pharmacol.*, **340**, 300–308.

PACICCA, C. VON DER WEID, P.-Y. & BÉNY, J.-L. (1992). Effect of nitro L-arginine on endothelium-dependent hyperpolarizations and relaxations of pig coronary arteries. *J. Physiol.*, **457**, 247–256.

RATZ, P.H. & FLAIM, S.F. (1985). Acetylcholine- and 5-hydroxytryptamine-stimulated contraction and calcium uptake in bovine coronary arteries: evidence for two populations of receptor-operated calcium channels. *J. Pharmacol. Exp. Ther.*, **234**, 641–647.

RICHARD, V., TANNER, F.C., TSCHUDI, M. & LÜSCHER, T.F. (1990). Different activation of L-arginine pathway by bradykinin, serotonin, and clonidine in coronary arteries. *Am. J. Physiol.*, **259**, H1433–H1439.

RUBANYI, G.M. & VANHOUTTE, P.M. (1990). Endothelium-derived relaxing factor. ed. G.M. Rubanyi & P.M. Vanhoutte. Basel (Switzerland): S. Krager.

SCHILLING, W.P. (1989). Effect of membrane potential on cytosolic calcium of bovine aortic endothelial cells. *Am. J. Physiol.*, **257**, H778–H784.

SCHOEFFTER, P. & HOYER, D. (1990). 5-Hydroxytryptamine (5-HT)-induced endothelium-dependant relaxation of pig coronary arteries is mediated by 5-HT receptors similar to the 5-HT$_{1D}$ receptor subtype. *J. Pharmacol. Exp. Ther.*, **252**, 387–395.

VAN NUETEN, J.M., JANSSEN, P.A.J., VAN BEEK, J., XHONNEUX, R., VERBEUREN, T.J. & VANHOUTTE, P.M. (1981). Vascular effects of ketanserin (R 41 468), a novel antagonist of 5-HT$_2$ serotonergic receptors. *J. Pharmacol. Exp. Ther.*, **218**, 217–230.

VANHOUTTE, P.M. (1987). Cardiovascular effects of serotonin. *J. Cardiovasc. Pharmacol.*, **10**, S8–S11.

VANHOUTTE, P.M., COHEN, R.A. & VAN NEUTEN, J.M. (1984). Serotonin and arterial vessels. *J. Cardiovasc. Pharmacol.*, **6**, S421–S428.

VON DER WEID, P.-Y. & BÉNY, J.-L. (1993). Simultaneous oscillations in the membrane potential of pig coronary artery endothelial and smooth muscle cells. *J. Physiol.*, **471**, 13–24.

(Received December 21, 1994
Accepted January 20, 1995)

British Journal of Pharmacology (1995) 115, 101-106

Regulation of cytosolic calcium by collagen in single human platelets

[1]Alastair W. Poole & Stephen P. Watson

University Department of Pharmacology, Mansfield Road, Oxford OX1 3QT

1 There is controversy in the literature as to whether collagen is able to induce directly a rise in cytosolic calcium concentration ($[Ca^{2+}]_i$) in human platelets. We have addressed this question by observing the cytosolic calcium response of single fura-2-loaded human platelets settling onto a collagen-coated surface using dynamic fluorescence ratio imaging.

2 Following a short lag phase after adherence to collagen fibres, platelets underwent a rapid rise in cytosolic calcium from basal values of 80 ± 13 nM ($n = 24$) to a peak of 475 ± 42 nM ($n = 24$) which was sustained for the remaining period of the experiment.

3 The tyrphostin protein tyrosine kinase inhibitor, ST271, reduced substantially the proportion of platelets which exhibited a rise in $[Ca^{2+}]_i$ on adherence to collagen and transformed the response in remaining cells to one of oscillations.

4 In contrast, and as a control for collagen, laminin-coated surfaces induced adherence of human platelets without elevating intracellular $[Ca^{2+}]$; the cells however remained responsive to ADP.

5 We conclude that collagen directly induces a rise in cytosolic calcium in single human platelets through a tyrosine kinase-mediated pathway.

Keywords: Human platelet; collagen; protein tyrosine kinase; staurosporine; tyrphostin; calcium; video imaging; single cell; Fc gamma

Introduction

Collagen is an adhesion molecule important in the primary activation of platelets during haemostasis. Despite this central role, its molecular basis of action remains unclear and its receptor is not defined although several candidates have been proposed. Among those put forward as the collagen receptor are the integrin $\alpha_2\beta_1$ (Niewenhuis *et al.*, 1985; Santoro, 1986; Coller *et al.*, 1989), glycoprotein IV (CD36) (Tandon *et al.*, 1989), C1q (or collectin) receptor (Peerschke *et al.*, 1993) and several uncharacterized surface proteins including p62 (Sugiyama *et al.*, 1987), p47 (Chiang *et al.*, 1993) and p65 (Chiang & Kang, 1982). None of these is known to possess the seven-transmembrane domain architecture associated with G protein-coupled receptors. It may be that signalling through these receptors requires clustering, in a manner similar to that for the low affinity IgG receptor on platelets (King *et al.*, 1990), FcγRIIA, which signals after receptor cross-linking (Anderson & Anderson, 1990).

It has become clear over recent years that many adhesion molecules mediate signal transduction from the extracellular matrix using non-receptor tyrosine kinases (for review see Shattil & Brugge, 1991). It is now also understood that protein tyrosine phosphorylation may play a role in calcium signalling through activation of phospholipase Cγ isoforms with subsequent formation of the Ca^{2+} mobilising messenger, inositol 1,4,5-trisphosphate (Ins 1,4,5-P_3; for review see Rhee & Choi, 1992). From our own work and that of others it has been shown that PLCγ2, but not PLCγ1, becomes, phosphorylated on tyrosine upon stimulation of platelets by collagen and antibody-mediated cross-linking of FcγRIIA (Blake *et al.*, 1994; Daniel *et al.*, 1994). Consistent with this, we have previously shown that collagen-induced formation of inositol phosphates in platelets is blocked by the nonselective inhibitor of tyrosine and serine/threonine kinases, staurosporine (Blake *et al.*, 1993).

Although collagen induces formation of inositol phosphates in platelets (Watson *et al.*, 1985), there is controversy as to whether this is associated with elevation of $[Ca^{2+}]_i$. In the presence of cyclo-oxygenase inhibitors, concentrations of collagen up to 20 μg ml^{-1} do not induce a measurable rise in cytosolic calcium in platelets loaded with the fluorescent indicators, fura-2 or quin2 (Rink *et al.*, 1983; Watson *et al.*, 1985; Pollock *et al.*, 1986), despite the fact that these are sufficient to induce activation of the phosphoinositide pathway. On the other hand, if the concentration of collagen is increased to 50 μg ml^{-1} a rise in cytosolic calcium is observed in the presence of a thromboxane receptor antagonist, ADP-scavenger system and fibrinogen antagonist (Smith *et al.*, 1992); however, despite the inclusion of these inhibitors, the possibility remains that other released substances underlie this response. In order to demonstrate definitively whether collagen induces elevation of $[Ca^{2+}]_i$ in platelets, we have performed studies in single cells which have undergone adhesion to collagen fibres. Part of this work has already been presented in abstract form (Poole *et al.*, 1993).

Methods

Platelet preparation

Human platelet suspensions were prepared as previously described (Watson *et al.*, 1985). Briefly, blood was drawn from volunteers who had denied taking medication in the previous two weeks, anticoagulated with acid-citrate-dextrose (ACD:blood, 1:7 by volume; to achieve a final citrate concentration of 22 mM) and platelet-rich plasma (PRP) prepared by centrifugation. The cyclo-oxygenase inhibitor, indomethacin (10 μM), was added during all subsequent stages of experimentation. PRP was incubated with fura-2-AM (4 μM) for 45 min at 30°C, washed by centrifugation (500 *g*, 15 min) and resuspended to a cell density of 2×10^8 ml^{-1} in a modified Tyrode-HEPES buffer (composition in mM: NaCl 134, $NaHCO_3$ 12, KCl 2.9, Na_2HPO_4 0.34, $MgCl_2$ 1, HEPES 20, glucose 5; buffered to pH 7.4).

[1] Author for correspondence.

Measurement of $[Ca^{2+}]_i$ in cell suspensions

$[Ca^{2+}]_i$ was calculated after measurement of the fluorescence ratio (R) at excitation wavelengths of 340 nm and 380 nm with emission at 510 nm, using a spectrofluorimeter with filter-wheel attachment (Perkin-Elmer LS50B). Cytosolic $[Ca^{2+}]$ was determined using the equation:

$$[Ca^{2+}]_i = K_d.\beta.[R - R_{min})/(R_{max} - R)]$$

where K_d is the dissociation constant of fura-2 for Ca^{2+} at room temperature (K_d taken as 115 nM), β is the ratio of intensities at $\lambda = 380$ nm at R_{min} and R_{max} ($I_{R=Rmin}/I_{R=Rmax}$), R_{min} is the intensity ratio (I^{340}/I^{380}) in the absence of Ca^{2+} and R_{max} is the intensity ratio in the presence of a saturating concentration of Ca^{2+}. Studies in which staurosporine was used demonstrated that this compound emitted a fluorescent signal within the range of interest for fura-2, and that this signal remained constant throughout the experiment. The staurosporine signal was determined for each experiment by measurement of the difference of both 340 and 380 nm signals before and after addition of staurosporine, and was subtracted accordingly. The tyrphostin ST271 absorbed much of the signal in the working spectrum for fura-2 and therefore measurements were proportionately normalised to the levels achieved prior to addition of ST271. All experiments were conducted at room temperature (22° ± 2°C) in the presence of extracellular Ca^{2+} (1 nM), indomethacin (10 μM) and apyrase (0.2 units ml^{-1}). In experiments involving activation of FcγRII, platelets were preincubated with mAb IV.3 for 1 min before cross-linking with anti-mouse-whole-IgG sheep $F(ab')_2$. Results are shown as representative traces of at least ten observations from four experiments and data are mean ± s.e.mean.

Single-platelet $[Ca^{2+}]_i$ studies

Glass coverslips were covered with a thin polythene film ('Clingfilm'), so as to provide an inert surface for platelets. Small droplets of collagen (10 μg ml^{-1}) or laminin (1 mg ml^{-1}) were pipetted onto the coated coverslip and allowed to dry at 37°C for 2 h. Fura-2-loaded platelets were added to the coverslip and allowed to settle onto the surface over a period of several minutes. Cells were visualised as they came into contact with the surface using a Zeiss Axiovert 35 microscope. Fluorescence video images were captured at 4 s intervals using IonVision software (Improvision, Warwick, U.K.) at excitation wavelengths of 340 nm and 380 nm with emission at 510 nm. Calculation of $[Ca^{2+}]_i$ from the 340:380 ratio was performed by use of a previously established calibration curve using standard solutions of various free Ca^{2+} concentrations (from Molecular Probes, OR, U.S.A.) applying a viscosity correction factor (Poenie, 1990). Analysis was performed with a Macintosh Quadra 900 running IonVision software (ImproVision, Warwick, U.K.). Experiments were carried out at room temperature (22° ± 2°C) in the presence of extracellular Ca^{2+} (1 mM), indomethacin (10 μM) and apyrase (0.2 units ml^{-1}).

Materials

All salts were Analar grade from BDH-Merck. Fura-2-AM was from Molecular Probes (Eugene, OR, U.S.A.), collagen (derived from equine achilles tendon) from Hormon-Chemie (Munich, Germany). Monoclonal antibody (mAb) IV.3 was purchased from Medarex Inc. (New Hampshire, U.S.A.). ST271 was a gift from Wellcome Foundation Laboratories (Kent, U.K.). Staurosporine, laminin, the thromboxane-mimetic U46619 ((15S)-hydroxy-11α, 9α-(epoxymethano) prosta-5z, 13E-dienoic acid), thrombin and sheep $F(ab')_2$ anti-mouse-IgG were from Sigma (Poole, U.K.). *Myo*-[^{3}H]-inositol was from Amersham International (Cardiff, U.K.).

Results

Populational cell studies

Smith & Dangelmaier (1990) have shown that high concentrations of collagen induce a rise in $[Ca^{2+}]_i$ in the presence of inhibitors of secondary mediators. Figure 1 confirms that in the presence of indomethacin (10 μM) and apyrase (0.2 units ml^{-1}), 10 μg ml^{-1} collagen induces no elevation in

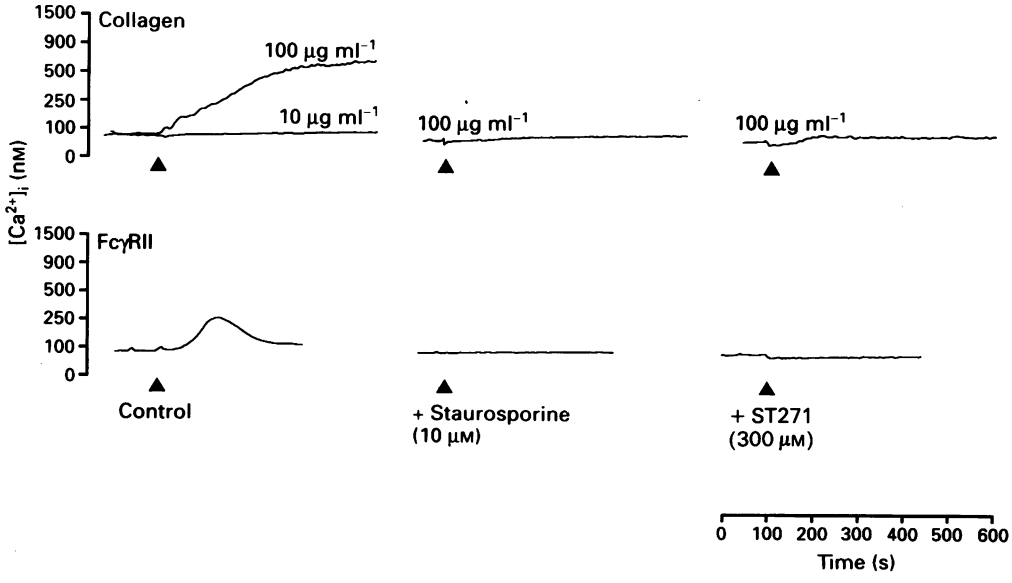

Figure 1 Tyrosine kinase inhibitors block the calcium response to collagen and FcγRII cross-linking in platelet suspensions. Suspensions of fura-2-loaded platelets were pre-incubated with staurosporine (10 μM), ST271 (300 μM) or dimethylsulphoxide (1% v:v) as a control, and stimulated with (a) collagen (100 μg ml^{-1}) or (b) FcγRII cross-linking (mAb IV.3, 1 μg ml^{-1} followed 60 s later by $F(ab')_2$ anti-mouse IgG, 30 μg ml^{-1}) at the point indicated (▲). In control platelets, both stimuli induce a marked rise in $[Ca^{2+}]_i$ although the time course for each stimulus differs. Both staurosporine and ST271 substantially inhibited the response, indicating an essential role for tyrosine phosphorylation in signalling induced by these agonists.

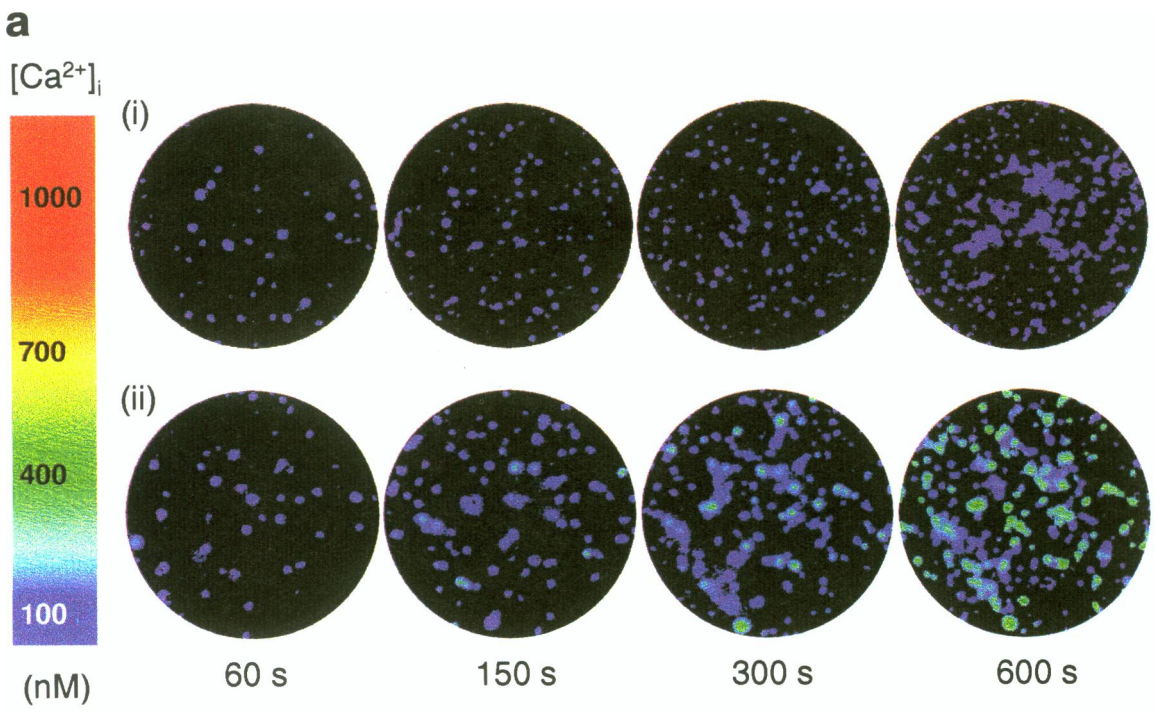

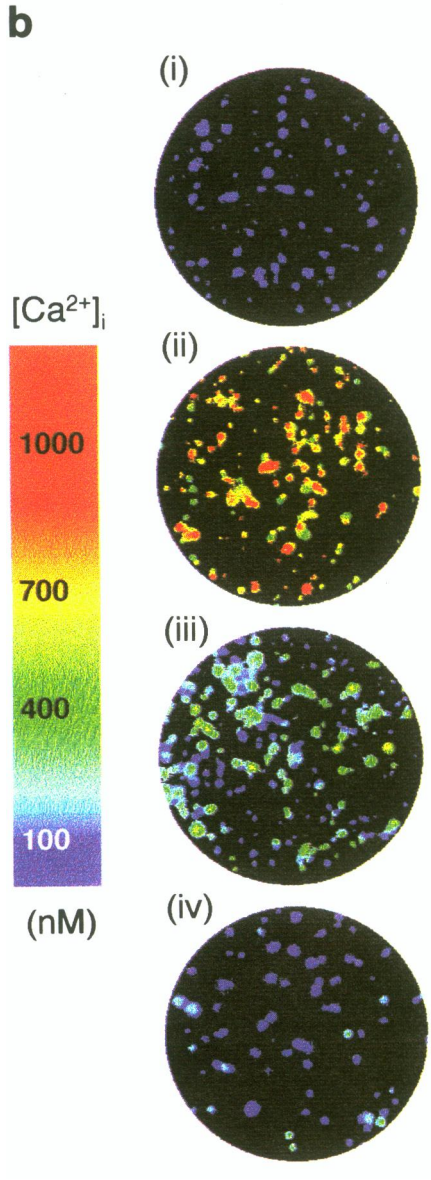

Figure 2 (a) Pseudo-colour images showing the cytosolic calcium response of single platelets settling onto collagen fibres. Fura-2-loaded platelets were allowed to settle onto a polythene-coated coverslip and images captured every 4 s at both 340 and 380 nm excitation wavelengths. Cytosolic calcium concentration was calculated from the 340/380 ratio and represented in pseudo-colour. Row (i) shows platelets settling onto the control surface without collagen. Platelets did not adhere to this surface and showed no signs of activation; their $[Ca^{2+}]_i$ remained at basal levels and under the light microscope they were seen to maintain a resting discoid shape. Row (ii) shows platelets settling onto a collagen-coated surface. Platelets moved over the surface until adhering to a collagen fibre and, after a variable lag phase (15–120 s), underwent a rapid rise in $[Ca^{2+}]_i$. (b) Pseudo-colour images of single platelets showing the effect of ST271 upon the calcium response to collagen. Fura-2-loaded platelets were allowed to settle onto a coverslip for 600 s after which 340 and 380 nm excitation wavelength images were captured and transformed into the pseudo-colour calcium images shown. (i) and (ii) are images of platelets on a collagen-free surface; (ii) was treated with thrombin (1 unit ml^{-1}) 20 s prior to image capture. (iii) and (iv) show the response of single platelets to collagen in the absence (iii) or presence (iv) of ST271 (300 μM). ST271 decreases the proportion of platelets which activate in contact with collagen, although the adhesive event appears unaffected.

cytosolic calcium, whereas 100 μg ml^{-1} collagen induces a slow steady rise in $[Ca^{2+}]_i$ to a plateau over a period of 10 min. Both collagen and cross-linking of FcγRII have been shown to induce phosphorylation of PLCγ2 on tyrosine (Blake *et al.*, 1994; Daniel *et al.*, 1994), an action which may underlie the elevation in cytosolic calcium. Consistent with this, Figure 1 shows that inhibitors of tyrosine kinases, the non-selective staurosporine and the more selective tyrphostin ST271, inhibit the calcium rise induced by these agonists.

Collagen induces a rise in $[Ca^{2+}]_i$ in single platelets

In order to investigate more directly the calcium response induced in platelets by collagen fibres, we used a single cell fluorescent imaging technique to visualise the interaction. A platelet suspension is added just above the collagen coated surface and as platelets settle onto the collagen-coated coverslip, an increasing number enter the plane of focus of the microscope. When visualised in real time it is evident that platelets move over the surface in an apparently random fashion until they find an anchor on a collagen fibre at which moment they become adherent. They remain fixed at this site throughout the duration of the recording. In contrast, platelets added to a control uncoated coverslip continue to move about the surface in a random fashion.

Figure 2a shows a sequence of images from a control coverslip and one in which the surface was coated with collagen. The time-dependent accumulation of platelets on the surface may be seen in both control and collagen-coated coverslips. On becoming adherent to collagen fibres and after a variable lag phase of 15–120 s, platelets undergo a rise in cytosolic $[Ca^{2+}]$ from a basal resting value of 80 ± 12 nM (n = 24 cells) to a peak of 475 ± 42 nM (n = 24 cells) which is maintained throughout the recording. The increase in $[Ca^{2+}]_i$ consists of an initial rapid peak which, in some cells, is followed by a slower phase that continues to rise over a period of 60–120 s. In contrast, platelets settling onto the control uncoated surface do not undergo a change in $[Ca^{2+}]_i$. Example traces illustrating the increase in $[Ca^{2+}]_i$ on adherence to collagen are shown in Figure 3a. In contrast, addition of thrombin to platelets on the control surface leads to an immediate increase in $[Ca^{2+}]_i$ in all cells in the field of view (Figure 2b); in many cases, this increase is in excess of 1 μM preventing accurate calibration.

The tyrphostin tyrosine kinase inhibitor, ST271, transforms the sustained $[Ca^{2+}]_i$ rise in single platelets to an oscillatory one and inhibits collagen-induced formation of inositol phosphates

The tyrphostin tyrosine kinase inhibitor, ST271 (300 μM) substantially reduced the proportion of single cells which underwent a rise in $[Ca^{2+}]_i$ on adherence to collagen (Figure 2b), but appeared to have no effect upon the number of platelets that adhered to collagen. The time course of the $[Ca^{2+}]_i$ rise in the small proportion of cells that did exhibit a response on adhesion to collagen was oscillatory in nature as exemplified by the traces in Figure 3b. These results are reminiscent of those seen in other cell types in which low concentrations of agonists, sufficient to induce only a small degree of activation of phospholipase C, induce oscillatory rises in $[Ca^{2+}]_i$ whereas much higher agonist concentrations generate sustained $[Ca^{2+}]_i$ increases (for review see Berridge & Galione, 1990). Studies using staurosporine in single platelets were prevented by the marked fluorescence of this compound.

Laminin induces no change in cytosolic calcium in single platelets

The results obtained with collagen were compared with those following adhesion of platelets to another integrin-binding protein, laminin, the receptor for which is the integrin $\alpha_6\beta_1$ (Sonnenberg *et al.*, 1988). After settling under gravity, platelets were found to bind rapidly to a laminin-coated surface and to remain fixed throughout the period of recording. When observed over a 10 min period, however, there was no increase in $[Ca^{2+}]_i$ in the vast majority of cells, although a small proportion (~1%) exhibited a single spike

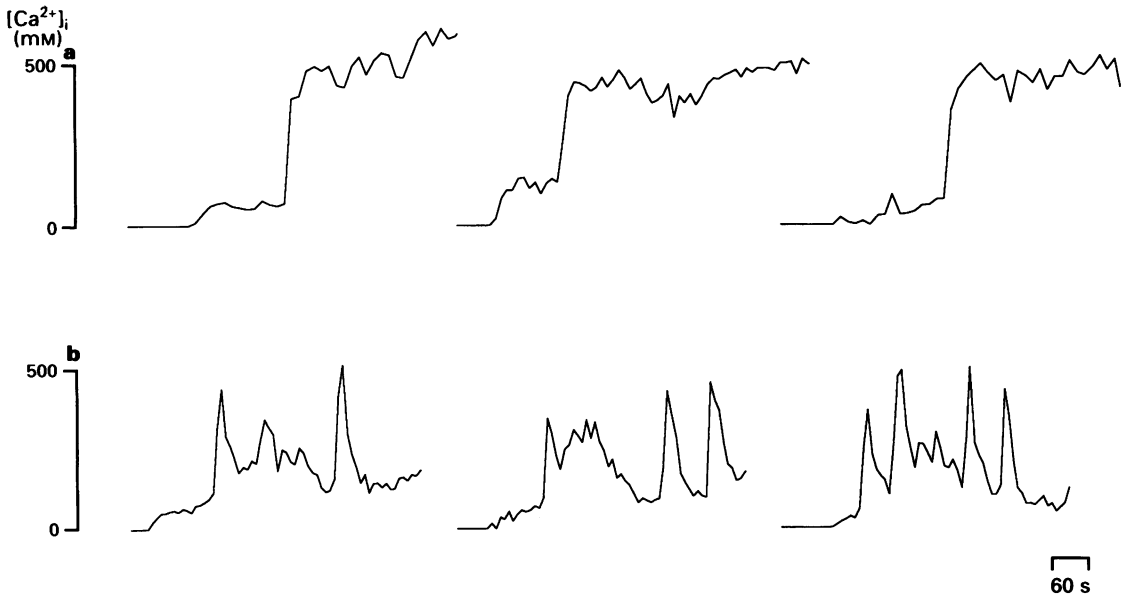

Figure 3 Collagen induces a rapid rise in $[Ca^{2+}]_i$ in single platelets; in the presence of ST271 collagen induces calcium oscillations. Three representative time plots are shown of the calcium response in individual platelets, which exhibit an elevation in $[Ca^{2+}]_i$, upon adherence to collagen under either control conditions treated with dimethylsulphoxide (1% v:v) (a) or treated with ST271 (300 μM) (b). Plots are formed by selecting the area where the platelet finally comes to rest and calculating the calcium concentration in that area for all time points recorded. The initial flat phase represents the time before the platelet entered the resting area, so the calculated calcium concentration defaults to zero. After a variable period of time the platelet enters the area of interest, shown by a rise in $[Ca^{2+}]_i$ to the resting value. Following a lag phase of 15–120 s the $[Ca^{2+}]_i$ rises rapidly to a plateau which, in control platelets, is sustained until the end of the recording (a), and in platelets treated with ST271 is transient followed by oscillations with 1–2 min interpeak interval (b).

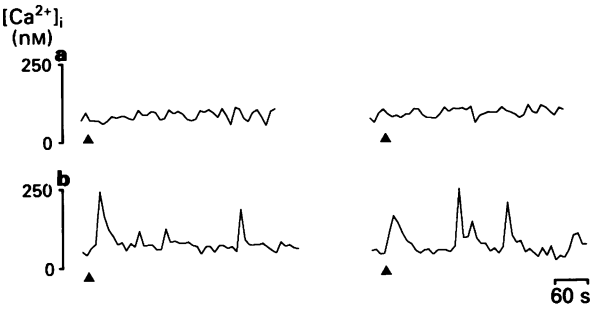

Figure 4 Calcium response of platelets adherent to a laminin-coated surface: response to the addition of ADP. Laminin (1 mg ml^{-1}) was dried onto polythene-coated coverslips. Fura-2-loaded platelets were added close to the surface as for the collagen experiments described earlier, and the calcium concentration monitored by capturing images at 340 and 380 nm excitation wavelength. Platelets rapidly became bound to the laminin-coated surface, but in contrast to collagen most platelets underwent no rise in $[Ca^{2+}]_i$ over the experimental period (two representative platelet responses are shown in (a)). ADP (1 μM) induced an initial transient spike in all platelets, and in 43% of cells this was followed by further repetitive spiking. (b) Shows two representative individual platelet calcium responses after addition of ADP (▲).

event (data not shown). The apparent strong interaction of platelets to laminin would appear to make this a suitable surface for investigation of the response of single cells to other agonists. Figure 4 illustrates the response of single platelets to ADP (1 μM) when bound to laminin. ADP induced an initial transient rise in $[Ca^{2+}]_i$, peaking at 252 ± 23 nM ($n = 100$), before declining to basal level; in approximately 50% of cells, this response was followed by additional transient peaks at irregular intervals (Figure 4).

Discussion

There are several reports of calcium measurements in single platelets (Nishio *et al.*, 1991; Heemskerk *et al.*, 1992; 1993). The procedure used in some of these studies involves attachment of cells to a glass coverslip surface coated with fibrinogen, followed by addition of agonist. This technique has the drawback that platelets are activated in contact with glass or immobilised fibrinogen, although in the latter case, inclusion of apyrase appears to block activation (Heemskerk *et al.*, 1992; Haimovich *et al.*, 1993). In the present study, we have coated coverslips with a thin polythene film which did not interfere with the optics of the microscope but provided an inert surface to the platelet. Collagen fibres could be dried on to this surface and adhesion of platelets monitored by light and fluorescence microscopy. This experimental set up also has the advantage of providing a more physiological presentation of collagen to the platelet, i.e. in the form of a solid surface.

Our results demonstrate that collagen induces a sustained increase in $[Ca^{2+}]_i$ in single platelets that have adhered to collagen fibres. This observation demonstrates that collagen is able to elevate $[Ca^{2+}]_i$ directly in single platelets. As a control, and for comparison with another adhesion ligand, we also investigated the effect of platelet adhesion to a laminin-coated surface. Platelets bind laminin through a membrane integrin, $\alpha_6\beta_1$ (Sonnenberg *et al.*, 1988), and although platelets adhere to the laminin-coated surface, they do not become activated over a period of several minutes, remaining responsive to other agonists, such as ADP. Laminin may therefore provide a important medium for single cell calcium studies in platelets using soluble agonists.

The explanation for the lack of an observed increase (Rink *et al.*, 1983; Watson *et al.*, 1985; Pollock *et al.*, 1986) in $[Ca^{2+}]_i$ in platelet populations using concentrations of collagen of 20 μg ml^{-1} or less is not known, but a number of factors are worthy of consideration. There is a much lower increase in $[Ca^{2+}]_i$ in single platelets adhered to collagen compared with the response to thrombin (see Figure 2b); thus, in a cell population low concentrations of collagen ($\leqslant$ 10 μg ml^{-1}), which induce less than 10% of cells to adhere (Smith & Dangelmaier, 1990), the weak signal generated by collagen may not be detected. It is also possible that formation of microaggregates of dye-loaded platelets on the collagen surface interferes with the fluorescence signal, similar to that previously reported for the decrease in fluorescence signal that occurs during platelet aggregation (Rink *et al.*, 1983).

The sustained nature of the response to collagen is unusual in that agonists that have been investigated thus far in single platelets, namely ADP (present study and Heemskerk *et al.*, 1992; 1993), thrombin (Heemskerk *et al.*, 1993; also Poole & Watson, unpublished work) and 5-hydroxytryptamine (Nishio *et al.*, 1991), induce an oscillatory rise. Several theories have been proposed to explain the molecular basis of $[Ca^{2+}]_i$ oscillations, the majority of which involve the repetitive emptying and refilling of intracellular calcium stores initiated by Ins 1,4,5P_3 (Berridge & Galione, 1990; Berridge, 1990; Harootunian *et al.*, 1991). The maintained response induced by collagen may therefore reflect a supramaximal and sustained formation of Ins 1,4,5P_3. For individual platelets therefore the response to collagen may be all-or-none, and in this respect collagen may be acting as a 'super-agonist'. This hypothesis may explain why the tyrphostin ST271 transforms the sustained response to one of oscillations. In the presence of ST271, collagen-induced formation of Ins 1,4,5P_3 is reduced substantially (data not shown), possibly to a level that allows regenerative emptying and refilling of calcium stores. It is also possible that the calcium stores are unable to refill in the presence of the tyrosine kinase inhibitor, since several recent reports suggest that tyrosine phosphorylation may play a role in controlling store-regulated calcium entry in platelets and other cell types (Vostal *et al.*, 1991; Sargeant *et al.*, 1993a,b; Lee *et al.*, 1993; Kruse *et al.*, 1994). In the absence of store refilling, it would become unlikely that a calcium rise could be sustained, and that an oscillatory response might be expected.

The underlying molecular mechanism of collagen-induced platelet activation is beginning to be elucidated. We, and others, have recently shown that PLCγ2 is phosphorylated on tyrosine in response to collagen (Blake *et al.*, 1994; Daniel *et al.*, 1994) and here we present evidence that is consistent with a requirement for tyrosine phosphorylation in collagen-induced elevation of cytosolic calcium, using two structurally distinct inhibitors of protein tyrosine kinases. In this paper we have demonstrated that collagen directly induces a rise in cytosolic calcium in human platelets through the use of dynamic video imaging. The single cell approach described here may prove a valuable technique for the study of platelet-extracellular matrix interaction.

This work was supported by the Wellcome Trust and British Heart Foundation. S.P.W. is a Royal Society University Research Fellow.

References

ANDERSON, G.P. & ANDERSON, C.L. (1990). Signal transduction by the platelet Fc receptor. *Blood*, **76**, 1165–1172.

BERRIDGE, M.J. (1990). Calcium oscillations. *J. Biol. Chem.*, **265**, 9583–9586.

BERRIDGE, M.J. & GALIONE, A. (1990). Cytosolic calcium oscillators. *FASEB J.*, **2**, 3074–3082.

BLAKE, R.A., SCHIEVEN, G.L. & WATSON, S.P. (1994). Collagen stimulates tyrosine phosphorylation of phospholipase Cγ2 but not phospholipase Cγ1 in human platelets. *FEBS Lett.*, **353**, 212–216.

BLAKE, R.A., WALKER, T.R. & WATSON, S.P. (1993). Activation of human platelets by peroxovanadate is associated with tyrosine phosphorylation of phospholipase Cγ and formation of inositol phosphates. *Biochem. J.*, **290**, 471–475.

CHIANG, T.M. & KANG, A.H. (1982). Isolation and purification of collagen alpha 1(I) receptor from human platelet membrane. *J. Biol. Chem.*, **257**, 7581–7586.

CHIANG, T.M., SEYER, J.M. & KANG, A.H. (1993). Collagen-platelet interaction: Separate receptor sites for types I and III collagen. *Thromb. Res.*, **71**, 443–456.

COLLER, B.S., BEER, J.H., SCUDDER, L.E. & STEINBERG, M.H. (1989). Collagen-platelet interactions: Evidence for a direct interaction of collagen with platelet GPIa/IIa and an indirect interaction with platelet GPIIb/IIIa mediated by adhesive proteins. *Blood*, **74**, 182–192.

DANIEL, J.L., DANGELMAIER, C. & SMITH, J.B. (1994). Evidence for a role for tyrosine phosphorylation of phospholipase Cγ2 in collagen-induced platelet cytosolic calcium mobilisation. *Biochem. J.*, **302**, 617–622.

HAIMOVICH, B., LIPFERT, L., BRUGGE, J.S. & SHATTIL, S.J. (1993). Tyrosine phosphorylation and cytoskeletal reorganization in platelets are triggered by interaction of integrin receptors with their immobilized ligands. *J. Biol. Chem.*, **268**, 15868–15877.

HAROOTUNIAN, A.T., KAO, J.P.Y., PARANJAPE, S. & TSIEN, R.Y. (1991). Generation of calcium oscillations in fibroblasts by positive feedback between calcium and IP3. *Science*, **251**, 75–78.

HEEMSKERK, J.W.M., HOYLAND, J., MASON, W.T. & SAGE, S.O. (1992). Spiking in cytosolic calcium concentration in single fibrinogen-bound fura-2-loaded human platelets. *Biochem. J.*, **283**, 379–383.

HEEMSKERK, J.W.M., VIS, P., FEIJGE, M.A.H., HOYLAND, J., MASON, W.T. & SAGE, S.O. (1993). Roles of phospholipase C and Ca^{2+}-ATPase in calcium responses of single, fibrinogen-bound platelets. *J. Biol. Chem.*, **268**, 356–363.

KING, M., MCDERMOTT, P. & SCHREIBER, A.D. (1990). Characterisation of the Fcγ receptor on human platelets. *Cell. Immunol.*, **128**, 462–479.

KRUSE, H.J., NEGRESCU, E.V., WEBER, P.C. & SIESS, W. (1994). Thrombin-induced Ca^{2+} influx and protein tyrosine phosphorylation in endothelial cells is inhibited by herbimycin A. *Biochem. Biophys. Res. Commun.*, **202**, 1651–1656.

LEE, K-M., TOSCAS, K. & VILLEREAL, M.L. (1993). Inhibition of bradykinin- and thapsigargin-induced Ca^{2+} entry by tyrosine kinase inhibitors. *J. Biol. Chem.*, **268**, 9945–9948.

NIEUWENHUIS, H.K., AKKERMAN, J.W.N., HOUDIJK, W.P.M. & SIAM, J.J. (1985). Human blood platelets showing no response to collagen fail to express surface glycoprotein Ia. *Nature*, **318**, 470–472.

NISHIO, H., IKEGAMI, Y. & SEGAWA, T. (1991). Fluorescence digital image analysis of serotonin-induced calcium oscillations in single blood platelets. *Cell Calcium*, **12**, 177–184.

PEERSCHKE, E.I.B., REID, K.B.M. & GREBREHIWET, B. (1993). Platelet activation by C1q results in the induction of alpha (IIb)/beta 3 integrins (GPIIb-IIIa) and the expression of P-selectin and

POENIE, M. (1990). Alteration of intracellular fura-2 fluorescence by viscosity: a simple correction. *Cell Calcium*, **11**, 85–91.

POLLOCK, W.K., RINK, T.J. & IRVINE, R.F. (1986). Liberation of (^{3}H)arachidonic acid and changes in cytosolic free calcium in fura-2-loaded human platelets stimulated by ionomycin and collagen. *Biochem. J.*, **235**, 869–877.

POOLE, A.W., BLAKE, R., ASSELIN, J. & WATSON, S.P. (1993). Tyrosine kinase inhibitors block the increase in Ca^{2+} that occurs on the adhesion of single platelets to collagen. *Br. J. Pharmacol.*, **110**, 41P.

RHEE, S.G. & CHOI, K.D. (1992). Regulation of inositol phospholipid-specific phospholipase C isozymes. *J. Biol. Chem.*, **267**, 12393–12396.

RINK, T.J., SANCHEZ, A. & HALLAM, T.J. (1983). Diacylglycerol and phorbol ester stimulate secretion without raising cytoplasmic free calcium in human platelets. *Nature*, **305**, 317–319.

SANTORO, S.A. (1986). Identification of a 160,000 dalton platelet membrane protein that mediates the initial divalent cation-dependent adhesion of platelets to collagen. *Cell*, **46**, 913–920.

SARGEANT, P., FARNDALE, R.W. & SAGE, S.O. (1993a). The tyrosine kinase inhibitors methyl 2,5-dihydroxycinnamate and genistein reduce thrombin-evoked tyrosine phosphorylation and Ca^{2+} entry in human platelets. *FEBS Lett.*, **315**, 242–246.

SARGEANT, P., FARNDALE, R.W. & SAGE, S.O. (1993b). ADP- and thapsigargin-evoked Ca^{2+} entry and protein-tyrosine phosphorylation are inhibited by the tyrosine kinase inhibitors genistein and methyl-2,5-dihydroxycinnamate in fura-2-loaded human platelets. *J. Biol. Chem.*, **268**, 18151–18156.

SHATTIL, S. & BRUGGE, J.S. (1991). Protein phosphorylation and the adhesive functions of platelets. *Curr. Op. Cell Biol.*, **3**, 869–879.

SMITH, J.B. & DANGELMAIER, C. (1990). Determination of platelet adhesion to collagen and the associated formation of phosphatidic acid and calcium mobilization. *Anal. Biochem.*, **187**, 173–178.

SMITH, J.B., SELAK, M.A., DANGELMAIER, C. & DANIEL, J. (1992). Cytosolic calcium as a second messenger for collagen-induced platelet responses. *Biochem. J.*, **288**, 925–929.

SONNENBERG, A., MODDERMAN, P.W. & HOGERVORST, F. (1988). Laminin receptor on platelets is the integrin VLA-6. *Nature*, **336**, 487–488.

SUGIYAMA, T., OKUMA, M., USHIKUBI, F., SENSAKI, S., KANAJI, K. & UCHINO, H. (1987). A novel platelet aggregating factor found in a patient with defective collagen-induced platelet aggregation and autoimmune thrombocytopenia. *Blood*, **69**, 1712–1720.

TANDON, N.N., KRALISZ, U. & JAMIESON, G.A. (1989). Identification of glycoprotein IV (CD36) as a primary receptor for platelet-collagen adhesion. *J. Biol. Chem.*, **264**, 7576–7583.

VOSTAL, J.G., JACKSON, W.L. & SHULMAN, N.R. (1991). Cytosolic and stored calcium antagonistically control tyrosine phosphorylation of specific platelet proteins. *J. Biol. Chem.*, **266**, 16911–16916.

WATSON, S.P., REEP, B., MCCONNELL, R.T. & LAPETINA, E.G. (1985). Collagen stimulates (^{3}H)inositol triphosphate formation in indomethacin-treated human platelets. *Biochem. J.*, **226**, 831–837.

(Received October 21, 1994
Accepted January 17, 1995)

British Journal of Pharmacology (1995) 115, 107-116

Characterization and distribution of putative 5-ht$_7$ receptors in guinea-pig brain

Z.P. To, D.W. Bonhaus, R.M. Eglen & [1]L.B. Jakeman

Institute of Pharmacology, Syntex Discovery Research, 3401 Hillview Ave., Palo Alto, CA 94303, U.S.A.

1 In the presence of (−)-cyanopindolol (1.0 μM) and sumatriptan (1.0 μM), 0.5 nM [^{3}H]-carboxamidotryptamine ([^{3}H]-5-CT) labelled a single population of receptors in guinea-pig cerebral cortex membranes.

2 5-HT-displaceable binding was rapid, saturable and reversible. A high affinity binding site was characterized both by equilibrium saturation (K_d = 0.76 ± 0.28 nM; B_{max} = 68.1 ± 26.7 fmol mg^{-1} protein) and kinetic (K_d = 0.18 ± 0.05 nM) analysis. The pharmacological profile of this site was similar to the profile obtained in transfected CHO-K1 cells expressing guinea-pig 5-ht$_7$ receptors.

3 Autoradiographic analysis revealed a discrete localization of binding sites in guinea-pig brain, with the highest density of sites in the medial thalamic nuclei and related limbic and cortical regions. Moderate levels of binding were detected in sensory relay nuclei, substantia nigra, hypothalamus, central grey and dorsal raphe nuclei. This distribution corresponded to that observed using *in situ* hybridization with [^{35}S]-UTP labelled riboprobes complementary to mRNA encoding the guinea-pig 5-ht$_7$ receptor.

4 In conclusion, under appropriate conditions, [^{3}H]-5-CT labelled a single population of saturable binding sites that corresponded to an endogenous 5-ht$_7$ receptor in guinea-pig brain. The distribution of 5-ht$_7$ receptors in thalamocortical and limbic brain regions suggests a role for these receptors in sensory and affective behaviours.

Keywords: 5-Carboxamidotryptamine; 5-hydroxytryptamine; 5-HT receptors; guinea-pig thalamus; guinea-pig limbic system; 5-ht$_7$; autoradiography; *in situ* hybridization

Introduction

5-Hydroxytryptamine (5-HT) exerts a wide variety of behavioural and physiological effects through actions on multiple receptor subtypes. Pharmacological and molecular cloning approaches have identified at least fourteen distinct subtypes of mammalian 5-HT receptors, classified into seven families with unique structural, transductional and operational characteristics (Martin & Humphrey, 1994; Hoyer *et al.*, 1994). Endogenous functional equivalents have been identified for four major classes (5-HT$_1$, 5-HT$_2$, 5-HT$_3$, 5-HT$_4$). Where functional correlates have not yet been identified (i.e. 5-ht$_5$, 5-ht$_6$, and 5-ht$_7$), the nomenclature recommendation has been to use the lowercase appellation (Hoyer *et al.*, 1994).

The 5-ht$_7$ receptor has been cloned from rat, mouse, guinea-pig and human cDNA (Plassat *et al.*, 1993; Ruat *et al.*, 1993; Shen *et al.*, 1993; Meyerhof *et al.*, 1993; Lovenberg *et al.*, 1993; Tsou *et al.*, 1994; Bard *et al.*, 1993). Despite a high degree of interspecies homology (95%), the receptor sequence exhibits low amino acid sequence homology (<40%) with other 5-HT receptors. The cDNA contains introns and predicts encoding of a seven-transmembrane receptor with a long carboxyl terminus. Cells transfected with the cDNA encoding the 5-ht$_7$ receptor express functional receptors coupled positively to adenylyl cyclase. The pharmacological profile of the 5-ht$_7$ receptor is unique but consistent across species (Eglen *et al.*, 1994b; Boess & Martin, 1994). 5-ht$_7$ receptors exhibit high affinity (pK_i 8.1–9.9) for 5-carboxamidotryptamine (5-CT), 5-HT, and 5-methoxytryptamine (5-MeOT), moderate affinity (pK_i 6.4–7.8) for (±)-2-dipropyl-amino-8-hydroxy-1,2,3,4,-tetrahydronaphthalene (8-OH-DPAT), methysergide, ergotamine, and spiperone, and low affinity (pK_i <6.0) for pindolol, sumatriptan, and buspirone. The greatest abundance of 5-ht$_7$ mRNA is found in the brain, where it is localized to the thalamus, hypothalamus, neocortex, olfactory tubercle, brainstem, and limbic regions (Plassat *et al.*, 1993; Ruat *et al.*, 1993; Shen *et al.*, 1993; Tsou *et al.*, 1994).

An important step for the classification of a cloned and expressed receptor is the demonstration of endogenous pharmacological correlates. Functional assays have revealed the presence of receptors that may correspond to the 5-ht$_7$ subtype in guinea-pig hippocampus (Shenker *et al.*, 1987; Tsou *et al.*, 1994; Alvarez *et al.*, unpublished) and several peripheral tissues including porcine vena cava (Sumner *et al.*, 1989), dog coronary artery (Cushing & Cohen, 1992), marmoset aorta (Dyer *et al.*, 1994) and guinea-pig ileum (Feniuk *et al.*, 1983; Eglen *et al.*, 1994a). To date, however, little is known about the binding characteristics or central nervous system distribution of endogenous 5-ht$_7$ receptors due, in part, to the lack of specific ligands.

The aim of the present study was to utilize [^{3}H]-5-carboxamidotryptamine ([^{3}H]-5-CT), to characterize, locate and quantify the density of endogenous 5-ht$_7$ receptors in guinea-pig brain. The binding profile of a pharmacologically isolated receptor was correlated with the cloned guinea-pig 5-ht$_7$ receptor. The distribution was examined by quantitative autoradiography and compared to that obtained using *in situ* hybridization of mRNA encoding this receptor.

A preliminary report of these data has been presented (Jakeman *et al.*, 1994a).

Methods

CHO-K1 cell binding studies

CHO-K1 cells were cotransfected with 4 mg pSW2-7c No. 3 (Tsou *et al.*, 1994) and 1 mg pSV2Neo in 100 mm dishes using the lipofectin method (Felgner *et al.*, 1987). Cells stably expressing the cloned guinea-pig 5-ht$_7$ receptor were grown in F-12 media supplemented with 10% foetal bovine serum (GIBCO-BRL) and harvested with 0.1% Na_2 EDTA diluted

[1] Author for correspondence at: Department of Neurosciences (MS S2-127), Institute of Pharmacology, Syntex Discovery Research, 3401 Hillview Ave., Palo Alto, CA, U.S.A. 94303.

1:10 in phosphate buffered saline. Cells were homogenized (0.5 million cells ml^{-1} of buffer) in Tris-EDTA buffer (composition, mM: Tris-base 50, Na_2 EDTA 0.5, $MgSO_4$ 10, $CaCl_2$ 2, pargyline 0.01, ascorbate 0.1%, pH 7.4 at 4°C). The cell homogenate was centrifuged at 45,000 *g* for 12 min, and the membrane pellet was washed, rehomogenized, and centrifuged twice.

For saturation experiments, cell membranes were incubated for 2 h at room temperature with 0.03–10 nM [^{3}H]-5-CT in the above buffer. In competition studies, membranes were incubated with approximately 0.5 nM [^{3}H]-5-CT for 2 h at room temperature in the presence or absence of competing drugs. Nonspecific binding was defined with 1.0 μM 5-HT. Bound and free radioactivity were separated by rapid filtration through 0.3% polyethylenimine (PEI) pretreated GF/B microplates and washed twice with ice-cold 50 mM Tris-HCl buffer (pH 7.4) on a Packard Filtermate cell harvester. Trapped radioactivity was counted in a Packard Top Count scintillation counter (Downers, Inc.).

Guinea-pig cortical membrane binding studies

Guinea-pig cerebral cortex tissue was dissected from whole guinea-pig brains (Rockland, Inc.), and homogenized (20 mg wet tissue ml^{-1} buffer) as described above. The tissue pellet was rehomogenized and incubated at 37°C for 20 min. The tissue homogenate was then resuspended and rehomogenized twice. Membranes were incubated with [^{3}H]-5-CT for 2 h in Tris-EDTA buffer (pH 7.4 at 21–23°C) containing 1.0 μM (−)-cyanopindolol and 1.0 μM sumatriptan, and filtered as described above.

For association studies, cortical membranes were incubated in 0.5 nM [^{3}H]-5-CT for 0 to 3 h in the absence (total) or presence (non-specific) of 1.0 μM 5-HT, and the binding was then dissociated with 1.0 μM 5-HT for 0 to 2.5 h. Kinetic experiments were terminated by rapid filtration with 50 mM Tris-HCl buffer through 0.3% PEI-pretreated GF/B glass fibre filters. Bound radioactivity was determined using a Packard 2500R scintillation analyzer.

Saturation experiments in cortical membranes were performed as described for the cells. Competition studies were performed using 0.30–0.75 nM [^{3}H]-5-CT. Filtermats were adhered to Multilex melt-on scintillator sheets and counted on a 1204 Betaplate TM BS Liquid Scintillation counter (Wallac Inc.).

Autoradiography

Six adult male Dunkin Hartley guinea-pigs (350–425 g) were killed by asphyxiation with CO_2 and the brains were removed and frozen on dry ice. Sequential sections of 20 μm thickness were cut at −20°C (2800E Jung Frigocut; Leica, Inc.), thaw-mounted onto gelatin-coated slides and stored for 1–7 days at −20°C. Sections were thawed and dried at room temperature, preincubated in 50 mM Tris buffer pH 7.4 for 30 min at room temperature, and then incubated for 2 h at room temperature in Tris-EDTA buffer containing 1.0 nM [^{3}H]-5-CT in the presence of 3.0 μM (−)-cyanopindolol and 3.0 μM sumatriptan. Higher concentrations of [^{3}H]-5-CT, (−)-cyanopindolol and sumatriptan were used in these experiments based on previous studies that have shown a 3–5 fold lower affinity of 5-HT ligands for receptors in tissue sections as compared with homogenate binding studies (Jakeman *et al.*, 1994b; Jakeman *et al.*, unpublished observations). Nonspecific binding was determined on adjacent sections by the addition of 1.0 μM 5-HT. After incubation, the slides were washed twice for 10 min in ice-cold 50 mM Tris (pH 7.4), dipped for 5 s in cold water, and dried quickly under a stream of cold air. Slides were apposed to autoradiographic film for 20 weeks and films developed in Kodak D-19.

In situ *hybridization*

The distribution of 5-ht_7 mRNA was determined in four separate experiments by *in situ* hybridization as described previously (Jakeman *et al.*, 1993; Tsou *et al.*, 1994). Briefly, [^{35}S]-UTP labelled cRNA probes were prepared from sense and antisense templates corresponding to the full open reading frame of the cloned guinea-pig 5-ht_7 receptor (Tsou *et al.*, 1994) using the Gemini II system (Promega Corp.). Sections were hybridized overnight at 55°C and washed for 1 h at 55°C in 0.1 × saline sodium citrate (SSC). Dried slides were apposed to autoradiographic film for 7–10 days.

Compounds

[^{3}H]-5-CT (50.4 Ci $mmol^{-1}$) was purchased from Dupont/New England Nuclear (Boston, MA, U.S.A.). Amoxapine, atropine sulphate, bufotenine monooxalate, (+)-butaclamol, 5-CT, clozapine, cyproheptadine hydrochloride, epidrine, haloperidol, histamine dihydrochloride, ketanserin tartrate, lisuride hydrogen maleate, (+)-lysergic acid diethylamide tartrate ((+)-LSD), mesulergine hydrochloride, metergoline, methiothepin mesylate, 5-MeOT, methylergonovine maleate, methysergide maleate, mianserin hydrochloride, naloxone hydrochloride, octoclothepin maleate, 8-OH-DPAT, oxymetazoline hydrochloride, pergolide methanesulphonate, pindobind$_{1A}$, (−)-pindolol, pirenperone, prochlorperazine dimaleate, ritanserin, 5-hydroxytryptamine hydrochloride (5-HT), spiperone hydrochloride, terguride hydrogen maleate, theophylline, and trifluroperazine dihydrochloride were purchased from Research Biochemicals International (Natick, MA, U.S.A.). 5-Benzyloxytryptamine (5-BeOT), dipropyl-5-carboxamidotryptamine (DP-5-CT), 5-hydroxy-N-ω-methyl-tryptamine (5-OH-NωMeT), 5-methody-*N*,*N*-dimethyltryptamine (5-MeDMT), 6-methoxytryptamine (6-MeOT) and tryptamine hydrochloride were obtained from Sigma Chemical Co. (St. Louis, MO, U.S.A.). Endo-N-(8-methyl-8-azabicyclo[3.2.1]oct-3-yl)-2,3dihydro-3-ethyl-2-oxo-1H-benzimidazole-1-carboxamide hydrochloride (BIMU-1), GR113808 (([1-[2-methylsulphonyl)amino]ethyl]-4-piperidinyl] methyl 1-methyl-1H-indole-3-carboxylate), DuP996 (3,3-bis(4-pyrindinyl methyl)-1-phenylindolin-2-one), ondansetron, and **R**-zacopride were synthesized in the Institute of Organic Chemistry (Syntex Discovery Research). All compounds were dissolved to 10 mM in 50% dimethyl sulphoxide (DMSO) and 50% ethanol and stored at −20°C up to 2 months. Stock solutions were then serially diluted over the range of 1 pM to 100 μM in experimental buffer.

Data analysis

The analyses of saturation and kinetic binding data were performed using non-linear curve fitting programmes by InPlot Scientific Graphics (GraphPad, Inc.) to yield K_d and B_{max} estimates. Kinetic data resulted in the observed association (K_{obs}) and dissociation rate constants (K_{-1}) which were used to calculate K_{+1} and K_d estimates (Molinoff *et al.*, 1981). Hill coefficients and IC_{50} values were obtained from the analysis of competition studies by use of a 4-parameter, logistic, iterative curve fitting programme. IC_{50} values were then converted to K_i values by the Cheng-Prusoff correction (Cheng & Prusoff, 1973). Affinity estimates were presented as the negative log of the K_i (pK_i). The correlation plot was analysed by linear regression (InPlot Scientific Graphics). All values are reported as mean ± s.e.mean from 3–8 experiments as indicated.

Autoradiographs were analysed by digital image analysis with the MCID imaging system (Imaging Research, Inc.). Specific regions of interest were defined on cresyl violet stained histological sections using a standard rat brain atlas (Paxinos & Watson, 1986). For receptor binding autoradiographs, the optical density of each region was converted to fmol radioligand bound mg^{-1} tissue equivalent (fmol mg^{-1}

t.e.) using ^3H standards (Amersham Co.) and a calibration curve was generated for each film. *In situ* hybridization autoradiographs were analysed qualitatively with optical film density scaled from 0 − + + + + for each brain region.

Results

Establishment of radioligand binding conditions

[^{3}H]-5-CT, at 0.5 nM, was predicted to bind to 5-HT_{1A}, 5-HT_{1D}, and 5-ht_7 receptors in guinea-pig cerebral cortex (Zifa & Fillion, 1992; Boess & Martin, 1994). To determine the appropriate concentrations of ligands required to mask binding to 5-HT_{1A} and 5-HT_{1D} receptors, the competition of 0.3–0.7 nM [^{3}H]-5-CT binding by (−)-cyanopindolol and sumatriptan was initially investigated. Both compounds recognized two distinct binding sites in guinea-pig cortical membranes. Thus, for (−)-cyanopindolol, a high affinity site accounted for 58% of the specific binding. The estimated affinity at this site (pK_i) was 7.0, which corresponded to its affinity at 5-HT_{1A} and 5-HT_{1B} receptors (Hoyer, 1991). A low affinity component was also observed, with an approximate pK_i of 5.8. Sumatriptan bound to approximately 20% of sites with high affinity ($pK_i = 6.8$), that corresponded to its affinity at 5-HT_{1D} receptors (Hoyer *et al.*, 1985; Boess & Martin, 1994). A low affinity component was also observed for sumatriptan with an approximate pK_i of 5.2. Therefore, in subsequent experiments, 1.0 μM (−)-cyanopindolol and 1.0 μM sumatriptan were included in the assay buffer to isolate operationally the (−)-cyanopindolol and sumatriptan insensitive components of specific [^{3}H]-5-CT binding.

In the presence of these ligands, the binding of 0.5 nM [^{3}H]-5-CT to guinea-pig cerebral cortex membranes was specific, heat-sensitive, and proportional with tissue concentration over a wide range (5 to 40 mg of wet tissue ml^{-1}). Specific (i.e. 5-HT-displaceable) binding accounted for approximately 75% of total binding and less than 1% of the total free radioligand bound to filters. The specific binding was reduced to 17% and 10% following preincubation of membranes for 20 min at 60°C and 90°C, respectively.

Receptor characterization in guinea-pig cortical membranes and comparison with cloned guinea-pig 5-ht_7 receptor

The specific binding of 0.5 nM [^{3}H]-5-CT in guinea-pig cortex membranes was best fit with monoexponential kinetic equations (Figure 1). Specific binding reached equilibrium within 90 min and remained stable for at least 3 h. Kinetic analysis yielded a K_{obs} value of 0.023 ± 0.003 min^{-1}. The binding was reversible by 1.0 μM 5-HT with an estimated dissociation constant (K_{-1}) value of $6.3 \pm 0.8 \times 10^{-3}$ min^{-1}. Thus, the kinetic K_d derived from these studies was 0.18 ± 0.05 nM ($n = 3$).

[^{3}H]-5-CT binding in guinea-pig cortex membranes was saturable and best described by a model for a single receptor population. Less than 10% of the free ligand bound over the concentration-range used (Figure 2). The mean estimated K_d and B_{max} values were 0.76 ± 0.28 nM and 68.5 ± 26.6 fmol mg^{-1} protein, respectively ($n = 4$; Figure 2). The affinity for [^{3}H]-5-CT was similar to that estimated in CHO-K1 cells

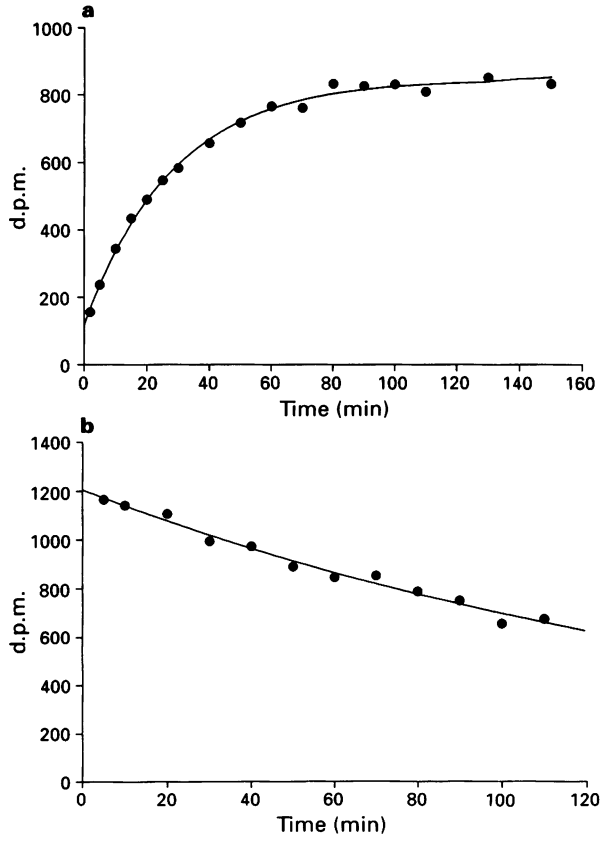

Figure 1 Kinetics of association (a) and dissociation (b) of [^{3}H]-carboxamidotryptamine ([^{3}H]-5-CT) binding in guinea-pig cerebral cortex membranes in the presence of 1.0 μM (−)-cyanopindolol and 1.0 μM sumatriptan. $K_{obs} = 0.033$; $K_{-1} = 5.99 \times 10^{-3}$; $K_d = 0.09$ nM. Similar results were obtained in 2 additional experiments ($n = 3$) as described in text.

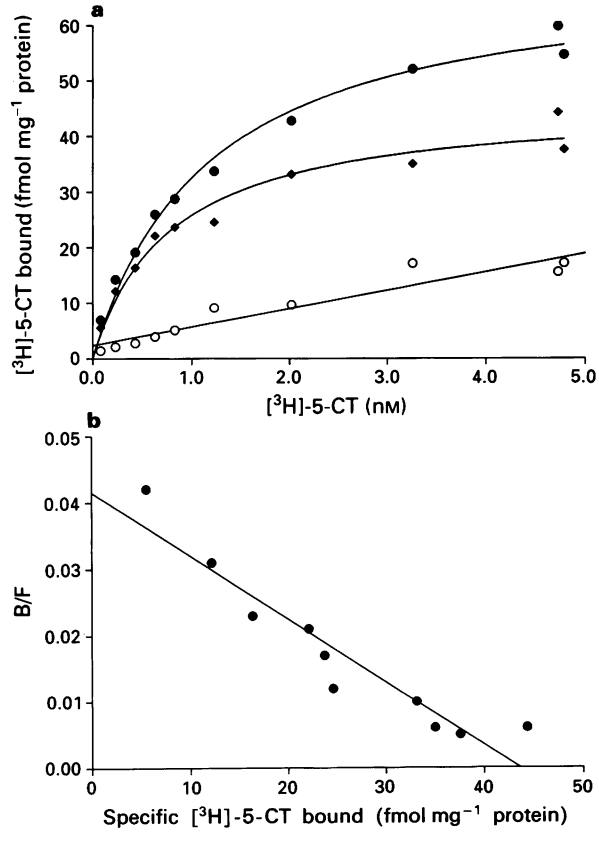

Figure 2 (a) Saturation analysis of [^{3}H]-5-carboxamidotryptamine ([^{3}H]-5-CT) binding to guinea-pig cerebral cortex membranes in the presence of 1.0 μM (−)-cyanopindolol and 1.0 μM sumatriptan. $K_d = 0.77$ nM; $B_{max} = 45.8$ fmol mg^{-1} protein. Total (●), non-specific (○), and specific (◆) binding. Similar results were obtained in 3 additional experiments ($n = 4$) to yield $K_d = 0.76 \pm 0.28$ nM and $B_{max} = 68.5 \pm 36.6$ fmol mg^{-1} protein. (b) Scatchard transformation of specific binding (●) from data in (a).

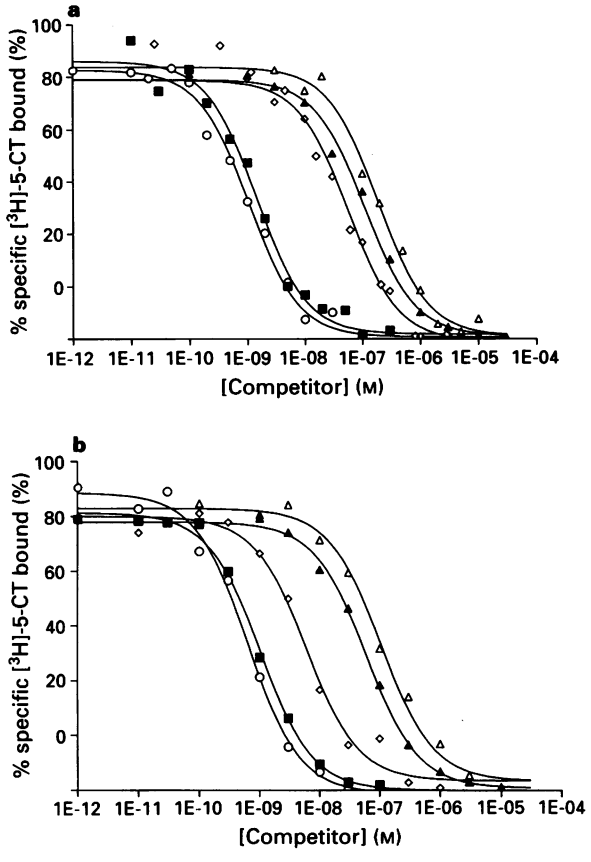

Figure 3 Displacement of 0.3–0.75 nM [^{3}H]-5-carboxamidotryptamine ([^{3}H]-5-CT) by selected compounds in guinea-pig cerebral cortex membranes (a) and membranes from CHO-K1 cells expressing the guinea-pig 5-ht$_7$ receptor (b). Displacement curves are representative of all compounds listed in Table 1. Representative compounds included 5-CT (○), 5-HT (■), methiothepin (◇), tryptamine (▲) and spiperone (△). Non-linear regression analysis yielded the following K_i values for each ligand in cerebral cortex (0.68, 1.05, 62, 65, 125 nM) and CHO-K1 cells (0.26, 0.40, 4.7, 21.6, 48.9 nM). All compounds displaced [^{3}H]-5-CT to the non-specific level defined in the presence of 1.0 μM 5-HT. Mean and s.e.mean of pK_i values for 3–8 determinations are listed in Table 1.

stably expressing the guinea-pig 5-ht$_7$ receptor (0.22 ± 0.02 nM). However, in the presence of masking compounds, the maximum binding capacity in the cortex was approximately one fifth that found in the transfected cells, i.e. 68.5 ± 26.6 fmol mg^{-1} protein compared to 393 ± 48 fmol mg^{-1} of protein.

Several ligands competed for [^{3}H]-5-CT binding in a monophasic manner, exhibiting a wide range of affinities (Figure 3). All ligands in Table 1 displaced [^{3}H]-5-CT to the nonspecific level defined by 1.0 μM 5-HT. Indoles, such as 5-CT, 5-HT, 5-MeOT, and 5-OHMeT, showed the highest affinity with pK_i values ranging from 8.2 to 9.0. Of the ergots, the two ligands with highest affinity, lisuride and pergolide, yielded pK_i values of 7.73 and 7.75, respectively. Derivatives of spiperone showed moderate affinity, the greatest affinity being exhibited by pirenperone with a pK_i value of 7.28. Octoclothepin and methiothepin exhibited affinity estimates of 7.49 and 7.34, respectively.

Several compounds failed to displace [^{3}H]-5-CT binding (pK_i < 5.0) including the derivatives of pindolol, ondansetron, GR113808, BIMU-1, R-zacopride, atropine, histamine, naloxone, epidrine, theophylline, γ-aminobutyric acid and DUP996.

A comparison of the affinities of ligands at [^{3}H]-5-CT binding sites in guinea-pig cortex and transfected cells yielded a statistically significant correlation (Figure 4; $r^2 = 0.96$; $P < 0.01$). The rank order of ligand affinity in both assays was: 5-CT, 5-HT, 5-MeOT > DP-5-CT, lisuride, pergolide > (+)-LSD, methiothepin, metergoline, tryptamine > spiperone, ritanserin, ergotamine, clozapine >> (−)-pindolol and (−)-butaclamol. All of the compounds in Table 1 showed a slightly lower affinity in the cortex binding assay than in the cloned CHO-K1 cell membranes. However, the Hill slope values (n_H) for all compounds were not different from unity.

Receptor distribution in guinea-pig brain

The binding of [^{3}H]-5-CT to guinea-pig brain sections was specific and heterogeneous (Figures 5 and 6, Table 2). The specific binding density following incubation with 1.0 nM [^{3}H]-5-CT ranged from 0.96 to 19.33 fmol mg^{-1}, t.e. Specific binding displaced by 5-HT accounted for more than 70% of total binding in all regions that bound 4.0 fmol of [^{3}H]-5-CT mg^{-1}, t.e. or more.

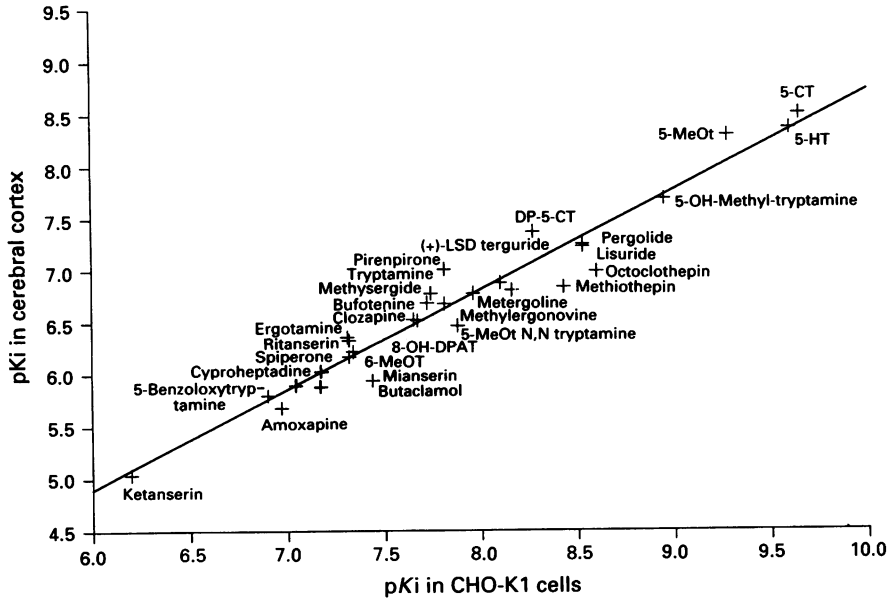

Figure 4 Correlation of the affinity of ligands at the [^{3}H]-5-carboxamidotryptamine ([^{3}H]-5-CT) binding site in guinea-pig cerebral cortex membranes and membranes from CHO-K1 cells expressing the 5-ht$_7$ receptor. Least squares linear regression equation $y = 0.96 \times - 0.34$; $r^2 = 0.96$; $P < 0.01$.

The highest receptor density was observed in the medial nuclei of the thalamus and associated limbic regions. The paraventricular nuclei of the thalamus (PVA, PV, PVP) displayed the greatest density of receptors (17–19 fmol mg^{-1}, t.e.). Other high density regions (> 10 fmol mg^{-1}, t.e.) included related midline thalamic nuclei (IMD, CM, and IAM) and limbic areas including the basomedial, basolateral and medial amygdala, dentate gyrus (stratum moleculare), and entorhinal cortex.

Moderate binding densities (> 8 fmol mg^{-1}, t.e.) were observed in superficial cortex (layers 2–4), hippocampal regions CA1-CA2 (stratum radiatum and stratum moleculare), substantia nigra, superior colliculus, and lateral septum. Slightly lower binding (> 6 fmol mg^{-1}, t.e.) was detected in medial and lateral portions of the medial geniculate nucleus, the medial hypothalamic nuclei (VMH, DMH, MPA), ventral pallidum and globus pallidus, superior colliculus, midbrain central gray, the parabrachial nuclei and dorsal raphe nucleus.

Low binding densities (< 5 fmol mg^{-1}, t.e.) were observed in several regions, including the lateral thalamic nuclei (LGN and LD), the deep layers of cortex, the medial septum, caudate putamen, midbrain interpeduncular nucleus, and several brainstem nuclei. Little to no specific binding was detected in the cerebellum.

5-ht7 mRNA distribution in guinea-pig brain

The distribution of guinea-pig 5-ht_7 receptor mRNA was determined in separate animals using *in situ* hybridization (Figures 5 and 6, Table 2). The highest levels of expression were found in the medial thalamic nuclei (PVA, PV, PVP, CM, IAD) and hippocampal formation (DG>CA3>CA2>>CA1). Moderate expression was found throughout the superficial layers of cortex (2-4), medial geniculate nucleus, amygdala, and hypothalamus. Low hybridization was associated with most midbrain and hindbrain regions. The cerebellar granule cell layer exhibited very high levels of hybridization with both sense and antisense probes. Hybridization with sense strand probes in all other brain regions was not above background.

Discussion

Selective ligands for the newer members of the 5-HT receptor family, including the 5-ht_5, 5-ht_6 and 5-ht_7 subtypes, have not yet been identified. While there are reports of endogenous responses that may correspond to 5-ht_6 and 5-ht_7 receptors (Shenker *et al.*, 1987; Cushing & Cohen, 1992; Feniuk *et al.*, 1993; Shoeffter & Waeber, 1994), endogenous correlates for

Table 1 Affinity of representative ligands competing for [^{3}H]-5-carboxamidotryptamine ([^{3}H]-5-CT) binding sites

	CHO-K1 cells (1)	*Guinea-pig cortex*	
	pK_i	pK_i	n_H
Compound	mean s.e.mean	mean s.e.mean	mean s.e.mean
5-CT	9.65 ± 0.09	9.01 ± 0.07	0.93 ± 0.04
5-HT	9.60 ± 0.24	8.87 ± 0.06	1.01 ± 0.10
5-MeOT	9.28 ± 0.07	8.80 ± 0.09	1.01 ± 0.12
5-OH-ME-Nw tryptamine	8.95 ± 0.02	8.19 ± 0.06	0.95 ± 0.09
DP-5-CT	8.27 ± 0.17	7.87 ± 0.02	0.96 ± 0.07
5-MeOT N,N tryptamine	7.88 ± 0.05	6.97 ± 0.18	0.92 ± 0.04
Tryptamine	7.72 ± 0.03	7.19 ± 0.10	0.94 ± 0.06
Bufotenine	7.67 ± 0.01	7.02 ± 0.14	0.91 ± 0.03
6-MeOT	7.44 ± 0.02	6.44 ± 0.03	0.86 ± 0.07
8-OH-DPAT	7.39 ± 0.03	6.87 ± 0.09	1.01 ± 0.05
5-Benzoloxytryptamine	6.59 ± 0.06	5.96 ± 0.16	1.05 ± 0.09
Lisuride	8.53 ± 0.12	7.73 ± 0.07	0.92 ± 0.03
Pergolide	8.53 ± 0.08	7.75 ± 0.09	0.87 ± 0.04
Metergoline	8.16 ± 0.11	7.31 ± 0.08	1.02 ± 0.07
Terguride	8.10 ± 0.10	7.38 ± 0.05	0.95 ± 0.05
Methylergonovine	7.96 ± 0.04	7.28 ± 0.08	1.20 ± 0.12
(+)-LSD	7.81 ± 0.03	7.51 ± 0.09	1.05 ± 0.04
Mesulergine	7.81 ± 0.06	7.18 ± 0.09	0.96 ± 0.06
Methysergide	7.65 ± 0.04	7.03 ± 0.07	0.96 ± 0.05
Ergotamine	7.31 ± 0.01	6.86 ± 0.07	1.17 ± 0.06
Pirenpirone	7.74 ± 0.04	7.28 ± 0.17	0.88 ± 0.04
Spiperone	7.32 ± 0.05	6.67 ± 0.07	0.92 ± 0.07
Ritanserin	7.34 ± 0.05	6.72 ± 0.11	1.05 ± 0.09
Ketanserin	6.20 ± 0.06	5.54 ± 0.09	0.94 ± 0.13
Haloperidol	5.48 ± 0.11	5.03 ± 0.12	1.00 ± 0.15
Octoclothepin	8.60 ± 0.20	7.49 ± 0.13	1.04 ± 0.08
Methiothepin	8.43 ± 0.09	7.34 ± 0.08	1.06 ± 0.06
Clozapine	7.32 ± 0.14	6.83 ± 0.12	0.83 ± 0.04
Mianserin	6.97 ± 0.10	6.18 ± 0.07	1.05 ± 0.15
Cyproheptadine	6.90 ± 0.03	6.30 ± 0.13	0.92 ± 0.04
Amoxapine	6.73 ± 0.09	5.85 ± 0.05	0.90 ± 0.05
Butaclamol	6.72 ± 0.01	6.06 ± 0.07	0.98 ± 0.04
Trifluoroperazine	5.84 ± 0.04	< 5	
Prochlorperazine	< 5	< 5	
Pindobind-5-HT_{1A}	5.72 ± 0.03	< 5	
(−)-Pindolol	< 4	< 5	

Values represent 3–8 determinations. [^{3}H]-5-CT (0.5 nM) binding in the presence of sumatriptan (1.0 μM) and (−)-cyanopindolol (1.0 μM). 5-HT (1.0 μM) was used to define non-specific binding. (1) Affinity values determined in CHO-K1 cells expressing guinea-pig 5ht_7 receptor. n_H values in cloned cells were not different from unity (Alvarez *et al.*, unpublished).

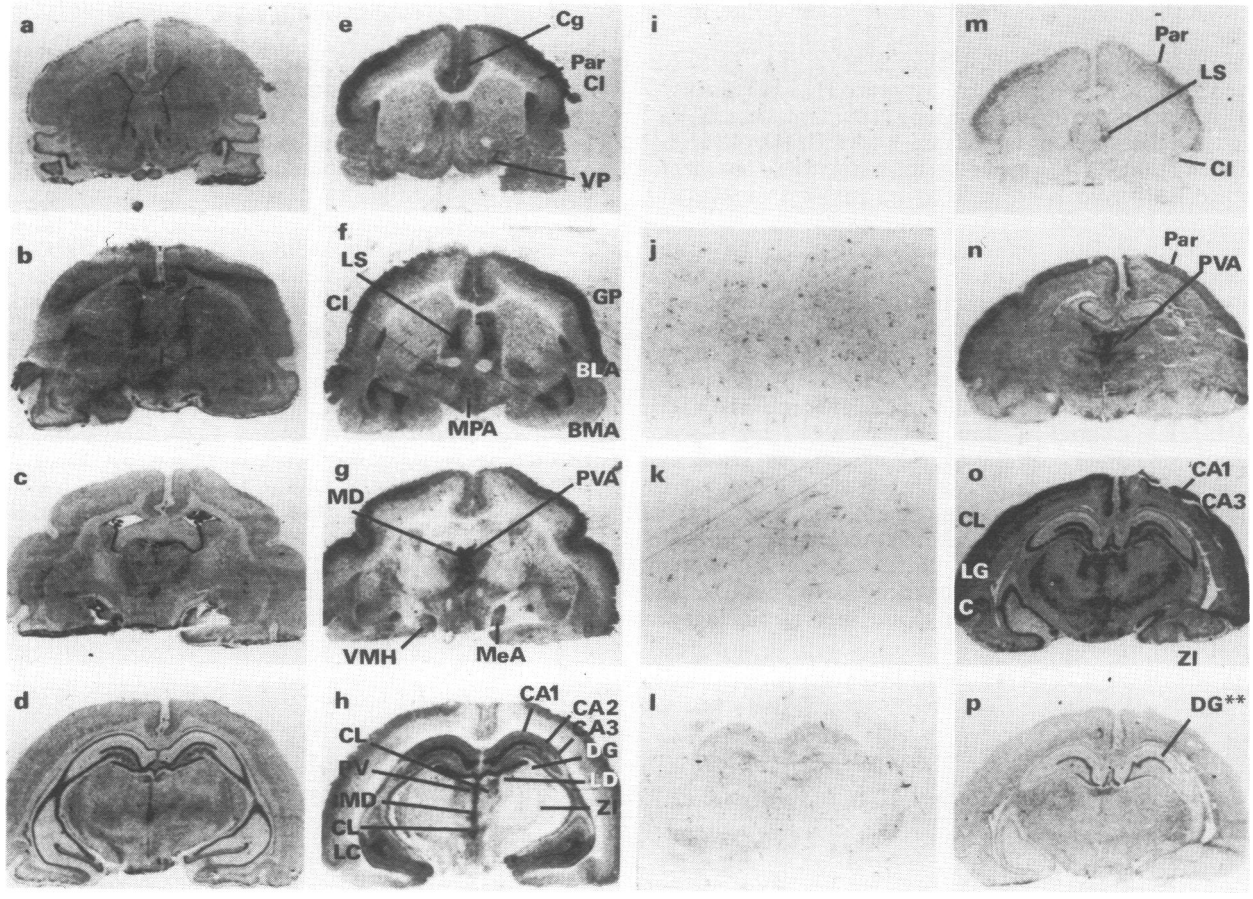

Figure 5 Distribution of 5-ht$_7$ receptor binding and mRNA in guinea-pig coronal forebrain sections. (a–d) Histological sections stained with 0.25% Cresyl violet. (e–h) Autoradiographs of total binding from same sections following incubation in 1.0 nM [^{3}H]-5-carboxamidotryptamine ([^{3}H]-5-CT) in the presence of (−)-cyanopindolol and sumatriptan. (i–l) Autoradiographs from sections adjacent to those in h–n, with non-specific binding defined in the presence of 1.0 μM 5-HT. (m–p) Autoradiographs following *in situ* hybridization using [^{35}S]-UTP-labelled antisense (m, n, o) and sense (p) strand riboprobes. Darker areas correspond to higher mRNA levels. Section in panel m from a different experiment from n–p. Hybridization in ventromedial hypothalamus is dense just lateral to suprachiasmatic nuclei (arrowhead). Hybridization using sense strand probe was not above background except in hippocampal dentate gyrus (DG**). Abbreviations are defined in Table 2.

these receptor subtypes have not been clearly isolated. In the present study, a distinct binding site in guinea-pig cerebral cortex membranes was evaluated. This site has a pharmacological profile that corresponds closely to the cloned 5-ht$_7$ receptor and a distribution similar to the distribution of 5-ht$_7$ mRNA in guinea-pig brain.

[^{3}H]-5-CT has been used previously to label 5-ht$_7$ receptors in transfected cells (Plassat *et al.*, 1993; Ruat *et al.*, 1993; Shen *et al.*, 1993; Bard *et al.*, 1993; Lovenberg *et al.*, 1993). However, this radioligand exhibits nanomolar affinity at 5-HT$_1$, 5-HT$_2$, 5-ht$_5$, 5-ht$_7$, and cloned 5-HT$_4$ receptors (Zifa & Fillion, 1992; Boess & Martin, 1994; Adham *et al.*, 1994). In contrast, [^{3}H]-5-CT is more selective, since it binds with nanomolar affinity only to 5-HT$_{1A}$, 5-HT$_{1B}$, 5-HT$_{1D}$ and 5-ht$_7$ subtypes (Hoyer *et al.*, 1985; Heuring & Peroutka, 1987; Hoyer, 1991; Nowak *et al.*, 1993). In the present study, a single population of receptors was isolated from guinea-pig cerebral cortex membranes using [^{3}H]-5-CT in the presence of (−)-cyanopindolol and sumatriptan to occupy 5-HT$_{1A}$ and 5-HT$_{1D}$ receptors. The specific binding under these conditions was saturable, reversible, and described by a single site receptor model in equilibrium, kinetic and competition analyses. All compounds displaced the radioligand to the non-specific level defined by 5-HT, indicating that no non-5-HT sites were labelled. However, it is likely that not all 5-HT$_7$ receptors were available for binding, as the masking compounds both have sufficient affinity for 5-ht$_7$ receptors to occupy a proportion of sites at 1.0 μM.

The affinities of several structurally diverse compounds that competed for [^{3}H]-5-CT binding sites was compared to those obtained in CHO-K1 cells stably expressing the cloned guinea-pig 5-ht$_7$ receptor. The rank orders of affinity were highly correlated, suggesting pharmacological identity. To verify an absence of other 5-HT receptor subtypes in the cortex binding assay, several compounds that distinguish known 5-HT receptors were used. A lack of 5-HT$_1$ and 5-ht$_5$ receptors was suggested by the low affinity of 8-OH-DPAT (5-HT$_{1A}$), pindolol derivatives (5-HT$_{1A}$, 5-HT$_{1B}$) and ergotamine (5-HT$_{1A}$, 5-HT$_{1B}$, 5-HT$_{1D}$, 5-ht$_{5A,5B}$). Subnanomolar concentrations of [^{3}H]-5-CT were not expected to label 5-HT$_{1E}$, 5-HT$_{1F}$, 5-HT$_2$, 5-HT$_3$, 5-HT$_4$ or 5-ht$_6$ receptors (Zifa & Fillion, 1992; Boess & Martin, 1994). The absence of these receptors was further suggested by the poor activity of sumatriptan (5-HT$_{1F}$), ritanserin and mianserin (5-HT$_2$), ondansetron (5-HT$_3$) and GR113808 (5-HT$_4$).

Although the correlation between brain tissue and cloned receptor binding is very good, all the compounds tested were weaker in the cortical membranes. The reason for this is not clear. A possible factor may be that the assay relies on binding of an agonist radioligand. Large differences have been reported for agonist binding affinity (K_d) and functional potency (EC_{50}) in the cloned 5-ht$_7$ receptors (Bard *et al.*, 1993; Tsou *et al.*, 1994), suggesting that coupling efficiency of this receptor can greatly affect potency. In addition, some differences may exist in the relationship between the receptor and associated G-proteins in the overexpressed conditions as

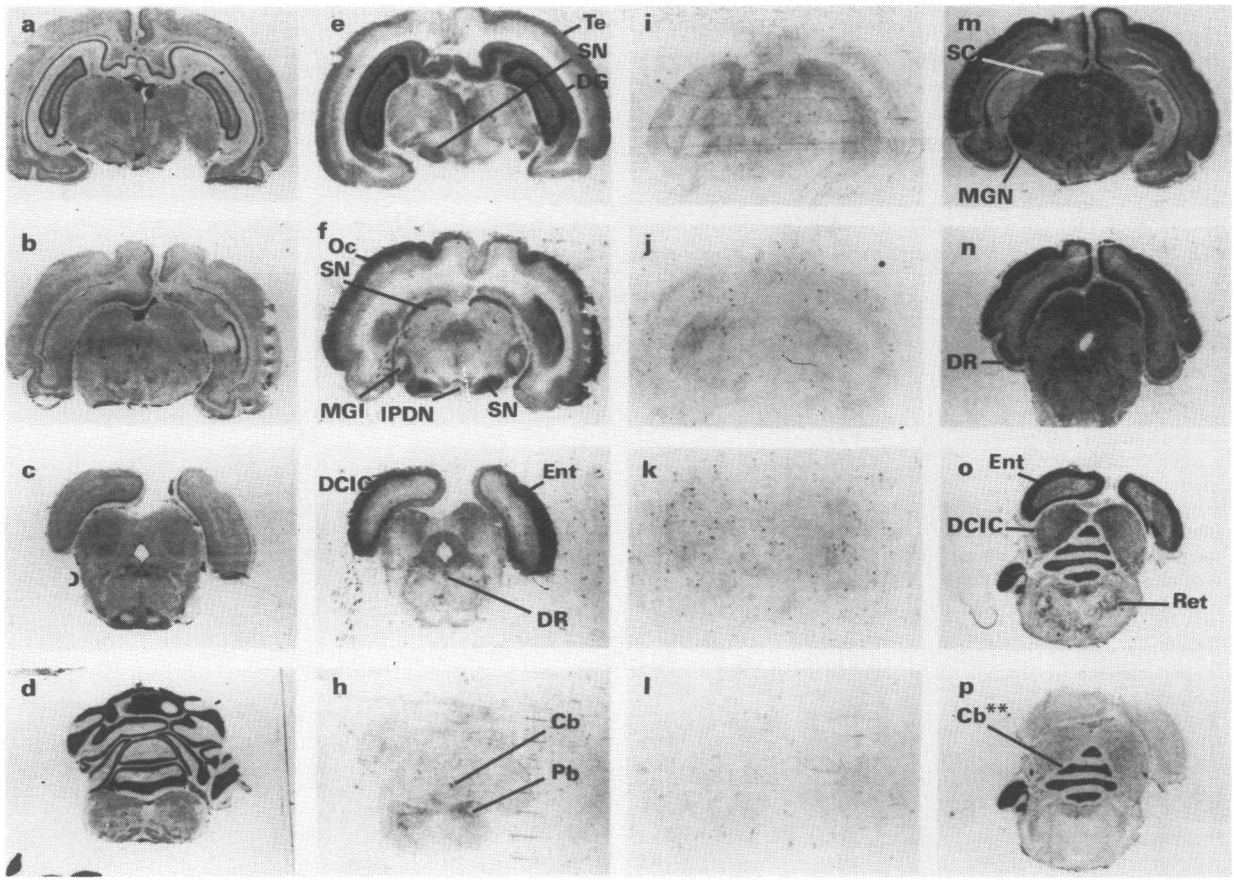

Figure 6 Distribution of 5-ht$_7$ receptor binding and mRNA in guinea-pig coronal midbrain and hindbrain sections. Sections labelled as in Figure 5 (a–d) Cresyl violet; (e–h) total binding, autoradiography; (i–l) non-specific binding, autoradiography; (m–p) *in situ* hybridization using antisense (m, n, o) and sense (p) strand ^{35}S-labelled riboprobes. Hybridization using sense strand probe was not above background except in cerebellar granule cell layer (Cb**). Abbreviations are defined in Table 2.

opposed to the endogenous tissues. Such differences might affect the observed affinity of ligands competing with an agonist binding site. Further studies using a radiolabelled antagonist may address this issue directly.

A heterogeneous distribution of [^{3}H]-5-CT binding sites was identified in guinea-pig brain sections with the highest binding densities in thalamo-cortical and limbic system areas. A qualitatively similar distribution was recently reported for 5-ht$_7$ receptors in rat and guinea-pig using [^{3}H]-5-CT in the presence of 100 nM PAPP (4-[2-[4-[3-(trifluoromethyl)phenyl]-1-piperazinyl]ethyl]benzene amide) and 160 nM (−)-pindolol (Branchek *et al.*, 1993).

This distribution corresponded closely to the distribution of 5-ht$_7$ mRNA, although some differences were observed. For example, 5-ht$_7$ mRNA in hippocampus was highest in the dentate gyrus and CA3 region, while [^{3}H]-5-CT binding was highest in the dentate gyrus and CA1-CA2 regions. These observations may suggest that 5-ht$_7$ receptors are located presynaptically on the Shaeffer collaterals and associational projections of CA3 pyramidal neurones. In contrast, receptors on dentate granule cells may be located both pre- and postsynaptically. The moderate binding density in brain regions with undetected mRNA levels, including the substantia nigra, central grey, superior colliculus and trigeminal nucleus (sp5) may reflect a presynaptic location of 5-ht$_7$ receptors in these brain areas (Branchek *et al.*, 1993).

In many brain areas, the distribution of binding sites was complementary to that of other 5-HT receptors, particularly the 5-HT$_1$ subtypes (Waeber *et al.*, 1989; Miquel *et al.*, 1991; Pompeiano *et al.*, 1992; del Arco *et al.*, 1993; Bruinvels *et al.*, 1994). Overlapping 5-ht$_7$ and 5-HT$_1$ receptor distributions were found in lateral septum, entorhinal cortex, CA1-CA2 subfields of the hippocampus, amygdala, substantia nigra, superior colliculi, and hypothalamus, and claustrum (5-HT$_{1E}$, Barone *et al.*, 1993). The areas of similar distribution may reflect opposing regulation of adenylyl cyclase activity by 5-HT.

Based on their distribution, functional implications of 5-ht$_7$ receptors may be suggested. Thus, binding in midline thalamic, limbic, and cortical structures suggest a role in affective behaviours (Paxinos, 1985; Turner & Herkenham, 1991). Moderate receptor densities in the medial geniculate nucleus, superior and inferior colliculi, central grey, and spinal trigeminal nuclei are also consistent with a role in the modulation of sensory information. Finally, receptors in substantia nigra and ventral pallidum would be consistent with possible actions of 5-ht$_7$ receptors in motor behaviours (Shen *et al.*, 1993; Branchek *et al.*, 1993).

Other roles for 5-ht$_7$ receptors activation can be inferred from the pharmacological binding profile. For example, 5-ht$_7$ receptors exhibit moderate to high affinity for clozapine, octoclothepin, pimozide, and risperidone. This has led to the hypothesis that activity at these receptors may contribute to the antipsychotic efficacy of these drugs (Roth *et al.*, 1994). Indeed, the low receptor density in striatum suggests that novel compounds acting selectively at the 5-ht$_7$ receptor subtype would have fewer extrapyramidal side effects.

The moderate affinity of 8-OH-DPAT at 5-ht$_7$ receptors is also important for proposing functional roles for these receptors. 8-OH-DPAT has been previously classified as a highly specific 5-HT$_{1A}$ receptor agonist (Gozlan *et al.*, 1983; Boess & Martin, 1994). However, 8-OH-DPAT also has moderate affinity for the 5-ht$_7$ receptor. Thus, several behavioural responses previously ascribed to 5-HT$_{1A}$ receptor activation may

also reflect involvement of 5-ht$_7$ receptors. For example, administration of 8-OH-DPAT can mimic 5-HT modulation of circadian rhythms in hypothalamic tissue slices. This effect has now been mimicked by cyclic AMP analogues and blocked by ritanserin, but not by pindolol, possibly implicating 5-ht$_7$ receptors in the modulation of circadian rhythms (Lovenberg *et al.*, 1993).

In summary, radioligand binding techniques have been used to identify a specific [^{3}H]-5-CT binding site in guinea-pig brain with a pharmacological profile and distribution similar to the cloned 5-ht$_7$ receptor. The development of a radioligand binding assay may prove useful for characterization of 5-ht$_7$ receptors.

Table 2 Distribution of 5-ht$_7$ receptors in coronal guinea-pig brain sections

Region		*Receptor autoradiography Specific bound* (fmol mg^{-1}, t.e.)	s.e.mean	*% spec. binding*	In situ *hybridization Optical density* (see footnote)
Thalamus					
paraventricular n., anterior	PVA	19.33	±2.25	94%	++++
paraventricular n., poster.	PVP	17.77	±1.76	92%	+++
paraventricular n.	PV	17.28	±2.48	88%	+++
intermediodorsal n.	IMD	13.05	±1.48	87%	++
central medial n.	CM	10.67	±2.01	83%	+++
interanterodorsal n.	IAM	11.74	±1.82	87%	+++
medial geniculate n., ventral	MGV	8.16	±1.01	84%	++
medial geniculate n., medial	MGM	7.29	±0.88	84%	++
mediodorsal n.	MD	6.96	±1.52	80%	++
centrolateral n.	CL	5.99	±0.60	80%	++
lateral geniculate n.	LGN	4.88	±0.75	71%	+
laterodorsal n.	LD	1.70	±0.40	49%	+
Hippocampus					
dentate gyrus (mol. layer)	DG	14.77	±1.17	86%	++++**
CA1 (all layers)	CA1	9.64	±0.60	77%	±
CA2 (all layers)	CA2	9.48	±0.39	80%	++
CA3 (all layers)	CA3	5.77	±0.54	81%	+++
Cerebral cortex					
entorhinal cortex	Ent	11.79	±1.12	87%	++
parietal cortex, layers 2-4	Par	10.27	±1.19	89%	++
occipital cortex, layers 2-4	Oc	9.91	±1.42	84%	++
frontal cortex, layers 2-4	Fr	9.21	±0.97	88%	++
temporal cortex, layers 2-4	Te	9.09	±1.09	84%	++
cingulate cortex	Cg	7.29	±0.87	83%	++
perirhinal cortex	PRh	7.06	±0.91	85%	++
parietal cortex, layers 5-6	Par (5-6)	4.24	±0.59	76%	±
Amygdala					
medial amygdala n.	MeA	11.42	±0.87	86%	+
basomedial n.	BMA	10.72	±1.84	87%	++
basolateral n.	BLA	10.58	±1.63	89%	++
Septum and hypothalamus					
lateral septum	LS	8.68	±1.05	85%	+
ventromedial hypothal n.	VMH	7.15	±0.96	86%	++*
dorsomedial hypothal n.	DMH	6.20	±0.85	76%	+
medial preoptic area	MPA	6.03	±1.04	83%	+
medial septum	MS	4.16	±0.99	75%	−
Basal ganglia					
claustrum	Cl	9.17	±0.96	88%	+
ventral pallidum	VP	7.21	±1.17	84%	−
globus pallidus	GP	6.83	±1.04	81%	−
caudate-putamen	CPu	2.85	±0.44	68%	−
Midbrain					
substantia nigtra, pars retic.	SNR	9.66	±1.04	87%	−
superior colliculus	SC	8.87	±0.76	84%	−
dorsal inferior colliculus	DCIC	6.76	±0.80	81%	++
central grey	CG	6.31	±1.01	78%	+
interpeduncular n.	IPDN	4.04	±0.32	76%	−
zona incerta	ZI	3.12	±0.45	64%	+
Hindbrain					
dorsal raphe n.	DR	7.14	±0.33	79%	±
parabrachial n.	PB	6.07	±0.83	81%	±
locus coeruleus	LC	5.82	±0.78	77%	−
spinal trigeminal n.	Sp5	5.36	±0.63	81%	−
prepositus hypoglossal n.	PrH	4.38	±0.41	74%	−
n. solitary tract	Sol	4.23	±0.35	74%	±
hindbrain reticular form.	Ret	3.88	±0.49	72%	+
median raphe n.	MR	3.80	±0.40	73%	−
cerebellum	Cb	0.96	±0.21	41%	++++**

Receptor autoradiography values obtained by digital image analysis of [^{3}H]-5-carboxamidotryptamine ([^{3}H]-5-CT) binding for $n = 6$ brains. Qualitative analysis of ^{35}S-labelled riboprobe *in situ* hybridization ($n = 4$) expressed as relative optical density from autoradiographs. Key: ++++, very dark; +++, dark; ++, moderate; +, light; ±, very light; −, none detected over sense control background.
*mRNA ventrolateral to suprachiasmatic nucleus; **dark hybridization in sense strand control sections.

The authors thank Ann Ping Tsou and Alan Kosaka for providing a stable cell line expressing GP2-7, I.S. Ramsey and Robert Alvarez for verification of receptor function in transfected cell lines by adenylyl cyclase assays, and Edward Leung and David E. Clarke for critical discussions of the data.

References

ADHAM, N., GERALD, C., SCHECHTER, L.E., WEINSHANK, R.L. & BRANCHEK, T.A. (1994). [^{3}H]5-HT labels the high affinity state of the cloned rat 5-HT$_4$ receptor. *Behav. Brain Res.*, (in press) (Abstract).

BARD, J.A., ZGOMBICK, J., ADHAM, N., VAYSSE, P., BRANCHEK, T.A. & WEINSHANK, R.L. (1993). Cloning of a novel human serotonin receptor (5-HT$_7$) positively linked to adenylate cyclase. *J. Biol. Chem.*, **268,** 23422–23426.

BARONE, P., MILLET, S., MORET, C., PRUDHOMME, N. & FILLION, G. (1993). Quantitative autoradiography of 5-HT$_{1E}$ binding sites in rodent brains: effect of lesion of serotonergic neurons. *Eur. J. Pharmacol.*, **249,** 221–230.

BOESS, F.G. & MARTIN, I.L. (1994). Review: molecular biology of 5-HT receptors. *Neuropharmacology*, **33,** 275–317.

BRANCHEK, T.A., GUSTAFSON, E.L., DURKIN, M.M., BARD, J.A. & WEINSHANK, R.L. (1994). Autoradiographic localization of 5-HT$_7$ and its mRNA in rat CNS by radioligand binding and *in situ* hybridization histochemistry. *Br. J. Pharmacol.*, **112,** 100P.

BRUINVELS, A.T., LANDWEHRMEYER, B., GUSTAFSON, E.L., DURKIN, M.M., MENGOD, G., BRANCHEK, T.A., HOYER, D. & PALACIOS, J.M. (1994). Localization of 5-HT$_{1B}$, 5-HT$_{1D\alpha}$, 5-HT$_{1E}$, and 5-HT$_{1F}$ receptor messenger RNA in rodent and primate brain. *Neuropharmacology*, **33,** 367–386.

CHENG, Y.C. & PRUSOFF, W.H. (1973). Relationship between inhibition constant (K$_i$) and the concentration of inhibitor which causes 50 percent inhibition (IC$_{50}$) of an enzymatic reaction. *Biochem. Pharmacol.*, **22,** 3099–3108.

CUSHING, D.J. & COHEN, M.L. (1992). Serotonin-induced relaxation in canine coronary artery smooth muscle. *J. Pharmacol. Exp. Ther.*, **263,** 123–129.

DEL ARCO, C., GALENDE, I. & PAZOS, A. (1993). Autoradiographic mapping of 5-HT$_1$ receptors in the guinea pig brain with particular reference to the 5-HT$_{1D}$ receptor sites. *Naunyn-Schmied. Arch. Pharmacol.*, **347,** 248–256.

DYER, S.M., DE LA LANDE, I.S., FREWIN, D.B. & HEAD, R.J. (1994). Characterisation of 5-hydroxytryptamine-induced, smooth muscle-mediated relaxation in the marmoset aorta. *Behav. Brain Res.*, (in press).

EGLEN, R.M., CHAMPNEY, M. & CARTER, D. (1994a). Characterization of post-junctional 5-hydroxytryptamine (5-HT) receptors mediating relaxations of guinea-pig isolated ileum. *Behav. Brain Res.*, (in press).

EGLEN, R.M., JAKEMAN, L. & ALVAREZ, R.A. (1994b). The 5-hydroxytryptamine$_7$ receptor. *Expert Opin. Invest. Drugs*, **3,** 175–177.

FELGNER, P.I., GADEK, T.R., HOLM, M., ROMAN, R., CHAN, H.W., WENZ, M., NORTHROP, J.P., RINGOLD, G.M. & DANIELSON, M. (1987). Lipofection: a highly efficient, lipid-mediated DNA-transfection procedure. *Proc. Natl. Acad. Sci. U.S.A.*, **84,** 7413–7417.

FENIUK, W., HUMPHREY, P.P.A. & WATTS, A.D. (1983). 5-Hydroxytryptamine-induced relaxation of isolated mammalian smooth muscle. *Eur. J. Pharmacol.*, **96,** 71–78.

GOZLAN, E., EL MESTIKAWY, S., PICHAT, L., GLOWINSKI, J. & HAMON, M. (1983). Identification of presynaptic serotonin autoreceptors using a new ligand ^{3}H-PAT. *Nature*, **305,** 140–142.

HEURING, R.E. & PEROUTKA, S.J. (1987). Characterization of a novel [^{3}H]5-HT binding site subtype in bovine brain membranes. *J. Neurosci.*, **7,** 894–903.

HOYER, D. (1991). The 5-HT receptor family: ligands, distribution and receptor-effector coupling. In *5-HT$_{1a}$ Agonists, 5-HT$_3$ Antagonists and Benzodiazepines: Their Comparative Behavioural Pharmacology*. ed. Rodgers, R.J. & Cooper, S.J. pp. 31–58. Chichester, UK: John Wiley & Sons Ltd.

HOYER, D., CLARKE, D.E., FOZARD, J.R., HARTIG, P.R., MARTIN, G.R., MYLECHARANE, E.J., SAXENA, P.R. & HUMPHREY, P.P.A. (1994). International union of pharmacology classification of receptors for 5-hydroxytryptamine (serotonin). *Pharmacol. Rev.*, **46,** 157–243.

HOYER, D., ENGEL, G. & KALKMAN, H.O. (1985). Molecular pharmacology of 5-HT$_1$ and 5-HT$_2$ recognition sites in rat and pig brain membranes: radioligand binding studies with [^{3}H]5-HT, [^{3}H]8-OH-DPAT, (−)-[^{125}I]iodocyanopindolol, [^{3}H]mesulergine and [^{3}H]ketanserin. *Eur. J. Pharmacol.*, **118,** 13–23.

JAKEMAN, L.B., ARMANINI, M., PHILLIPS, H.S. & FERRERA, N. (1993). Developmental expression of binding sites and messenger ribonucleic acid for vascular endothelial growth factor suggests a role for this protein in vasculogenesis and angiogenesis. *Endocrinology*, **133,** 848–859.

JAKEMAN, L.B., TO, Z.P., BONHAUS, D.W. & EGLEN, R.M. (1994a). Pharmacological characterization of an endogenous 5-HT$_7$ receptor in guinea pig cerebral cortex by radioligand binding. *Behav. Brain Res.*, (in press).

JAKEMAN, L.B., TO, Z.P., EGLEN, R.M., WONG, E.H.F. & BONHAUS, D.W. (1994b). Quantitative autoradiography of 5-HT$_4$ receptors in brains of three species using two structurally distinct radioligands, [^{3}H] GR 113808 and [^{3}H]BIMU-1. *Neuropharmacology*, **33,** 1027–1038.

LOVENBERG, T.W., BARON, B.M., DE LECEA, L., MILLER, J.D., PROSSER, R.A., REA, M.A., FOYE, P.E., RACKE, M., SLONE, A.L., SIEGEL, B.W., DANIELSON, P.E., SUTCLIFFE, J.G. & ERLANDER, M.G. (1993). A novel adenylyl cyclase-activating serotonin receptor (5-HT$_7$) implicated in the regulation of mammalian circadian rhythms. *Neuron*, **11,** 449–458.

MARTIN, G.R. & HUMPHREY, P.P.A. (1994). Classification review: receptors for 5-hydroxytryptamine: current perspectives on classification and nomenclature. *Neuropharmacology*, **33,** 261–273.

MEYERHOF, W., OBERMULLER, F., FEHR, S. & RICHTER, D. (1993). A novel rat serotonin receptor: primary structure, pharmacology, and expression pattern in distinct brain regions. *DNA Cell Biol.*, **12,** 401–409.

MIQUEL, M.-C., DOUCET, E., BONI, C., MESTIKAWY, S.E., MATTIESSEN, L., DAVAL, G., VERGE, D. & HAMON, M. (1991). Central serotonin$_{1A}$ receptors: respective distributions of encoding mRNA, receptor protein and binding sites by in situ hybridization histochemistry, radioimmunohistochemistry, and autoradiographic mapping in rat brain. *Neurochem. Int.*, **19,** 453–465.

MOLINOFF, P.B., WOLFE, B.B. & WEILAND, G.A. (1981). Quantitative analysis of drug-receptor interactions: II. Determination of the properties of receptor subtypes. *Life Sci.*, **29,** 427–443.

NOWAK, H.P., MAHLE, C.D. & YOCCA, F.D. (1993). [^{3}H]5-carboxamidotryptamine labels 5-HT$_{1D}$ binding sites in bovine substantia nigra. *Br. J. Pharmacol.*, **109,** 1206–1211.

PAXINOS, G. (1985). *The Rat Nervous System*. Sydney, Australia: Academic Press, Inc.

PAXINOS, G. & WATSON, C. (1986). *The Rat Brain in Stereotaxic Coordinates*. New York: Academic Press.

PLASSAT, J.-L., AMLAIKY, N. & HEN, R. (1993). Molecular cloning of a mammalian serotonin receptor that activates adenylate cyclase. *Mol. Pharmacol.*, **44,** 229–236.

POMPEIANO, M., PALACIOS, J.M. & MENGOD, G. (1992). Distribution and cellular localization of mRNA coding for 5-HT$_{1A}$ receptor in the rat brain: correlation with receptor binding. *J. Neurosci.*, **12,** 440–453.

ROTH, B.L., CRAIGO, S.C., CHOUDHARY, M.S., ULUER, A., MONSMA, F.J., SHEN, Y., MELTZER, H.Y. & SIBLEY, D.R. (1994). Binding of typical and atypical antipsychotic agents to 5-hydroxytryptamine-6 and 5-hydroxytryptamine-7 receptors. *J. Pharmacol. Exp. Ther.*, **268,** 1403–1410.

RUAT, M., TRAIFFORT, E., LEURS, R., TARDIVEL-LACOMBE, J., DIAZ, J., ARRANG, J.-M. & SCHWARTZ, J.-C. (1993). Molecular cloning, characterization, and localization of a high-affinity serotonin receptor (5-HT$_7$) activating cAMP formation. *Proc. Natl. Acad. Sci. U.S.A.*, **90,** 8547–8551.

SCHOEFFTER, P. & WAEBER, C. (1994). 5-hydroxytryptamine receptors with a 5-HT_6 receptor-like profile stimulating adenylyl cyclase activity in pig caudate membranes. *Naunyn-Schmied. Arch. Pharmacol.*, **350,** 356–360.

SHEN, Y., MONSMA, F.J., METCALF, M.A., JOSE, P.A., HAMBLIN, M.W. & SIBLEY, D.R. (1993). Molecular cloning and expression of a 5-hydroxytryptamine$_7$ serotonin receptor subtype. *J. Biol. Chem.*, **268,** 18200–18204.

SHENKER, A., MAAYANI, S., WEINSTEIN, H. & GREEN, J.P. (1987). Pharmacological characterization of two 5-hydroxytryptamine receptors coupled to adenylate cyclase in guinea pig hippocampal membranes. *Mol. Pharmacol.*, **31,** 357–367.

SUMNER, M.J., FENIUK, W. & HUMPHREY, P.P.A. (1989). Further characterisation of the 5-HT receptor mediating vascular relaxation and elevation of cyclic AMP in porcine isolated vena cava. *Br. J. Pharmacol.*, **97,** 292–300.

TSOU, A.P., KOSAKA, A., BACH, C., ZUPPAN, P., YEE, C., TOM, L., ALVAREZ, R., RAMSEY, S., BONHAUS, D.W., STEFANICH, E., JAKEMAN, L., EGLEN, R.M. & CHAN, H.W. (1994). Cloning and expression of a 5-hydroxytryptamine$_7$ receptor positively coupled to adenylyl cyclase. *J. Neurochem.*, **63,** 456–464.

TURNER, B.H. & HERKENHAM, M. (1991). Thalamoamygdaloid projections in the rat: a test of the amygdala's role in sensory processing. *J. Comp. Neurol.*, **313,** 295–325.

WAEBER, C., DIETL, M.M., HOYER, D. & PALACIOS, J.M. (1989). 5.HT_1 Receptors in the vertebrate brain. Regional distribution examined by autoradiography. *Naunyn-Schmied. Arch. Pharmacol.*, **340,** 486–494.

ZIFA, E. & FILLION, G. (1992). 5-hydroxytryptamine receptors. *Pharmacol. Rev.*, **44,** 401–458.

(Received October 20, 1994
Revised January 11, 1995
Accepted January 12, 1995)

British Journal of Pharmacology (1995) 115, 117-127

Time-dependent fading of the activation of K_{ATP} channels, induced by aprikalim and nucleotides, in excised membrane patches from cardiac myocytes

[1]Dominique Thuringer, *Icilio Cavero & Edouard Coraboeuf

Hôpital Marie Lannelongue, Département de Recherche Médicale, CNRS URA 1159, Laboratoire de Cardiologie Moléculaire et Cellulaire, 133 Avenue de la Résistance, 92350 Le Plessis Robinson, France and *Rhône-Poulenc Rorer Central Research, CRVA, 13 Quai Jules Guesde, B.P.14, 94403 Vitry-sur-Seine, France

1 The effects of the potassium channel opener (KCO) aprikalim (RP 52891) on the nucleotide-induced modulation of ATP-sensitive K^+ (K_{ATP}) channels in freshly dissociated ventricular myocytes of guinea-pig heart, were studied by use of the inside-out patch-clamp technique. The internal surface of the excised membrane patch was initially bathed with a standard solution (Mg^{2+}-free with EDTA), then sequentially superfused with solutions containing nucleoside diphosphates (NDPs: 200 μM ADP and 50 μM GDP) and NDPs plus 1 mM $MgCl_2$ (with EGTA; referred to as Mg-NDP solution).

2 The normalized concentration-response (channel closing) relationship to ATP was shifted to the right when the standard solution was replaced by the Mg-NDP solution. Hence, the internal concentration of ATP ($[ATP]_i$) inhibiting the channel activity by half (K_i) increased from 56 μM to 180 μM, with an apparently constant slope factor ($s = 2.37$). NDPs in the absence of Mg^{2+} did not decrease the sensitivity of the channels to ATP.

3 In standard solution, aprikalim (100 μM) activated K_{ATP} channels in the presence of a maximally inhibitory $[ATP]_i$ (500 μM). This effect was strongly enhanced when aprikalim was applied to patches exposed to Mg-NDP solution, as demonstrated by the 9 fold increase in K_i *for* $[ATP]_i$ *(from 180* μM to 1.5 mM and $s = 2.37$).

4 The ability of aprikalim to overcome the channel closing effects of ATP in Mg-NDP solution waned rapidly. Similarly, the NDP-induced activation of ATP-blocked channels was also time-dependent. Both activation processes disappeared before the channel run-down phenomenon appeared in ATP-free conditions.

5 In conclusion, aprikalim is much more potent in opening K_{ATP} channels in membrane patches bathed in Mg-NDP solution than in standard solution. However, under the former experimental conditions, the effect of aprikalim waned rapidly. It is proposed that the waning phenomenon results from changes in the intrinsic enzymatic activity of the K_{ATP} channel protein (possibly linked to the experimental conditions) which lead to the channel closure.

Keywords: ATP-sensitive K^+ channel; aprikalim (RP 52891); patch-clamp; potassium channel opener (KCO); magnesium (Mg^{2+}); nucleoside diphosphates (NDPs); adenosine triphosphate (ATP); guinea-pig heart; ventricular myocytes

Introduction

Potassium channel openers (KCOs) constitute a class of chemically diverse compounds (Edwards & Weston, 1990) which increase cell membrane permeability to K^+ in various tissues (for review see Longman & Hamilton, 1992). The primary action of KCOs is to overcome the closure of K_{ATP} channels produced by intracellular ATP concentrations ($[ATP]_i$), although these agents may alter other K^+ currents (for review see Ashcroft & Ashcroft, 1990; Longman & Hamilton, 1992; Quast, 1993). In experiments with excised inside-out patches, micromolar concentrations of KCOs shift the $[ATP]_i$-response (closing channel) curve towards the right. Hence, in the presence of the KCO, RP 49356 (30 μM), the $[ATP]_i$ necessary to close 50% of the K_{ATP} channels increases by approximately 9 fold (from 56 to 500 μM; Thuringer & Escande, 1989). While this provides evidence that KCOs open K_{ATP} channels, it is not immediately evident how, in isolated heart preparations in which physiological $[ATP]_i$ is 5-10 mM (Elliot *et al.*, 1989), RP 49356 and other KCOs at this concentration can markedly shorten action potential duration and depress contractile activity. Several proposals have been made to account for this apparent paradox. Firstly, the activation of a very small fraction of cellular K_{ATP} channels is sufficient to shorten markedly the action potential duration (Findlay *et al.*, 1989; Carmeliet *et al.*, 1990; Faivre & Findlay, 1990; Nichols *et al.*, 1991). Secondly, catabolites of high energy phosphates, in addition to or independently of ATP, modulate channel activity in intact cells (for review see Ashcroft & Ashcroft, 1990; Deutsch *et al.*, 1991; Standen, 1992; Deutsch & Weiss, 1993; Weiss & Venkatesh, 1993); indeed, cytosolic ADP or GDP increases channel activity in the presence of Mg^{2+} (Findlay, 1988a; Lederer & Nichols, 1989; Tung & Kurachi, 1991) by shifting towards the right the concentration-response curve for closing channels induced by a change in [ATP] (Nichols & Lederer, 1990; Tung & Kurachi, 1991). Thirdly, there may be an intracellular compartmentalization of ATP. Finally, some unknown channel regulatory proteins may exist in intact cells, and these may be lost following patch excision (Noma & Shibasaki, 1985; Elliot *et al.*, 1989). The identification of any of these possible modulators might help to understand not only the paradox that KCOs can open K_{ATP} channels at physiological $[ATP]_i$, but also some discrepant observations that have been made with inside-out patches, such as that KCOs do (Escande *et al.*, 1989; Thuringer & Escande, 1989; Shen *et al.*, 1991; Tung & Kurachi, 1991) or do not (Ripoll *et al.*, 1990) activate channels following run-down. Thus, differences in channel response to KCOs might be linked to some as yet uncontrollable changes in channel modulatory mechanisms which take place after the membrane is excised from the cell.

[1] Author for correspondence.

The purpose of the present work was to analyse the activation of cardiac K_{ATP} channels by aprikalim (the eutomer of RP 49356) in order to provide new insights into the mechanisms regulating channel function. We have shown previously that in Mg^{2+}-free high-K^+ solution containing EGTA, cardiac K_{ATP} channels need to be partially closed either by ATP or by run-down before RP 49356 exerts its effect (Thuringer & Escande, 1989). Since that time, much evidence has come to light pointing to the amplification of KCO-induced channel activation by NDPs and Mg^{2+} (Shen *et al.*, 1991; Tung & Kurachi, 1991; Larsson *et al.*, 1993). The Mg^{2+}-dependent activation site proposed for NDPs (Findlay 1988a; Lederer & Nichols, 1989; Shen *et al.*, 1991; Tung & Kurachi, 1991) has been recently advanced for KCOs in skeletal muscle (Hussain *et al.*, 1994). The aim of this investigation was to assess whether the same basal mechanism might be involved in NDP- and KCO-induced activation of K_{ATP} channels in excised membrane patches from guinea-pig cardiac myocytes. To this end, we examined drug-channel interactions for aprikalim in the absence (EDTA with no $MgCl_2$) or presence of ADP, GDP and Mg^{2+} (EGTA), before and during channel run-down.

Methods

Cell isolation

Ventricular myocytes were isolated from hearts of guinea-pig weighing 200–300 g by a standard dissociation technique. Briefly, the heart was mounted on a Langendorff-type apparatus and successively perfused (at 37°C) with Ca^{2+}-free Tyrode solution (see below) and the digesting Tyrode solution containing 1 mg ml^{-1} collagenase (Type I, Sigma) plus 0.28 mg ml^{-1} protease (Type XIV, Sigma). The ventricles were then separated from the heart, cut into small pieces in standard Tyrode solution containing additional $CaCl_2$ (200 μM). Myocytes were dispersed mechanically, reseeded in Petri dishes filled with the latter solution and then kept at room temperature (22°–24°C) until their use.

Solutions and drugs

The Ca^{2+}-free Tyrode solution contained (in mM): NaCl 136, KCl 5.4, $MgCl_2$ 1.0, HEPES (*N*-2-hydroxyethylpiperazine-*N'*-2-ethane sulphonic acid) 10, NaH_2PO_4 0.33, glucose 10, adjusted to pH 7.3 with NaOH. The composition of the pipette solution was (in mM): KCl 140, $CaCl_2$ 2, $MgCl_2$ 1, HEPES 10, glucose 10, adjusted to pH 7.3 with KOH. Inside-out patches were formed in the standard solution containing (in mM): KCl 130, KOH 10, HEPES 10, EDTA (ethylenediamine tetraacetic acid) 3, glucose 10, adjusted to pH 7.3 with KOH. The Mg-NDP containing solution was prepared by adding 200 μM ADP and 50 μM GDP in the form of K^+ salts, plus 1 mM $MgCl_2$ to the standard solution in which 1 mM EGTA (ethylene glycol-*bis*-(β-aminoethyl ether)-*N,N,N', N'*-tetraacetic acid) was substituted for 3 mM EDTA (Nichols & Lederer, 1990). A flow of solution from one of a series of five pipette outlets continuously superfused the inside-out membrane patch. The flow rate of perfusion solutions was 50–100 μl min^{-1}. Thus, the solution exchange can be considered quasi-instantaneous in the patch area. In all experiments, ATP was used as Mg^{2+}-salt. A solution of 2 mM aprikalim in 1% DMSO (dimethyl sulphoxide) was prepared daily. Nucleotides and drugs were added at various concentrations to bath solutions. The pH of these solutions was always adjusted to 7.3 with KOH just before use. All chemical compounds were purchased from Sigma Chemical (St. Louis, MO, U.S.A.) except for aprikalim, which was provided by Rhône-Poulenc Rorer (Vitry-sur-Seine, France).

Patch-clamp recordings and data analysis

Patch-clamp experiments were performed at room temperature. Membrane currents were recorded in the inside-out patch-clamp configuration with a RK300 Bio-Logic amplifier (Bio-Logic, Echirolles, France). Patch pipettes were pulled from Pyrex capillaries (Corning 7740) and had resistances ranging between 5 and 8 MΩ. Current traces recorded on tapes (Bio-Logic DTR 1202 recorder) were retrieved on a Brush recorder (TA240, Gould Inc.) and filtered at 300 Hz using a five-pole Tchebicheff filter (Bio-Logic, Echirolles, France) or digitalized at a minimum sampling rate of 2 kHz using software Acquis1 (G.Sadoc, CNRS-URA 1121, Orsay, France). For each period of drug application, the current flowing through the patch was calculated with respect to the zero current level determined in the presence of an ATP concentration high enough to produce complete closure of all active K_{ATP} channels in the patch area. The mean patch current amplitude per time unit (calculated over periods of 20–30 s) is expressed as a fraction of the current measured in ATP-free standard solution in order to obtain relative current values. Data for the dose-response curve were fitted with the following general equation:

$$\text{Relative current} = 1/[1 + ([ATP]_i/K_i)^s]$$

where K_i is the $[ATP]_i$ causing half-maximal inhibition (50%) and s is the slope factor (pseudo Hill coefficient). When possible, data are given as mean ± standard deviation (s.d. vertical bar) of n different experiments.

Results

NDPs decrease the ATP sensitivity of channels

In most inside-out patch experiments, inward unitary K^+ currents flowing through K_{ATP} channels were recorded at negative potentials. These channels rapidly fluctuate between open and closed states and are characterized by an elementary conductance of 76.1 ± 2.5 pS ($n = 5$) with 140 mM K^+ on both sides of the patch membrane. In all experiments, a patch superfused with the standard solution (NDP- and Mg^{2+}-free with EDTA) was used as control. Concentrations of NDPs used are probably in the upper limits of those proposed to occur during an ischaemic stress (Lederer & Nichols, 1989; Nichols & Lederer; 1990) because we wanted to obtain maximal effects on the K_{ATP} channel activity. Indeed, the effects of NDPs are concentration-dependent (Lederer & Nichols, 1989; Tung & Kurachi, 1991).

In the first series of experiments, the concentration-dependence of the channel inhibition by internal ATP in standard solution and solutions containing NDP was investigated. The effects of two or three short ATP applications were checked rapidly after patch excision to minimize the channel run-down normally observed during single-channel current recordings (Thuringer & Escande, 1989). An example of current traces from three different patches is shown in Figure 1. Under ATP-free standard conditions, K_{ATP} channels were fully active (Figure 1a). The application of 300 μM ATP rapidly suppressed this activity almost totally and revealed an additional type of channel activity of smaller current amplitude (about −0.9 pA) with long-lasting openings identified as the inwardly-rectifying K^+ current flowing through iK1 channels. The removal of ATP routinely reactivated quickly and completely all K_{ATP} channels present in the patch. For patches bathed in the Mg-NDP solution (200 μM ADP, 50 μM GDP, 1 mM $MgCl_2$ with EGTA), 300 μM ATP also inhibited the K_{ATP} channel activity, but did so only partially (Figure 1b; $n = 3$ different experiments). Comparable results were obtained at positive potentials ($n = 10$), except that the unitary current amplitudes of both iK1 and K_{ATP} channels decreased, probably due to the fast voltage-dependent block by internal Mg^{2+} (Horie *et al.*, 1987;

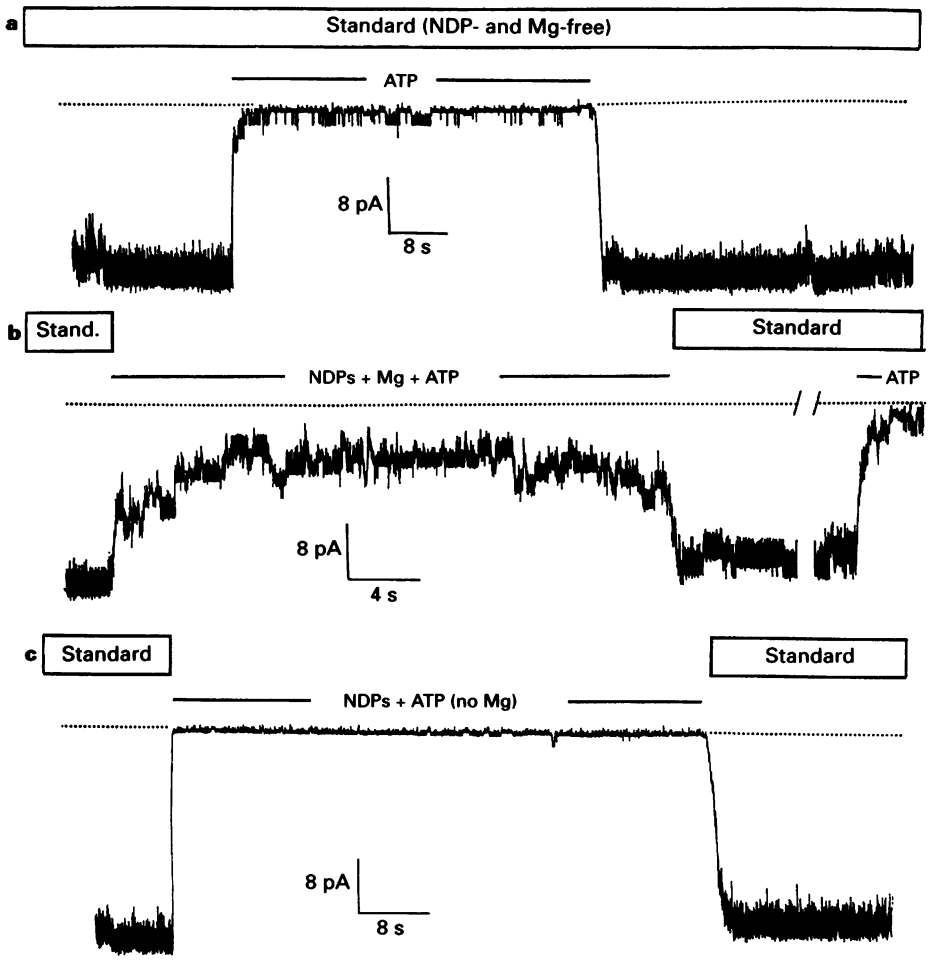

Figure 1 Effects of intracellular nucleotides and Mg^{2+} on single K_{ATP} channel currents in inside-out membrane patches. Current traces recorded from three different patches. The inhibitory effect of 300 μM ATP was tested in standard solution (Mg^{2+}-free with EDTA; a), in Mg-NDP solution (200 μM ADP, 50 μM GDP, 1 mM $MgCl_2$ with EGTA; b) and in NDP solution (200 μM ADP, 50 μM GDP, Mg^{2+}-free with EDTA; c) as indicated above each trace. The K_{ATP} channel activation appears as fast openings superimposed on slow current fluctuations resulting from iK1 channel openings, as observed in both (a) and (c) traces during ATP exposure. At least 10 simultaneous openings of K_{ATP} channels were observable on each trace in ATP-free conditions. Internal NDPs reduced markedly the blocking effect of ATP on K_{ATP} channels only in the presence of Mg^{2+} (b). In Mg-free solution, NDPs appear to be slightly inhibitory upon ATP application (c). In this and subsequent figures, the patch membrane potential (Em) was −30 mV and downward deflections represent inwardly directed unitary K^+ currents (symmetrical high K^+ conditions). Traces were filtered at 300 Hz. Dotted lines mark the current level when all channels were closed. Rectangular boxes indicate the kind of solution used and lines mark drug applications. Experiments were performed at 22°–24°C.

Matsuda, 1991). ADP and GDP activated K_{ATP} channels exclusively in the presence of internal Mg^{2+}. In the absence of this cation (EDTA with no $MgCl_2$), the effectiveness of ATP in blocking K_{ATP} channels was slightly increased by purine diphosphates, as shown in Figure 1 (c; $n = 3$ different experiments), a result that is in line with previous reports (Findlay, 1988a; Lederer & Nichols, 1989; Nichols & Lederer, 1990; Nichols *et al.*, 1991; Tung & Kurachi, 1991). The concentration-response curves for ATP closing K_{ATP} channels in standard and Mg-NDP solutions are illustrated in Figure 2. In standard solution, the equation fitting data provided a K_i of 56 μM and a slope value of 2.37 (see Methods). These results are in good agreement with previous observations of ventricular myocytes (Findlay, 1988b; Thuringer & Escande, 1989). In Mg-NDP solution, data were also well fitted by the equation which provided a K_i of 180 μM and a slope value of 2.37. Therefore, the inefficiency of 300 μM ATP in blocking all channels in the presence of ADP, GDP and Mg^{2+}, as illustrated in Figure 1 (middle trace), results from a parallel shift towards substantially higher $[ATP]_i$ of the ATP-dependence of channel activity (Figure 2).

Aprikalim counteracts the inhibitory effect of ATP

Under standard conditions, aprikalim was weakly activating in the presence of ATP (Figure 3). Aprikalim (10 μM) failed to activate significantly the K_{ATP} channel activity in the presence of 500 μM ATP. The iK1 channel activity was still present after ATP had inhibited K_{ATP} channels. A modest activation of K_{ATP} channels was observed when the concentration of aprikalim was increased to 100 μM; this activation was suppressed when the solution was replaced by one containing 10 μM aprikalim. That the level of activity induced by aprikalim was low cannot be attributed to the run-down of K_{ATP} channels, because the level of simultaneous channel openings recorded after ATP removal (Figure 3d) was similar to that recorded at the beginning of the experiment (Figure 3a). Similar results were obtained in six other experiments.

Because the extent of KCO effects in some circumstances depends on the degree of channel activity under nucleotide-free conditions (Thuringer & Escande, 1989; Fan *et al.*, 1990; Allard & Lazdunski, 1993), we also tested aprikalim in the absence of internal ATP (Figure 4). A few seconds after the

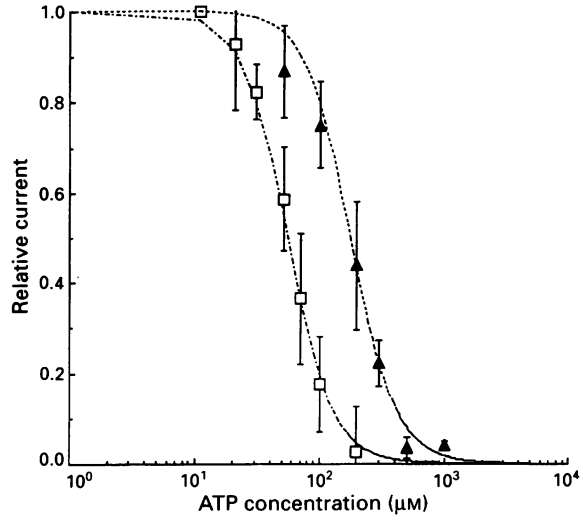

Figure 2 Concentration-response relationships for the closing of K_{ATP} channels by ATP in standard solution (Mg^{2+}- free with EDTA; □) and in Mg-NDP solution (200 μM ADP, 50 μM GDP, 1 mM $MgCl_2$ with EGTA; ▲). The relative current represents the mean patch current in the presence of ATP as a fraction of that in ATP-free solution. Values are mean ± s.d. ($n = 3$ to 5 in each case). The dashed lines are fitted by regression analysis with $K_i = 56$ μM (standard) or 180 μM (NDPs + Mg) and a slope factor $s = 2.37$.

patch was formed in standard solution, the high level of channel activity generally recorded in all patches was neither increased nor reduced by the internal application of 100 μM aprikalim (Figure 4a; $n = 5$ experiments). Moreover, after several minutes of recording, during which the channel activity decreased spontaneously, 100 μM aprikalim did not activate more K_{ATP} channels (Figure 4b; $n = 4$ experiments).

Whether aprikalim would open ATP-blocked channels in patches maintained in the Mg-NDP solution was also tested in the presence of 500 μM ATP, which reduces channel activity by ≈90% (see Figure 2). As shown in Figure 5a, only one K_{ATP} channel briefly opened during ATP superfusion. Returning to ATP-free standard conditions invariably reactivated K_{ATP} channels present in the patch area to a maximal extent (13 simultaneous openings). This high level of activity persisted when the patch was superfused with Mg-NDP solution containing 100 μM aprikalim. Under the latter conditions, exposing the patch to 500 μM ATP reduced channel activity only slightly (10–12 simultaneous openings; Figure 5b). Decreasing the concentration of aprikalim to 10 μM was accompanied by a substantial decrease in activity and channels attained a new steady-state level (1–3 levels of activity) in approximately 15 s (Figure 5c). The removal of aprikalim but not ATP resulted in a rapid and almost complete loss of K_{ATP} channel activity (only one channel opened from time to time). The maximal sustained activity of K_{ATP} channels could be restored by removing ATP and adding 100 μM aprikalim, indicating that no run-down occurred dur-

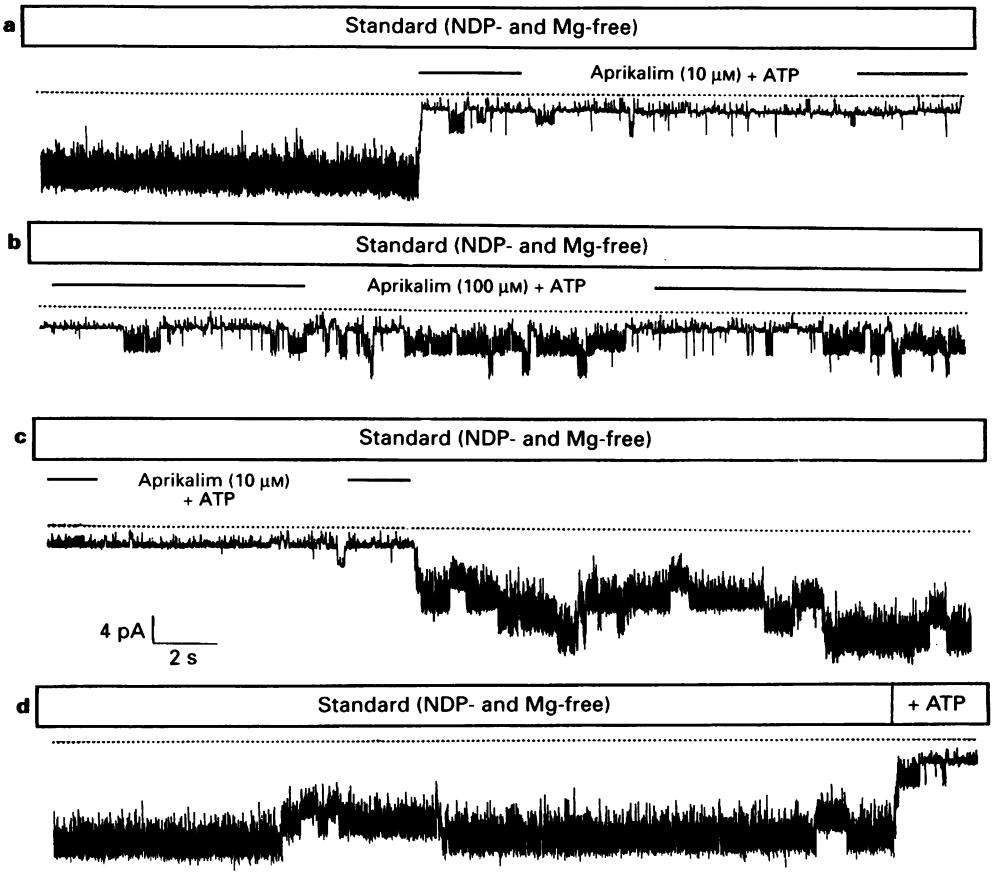

Figure 3 Effect of aprikalim on K_{ATP} channels in NDP- and Mg^{2+}-free conditions. Continuous current traces recorded from one inside-out patch containing at least four K_{ATP} channels. Patch was perfused with standard solution (NDP- and Mg^{2+}-free, EDTA) initially, then both ATP (500 μM) and aprikalim (10 μM then 100 μM) were added, before returning to standard solution. Aprikalim (10 μM) did not induce K_{ATP} channel activity in presence of ATP. Increasing the dose of aprikalim (100 μM) caused a slight and reversible activation of ATP-blocked channels. Comparison of channel activity in drug-free standard solution at the beginning (a) and at the end (d) of current recording indicates the absence of channel run-down.

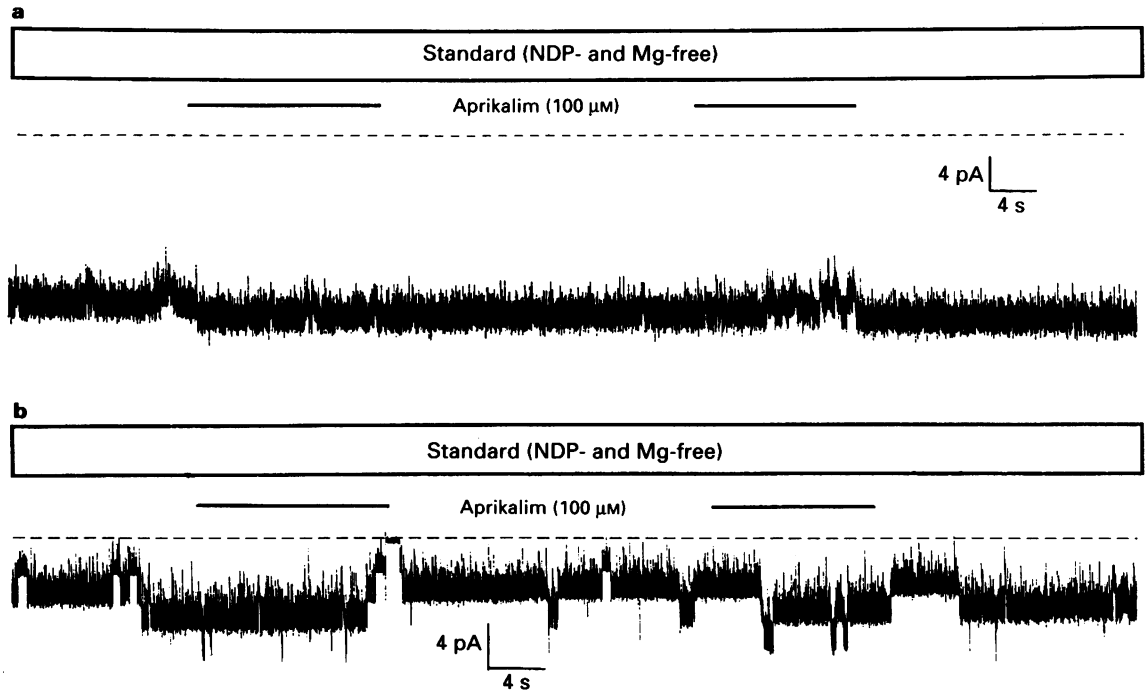

Figure 4 Effect of aprikalim on K_{ATP} channels in nucleotide-free standard conditions. Current traces recorded from two separate inside-out patches continuously superfused with the standard solution (NDP- and Mg^{2+}-free, EDTA). The effect of 100 μM aprikalim added to the standard solution was tested in a patch with high activity (a; few seconds after its excision) and in a patch with low activity (b; after 5 min of recording). In ATP-free conditions, aprikalim did not affect the K_{ATP} channel activity.

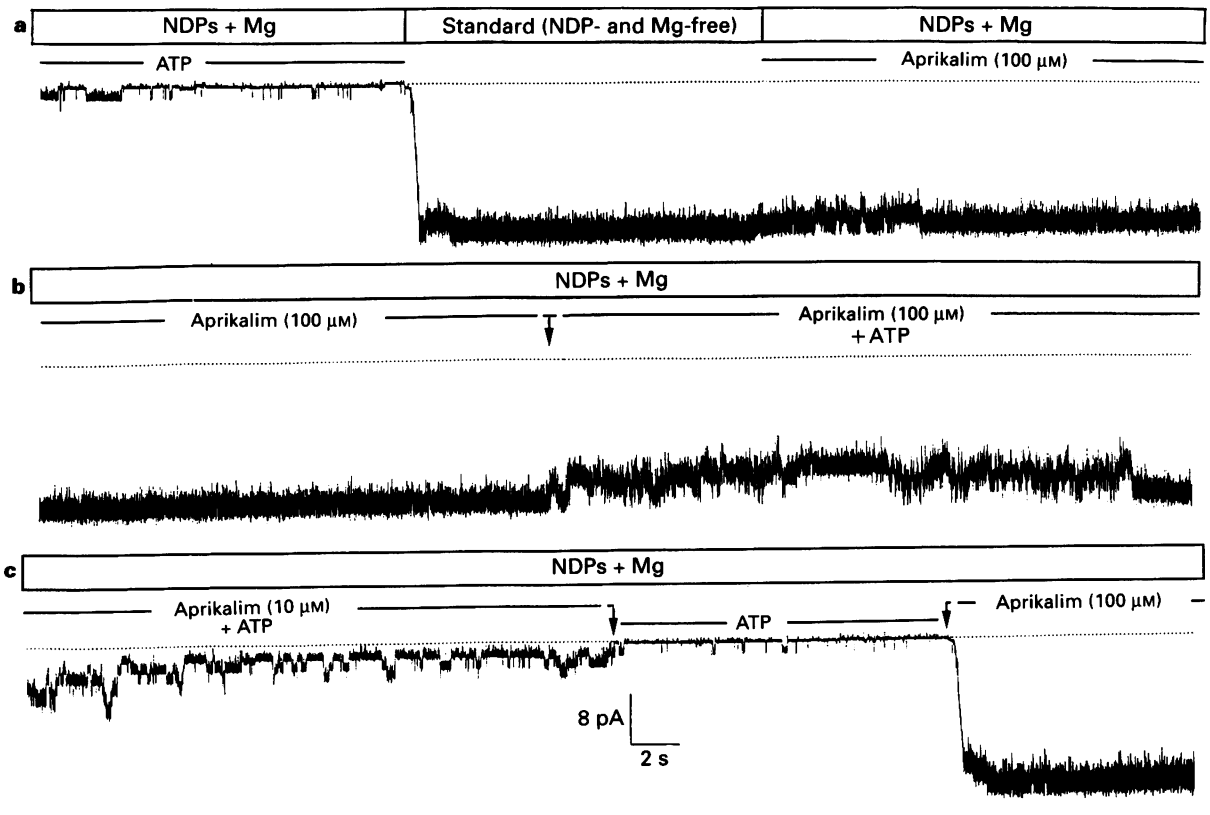

Figure 5 Effect of aprikalim on K_{ATP} channels in the presence of NDPs and Mg^{2+}. Current traces recorded from one inside-out patch. Patch was excised in standard solution (NDP- and Mg^{2+}-free; not shown), then superfused with Mg-NDP solution containing 500 μM ATP, before returning to standard solution. Aprikalim (100 μM then 10 μM) was added to the Mg-NDP solution (200 μM ADP, 50 μM GDP, 1 mM $MgCl_2$ with EGTA) with or without 500 μM ATP. Change of successive drug applications is marked by arrow. At least fifteen simultaneous openings of K_{ATP} channels can be detected in the standard solution as in the Mg-NDP solution containing aprikalim.

ing the course of this experimental procedure. Similar results were obtained with four additional inside-out membrane patches from different myocytes. Therefore, aprikalim activated K_{ATP} channels despite the continued presence of almost maximally inhibitory $[ATP]_i$.

In subsequent experiments, the effects of 100 μM aprikalim on K_{ATP} channels were more extensively studied by determining a concentration-response curve to $[ATP]_i$. The results obtained from 3 to 7 experiments for each $[ATP]_i$ are shown in Figure 6. The aprikalim-induced activation of K_{ATP} channels occurred at millimolar $[ATP]_i$. Fitting of experimental data obtained by superfusing the patch with Mg-NDP solution containing 100 μM aprikalim yield a K_i for $[ATP]_i$ of 1.5 mM with a slope value of 2.37 (unbroken line; Figure 6).

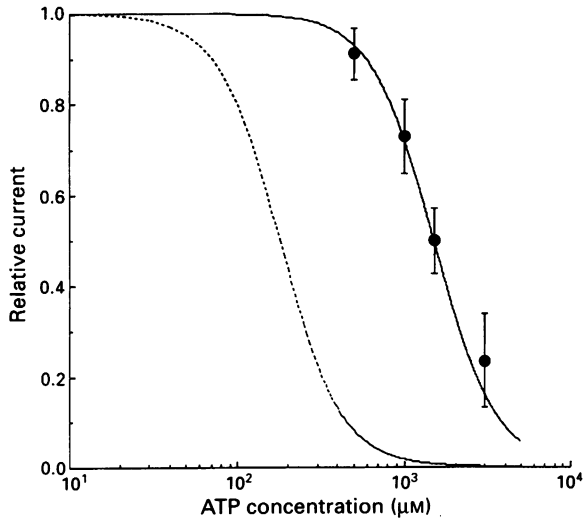

Figure 6 Concentration-response relationships for the closing of K_{ATP} channels by ATP in Mg-NDP solution in the absence (dotted curve redrawn from Figure 2) and the presence of 100 μM aprikalim (● and continuous curve). The relative current represents the mean patch current in test [ATP] as a fraction of that in ATP-free conditions. Values are mean ± s.d. ($n = 3$ to 7 in each case). The continuous line is fitted by regression analysis ($K_i = 1.5$ mM and $s = 2.37$).

Activating action of aprikalim depends on time after patch excision

In preliminary experiments, we observed that the activating effect of aprikalim, which was strong during the first few minutes that the patches were bathed in Mg-NDP solution, tended to vanish rapidly with time. Specific experiments ($n = 10$) were then carried out to determine whether this decay differed from the run-down process. Just after inside-out patch formation, the channel activity in standard solution was briefly recorded, then the standard solution was replaced by the Mg-NDP solution in which 100 μM aprikalim were added alone or with ATP (at one or several concentrations). This protocol was repeated several times and the channel run-down estimated by returning the patches to standard solution after each drug application. To quantify these effects more precisely, we calculated the current through the patch as the ratio of the mean current amplitude to a time unit (averaged over 20–30 s after reaching a steady level). This ratio was determined both for patches in test solutions and for patches in the standard solution at the onset of the current recording. A typical experiment is illustrated in Figure 7, where 100 μM aprikalim was applied in the absence of ATP and then in the presence of 1 mM ATP. Excision of the patch in the standard medium maximally activated K_{ATP} channels present in the patch area (9–10 levels of activity, patch current taken as unity; Figure 7a). The internal app-

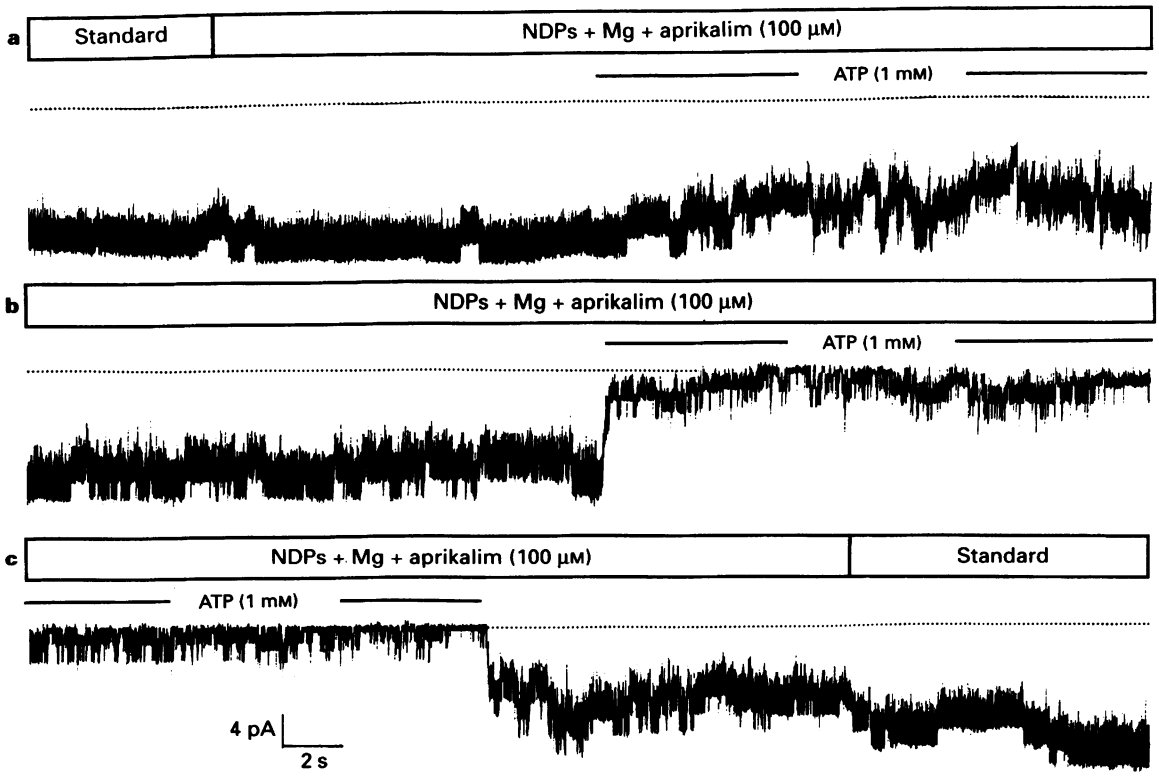

Figure 7 Time-dependent decline of aprikalim-induced channel activity. Current traces recorded from one inside-out patch. Trace (a) started 20 s after patch excision in standard solution (NDP- and Mg^{2+}-free) whereas trace (b) was obtained 4 min later. Traces (b) and (c) represent a continuous recording. ATP (1 mM) was added to Mg-NDP solution (200 μM ADP, 50 μM GDP, 1 mM $MgCl_2$) containing aprikalim (100 μM), as indicated above each trace. Comparison of channel activity in standard solution at the beginning (a) and at the end (c) of the current recording indicates the absence of channel run-down.

lication of 100 μM aprikalim (in Mg-NDP solution) did not affect this sustained channel activity; further addition of 1 mM ATP inhibited it partially and reversibly (3–10 simultaneous channel openings; relative current = 0.724). However, after ATP was removed, the number of active channels progressively decreased despite the presence of aprikalim (4–8 levels of activity about 4 min following the patch excision; relative current = 0.797; Figure 7b), and a second addition of 1 mM ATP further reduced the channel activity to 0–4 levels (relative current = 0.145). This gradual loss of aprikalim-induced activation might be attributed to a concurrently arising run-down phenomenon which routinely occurs in isolated patches with kinetics depending on the patch tested. However, this was clearly not the case, since, when patches were returned to standard solution, the channel activity attained a new steady-state level of 9 simultaneous openings (relative current = 0.908), as shown in Figure 7c. Although the kinetics of this time-dependent process varied greatly from patch to patch, a comparable lack of effect of aprikalim on ATP-blocked channels was observed after a few minutes in all the patches ($n = 9$), even in the presence of micromolar [ATP]. A more complete example of such a

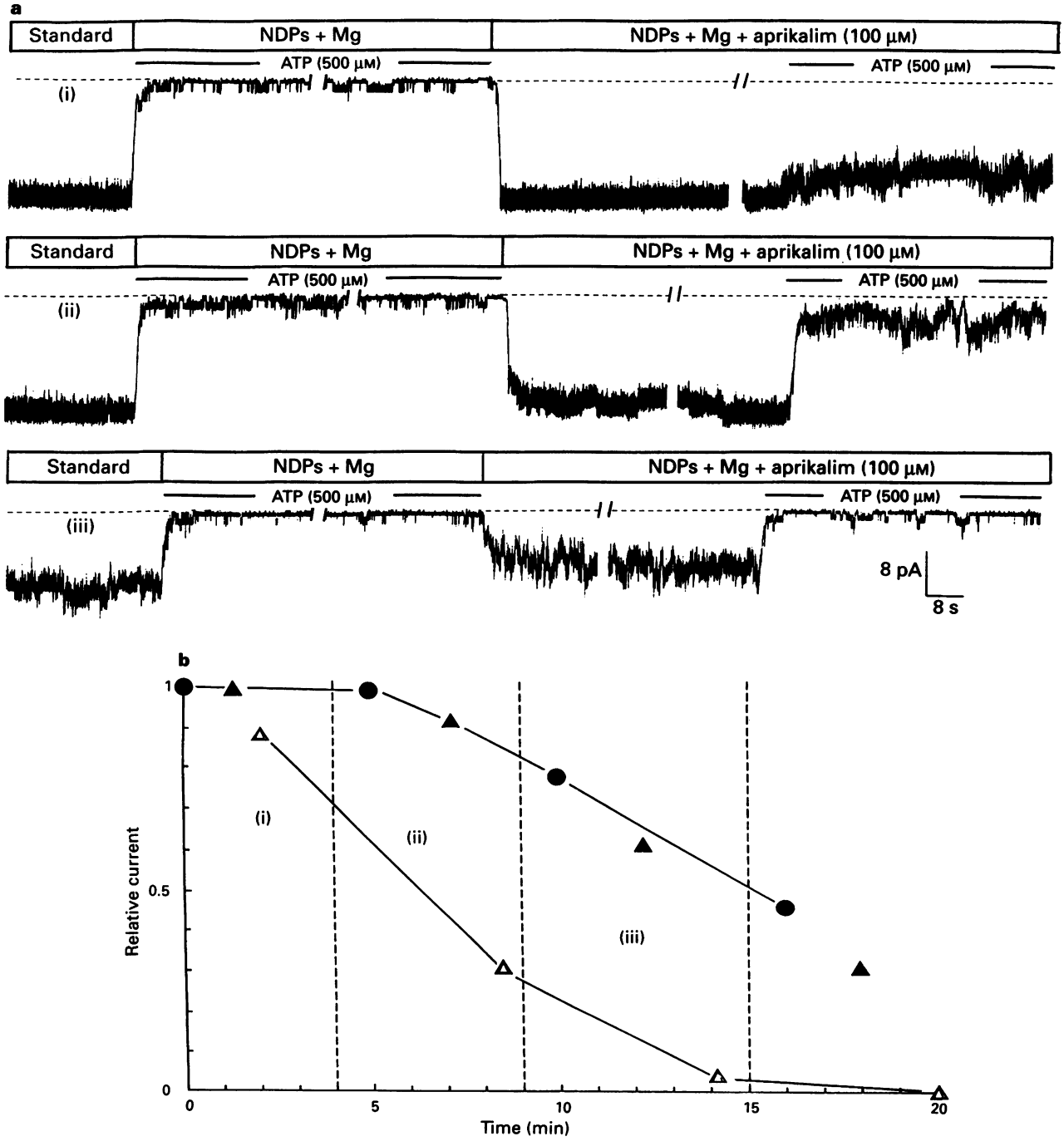

Figure 8 Comparative evolution with time after patch excision of aprikalim-induced channel activity and channel run-down. (a) Current traces recorded from one inside-out patch: 30 s after patch excision (i), 5 min later (ii), and 10 min later (iii). Just after patch excision, the K_{ATP} channel activity was recorded in standard solution, then in Mg-NDP solution in which aprikalim (100 μM) and/or ATP (500 μM) were added, as indicated. After each series of drug applications, the channel run-down was estimated by returning to standard solution. (b) Time course of the relative current measured during repetitive applications of 100 μM aprikalim (▲) and 100 μM aprikalim plus 500 μM ATP (△) in Mg-NDP conditions, and during exposure to standard solution (●). Relative current is the mean patch current measured in the different conditions expressed as a fraction of that measured in standard solution immediately after patch excision. Data in (i), (ii) and (iii) are obtained from the corresponding traces in (a).

gradual decrease in the effectiveness of aprikalim, different from the run-down process, is shown in Figure 8: diminishing responses to successive applications of 100 μM aprikalim were observed in the presence of 500 μM ATP. The maximal level of channel activity normally recorded for patches in the standard solution (11 simultaneous openings) during the first minutes after inside-out patch formation (upper trace) was the same as that observed for patches in Mg-NDP solution containing aprikalim. Applying ATP alone to patches in Mg-NDP solution drastically inhibited K_{ATP} channel activity (1 level of activity), whereas applying ATP in the presence of aprikalim only slightly inhibited it (8–9 levels of activity), as already described (see Figures 4 to 6). Five minutes after patch excision (Figure 8a(ii)), all K_{ATP} channels were maximally activated upon returning the patches to standard solution (11 levels of activity), and the subsequent application of ATP in Mg-NDP solution still strongly reduced channel activity (1 level of activity). The second application of aprikalim did not reactivate all K_{ATP} channels (8–10 simultaneous channel openings) and the concomitant addition of ATP even more drastically reduced channel activity (1–4 levels of activity). Ten minutes after patch excision (Figure 8a(iii)), a modest run-down of K_{ATP} channel activity was noted when patches were returned to standard solution (5–8 levels of activity). A stronger inhibition of this activity was induced by ATP alone in Mg-NDP solution, probably as a consequence of the spontaneous loss of active channels (one opening). The subsequent application of aprikalim partially activated the channels (3–6 levels of activity), an activation which was almost entirely suppressed by ATP (1–2 brief openings). Quantitative analysis of the data (Figure 8b) indicated that, despite the presence of aprikalim, the patch current fell rapidly upon successive ATP applications during the first 10 min of recording (by 11.5% at the first application and by 69% at the second) whereas its value was reduced in the absence of ATP only slightly and only at the second application by 8%. Thereafter, the channel activity recorded in standard solution waned (run-down; reduction of 22% at the third application) at a rate somewhat slower than that found for patches in Mg-NDP solution containing aprikalim (reduction of 38.5% at the third application). Aprikalim lost its ability to overcome ATP inhibition much faster, since ATP almost completely inhibited the patch current within 14 min (reduction of 96% at the third application), whereas reductions of 54% and 69% were subsequently observed for patches bathed in standard solution and in Mg-NDP solution containing aprikalim, respectively. Therefore the progressively developing ineffectiveness of aprikalim in counteracting the inhibitory effect of ATP was faster than, and different from, the spontaneous loss of channel activity due to run-down.

Activating action of Mg-NDPs wanes rapidly

The time-dependence of K_{ATP} channel activation induced by NDPs was also tested on inside-out patches ($n = 7$) successively superfused with standard solution then with Mg-NDP solution containing ATP at various concentrations. Before studying low [ATP], the patch was exposed to 1 mM ATP for at least 20–30 s to delay channel run-down. As observed in Figure 9a, 1 mM ATP inhibited strongly K_{ATP} channel activity when applied together with Mg^{2+} and NDPs. This basal activity was enhanced by decreasing the [ATP] to 200 μM, as already illustrated in Figure 2. Following a 5 min period of recording, during which a loss of four levels of channel activity was observed in the standard solution (Figure 9b), an inhibition of channel openings, much stronger than that shown in the upper trace, was produced by 200 μM ATP. Some rare single-channel openings could still be detected in the presence of 1 mM ATP. The run-down of channel activity took place 3 min later under standard conditions. The time-course of the NDP-induced modulation of K_{ATP} channel activity recorded from another inside-out patch is illustrated in Figure 10. After patch formation in standard solution, the membrane was exposed to 1 mM, 200 μM, 100 μM then 50 μM ATP in Mg-NDP conditions, before being re-exposed to the standard solution. It can be seen that (i) some channel activity persisted throughout the

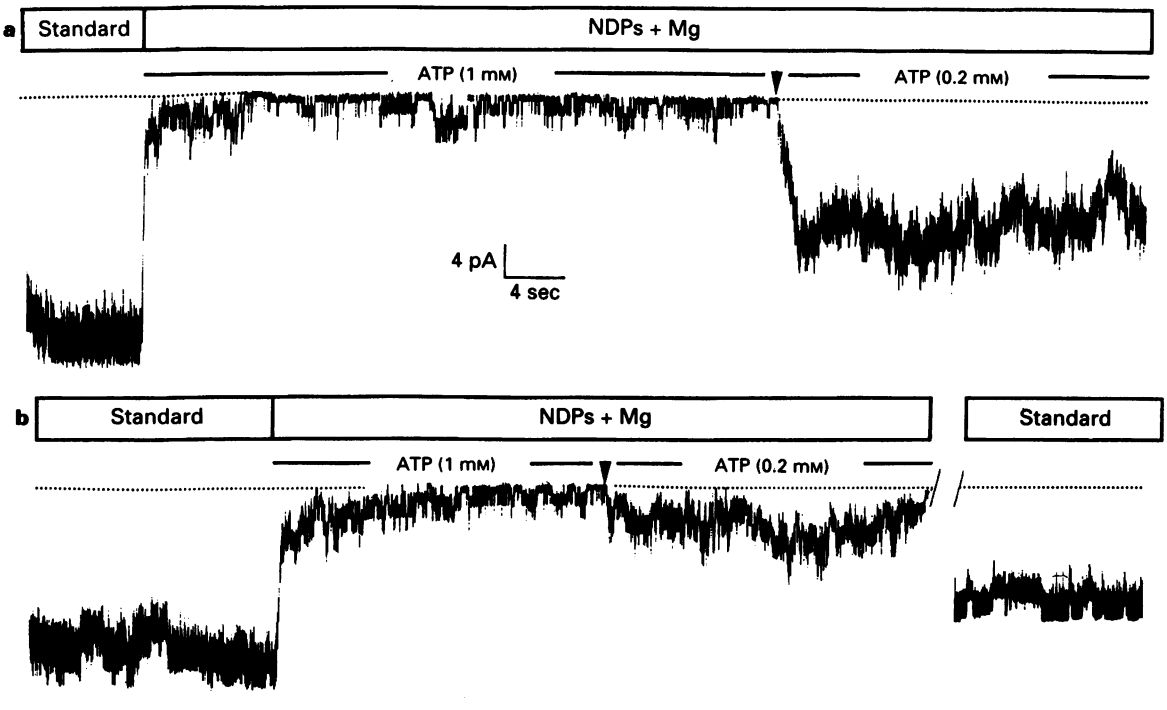

Figure 9 Time-dependent decline of NDP-induced channel activity. Current traces recorded from one inside-out patch at different times after patch excision: 10 s (a), 5 min (b) and 8 min (right part of b). Just after patch excision, the K_{ATP} channel activity was recorded in standard solution initially, then in Mg-NDP solution containing ATP at two different concentrations (1 mM then 200 μM) as indicated. Change of [ATP] is marked by arrow. After each series of ATP applications, the channel run-down was estimated by returning to standard solution.

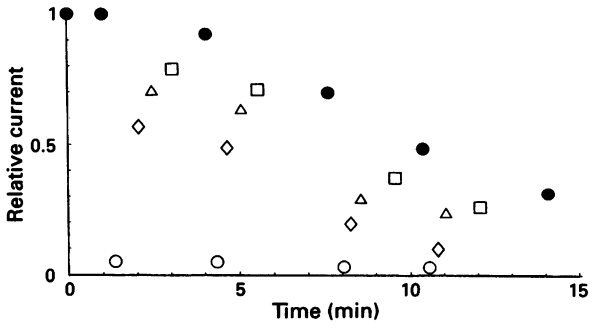

Figure 10 Comparative evolution with time after patch excision of NDP-induced channel activity and channel run-down. Data were obtained from one inside-out patch repeatedly exposed to various [ATP]: 1 mM (○), 200 μM (◇), 100 μM (△) and 50 μM (□) in Mg-NDP solution, and then patch was re-exposed to standard solution (●) in order to estimate channel run-down. Ordinate scale shows patch current relative to the current recorded in standard solution immediately after patch excision.

experimental procedure when 1 mM ATP was applied to the patch under Mg-NDP conditions, (ii) the inhibitory effect of moderate ATP concentrations increased markedly as a function of time, and (iii) the channel activity recorded in the standard solution was consistently lower than that recorded prior to inhibition by a series of successive ATP applications. For instance, the patch current declined from 1 to 0.482 (i.e., 51.8%) 10 min after patch excision. Repeated applications of micromolar [ATP] also caused progressively smaller responses, i.e. from 0.567 to 0.1 in 200 μM ATP (82.4%), from 0.699 to 0.234 in 100 μM ATP (66.5%) and from 0.786 to 0.257 in 50 μM ATP (67.3%) after a comparable period of time. Although the kinetics of this time-dependent process varied from patch to patch, a comparable lack of effect of NDPs on ATP-blocked channels was observed in the six other experiments. Thus, the NDP-induced activation of ATP-blocked channels waned faster than the channel run-down appeared.

Discussion

Our study provides two major pieces of information about the electrophysiological profile of aprikalim (RP 52891, the eutomer of RP 49356), as observed with inside-out membrane patches from guinea-pig ventricular myocytes. First, aprikalim is much more potent in opening ATP-blocked K_{ATP} channels in the presence than in the absence of internal Mg-NDPs. Second, this channel activation induced by aprikalim wanes more rapidly than can be accounted for by channel run-down.

Many features of the interaction between aprikalim and K_{ATP} channels reported here are common to other KCOs (for review, see Ashcroft & Ashcroft, 1990): (i) the internal application of aprikalim reduced, in a concentration-dependent manner, the ATP sensitivity of cardiac K_{ATP} channels; (ii) the aprikalim-induced activation of K_{ATP} channels occurred even in the absence of internal Mg^{2+}; and (iii) this effect was markedly enhanced by NDPs in the presence of Mg^{2+}. The ability of aprikalim and some other KCOs (Shen *et al.*, 1991; Tung & Kurachi, 1991; Allard & Lazdunski, 1993; Larsson *et al.*, 1993) to facilitate the opening of K_{ATP} channels and to hasten strongly their recruitment once this has been initiated by an endogenous event (i.e. increases in $[ADP]_i$ from 10 to 200 μM; Allen *et al.*, 1985) may be of a particular relevance for the therapeutic potential of this class of compounds protecting the heart against an ischaemic/perfusion injury (Richer *et al.*, 1990; Auchampach *et al.*, 1991; Anderson, 1992; Escande & Cavero, 1992; Gross & Auchampach, 1992; Lynch *et al.*, 1992; Opie, 1993). Through the additional stimulating effects of H^+ (Fan & Makielski, 1993), lactate (Han *et al* 1994) and adenosine (Li *et al.*, 1993), KCOs might even further accelerate the opening of K_{ATP} channels when $[ATP]_i$ is higher than that generally required for such an opening to occur in the absence of a KCO. The beneficial consequence which may be expected from this effect of KCOs is to prolong cell viability during oxygen deprivation, since the cardiac myocyte can rapidly adopt a strategy of defence against ischaemia/reperfusion damage before the drastic fall of its $[ATP]_i$ (Auchampach *et al.*, 1991).

The mechanism of action of aprikalim seems to be somewhat different from that of the racemic compound, RP 49356 (Thuringer & Escande, 1989; Weik & Neumcke, 1990), since aprikalim required the presence of internal ATP for its effects and only weakly activated K_{ATP} channels in patches bathed in Mg^{2+}-free solution. Similar differences have also been reported for other KCOs (Escande *et al.*, 1989; Kozlowski *et al.*, 1989; Fan *et al.*, 1990; Takano & Noma, 1990; Shen *et al.*, 1991; Tung & Kurachi, 1991; Larsson *et al.*, 1993; Hussain *et al.*, 1994). The exact reason for these observations remains unclear. However, it is difficult to be sure that, for aprikalim and RP 49356, such discrepancies are entirely independent of the experimental conditions, since we did not study these two compounds at the same time. In the present experiments, the continuous and direct superfusion of the patch with Mg^{2+}-free standard solution containing EDTA very likely washed out any Mg^{2+} bound to the internal surface of the excised membrane. Levcromakalim (formerly called lemakalim; the eutomer of cromakalim) has been recently proposed to have a Mg^{2+}-dependent mechanism of K_{ATP} channel activation in skeletal muscle (Hussain *et al.*, 1994); intracellular Mg^{2+}, therefore, may also be required for channel activation by KCOs in the heart. However, the possibility that aprikalim-induced channel activation is mediated through a Mg^{2+}-dependent binding site can be discarded in view of the observation that a high concentration of aprikalim still activated ATP-blocked channels in Mg^{2+}-free conditions, as also reported for pinacidil in cardiac myocytes (Fan *et al.*, 1990). A simple interpretation of these results would be that the inhibitory nucleotide binding site and the site for KCOs allosterically interact, as proposed for pinacidil in skeletal muscle cells (Allard & Lazdunski, 1993). Such an interaction could also account for the strongly facilitating effect of NDPs on aprikalim action in the presence of Mg^{2+}.

One interesting observation we made is that aprikalim or NDPs in Mg^{2+}-containing solutions can lose their effects against the inhibitory action of ATP faster than K_{ATP} channels run down. Previous reports have shown that in cardiac myocytes KCOs alone (Escande *et al.*, 1989; Thuringer & Escande, 1989; Takano & Noma, 1990; Ashford *et al.*, 1994) or co-applied with Mg-NDPs (Shen *et al.*, 1991; Tung & Kurachi, 1991) can temporarily restore channel activity after complete run-down. However, the experimental conditions used in these studies differ substantially from ours, since we analysed the progressive inability of aprikalim to counteract the inhibitory action of internal ATP over time. In agreement with out results, Ripoll *et al.* (1990) have observed that cromakalim in NDP-free solution no longer counteracts the inhibitory action of ATP after the run-down process has taken place. In addition, diminishing responses to repeated applications of levcromakalim in nucleotide-free solutions have also been reported to occur in skeletal muscle cells (Hussain *et al.*, 1994). Therefore, the time-dependent fading of the aprikalim-induced activation of K_{ATP} channels is probably not linked to the presence of NDPs. Like aprikalim, Mg-NDPs failed to activate partially run-down K_{ATP} channels in the presence of micromolar $[ATP]_i$. Such an increase in channel sensitivity to micromolar $[ATP]_i$ as channel activity runs down is in line with previous observations (Thuringer & Escande, 1989; Nichols & Lederer, 1991; Deutsch & Weiss, 1993). That the channel activity after the removal of Mg-NDPs and ATP was consistently lower than

the control activity prior to inhibition by ATP suggests that no phosphorylation occurred under our experimental conditions. In apparent contrast with our results, Ashford *et al.* (1994) have recently shown that, like native cardiac K_{ATP} channels (Shen *et al.*, 1991; Tung & Kurachi, 1991), the cloned cardiac channel (rcK_{ATP}-1) undergoing run-down can be reactivated by NDPs, exclusively at very high concentrations (10 mM) in the presence of 2 mM Mg^{2+} and that this effect is drastically increased when micromolar $[ATP]_i$ is co-applied with Mg-NDP. However, it is possible that the high $[NDPs]_i$ used by these authors triggered an additional mechanism of channel opening. Indeed, the channel reactivation following run-down requires energy necessarily derived from high energy phosphates (Furukawa *et al.*, 1994). It may be speculated that millimolar $[NDPs]_i$ can also supply this energy to restore the channel protein to its active conformational state.

We have difficulties in offering a satisfactory interpretation for the time-dependent fading of K_{ATP} channel activation by aprikalim or NDPs for which the same basal mechanism (different from the run-down due to channel dephosphorylation; Findlay, 1988b; Furukawa *et al.*, 1994) may be responsible. Our data exclude the possibility that channel phosphorylation may be part of the mechanism underlying the action of aprikalim or NDPs in the presence of internal Mg^{2+}. This, however, does not mean that the degree of channel phosphorylation and the potency of aprikalim or NDPs in activating channels are fully independent and cannot exert reciprocal influences. Interestingly, Shen *et al.* (1991) have reported that other KCOs (except nicorandil) can activate cardiac K_{ATP} channels only if the channels are not completely dephosphorylated. Our data, which are quite similar to theirs, perhaps could be explained on the basis of variable degrees of channel phosphorylation resulting from our experimental conditions. It may be speculated that, in our experimental conditions, K_{ATP} channels would become dephosphorylated over short periods of time (5–10 min) because the continuous superfusion of the patch with Mg-free standard solution (EDTA) would wash out any superficial membranous ATP, Mg^{2+} or other regulatory molecules, such as kinases, associated with the channel protein (Larsson *et al.*, 1993; Hussain *et al.*, 1994). Whether any activating substances are actually lost during patch excision is still unknown. It is tempting to suggest that one of the G proteins proposed to prevent the ATP-dependent closure of K_{ATP} channels (Terzic *et al.*, 1994) might be involved in transducing the signal generated by the KCO or NDP binding to the channel protein. Presumably, this G protein could be washed out from the excised patch during the experimental procedure. Further studies are necessary to elucidate such possible regulatory mechanisms which are hinted at by our inside-out patch experiments.

In summary, we have shown that aprikalim is much more potent in opening ATP-blocked K_{ATP} channels in the presence than in the absence of internal Mg-NDPs, although its action wanes rapidly in excised membrane patches. This fading, like channel run-down, appears to be linked to the excised patch itself as well as to the experimental conditions. Therefore, the failure of aprikalim to produce in our experiments a sustained K_{ATP} channel activity cannot be considered an intrinsic property of the compound since it is not observed with intact tissues (Richer *et al.*, 1990; Auchampach *et al.*, 1991; Escande & Cavero, 1992). In conclusion, our results favour the hypothesis that cardiac myocytes suffering a transient ischaemic stress and treated with aprikalim (or more generally with KCO) are likely to adopt much sooner a strategy of protection and resume their contractile function more easily, upon timely reperfusion, than untreated cells (Cavero & Premmereur, 1994).

The authors would like to acknowledge the assistance of P. Richer in cell preparations. We are grateful to I. Findlay, A. Coulombe and J-J. Mercadier for helpful comments, to E. Deroubaix and D. Escande for kindly lending the set-up and Brush recorder, and to K. Pepper for her help in restyling the English. This work was supported by a grant from CRVA Rhône-Poulenc Rorer Central Research, 13 Quai Jules Guesde, 94403 Vitry-sur-Seine, France.

References

ALLARD, B. & LAZDUNSKI, M. (1993). Pharmacological properties of ATP-sensitive K^+ channels in mammalian skeletal muscle cells. *Eur. J. Pharmacol.*, **236**, 419–426.

ALLEN, D.G., MORRIS, P.G., ORCHARD, C.H. & PIROLO, J.S. (1985). A nuclear magnetic resonance study of metabolism in the ferret heart during hypoxia and inhibition of glycolysis. *J. Physiol.*, **361**, 185–204.

ANDERSSON, K.E. (1992). Clinical pharmacology of potassium channel openers. *Pharmacol & Toxicol.*, **70**, 244–254.

ASHCROFT, S.J.H. & ASHCROFT, F.M. (1990). Properties and functions of ATP-sensitive K^+ channels. *Cellular Signalling*, **2**, 197–214.

ASHFORD, M.L.J., BOND, C.T., BLAIR, T.A. & ADELMAN, J.P. (1994). Cloning and functional expression of a rat heart KATP channel. *Nature*, **370**, 456–459.

AUCHAMPACH, J.A., MARUYAMA, M., CAVERO, I. & GROSS, G.J. (1991). The new K^+ channel opener aprikalim (RP 52891) reduces experimental infarct size in dogs in the absence of systemic hemodynamic changes. *J. Pharmacol. Exp. Ther.*, **259**, 961–967.

CARMELIET, E., STORMS, L. & VEREECKE, J. (1990). The ATP-dependent K^+ channel and metabolic inhibition. In *Cardiac Electrophysiology. From Cell to Bedside.* ed. Zipes, D.P. & J. Jalife. pp. 103–108. Philadelphia: WB Saunders.

CAVERO, I. & PREMMEREUR, J. (1994). ATP sensitive potassium channel openers are of potential benefit in ischaemic heart disease. *Cardiovasc. Res.*, **28**, 32–33.

DUETSCH, N., KLITZNER, T.S., LAMP, S.T. & WEISS, J. N. (1991). Activation of cardiac ATP-sensitive K^+ current during hypoxia: correlation with tissue ATP levels. *Am. J. Physiol.*, **261**, H671–H676.

DUETSCH, N. & WEISS, J.N. (1993). ATP-sensitive K^+ channel modification by metabolic inhibition in isolated guinea-pig ventricular myocytes. *J. Physiol.*, **465**, 163–179.

EDWARDS, G. & WESTON, A.H. (1990). Structure-activity relationships of K^+ channel openers. *Trends Pharmacol. Sci.*, **11**, 417–422.

ELLIOT, A.C., SMITH, G.L. & ALLEN, D.G. (1989). Simultaneous measurements of action potential duration and intracellular ATP in isolated ferret hearts exposed to cyanide. *Circ. Res.*, **64**, 583–591.

ESCANDE, D. & CAVERO, I. (1992). K^+ channel openers and 'natural' cardioprotection. *Trends Pharmacol. Sci.*, **13**, 269–272.

ESCANDE, D., THURINGER, D., LE GUERN, S., COURTEIX, J., LAVILLE, M. & CAVERO, I. (1989). Potassium channel openers act through an activation of ATP-sensitive K^+ channels in guinea-pig cardiac myocytes. *Pflügers Arch.*, **414**, 669–675.

FAIVRE, J-F. & FINDLAY, I. (1990). Action potential duration and activation of ATP-sensitive potassium channel in isolated guinea-pig ventricular myocytes. *Biochem. Biophys. Acta*, **1029**, 167–172.

FAN, Z. & MAKIELSKI, M.C. (1993). Intracellular H^+ and Ca^{2+} modulation of trypsin-modified ATP-sensitive K^+ channels in rabbit ventricular myocytes. *Circ. Res.*, **72**, 715–722.

FAN, Z., NAKAYAMA, K. & HIRAOKA, M. (1990). Multiple actions of pinacidil on adenosine trisphosphate-sensitive potassium channels in guinea-pig ventricular myocytes. *J. Physiol.*, **430**, 273–282.

FINDLAY, I. (1988a). Effects of ADP upon the ATP-sensitive K^+ channel in rat ventricular myocytes. *J. Memb. Biol.*, **101**, 83–92.

FINDLAY, I. (1988b). ATP^{4+} and ATP-Mg inhibit the ATP-sensitive K^+ channel of rat ventricular myocytes. *Pflügers Arch.*, **412**, 37–41.

FINDLAY, I., DEROUBAIX, E., GUIRAUDOU, P. & CORABOEUF, E. (1989). Effects of activation of ATP-sensitive K^+ channels in mammalian ventricular myocytes. *Am. J. Physiol.*, **257**, H1551–H1559.

FURUKAWA, T., VIRAG, L., FURUKAWA, N., SAWANOBORI, T. & HIRAOKA, M. (1994). Mechanism for reactivation of the adenosine 5'-triphosphate-sensitive K^+ channel by MgATP complexes in guinea-pig ventricular myocytes. *J. Physiol.*, **479**, 95–107.

GROSS, G.J. & AUCHAMPACH, J.A. (1992). Role of ATP dependent potassium channels in myocardial ischaemia. *Cardiovasc. Res.*, **26**, 1011–1016.

HAN, J., SO, I., KIM, E.-Y. & EARM, Y.E. (1994). ATP-sensitive potassium channels are modulated by intracellular lactate in rabbit ventricular myoctyes. *Pflügers. Arch*, **425**, 546–548.

HORIE, M., IRISAWA, H. & NOMA, A. (1987). Voltage-dependent block of adenosine-triphosphate-sensitive potassium channel in guinea-pig ventricular cells. *J. Physiol.*, **387**, 251–272.

HUSSAIN, M., WAREHAM, A.C. & HEAD, S.I. (1994). Mechanism of action of a K^+ channel activator BRL 38227 on ATP-sensitive K^+ channels in mouse skeletal muscle fibres. *J. Physiol.*, **478**, 523–532.

KOZLOWSKI, R.Z., HALES, C.N. & ASHFORD, M.L. (1989). Dual effect of diazoxide on ATP K currents recorded from an insulin-secreting cell line. *Br. J. Pharmacol.*, **97**, 1039–1050.

LARSSON, O., AMMALA, C., BOKVIST, K., FREDHOLM, B. & RORSMAN, P. (1993). Stimulation of the KATP channel by ADP and diazoxide requires nucleotide hydrolysis in mouse pancreatic β-cells. *J. Physiol.*, **463**, 349–365.

LEDERER, W.J. & NICHOLS, C.G. (1989). Nucleotide modulation of the activity of rat heart ATP-sensitive K^+ channels in isolated membrane patches. *J. Physiol.*, **419**, 193–211.

LI, G.R., FENG, J. SHRIER, A. & NATTEL, S. (1993). Does adenosine produce its electrophysiologic effects via IK-ATP? *Circulation*, **88**, I–232.

LONGMAN, S.D. & HAMILTON, T.C. (1992). Potassium channel activator drugs: mechanism of action, pharmacological properties, and therapeutic potential. *Med. Res. Rev.*, **12**, 73–148.

LYNCH, J.J., SANGUINETTI, M.C., KIMURA, S. & BASSETT, L.A. (1992). Therapeutic potential of modulating potassium currents in the diseased myocardium. *FASEB J.*, **6**, 2952–2960.

MATSUDA, H. (1991). Effects of external and internal K^+ ions on magnesium block of inwardly rectifying K^+ channels in guinea-pig heart cells. *J. Physiol.*, **435**, 83–99.

NICHOLS, C.G. & LEDERER, W.J. (1990). The regulation of ATP-sensitive K^+ channel activity in intact and permeabilized rat ventricular myocytes. *J. Physiol.*, **423**, 91–110.

NICHOLS, C.G., RIPOLL, C. & LEDERER, W.J. (1991). ATP-sensitive potassium channel modulation of guinea-pig ventricular action potential and contraction. *Circ. Res.*, **68**, 280–287.

NOMA, A. & SHIBASAKI, T. (1985). Membrane current through adenosine-triphosphate regulated potassium channels in guinea-pig ventricular cells. *J. Physiol.*, **363**, 463–480.

OPIE, L.H. (1993). Modulation of ischemia by regulation of the ATP-sensitive potassium channel. *Cardiovasc. Drugs Ther.*, **7**, 507–513.

QUAST, U. (1993). Do the K^+ channel openers relax smooth muscle by opening K^+ channels? *Trends Pharmacol. Sci.*, **14**, 332–337.

RICHER, C., PRATZ, J., MULDER, P., MONDOT, S., GIUDICELLI, J.F. & CAVERO, I. (1990). Cardiovascular and biological effects of K^+ channel openers, a class of drugs with vasorelaxant and cardioprotective properties. *Life Sci.*, **47**, 1693–1705.

RIPOLL, C., LEDERER, J.W. & NICHOLS, C.G. (1990). Modulation of ATP-sensitive K^+ channel activity and contractile behavior in mammalian ventricle by the potassium channel openers cromakalim and RP 49356. *J. Pharmacol. Exp. Ther.*, **255**, 429–435.

SHEN, W.K., TUNG, R.T., MACHULDA, M.M. & KURACHI, Y. (1991). Essential role of nucleotide diphosphates in nicorandil-mediated activation of cardiac ATP-sensitive K^+ channels. *Circ. Res.*, **69**, 1152–1158.

STANDEN, N.B. (1992). Potassium channels, metabolism and muscle. *Exp. Physiol.*, **77**, 1–25.

TAKANO, M. & NOMA, A. (1990). Selective modulation of the ATP-sensitive K^+ channel by nicorandil in guinea-pig cardiac myoctes. *Naunyn-Schmied. Arch. Pharmacol.*, **342**, 592–597.

TERZIC, A., TUNG, R.T., INANOBE, A., KATADA, T. & KURACHI, Y. (1991). G proteins activate ATP-sensitive K^+ channels by antagonizing ATP-dependent gating. *Neuron*, **12**, 885–893.

THURINGER, D. & ESCANDE, D. (1989). Apparent competition between ATP and the potassium channel opener RP 49356 on ATP-sensitive K^+ channels of cardiac myocyte. *Mol. Pharmacol.*, **36**, 897–902.

TUNG, R.T. & KURACHI, Y. (1991). On the mechanism of nucleotide diphosphate activation of the cardiac ATP-sensitive K^+ channel in ventricular cell of guinea-pig. *J. Physiol.*, **437**, 239–256.

WEIK, R. & NEUMCKE, B. (1990). ATP-sensitive potassium channels in adult mouse skeletal muscle: characterization of the ATP-binding site. *J. Memb. Biol.*, **110**, 217–225.

WEISS, J.N. & VENKATESH, N. (1993). Metabolic regulation of cardiac ATP-sensitive K^+ channels. *Cardiovasc. Drugs Ther.*, **7**, 499–505.

(Received November 24, 1994
Revised January 3, 1995
Accepted January 27, 1995)

British Journal of Pharmacology (1995) 115, 128–132

Involvement of tachykinins in plasma extravasation induced by bradykinin and low pH medium in the guinea-pig conjunctiva

Michela Figini, Panthea Javdan, Fabio Cioncolini & [1]Pierangelo Geppetti

Institute of Internal Medicine and Therapeutics IV, Laboratory of Clinical Pharmacology, University of Florence, Viale Pieraccini 6, 50139 Florence, Italy

1 The effect of bradykinin, capsaicin, substance P and low pH medium on plasma extravasation in the guinea-pig conjunctiva has been studied. Evans blue dye was measured in the conjunctiva after local instillation of the agents into the conjunctival sac.

2 Bradykinin (2–50 nmol), capsaicin (20–50 nmol) and substance P (0.5–5 nmol) caused a dose-dependent increase in plasma extravasation with the following order of potency: substance P > bradykinin = capsaicin. The effect of capsaicin (50 nmol) and substance P (5 nmol) was abolished by the tachykinin NK_1 receptor antagonist, CP-99,994 (8 μmol kg^{-1}, i.v.) ($P<0.01$), whereas CP-100,263 (8 μmol kg^{-1}, i.v.) the inactive enantiomer of CP-99, 994 was without effect. CP-99,994 inhibited by 70% ($P<0.01$) the effect of bradykinin.

3 The kinin B_2 receptor antagonist, Hoe 140 (icatibant, 10 nmol kg^{-1}, i.v.) abolished the response to bradykinin (50 nmol) ($P<0.01$), but did not affect the responses to capsaicin (50 nmol) or substance P (5 nmol). Plasma extravasation induced by low pH medium (pH 1) was abolished by CP-99,994 ($P<0.01$) and by Hoe 140 ($P<0.01$).

4 The present findings suggest that: endogenous or exogenous tachykinins increase plasma extravasation in the guinea-pig conjunctiva by activation of NK_1 receptors; bradykinin-induced plasma extravasation is mediated by tachykinin release from sensory nerve endings; low pH media cause plasma extravasation via release of kinins that by activation of B_2 receptors release tachykinins from sensory nerve endings.

Keywords: Neurogenic inflammation; conjunctiva; substance P; capsaicin; tachykinin NK_1 receptors; bradykinin; kinin B_2 receptors; low pH

Introduction

A subpopulation of primary sensory neurones is characterized by the ability to release neuropeptides from their peripheral endings, thus causing a series of effects collectively referred to as neurogenic inflammation. In most tissues these effects consist of arterial vasodilatation, leakage of plasma proteins and recruitment of inflammatory cells. The neuropeptides released from primary sensory neurones include calcitonin gene-related peptide (CGRP) and the tachykinins, substance P and neurokinin A. CGRP mediates vasodilatation in certain tissues and organs, whereas the tachykinins increase plasma protein extravasation and promote leukocyte adhesion to the vascular endothelium (Holzer, 1988; Maggi *et al.*, 1989). These effects of tachykinins are mediated, with a few exceptions (Tousignant *et al.*, 1993), by activation of tachykinin NK_1 receptors (Eglezos *et al.*, 1992), probably located on the endothelial cells of postcapillary venules (Bowden *et al.*, 1994).

The conjunctiva is innervated by peptide-containing sensory nerves (Elsas *et al.*, 1994). These nerves are sensitive to the excitatory action of capsaicin, the pungent principle contained in the plants of the genus *Capsicum*. Early studies by N. Jancso and coworkers reported that capsaicin or other congeners of capsaicin cause oedema or interendothelial gap formation in the venules in the conjunctiva of the rat and guinea-pig (Jancso, 1955; Jancso *et al.*, 1968). More recently, Saria and coworkers (1983) showed that a variety of exogenous or endogenous agents, including the proinflammatory peptide, bradykinin, induce plasma extravasation in rodent conjunctiva. The kinins, bradykinin and kallidin, are formed during injury and inflammation from plasma or tissue precursor, respectively (Regoli & Barabe, 1980). Kinins acting directly on effector cells or indirectly by releasing other inflammatory mediators increase and sustain the inflammatory response.

The aim of the present paper was to investigate the mechanism and possible pathophysiological implications of the bradykinin-induced plasma extravasation in the guinea-pig conjunctiva. Because in other tissues the increase in plasma extravasation induced by bradykinin is mediated by activation of a neurogenic inflammatory mechanism (Lundberg & Saria, 1983; Ichinose *et al.*, 1990; Bertrand *et al.*, 1993a; Geppetti, 1993), this possibility was explored in the guinea-pig conjunctiva. To determine whether kinin B_2 receptors mediate the response to bradykinin the peptide B_2 receptor antagonist, Hoe 140 (icatibant) (Wirth *et al.*, 1991) was used. To determine whether the action of kinin and capsaicin was due to tachykinin release, the NK_1 receptor antagonist, CP-99,994 (McLean *et al.*, 1993) was used. Finally, the involvement of kinin formation and of neurogenic inflammatory mechanisms in the plasma extravasation induced by acid media was investigated.

Methods

Animals and experimental procedure

Male albino Hartley guinea-pigs (Rodentia, Bergamo, Italy) were used in this study. They were kept in a temperature-controlled environment with standard laboratory food and water freely available. The animals (body weight, 350–450 g) were anaesthetized with sodium pentobarbitone (45 mg kg^{-1}, i.p.) and the jugular vein was cannulated. Deep anaesthesia

[1] Author for correspondence.

was monitored throughout the experiment and additional anaesthetic administered as required. Evans blue dye (3% solution in 0.9% NaCl; Sigma, St. Louis, MO, U.S.A.) was used to measure plasma extravasation, which was injected (30 mg kg^{-1}, i.v. over 5 s) via the jugular vein. Immediately after Evans blue administration, agents were given by local instillation (dissolved in 10 µl of saline) into the conjunctival sac by means of a micropipette. The solution was applied uniformly throughout the conjunctival surface. One single conjunctiva, chosen at random, was treated with the stimulus in each animal. Local application of drugs or agents to the conjunctiva did not cause any adverse reaction of any aversive behavioural response.

Terminal anaesthesia (pentobarbitone, 40 mg kg^{-1}, i.v.) was always administered 30 s before terminating the experiments. At this time it is assumed that the increase in vascular permeability is already completed. Experiments were terminated by opening of the chest 5 min after injection of the tracer, inserting a cannula into the ascending aorta through the left ventricle, and perfusing the circulation for 2 min with phosphate buffer (pH 5; Sigma Chemical, St. Louis, MO) at a pressure of 130 mmHg. The conjunctiva adherent to either the palpebra or the sclera was removed. Tissues were blotted on paper and weighed. All tissues were incubated in 1 ml of formamide (Merk, Darmstadt, Germany) at 60°C for 18 h to extract the extravasated Evans blue dye (Lundberg & Saria, 1983).

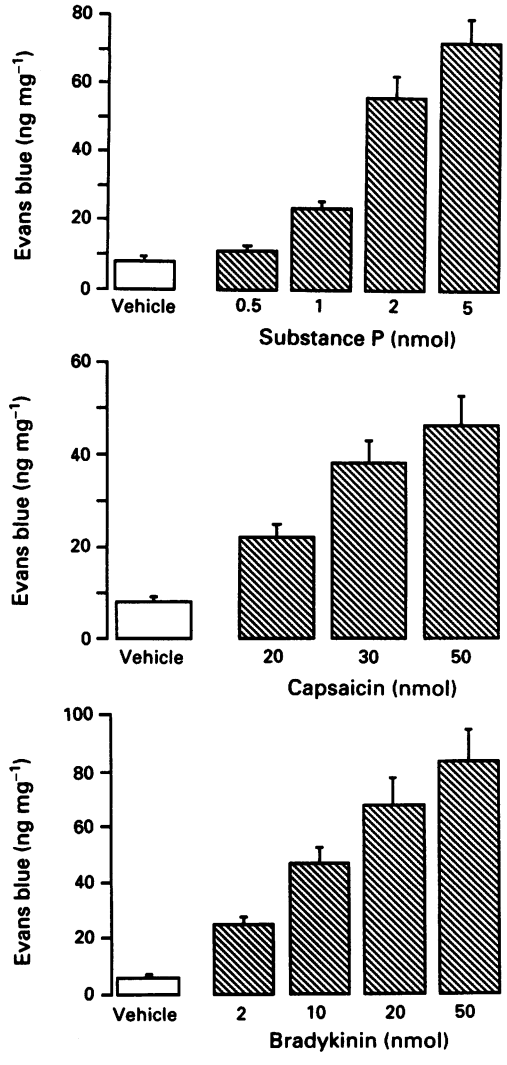

Figure 1 Effect of increasing doses of substance P, bradykinin and capsaicin (hatched columns) on the Evans blue dye extravasation in the conjunctiva of guinea-pigs. Drugs were applied in a volume of 10 µl to the conjunctiva. Open columns indicate the Evans blue dye extravasation produced by the vehicle of each drug (10 µl). Columns are mean ± s.e.mean of at least 4 experiments.

Capsaicin (50 nmol) was dissolved in a solution containing 10% ethanol, 5% Tween 80 and 85% 0.9% NaCl. Further dilutions were in 0.9% NaCl. All the other drugs were dissolved in 0.9% NaCl. CP-99,994 and CP-100,263 were given 5 min before the stimulus, and Hoe 140 15 min before the stimulus by i.v. administration through the jugular vein. Low pH media were obtained by adding HCl to the saline solution until the desired pH was obtained.

Measurement of plasma extravasation

The extravasation of Evans blue dye-labelled macromolecules from the microcirculation in the tissue was quantified by measuring the optical density of the formamide extracts at a wavelength of 620 nm with a spectrophotometer (Model UV1204, Shimatzu Scientific Instruments, Inc., Japan). The amount of Evans blue dye extravasated in the tissues, expressed in ng mg^{-1} of wet weight, was interpolated from a standard curve of Evans blue concentrations (0.1 to 5 µg ml^{-1}).

Drugs

CP-99,994 (+)-(2S,3S)-3-(2-methoxybenzyl-amino)-2-phenylpiperidine) and CP-100,263 (−)-(2R,3R)-3-(2-methoxybenzyl-amino)-2-phenylpiperidine) were kind gifts from Dr J.A. Lowe III (Pfizer Inc., Groton, CT, U.S.A.), and Hoe 140 (D-Arg-[Hyp^3, Thi^5, D-Tic^7, Oic^8]-bradykinin) was a kind gift from Dr K.J. Wirth (Hoechst, Germany). Substance P and bradykinin were purchased from Peninsula Laboratories, Inc. (Merseyside, UK); capsaicin was obtained from Sigma Chemical Co. (St. Louis, MO, U.S.A.).

Statistical analysis

All data are expressed as mean ± s.e.mean. Mean values of spectrophotometric measurements of Evans blue dye extravasation were analysed by one-way analysis of variance. Comparisons between means in each condition were performed by Bonferroni's multiple range test. Student's t test for paired or unpaired data was used when applicable. Differences of $P<0.05$ were considered significant.

Results

Effect of bradykinin, capsaicin and substance P

Baseline Evans blue dye extravasation in untreated conjunctiva of guinea-pigs was 11.2 ± 1.3 ng mg^{-1} ($n = 6$). Instillation of 10 µl of saline into the conjunctiva contralateral to the untreated side did not increase plasma extravasation significantly (12.4 ± 1.1 ng mg^{-1}, $n = 6$). Instillation of bradykinin and substance P caused a dose-dependent increase in Evans blue dye extravasation (Figure 1). The vehicle of 50 nmol capsaicin (10% ethanol, 5% Tween 80 and 85% 0.9% NaCl) did not induce any increase in the extravasation of the Evans blue dye (9.7 ± 1.1 ng ml^{-1}, $n = 5$) as compared with the effect of saline (10.9 ± 1.6 ng ml^{-1}, $n = 5$) applied to the contralateral eye. Capsaicin caused a dose-dependent increase in plasma extravasation (Figure 1). Substance P was approximately 10 times more potent in increasing the extravasation of the Evans blue dye in the conjunctiva than capsaicin and bradykinin. Bradykinin and capsaisin were virtually equipotent.

Effect of tachykinin and kinin receptor antagonists

Both CP-99,994 (8 µmol kg^{-1}, i.v.) and CP-100,263 (8 µmol kg^{-1}, i.v.), the inactive enantiomer of CP-99,994 did not affect baseline Evans blue dye extravasation (data not

shown). Pretreatment with CP-99,994 (8 μmol kg^{-1}, i.v.) abolished the response to substance P (5 nmol), whereas pretreatment with 8 μmol kg^{-1} of CP-100,263 (i.v.), did not affect the response to substance P (Figure 2). Pretreatment with CP-99,994 (8 μmol kg^{-1}, i.v.) abolished the increase in Evans blue dye extravasation induced by capsaicin (50 nmol) and reduced by about 70% the response to bradykinin (50 nmol) (Figure 2).

Hoe 140 (10 nmol kg^{-1}, i.v.) did not affect basal plasma extravasation in the guinea-pig conjunctiva (data not shown). Pretreatment with Hoe 140 abolished the Evans blue dye extravasation caused by bradykinin (50 nmol), but did not affect the response induced by substance P (5 nmol) (Figure 3).

Effect of low pH media

Application of low pH media (10 μl) to the conjunctival surface increased Evans blue dye extravasation in a manner inversely related to the pH of the medium. Media at pH higher than 2 did not affect plasma extravasation. A medium at pH 1.5 increased Evans blue dye extravasation to 24.3 ± 3.5 ng mg^{-1} ($n = 4$). Medium at pH 1 caused an increase in Evans blue dye extravasation (43.7 ± 6.8 ng mg^{-1}, $n = 5$), that was comparable to that induced by submaximal doses of substance P or bradykinin (Figure 4), without causing any macroscopical damage to the conjunctiva. Media at pH 0.5 or lower caused macroscopical damage of the conjunctiva and therefore were not further investigated. Pretreatment with CP-99,994 (8 μmol kg^{-1}, i.v.) or pretreatment with Hoe 140 (10 nmol kg^{-1}, i.v.) abolished the extravasation induced by pH 1 medium (Figure 4).

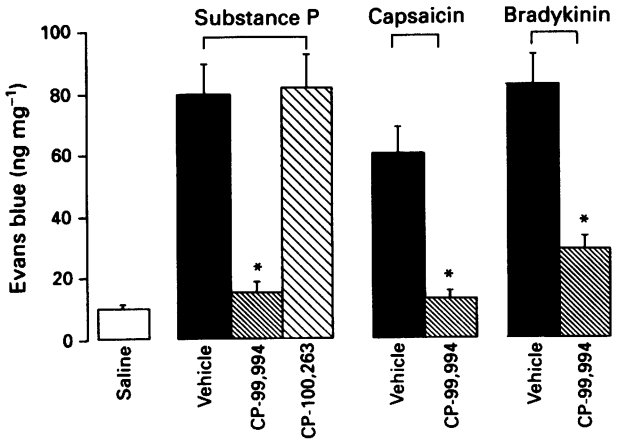

Figure 2 Effect of pretreatment with the tachykinin NK_1 receptor antagonist, CP-99,994 (8 μmol kg^{-1}, i.v.), or its enantiomer CP-100,263 (8 μmol kg^{-1}, i.v.), on the Evans blue dye extravasation evoked by the instillation of substance P (5 nmol), capsaicin (50 nmol) or bradykinin (50 nmol) in the guinea-pig conjunctiva. Open column indicates the Evans blue dye extravasation induced by 0.9% saline (10 μl). Drugs were applied in a volume of 10 μl to the conjunctiva. Columns are mean ± s.e.mean of at least 4 experiments. *$P < 0.01$ versus vehicle.

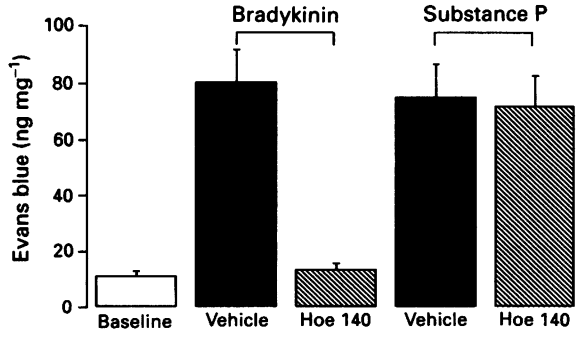

Figure 3 Effect of pretreatment with the kinin B_2 receptor antagonist, Hoe 140 (10 nmol kg^{-1}, i.v.), on the Evans blue dye extravasation evoked by the instillation of substance P (5 nmol) or bradykinin (50 nmol) in the guinea-pig conjunctiva. Open column indicates the Evans blue dye extravasation induced by 0.9% saline (10 μl). Drugs were applied in a volume of 10 μl to the conjunctiva. Columns are mean ± s.e.mean of at least 4 experiments. *$P < 0.01$ versus vehicle.

Discussion

The stimuli used in the present investigation were all able to cause plasma extravasation in the guinea-pig conjunctiva. Substance P, capsaicin and bradykinin induced a dose-dependent increase in plasma extravasation. Low pH media increased plasma extravasation in a manner inversely related to the pH value of the medium. Plasma extravasation evoked by substance P was completely abolished by the tachykinin NK_1 receptor antagonist, CP-99,994. This compound exhibits a lesser calcium antagonist property than the parent molecule CP-96,345 (McLean *et al.*, 1993). In addition, the observation that CP-100,263, the enantiomer of CP-99,994, which is inactive on tachykinin NK_1 receptors, did not show any effect on the substance P-induced response indicates that CP-99,994 acted selectively to inhibit the NK_1 receptor. Therefore, the present data suggest that the plasma extravasation caused by exogenously applied substance P to the guinea-pig conjunctiva is entirely mediated by activation of NK_1 receptors. Capsaicin excites sensory nerves causing the release of tachykinins and CGRP from the peripheral endings of these nerves. The finding that CP-99,994 blocked the plasma extravasation induced by capsaicin suggests that the plasma extravasation mediated by the release of endogenous tachykinins is also due to the activation of NK_1 receptors. This conclusion is in agreement with recent data reporting that plasma extravasation caused by capsaicin i.v. in the guinea-pig conjunctiva was abolished by the tachykinin NK_1 receptor antagonist, RPR 100893 (Lee *et al.*, 1994). CGRP is released with tachykinins from sensory nerve endings, and regulates blood flow in various organs of different species. The present findings, do not exclude the possibility that CGRP by regulating conjunctival blood flow may modulate plasma extravasation induced by stimulation of sensory nerves. However, they exclude the possibility that CGRP

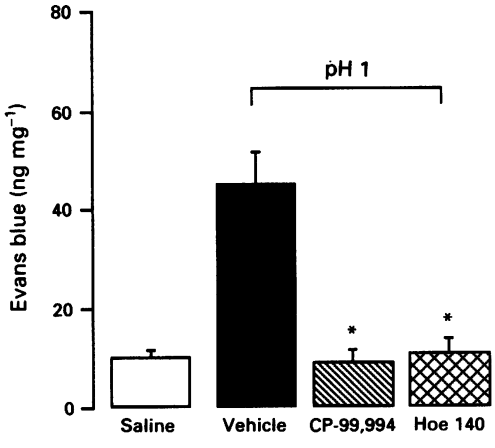

Figure 4 Effect of pretreatment with the tachykinin NK_1 receptor antagonist, CP-99,994 (8 μmol kg^{-1}, i.v.), and the kinin B_2 receptor antagonist, Hoe 140 (10 nmol kg^{-1}, i.v.), on the Evans blue dye extravasation evoked by the instillation of a medium at pH 1 in the guinea-pig conjunctiva. Open column indicates the Evans blue dye extravasation induced by 0.9% saline (10 μl). Drugs were applied in a volume of 10 μl to the conjunctiva. Columns are mean ± s.e.mean of at least 4 experiments. *$P < 0.01$ versus vehicle.

plays a direct role in neurogenic plasma extravasation in the conjunctiva.

The effects of bradykinin are mediated by stimulation of B_1 and B_2 receptors (Regoli & Barabe 1980). Since the selective kinin B_2 receptor antagonist, Hoe 140 (Wirth *et al.*, 1991) abolished plasma extravasation induced by locally applied bradykinin, it is concluded that this effect of bradykinin is mediated by activation of B_2 receptors. This antagonist did not affect substance P-induced plasma extravasation, which indicates that kinin release is not involved in the plasma extravasation evoked by substance P in the guinea-pig conjunctiva.

Bradykinin stimulates inflammatory responses, including plasma extravasation, via its own receptors on effector cells or indirectly by releasing mediators from intermediate cells. Bradykinin-induced plasma extravasation in the guinea-pig conjunctiva is markedly inhibited by CP-99,994, thus indicating that NK_1 receptor activation is involved in this response. Bradykinin stimulates sensory nerves and causes the release of sensory neuropeptides from peripheral endings of these neurones (Geppetti, 1993). It is proposed that local application of bradykinin to the guinea-pig conjunctiva increases the leakage of plasma proteins mainly by a neurogenic inflammatory mechanism. CP-99,994, at a dose that completely blocked substance P- and capsaicin-induced plasma extravasation, significantly inhibited, but did not abolish the response caused by bradykinin. It is probable that the CP-99,994-resistant component of the bradykinin-induced response is mediated by the activation of bradykinin B_2 receptors on the venular endothelium. A dual mechanism, in large part neurogenic, and in minor part non-neurogenic for inducing plasma extravasation by locally applied bradykinin has also been shown in other organs and tissues including the trachea (Lundberg & Saria, 1983) and the nasal mucosa (Bertrand *et al.*, 1993a).

The pH of the medium during tissue injury, ischaemia or inflammation may fall to values around 5 or 4, and hyperaemia may lower the pH of the lachrymal fluid. In addition, acid solution may accidentally come in contact with the conjunctival surface. The observation that CP-99,994 blocked plasma extravasation evoked by low pH medium suggests that in the guinea-pig conjunctiva, protons increase plasma extravasation by releasing tachykinins from sensory nerve endings. Recently, protons have been shown to activate a cation conductance and to release neuropeptides selectively in capsaicin-sensitive primary sensory neurones (Geppetti *et al.*, 1990; Bevan & Yeats, 1991). Hence, at least part of the proinflammatory action of hydrogen ions may derive from their ability to excite sensory nerves and cause neurogenic inflammation. Evidence obtained in dorsal root ganglion neurones in culture or in slices of peripheral tissues suggests protons may have a direct action on sensory nerves where they activate the channel non selective for cations opened by capsaicin (Geppetti *et al.*, 1991; Liu & Simon, 1994). However, the present data showing that Hoe 140 abolished the plasma extravasation induced by low pH medium in the conjunctiva raise the possibility that kinins play an initial role in mediating the inflammatory response to protons.

Since both kinin and tachykinin receptor antagonists blocked the plasma extravasation evoked by low pH media, the hypothesis may be advanced that these two classes of peptide mediators do not act independently, but rather utilize a common final pathway. The observation that Hoe 140 did not affect the plasma extravasation evoked by substance P, whereas CP-99,994 reduced markedly the response to bradykinin suggests that protons promote the following cascade of events: low pH medium releases kinins which by stimulating sensory neuropeptide release increase plasma extravasation. Examples of kinins formed following different types of inflammatory insult, and causing inflammatory responses through the release of sensory neuropeptides have been reported recently (Bertrand *et al.*, 1993b; Ahluwalia *et al.*, 1994; Ricciardolo *et al.*, 1994; Yoshihara *et al.*, 1994). There is also pharmacological evidence that the increase in mucosal blood flow of the gastric wall induced by acid back diffusion is in part mediated by kinins (Holzer & Petho, 1994). Mucosal hyperaemia induced by acid back diffusion is mediated by sensory nerve stimulation (Holzer, 1992), thus suggesting that a mechanism similar to that reported here for the conjunctiva may also be present in the stomach.

Conjunctivitis may derive from several types of insult. Here, we report that certain stimuli cause plasma extravasation in the conjunctiva by a neurogenic inflammatory mechanism. We also show that a pathway involving kinin generation and the subsequent release of sensory neuropeptides plays a major role in the inflammatory response to low pH media. Hence, drugs which inhibit kinin B_2 and tachykinin NK_1 receptors may be of value in the treatment of conjunctivitis.

This work was supported by grant from MURST (60%, Florence, Italy) and Consiglio Nazionale delle Ricerche (Rome, Italy), Progetto Bilaterale.

References

AHLUWALIA, A., MAGGI, C.A. SANTICIOLI, P., LECCI, A. & GIULIANI, S. (1994). Characterization of the capsaicin-sensitive component of cyclophosphamide-induced inflammation in the rat urinary bladder. *Br. J. Pharmacol.*, **111**, 1017–1022.

BERTRAND, C., GEPPETTI, P., BAKER, J., YAMAWAKI, I., PETERSSON, G., PIEDIMONTE, G. & NADEL, J.A. (1993a). Role of peptidases and NK-1 receptors in the increased vascular extravasation induced by bradykinin in the rat nasal mucosa. *J. Appl. Physiol.*, **74**, 2456–2461.

BERTRAND, C., NADEL, J.A., YAMAWAKI, I. & GEPPETTI, P. (1993b). Role of kinins in the vascular extravasation evoked by antigen and mediated by tachykinins in guinea-pig trachea. *J. Immunol.*, **151**, 4902–4907.

BEVAN, S. & YEATS, J. (1991). Protons activate a cation conductance in a subpopulation of rat dosal root neurones. *J. Physiol.*, **433**, 145–161.

BOWDEN, J.J., GARLAND, A.M., BALUK, P., LEFEVRE, P.M., GRADY, E.F., VIGNA, S.R., BUNNETT, N.W. & MCDONALD, D.M. (1994). Direct observation of substance P-induced internalization of NK_1 receptor at sites of inflammation. *Proc. Natl. Acad. Sci. U.S.A.*, **91**, 8964–8968.

EGLEZOS, A., GIULIANI, S., VITI, G. & MAGGI, C.A. (1992). Direct evidence that capsaicin-induced plasma protein extravasation is mediated through tachykinin NK_1 receptors. *Eur. J. Pharmacol.*, **209**, 277–279.

ELSAS, T., EDVINSSON, L., SUNDLER, F. & UDDMAN, R. (1994). Neuronal pathways to the rat conjunctiva revealed by retrograde tracing and immunocytochemistry. *Exp. Eye Res.*, **58**, 117–126.

GEPPETTI, P. (1993). Sensory neuropeptides release of bradykinin: mechanisms and pathophysiological implications. *Regul. Pept.*, **47**, 1–23.

GEPPETTI, P., DEL BIANCO, E., PATACCHINI, R., SANTICIOLI, P., MAGGI, C.A. & TRAMONTANA, M. (1991). Low pH-induced release of calcitonin gene-related peptide from capsaicin-sensitive sensory nerves: mechanism of action and biological response. *Neuroscience*, **41**, 295–301.

GEPPETTI, P., TRAMONTANA, M., PATACCHINI R., DEL BIANCO, E., SANTICIOLI, P. & MAGGI, C.A. (1990). Neurochemical evidence for the activation of the 'efferent' function of capsaicin-sensitive nerves by lowering of the pH in the guinea-pig urinary bladder. *Neurosci. Lett.*, **114**, 101–106.

HOLZER, P. (1988). Local effector functions of capsaicin-sensitive sensory nerves endings: involvement of tachykinins, calcitonin gene-related peptide and other neuropeptides. *Neuroscience*, **24**, 739–768.

HOLZER, P. (1992). Peptidergic sensory neurones in the control of vascular functions: mechanisms and significance in the cutaneous and splanchinc vascular beds. *Rev. Physiol. Biochem. Pharmacol.*, **121**, 49–146.

HOLZER, P. & PETHO, G. (1994). Role of bradykinin in the regulation of gastric blood flow in the face of acid injury. *Gastroenterology*, **106**, A238.

ICHINOSE, M., BELVISI, M.G. & BARNES, P.J. (1990). Bradykinin-induced bronchoconstriction in guinea-pig in vivo: role of neural mechanisms. *J. Pharmacol. Exp. Ther.*, **253**, 594–599.

JANCSÓ, N. (1955). *Speicherung Stoffanreichenung in Retikuloendothel und in der Diere*. Budapest: Akademiai Kiado.

JANCSÓ, N., JANCSÓ-GABOR, A. & SZOLCSÁNYI, J. (1968). The role of sensory nerve endings in neurogenic inflammation induced in human skin and in the eye and paw of the rat. *Br. J. Pharmacol.*, **32**, 32–41.

LEE, W.S., MOUSSAOUI, S. & MOSKOWITZ, M.A. (1994). Blockade by oral or parenteral RPR 100893 (a non-peptide NK_1 receptor antagonist) of neurogenic plasma extravasation within guinea-pig dura mater and conjunctiva. *Br. J. Pharmacol.*, **112**, 920–924.

LIU, L. & SIMON, S.A. (1994). A rapid capsaicin-activated current in rat trigeminal ganglion neurons. *Proc. Natl. Acad. Sci. U.S.A.*, **91**, 738–741.

LUNDBERG, J.M. & SARIA, A. (1983). Capsaicin induced desensitization of the airway mucosa to cigarette smoke, mechanical and chemical irritants. *Nature*, **302**, 251–253.

MAGGI, C.A., PATACCHINI, R., SANTICIOLI, P., GIULIANI, S., DEL BIANCO, E., GEPPETTI, P. & MELI, A. (1989). The 'efferent' function of capsaicin-sensitive nerves: ruthenium red discriminates between different mechanisms of activation. *Eur. J. Pharmacol.*, **170**, 167–177.

MCLEAN, S., GANONG, A., SEYMOUR, P.A., SNIDER, R.M., DESAI, M.C., ROSEN, T., BRYCE, D.K., LONGO, K.P., REYNOLDS, L.S., ROBINSON, G., SCHMIDT, A.W., SIOK, C. & HEYM, J. (1993). Pharmacology of CP-99,994; a nonpeptide antagonist of the tachykinin neurokinin-1 receptor. *J. Pharmacol. Exp. Ther.*, **267**, 472–479.

REGOLI, D. & BARABÉ, J. (1980). Pharmacology of bradykinin and related kinins. *Pharmacol. Rev.*, **32**, 1–46.

RICCIARDOLO, F.L.M., NADEL, J.A., BERTRAND, C., YAMAWAKI, I., CHAN, B. & GEPPETTI, P. (1994). Tachykinins and kinins in antigen-evoked plasma extravasation in guinea-pig nasal mucosa. *Eur. J. Pharmacol.*, **261**, 127–132.

SARIA, A., LUNDBERG, J., SKOFITSCH, G. & LEMBECK, F. (1983). Vascular protein leakage in various tissues induced by substance P, capsaicin, bradykinin, serotonin, histamine and antigen challenge. *Naunyn Schmied. Arch. Pharmacol.*, **324**, 212–218.

TOUSIGNANT, C., CHAN, C.-C., GUEVREMONT, D., BRIDEAU, C., HALE, J.J, MACCROSS, M. & RODGER, I.W. (1993). NK_2 receptors mediate plasma extravasation in guinea-pig lower airways. *Br. J. Pharmacol.*, **108**, 383–386.

WIRTH, K., HOCK, F.J., ALBUS, U., LINZ, W., ALPERMANN, H.G., ANAGNOSTOPOULOS, H., HENKE, S., BREIPOHL, G., KÖNIG, W., KNOLLE, J. & SCHÖLKENS, B.A. (1991). Hoe 140 a new potent and long acting bradykinin-antagonist: *in vivo* studies. *Br. J. Pharmacol.*, **102**, 774–777.

YOSHIHARA, S., CHAN, B., YAMAWAKI, I., GEPPETTI, P., RICCIARDOLO, F.L.M. & NADEL, J.A. (1994). Exposure to cold air increases plasma extravasation in the rat trachea by tachykinin release from sensory nerves. *Am. J. Respir, Crit. Care Med.*, **149**, A891.

(Received October 3, 1994
Revised December 6, 1994
Accepted January 6, 1995)

British Journal of Pharmacology (1995) 115, 133-141

Caffeine-evoked, calcium-sensitive membrane currents in rabbit aortic endothelial cells

[1]J. Rusko, G. Van Slooten & [2]D.J. Adams

Department of Molecular & Cellular Pharmacology, University of Miami School of Medicine, Miami, FL 33101, U.S.A.

1 Single cell photometry and whole-cell patch clamp recording were used to study caffeine-induced intracellular Ca^{2+} signals and membrane currents, respectively, in endothelial cells freshly dissociated from rabbit aorta.

2 Caffeine (5 mM) evoked a transient increase in $[Ca^{2+}]_i$ in fura-2-loaded endothelial cells. Pretreatment of cells with 10 μM ryanodine did not alter resting $[Ca^{2+}]_i$ but irreversibly inhibited the caffeine-induced rise in $[Ca^{2+}]_i$. The caffeine-induced increase in $[Ca^{2+}]_i$ was not attenuated by the removal of extracellular Ca^{2+} and did not stimulate the rate of Mn^{2+} quench of fura-2 fluorescence.

3 Bath application of caffeine evoked a dose- and voltage-dependent outward current. The rate of onset and amplitude of the caffeine-evoked outward current increased with higher caffeine concentrations and membrane depolarization. The relationship between caffeine-evoked current amplitude and membrane potential was non linear, suggesting that the channels underlying the current are voltage-sensitive.

4 In the absence of extracellular Ca^{2+}, the amplitude of the caffeine-evoked outward current was reduced by approximately 50% but the duration of the current was prolonged compared to that observed in the presence of external Ca^{2+}. Ca^{2+}-free external solutions produced an unexpected increase in both the frequency and amplitude of spontaneous transient outward currents (STOCs).

5 Inclusion of heparin (10 μg ml^{-1}) in the patch pipette abolished the acetylcholine (ACh)-induced outward current but failed to inhibit either STOCs or the caffeine-evoked outward current in native endothelial cells. In the absence of extracellular Ca^{2+}, heparin did not affect either STOCs or the caffeine-induced outward current.

6 Externally applied tetraethylammonium ions (TEA, 3-10 mM) reversibly inhibited unitary Ca^{2+}-activated K^+ currents and STOCs in endothelial cells but failed to inhibit completely the outward current evoked by 20 mM caffeine.

7 Bath application of 0.1 mM zinc ion (Zn^{2+}), a chloride channel blocker, did not affect unitary currents or STOCs but reduced the amplitude of the caffeine-evoked current by >75% compared to control. Replacement of extracellular NaCl with Na gluconate also reduced the amplitude of the caffeine-induced outward current. Bath application of 0.1 mM Zn^{2+} and 10 mM TEA completely blocked the caffeine-evoked outward current in endothelial cells.

8 Caffeine-induced Ca^{2+} release from intracellular stores evokes a transient rise in $[Ca^{2+}]_i$ which is correlated with a large, transient outward current. The ionic dependence and inhibition of the caffeine-sensitive current by TEA and Zn^{2+} suggests that Ca^{2+}-activated K^+ and Cl^- conductances contribute to the caffeine response in rabbit aortic endothelial cells.

Keywords: Caffeine; ryanodine; endothelium; internal calcium stores; tetraethylammonium; heparin; calcium-activated K^+ currents; calcium-activated Cl^- currents

Introduction

The secretion of endothelium-derived factors such as prostacyclin (PGI_2), nitric oxide and von Willebrand factor (vWf), is closely associated with the intracellular free calcium ion concentration ($[Ca^{2+}]_i$). Electrophysiological studies of endothelial cells freshly dissociated from rabbit aorta have shown that intracellular Ca^{2+} levels also regulate single channel activity and spontaneous transient outward currents (STOCs; Rusko *et al.*, 1992). These currents were identified as K^+ currents by their ionic dependence and sensitivity to block by the K channel blockers, tetraethylammonium ions (TEA) and charybdotoxin. The dependence of outward K^+ current activity on $[Ca^{2+}]_i$ suggests that the opening of plasmalemmal Ca^{2+}-dependent K channels is triggered by the cyclical release of Ca^{2+} from internal stores. The activation of Ca^{2+}-dependent K channels has been used to monitor the functional status of the intracellular Ca^{2+} stores in smooth muscle cells (Benham & Bolton, 1986).

The activation of cell-surface receptors by vasoactive agents (e.g. bradykinin, acetylcholine and ATP) in native aortic endothelial cells produces a biphasic increase in both the open probability of unitary currents and the amplitude of STOCs (Sauvé *et al.*, 1988; Rusko *et al.*, 1992). This current activation is correlated with a biphasic elevation in $[Ca^{2+}]_i$: an initial discharge of Ca^{2+} from intracellular stores, and a subsequent prolonged entry of Ca^{2+} from the extracellular space (see reviews by Adams *et al.*, 1993; Himmel *et al.*, 1993). In the absence of extracellular Ca^{2+}, a decrease in the magnitude of the initial agonist-evoked transient increase of $[Ca^{2+}]_i$ was observed in bovine aortic endothelial cells (Schilling *et al.*, 1988; Lückhoff *et al.*, 1988). Furthermore, depletion of the intracellular Ca^{2+} stores has been reported to be linked to the agonist-induced Ca^{2+} influx from the extracellular space (Hallam *et al.*, 1989; Jacob, 1990; Schilling *et al.*, 1992). The precise mechanism(s) which brings about these changes in cytoplasmic $[Ca^{2+}]$ in native endothelial cells is ill-defined.

The receptor-stimulated turnover of inositol phosphate has

[1] Present address: Department of Pharmacology & Therapeutics, Faculty of Medicine, University of British Columbia, B.C. Canada V6T 1Z3.

[2] Author for correspondence at present address: Department of Physiology & Pharmacology, University of Queensland, Brisbane, QLD 4072, Australia.

been shown to trigger directly the initial, transient release of intracellular Ca^{2+} from endoplasmic reticulum of cultured endothelial cells (Jaffe *et al.*, 1987; Pollock *et al.*, 1988; Freay *et al.*, 1989). There is also evidence for the release of Ca^{2+} from intracellular stores by actions of methylxanthines, such as caffeine, which are known to translocate Ca^{2+} from intracellular Ca^{2+} stores into the cytosol of skeletal, cardiac and vascular smooth muscle cells by enhancing Ca^{2+}-induced Ca^{2+}-release (see Endo, 1985). Caffeine is also able to release Ca^{2+} from the agonist-releasable intracellular Ca^{2+} stores (Benham & Bolton, 1986; Bolton & Lim, 1989). This Ca^{2+}-induced Ca^{2+} release mechanism has been shown to be present in addition to the inositol-1,4,5-trisphosphate ($InsP_3$)-mediated Ca^{2+}-release mechanism in a variety of excitable and non-excitable cells (see Tsien & Tsien, 1990; Pozzan *et al.*, 1994). Evidence for the coexistence of $InsP_3$-sensitive and caffeine-sensitive Ca^{2+} stores has also recently been shown in cultured endothelial cells from bovine aorta (Thuringer & Sauvé, 1992).

This study examines caffeine-induced Ca^{2+} release from $InsP_3$-insensitive intracellular stores in endothelial cells freshly dissociated from rabbit aorta as shown by the activation of Ca^{2+}-sensitive membrane conductances. Caffeine activates an outward current correlated with the rise in $[Ca^{2+}]_i$ which is not completely blocked by bath-applied TEA and is sensitive to the external Cl^- concentration and zinc ions. Preliminary reports of some of these results has been presented previously (Adams *et al.*, 1993; Rusko *et al.*, 1993).

Methods

Experiments were carried out on freshly dissociated endothelial cells obtained from rabbit aorta. Procedures for the preparation of endothelial cells and electrophysiological recordings were as previously described (Rusko *et al.*, 1992). Briefly, pieces of endothelium were peeled from the thoracic aorta of a rabbit killed by CO_2 asphyxiation and incubated for 35 min in a solution containing 0.9 mg ml^{-1} papain and 0.8 mg ml^{-1} dithiothreitol. The tissue was washed and gently triturated in Dulbecco's phosphate-buffered saline (DPBS, pH 7.35; GIBCO Laboratories, NY, U.S.A.) containing 20% foetal calf serum. Following centrifugation, the cells were plated on glass coverslips and stored at 4°C for at least 4 h prior to use that day. Positive identification of cells as endothelial was based on morphological characteristics and specific uptake of rhodamine-fluorescent acetylated low density lipoprotein (1,1,-dioctadecyl-3,3,3,3'-tetramethyl-indocarbocyanine (DiI-Ac-LDL), Biomedical Technologies, Stoughton MA, U.S.A.) as previously described (Rusko *et al.*, 1992).

The physiological saline solution (PSS) used as the external bathing media had the following composition (mM): NaCl 125.4, KCl 5.9, $MgCl_2$ 1.2, $CaCl_2$ 1.5, glucose 11.5, N-2-hydroxy-ethylpiperazine-*N'*-2-ethansulphonic acid (HEPES) 10, titrated to pH 7.35 with NaOH. Whole-cell currents were recorded using a patch pipette filled with an intracellular solution with the following composition (mM): KCl 126, NaCl 5, $MgCl_2$ 1.2, glucose 11, ethyleneglycol-bis-(β-aminoethylether) *N,N,N',N'*-tetraacetic acid (EGTA) 0.8, HEPES 10, titrated to pH 7.2 with KOH. The experiments were carried out at room temperature (23 ± 2°C).

Microfluorometric measurements

Fluorescence measurements of cytoplasmic free Ca^{2+} concentration in single, nonconfluent endothelial cells were carried out with the fluorescent Ca^{2+} indicator dye, fura-2. Freshly dissociated endothelial cells were incubated in PSS containing 1 μM of the acetoxymethyl ester of fura-2 (fura-2/AM dissolved in dimethylsulphoxide, DMSO) at room temperature (23°C) for 30 min, and excess ester was rinsed away with buffered PPS. Endothelial cells on glass coverslips were mounted in an open perfusion microincubator (PDMI-2, Medical Systems Corp., N.Y., U.S.A.) on the stage of an inverted phase contrast microscope (Nikon Diaphot) and continuously superfused at 2 ml min^{-1} with PSS. The temperature of the microincubator and bathing solution was maintained at 37°C by a bipolar temperature controller (TC-202, Medical Systems Corp., N.Y., U.S.A.). Cells were alternatively excited (60 Hz) at 340 nm and 380 nm wavelengths with an optical chopper (OC-4000, PTI) in the path of the u.v. light provided by a 75 W xenon arc lamp. Fura-2 fluorescence viewed with a × 100 Fluor objective (Nikon, 1.3 numerical aperture) was measured at 510 nm wavelength with a photon counter (Hamamatsu R928). Signals were digitized by an A-D converter and analysed with Deltascan software (PTI) on a PC 80486/50 MHz computer. Only single cells with an even dye distribution within the cytoplasm were used. The ratio of signals at the two excitation wavelengths (F_{340}/F_{380}) was determined after subtraction of autofluorescence. $[Ca^{2+}]_i$ was calculated following the method of Grynkiewicz *et al.* (1985).

In a series of experiments, quenching of intracellular fura-2 fluorescence by external Mn^{2+} was carried out to evaluate unidirectional Ca^{2+} movement into endothelial cells (Jacob, 1990). Endothelial cells were bathed in Ca^{2+}-free PSS containing 0.5 mM $MnCl_2$ and the rate of Mn^{2+} influx was determined from the rate of decrease of fura-2 fluorescence from cells excited at 360 nm wavelength. The slope of the fura-2 fluorescence, under control conditions, remained linear for ⩾ 300 s during which time either caffeine or ionomycin were bath applied. Simultaneous monitoring of the emission due to 380 nm excitation and ratioing with the 360 nm signal was used to correlate $[Ca^{2+}]_i$ changes to Mn^{2+} influx.

Electrical recordings

The membrane currents were measured by the whole-cell recording configuration of the patch clamp technique (Hamill *et al.*, 1981) and a List L/M-EPC7 patch-clamp amplifier (List Electronics, Darmstadt, Germany). Voltage ramps (−150 to +100 mV, 4 s duration) were applied using pCLAMP programmes (Axon Instruments Inc, CA, U.S.A.) generated protocols and a PC 80386/33 MHz computer equipped with an A-D/D-A converter (12 bit resolution; Tecmar Labmaster DMA TM-40). Membrane currents were filtered at 2.5 kHz (−3dB, 4-pole Bessel Filter; Ithaco 4302), digitized using a digital VCR recorder adaptor (PCM-1; Medical Systems Corp., N.Y., U.S.A.) and stored for later analysis on videotape. Membrane currents were continuously monitored and the current amplitude was analysed by direct measurement on a digital oscilloscope (Tektronix 5223). Whole-cell and unitary currents were displayed on a chart recorder (Gould 2200S) and outward currents are shown as upward deflections. Numerical data are represented as the mean ± one standard error of the mean (s.e.mean).

Reagents

All chemical reagents used were of analytical grade. The following drugs were used: acetylcholine chloride, caffeine, papain, theophylline, ethylene glycol-*bis*(β-aminoethyl ether) *N,N,N,N*-tetraacetic acid (EGTA), heparin, sodium salt (mol. wt. 4,000–6,000), dimethyl sulphoxide (DMSO) (obtained from Sigma Chemical Co., St. Louis, MO, U.S.A.), tetraethylammonium chloride (TEA; Eastman Kodak Co., Rochester, N.Y., U.S.A.), D-gluconic acid, sodium salt (Aldrich Chemical Co., Milwaukee, WI, U.S.A.) and ryanodine, ionomycin (Calbiochem Corp., La Jolla, CA, U.S.A.).

Results

Caffeine-induced Ca^{2+} release from ryanodine-sensitive intracellular stores

Fura-2-loaded endothelial cells freshly dissociated from rabbit aorta exhibit a resting F_{340}/F_{380} ratio of 0.56 ± 0.01 ($n = 64$) which corresponds to a $[Ca^{2+}]_i$ of 82 ± 4 nM. Bath application of 5 mM caffeine evokes a transient increase in $[Ca^{2+}]_i$. Superfusion of endothelial cells with PSS containing 5 mM caffeine produced a rise in $[Ca^{2+}]_i$ to a peak F_{340}/F_{380} ratio of 2.11 ± 0.08 (866 ± 83 nM, $n = 64$) which corresponds to an approximately ten fold increase in $[Ca^{2+}]_i$ (Figure 1a). Another methylxanthine, theophylline (5 mM), also evoked a transient increase in $[Ca^{2+}]_i$ of similar magnitude and time course to that observed in response to caffeine (not shown). Pretreatment of the cells with 10 μM ryanodine did not alter resting $[Ca^{2+}]_i$; however, following >20 min exposure to ryanodine, the caffeine-induced rise in $[Ca^{2+}]_i$ was completely blocked (Figure 1b). This block was irreversible even after >30 min washout ($n = 6$).

Figure 2 shows that a higher caffeine concentration (20 mM) evokes a biphasic increase in $[Ca^{2+}]_i$: an initial transient increase, of similar magnitude to that produced by 5 mM caffeine, which decreases to a plateau phase of variable amplitude ($n = 11$). In a Ca^{2+}-free (1 mM EGTA) external solution the plateau phase following the caffeine-induced transient rise in $[Ca^{2+}]_i$ was abolished (Figure 2b). Analogous to the agonist-induced $[Ca^{2+}]_i$ response observed in endothelial cells, the transient $[Ca^{2+}]_i$ peak most probably reflects Ca^{2+} release from intracellular stores whereas the external Ca^{2+}-dependent plateau phase of the caffeine-induced $[Ca^{2+}]_i$ response may be due to an increased plasmalemmal Ca^{2+} influx.

To determine if Ca^{2+} influx is stimulated by bath application of caffeine, the fluorescence of fura-2-loaded cells was measured at excitation wavelengths of 360 and 380 nm with 0.5 mM $MnCl_2$ added to Ca^{2+}-free PSS. Assuming Mn^{2+} is a suitable marker for Ca^{2+} entry in endothelial cells (Jacob, 1990), Ca^{2+} influx can be inferred from the decrease of the fluorescence signal obtained at 360 nm excitation. The slope of the 360 nm fluorescence signal, reflecting the rate of Mn^{2+}

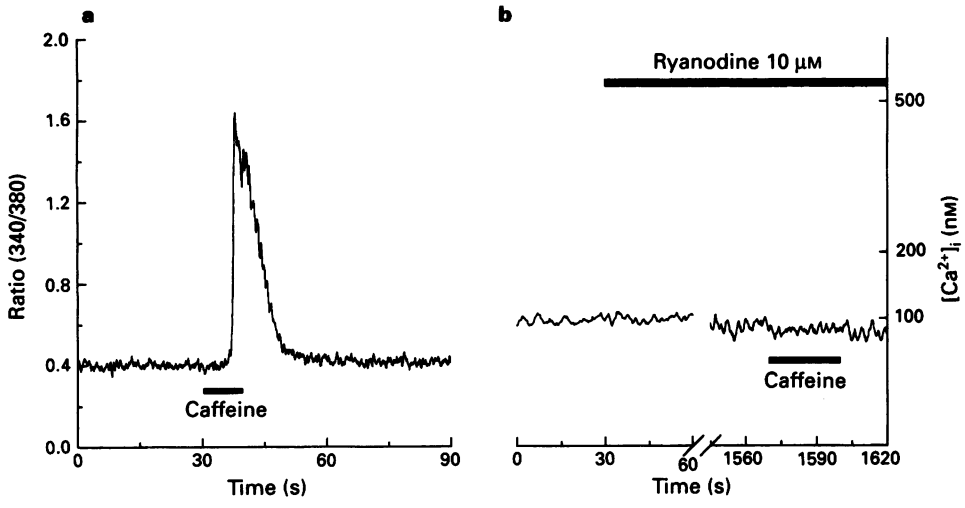

Figure 1 Caffeine- and ryanodine-sensitive $[Ca^{2+}]_i$ responses in rabbit aortic endothelial cells. (a) The intracellular Ca^{2+} response of an isolated, fura-2-loaded rabbit aortic endothelial cell to bath (PSS)-application of 5 mM caffeine. (b) Blockade of the caffeine-induced transient rise in $[Ca^{2+}]_i$ following treatment of an endothelial cell with 10 μM ryanodine for 25 min. This trace is representative of six experiments.

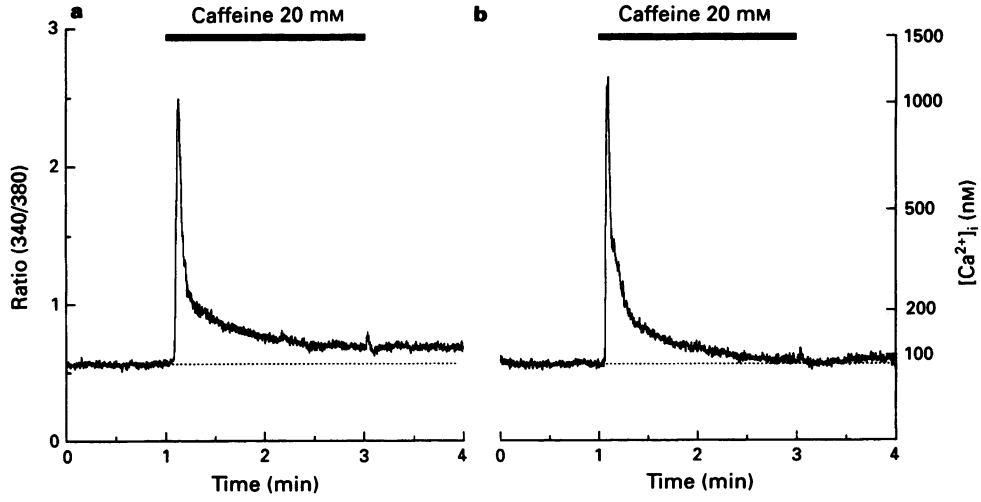

Figure 2 Caffeine-induced increase in $[Ca^{2+}]_i$ in the presence (a) and absence (b) of extracellular Ca^{2+}. Caffeine (20 mM)-induced increase in $[Ca^{2+}]_i$ in an isolated, fura-2-loaded rabbit aortic endothelial cell obtained in normal PSS containing 1.5 mM Ca^{2+} (a) and in a Ca^{2+}-free external solution containing 1 mM EGTA (b). These traces are representative of 11 experiments for each condition.

quench of fura-2 fluorescence, remained unchanged following the addition of 5–20 mM caffeine ($n = 8$). The F_{360}/F_{380} ratio exhibited a transient increase in response to caffeine due to Ca^{2+} release from intracellular stores (not shown). As a positive control, superfusion of endothelial cells with Ca^{2+}-free PSS containing 1 μM ionomycin, a divalent cation ionophore, produced a 11.9 ± 1.9-fold ($n = 3$) increase in the rate of Mn^{2+} quench of fura-2 fluorescence.

Caffeine-induced outward currents in native endothelial cells

Unitary currents and STOCs due to the activation of Ca^{2+}-dependent K^+ channels were observed in freshly dissociated endothelial cells from rabbit aorta at membrane potentials positive to −40 mV (Rusko *et al.*, 1992). Bath application of caffeine (5 and 20 mM) evoked a dose- and voltage-dependent

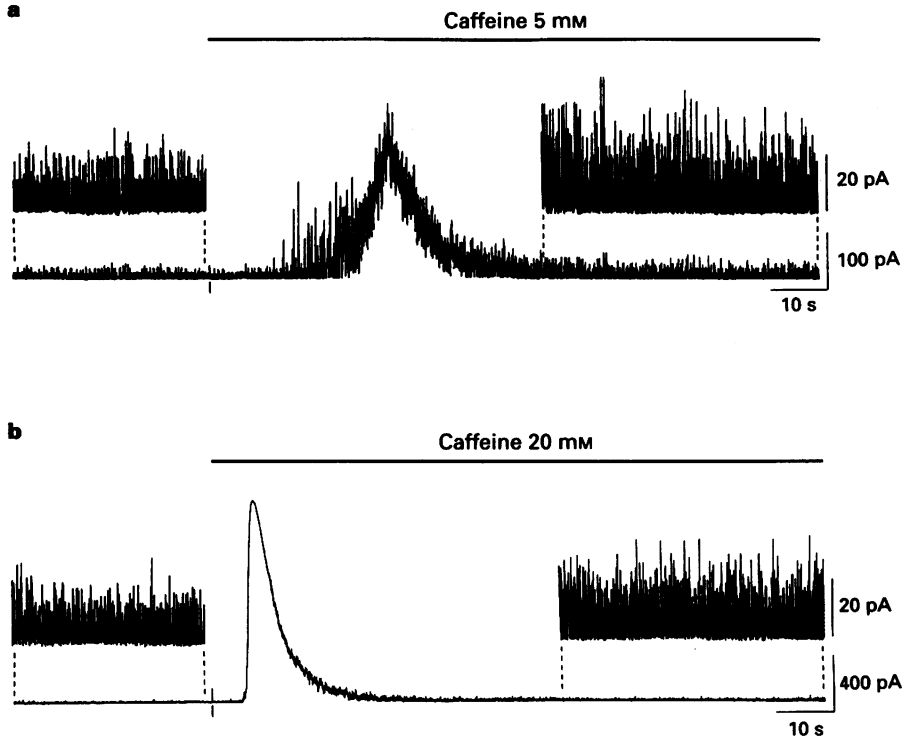

Figure 3 Caffeine-evoked outward currents in rabbit aortic endothelial cells. Continuous traces of unitary currents and STOCs recorded prior to and during exposure to 5 mM caffeine (a) and in the presence of 20 mM caffeine (b). Bath-applications of PSS containing caffeine are indicated by the horizontal bars. Upper traces show current activities at expanded current scales. Holding potential, +20 mV. Traces shown are representative of 3 experiments.

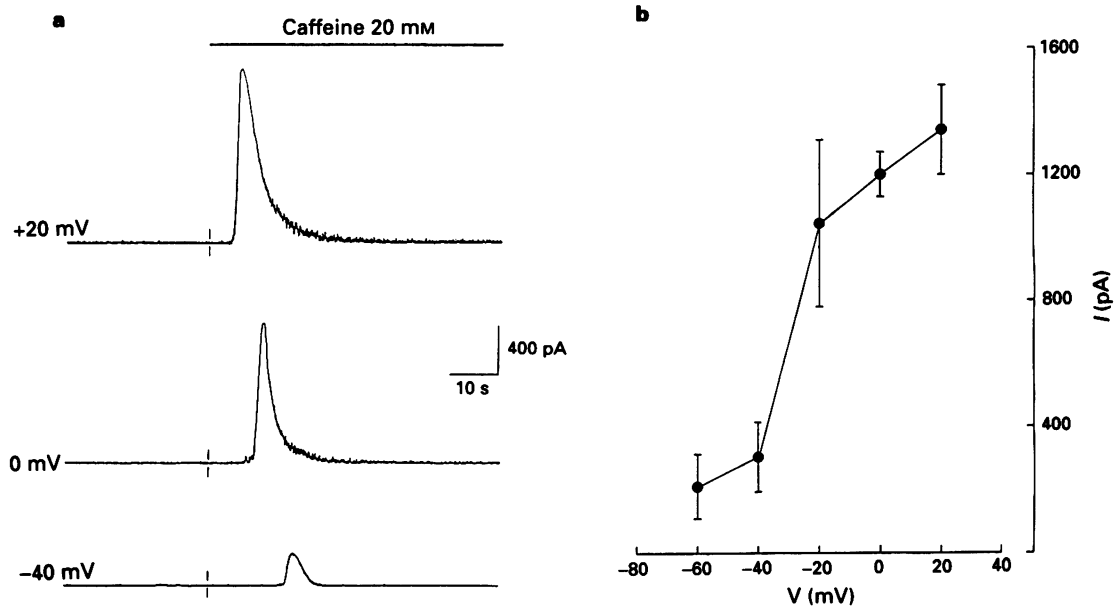

Figure 4 Voltage-dependence of transient whole-cell outward currents evoked by caffeine in rabbit aortic endothelial cells. (a) Traces of the outward currents evoked by PSS containing 20 mM caffeine at holding potentials of +20, 0, and −40 mV. (b) The current-voltage relationship obtained for the peak amplitude of the caffeine-induced outward current determined in six cells.

outward current in these endothelial cells. Figure 3a shows a typical whole-cell current response to bath application of 5 mM caffeine, producing an increase in the frequency and amplitude of unitary currents and STOCs. The frequency of STOCs increased 304 ± 18% ($n = 3$) following 3 min bath perfusion of PSS containing 5 mM caffeine ($n = 3$). The initial burst of these currents is superimposed on a slowly developing outward current which peaks at approximately 375 pA amplitude (Figure 3a). At a higher caffeine concentration (20 mM), the transient outward current amplitude increased to >1 nA (1.3 ± 0.14 nA, $n = 5$) and had durations of 7–15 s in endothelial cells held at +20 mV (Figure 3b). In the continued presence of caffeine, the frequency and amplitude of unitary currents and STOCs were increased compared to control conditions prior to caffeine application. The rapid onset of the outward current evoked by caffeine suggests a close spatial relationship between the intracellular Ca^{2+} stores and plasmalemmal Ca^{2+}-dependent K^+ channels. A long-lasting outward current in response to a second application of caffeine was not observed after >5 min washout (not shown).

Figure 4 describes the voltage-dependence of the caffeine-induced outward current in voltage-clamped endothelial cells. Bath application of 20 mM caffeine evoked an outward current that increased in amplitude with membrane depolarization, saturating at approximately +20 mV. Representative whole-cell outward currents evoked by 20 mM caffeine at three different membrane potentials are shown in Figure 4a.

The relationship between caffeine-induced current amplitude and membrane potential averaged from six cells is shown in Figure 4b. The activation of the outward current is non-linear suggesting that the ionic channels underlying the caffeine-induced current are voltage-sensitive. The membrane potential at which half-maximal activation of the caffeine-induced outward current is observed is shifted by approximately −40 mV compared to that obtained for activation of the Ca^{2+}-dependent K^+ current in rabbit aortic endothelial cells (Demirel *et al.*, 1994) suggesting that another ionic conductance may contribute to the caffeine-evoked outward current.

Dependence of outward currents on extracellular Ca^{2+}

The open-state probability of the unitary K^+ currents in rabbit aortic endothelial cells is sensitive to $[Ca^{2+}]_i$ (Rusko *et al.*, 1992; Demirel *et al.*, 1994). The unitary current activity was also affected by the extracellular $[Ca^{2+}]$. A decrease in the extracellular $[Ca^{2+}]$ may be expected to affect $[Ca^{2+}]_i$ by increasing Ca^{2+} efflux and reducing Ca^{2+} influx across the cell membrane. The dependence of unitary currents, STOCs and the caffeine-induced outward current on the extracellular $[Ca^{2+}]$ was examined in endothelial cells bathed in Ca^{2+}-free

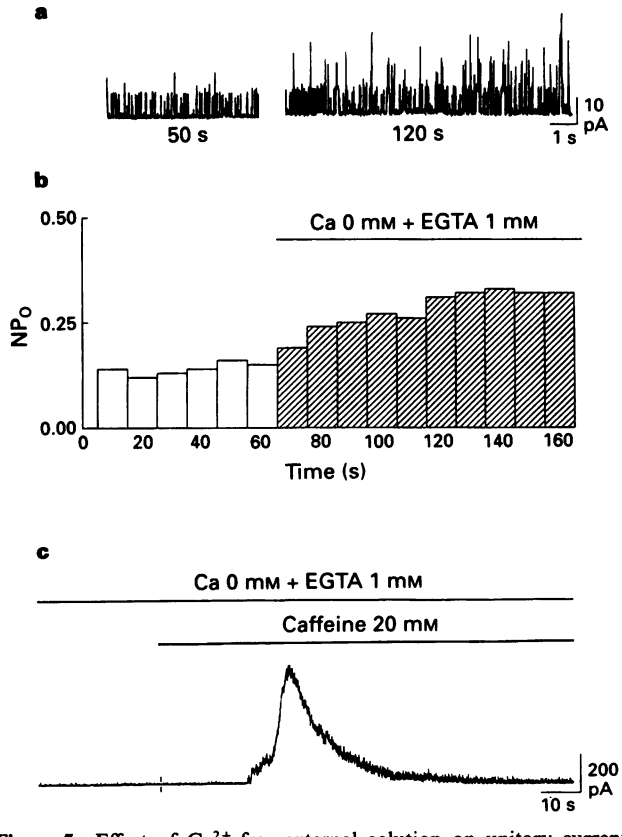

Figure 5 Effect of Ca^{2+}-free external solution on unitary currents and STOCs in aortic endothelial cells. (a) Unitary currents and STOCs recorded at holding potential +20 mV before (control, $t = 50$ s) and during exposure to Ca^{2+}-free (0 mM Ca^{2+}, $t = 120$ s) external solution. Traces shown are representative of 9 experiments. (b) Time course of change in NP_0 (10 s bin width) of unitary and STOCs before and during exposure to a Ca^{2+}-free external solution (horizontal bar). (c) Continuous record of membrane current observed following exposure to 20 mM caffeine in the presence of Ca^{2+}-free, EGTA containing solution for the periods indicated by the horizontal bars. Holding potential, +20 mV. Trace shown is representative of 4 experiments.

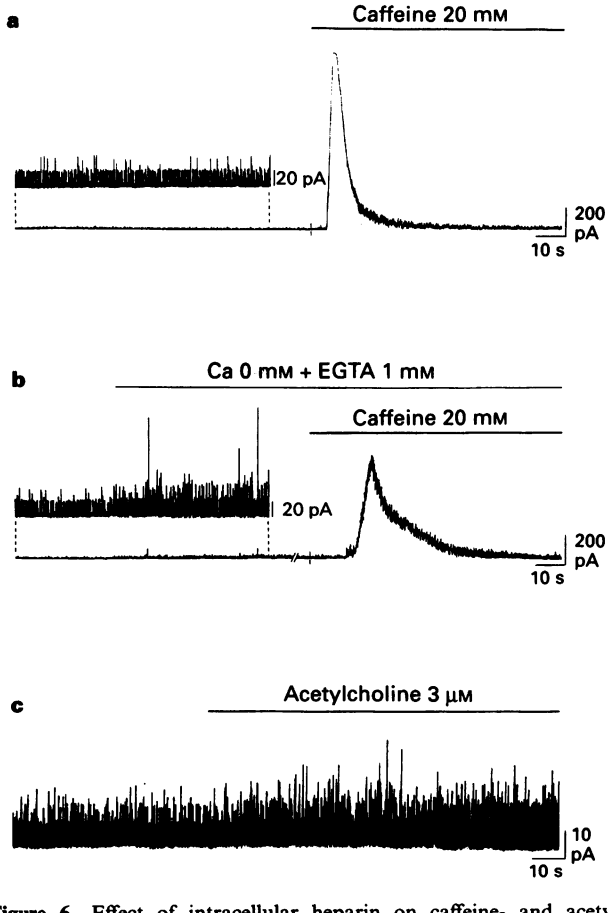

Figure 6 Effect of intracellular heparin on caffeine- and acetylcholine (ACh)-evoked outward currents in endothelial cells. (a). Caffeine-evoked outward current recorded at a holding potential of +20 mV from a cell bathed in PSS containing 1.5 mM $CaCl_2$. (b) Caffeine-evoked outward current obtained in the absence of extracellular Ca^{2+} (1 mM EGTA). (c) Unitary outward currents recorded in the absence and presence of bath applied 3 μM acetylcholine. Whole-cell currents recorded from endothelial cells dialyzed with pipette solution containing 10 μg ml^{-1} heparin. Traces shown are representative of at least 5 experiments for each condition. Horizontal bars indicate period during which the cell was bathed in an extracellular solution containing caffeine (20 mM), no added Ca^{2+}(0 mM Ca^{2+} + 1 mM EGTA) or acetylcholine (3 μM). Holding potential +20 mV.

medium containing 1 mM EGTA. Figure 5a shows an unexpected increase in both the frequency and the amplitude of STOCs produced by exposure to a Ca^{2+}-free external solution ($n = 9$). A plot of the open-channel probability (NP_0) of the unitary Ca^{2+}-dependent K^+ currents as a function of time is shown in Figure 5b.

In the absence of extracellular Ca^{2+}, caffeine (20 mM) continued to evoke a transient, outward current but the amplitude (572 ± 138 pA, $n = 4$) was reduced by approximately 50% compared to that observed in the presence of extracellular Ca^{2+} (Figure 5c). However, the caffeine-induced outward current was significantly prolonged lasting 35–45 s, a >30% increase. Moreover, the transient outward current evoked by caffeine in Ca^{2+}-free solution appears to be composed of two superimposed currents: the initial increase in current appears as a shoulder preceding a second current of larger amplitude. In the continued presence of caffeine in Ca^{2+}-free solution, unitary currents and STOCs occurred at both a higher frequency and amplitude than that observed under control conditions prior to caffeine application.

The effects of heparin on Ca^{2+} release from intracellular stores

Heparin, a specific competitive antagonist of the $InsP_3$ receptor, has been shown to inhibit $InsP_3$-mediated Ca^{2+} release from intracellular stores in a variety of cell types (Ghosh *et al.*, 1988). Inclusion of heparin (10 μg ml^{-1}) in the patch pipette had no noticeable influence on either unitary currents or STOCs in native aortic endothelial cells under resting conditions. Heparin failed to prevent the increase in both frequency and amplitude of unitary currents and STOCs observed following the removal of extracellular Ca^{2+}.

The effects of intracellular heparin on the caffeine-induced current activation were examined in voltage-clamped endothelial cells. Figure 6a shows membrane currents obtained in response to bath application of 20 mM caffeine in cells held at +20 mV in the presence of 10 μg ml^{-1} heparin in the patch pipette solution. The large, long-lasting outward current evoked by caffeine in normal PSS (1108 ± 363 pA, $n = 5$) appears similar to that observed in the absence of intracellular heparin (Figure 3b). Similarly the presence of heparin in the pipette (Figure 6b) failed to abolish the caffeine-evoked outward current in the absence of extracellular Ca^{2+}. The amplitude of the caffeine-evoked current was approximately half (557 ± 132 pA, $n = 6$) of that observed in the presence of 1.5 mM extracellular Ca^{2+}. Figure 6c shows the result of a control experiment indicating that heparin had diffused into the cell. The addition of 10 μg ml^{-1} heparin to the pipette inhibited the ACh (3 μM)-induced outward K^+ current ($n = 5$) observed in the absence of intracellular heparin (*cf.* Figure 6, Rusko *et al.*, 1992).

Pharmacological block of caffeine-induced outward currents

Evidence that Ca^{2+}-dependent K channels underlie the unitary and spontaneous transient outward currents observed in rabbit aortic endothelial cells is provided, in part, by the inhibition of these currents by Ca^{2+}-dependent K channel blockers, tetraethylammonium ions (TEA) and charybdotoxin (Rusko *et al.*, 1992). Externally applied TEA

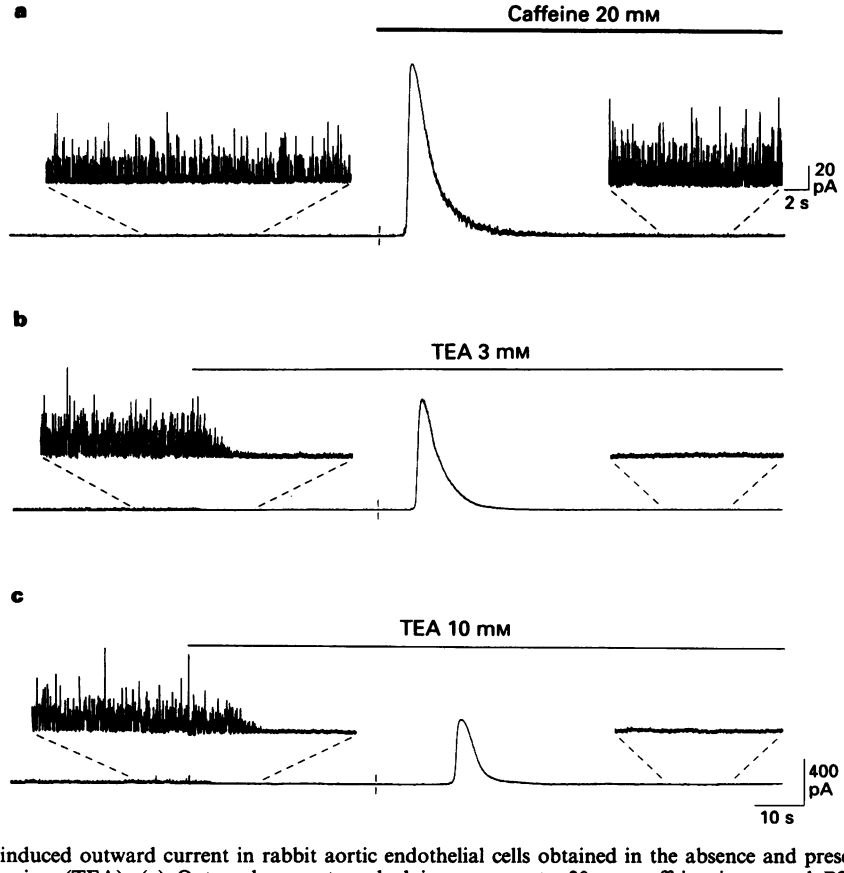

Figure 7 Caffeine-induced outward current in rabbit aortic endothelial cells obtained in the absence and presence of bath applied tetraethylammonium ion (TEA). (a) Outward current evoked in response to 20 mM caffeine in normal PSS. Caffeine-induced outward currents obtained in the presence of either 3 mM (b) or 10 mM (c) TEA. The top horizontal bar indicates the times at which caffeine was bath applied for all three traces. The horizontal bars shown in (b) and (c) indicate times at which TEA was bath-applied. Holding potential, +20 mV. Lower scale bars indicate the time and current magnitude for traces in (a), (b) and (c). Upper scale bars indicate time and current magnitudes for all expanded inserts. Traces shown are representative of at least 3 experiments.

(3–10 mM) reversibly inhibited unitary currents and STOCs observed in endothelial cells clamped at +20 mV but failed to inhibit completely the large, prolonged outward current evoked by caffeine (Figure 7b,c). Figure 7 shows that the prolonged outward current evoked by 20 mM caffeine was reduced in a concentration-dependent manner by extracellular TEA. The amplitude of the caffeine-induced outward current was reduced by 16% (1095 ± 209 pA, $n = 4$) and by 63% (480 ± 35 pA, $n = 3$) in the presence of 3 mM and 10 mM TEA, respectively. In the maintained presence of TEA, unitary currents and STOCs were not observed following caffeine stimulation. Although TEA partially inhibited the caffeine-evoked outward current, the inability of TEA to block completely the prolonged outward current evoked by caffeine suggests that another ionic conductance may be activated in the presence of caffeine.

In order to examine the contribution of a chloride conductance to the caffeine-induced outward current, zinc ion (Zn^{2+}), a chloride channel blocker, was bath-applied to voltage-clamped endothelial cells. Bath-application of 0.1 mM Zn^{2+} produced a small, sustained inward current of <5 pA amplitude but did not affect unitary currents or STOCs. The peak amplitude of the caffeine (20 mM)-induced outward current, however, was reduced by $>75\%$ (246 ± 35 pA, $n = 4$) in the presence of 0.1 mM Zn^{2+} (Figure 8a) compared to that obtained in normal PSS (Figure 3a). The caffeine-induced outward current was examined in the presence of both Zn^{2+} and TEA. Bath application of 0.1 mM Zn^{2+} and 10 mM TEA abolished unitary currents and STOCs and inhibited the caffeine (20 mM)-evoked outward current by $>95\%$ (<50 pA) after 5 min perfusion (Figure 8b). In 19 of 21 cells, bath application of both Zn^{2+} and TEA completely blocked the caffeine-induced outward current within 5 min, and longer exposure abolished the response in all 21 cells. Replacement of extracellular NaCl with Na gluconate reduced the amplitude of the caffeine (20 mM)-evoked outward current by approximately 30% (930 ± 144 pA, $n = 3$) compared to that obtained in normal PSS (not shown). Taken together, these results indicate that caffeine-induced Ca^{2+} release activates a Cl^--conductance in addition to a K^+ conductance in arterial endothelial cells.

Discussion

Results from this study demonstrate that caffeine stimulates Ca^{2+} release from intracellular stores, elevating cytoplasmic $[Ca^{2+}]$ which activates membrane currents in native endothelial cells from rabbit aorta. Ca^{2+}-dependent K^+ currents have been shown to be regulated by the $[Ca^{2+}]_i$ which is influenced by plasmalemmal Ca^{2+} influx and Ca^{2+} release from internal stores (Rusko *et al.*, 1992; Adams *et al.*, 1993). Bath application of caffeine, which stimulates Ca^{2+} release from internal stores, evoked a transient increase in $[Ca^{2+}]_i$ and an outward current both of which were sustained in the absence of extracellular Ca^{2+}. Caffeine-induced Ca^{2+} release from intracellular stores was dose-dependent and inhibited by prolonged exposure to ryanodine (10^{-5} M), an inhibitor of the Ca^{2+} release channel of sarcoplasmic reticulum (Nagasaki & Fleischer, 1988). These data indicate the presence of functional caffeine- and ryanodine-sensitive intracellular Ca^{2+} stores in freshly dissociated endothelial cells from rabbit aorta.

The inability of Ca^{2+}-free external solutions to inhibit unitary currents and STOCs suggests that Ca^{2+} entry from the extracellular space is not necessary for maintaining the activity of these currents and that the release of intracellular stores is a sufficient source of Ca^{2+} for activation of Ca^{2+}-dependent K channels in native endothelial cells. The increase in both the frequency and amplitude of unitary currents and STOCs observed in the presence of Ca^{2+}-free external solution contrasts with the inhibition of STOCs observed in jejunal and arterial smooth muscle cells (Benham & Bolton, 1986). Differences in the Ca^{2+} sensitivity of the Ca^{2+}-dependent K channels may be related to the different functions of these three cell types. Our data suggest that in the absence of extracellular Ca^{2+}, stored Ca^{2+} may be released into the cytoplasm and subsequently resequestered into intra-

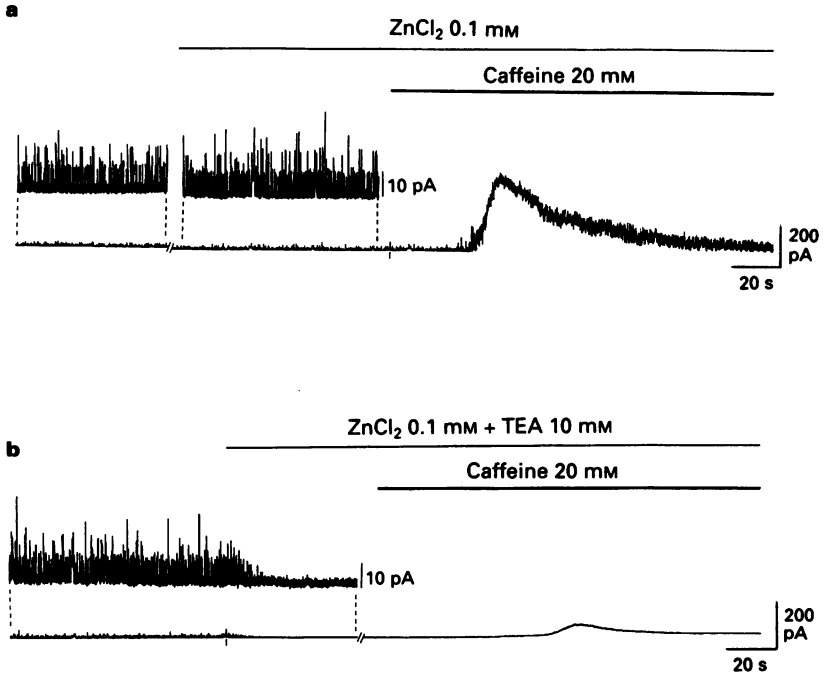

Figure 8 Caffeine-induced membrane currents in the presence of tetraethylammonium (TEA) and zinc ions. (a) Outward currents recorded in response to 20 mM caffeine in the presence of 0.1 mM $ZnCl_2$. Traces shown are representative of 4 experiments. (b) Response of a cell to 20 mM caffeine following 5 min incubation in PSS containing 0.1 mM $ZnCl_2$ and 10 mM TEA. Horizontal bars indicate times at which $ZnCl_2$, TEA and caffeine were applied. Holding potential, +20 mV.

cellular stores rather than lost from the endothelial cell. Transient local fluctuations in $[Ca^{2+}]_i$ from superficial Ca^{2+} stores adjacent to the plasmalemma may contribute to the rapid repetitive discharges of unitary currents and STOCs even in the prolonged absence (> 30 min) of extracellular Ca^{2+}. The mechanisms by which the amplitude and frequency of unitary currents and STOCs are modulated by external Ca^{2+} are not yet understood.

The ability of caffeine to evoke a long-lasting outward current in Ca^{2+}-free external solution, albeit of smaller amplitude than that obtained in the presence of extracellular Ca^{2+}, also suggests that the release of intracellular Ca^{2+} stores may be an important source of Ca^{2+} for activation of Ca^{2+}-sensitive ion channels in native endothelial cells. However, it is not possible to determine whether the reduced amplitude of the caffeine-induced outward current observed in Ca^{2+}-free solution is due to a partial depletion of intracellular Ca^{2+} stores or to an impaired ability to release the complete amount of intracellular stored Ca^{2+}. Microfluorometric measurements of fura-2-loaded endothelial cells suggest that the increased unitary current activity induced by prolonged application of caffeine is probably due to sustained elevation of $[Ca^{2+}]_i$. The lack of effect of caffeine on the rate of Mn^{2+} quench of fura-2 fluorescence suggests that the sustained elevation of $[Ca^{2+}]_i$ induced by caffeine is primarily due to release of Ca^{2+} from intracellular stores rather than due to Ca^{2+} influx. In bovine cultured aortic endothelial cells, caffeine has been shown to release only a small fraction of Ca^{2+} from the intracellular stores in the absence of extracellular Ca^{2+} (Buchan & Martin, 1991). By contrast, our results obtained in freshly dissociated rabbit aortic endothelial cells indicate that a significant amount of Ca^{2+} is mobilized by caffeine. The preservation of approximately one half (~52%) of the caffeine-induced outward current following prolonged superfusion with Ca^{2+}-free solution, suggests that the release of Ca^{2+} from intracellular stores plays a significant role in caffeine-induced Ca^{2+} stimulation of vascular endothelial cells.

There is considerable evidence demonstrating that $InsP_3$ triggers the initial phase of the agonist-induced Ca^{2+} mobilization from endoplasmic reticulum in endothelial cells (Pollock *et al.*, 1988; Freay *et al.*, 1989). However, the possibility that outward currents in native endothelial cells are stimulated by cyclical release of Ca^{2+} from $InsP_3$-sensitive Ca^{2+} stores can be ruled out from the results of experiments using heparin as an inhibitor of the $InsP_3$-induced Ca^{2+} release mechanism. ACh-evoked outward K^+ currents were inhibited by the inclusion of 10 $\mu g\ ml^{-1}$ heparin in the patch pipette solution (see Figure 5c; Sakai, 1990). Heparin, however, had no effect on either the caffeine-induced long-lasting outward currents or the increased frequency and amplitude of unitary currents and STOCs evoked by Ca^{2+}-free external solutions. These results suggest the presence of $InsP_3$-insensitive Ca^{2+} stores in freshly dissociated endothelial stores which may be activated by a Ca^{2+}-induced Ca^{2+} release mechanism.

The presence of anti-ryanodine receptor antibody binding sites has recently been demonstrated in vascular and endocardial endothelium (Lesh *et al.*, 1993). Furthermore, the light microscopic distribution of endothelial immunofluorescence indicates that the binding sites are localized on the endoplasmic reticulum (ER). The presence of functional ryanodine-sensitive Ca^{2+} stores has recently been shown by both a direct effect of ryanodine on resting $[Ca^{2+}]_i$ in human cultured aortic, umbilical vein and bovine pulmonary artery endothelial cells, and by attenuation of the agonist-induced $[Ca^{2+}]_i$ transient increase in rat aortic endothelial cells by ryanodine (Ziegelstein *et al.*, 1994). These results suggest that ryanodine-sensitive Ca^{2+} stores in cultured endothelial cells can effectively deplete the $InsP_3$-sensitive intracellular Ca^{2+} pool. In contrast, our data obtained in the presence of intracellular heparin suggests that in rabbit aortic endothelial cells the caffeine- and ryanodine-sensitive Ca^{2+} stores may be functionally distinct from the agonist-sensitive Ca^{2+} stores (see Figure 6). However, ryanodine (10^{-5} M) has been shown to produce a time-dependent decrease in ACh-induced outward current amplitude in rabbit aortic endothelial cells (Sakai, 1990). A recent study of endothelial cells freshly dispersed from porcine coronary arteries suggests a heterogeneity in functional organization of endothelial Ca^{2+} stores, whereby, in a population of cells (quiet-responders), caffeine translocates Ca^{2+} towards the bradykinin ($InsP_3$)-sensitive store, while in another population (overt-responders), caffeine empties the $InsP_3$-sensitive store (Graier *et al.*, 1994).

TEA, an inhibitor of Ca^{2+}-dependent K^+ currents and STOCs in rabbit aortic endothelial cells, failed to inhibit completely the caffeine-induced outward current suggesting the presence of a TEA-insensitive component of the outward current. Evidence that Cl^- may contribute to the caffeine-evoked outward current was obtained from results of measurements made in the presence of external Zn^{2+} and when external Cl^- was replaced with gluconate. Extracellular Zn^{2+} has been shown to block a Cl^- conductance in skeletal muscle (Hutter & Warner, 1967) and inhibit unitary Cl^- currents in excised muscle membrane patches (Woll *et al.*, 1987). In the present study, external Zn^{2+} reduced the amplitude but did not completely block the caffeine-evoked outward current. However, bath-application of both Zn^{2+} and TEA completely blocked this outward current in most endothelial cells. These results suggest that both K^+ and Cl^- contribute as charge carriers to the caffeine-evoked outward current in endothelial cells. Whole-cell and single channel Cl^- currents which are blocked by Zn^{2+}, have been described in bovine pulmonary artery endothelial cells (Shapiro & DeCoursey, 1991). Ca^{2+}-activated Cl^- currents have also been recently reported in arterial endothelial cells, suggesting that the elevation of $[Ca^{2+}]_i$ may activate these Cl^- channels and produce an outward current depending on the Cl^- equilibrium potential (Groschner & Kukovetz, 1992; Vaca & Kunze, 1993).

Caffeine not only releases Ca^{2+} from intracellular stores but also affects a number of other cellular functions including membrane electrical properties, Ca^{2+} influx, Ca^{2+} extrusion and modulation of phosphodiesterases which regulate cyclic AMP levels. Caffeine has also been shown to inhibit voltage-dependent calcium channels in smooth muscle cells (Hughes *et al.*, 1990; Zholos *et al.*, 1991). Additionally, we found that prolonged exposure of endothelial cells to caffeine induces cell shrinkage. Although the mechanism underlying the caffeine-induced shrinkage is unknown, it has been shown that hypotonic volume increases activate a Cl^- current in human endothelial cells (Nilius *et al.*, 1994) suggesting that caffeine-sensitive, Ca^{2+}-activated Cl^- currents may regulate cell volume.

In conclusion, these findings suggest that Ca^{2+}-induced Ca^{2+} release may modulate ER Ca^{2+} release in arterial endothelial cells. The activation of plasmalemmal ion channels by an elevation of $[Ca^{2+}]_i$ due to caffeine-induced Ca^{2+} release from intracellular stores is characterized by a large, transient outward current. The ionic dependence and pharmacological profile of the caffeine-evoked current suggests that Ca^{2+}-sensitive K^+ and Cl^- conductances contribute to the caffeine response in rabbit aortic endothelial cells.

We thank Drs Christopher Katnik and Richard Kramer for their constructive criticism of a draft of this manuscript. This research was supported by National Institutes of Health grants RO1 HL-39831 and HL-35422. G.V.S. was supported by NIH training grant HL-07188.

References

ADAMS, D.J., RUSKO, J. & VAN SLOOTEN, G. (1993). Calcium signalling in vascular endothelial cells: Ca^{2+} entry and release. In *Ion Flux in Pulmonary Vascular Control.* ed. Weir, E.K., Hume, J.R. & Reeves, J.T. NATO ASI Series, Vol. 251, pp. 259–275. New York: Plenum Press.

BENHAM, C.D. & BOLTON, T.B. (1986). Spontaneous transient outward currents in single visceral and vascular smooth muscle cells of rabbit. *J. Physiol.*, **381,** 385–406.

BOLTON, T.B. & LIM, S.P. (1989). Properties of calcium stores and transient outward currents in single smooth muscle cells of rabbit intestine. *J. Physiol.*, **409,** 385–401.

BUCHAN, K.W. & MARTIN, W. (1991). Bradykinin induces elevations of cytosolic calcium through mobilization of intracellular and extracellular pools in bovine aortic endothelial cells. *Br. J. Pharmacol.*, **102,** 35–40.

DEMIREL, E., RUSKO, J., LASKEY, R.E., ADAMS, D.J. & VAN BREEMEN, C. (1994). TEA inhibits ACh-induced EDRF release: endothelial Ca^{2+}-dependent K^+ channels contribute to vascular tone. *Am. J. Physiol.*, **267,** H1135–H1141.

ENDO, M. (1985). Calcium release from sarcoplasmic reticulum. *Curr. Top. Membr. Transp.*, **25,** 181–230.

FREAY, A., JOHNS, A., ADAMS, D.J., RYAN, U.S. & VAN BREEMEN, C. (1989). Bradykinin and inositol-1,4,5-triphosphate stimulated calcium release from intracellular stores in cultured bovine endothelial cells. *Pflügers Arch.*, **414,** 377–384.

GHOSH, T.K., EIS, P.S., MULLANEY, J.M., EBERT, C.L. & GILL, D.L. (1988). Competitive, reversible, and potent antagonism of inositol 1,4,5-trisphosphate-activated calcium release by heparin. *J. Biol. Chem.*, **263,** 11075–11079.

GRAIER, W.F., SIMECEK, S., BOWLES, D.K. & STUREK, M. (1994). Heterogeneity of caffeine- and bradykinin-sensitive Ca^{2+} stores in vascular endothelial cells. *Biochem. J.*, **300,** 637–641.

GROSCHNER, K. & KUKOVETZ, W.R. (1992). Voltage-sensitive chloride channels of large conductance in the membrane of pig aortic endothelial cells. *Pflügers Arch.*, **421,** 209–217.

GRYNKIEWICZ, G., POENIE, M. & TSIEN, R.Y. (1985). A new generation of Ca^{2+} indicators with greatly improved fluorescence properties. *J. Biol. Chem.*, **260,** 3440–3450.

HALLAM, T.J., JACOB, R. & MERRITT, J.E. (1989). Influx of bivalent cations can be independent of receptor stimulation in human endothelial cells. *Biochem. J.*, **259,** 125–129.

HAMILL, O.P., MARTY, A., NEHER, E., SAKMANN, B. & SIGWORTH, F.J. (1981). Improved patch-clamp techniques for high resolution current recording from cells and cell-free membrane patches. *Pflügers Arch.*, **391,** 85–100.

HIMMEL, H.M., WHORTON, A.R. & STRAUSS, H.C. (1993). Intracellular calcium, currents, and stimulus-response coupling in endothelial cells. *Hypertension*, **21,** 112–127.

HUGHES, A.D., HERING, S. & BOLTON, T.B. (1990). The action of caffeine on inward barium current through voltage-dependent calcium channels in single rabbit ear artery cells. *Pflügers Arch.*, **416,** 462–466.

HUTTER, O.F. & WARNER, A.E. (1967). Action of some foreign cations and anions on the chloride permeability of frog muscle. *J. Physiol.*, **189,** 445–460.

JACOB, R. (1990). Agonist-stimulated divalent cation entry into single cultured human umbilical vein endothelial cells. *J. Physiol.*, **421,** 55–77.

JAFFE, E.A., GRULICH, J., WEKSLER, B.B., HAMPEL, G. & WATANABE, K. (1987). Correlation between thrombin-induced prostacyclin production and inositol trisphosphate and cytosolic free calcium levels in cultured human endothelial cells. *J. Biol. Chem.*, **262,** 8557–8565.

LESH, R.E., MARKS, A.R., SOMLYO, A.V., FLEISCHER, S. & SOMLYO, A.P. (1993). Anti-ryanodine receptor antibody binding sites in vascular and endocardial endothelium. *Circ. Res.*, **72,** 481–488.

LÜCKHOFF, A., POHL, U., MÜLSCH, A. & BUSSE, R. (1988). Differential role of extra- and intracellular calcium in the release of EDRF and prostacyclin from cultured endothelial cells. *Br. J. Pharmacol.*, **95,** 189–196.

NAGASAKI, K. & FLEISCHER, S. (1988). Ryanodine sensitivity of the calcium release channel of sarcoplasmic reticulum. *Cell Calcium*, **9,** 1–7.

NILIUS, B., OIKE, M., ZAHRADNIK, I. & DROOGMANS, G. (1994). Activation of a Cl^- current by hypotonic volume increase in human endothelial cells. *J. Gen. Physiol.*, **103,** 787–805.

POLLOCK, W.K., WREGGETT, K.A. & IRVINE, R.F. (1988). Inositol phosphate production and Ca^{2+} mobilization in human umbilical-vein endothelial cells stimulated by thrombin and histamine. *Biochem. J.*, **256,** 371–376.

POZZAN, T., RIZZUTO, R., VOLPE, P. & MELDOLESI, J. (1994). Molecular and cellular physiology of intracellular calcium stores. *Physiol. Rev.*, **74,** 595–636.

RUSKO, J., TANZI, F., VAN BREEMEN, C. & ADAMS, D.J. (1992). Calcium-activated potassium channels in native endothelial cells from rabbit aorta: Conductance, Ca^{2+} sensitivity and block. *J. Physiol.*, **455,** 601–621.

RUSKO, J., VAN BREEMEN, C. & ADAMS, D.J. (1993) Caffeine-induced Ca^{2+} release from intracellular stores in freshly dissociated endothelial cells from rabbit aorta. *J. Physiol.*, **459,** 256P.

SAKAI, T. (1990). Acetylcholine induces Ca-dependent K currents in rabbit endothelial cells. *Jpn. J. Pharmacol.*, **53,** 235–246.

SAUVÉ, R., PARENT, L., SIMONEAU, C. & ROY, G. (1988). External ATP triggers a biphasic activation process of a calcium-dependent K^+ channel in cultured bovine aortic endothelial cells. *Pflügers Arch.*, **412,** 469–481.

SCHILLING, W.P., CABELLO, O.A. & RAJAN, L. (1992). Depletion of the inositol 1,4,5-trisphosphate-sensitive intracellular Ca^{2+} store in vascular endothelial cells activates the agonist-sensitive Ca^{2+}-influx pathway. *Biochem. J.*, **284,** 521–530.

SCHILLING, W.P., RITCHIE, A.K., NAVARRO, L.T. & ESKIN, S.G. (1988). Bradykinin stimulated calcium influx in cultured bovine aortic endothelial cells. *Am. J. Physiol.*, **255,** H219–H227.

SHAPIRO, M.S. & DECOURSEY, T.E. (1991). Chloride currents in bovine pulmonary artery endothelial cells. In *Ion Channels of Vascular Smooth Muscle Cells and Endothelial Cells*, e.d. Sperelakis, N. & Kuriyama, H. pp. 327–336. New York: Elsevier Science Publishing Co.

THURINGER, D. & SAUVÉ, R. (1992). A patch clamp study of the Ca^{2+} mobilization from internal stores in bovine aortic endothelial cells. I. Effects of caffeine on intracellular Ca^{2+} stores. *J. Membr. Biol.*, **130,** 125–137.

TSIEN, R.W. & TSIEN, R.Y. (1990). Calcium channels, stores and oscillations. *Annu. Rev. Cell. Biol.*, **6,** 715–760.

VACA, L. & KUNZE, D.L. (1993). cAMP-dependent phosphorylation modulates voltage gating in an endothelial Cl^- channel. *Am. J. Physiol.*, **264,** C370–C375.

WOLL, K.H., LEIBOWITZ, M.D., NEUMCKE, B. & HILLE, B. (1987). A high-conductance anion channel in adult amphibian skeletal muscle. *Pflügers Arch.*, **410,** 632–640.

ZIEGELSTEIN, R.C., SPURGEON, H.A., PILI, R., PASSANITI, A., CHENG, L., CORDA, S., LAKATTA, E.G. & CAPOGROSSI, M.C. (1994). A functional ryanodine-sensitive intracellular Ca^{2+} store is present in vascular endothelial cells. *Circ. Res.*, **74,** 151–156.

ZHOLOS, A.V., BAIDAN, L.V. & SHUBA, M.F. (1991). The inhibitory action of caffeine on calcium currents in isolated intestinal smooth muscle cells. *Pflügers Arch.*, **419,** 267–273.

(Received August 15, 1994
Revised December 20, 1994
Accepted January 9, 1995)

British Journal of Pharmacology (1995) 115, 142-146

Characterization of α_1-adrenoceptor subtypes in tension response of human prostate to electrical field stimulation

Jih-Hwa Guh, *Shih-Chieh Chueh, Feng-Nien Ko & [1]Che-Ming Teng

Pharmacological Institute and *Department of Urology, College of Medicine, National Taiwan University, Taipei, Taiwan

1 The effects of various α_1-adrenoceptor antagonists and nifedipine on tension responses of human prostate to electrical field stimulation were evaluated in this study.

2 Prazosin (3×10^{-10} to 10^{-8} M) and 5-methyl-urapidil (10^{-9} to 3×10^{-8} M) blocked concentration-dependently the tension responses to electrical field stimulation and completely abolished them in the maximal concentrations (10^{-8} M and 3×10^{-8} M, respectively); in contrast, chloroethylclonidine (CEC), in the maximal concentration of 100 μM, blocked these effects by only 50%.

3 The contractile responses of rat vas deferens and spleen to exogenously-applied α_1-adrenoceptor agonists were competitively inhibited by prazosin and 5-methyl-urapidil; in addition, the pA_2 values were calculated and the relative potencies with reference to prazosin were obtained. The relative potency of 5-methyl-urapidil in human prostate (0.105) was close to that in rat vas deferens (0.257), which contains primarily putative α_{1A}-adrenoceptors. However, it was much more than that in rat spleen (0.011), which contains primarily putative α_{1B}-adrenoceptors.

4 Nifedipine (10^{-8} to 10^{-6} M) inhibited concentration-dependently the contractile responses to electrical field stimulation in human prostate; in addition, the inhibition percentages were similar to those to exogenously-applied noradrenaline in rat vas deferens. In contrast, CEC (10 μM), which almost flattened the concentration-response curve of the rat spleen to phenylephrine, only partially inhibited (by 33.1%) the nerve-mediated contraction of human prostate.

5 The involvement of prejunctional α_2-adrenoceptors situated on the sympathetic nerve terminals of human prostate was also examined. Clonidine (3×10^{-9} to 3×10^{-7} M) blocked concentration-dependently the contractile response to electrical field stimulation of human prostate and this inhibitory effect was reversed by yohimbine (10^{-7} M). Additionally, the inhibitory effect of CEC (3×10^{-6} to 3×10^{-4} M) to the nerve-mediated contraction was also partially reversed by yohimbine (10^{-7} M).

6 It is suggested that the putative α_{1A}-adrenoceptors in human prostate may be functionally confined to the synaptic region whereas only minor populations of the putative α_{1B}- and/or α_{1C}-adrenoceptors exist in this region.

Keywords: Human prostate; electrical field stimulation; α_1-adrenoceptor subtypes; 5-methyl-urapidil; chloroethylclonidine

Introduction

A substantial amount of pharmacological research (Hedlund *et al.*, 1985; Kitada & Kumazawa, 1987; Yamada *et al.*, 1987) and clinical trials (Caine *et al.*, 1978; Shapiro *et al.*, 1981; Kirby *et al.*, 1987; Jardin *et al.*, 1991) on benign prostatic hypertrophy (BPH) has recently been undertaken. In these studies, it is well established that α-adrenoceptors are present in smooth muscle in BPH; in addition, α-adrenergic stimulation is an important factor in the development of urinary obstruction in BPH. Although both α_1- and α_2-adrenoceptors are identified within the human prostate, the contractile properties of the human prostate adenoma are mediated primarily by α_1-adrenoceptors (Hedlund *et al.*, 1985; Hieble *et al.*, 1985; Kitada & Kumazawa, 1987; James *et al.*, 1989).

More recently, at least three α_1-adrenoceptor subtypes have been demonstrated to exist by gene coding, i.e., $\alpha_{1A/D}$, α_{1B} and α_{1C} (Cotecchia *et al.*, 1988; Lomasney *et al.*, 1991; Schwinn *et al.*, 1991; Garcia-Sainz *et al.*, 1992; Schwinn & Lomasney, 1992). In human prostate, Chapple *et al.* (1991) suggested that the α_{1B} subtype forms the majority of the α_1-adrenoceptors, whereas Lepor *et al.* (1993) and Testa *et al.* (1993) using binding tests suggested that the dominant α_1-adrenoceptor subtype in the human prostate is the α_{1A} subtype. Price *et al.* (1993) investigated the mRNA expression of α_1-adrenoceptors in the human prostate with specific probes for the $\alpha_{1A/D}$, α_{1B} and α_{1C} subtypes, indicating that the predominant subtype is α_{1C}. In addition to exogenous adrenergic stimulation, endogenous adrenergic stimulation plays an important role in human prostate since the tone of prostatic smooth muscle regulated by the autonomic nervous system is thought to be the 'dynamic' component of bladder outlet obstruction by BPH (Caine, 1986). Furthermore, a rather dense network of adrenergic nerve fibres has been found within the smooth muscle layer of the prostatic glandular stroma (Vaalasti & Hervonen, 1980).

This study seeks to characterize the α_1-adrenoceptor subtypes involved in contraction after endogenous adrenergic stimulation in the smooth muscle of human prostate. We have employed 5-methyl-urapidil, selective for α_{1A}-adrenoceptors (Gross *et al.*, 1988; Hanft & Gross, 1989); chloroethylclonidine (CEC), which alkylates α_{1B}-adrenoceptors (Han *et al.*, 1978; Minneman, 1988); prazosin, which is a non-selective α_1-adrenoceptor antagonist (Hanft & Gross, 1989; Aboud *et al.*, 1993) and nifedipine, which inhibits $[Ca^{2+}]_0$ influx (Rampe *et al.*, 1985), to distinguish between the various α_1-adrenoceptor subtypes.

Methods

Human hyperplastic prostates were obtained at operation from 28 males, aged 53-78 years, by open prostatectomy or transurethral resection of the prostate. All these patients had

[1]Author for correspondence at: Pharmacological Institute, College of Medicine, National Taiwan University, No. 1, Jen-Ai Road, 1st Section, Taipei, 10018, Taiwan.

histories of prostatism, and were diagnosed to have BPH by a combination of rectal digital examinations, transrectal sonography of prostate and urodynamic studies (including uroflowmetry, urethral pressure profile and cystometry). The specimens were used for *in vitro* isometric tension experiments.

In vitro *isometric tension experiments*

Immediately after removal, the prostatic tissue was placed in Krebs solution. The specimens were cut into strips (1 × 3 × 15 mm), and mounted vertically between two parallel platinum ring electrodes in organ baths containing 5 ml of Krebs solution which was continuously bubbled with 95% O_2 plus 5% CO_2 at 37°C. Tissues were equilibrated for 60 min with three changes of solution and maintained under a resting tension of 1 g before specific experimental protocols were initiated. Intramural nerve stimulation was performed by means of an electronic stimulator (Grass model S88) delivering square pulses of 0.2 ms duration at supramaximum voltage (80 V over the electrodes) and 20 Hz for 5 s. Contractions were recorded isometrically via a force-displacement transducer (Grass, Model 7DAG) connected to a Grass polygraph. The almost complete inhibition of the response by tetrodotoxin (0.1 μM) confirmed that the contractions induced by transmural stimulation were nerve-mediated.

Rat vas deferens contraction

Whole rat vas deferens were mounted and equilibrated under the same conditions as human prostate for 60 min under a resting tension of 0.5 g. After the equilibration period, rat vas deferens were contracted twice to 10 μM noradrenaline and then washed and equilibrated for a further 30 min. Non-cumulative concentration-response curves for noradrenaline-induced contractions were determined in the absence or presence of the indicated antagonists and tissues were allowed to equilibrate with each antagonist for 30 min.

Rat spleen contraction

Rat spleens were hemisected and equilibrated under the same conditions as human prostate at a resting tension of 1 g and a concentration-response curve to phenylephrine was obtained in a cumulative manner in the absence or presence of the indicated antagonists.

Drugs and solutions

The composition of the Krebs solution (pH 7.4) used was (mM): NaCl 118.0, KCl 4.0, $MgSO_4$ 1.2, $CaCl_2$ 1.9, KH_2PO_4 1.2, $NaHCO_3$ 25.0 and glucose 11.7. Additionally, desmethylimipramine (10 nM), corticosterone (40 μM) and propranolol (1 μM), known to block neuronal and extraneuronal uptake of noradrenaline and β-adrenoceptors, respectively, were present.

The following drugs were used: noradrenaline HCl, prazosin HCl, yohimbine HCl, clonidine HCl, nifedipine, propranolol HCl, desmethylimipramine HCl and corticosterone (all purchased from Sigma Chemical Co., St. Louis, U.S.A.); chloroethylclonidine dihydrochloride and 5-methyl-urapidil (Research Biochemical Inc. Natick, MA, U.S.A.); phenylephrine HCl (Denmarks Apotekerforening). Drugs were dissolved in distilled water, except for corticosterone (100% ethanol) and nifedipine (dimethylsulphoxide). The final concentration of dimethylsulphoxide in the bathing solution did not exceed 0.1% and had no effect on the muscle contraction.

Data analysis

Agonist elicited concentration-response curves in the presence of the indicated concentrations of each antagonist were related to the control concentration-response curves, of which the maximal response was taken as 100%. The concentration of antagonist necessary to give a half-maximal response in the presence of each concentration of antagonist was divided by the concentration giving a half-maximal response in the absence of antagonist to determine the dose ratio (DR). Data were plotted by the method of Arunlakshana & Schild (1959) as the −log (antagonist concentration) (M) vs the log (DR − 1) and when DR was 2, the −log (antagonist concentration) was taken as the pA_2 value from the Schild plot (Mackay, 1978).

The experimental results are expressed as means ± s.e. mean and accompanied by the number of observations. Statistical significance was assessed by Student's t test and P values less than 0.05 were considered significant.

Results

Effects of α_1-adrenoceptor antagonists on electrical field stimulation of human prostate

The contractile responses to transmural field stimulation were concentration-dependently blocked by pretreatment with prazosin (3×10^{-10} to 10^{-8} M), 5-methyl-urapidil (10^{-9} to 3×10^{-8} M) or CEC (3×10^{-6} to 10^{-4} M). At the maximal concentrations, both prazosin (10^{-8} M) and 5-methyl-urapidil (3×10^{-8} M) almost completely abolished these responses whilst CEC (10^{-4} M) inhibited these responses by only approximately 50% (Figure 1). Yohimbine (10^{-8} to 10^{-6} M) was also examined but had no effect on these responses (data not shown).

Effects of nifedipine on rat vas deferens and human prostate

Exogenously-applied noradrenaline stimulated concentration-dependently the contractions in rat vas deferens. Nifedipine (10^{-8} to 10^{-6} M) caused concentration-related reductions in these responses (Figure 2a, Table 1); in contrast, CEC (30 μM) was ineffective against these responses. In comparison with rat vas deferens, nifedipine (10^{-8} to 10^{-6} M) also inhibited concentration-dependently the contractions to electrical field stimulation in human prostate (Figure 2b). Furthermore, the inhibition percentages were similar to those for exogenously-applied noradrenaline in rat vas deferens (Table 1).

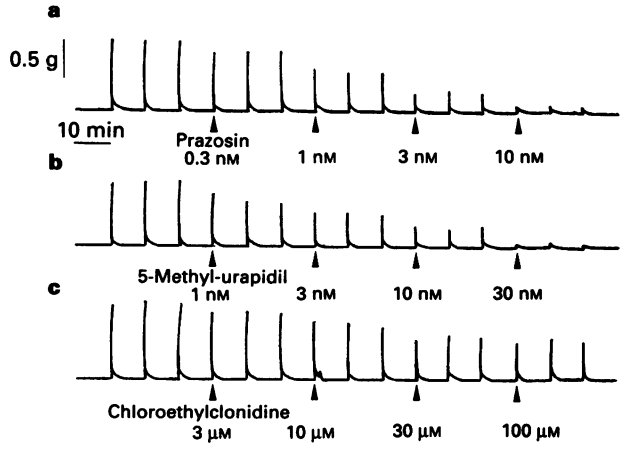

Figure 1 Representative traces of the inhibitory effect of prazosin (a), 5-methyl-urapidil (b) and chloroethylclonidine (c) on the contraction induced by transmural field stimulation in human hyperplastic prostates. Electrical stimulation was given at intervals of 10 min as described in Methods. The depicted traces were obtained from one of the five experiments.

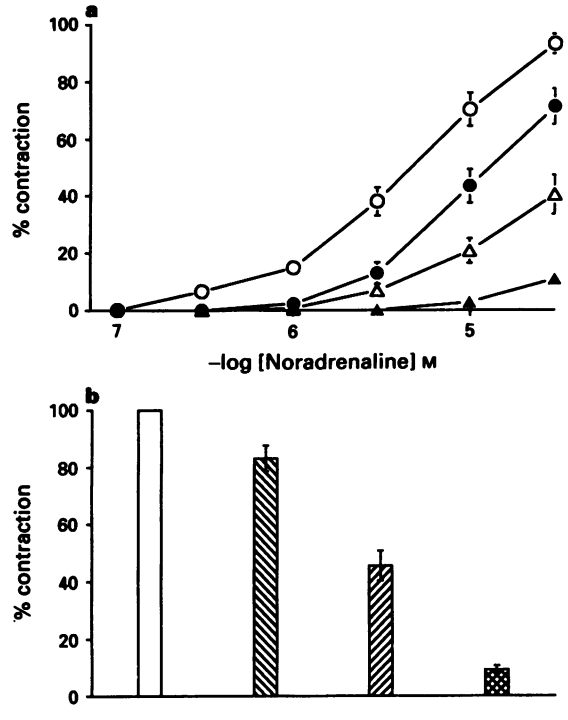

Figure 2 Effects of nifedipine on contractions to noradrenaline in rat vas deferens (a) and to transmural field stimulation in human hyperplastic prostates (b). Dimethylsulphoxide (0.05%, control) (○, □) or nifedipine, 10^{-8} M (●, ▨), 10^{-7} M (△, ▨) and 10^{-6} M (▲, ▨) was preincubated with tissues for 30 min. Values are the mean ± s.e.mean ($n = 5$).

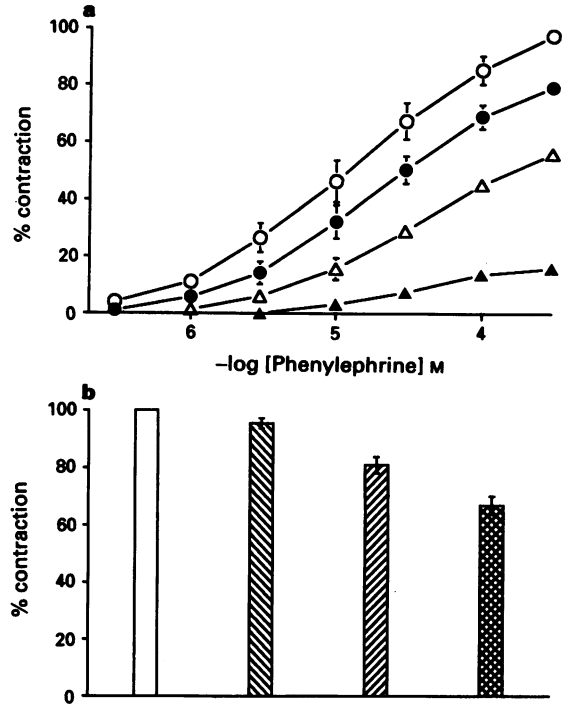

Figure 3 Effects of chloroethylclonidine on contractions to phenylephrine in rat spleens (a) and to transmural field stimulation in human hyperplastic prostates (b). Distilled water (control) (○, □) or chloroethylclonidine, 10^{-6} M (●, ▨), 3×10^{-6} M (△, ▨) and 10^{-5} M (▲, ▨) was preincubated with tissues for 30 min. Each values represents the mean ± s.e.mean ($n = 5$).

Table 1 The inhibitory effects of nifedipine and chloroethylclonidine on contractions to noradrenaline (30 μM) in rat vas deferens, to phenylephrine (300 μM) in rat spleens and to transmural field stimulation in human hyperplastic prostates

		Inhibition (%)		
Drugs (M)		*Vas deferens*	*Spleens*	*Prostate*
Nifedipine	10^{-8}	23.4 ± 6.7	-	16.8 ± 4.5
	10^{-7}	56.8 ± 7.3	-	54.4 ± 5.2
	10^{-6}	88.5 ± 1.6	-	90.8 ± 1.5
Chloroethylclonidine	10^{-6}	-	18.8 ± 0.7	4.6 ± 1.8
	3×10^{-6}	-	42.5 ± 1.8	19.0 ± 2.8
	10^{-5}	-	83.7 ± 1.6	33.1 ± 3.1

Values are expressed as means ± s.e.mean of 5 individual experiments.

Effects of CEC on rat spleen and human prostate

Phenylephrine stimulated concentration-dependently the contractions in rat spleen. CEC (1 to 10 μM) caused concentration-related reductions in these responses (Figure 3a, Table 1) and at a concentration of 10 μM, CEC almost flattened the concentration-response curve to phenylephrine; in contrast, nifedipine (1 μM) was ineffective on these responses. In comparison with rat spleen, CEC (1 to 10 μM) also concentration-dependently inhibited the contractions to electrical field stimulation in human prostate. At a concentration of 10 μM, however, CEC inhibited these responses by only 33.1% (Figure 3b, Table 1).

Effects of prazosin and 5-methyl-urapidil on rat vas deferens, rat spleen and human prostate

Prazosin and 5-methyl-urapidil produced parallel rightward shifts in the concentration-response curves of rat vas deferens to exogenously-applied noradrenaline and of rat spleens to phenylephrine without diminishing the maximal responses. The slopes of Schild plots were not significantly different from negative units (vas deferens: -1.10 ± 0.06 and -1.06 ± 0.04, respectively; spleen: -1.08 ± 0.07 and -1.04 ± 0.04, respectively); the pA_2 values were calculated (Table 2). Prazosin and 5-methyl-urapidil inhibited concentration-dependently the contractions to electrical field stimulation of human prostate and the half-maximal inhibition (IC_{50}) was determined (Table 2). In addition, the relative potencies of 5-methyl-urapidil with reference to prazosin in these tissues were obtained. Table 2 shows that the relative potency of 5-methyl-urapidil in human prostate (0.105) is close to that in rat vas deferens (0.257), but is about 10 fold that in rat spleen (0.011).

Effects of yohimbine on clonidine- and CEC-induced inhibitory responses in human prostate

Both clonidine (3×10^{-9} to 3×10^{-7} M) and CEC (3×10^{-6} to 10^{-4} M) inhibited concentration-dependently the contractions to electrical field stimulation in human prostate. The inhibitory effects were partially reversed by yohimbine (10^{-7} M); subsequently, the concentration-response curves were shifted to the right (Figure 4).

Discussion

This study has examined the effects of α_1-adrenoceptor antagonists on contractile responses to electrical field stimulation in human prostate. Prazosin, 5-methyl-urapidil and CEC all concentration-dependently blocked these responses. Both prazosin and 5-methyl-urapidil, at maximal concentrations, almost completely abolished these nerve-mediated responses whereas CEC only partially inhibited them. Also, further characterization of α_1-adrenoceptor subtypes mediat-

Table 2 Effects of α_1-adrenoceptor antagonists and nifedipine on tension responses stimulated by noradrenaline of rat vas deferens, by phenylephrine of rat spleens and by transmural field stimulation of human hyperplastic prostates

	Vas deferens (α_{1A})		*Spleen* (α_{1B})		*Prostate*	
Drugs	pA_2	*Relative potency*	pA_2	*Relative potency*	pIC_{50}	*Relative potency*
Prazosin	9.41 ± 0.41	1	9.11 ± 0.25	1	8.99 ± 0.13	1
5-MU	8.82 ± 0.43	0.257	7.15 ± 0.19	0.011	8.01 ± 0.17	0.105
CEC	No effect		Effective		Effective	
Nifedipine	Effective		No effect		Effective	

Values are expressed as means ± s.e.mean of 5 to 8 individual experiments. Abbreviations: 5-MU, 5-methyl-urapidil; CEC, chloroethylclonidine

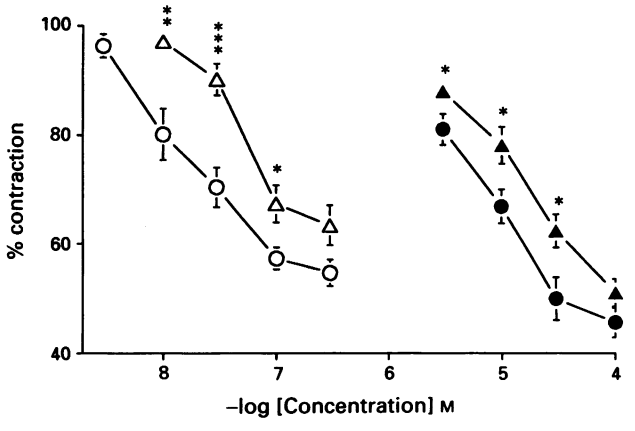

Figure 4 Effect of yohimbine on clonidine- and chloroethylclonidine-induced inhibition on contractions to transmural field stimulation in human hyperplastic prostates. Clonidine (○, △) or chloroethylclonidine (●, ▲) was preincubated in the absence (control) (○, ●) or presence (△, ▲) of yohimbine (10^{-7} M) with tissues for 30 min. Each point represents the mean ± s.e.mean ($n = 5$). $^*P < 0.05$, $^{**}P < 0.01$ and $^{***}P < 0.001$ as compared with the respective control.

ing contractions elicited by neuronally-released noradrenaline was performed.

Based on affinities of a series of ligands for binding sites in rat vas deferens and spleen (Han *et al.*, 1987; Gross *et al.*, 1988), and on the ability of CEC to inactivate the α_{1B} but not the α_{1A}-adrenoceptor subtypes (Han *et al.*, 1987; Minneman *et al.*, 1988), it has been suggested that contractions to exogenously-applied noradrenaline are mediated predominantly by α_{1A}-adrenoceptors in rat vas deferens (Han *et al.*, 1987; Hanft & Gross, 1989), and by α_{1B}-adrenoceptors in rat spleen (Han *et al.*, 1987). In the present study, the contractions of rat vas deferens to noradrenaline have been used as a model for α_{1A}-adrenoceptors and contractions of rat spleen to phenylephrine as a model for α_{1B}-adrenoceptors. We found prazosin, a nonselective α_1-adrenoceptor antagonist (Hanft & Gross, 1989; Aboud *et al.*, 1993), and 5-methyl-urapidil, a selective α_{1A}-adrenoceptor antagonist (Gross *et al.*, 1988; Hanft & Gross, 1989), competitively inhibited the contractions to noradrenaline in rat vas deferens and those to phenylephrine in rat spleen. In rat spleen, phenylephrine but not noradrenaline was used because of the involvement of α_2- as well as α_1-adrenoceptors in the contractile responses (Kenakin & Novak, 1988). Table 2 shows that prazosin had similar pA_2 values in rat vas deferens and spleen; 5-methyl-urapidil exhibited greater potency (47 fold) in rat vas deferens than in rat spleen. However, it is difficult to obtain pA_2 values for prazosin and 5-methyl-urapidil to electrical field stimulation in human prostate. Therefore, the pIC_{50} values were calculated and the relative potencies with reference to prazosin were determined. The observed data revealed that the relative potency of 5-methyl-urapidil in human prostate was close to that in rat vas deferens whereas it was about 10 fold that in rat spleen.

A number of authors have reported that the smooth muscle contractions elicited by α_{1A}-adrenoceptor activation are dependent on Ca^{2+} influx through dihydropyridine-sensitive channels, while contractions elicited by the activations of other α_1-adrenoceptors are independent of extracellular Ca^{2+} influx (Han *et al.*, 1987; Minneman, 1988; Han & Minneman, 1990). In the present study, nifedipine (10^{-8} to 10^{-6} M) induced concentration-related reductions in noradrenaline-stimulated concentration-response curves in rat vas deferens but was ineffective against those in rat spleen. In addition, nifedipine also concentration-dependently inhibited the contractions to electrical field stimulation in human prostate; moreover, the respective inhibition percentage was consistent with that in rat vas deferens (Table 1). In rat spleen, the concentration-response curve to phenylephrine remained unaffected by nifedipine (1 μM) but was reduced in a concentration-related manner by CEC; moreover, it was almost flattened by 10 μM CEC. In contrast, CEC (10 μM) only partially inhibited (by 33.1%) the nerve-mediated contractions in human prostate. These data imply that the contractions elicited by neuronally-released noradrenaline in human prostate are mediated predominantly by the putative α_{1A}-adrenoceptors.

In a number of studies, 5-methyl-urapidil has been reported to have a high affinity for cloned α_{1C}-adrenoceptors (Goetz *et al.*, 1993; Kenny *et al.*, 1994; Michel & Insel, 1994). Furthermore, it has been suggested that α_{1C}-subtype forms the majority of the α_1-adrenoceptors in human prostate (Price *et al.*, 1993). However, α_{1C}-adrenoceptors are sensitive to alkylation by CEC (Garcia-Sainz *et al.*, 1992; Michel *et al.*, 1992). In the present study, the nerve-mediated contractions in human prostate was sensitive to blockade by 5-methyl-urapidil; but was only partially reduced by CEC. This response was unlikely to be mediated predominantly by α_{1C}-adrenoceptors. In addition, the concentrations of CEC used to block these responses were markedly higher than those required to inhibit the contractions to phenylephrine in rat spleen. Whether these inhibitions to neuronally-released noradrenaline by CEC in human prostate result from the alkylation of α_{1B} and/or α_{1C}-adrenoceptors remains doubtful since CEC also has an affinity for α_2-adrenoceptors (Michel *et al.*, 1993).

Clonidine, a selective prejunctional α_2-adrenoceptor agonist, was examined to assess the contribution of α_2-adrenoceptors in nerve-mediated contractions of human prostate. Clonidine (3×10^{-9} to 3×10^{-7} M) concentration-dependently inhibited the contractions to electrical field stimulation in human prostate; at the high concentration of 3×10^{-7} M, it produced maximal inhibition (by 42.7%) of these nerve-mediated responses. The clonidine-elicited inhibition was reversed by yohimbine (10^{-7} M) confirming the involvement of prejunctional α_2-adrenoceptors. In addition, yohimbine (10^{-7} M) also partially reversed the inhibitory effect of CEC on nerve-mediated contractions in human prostate. This implies that the observed CEC-sensitive effects in human pros-

tate are related at least partially to the activation of prejunctional α_2-adrenoceptors.

In summary, we have demonstrated in this paper that the major subtype mediating contractions to neuronally-released noradrenaline is the α_{1A}-adrenoceptor; in addition, activation of prejunctional α_2-adrenoceptors may partially inhibit these responses. Furthermore, the CEC-sensitive effects may be accounted for at least partially by the activation of prejunctional α_2-adrenoceptors.

We appreciate the generous supply of human prostate tissues by Drs Jun Chen and Shyn-Chyan Chen of the Department of Urology, National Taiwan University Hospital, Taipei, Taiwan. This work was supported by a research grant of the National Science Council of the Republic of China (NSC 84-0425-B002-001).

References

ABOUD, R., SHAFII, M. & DOCHERTY, J.R. (1993). Investigation of the subtypes of α_1-adrenoceptor mediating contractions of rat aorta, vas deferens and spleen. *Br. J. Pharmacol.*, **109**, 80–87.

ARUNLAKSHANA, O. & SCHILD, H.O. (1959). Some quantitative uses of drug antagonists. *Br. J. Pharmacol. Chemother.*, **14**, 48–52.

CAINE, M. (1986). Clinical experience with α-adrenoceptor antagonists in benign prostatic hypertrophy. *Fed. Proc.*, **45**, 2604–2608.

CAINE, M., PERLBERG, S. & MERETYK, S. (1978). A placebo-controlled double-blind study of the effect on phenoxybenzamine in benign prostatic obstruction. *Br. J. Urol.*, **50**, 551–554.

CHAPPLE, C.R., BURT, R.P. & MARSHALL, I. (1991). α_1-Adrenoceptor subtypes in the human prostate and inferior epigastric artery. *Neurourol. Urodyn.*, **10**, 306–308.

COTECCHIA, S., SCHWINN, D.A., RANDALL, R.R., LEFKOWITZ, R.J., CARON, M.G. & KOBILKA, K.K. (1988). Molecular cloning and expression of the cDNA for the hamster α_1-adrenoceptors. *Proc. Natl. Acad. Sci. U.S.A.*, **85**, 7159–7163.

GARCIA-SAINZ, J.A., ROMERO-AVILA, M.T., HERNANDEZ, R.A., MACIAS-SILVA, M., OLIVARES-REYES, A. & GONZALEZ-ESPINOSA, C. (1992). Species heterogeneity of hepatic α_1-adrenoceptors: α_{1A}-, α_{1B}- and α_{1C}-subtypes. *Biochem. Biophys. Res. Commun.*, **186**, 760–767.

GOETZ, A., LUTZ, M., CARPI, E., RIMELE, T. & SAUSSY, D. (1993). Comparison of ligand affinities for cloned α_1-adrenoceptor subtypes. *FASEB J.*, **7**, A696.

GROSS, G., HANFT, G. & RUGEVICS, C. (1988). 5-Methyl-urapidil discriminates between subtypes of the α_1-adrenoceptor. *Eur. J. Pharmacol.*, **151**, 333–335.

HAN, C., ABEL, P.W. & MINNEMAN, K.P. (1987). α_1-Adrenoceptor subtypes linked to different mechanisms for increasing intracellular Ca^{2+} in smooth muscle. *Nature*, **329**, 333–335.

HAN, C., LI, J. & MINNEMAN, K.P. (1990). Subtypes of α_1-adrenoceptors in rat blood vessels. *Eur. J. Pharmacol.*, **190**, 97–104.

HANFT, G. & GROSS, G. (1989). Subclassification of α_1-adrenoceptor recognition sites by urapidil derivatives and other selective antagonists. *Br. J. Pharmacol.*, **97**, 691–700.

HEDLUND, H., ANDERSSON, K.E. & LARSSON, B. (1985). Alpha-adrenoceptors and muscarinic receptors in the isolated human prostate. *J. Urol.*, **134**, 1291–1298.

HIEBLE, J.P., CAINE, M. & ZALAZNIK, E. (1985). In vitro characterization of the α-adrenoceptors in human prostate. *Eur. J. Pharmacol.*, **107**, 111–117.

JAMES, S., CHAPPLE, C.R., PHILLIPS, M.I., GREENGRASS, P.M., DAVEY, M.J., TURNER-WARWICK, T., MILORY, E.J.G. & BURNSTOCK, G. (1989). Autoradiographic analysis of α-adrenoceptors and muscarinic cholinergic receptors in the hyperplastic human prostate. *J. Urol.*, **142**, 438–444.

JARDIN, A., BENSADOUN, H., DELAUCHE-CAVALLIER, M.C., ATTALI, P. & THE BPH-ALF GROUP. (1991). Alfuzosin for treatment of benign prostatic hypertrophy. *Lancet*, **337**, 1457–1461.

KENAKIN, T.P. & NOVAK, P.J. (1988). Classification of phenoxybenzamine/prazosin resistant contractions of rat spleens to postsynaptic alpha-2 adrenoceptors. *J. Pharmacol. Exp. Ther.*, **244**, 206–212.

KENNY, B.A., NAYLOR, A.M., GREENGRASS, P.M., RUSSELL, M.J., FRIEND, S.J., READ, A.M. & WYLLIE, M.G. (1994). Pharmacological properties of the cloned $\alpha_{1A/D}$-adrenoceptor subtype are consistent with the α_{1A}-adrenoceptor characterized in rat cerebral cortex and vas deferens. *Br. J. Pharmacol.*, **111**, 1003–1008.

KIRBY, R.S., COPPINGER, S.W.C. & CORCORAN, M.O. (1987). Prazosin in the treatment of prostatic obstruction. A placebo-controlled study. *Br. J. Urol.*, **60**, 136–142.

KITADA, S. & KUMAZAWA, J. (1987). Pharmacological characteristics of smooth muscle in benign prostatic hyperplasia and normal prostatic tissue. *J. Urol.*, **138**, 158–160.

LEPOR, H., TANG, R., MERETYK, S. & SAPIRA, E. (1993). Alpha1-adrenoceptor subtypes in the human prostate. *J. Urol.*, **149**, 640–642.

LOMASNEY, J.W., COTECCHIA, S., LORENZ, W., LEUNG, W.Y., SCHWINN, D.A., YANG-FENG, T.L., BROWNSTEIN, M., LEFKOWITZ, R.J. & CARON, M.G. (1991). Molecular cloning and expression of the cDNA for the α_{1A}-adrenoceptor: the gene for which is located on human chromosome 5. *J. Biol. Chem.*, **266**, 6365–6369.

MACKAY, D. (1978). How should values of pA_2 and affinity constants for pharmacological competitive antagonists be estimated? *J. Pharm. Pharmacol.*, **30**, 312–313.

MICHEL, M.C. & INSEL, P.A. (1994). Comparison of drug affinities at cloned and rat tissue α_1-adrenoceptor subtypes. *Br. J. Pharmacol.*, **112**, 59P.

MICHEL, M.C., KERKER, J., BRANCHEK, T.A. & FORRAY, C. (1993). Selective irreversible binding of chloroethylclonidine at α_1 and α_2-adrenoceptor subtypes. *Mol. Pharmacol.*, **44**, 1165–1170.

MICHEL, M.C., PHILIPP, T. & BRODDE, O.-E. (1992). α- and β-adrenoceptors in hypertension: molecular biology and pharmacological studies. *Pharmacol. Toxicol.*, **70** (Suppl. II), S1–S10.

MINNEMAN, K.P. (1988). α_1-Adrenergic receptor subtypes, inositol phosphates, and sources of cell calcium. *Pharmacol. Rev.*, **40**, 87–119.

MINNEMAN, K.P., HAN, C. & ABEL, P.W. (1988). Comparison of α_1-adrenergic receptor subtypes distinguished by chloroethylclonidine and WB4101. *Mol. Pharmacol.*, **33**, 509–514.

PRICE, D.T., SCHWINN, D.A., LOMASNEY, J.W., ALLEN, L.F., CARON, M.G. & LEFKOWITZ, R.J. (1993). Identification, quantification and localization of mRNA for three distinct alpha1 adrenergic receptor subtypes in human prostate. In 88th Annual Meeting of the American Urological Association, San Antonio, TX, May 15–20.

RAMPE, D., SU, C.M., YOUSIF, F. & TRIGGLE, D.J. (1985). Calcium channel antagonists: pharmacological considerations. *Br. J. Clin. Pharmacol.*, **20**, 247s–254s.

SCHWINN, D.A. & LOMASNEY, J.W. (1992). Pharmacologic characterization of cloned α_1-adrenoceptor subtypes: selective antagonists suggest the existence of a fourth subtype. *Eur. J. Pharmacol. Mol. Pharmacol.*, **227**, 433–436.

SCHWINN, D.A., PAGE, S.O., MIDDLETON, J.P., LORENZ, W., LIGGETT, S.B., YAMAMOTO, K., LAPETINA, E.G., CARON, M.G., LEFKOWITZ, R.J. & COTECCHIA, S. (1991). The α_{1C}-adrenoceptor: characterization of signal transduction pathways and mammalian tissue heterogeneity. *Mol. Pharmacol.*, **40**, 619–626.

SHAPIRO, A., MAZOUZ, B. & CAINE, M. (1981). The alpha-adrenergic blocking effect of prazosin on the human prostate. *Urol. Res.*, **9**, 17–20.

TESTA, R., GUARNERI, L., IBBA, M., STRADA, G., POGGESI, E., TADDEI, C., SIMONAZZI, I. & LEONARDI, A. (1993). Characterization of α_1-adrenoceptor subtypes in prostate and prostatic urethra of rat, rabbit, dog and man. *Eur. J. Pharmacol.*, **249**, 307–315.

VAALASTI, A. & HERVONEN, A. (1980). Autonomic innervation of the human prostate. *Invest. Urol.*, **17**, 293–297.

YAMADA, S., ASHIZAWA, N., USHIJIMA, H., NAKAYAMA, K., HAYASHI, E. & HONDA, K. (1987). Alpha-1 adrenoceptors in human prostate: characterization and alteration in benign prostatic hypertrophy. *J. Pharmacol. Exp. Ther.*, **242**, 326–330.

(Received October 21, 1994
Accepted January 17, 1995)

British Journal of Pharmacology (1995) 115, 147-157

Effects of GTPγS on muscarinic receptor-stimulated inositol phospholipid hydrolysis in permeabilized smooth muscle from the small intestine

[1]S.A. Prestwich, [2]H. Miyazaki & T.B. Bolton

Department of Pharmacology and Clinical Pharmacology, St George's Hospital Medical School, Cranmer Terrace, London SW17 0RE

1 Smooth muscle fragments from the longitudinal layer of the small intestine of the guinea-pig were permeabilized with *Staphylococcus aureus* alpha toxin (α-toxin) and used to investigate the role of G-protein activation in the regulation of muscarinic acetylcholine receptor (AChR)-stimulated inositol phospholipid hydrolysis.

2 The efficiency of α-toxin permeabilization was estimated by the release of [^{3}H]-2-deoxyglucose ([^{3}H]-2DG) after prior loading or lactate dehydrogenase (LDH) enzyme release from the smooth muscle fragments.

3 In α-toxin-permeabilized smooth muscle, but not in non-permeabilized muscle, GTPγS induced time- and concentration-dependent increases in labelled inositol phosphates. Carbachol (CCh) increased labelled inositol phosphates in both permeabilized and non-permeabilized muscle, although the increases were greater in non-permeabilized smooth muscle. The response to 100 μM CCh was severely reduced by 0.5 μM atropine.

4 In permeabilized muscle the effects of GTPγS or CCh on inositol phosphate levels were reduced by treatment with pertussis toxin (PTX) and completely inhibited by GDPβS.

5 GTPγS caused a concentration-dependent inhibition of the CCh-induced increases in the levels of labelled inositol phosphates. Dibutyryl cyclic AMP or Sp-cAMPs (adenosine-3',5'-cyclic phosphorothiolate-Sp) reduced the effects of CCh on inositol phosphate levels.

6 The results suggest that muscarinic AChR activation induces inositol phospholipid hydrolysis via more than one G-protein in this smooth muscle and that several mechanisms may contribute to the modulation of both stimulatory and inhibitory responses observed.

Keywords: Smooth muscle; permeabilization; inositol phosphates; G-proteins; GTPγS; GDPβS; pertussis toxin; cyclic AMP

Introduction

Stimulation of muscarinic acetylcholine receptors (AChRs) in longitudinal smooth muscle of small intestine results in an increase in inositol phospholipid hydrolysis by activation of a phospholipase C (PLC) producing inositol (1,4,5) trisphosphate (Ins(1,4,5)P_3) and 1,2-diacylglycerol (Jafferji & Michell, 1976; Best & Bolton, 1986). This effect is believed to be mediated by G-proteins. The Ins(1,4,5)P_3 causes Ca^{2+} release from the stores in the sarcoplasmic reticulum and this contributes to tension generations in this excitable smooth muscle (Pacaud & Bolton, 1992).

The structures of cloned muscarinic AChRs and the dependence of muscarinic AChR-induced responses on the presence of GTP in membranes and in permeabilized cells support the idea that agonist-induced increases in inositol phospholipid turnover are mediated by G-proteins (Cockcroft & Gomperts, 1985; Litosch *et al.*, 1985; Casey & Gilman, 1988). GTPγS is a slowly hydrolysable, non permeable analogue of GTP that causes stimulation of inositol phospholipid hydrolysis in many cell types including smooth muscle (Honkanen & Abdel-Latif, 1989). GTPγS also increases the Ca^{2+} sensitivity of myosin phosphorylation in both tonic and phasic smooth muscles but these effects may be separate from the effects of GTPγS on inositol phospholipid hydrolysis which have been investigated in this study (Kitazawa *et al.*, 1991; Ono *et al.*, 1992) although others believe they may be involved (Nishimura *et al.*, 1990).

Intact receptors and signal transduction systems are retained following permeabilization of smooth muscle with α-toxin and it has been used by various workers to investigate the mechanisms of excitation-contraction coupling (Nishimurar *et al.*, 1988; Kitazawa *et al.*, 1991). α-Toxin is a cytolytic exotoxin secreted by *Staphylococcus aureus*. Hexamerization of the α-toxin molecules results in the formation of pores of 2-3 nm in diameter in the plasma membrane (Füssle *et al.*, 1981; Hohman, 1988) but as the α-toxin monomer is 34 kDa it does not enter the cell and so its action is restricted to the plasma membrane (Bhakdi & Tranum-Jensen, 1987). The small pore size allows equilibration of cytoplasm, inorganic ions and small molecules such as GTP analogues, contained in experimental solutions, without losing larger molecules such as calmodulin, protein kinases and other enzymes.

We have shown previously that AlF interacts with G-proteins to inhibit muscarinic AChR-induced stimulation of inositol phospholipid hydrolysis (Prestwich & Bolton, 1995). The purpose of the present experiments was to examine further the role of G-proteins in the muscarinic AChR-induced increases in the levels of [^{3}H]-inositol phosphates observed in this tissue. The interaction between CCh and GTPγS was determined to see if GTPγS could potentiate the muscarinic AChR responses as described in other systems (Cockcroft & Gomperts, 1985; Litosch *et al.*, 1985; Smith *et al.*, 1985; Uhing *et al.*, 1986; Cockcroft, 1987; Cattaneo & Vicentini, 1989). For these experiments on smooth muscle fragments, attempts were made to permeabilize completely with α-toxin so that the increases in [^{3}H]-inositol phosphates

[1] Author for correspondence.
[2] Now deceased.

observed occurred only in permeabilized fragments. These fragments were used to determine the effects of GTPγS and GDPβS (more stable analogues of GTP and GDP) and treatment with PTX, on the levels of [^{3}H]-inositol phosphates generated by muscarinic AChR activation with CCh. In addition to measurements of levels of [^{3}H]-inositol phosphates, levels of adenosine 3′:5′-cyclic monophosphate (cyclic AMP) were determined to see if increases in cyclic AMP levels could account for some of the observed effects.

Methods

Guinea-pigs were stunned and exsanguinated and longitudinal muscle of the small intestine removed. Fragments were prepared by tissue chopping as previously described (Prestwich & Bolton, 1995).

Permeabilization of fragments

Preliminary experiments described in Results showed that incubation with 2500 u ml^{-1} α-toxin for 30 min in internal substitution solution (ISS, see below) resulted in satisfactory permeabilization of the smooth muscle fragments and this treatment was used in all experiments where permeabilization was required.

After washing the [^{3}H]-inositol-labelled fragments (fragments were incubated with 1.85 MBq ml^{-1} [^{3}H]-inositol for 20 h at 30°C) with Krebs ringer buffer (KRB) they were rinsed several times in ISS, suspended in 1 ml of this solution containing 2500 u ml^{-1} α-toxin and 925 kBq [^{3}H]-inositol and then incubated at 37°C for 30 min with occasional gentle mixing. At the end of 30 min incubation, the α-toxin was removed with several washes of 10 ml ISS.

Permeabilized fragments were aliquoted to give about 1 mg protein per pot into 'mesh pots' ('mesh pots' were 5 ml Gilson pipette tips which had been cut so that a small circle of nylon mesh could be placed over the end and secured with a ring and they would easily fit into a 5 ml beta vial); these were placed in a beta vial containing 3 ml ISS. The assay procedure was as follows: a mesh pot was removed, blotted onto blotting paper, and immersed in 3 ml ISS at 37°C for 30 s; this was repeated. The sample was then blotted and immersed in the test solution (500 μl). At the end of the incubation, 500 μl 20% trichloroacetic acid (TCA) and 50 μl 50 mM EDTA were added to stop the assay and after rinsing the fragments on the mesh with a small volume of buffer, the samples were vortexed, placed on ice for 20 min and then centrifuged at 4000 *g* for 10 min. The supernatant was removed and the TCA extracted by the addition of 4 × 5 ml water-saturated diethyl ether; the residual ether was removed with nitrogen and the pH of the samples adjusted to 7.0 with 1 M NaOH. The pellet was stored for protein determination by the method of Lowry *et al.* (1951) (there was no interference in the protein assay from anything leaching off the mesh). Samples were assayed for [^{3}H]-inositol phosphates by anion-exchange h.p.l.c. within 7 days.

In some experiments the tissue part was separated from the supernatant part at the end of the incubation period. For these experiments, at the end of the incubation period the inner pot was raised, 500 μl buffer pipetted into it to wash excess supernatant off the tissue and the tissue part was then immersed in a solution of 10% TCA. TCA was then added to the supernatant to give 10% final.

The composition of the high K^+ intracellular substitution solution (ISS) was as follows: (final, mM) K^+ aspartate 130, $MgCl_2$ 3.1, Na_2ATP 2, EGTA 2, creatine PO_4 20, HEPES 20, $CaCl_2$ 1 (free concentration = 0.137 μM) pH 7.2 with KOH. The pores in the plasma membrane made by α-toxin treatment did not allow molecules greater than 1000 Da to pass, therefore creatine kinase and calmodulin would be retained and so did not need to be added to the intracellular solution.

The concentration of free Ca^{2+}, Mg^{2+} and ATP were calculated with a computer programme called EQCAL (Biosoft, U.K.). This programme uses the stability constants for metal-chelate and metal-nucleotide complexes reported by Martell & Smith (1975).

Measurement of [^{3}H]-2DG release

Loss of ^{3}H from fragments which had been previously loaded with [^{3}H]-2-deoxyglucose ([^{3}H]-2DG) in the absence and presence of increasing concentrations of α-toxin was used to assess the degree of permeabilization by different concentrations of α-toxin. Permeabilization by this toxin was also compared with permeabilization by saponin, Triton-X-100 and by hypo-osmotic shock with pure water (distilled water passed through a Milli-Q deionization system). Release of the enzyme lactate dehydrogenase (LDH) was also determined to compare the effect of permeabilization by α-toxin with other permeabilizing agents.

Fragments from the longitudinal smooth muscle layer of the small intestine were incubated in KRB for 30 min at 37°C, followed by washing several times in KRB minus glucose and incubated with 185 kBq [^{3}H]-2DG in KRB minus glucose for 2 h at 37°C (based on the method of Olefsky, 1978). At the end of this period the fragments were washed several times in the high K^+ internal substitution solution (ISS). To estimate the extent of permeabilization of the fragments the escape of [^{3}H]-2DG was estimated as d.p.m. appearing in the supernatant or as d.p.m. remaining in the tissue fragments. Fragments were divided into mesh pots in a total volume of 1 ml containing either ISS alone or ISS in the presence of one of the following: α-toxin in concentrations from 250 u ml^{-1} to 8000 u ml^{-1}; saponin, 1 mg ml^{-1}; Triton-X-100, 1% or pure water to cause hypotonic lysis of cells. The temperature was 37°C (except that 22°C was used for saponin). At selected time intervals, 50 μl aliquots were removed to determine the amount of ^{3}H which had been released into the supernatant (Figure 1a). At the end of the incubation period residual d.p.m. in the supernatant were counted and 10% trichloroacetic acid added to the tissue portion to determine the number of d.p.m. remaining in the tissue. Hisafe 3 (LKB) (4 ml) was added to each pot and the d.p.m. determined in a Beckman scintillation counter. After correcting for the volume in the pot remaining at each time point, the amount of ^{3}H released (Figure 1a) or the ^{3}H remaining (Figure 1b) was calculated as a percentage of the total number of d.p.m. in the tissue at the beginning of the experiment.

Measurement of LDH release

The enzyme LDH was chosen for assay as an example of a molecule too large to escape through the membrane pores created by α-toxin. Smooth muscle fragments were rinsed several times after preparation in ISS and then incubated in either ISS alone, 5000 u ml^{-1} α-toxin, 1 mg ml^{-1} saponin or 1% Triton-X-100 for up to 60 min. At selected time intervals aliquots were removed, placed on ice and assayed immediately for LDH activity. At the end of the experiment the remaining LDH in the tissue was extracted with TCA.

The assay for LDH activity was based on the method of Bergmeyer & Bernt (1974). LDH activity was determined spectrophotometrically by observing the oxidation of NADH in the presence of pyruvate to produce lactate; 3 ml of 0.63 mM pyruvate and 50 mM phosphate buffer pH 7.5 was mixed with 50 μl of 11.3 mM NADH (buffered to pH 7.5 with $NaHCO_3$) and 100 μl of sample. The absorbance was read at 365 nm in a cuvette at 22°C, immediately after mixing and again exactly 5 min later in a Beckman spectrophotometer. The reduction in the optical extinction during this time was taken as a measure of LDH activity. The results are expressed as % of total LDH remaining at each time point.

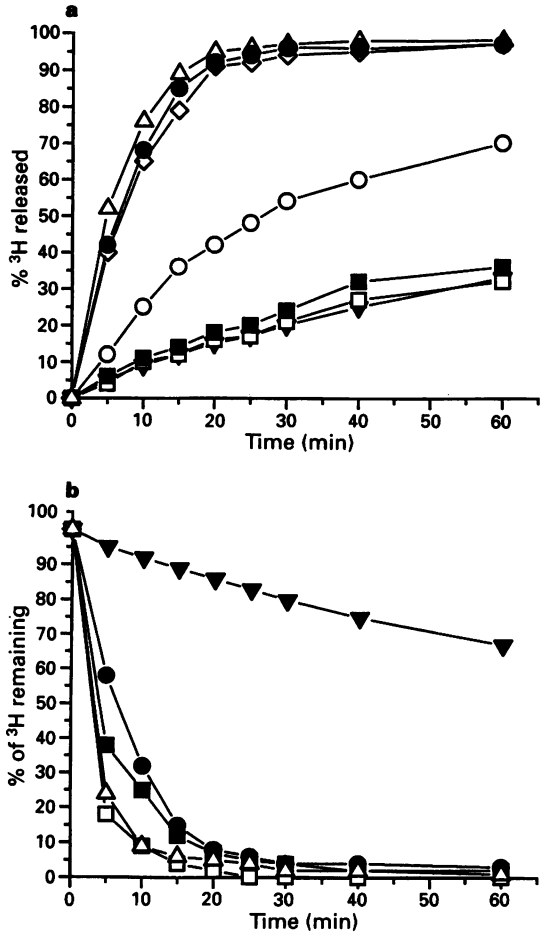

Figure 1 (a) Permeabilization of smooth muscle fragments with α-toxin. [^{3}H]-2DG-labelled smooth muscle fragments prepared as described, were incubated in the absence (ISS) (▼) or in the presence of ISS containing either 250 (□), 500 (■), 1000 (○), 2500 (◇), 5000 (●) or 8000 (△) u ml^{-1} α-toxin from zero time. The % of ^{3}H released with time during incubation with or without the α-toxin for up to 60 min at 37°C was determined. Results are expressed as the mean % release of ^{3}H into the supernatant compared to the total number of d.p.m. in each aliquot of tissue ($n = 2$). (b) Measurement of ^{3}H-efflux during permeabilization. [^{3}H]-2DG-labelled fragments were incubated in the absence (▼) ($n = 3$) of any permeabilizing agent (ISS alone) or in the presence of ISS containing either 2500 u ml^{-1} α-toxin (●) ($n = 3$), 1 mg ml^{-1} saponin (■) ($n = 2$), 1% Triton-X-100 (□) ($n = 2$) or pure H_2O (△) ($n = 2$) with no added solutes for up to 60 min at 22°C for the saponin and at 37°C for the rest. Results are expressed as the mean amount of ^{3}H remaining in the fragments at any time compared to the total d.p.m. in the aliquot of tissue. For abbreviatons in this and subsequent legends, see text.

Figure 2 shows the ability of the smooth muscle fragments to retain LDH under the different conditions.

Labelling and measurement of [^{3}H]-inositol phosphates by h.p.l.c.

The labelling (20 h incubation) and measurement of the [^{3}H]-inositol phosphate isomers was the same as in Prestwich & Bolton (1991; 1995). Briefly, chopped fragments (350 × 350 μm) were incubated in Krebs Ringer buffer of the following composition (final, mM): NaCl 120, KCl 5.9, $NaHCO_3$ 15.4, NaH_2PO_4 1.2, glucose 11.5, $MgCl_2$ 1.2, $CaCl_2$ 2.5 (pH was 7.25 when equilibrated) containing 1.85 MBq ml^{-1} [^{3}H]-inositol and kept in a humidified atmosphere containing 95% O_2/5% CO_2 at 30°C for 20 h. Contraction of the muscle to CCh could still be observed after this period of incubation.

For the majority of the studies the [^{3}H]-inositol phosphate isomers were separated by h.p.l.c. with a method modified

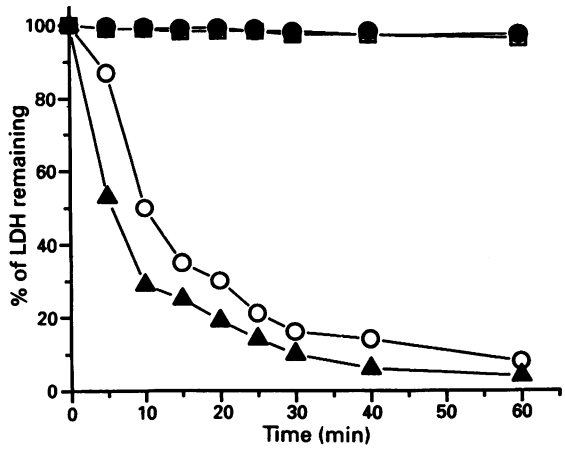

Figure 2 Measurement of loss of lactic dehydrogenase (LDH) during permeabilization. The smooth muscle fragments were incubated in ISS in the absence (●) ($n = 2$) or presence of 5000 u ml^{-1} α-toxin (□) ($n = 3$), 1 mg ml^{-1} saponin (○) ($n = 3$) or 1% Triton-X-100 (▲) ($n = 2$). Aliquots were removed at different times up to 60 min and the LDH activity determined. Results are expressed as the mean % of LDH remaining out of the total in each aliquot at each time point. The amount of LDH at time zero was calculated from the cumulative amount plus the total remaining at the end of the experiment.

from Irvine *et al.* (1985) and Batty *et al.* (1985). A Partisal SAX (strong anion exchange) column was used and the inositol phosphates eluted using an ammonium formate gradient from 0 to 2 M brought to pH 3.7 with H_3PO_4. The eluate was collected in a fraction collector. Elution profiles were determined by scintillation counting using a Beckman LS1701 scintillation counter. The identity of the various [^{3}H]-inositol phosphate isomers except for one of the [^{3}H]-inositol bisphosphates, was determined by comparing their elution profiles from the h.p.l.c. with those of labelled standards (see Prestwich & Bolton, 1991). From these standards the following inositol phosphate isomers were identified: [^{3}H]-inositol monophosphates ([^{3}H]-inositol (1) phosphate and [^{3}H]-inositol (4) phosphate) ($InsP_1$); [^{3}H]-inositol (1,4) bisphosphate ($Ins(1,4)P_2$); [^{3}H]-inositol (1,3,4) trisphosphate ($Ins(1,3,4)P_3$); [^{3}H]-inositol (1,4,5) trisphosphate ($Ins(1,4,5)P_3$) and [^{3}H]-inositol tetrakisphosphates ($InsP_4$). From the elution profiles of other workers, the other [^{3}H]-inositol bisphosphate is likely to be [^{3}H]-inositol (3,4) bisphosphate (labelled $sInsP_2$ in the Figures). Agonist-stimulated responses were compared with control values and the results usually expressed as % change compared to control. For the studies using dibutyryl cyclic AMP and Sp-cAMPs the [^{3}H]-inositol phosphate isomers were separated on Agl-X-8 columns following the method of Downes & Michell (1981).

Measurement of cyclic AMP

Smooth muscle fragments were prepared and incubated as previously described (Prestwich & Bolton, 1991) when measuring [^{3}H]-inositol phosphates. Initial experiments to determine agonist responses (data not shown) were carried out in the absence of the phosphodiesterase inhibitor, isobutylmethylxanthine (IBMX) but no changes in the basal cyclic AMP levels could be seen. Therefore the fragments were incubated in KRB containing 1 mM IBMX for the cyclic AMP experiments. After incubation with or without CCh for the desired time the reaction was terminated by addition of 10% (final) TCA. The TCA was removed by diethyl ether extraction, and the samples neutralized, lyophilized and reconstituted in water. The cyclic AMP formed was determined by competition binding assay with a radiolabelled kit from Amersham International Ltd.

Materials

GDPβS (trilithium salt), GTPγS (tetralithium salt), α-toxin and pertussis toxin (PTX) were obtained from Boehringer. Dibutyryl cyclic AMP and Sp-cAMPs were obtained from Calbiochem. [^{3}H]-2DG, [^{3}H]-inositol and the [^{3}H]-cyclic AMP assay kit were obtained from Amersham International Ltd. [^{3}H]-inositol contained a PT6 tablet which absorbed any radiolysis products, which meant no purification of the label was necessary before use. All other chemicals and drugs were obtained from Sigma Chemical Company Ltd or BDH.

Data analysis

The data are expressed as the mean ± s.e.mean of at least three paired experiments performed on different occasions. Intra-assay variation was very small and the main variability was seen between guinea-pigs. The statistical significance was assessed by use of Student's paired *t* test. *P* values that were less than 0.05 were considered to be significant. Calculations were performed using the computer programme INSTAT (GraphPAD software, U.S.A.).

Results

[^{3}H]-2DG experiments

The efflux of ^{3}H from smooth muscle fragments labelled with [^{3}H]-2DG increased with increasing concentrations of α-toxin reflecting the degree of permeabilization of the fragments (Figure 1a). In non-permeabilized fragments 33% of the total ^{3}H was released by the end of the 60 min incubation period. This may be because the ISS contains only 0.1 μM Ca^{2+} and this would make the fragments leaky. Incubation with up to 500 u ml^{-1} of α-toxin for up to 60 min at 37°C showed no increase in the rate of release of ^{3}H when compared with non-α-toxin treated fragments (Figure 1a). Increasing the concentration of α-toxin to 1000 u ml^{-1} resulted in an increased efflux of ^{3}H compared to control so that at 30 min, 50% of the ^{3}H had been released compared to only 20% in control. Incubation with concentrations of 2500 u ml^{-1} or greater resulted in more than 90% of the ^{3}H in the fragments being released by 20 min. Measurement of ^{3}H may include substances other than [^{3}H]-2DG: derived from the cell.

Measurement of the amount of ^{3}H remaining in the smooth muscle fragments showed that after 30 min incubation in ISS, the non-permeabilized fragments had lost only 20% of the ^{3}H taken up. However, following 30 min incubation with 2500 u ml^{-1} α-toxin, only 4% of the ^{3}H remained in the fragments (Figure 1b). After 30 min incubation with saponin (1 mg ml^{-1}, 20 min, 22°C), less than 10% of the ^{3}H remained and incubation with Triton-X-100 or distilled water resulted in almost complete loss of ^{3}H taken up by the end of the incubation period.

Since greater than 90% of the ^{3}H from [^{3}H]-2DG labelled fragments had been lost by 20 min when the fragments were permeabilized with 2500 u ml^{-1} or more α-toxin it was decided to use 2500 u ml^{-1} α-toxin and incubate for 30 min in order to permeabilize the fragments prior to the experiments.

LDH experiments

There was no detectable loss of LDH during incubation of smooth muscle fragments in ISS alone or during treatment with 5000 u ml^{-1} α-toxin (Figure 2) a concentration that has been shown to release more than 95% of the [^{3}H]-2DG taken up (Figure 1a) by the end of the 60 min incubation period. However, permeabilization of the fragments with Triton-X-

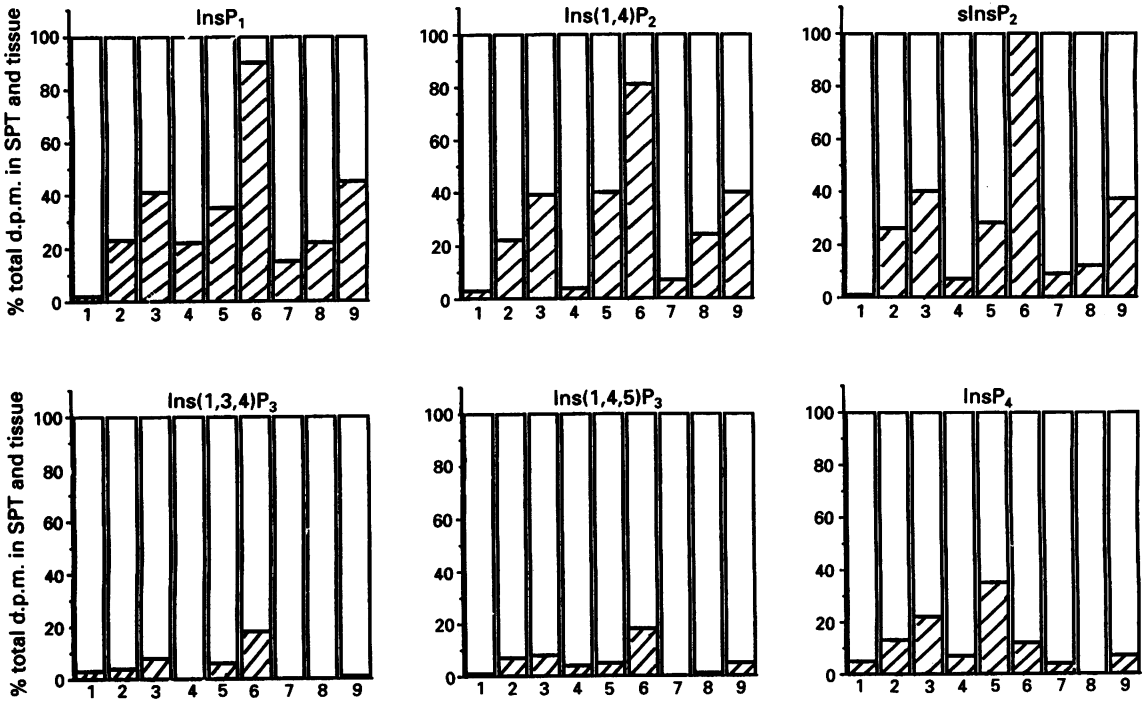

Figure 3 The distribution of d.p.m. between supernatant (SPT) and tissue in permeabilized fragments. Increases in the levels of [^{3}H]-inositol phosphates were determined in [^{3}H]-inositol-labelled fragments permeabilized with α-toxin in the presence of ISS alone, GTPγS or CCh for different times and the tissue part separated from the supernatant as described in the Methods. Results represent the % of the total d.p.m. for each isomer found in the supernatant (hatched) or tissue part (open). (1), (2), and (3) represent distribution of basal d.p.m. after incubation in ISS for 30 s, 5 min or 20 min respectively. (4), (5), and (6) represent distribution of d.p.m. after subtraction of basal levels following stimulation with 100 μM GTPγS for 30 s, 5 min or 20 min respectively and (7), (8), and (9) represent the distribution of d.p.m. after subtraction of basal levels following stimulation with 100 μM CCh for 30 s, 5 min or 20 min respectively. The results represent the values from one experiment. Separation of supernatant from the tissue and analysis of [^{3}H]-inositol phosphates was performed on many samples with similar results.

100 or saponin resulted in a rapid loss of the enzyme LDH, such that greater than 50% of the LDH was lost from the fragments in the first 5 min incubation with Triton-X-100 and 10 min incubation with saponin (Figure 2). Concentrations of α-toxin up to 8000 u ml^{-1} also failed to cause detectable release of LDH (data not shown).

Basal levels of [^{3}H]-inositol phosphates

In contrast to experiments on non-permeabilized fragments (Prestwich & Bolton, 1995) the basal levels of [^{3}H]-inositol phosphates increased with time after permeabilization. The increases were 83%, 59%, 36%, 59% and 75% for the [^{3}H]-$InsP_1$, [^{3}H]-Ins(1,4)P_2, [^{3}H]-Ins(1,3,4)P_3, [^{3}H]-Ins(1,4,5)P_3 and [^{3}H]-$InsP_4$ respectively at 5 min compared to the values at 10 s. The increase in inositol phosphates observed may be related to the contractile effects of mM ATP concentrations present in ISS on longitudinal muscle of guinea-pig ileum (Burnstock *et al.*, 1970). Also the loss of [^{3}H]-$InsP_1$ and [^{3}H]-Ins(1,4)P_2 through the 'pores' formed during permeabilization may cause a shift in the equilibrium resulting in increased intracellular turnover.

Distribution of d.p.m. between the supernatant and tissue

Measurement of the distribution of d.p.m. between the supernatant part and tissue part of a sample showed that in non-permeabilized fragments incubated in normal KRB for 10 min, no detectable amounts of radioactivity eluting on the h.p.l.c. corresponding to the [^{3}H]-inositol phosphates were observed. Only 3% of total radioactivity was found in the supernatant of non-permeabilized fragments after incubating in ISS for 10 min.

Following permeabilization, inositol phosphates escaped into the supernatant. Several experiments were performed to determine the distribution of inositol phosphates in the supernatant compared with the tissue portion. Saponin (1 mg ml^{-1}) also increased inositol phosphates in a similar way to α-toxin but the effects were much smaller. Measurement of individual [^{3}H]-inositol phosphates in the supernatant and tissue fractions from permeabilized fragments during different experimental conditions is shown in Figure 3. The first three columns are from control samples incubated for 30 s, 5 min and 20 min and it can be seen that there is a time-dependent increase in the percentage of d.p.m. found in the supernatant fraction for all the [^{3}H]-inositol phosphates. The other six columns have had the basal d.p.m. subtracted and represent the distribution during either GTPγS (100 μM) stimulation for 30 s (4), 5 min (5) or 20 min (6) or CCh (100 μM) stimulation for 30 s (7), 5 min (8) or 20 min (9). The general trend is that the longer the incubation the greater percentage of [^{3}H]-$InsP_1$, [^{3}H]-Ins(1,4)P_2 and [^{3}H]-sInsP_2 that appears in the supernatant but for the [^{3}H]-Ins(1,3,4)P_3, [^{3}H]-Ins(1,4,5)P_3 and [^{3}H]-$InsP_4$ the majority of the d.p.m. remained in the tissue part (Figure 3).

Effect of CCh and GTPγS on [^{3}H]-inositol phosphate levels

Incubation of α-toxin permeabilized, [^{3}H]-inositol-labelled, smooth muscle fragments with CCh (in the absence of added GTP) or GTPγS resulted in time- and concentration-dependent increases in the levels of all the [^{3}H]-inositol phosphates in combined tissue fragments and supernatant (Figures 4 and 5). The time courses and % increases produced by CCh and GTPγS in the levels of [^{3}H]-inositol phosphate isomers were very similar except for [^{3}H]-Ins(1,4,5)P_3 and [^{3}H]-$InsP_4$'s at the early times (Figure 4). Increases in the levels of [^{3}H]-Ins(1,4,5)P_3 were significantly less with GTPγS than with CCh at all time points ($P<0.05$). GTPγS (up to 1 mM) had no significant effect on [^{3}H]-inositol phosphate levels in non-permeabilized muscle fragments

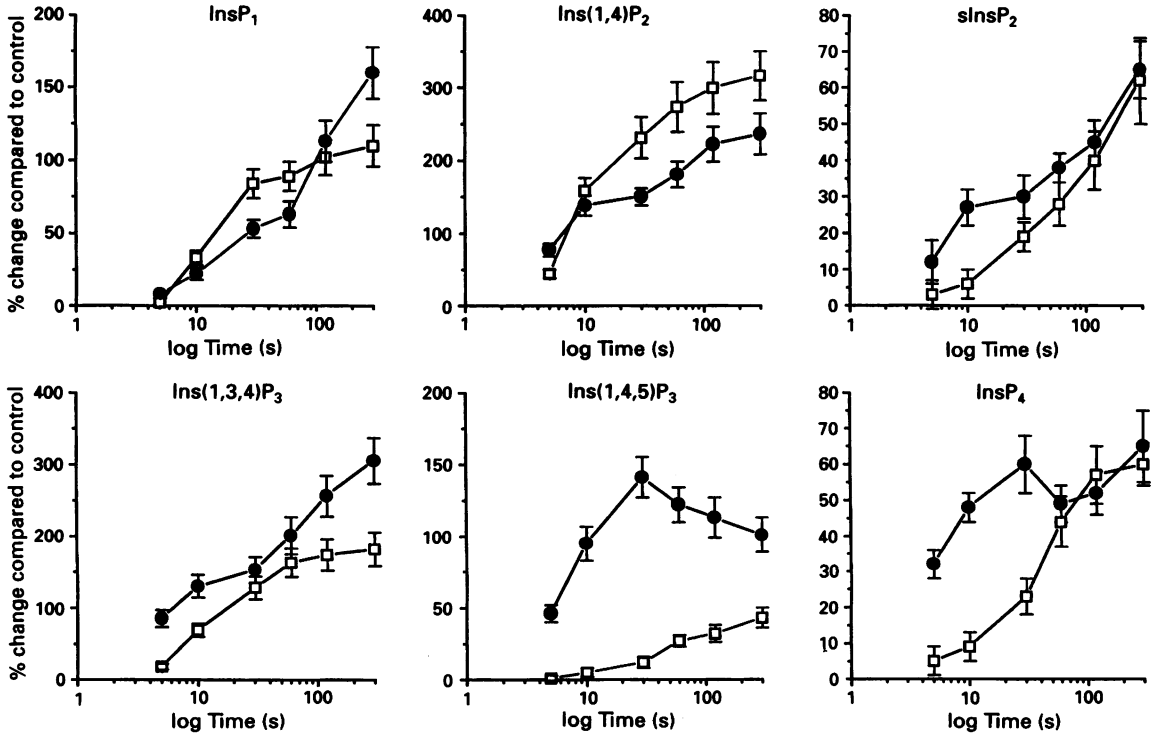

Figure 4 Effects of time of incubation with GTPγS or CCh on [^{3}H]-inositol phosphate levels in permeabilized smooth muscle fragments and their supernatant combined. [^{3}H]-inositol-labelled, α-toxin permeabilized fragments were incubated with 100 μM CCh (●) or 100 μM GTPγS (□) for 5 s, 10 s, 30 s, 60 s, 120 s or 5 min. Results represent the mean ± s.e.mean of three experiments performed on separate occasions and are expressed as the % change compared to control, where the control is taken as the value in the absence of added drug. Increases in the levels of [^{3}H]-$InsP_1$, [^{3}H]-Ins(1,4)P_2, [^{3}H]-sInsP_2, [^{3}H]-Ins(1,3,4)P_3, [^{3}H]-Ins(1,4,5)P_3 and [^{3}H]-$InsP_4$ are shown.

indicating that α-toxin treatment is essential to allow GTPγS access to the cell interior. Incubation of the permeabilized fragments with 0.5 μM atropine for 10 min prior to addition of 100 μM CCh reduced the CCh-induced increases in the levels of all the labelled inositol phosphates by an average of 79% (2 experiments). In non-permeabilized fragments the reduction of the response to 100 μM CCh was 95 ± 1.3% ($n = 6$). These effects are compatible with an equilibrium dissociation constant of atropine for the receptor of 3×10^{-9} M.

Effect of simultaneous addition of GTPγS and CCh on the levels of [^{3}H]-inositol phosphates

Although CCh-induced increases in the levels of [^{3}H]-inositol phosphates could be observed in permeabilized fragments and their supernatants in the absence of any added GTP, the absolute increase in d.p.m. was less than with non-permeabilized fragments for some of the isomers (Figure 6) and the maximum increase in [^{3}H]-Ins(1,4,5)P_3 was later in permeabilized fragments (30 s in permeabilized fragments, 10 s in non-permeabilized) and did not decline. The [^{3}H]-Ins(1,4)P_2 isomer increased slowly up to 2 min incubation, compared with the non-permeabilized fragments where the response peaked at 30 s (Figure 6).

Addition of 20 μM GTPγS at the same time as different concentrations of CCh, followed by incubation for 2 min did not further increase the levels of any of the [^{3}H]-inositol phosphates over the effect of CCh alone (data not shown). Incubation of permeabilized fragments with 100 μM GTPγS and various concentrations of CCh for 5 min however, significantly inhibited the CCh-induced increases in the levels of all the [^{3}H]-inositol phosphates ($P < 0.05$) (Figure 7). Incubation with 3 μM CCh for 5 min increased the levels of all the [^{3}H]-inositol phosphates and these increases were inhibited in the presence of 1–100 μM GTPγS when added at the same time as the CCh. The IC_{50} for GTPγS inhibition was between 5 μM and 8 μM for all the [^{3}H]-inositol phosphate isomers and at 100 μM GTPγS, almost all (95 ± 4.2%) the CCh response was inhibited.

In fragments permeabilized with saponin (1 mg ml^{-1} for 20 min at 22°C) CCh alone (without GTP) increased inositol phosphate levels as did GTPγS. The effects of CCh or GTPγS were generally smaller on the inositol phosphate isomers measured than when α-toxin was used.

The effect of incubation with GTPγS prior to CCh addition

When permeabilized smooth muscle fragments were incubated in the presence of increasing concentrations of GTPγS for 5 min before the addition of 100 μM CCh for a further 30 s, GTPγS above 1 μM caused a significant inhibition of the CCh-induced increases in the levels of all the [^{3}H]-inositol phosphates (Figure 8).

Effect of PTX treatment on CCh and GTPγS effects in permeabilized fragments

The CCh-induced increases and the GTPγS-induced increases in the levels of [^{3}H]-inositol phosphates were greatly reduced following treatment with PTX (6 μg ml^{-1} for 20 h at 30°C) (Figures 8 and 9). GTPγS inhibited the effect of CCh on [^{3}H]-inositol phosphate levels and this was, in general, also true when the effect of CCh was substantially reduced by PTX pretreatment. However, in different experiments there was some variation in the effects of GTPγS on the PTX-insensitive CCh response (compare Figures 8 and 9).

Effect of GDPβS

GDPβS (5 mM) had no effect on the basal levels of the [^{3}H]-inositol phosphates. However it almost completely inhibited (by 92% and 96% respectively) the CCh-(100 μM)

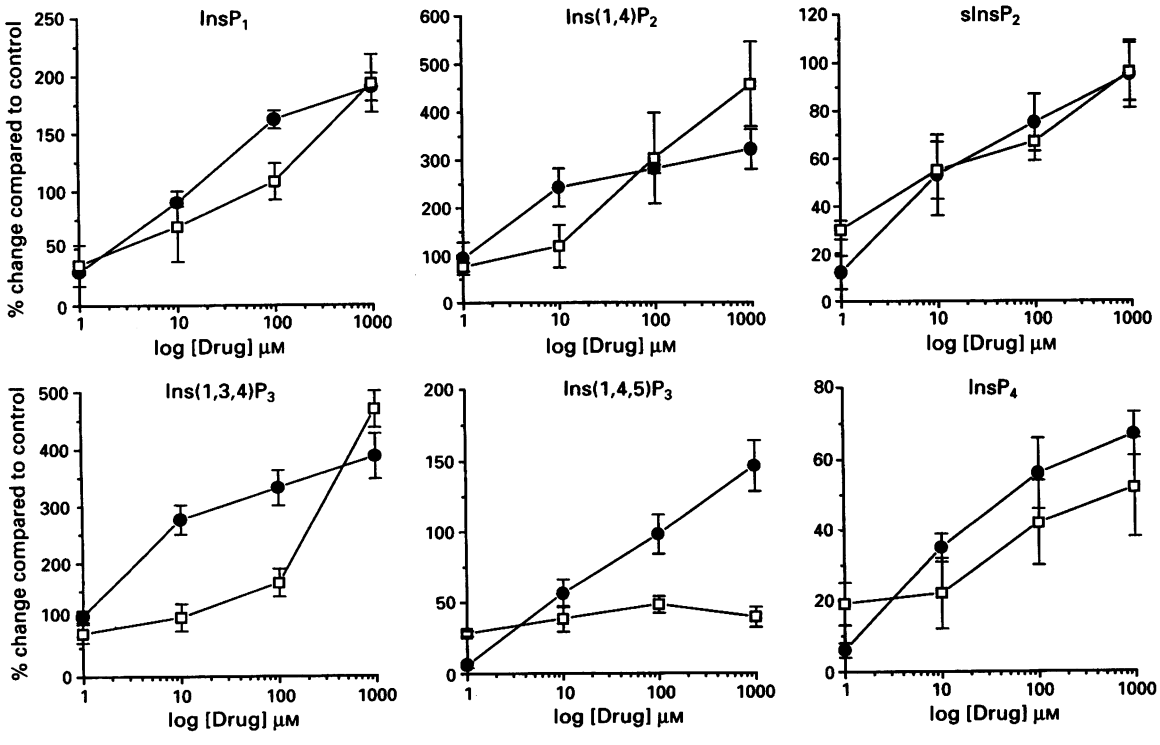

Figure 5 Concentration-response curves for the effects of CCh and GTPγS on [^{3}H]-inositol phosphates in permeabilized smooth muscle fragments and their supernatant combined. Permeabilized fragments were incubated in the presence of different concentrations of CCh (●) or GTPγS (□) for 5 min. Results represent the mean ± s.e.mean of three experiments performed on separate occasions and are expressed as the % change compared to control, where the control is taken as the value in the absence of added drug.

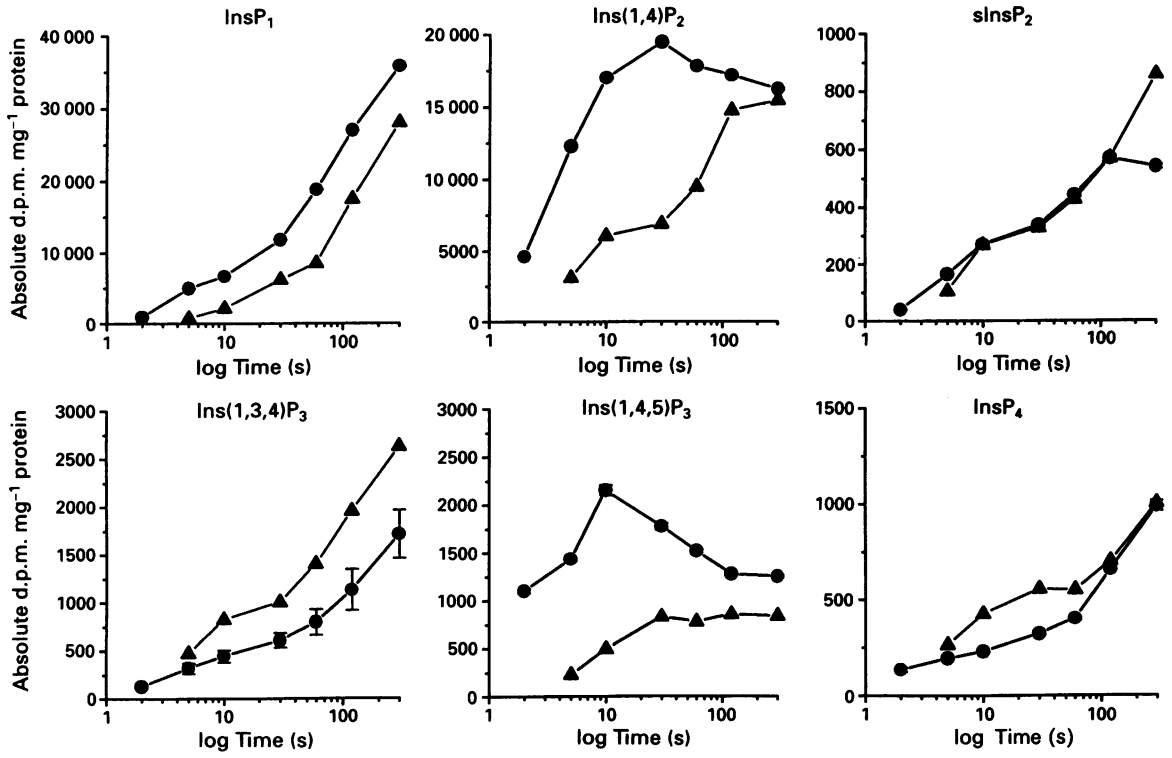

Figure 6 Comparison of CCh-induced increases in [^{3}H]-inositol phosphates in non-permeabilized and permeabilized fragments with their supernatant. CCh-induced increases in the levels of [^{3}H]-inositol phosphates were determined in non-permeabilized fragments and fragments permeabilized with 2500 u ml^{-1} α-toxin for 30 min. Results show the time-dependent increases in the levels of [^{3}H]-inositol phosphates in the presence of 100 μM CCh in non-permeabilized fragments (●) or permeabilized (▲) fragments and are the mean ± s.e.mean (where it exceeds symbol width) of three unpaired experiments performed on separate occasions, on separate guinea-pigs and are expressed as absolute d.p.m. minus basal values.

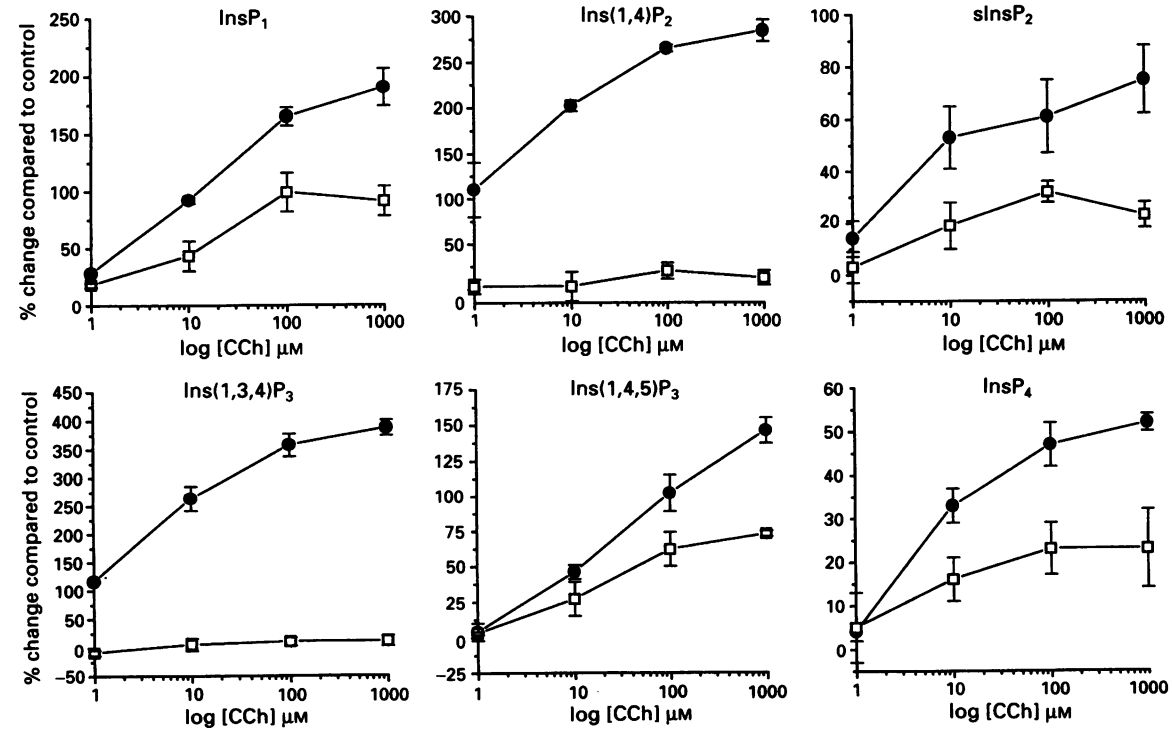

Figure 7 Effect of GTPγS on the response to CCh in permeabilized fragments. Permeabilized fragments were incubated with either 1 μM, 10 μM, 100 μM or 1 mM CCh for 5 min in the absence (●) or presence (□) of 100 μM GTPγS for 5 min added with the CCh. Results represent the mean ± s.e.mean of three experiments performed on separate occasions and are expressed as the % change compared to control, where the control is taken as the value in the absence of CCh.

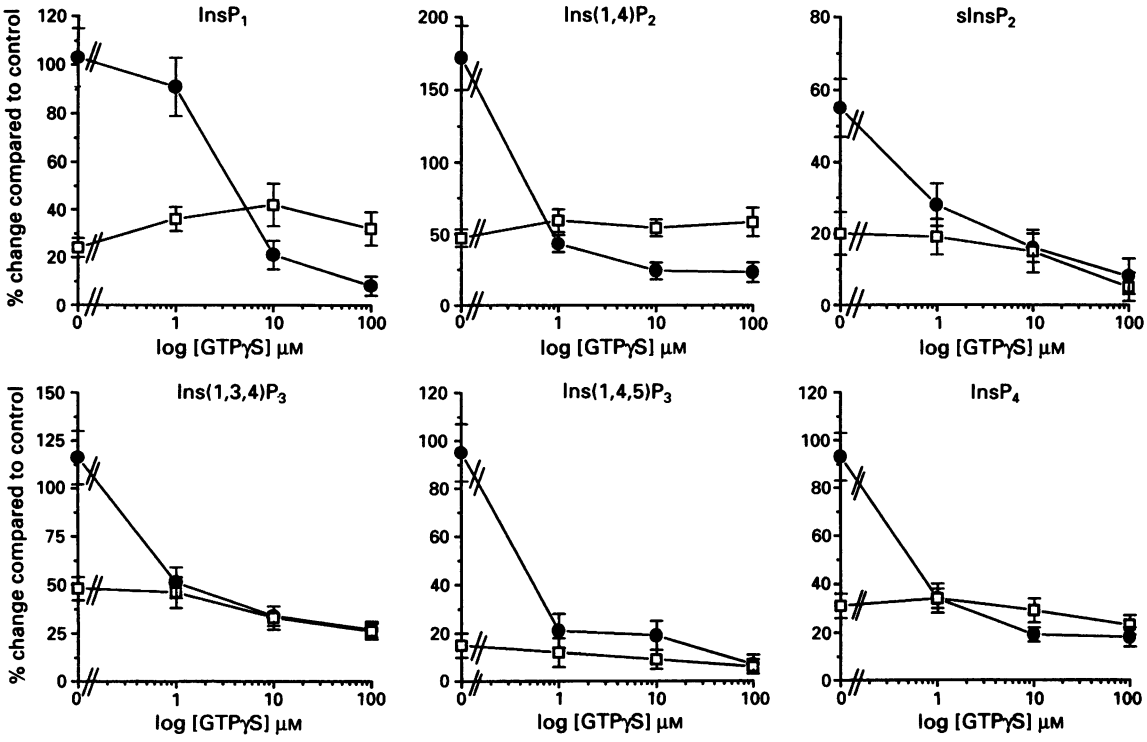

Figure 8 GTPγS inhibition of the CCh response and the effect of PTX on this. Smooth muscle fragments were incubated for 20 h at 30°C in either normal KRB or KRB containing 6 μg ml^{-1} PTX; [^{3}H]-inositol was present in the incubation solutions. The fragments were then permeabilized and incubated for 5 min in the absence or in the presence of 1 μM, 10 μM or 100 μM GTPγS. At the end of the 5 min incubation period, 100 μM CCh was added for a further 30 s and the reaction stopped. Results are shown as the % increase over the level of [^{3}H]-inositol phosphate without CCh. The inhibitory effect of GTPγS on the % increase of the response to 100 μM CCh in fragments with no PTX (●) and with PTX treatment is shown (□). Results represent the mean ± s.e.mean of three experiments performed on separate occasions.

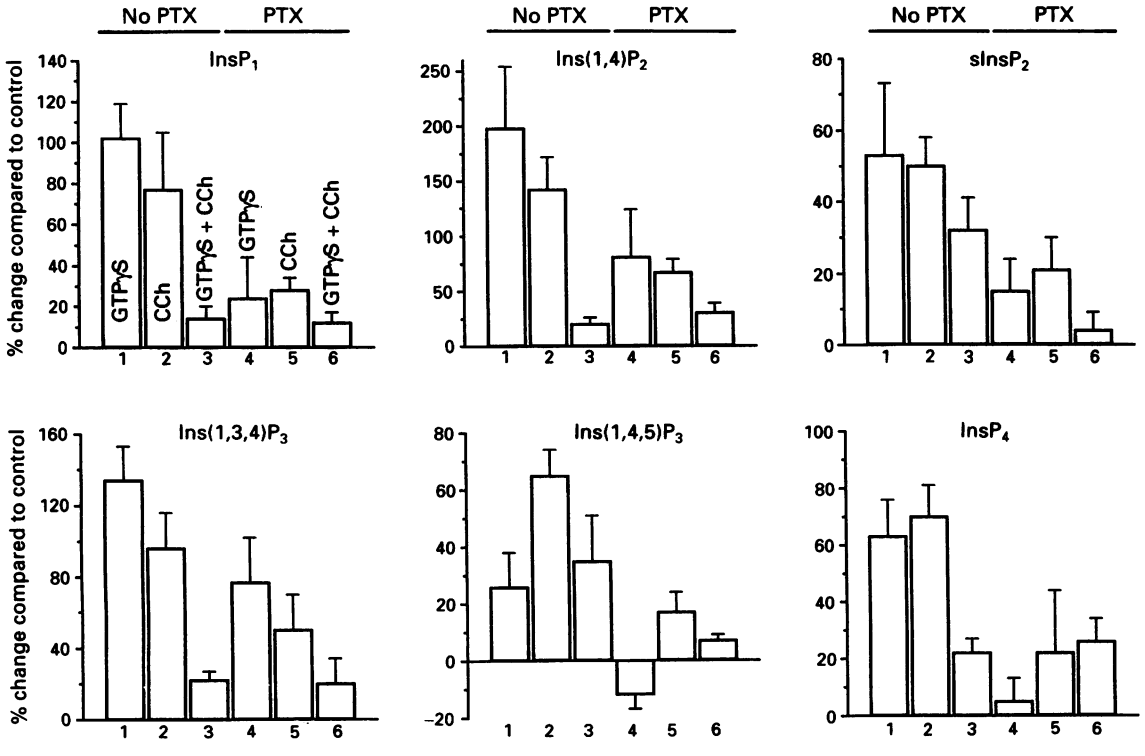

Figure 9 Effect of PTX on the interaction between CCh and GTPγS. [^{3}H]-inositol-labelled smooth muscle fragments were incubated for 20 h at 30°C in either normal KRB or KRB containing 6 μg ml^{-1} PTX. The fragments were then permeabilized and incubated in 100 μM GTPγS for 5.5 min, incubated for 5 min in ISS alone followed by 100 μM CCh for 30 s or 100 μM GTPγS for 5 min followed by 30 s application of 100 μM CCh. Columns (1), (2) and (3) are without PTX and (4), (5), and (6) are with PTX treatment. (1) and (4) represent 100 μM GTPγS for 5 min, (2) and (5) represent 100 μM CCh for 30 s and (3) and (6) represent 30 s application of 100 μM CCh in the presence of 100 μM GTPγS previously present for 5 min. Results represent the mean ± s.e.mean of three experiments performed on separate occasions and are expressed as the % change compared to control, where the control is taken as the value in the absence of CCh for (2), (3), (5) and (6) and the absence of GTPγS for (1) and (4).

and GTPγS-(100 μM) induced increases in the levels of [^{3}H]-$InsP_1$ and [^{3}H]-Ins(1,4,5)P_3. The increases in [^{3}H]-Ins(1,4)P_2, [^{3}H]-Ins(1,3,4)P_3 and [^{3}H]-$InsP_4$ levels due to GTPγS stimulation were inhibited by 82%, 81% and 82% respectively and increases due to CCh stimulation were inhibited by 81%, 80% and 96% respectively.

Effect of dibutyryl cyclic AMP and Sp-cAMPs on CCh-induced increases in [^{3}H]-inositol phosphate levels

Incubation of permeabilized fragments in the presence of either 10 μM dibutyryl cyclic AMP or 10 μM Sp-cAMPs for 10 min prior to application of CCh (100 μM) for a further 10 s resulted in a substantial reduction in the response to CCh. The average % reduction ($n = 3$) in the CCh response for [^{3}H]-$InsP_1$, [^{3}H]-$InsP_2$, [^{3}H]-$InsP_3$ and [^{3}H]-$InsP_4$ isomers in the presence of dibutyryl cyclic AMP was 93 ± 11, 89 ± 13, 86 ± 11 and 69 ± 11 and in the presence of Sp-cAMPs was 56 ± 6, 78 ± 6, 71 ± 7 and 79 ± 7 respectively.

Cyclic AMP measurements

Basal cyclic AMP values for non-permeabilized smooth muscle fragments incubated in the absence of added IBMX rose from 0.98 to 2.12 pmol mg^{-1} protein during a 10 min incubation period. Changes in these levels in the absence of IBMX upon β-adrenoceptor activation or following treatment of fragments with ChTX could not be observed (data not shown). Basal cyclic AMP levels incubated in the presence of 1 mM IBMX increased from 10 to 36 pmol mg^{-1} protein over a 10 min incubation period. This indicates that there is very efficient metabolism of cyclic AMP by phosphodiesterases present in these fragments. Increases in the levels of cyclic AMP were observed when a β-adrenoceptor agonist was added if 1 mM IBMX was present. However, up to 100 μM CCh (for 10 min) had no significant effect on the levels of cyclic AMP (20 ± 6 pmol mg^{-1} protein, $n = 6$) whereas incubation with 100 μM GTPγS (for 10 min) significantly increased cyclic AMP levels to 174 ± 18 pmol mg^{-1} protein ($P < 0.01$, $n = 3$). However, 10 mM NaF/10 μM $AlCl_3$ had no significant effect on cyclic AMP levels (28 ± 8 pmol mg^{-1} protein, $n = 3$). GDPβS (5 mM, for 10 min) had no effect on the basal levels of cyclic AMP but significantly inhibited the increases produced by 100 μM GTPγS by 55 ± 9.2% ($P < 0.05$, $n = 3$) (incubated together for 10 min).

Discussion

Permeabilization

The studies on the loss of [^{3}H]-2DG and LDH indicate that a sufficient concentration of α-toxin will permeabilize the cell membranes allowing small, but not large, molecules to escape. Further evidence for this came from the loss of [^{3}H]-inositol phosphates which also escaped from the tissue after α-toxin treatment; in fragments not so treated, escape of [^{3}H]-inositol phosphates was negligible. Also, GTPγS normally without effect on [^{3}H]-inositol phosphate levels, increased these substantially after α-toxin treatment indicating that adequate access to the interior of cells was achieved. The question of whether some cells in the tissue fragments remained unpermeabilized is an important one, because if permeabilized and non-permeabilized cells are both present in significant numbers, the total tissue response will represent events taking place in two separate populations and not, as is required for the interpretation of these experiments, in the same cells. Increasing α-toxin concentration from 2500 to 8000 u ml^{-1} only marginally increased the rate of loss of [^{3}H]-2DG over the first 5 min. Thus increasing the rate of formation of membrane pores more than 3 fold by increasing the α-toxin concentration had only a marginal effect on exchange. It is possible that treatment with 2500 u ml^{-1} or more of α-toxin for only 5 min is sufficient to produce exchange of small molecules at a near maximum rate although this possibility was not tested and α-toxin was routinely applied for 30 min. Presumably, at concentrations above 2500 u ml^{-1} other factors limit the escape of small molecules from the tissue fragments. Triton-X-100 (1%) and saponin (1 mg ml^{-1}) caused a greater loss of [^{3}H]-2DG but these agents also caused loss of large molecules such as LDH. The loss of these larger molecules and the resultant alterations in the cell molecular architecture may explain the faster loss of [^{3}H]-2DG seen with these detergents. Saponin and Triton-X-100 have been used to permeabilize smooth muscle (Endo *et al.*, 1977; Obara & Yamada, 1984) but loss of receptor function (Itoh *et al.*, 1983; Somlyo *et al.*, 1985) and destruction of intracellular membranes have been observed (Knight & Scrutton, 1986). However, agonist-induced contraction has been shown to occur in smooth muscle permeabilized with saponin in the absence of GTP (Fermum *et al.*, 1991). In the present study, both GTPγS and CCh increased inositol phosphate levels in saponin-treated fragments although the effects were less than in α-toxin treated tissue.

The increase in most [^{3}H]-inositol phosphate isomers in α-toxin permeabilized fragments was less than in non-permeabilized fragments. After permeabilization, $[Ca^{2+}]_i$ was held at 0.13 μM by the use of EGTA and there is presumably no membrane potential change. Phospholipase C (PLC) is an enzyme stimulated by Ca^{2+} (Low *et al.*, 1986; Ryu *et al.*, 1987) and depolarization of the membrane may increase inositol phosphate formation (Jafferji & Michell, 1976; Best & Bolton, 1986); both these effects may contribute in the non-permeabilized fragments to the increase in [^{3}H]-inositol phosphate levels produced by CCh. Also, increases in the levels of all the [^{3}H]-inositol phosphates following incubation of permeabilized fragments with CCh occurred in the absence of any added GTP. However, commercial ATP may be contaminated with GTP (Ross & Gilman, 1980) and ATP may also be transphosphorylated to GTP (Sternweis & Gilman, 1982; Otero, 1990).

From the distribution of [^{3}H]-inositol phosphates between the supernatant and tissue of the samples it was found that as the basal levels increase with time so does the percentage of d.p.m. found in the supernatant (Figure 3). As the levels of [^{3}H]-$InsP_1$, [^{3}H]-Ins(1,4)P_2 and [^{3}H]-s$InsP_2$ increase with time when GTPγS is present a substantial proportion of these isomers move into the supernatant part suggesting the levels rose in the cytosol of the cells. Although the time-dependent increases in these [^{3}H]-inositol phosphates are similar in the presence of CCh or GTPγS, the movement of isomers into the supernatant is not as great in the presence of CCh (Figure 3). This may reflect a faster turnover of the [^{3}H]-inositol phosphates in the presence of CCh so that they are not so available for diffusion out of the cell. Also the d.p.m. for the higher [^{3}H]-inositol phosphates, [^{3}H]-Ins(1,3,4)P_3, and [^{3}H]-Ins(1,4,5)P_3 stay mainly in the tissue fragments in the presence of both GTPγS or CCh. This may also reflect a higher turnover of these isomers and indicates that these isomers are readily metabolized and therefore do not have a chance to pass out of the cell and/or there is some compartmentalization within the cell. The changeable results in the distribution of the [^{3}H]-$InsP_4$ isomer may reflect a possible mixture of isomers which change with time.

GTPγS and CCh

GTPγS inhibited the action of CCh when added at the same time and was an even more effective inhibitor when added prior to CCh application. Previously we have shown that although AlF increased basal levels of [^{3}H]-inositol phosphates, it completely inhibits the CCh-induced increases in [^{3}H]-inositol phosphates in non-permeabilized fragments (Prestwich & Bolton, 1995). In this study, GTPγS also both increased the levels of [^{3}H]-inositol phosphates in perme-

abilized fragments and inhibited the CCh response suggesting that both AlF and GTPγS may act through G-proteins both to stimulate basal levels of [^{3}H]-inositol phosphates and to inhibit CCh-induced increases in [^{3}H]-inositol phosphate levels.

However, incubation with GTPγS also increased basal levels of cyclic AMP. Increases in cyclic AMP result in increased activity of protein kinase A and phosphorylation of proteins so that part of the inhibition of CCh-stimulated increases in the levels of [^{3}H]-inositol phosphates by GTPγS could be due to activation of protein kinase A. Increases in protein kinase A activity via activation of Gsα could result in phosphorylation of the muscarinic AChR, G-protein or PLC mimicking a negative feedback mechanism. This mechanism for GTPγS action seems likely since incubation of the smooth muscle fragments in the presence of either of the cyclic AMP analogues, dibutyryl cyclic AMP or Sp-cAMPs, also substantially reduced the CCh-induced stimulation of labelled inositol phosphates. However, incubation with AlF under conditions which completely inhibited CCh-induced increases in labelled inositol phosphates (Prestwich & Bolton, 1995) had no effect on the levels of cyclic AMP. Therefore other mechanisms for this inhibition by both G-protein activators must also be considered.

Activation of PLC by GTPγS or AlF would also increase 1,2-diacylglycerol levels and activate protein kinase C. Protein kinase C activation could result in the phosphorylation of the G-protein (Katada *et al.*, 1985) or the muscarinic AChR itself (Woods *et al.*, 1987) resulting in a reduced ability of the system to increase [^{3}H]-inositol phosphates in response to further agonist being present. However G-protein-mediated inhibition of PLC activity itself has also been observed (Bizzarri *et al.*, 1990; Geet *et al.*, 1990; Gutowski *et al.*, 1991).

Recent studies have suggested that both βγ subunits and α subunits can both stimulate and inhibit the activity of PLC (Sternweis & Smrcka, 1992). PLCβ2 can be modulated independently by α and βγ subunits acting at different sites (Bong Lee *et al.*, 1993). Both α and βγ subunits can regulate cardiac K^+ channel opening (Logothetis *et al.*, 1988). Thus there are several ways α and βγ can modulate PLC: α alone, βγ alone, or both acting independently; both acting synergistically or both acting antagonistically.

PLC exists in several isoforms some of which e.g. PLCβ1-4 are regulated by G-proteins whereas others are not e.g. PLCγ. PLCβ forms 1-3 are regulated both by Gα subunits of the Gq class, and by Gβγ subunits (Katz *et al.*, 1992; Park *et al.*, 1993). PLCβ4 is not regulated by Gβγ. Activation of PLCβ isoforms by Gαq/11 and Gβγ is independent and not conditional on priming by either subunit. However, the concentration of βγ subunits required to activate PLCβ3 was shown to be much higher (40 fold) than that of α subunits required to activate PLCβ1 (Park *et al.*, 1993). In longitudinal muscle of guinea-pig small intestine it is conceivable that the PTX-insensitive component of muscarinic AChR activation of inositol phospholipid hydrolysis may occur via α subunits from a G-protein of the Gq family interacting with a PLCβ1 isozyme, and PTX-sensitive component arise from the interaction of the muscarinic AChR with Gi (associated with adenylyl cyclase inhibition) freeing up βγ subunits to interact with the PLCβ2 isozyme.

As well as reducing the CCh-induced increases in [^{3}H]-inositol phosphate levels, PTX treatment also reduced the increases produced by GTPγS, which is a receptor-independent process. This may be explained by failure of αβγ subunits to dissociate into α and free βγ following α subunit ribosylation. The carboxyl terminal (where ADP-ribosylation by PTX of a cysteine residue occurs) is thought to be involved in binding to the receptor and the major effect of ADP-ribosylation by PTX is an uncoupling of the receptor from the G-protein. This sensitivity of both CCh and GTPγS to PTX suggests that PTX not only uncoupled the muscarinic AChR from PLC but also uncoupled the G-protein from PLC activity.

Muscarinic AChR types

The effects observed due to muscarinic AChR activation may be mediated by only one type or several types of muscarinic AChRs. It has been suggested that M_2 and M_3 receptors are present in this tissue (Michel & Whiting, 1990) and contraction via stimulation of mainly the M_3 type has been suggested to occur (Barocelli *et al.*, 1993). However transfection studies have shown that stimulation of the m3 AChR can result in inositol phospholipid hydrolysis and activation of the m2 AChR can result in both adenylyl cyclase inhibition and inositol phospholipid hydrolysis (Ashkenazi *et al.*, 1989). The response to activation of both transfected m2 and m3 receptors in oocytes was inhibited by heparin suggesting that both receptors acted through an Ins(1,4,5)P_3-dependent pathway. The precise type of muscarinic AChR involved in this study awaits either highly selective antagonists or transfection and analysis of the specific subtypes present in this tissue.

The authors thank the MRC for financial support.

References

ASHKENAZI, A., PERALTA, E.G., WINSLOW, J.W., RAMACHANDRAN, J. & CAPON, D.J. (1989). Functionally distinct G-proteins selectively couple different receptors to phosphatidylinositol hydrolysis in the same cell. *Cell*, **56**, 487–493.

BAROCELLI, E., CHIAVARINI, M., BALLABENI, V. & IMPICCIATORE, M. (1993). Interaction of selective compounds with muscarinic receptors at dispersed intestinal smooth muscle cells. *Br. J. Pharmacol.*, **108**, 393–397.

BATTY, I.H., NAHORSKI, R. & IRVINE, R.F. (1985). Rapid formation of inositol 1,3,4,5-tetrakisphosphate following muscarinic receptor stimulation of rat cerebral cortical slices. *Biochem. J.*, **232**, 211–215.

BERGMEYER, H.U. & BERNT, S. (1974). Lactate dehydrogenase: UV-assay with pyruvate and NADH. In *Methods of Enzymatic Analysis*. ed. Bergmeyer, H.U. Vol. 2. pp. 574–579. New York, London: Verlag Chemie Weinheim, Academic Press, Inc.

BEST, L. & BOLTON, T.B. (1986). Depolarization of guinea-pig visceral smooth muscle causes hydrolysis of inositol phospholipids. *Naunyn-Schmied. Arch. Pharmacol.*, **333**, 78–82.

BHAKDI, S. & TRANUM-JENSEN, J. (1987). Damage to mammalian cells by proteins that form transmembrane pores. *Rev. Physiol. Biochem. Pharmacol.*, **107**, 147–223.

BIZZARRI, C., GIOLAMO, M.D., D'ORAZIO, M.C. & CORDA, D. (1990). Evidence that a guanine nucleotide binding protein linked to muscarinic receptor inhibits directly phospholipase C. *Proc. Natl. Acad. Sci. U.S.A.*, **87**, 4889–4893.

BONG LEE, S., SHIN, S.H., HEPLER, J.R., GILMAN, A.G. & RHEE, S.G. (1993). Activation of phospholipase C-β2 mutants by G protein αq and βγ subunits. *J. Biol. Chem.*, **268**, 25952–25957.

BURNSTOCK, G., CAMPBELL, G., SATCHELL, D. & SMYTHE, A. (1970). Evidence that adenosine triphosphate or a related nucleotide is the transmitter substance released by non-adrenergic inhibitory nerves in the gut. *Br. J. Pharmacol.*, **40**, 668–688.

CASEY, P. & GILMAN, A.G. (1988). G protein involvement in receptor-effector coupling. *J. Biol. Chem.*, **263**, 2577–2580.

CATTANEO, M.G. & VICENTINI, L.M. (1989). Differential mechanisms of inositol phosphate generation at the receptors for bombesin and platelet-derived growth factor. *Biochem. J.*, **262**, 665–668.

COCKCROFT, S. (1987). Polyphosphoinositide phosphodiesterase: regulation by a novel guanine nucleotide binding protein Gp. *Trends Biochem. Sci.*, **12**, 75–78.

COCKCROFT, S. & GOMPERTS, B.D. (1985). Role of guanine nucleotide binding protein in the activation of polyphosphoinositide phosphodiesterase. *Nature*, **314**, 534–536.

DOWNES, C.P. & MICHEL, R.H. (1981). The phosphoinositide phosphodiesterase of erythrocyte membranes. *Biochem. J.*, **198**, 133–140.

ENDO, M., KITAZAWA, T., YAGI, S., IINO, M. & KAKUTA, Y. (1977). Some properties of chemically skinned smooth muscle fibres. In *Excitation-Contraction Coupling in Smooth Muscle*. ed. Casteels, R., Godfriend, T & Rüegg, J.C. pp. 199–209. New York: Elsevier/North Holland.

FERMUM, R., KOSCHE, D. & MÖRITZ, K.-U. (1991). Membrane-associated signal transduction modulates contractile responses to Ca^{2+} in saponin-skinned coronary smooth muscle. *Naunyn-Schmied. Arch. Pharmacol.*, **343**, 209–216.

FÜSSLE, R., BHAKDI, S., SZIEGOLEIT, A., TRANUM-JENSEN, J., KRANZ, T. & WELLENSIEK, H.-J. (1981). On the mechanism of membrane damage by *Staphylococcus aureus* α-toxin. *J. Cell Biol.*, **91**, 83–94.

GEET, C.V., DECKMYN, H., KIENAST, J., WITTEVRONGEL, C. & VERMYLEN, J. (1990). Guanine nucleotide-dependent inhibition of phospholipase C in human endothelial cells. *J. Biol. Chem.*, **265**, 7920–7926.

GUTOWSKI, S., SMRCKA, A., NOWAK, L., WU, D.G., SIMON, M. & STERNWEIS, P.C. (1991). Antibodies to the αq subfamily of guanine nucleotide-binding proteins α subunits attenuate activation of phosphatidylinositol 4,5-bisphosphate hydrolysis by hormones. *J. Biol. Chem.*, **266**, 20519–20524.

HOHMAN, R.J. (1988). Aggregation of IgE receptors induces degranulation in rat basophilic leukemia cells permeabilized with α-toxin from *Staphylococcus aureus*. *Proc. Natl. Acad. Sci. U.S.A.*, **85**, 1624–1628.

HONKANEN, R.E. & ABDEL-LATIF, A.A. (1989). Muscarinic-agonist and guanine nucleotide stimulation of myo-inositol trisphosphate formation in membranes isolated from bovine sphincter smooth muscle: effects of short-term cholinergic desensitization. *Mem. Biochem.*, **8**, 39–59.

IRVINE, R.F., ÄNGGÄRD, E.E., LETCHER, A.J. & DOWNES, C.P. (1985). Metabolism of inositol 1,4,5-trisphosphate and inositol 1,3,4-trisphosphate in rat parotid glands. *Biochem. J.*, **229**, 505–511.

ITOH, T., KURIYAMA, H. & SUZUKI, H. (1983). Differences and similarities in the noradrenaline- and caffeine-induced mechanical responses in the rabbit mesenteric artery. *J. Physiol.*, **337**, 609–629.

JAFFERJI, S.S. & MICHELL, R.H. (1976). Muscarinic cholinergic stimulation of phosphatidylinositol turnover in the longitudinal smooth muscle of the guinea-pig ileum. *Biochem. J.*, **154**, 653–657.

KATADA, T., GILMAN, A.G., WATANABE, Y., BAUER, S. & JAKOBS, K.H. (1985). Protein kinase C phosphorylates inhibitory guanine-nucleotide-binding regulatory component and apparently suppresses its function in hormonal inhibition of adenylate cyclase. *Eur. J. Biochem.*, **151**, 431–437.

KATZ, A., WU, D. & SIMON, M.I. (1992). Subunits βγ of heterotrimeric G protein β2 isoform of phospholipase C. *Nature*, **360**, 686–689.

KITAZAWA, T., GAYLINN, B.D., DENNEY, G.H. & SOMLYO, A.P. (1991). G-protein-mediated Ca^{2+} sensitization of smooth muscle contraction through myosin light chain phosphorylation. *J. Biol. Chem.*, **266**, 1708–1715.

KNIGHT, D. & SCRUTTON, M. (1986). Gaining access to the cytosol: the technique and some applications of electropermeabilization. *Biochem. J.*, **234**, 497–506.

LITOSCH, I., WALLIS, C. & FAIN, J.N. (1985). 5-Hydroxytryptamine stimulates inositol phosphate production in a cell-free system from blowfly salivary glands. *J. Biol. Chem.*, **260**, 5464–5471.

LOGOTHETIS, D.E., KIM, D., NORTHUP, J.K., NEER, E.J. & CLAPHAM, D.E. (1988). Specificity of action of guanine nucleotide binding regulatory protein subunits on the cardiac muscarinic K^+ channel. *Proc. Natl. Acad. Sci. U.S.A.*, **85**, 5814–5818.

LOW, M.G., CARROLL, R.C. & COX, A.C. (1986). Characterization of multiple forms of phosphoinositide-specific phospholipase C purified from human platelets. *Biochem. J.*, **237**, 139–145.

LOWRY, O.H., ROSEBROUGH, N.J., FARR, A.L. & RANDALL, R.J. (1951). Protein measurement with the folin phenol reagent. *J. Biol. Chem.*, **193**, 265–275.

MARTELL, A.E. & SMITH, R.M. (1975). *Critical Stability Constants*. pp. 269–284. New York: Plenum Press.

MICHEL, A.D. & WHITING, R.L. (1990). The binding of [^{3}H]4-diphenylacetoxy-N-methylpiperidine methiodide to longitudinal ileal smooth muscle muscarinic receptors. *Eur. J. Pharmacol.*, **176**, 197–206.

NISHIMURA, J., KHALIL, R.A., DRENTH, J.P. & VAN BREEMEN, C. (1990). Evidence for increased myofilament Ca^{2+} sensitivity in norepinephrine-activated vascular smooth muscle. *Am. J. Physiol.*, **259**, H2–H8.

NISHIMURA, J., KOLBER, M. & VAN BREEMEN, C. (1988). Norepinephrine and GTPγS increase myofilament Ca^{2+} sensitivity in alpha-toxin permeabilized arterial smooth muscle. *Biochem. Biophys. Res. Commun.*, **157**, 677–683.

OBARA, K. & YAMADA, T. (1984). Some properties of chemically skinned smooth muscle cells. *Jpn. J. Physiol.*, **34**, 1089–1104.

OLEFSKY, J.M. (1978). Mechanisms of the ability of insulin to activate the glucose-transport system in rat adipocytes. *Biochem. J.*, **172**, 137–142.

ONO, T., MITA, M., SUGA, O., HASHIMOTO, T., OISHI, K. & UCHIDA, M.K. (1992). Receptor-coupled shortening of alpha-toxin-permeabilized single smooth muscle cells from the guinea-pig stomach. *Br. J. Pharmacol.*, **106**, 539–543.

OTERO, A. DE. S. (1990). Transphosphorylation and G-protein activation. *Biochem. Pharmacol.*, **39**, 1399–1404.

PACAUD, P. & BOLTON, T.B. (1992). Relation between muscarinic receptor cationic current and internal calcium in guinea-pig jejunal smooth muscle cells. *J. Physiol.*, **441**, 477–499.

PARK, D., JHON, D.-Y., LEE, C.W., LEE, K.-H. & RHEE, S.G. (1993). Activation of phospholipase C isozymes by G protein βγ subunits. *J. Biol. Chem.*, **268**, 4573–4576.

PRESTWICH, S.A. & BOLTON, T.B. (1991). Measurement of picomole amounts of any inositol phosphate isomer separable by h.p.l.c. by means of a bioluminescence assay. *Biochem. J.*, **274**, 663–672.

PRESTWICH, S.A. & BOLTON, T.B. (1995). G-protein involvement in muscarinic receptor-stimulated inositol phosphate production in longitudinal smooth muscle from the small intestine of the guinea pig. *Br. J. Pharmacol.*, **114**, 119–126.

ROSS, E.M. & GILMAN, A.G. (1980). Biochemical properties of hormone-sensitive adenylate cyclase. *Annu. Rev. Biochem.*, **49**, 533–564.

RYU, S.H., LEE, S.Y., LEE, K.Y. & RHEE, S.G. (1987). Catalytic properties of inositol trisphosphatase kinase: activation by Ca^{2+} and calmodulin. *FASEB J.*, **1**, 388–393.

SMELLIE, F.E., DAVIS, C.W., DALY, J.W. & WELLS, J.N. (1979). Alkylxanthines: inhibition of adenosine elicited accumulation of cyclic AMP in brain slices and of brain phosphodiesterase activity. *Life Sci.*, **24**, 2475–2482.

SMITH, C.D., LANE, B.C., KUSAKA, I., VERGHESE, M.W. & SNYDERMAN, R. (1985). Chemoattractant receptor-induced hydrolysis of phosphatidylinositol 4,5-bisphosphate in human polymorphonuclear leucocyte membranes: requirement for guanine nucleotide regulatory protein. *J. Biol. Chem.*, **260**, 5875–5878.

SOMLYO, A.V., BOND, M., SOMLYO, A.P. & SCARPA, A. (1985). Inositol trisphosphate-induced calcium release and contraction in vascular smooth muscle. *Proc. Natl. Acad. Sci. U.S.A.*, **82**, 5231–5235.

STERNWEIS, P.C. & GILMAN, A.G. (1982). Aluminium: a requirement for activation of the regulatory component of adenylate cyclase by fluoride. *Proc. Natl. Acad. Sci. U.S.A.*, **99**, 4888–4891.

STERNWEIS, P.C. & SMRCKA, A.V. (1992). Regulation of phospholipase C by G proteins. *Trends Pharmacol. Sci.*, **17**, 502–506.

UHING, R.J., PRPIC, V., JIANG, H. & EXTON, J.H. (1986). Hormone-stimulated polyphosphoinositide breakdown in rat liver plasma membranes. Roles of guanine nucleotides and calcium. *J. Biol. Chem.*, **261**, 2140–2146.

WOODS, N.M., CUTHBERTSON, K.S.R. & COBBOLD, P.H. (1987). Phorbol ester-induced alterations of free Ca^{2+} ion transients in single rat hepatocytes. *Biochem. J.*, **246**, 619–626.

(Received October 20, 1994
Revised January 12, 1995
Accepted January 17, 1995)

British Journal of Pharmacology (1995) 115, 158–162

Pharmacological identification of different inhibitory mediators involved in the innervation of the internal anal sphincter

[1]A. Tøttrup, M.A. Knudsen, F. Hanberg Sørensen & E.B. Glavind

Dept of Surgical Research, University Hospital of Aarhus, Amtssygehuset, 8000 Aarhus C, Denmark

1 Inhibitory non-adrenergic, non-cholinergic (NANC) responses were studied in isolated strips from the rabbit internal anal sphincter.

2 In the presence of atropine and guanethidine, transmural field stimulation induced frequency-dependent relaxations that reached a plateau at frequencies ≥ 4 Hz.

3 These relaxations were inhibited by apamin (10^{-6} M) and by N^{ω}-nitro-L-arginine (L-NOARG, 10^{-4} M). With these two substances in combination, relaxations were still seen in response to field stimulation, but only at frequencies >2 Hz.

4 In the presence of both apamin (10^{-6} M) and L-NOARG (10^{-4} M), responses at high frequencies consisted of a fast relaxation followed by a slow return to prestimulus tension level. α-Chrymotrypsin hastens the return of tension to prestimulus level after high frequency stimulation.

5 Zinc-protoporphyrin IX, an inhibitor of haeme oxygenase, had a significant inhibitory effect on relaxations induced by transmural field stimulation. It was found, however, that responses to sodium nitroprusside and to isoprenaline (both 10^{-9}–10^{-4} M) were reduced comparably, indicating that the effect of zinc-protoporphyrin IX was unspecific.

6 It is concluded that pharmacological analysis allows identification of at least three distinguishable components of the inhibitory NANC innervation of the rabbit internal anal sphincter. The study does not allow conclusions about the role of carbon monoxide, a recently proposed mediator of NANC responses in opossum internal anal sphincter.

Keywords: ATP; nitric oxide; L-arginine; NANC; apamin; carbon monoxide; zinc protoporphyrin

Introduction

Until a few years ago, the bee venom, apamin, was the only agent that efficiently and specifically affected responses to stimulation of inhibitory non-adrenergic, non-cholinergic (NANC) nerves of the intestine. Apamin blocks the opening of Ca^{2+}-sensitive potassium channels (Banks *et al.*, 1979), and although not firmly established, the purine ATP seems to be a likely transmitter candidate for this response. It is evident that apamin has dramatic effects in some tissues (Maas, 1981; Lim & Muir, 1986) while no influence on NANC responses can be detected in others (Jury *et al.*, 1985). Moreover, some portions of the gut show both apamin-sensitive and -insensitive responses (Costa *et al.*, 1986). The identification of NO or a related molecule generated from the L-arginine-NO pathway as a mediator of NANC neurotransmission (Gillespie *et al.*, 1989; Li & Rand, 1989) has given us the opportunity to differentiate further between types of NANC responses in various organs. Analogues of L-arginine are efficient inhibitors of NO formation (Rees *et al.*, 1989; Moore *et al.*, 1990), and again, in some tissues very convincing effects of the substances can be demonstrated (Bult *et al.*, 1990; O'Kelly *et al.*, 1993; Tøttrup *et al.*, 1991; 1992), while NANC responses in other tissues are not significantly affected (Knudsen & Tøttrup, 1992). The peptide vasoactive intestinal polypeptide (VIP), which is present abundantly in myenteric neurones, definitely seems to be an inhibitory NANC transmitter (for review, see Dockray, 1987). A precise definition of the role of VIP has so far been limited because specific VIP antagonists with well-documented actions in smooth muscle are not at present available. To complicate things further, very recent papers have proposed that carbon monoxide may be a neural messenger (Verma *et al.*, 1993), and may be involved in the mediation of inhibitory NANC responses of the internal anal sphincter (Rattan & Chakder, 1993). Haeme oxygenase converts haeme to CO and biliverdin (Maines, 1988), and this conversion may be blocked by zinc protoporphyrin IX (Zn-PP-IX; Maines, 1981). The present experiments were carried out to characterize the NANC inhibitory innervation of the rabbit internal anal sphincter in order to estimate the impact of the different mediator systems mentioned above.

Methods

Sixteen female rabbits weighing 2.4–3.1 kg were killed by a blow to the neck, and the anal canal and rectum excised and immediately transferred to 4°C Krebs solution (for composition, see below). The tissue was placed on a dissection tray containing cold Krebs solution. The anal canal and rectum was opened by an incision along the ventral longitudinal axis and pinned flat with the mucosal surface up. The mucosa was removed by sharp dissection with the aid of a dissecting microscope thereby exposing the underlying circular muscle. A 2 mm wide strip of the most distal part of the muscle was excised in the whole circumference. From these crude preparations, 3–4 strips were prepared with silk ligatures placed in both ends measuring 2–4 mm in length (between the ligatures) and 1–2 mm in width. The strips were transferred to 5 ml organ baths containing Ca^{2+}-free medium (for composition, see below). The baths were constantly bubbled with 5% CO_2 in O_2, maintaining pH at 7.40 ± 0.05. Bath temperature was thermostatically controlled at 37 ± 0.5°C.

The strips were mounted horizontally between 2 small L-shaped hooks. One hook was attached to an isometric force transducer (Grass FT.03), and the other was fastened to a sledge for adjustment of strip length. Tension was registered on an eight-channel Grass Polygraph (model 7E). Initially, resting length was measured with the preparations hanging slack between the hooks by the aid of a micrometer

[1] Author for correspondence.

mounted on the dissecting microscope. The length was then slowly increased to 200% of resting length, and strip diameter was measured. Efforts were made to prepare strips with an even diameter, and in case of measurable differences, diameter was measured at the thinnest portion of the strip. Final adjustment of strip length was then performed in order to achieve a resting tension at 5 mN per mm^2 (cross sectional area calculated from strip diameter at 200% of resting length). In separate experiments, this procedure has been shown to secure optimal suspension of rabbit internal anal sphincter strips (Glavind *et al.*, unpublished). The Ca^{2+}-free medium was then replaced with Krebs solution, and tension immediately increased to a stable level with superimposed phasic activity within 10–25 min. For all tensions subsequently given, zero level is the tension measured in Ca^{2+}-free medium.

Transmural field stimulation was applied through two platinum wire electrodes placed on either side of the preparations. Square wave impulses of 0.4 ms duration at supramaximal voltage (140–160 V) was delivered in 5 s trains of impulses every 2–4 min from a Grass S88 stimulator through 4 isolation units (Grass SIU5). Frequency was varied between 1 impulse s^{-1} to 32 Hz (alternating high/low frequency). All experiments were carried out in the presence of atropine (10^{-6} M) and guanethidine (10^{-6} M).

Composition of solutions

The Krebs solution contained (in mM): NaCl 119, KCl 4.6, $NaHCO_3$ 15, $CaCl_2$ 1.5, $MgCl_2$ 1.2, NaH_2PO_4 1.2, glucose 11. The Ca^{2+}-free medium contained (in mM): NaCl 119, KCl 4.6, $NaHCO_3$ 15, $MgCl_2$ 1.2, NaH_2PO_4 1.2, glucose 11, ethyleneglycol-*bis*-β-amino-N-N tetraacetate (EGTA) 0.01.

Drugs

Atropine sulphate (Danish Pharmacy Labs), α-chymotrypsin (Sigma), guanethidine (Sigma), apamin (Sigma), isoprenaline sulphate (Sigma), tetrodotoxin (Sigma), zinc protoporphyrin IX (Zn-PP-IX, Sigma), N^{ω}-nitro-L-arginine (L-NOARG, Sigma), L-arginine (Sigma), sodium nitroprusside (SNP, Sigma). The stock solutions of Zn-PP-IX were prepared in the dark by first dissolving Zn-PP-IX in a small volume of 0.2 N sodium hydroxide solution and then diluting with distilled water. The pH of the solution was adjusted to 7.4 with 0.2 N HCl. All other compounds were dissolved in 0.9% NaCl containing 1.0 mM ascorbic acid. Ultrasonic disruption of L-NOARG powder was required to dissolve this agent.

Drugs were added in cumulatively increasing concentrations to the baths (all concentrations given are final bath concentrations), allowing the responses to reach new stable levels between each increment of concentration.

Data analysis

Responses to drugs were measured and calculated as % change of spontaneous active tension. The spontaneous active tension level was determined by the difference between passive tension (the tension in Ca^{2+}-free medium) and the lower level of the phasic contractions. Amplitudes of the relaxations induced during transmural field stimulation were measured as the difference between the lower level of phasic activity and the peak of relaxation. In experiments where maximal relaxation (E_{max}) could be determined, calculation of the frequency inducing half-maximum response (F_{50}) was made by linear interpolation on the semi-logarithmic frequency-response curve, and expressed as log F_{50}. All data are expressed as the mean ± s.e.mean. Statistical differences between two means were determined by Student's paired or an unpaired *t* test where applicable. *n* refers to the number of independent observations.

Results

Basal pattern

In normal Krebs solution spontaneous active tension was 12.9 ± 2.1 mN with superimposed phasic activity. Transmural field stimulation induced frequency-dependent relaxations in all strips (Figures 1 and 2). Maximal relaxation induced by transmural field stimulation was 94 ± 1%. A plateau in the frequency-response curve was noted from 4 Hz to 32 Hz. The responses to transmural field stimulation were abolished by tetrodotoxin (10^{-6} M).

Effects of drugs on transmural field stimulation responses

Apamin (10^{-6} M) increased tension from 6.0 ± 1.0 mN to 8.7 ± 1.6 mN ($P<0.05$) and significantly inhibited responses to transmural field stimulation as shown by a shift to the right of the frequency-response curve (Figure 2, Table 1; $n = 7$). E_{max} was unchanged. L-NOARG (10^{-4} M) increased tension from 12.8 ± 2.3 mN to 16.2 ± 2.9 mN ($P<0.01$), shifted the frequency-response curve to the right, and reduced maximal relaxation in response to transmural field stimulation (Figure 2 and Table 1; $n = 7$). This effect was not seen when the preparations were preincubated with L-arginine (10^{-4} M, data not shown). Responses to transmural field stimulation were abolished at frequencies ≤ 2 Hz in the presence of both apamin and L-NOARG (Figure 2; $n = 7$). Zn-PP-IX in a concentration of 10^{-4} M had no effect on tension or on responses to transmural field stimulation ($n = 4$), but a profound reduction in relaxation was noticed at a concentration of 10^{-3} M (Figure 3c; $n = 4$). By combining apamin, L-NOARG and Zn-PP-IX, the responses to transmural field stimulation were abolished ($n = 7$).

α-Chymotrypsin (5 u ml^{-1}) did not affect peak relaxation induced by transmural field stimulation at any frequency (Figure 2; $n = 7$). In the presence of L-NOARG and apamin, α-chymotrypsin shortened the return of tension to prestimulus level after high frequency stimulation (Figure 4). The

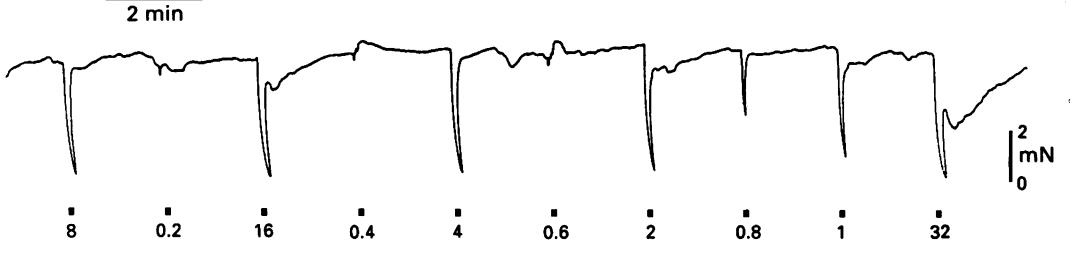

Figure 1 Original tracing illustrating the effect of transmural field stimulation (5 s trains, supramaximal voltage, 0.4 ms impulse duration) on resting tension of the rabbit internal anal sphincter. The frequency applied is given below. The baths were preincubated with atropine 10^{-6} M and guanethidine 10^{-6} M.

time elapsed for tension to regain 50% of the tension in response to 32 Hz stimulation was 50 s ± 9 and 5 s ± 2 without and with α-chymotrypsin ($P<0.01$; $n=3$).

Responses to isoprenaline and sodium nitroprusside

Isoprenaline induced concentration-dependent relaxations of the internal anal sphincter. At 3×10^{-6} M full relaxation was obtained ($n=4$). The response was not affected by preincubation with Zn-PP-IX (10^{-4} M, $n=4$), but a notable reduction of the effect was noticed with Zn-PP-IX at a concentration of 10^{-3} M (Figure 3a; $n=4$). Sodium nitroprusside had inhibitory effects on the internal anal sphincter resulting in 100% relaxation at 10^{-4} M ($n=4$). The effect was not influenced by the presence of Zn-PP-IX 10^{-4} M ($n=4$), but 10^{-3} M Zn-PP-IX significantly reduced the response to sodium nitroprusside (Figure 3b; $n=4$).

Table 1 Effect of apamin and N$^{\omega}$-nitro-L-arginine (L-NOARG) on responses to transmural field stimulation

	E_{max}	log F_{50}	F_{50}
Control	95 ± 2	−0.118 ± 0.003	0.76
Apamin 10^{-6} M	94 ± 4	0.037 ± 0.003*	1.09
Control	94 ± 4	−0.121 ± 0.002	0.76
L-NOARG 10^{-4} M	83 ± 3*	0.251 ± 0.004*	1.78

*$P<0.001$.

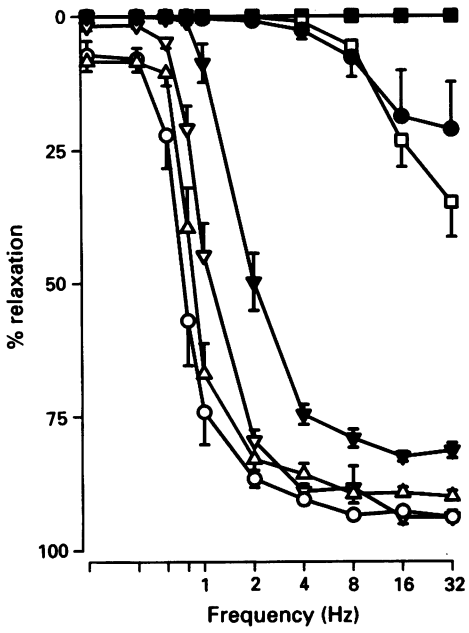

Figure 2 The effect of transmural field stimulation (5 s trains, supramaximal voltage, 0.4 ms impulse duration, varying frequency) on resting tension of the rabbit internal anal sphincter. The preparations were preincubated with atropine 10^{-6} M and guanethidine 10^{-6} M: (○) control; (△) α-chymotrypsin (5 u ml^{-1}); (●) Zn-PP-IX (10^{-3} M); (▽) apamin (10^{-6} M); (▼) L-NOARG (10^{-4} M); (□) apamin (10^{-6} M) and L-NOARG (10^{-4} M); (■) apamin (10^{-6} M), L-NOARG (10^{-4} M) and Zn-PP-IX (10^{-3} M). Values are mean ± s.e.mean. For abbreviations, see text.

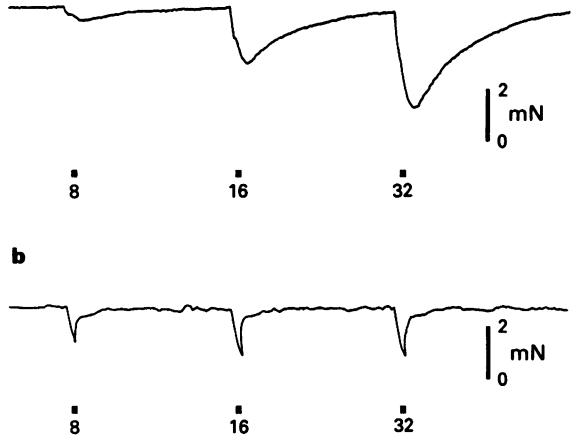

Figure 4 Original tracings illustrating the effect of transmural field stimulation (5 s trains, supramaximal voltage, 0.4 ms impulse duration) on resting tension of the rabbit internal anal sphincter in the presence of atropine (10^{-6} M), guanethidine (10^{-6} M), N$^{\omega}$-nitro-L-arginine (10^{-4} M) and apamin (10^{-6} M). (a) Without α-chymotrypsin; (b) with α-chymotrypsin (5 u ml^{-1}). The frequency applied is given below each curve.

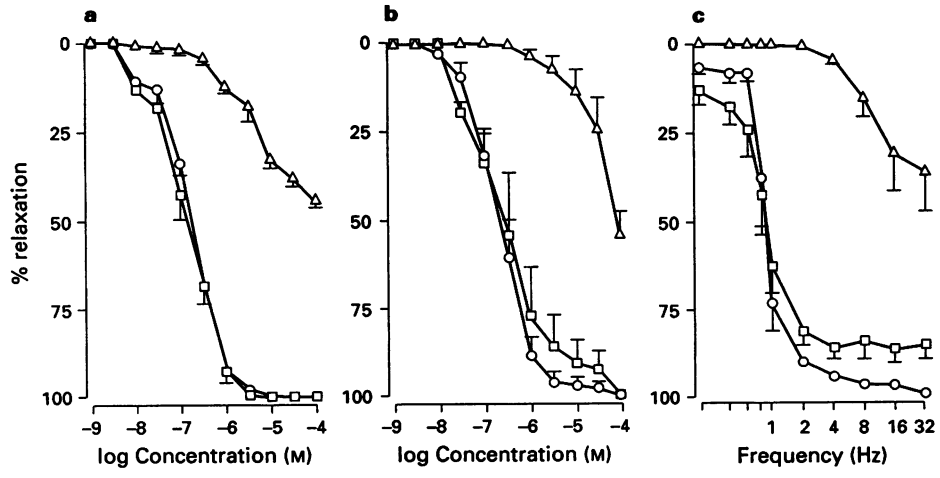

Figure 3 (a) The effect of isoprenaline on resting tension of the rabbit internal anal sphincter. (b) The effect of sodium nitroprusside on resting tension of the rabbit internal anal sphincter. (c) The effect of transmural field stimulation (5 s trains, supramaximal voltage, 0.4 ms impulse duration, varying frequency) on resting tension of the rabbit internal anal sphincter. (○) Control; (□) after preincubation with zinc protoporphyrin-IX (Zn-PP-IX, 10^{-4} M); (△) after preincubation with Zn-PP-IX (10^{-3} M). The preparations were preincubated with atropine 10^{-6} M and guanethidine 10^{-6} M. Values are mean ± s.e.mean.

Discussion

In the presence of atropine and guanethidine, the response to stimulation of intrinsic nerves of the internal anal sphincter was inhibitory at all frequencies studied. This NANC inhibition was found to be composed of at least three distinguishable components. One component was probably mediated by NO or a related molecule, since L-NOARG significantly inhibited the response to transmural field stimulation. L-NOARG is also capable of inhibiting NANC relaxation of the opossum (Tøttrup *et al.*, 1992) and human (O'Kelly *et al.*, 1993) internal anal sphincter, but the effect of L-NOARG seems much larger in these species than in rabbits.

In the present experiments, apamin significantly shifted the frequency-response curve to the right, but the effect was more pronounced when apamin was added in the presence of L-NOARG. In a study of different regions of the guinea-pig gastrointestinal tract, Costa and co-workers found that some regions of the gut exhibited NANC responses that were almost abolished by apamin, while apamin had no effect in others (Costa *et al.*, 1986). The antrum, ileum and distal colon had responses that were partly sensitive to apamin. In the guinea-pig internal anal sphincter, apamin abolished both the electrical and the mechanical response to field stimulation (Lim & Muir, 1986), and rabbits and guinea-pigs are therefore clearly different in the quantitative importance of the apamin-sensitive response. Apamin blocks Ca^{2+}-dependent increase in potassium conductance (Banks *et al.*, 1979), and converts membrane hyperpolarization in response to ATP to depolarization (Maas & Den Hertog, 1979; Shuba & Vladimirova, 1980). It is still an open question whether ATP is the transmitter responsible for the apamin-sensitive responses, but our experiments do not allow any statements for or against this hypothesis.

It is noteworthy that apamin and L-NOARG when added alone to the baths had rather small effects, but in combination the effect seemed superadditive. In other words, a complete dropout of one of the components has relatively little influence on the resulting inhibition, while interference with both systems has tremendous impact. This could imply that the released mediators act by different mechanisms. The non-L-NOARG non-apamin-sensitive relaxations were characterized by longer duration, and by being absent at frequencies $\leqslant 2$ Hz. The amplitude of the relaxations induced by transmural field stimulation were not reduced by α-chymotrypsin, but the duration of the relaxation was profoundly reduced. Therefore, a part of the the NANC response in the internal anal sphincter may be peptidergic.

A recent report has proposed that CO may be involved in the mediation of NANC responses in the internal anal sphincter. CO may be formed from haeme by the activation of haeme oxygenase (Maines, 1988), and Zn-PP-IX is an inhibitor of this formation (Maines, 1981). As seen in both Figures 1 and 2a, a very significant reduction in NANC relaxation was achieved with Zn-PP-IX. In fact the combination of L-NOARG, apamin and Zn-PP-IX abolished relaxations at all frequencies studied. Our concern about the finding of the present study is the fact that responses to both isoprenaline and SNP were inhibited almost to the same extent as the NANC responses, suggesting that Zn-PP-IX at 10^{-3} M has other actions than haeme oxygenase inhibition. This makes it impossible to draw conclusions concerning the involvement of CO in the mediation of NANC inhibition in the rabbit internal anal sphincter.

Inhibitory responses of smooth muscles are not always dependent on membrane potential changes, and therefore it is important to characterize inhibitory neurotransmission with both electrical and mechanical recording. The rabbit internal anal sphincter is a valuable tissue for studying relaxant effects because unlike several other gut muscles, it has the ability to generate spontaneous and sustained tone, which allows relaxant responses to be evaluated precisely. NANC relaxation of the rabbit internal anal sphincter seems to be mediated by at least three agents that can be distinguished pharmacologically. All three components have previously been reported to exist in other parts of the gut, but not in the same tissue. We are unable to provide conclusive evidence of a role for the newly reported mediator, CO, due to the non-specific effects of the inhibitor used.

This study was supported by the NOVO Foundation and The Aarhus University Research Foundation.

References

BANKS, B.E.C., BROWN, C., BURGESS, G.M., BURNSTOCK, G., CLARET, M., COCKS, T.M. & JENKINSON, D.H. (1979). Apamin blocks certain neurotransmitter-induced increases in potassium permeability. *Nature*, **182**, 415.

BULT, H., BOECKXSTAENS, G.E., PELCKMANS, P.A., JORDAENS, F.H., MAERCKE, Y.M. & VAN HERMAN, A.G. (1990). Nitric oxide as an inhibitory non-adrenergic non-cholinergic neurotransmitter. *Nature*, **345**, 346–347.

COSTA, M., FURNESS, J.B. & HUMPHREYS, C.M.S. (1986). Apamin distinguishes two types of relaxation mediated by enteric nerves in the guinea-pig gastrointestinal tract. *Naunyn-Schmied. Arch. Pharmacol.*, **332**, 79–88.

DOCKRAY, G.J. (1987). Physiology of enteric neuropeptides. In *Physiology of the Gastrointestinal Tract*, Second Edition. ed. Johnson, L.R. pp. 41–66. New York: Raven Press.

GILLESPIE, J.S., LIU, X. & MARTIN, W. (1989). The effects of L-arginine and N^G-monomethyl L-arginine on the response of the rat anococcygeus muscle to NANC nerve stimulation. *Br. J. Pharmacol.*, **98**, 1080–1082.

JURY, J., JAGER, L.P. & DANIEL, E.E. (1985). Unusual potassium channels mediate nonadrenergic noncholinergic nerve-mediated inhibition in opossum esophagus. *Can. J. Physiol. Pharmacol.*, **63**, 107–112.

KNUDSEN, M.A. & TØTTRUP, A. (1992). A possible role of the L-arginine-nitric oxide pathway in the modulation of cholinergic transmission in the guinea-pig taenia coli. *Br. J. Pharmacol.*, **107**, 837–841.

LI, C.G. & RAND, M.J,. (1989). Evidence for a role of nitric oxide in the neurotransmitter system mediating relaxation of the rat anococcygeus muscle. *Clin. Exp. Pharmacol. Physiol.*, **16**, 933–938.

LIM, S.P. & MUIR, T.C. (1986). Neuroeffector transmission in the guinea-pig internal anal sphincter: an electrical and mechanical study. *Eur. J. Pharmacol.*, **128**, 17–24.

MAAS, A.J.J. (1981). The effect of apamin on responses evoked by field stimulation in the guinea-pig taenia caeci. *Eur. J. Pharmacol.*, **73**, 1–9.

MAAS, A.J.J. & DEN HERTOG, A. (1979). The effect of apamin on the smooth muscle cells of the guinea-pig taenia coli. *Eur. J. Pharmacol.*, **58**, 151–156.

MAINES, M.D. (1981). Zinc protoporphyrin is a selective inhibitor of heme oxygenase in the neonatal rat. *Biochem. Biophys. Acta*, **673**, 339–350.

MAINES, M.D. (1988). Heme oxygenase: function, multiplicity, regulatory mechanisms, and clinical implications. *FASEB J.*, **2**, 2557–2568.

MOORE, P.K., AL-SWAYEH, O.A., CHONG, N.W.S., EVANS, R.A. & GIBSON, A. (1990). L-N^G-nitro arginine (L-NOARG), a novel, L-arginine reversible inhibitor of endothelium-dependent vasodilatation *in vitro*. *Br. J. Pharmacol.*, **99**, 408–412.

O'KELLY, T., BRADING, A. & MORTENSEN, N. (1993). Nerve mediated relaxation of the human anal sphincter: the role of nitric oxide. *Gut*, **34**, 689–693.

RATTAN, S. & CHAKDER, S. (1993). Inhibitory effect of carbon monoxide (CO) on internal anal sphincter: Heme oxygenase inhibitor inhibits NANC relaxation. *Am. J. Physiol.*, **265**, G799–G804.

REES, D.D., PALMER, R.M.J., HODSON, H.F. & MONCADA, S. (1989). A specific inhibitor of nitric oxide formation from L-arginine attenuates endothelium-dependent relaxation. *Br. J. Pharmacol.*, **96**, 418–424.

SHUBA, M.F. & VLADIMIROVA, I.A. (1980). Effect of apamin on the electrical responses of smooth muscle to adenosine 5'-triphosphate and to non-adrenergic, non-cholinergic nerve stimulation. *Neuroscience*, **5**, 853–859.

TØTTRUP, A., GLAVIND, E.B. & SVANE, D. (1992). Involvement of the L-arginine-nitric oxide pathway in internal anal sphincter relaxation. *Gastroenterology*, **102**, 409–415.

TØTTRUP, A., SVANE, D. & FORMAN, A. (1991). Nitric oxide as a mediator of NANC inhibition in opossum lower esophageal sphincter. *Am. J. Physiol.*, **260**, G385–G389.

VERMA, A., HIRSCH, J., GLATT, C.E., RONNETT, G.V. & SNYDER, S.H. (1993). Carbon monoxide: a putative neural messenger. *Science*, **259**, 381–384.

(Received December 2, 1994
Revised January 3, 1995
Accepted January 6, 1995)

British Journal of Pharmacology (1995) 115, 163-171

Inhibition of rat colon contractility by prostacyclin (IP-) receptor agonists: involvement of NANC neurotransmission

Yue-ming Qian & [1]Robert L. Jones

Department of Pharmacology, Faculty of Medicine, Chinese University of Hong Kong, Shatin, NT, Hong Kong

1 The possibility that prostacyclin (IP-) receptor agonists inhibit spontaneous contractions of the rat isolated colon by activating enteric neurones has been investigated. Cicaprost was used as the test agonist because of its high stability, selectivity and potency (IC_{50} = 3.8 nM).

2 The Na^+ channel blockers saxitoxin (STX, 1 nM) and tetrodotoxin (TTX, 1 μM), whilst having little effect on resting spontaneous activity, virtually abolished the inhibitory actions of cicaprost (10 nM) and nicotine (3 μM); inhibitory responses to isoprenaline (20 nM) were not affected. Phentolamine (1 μM), propranolol (1 μM) and atropine (1 μM) had no effect on cicaprost inhibition. These data are compatible with release of inhibitory NANC transmitter(s) by cicaprost.

3 A transmitter role for nitric oxide was investigated. The nitric oxide synthase (NOS) inhibitor N^{ω}-nitro-L-arginine methyl ester (L-NAME, 100 μM) inhibited the actions of both cicaprost (10 nM) and nicotine (3 μM) by 50–60%, but did not affect responses to isoprenaline (20 nM) or sodium nitroprusside (1–5 μM). The enantiomeric D-NAME (100 μM), which has negligible NOS inhibitory activity, had no effect on the action of cicaprost.

4 The involvement of purinergic transmitters was also investigated. Desensitization to the inhibitory action of ATP did not affect cicaprost responses. The P_{2X}/P_{2Y}-receptor antagonist, suramin, at 300 μM blocked ATP responses, but not those due to adenosine; it did not affect cicaprost inhibition. The selective adenosine A_1-receptor antagonist, DPCPX, used at a sufficiently high concentration (5 μM) to block adenosine A_2-receptors, did not affect cicaprost inhibition. Apamin (25 nM), a blocker of calcium-activated K^+ channels on smooth muscle, abolished or markedly reduced the inhibitory actions of ATP and adenosine, and partially inhibited cicaprost and nicotine responses. The combination of L-NAME (100 μM) and apamin (25 nM) abolished cicaprost and nicotine responses.

5 Investigation of vasoactive intestinal peptide (VIP) as a potential transmitter showed that its inhibitory action on the colon (IC_{50} = 50 nM) was partially inhibited by TTX (1 μM). α-Chymotrypsin abolished the effect of VIP but had no effect on cicaprost inhibition. Attempts to inhibit VIP responses using peptide antagonists and by agonist desensitization were unsuccessful.

6 KCl (40 mM) contracted the colon and abolished spontaneous activity. Under these conditions, isoprenaline, sodium nitroprusside and ATP induced relaxation, whereas cicaprost (10–310 nM) had no effect. Cicaprost inhibited both the tone and the spontaneous activity induced by the EP_1/EP_3-receptor agonist, sulprostone (8.6 nM) but not when either TTX (1 μM) or KCl (40 mM) was also present. On KCl-treated preparations, the prostacyclin analogue, iloprost (10–500 nM), induced contraction, presumably due to activation of EP-receptors.

7 It is concluded that IP-receptor agonists inhibit the contractility of rat colon by stimulating the release of at least two transmitters from NANC enteric neurones. Nitric oxide appears to be one of the transmitters. The second transmitter mechanism is apamin-sensitive; the experimental results do not support ATP, adenosine or VIP as transmitter candidates. However, further studies using more potent and selective receptor antagonists are required.

Keywords: Prostacyclin receptor agonist; cicaprost; colonic smooth muscle; enteric neurones; tetrodotoxin; nitric oxide; ATP; purinoceptor antagonists; adenosine receptor antagonists; vasoactive intestinal peptide

Introduction

Prostacyclin inhibits the spontaneous activity and tone of the rat isolated colon, whereas other products of prostaglandin H_2 (PGH_2) metabolism, such as PGE_2 and $PGF_{2\alpha}$, are contractile; this distinction was particularly useful in the early identification of prostacyclin by superfusion bioassay (Gryglewski *et al.*, 1976). The rat colon was also included in our investigations of the agonist specificity of some of the first stable analogues of prostacyclin (Dong *et al.*, 1986). We showed that iloprost and isocarbacyclin activate both prostacyclin (IP-) and prostaglandin E (EP-) receptors to produce a combination of inhibitory and excitatory actions on the colon (see Watson & Girdlestone, 1994, for nomenclature of prostanoid receptors). On the other hand, cicaprost (Stürzebecher *et al.*, 1986) invariably inhibited the spontaneous activity of the colon and, using data from other smooth muscle preparations, we proposed it as a highly specific IP-receptor agonist (Dong *et al.*, 1986; Lawrence *et al.*, 1992).

IP-receptors on blood platelets can be activated by a range of diphenylalkanoic acids (e.g. EP 157, octimibate), which bear little structural relationship to prostacyclin (see Jones *et al.*, 1993 and Meanwell *et al.*, 1994). In our studies of some of the more lipophilic compounds on the rat colon, inconsistent inhibition of contractility was observed. This appeared to be related to the presence of ethanol, which was essential to the preparation of homogeneous stock solutions. We therefore investigated whether a more robust assay would be obtained if the IP-receptor agonists acted against tone induced by an exogenous agent. To our surprise, we found that cicaprost did not relax colon preparations contracted submaximally with KCl. Further investigations showed that the Na^+ channel blocker, tetrodotoxin (TTX), could abolish the inhibitory action of cicaprost but not that of

[1] Author for correspondence.

isoprenaline. A neuronal site of action for cicaprost within the colon seemed possible; this paper describes experiments to define the nature of this action.

Methods

Isolated colon preparations

Male Sprague-Dawley rats, weighing 250–300 g, were fasted overnight and killed by stunning and exsanguination. A 4 cm length of the ascending colon was removed and cleaned of mesenteric tissue. Two segments were cut and, without further dissection, were suspended in 10 ml organ baths containing Krebs solution of the following composition (mM): NaCl 118, KCl 4.7, $CaCl_2$ 2.5, $MgSO_4$ 1.0, KH_2PO_4 1.18, $NaHCO_3$ 25 and glucose 10. The bathing solution was gassed with 95% O_2/5% CO_2, maintained at 37°C, and contained 1 μM indomethacin. Washout of the organ bath was by upward displacement and overflow. Contractions of the longitudinal muscle were measured with Grass FT03 isometric transducers connected to a MacLab data acquisition system (ADInstruments Pty Ltd, Australia). An initial basal tension of 0.5 g was applied; on relaxation further tension was repeatedly applied until the basal tension remained steady at 0.3 g.

Experimental protocols

In all experiments, proximal and distal sections of colon from the same rat were used as matched preparations. After about 60 min equilibration, with frequent washing, several submaximal doses of the appropriate inhibitory agonist were tested on each preparation to ensure that a stable and acceptable level of sensitivity had been reached before the following experimental procedures were begun. Agonist doses were allowed 3–4 min contact with the preparations; blockers/inhibitors were added 10 or 15 min before the agonist dose(s).

Effects of cicaprost and isoprenaline on spontaneous activity and KCl- and sulprostone-induced tone Spontaneous activity: non-cumulative dose-response relationships for cicaprost and isoprenaline were obtained on proximal and distal preparations respectively from 3 rats, and also on distal and proximal preparations respectively from 3 different rats (data combined and quoted as $n = 6$ in Results); this procedure was repeated with cumulative dosing for cicaprost and isoprenaline on KCl-induced tone (6 different rats), and for cicaprost on sulprostone- and KCl/sulprostone-induced tone (6 different rats).

Effects of blockers/inhibitors on responses to single doses of inhibitory agonist Responses to single doses of both cicaprost and isoprenaline were obtained on both proximal and distal preparations from 3 rats, before and after treatment(s) with blocker/inhibitor (sequentially increasing concentrations) ($n = 6$ in Results). In the case of N^{ω}-nitro-L-arginine methyl ester (L-NAME) and/or apamin on nicotine responses, either the distal or proximal preparation was always used as a non-treated preparation to assess the extent of agonist desensitization; during the first treatment period, either L-NAME or apamin was present ($n = 3$), and during the second period, a combination of L–NAME and apamin ($n = 6$).

Effects of blockers/inhibitors on purinoceptor agonists Cumulative dose-response relationships were obtained for a purinoceptor agonist on both proximal and distal preparations from 2 rats. One preparation was used as control and other treated with antagonist/inhibitor/desensitizing agent; second agonist dose-response relationships were then established. This procedure was repeated using 2 different rats with exchange of control and treatment on the proximal and distal preparations ($n = 4$ in Results).

Data analysis and statistical tests

Using the MacLab Chart 3.3 programme, spontaneous activity was measured as the average contractile force over a 2 min period (480 data points). The baseline tension value was set by eye. The response to an inhibitory agonist was taken as the percentage change from the resting spontaneous activity (e.g. −100% corresponds to abolition of spontaneous activity). Using data from a number of experiments, mean agonist responses elicited during control and treatment (receptor antagonist/channel blocker/enzyme inhibitor) periods were compared by Student's unpaired t test; statistical significance was accepted when $P < 0.05$.

Drugs

Cicaprost, iloprost and sulprostone were gifts from Schering AG, Berlin, Germany; ethanolic stock solutions of 5 mg ml^{-1} were kept at −20°C and diluted with 0.9% w/v NaCl (saline) solution for use. Indomethacin, isoprenaline (racemic), phenylephrine, tetrodotoxin (TTX), vasoactive intestinal peptide (VIP), [D-*p*-chloro-Phe^6,Leu^{17}]-VIP, [Lys^1,$Pro^{2,5}$,$Arg^{3,4}$, Tyr^6]-VIP, N^{ω}-nitro-L-arginine methyl ester (L-NAME), D-NAME, ATP, and adenosine were purchased from the Sigma Chemical Company, U.S.A.; saxitoxin (STX) from Calbiochem-Novabiochem Corp., U.S.A.; 2-methylthio ATP, 8-cyclopentyl-1,3-dipropylxanthine (DPCPX), and apamin from Research Biochemicals International, U.S.A., and suramin from Biomol Research Laboratories, U.S.A. A stock solution of TTX (500 μM) was prepared in saline containing 0.01% acetic acid and diluted with saline. VIP, the VIP analogues, L-NAME and D-NAME were dissolved in distilled water and diluted with saline before use. Stock solutions of purines were prepared in distilled water each day.

Results

In virtually all cases, responses of the proximal and distal sections of the rat colon to the drugs investigated were similar in magnitude, and it was decided to combine the data for graphical and statistical analyses.

Log concentration-response curves for inhibition of the spontaneous activity of the rat colon by cicaprost ($IC_{50} = 3.8$ nM) and isoprenaline (12.5 nM) are shown in Figure 1. In subsequent experiments, the effects of antagonists and inhibitors were assessed against submaximal responses elicited by standard concentrations of 10 nM cicaprost and 20 nM isoprenaline; these responses remained constant or in the case of cicaprost sometimes slightly increased in size (5–10%) over a period of 2–3 h. Nicotine also inhibited the spontaneous activity of the colon ($IC_{50} = 1–2$ μM), but was prone to tachyphylaxis. In subsequent studies, the reduction in response to a standard concentration of 3 μM nicotine applied every 20 min was small enough to allow the testing of inhibitory agents. Deliberate desensitization to nicotine, with three or four 10 μM challenges at 15 min intervals, had no effect on cicaprost inhibition (Figure 3c).

Evidence that cicaprost activates NANC enteric neurones

The Na^+ channel blockers, saxitoxin (STX, 0.1 and 1 nM) and TTX (0.1 and 1 μM), slightly slowed the rate of spontaneous contractions and tended to make the contraction pattern more regular. TTX (1 μM) markedly reduced and in some cases abolished cicaprost responses (Figures 2a and 3a), always abolished nicotine responses (not shown), but had no

effect on isoprenaline responses (Figure 3a). Cicaprost responses (−76.8 ± 2.4%, $n = 5$) were inhibited by STX at 0.1 nM (−57.3 ± 8.9%, $P > 0.05$) and 1 nM (−4.8 ± 1.6%, $P < 0.001$).

Phentolamine at 1 μM did not significantly affect the spontaneous activity of the colon, although in some preparations the basal tension was slightly decreased. Inhibitory responses (−70 to −80%) to phenylephrine (3 μM) were abolished by 1 μM phentolamine, whereas cicaprost and isoprenaline responses were unaffected (Figure 3b). Propranolol at a concentration of 1 μM (which had no significant effect on spontaneous activity or basal tone) markedly inhibited isoprenaline responses, but had no effect on cicaprost responses (Figure 3b). The response of the colon preparation to atropine was complex. Following exposure to 50 nM atropine, there was a small reduction in basal tension and spontaneous activity was reduced by about 20%. Subsequent doses of atropine (0.1–1 μM) produced no further effects. If however a preparation was initially exposed to 1 μM atropine, resting tension was markedly reduced and spontaneous activity abolished for several minutes; these parameters recovered to 60–70% of control values over a period of 20 min. After washout of 1 μM atropine from the organ bath, TTX (1 μM) did not slow the rate, but slightly increased the amplitude of spontaneous contractions. The presence of atropine (1 μM) did not significantly affect responses to either cicaprost or isoprenaline (Figure 3b).

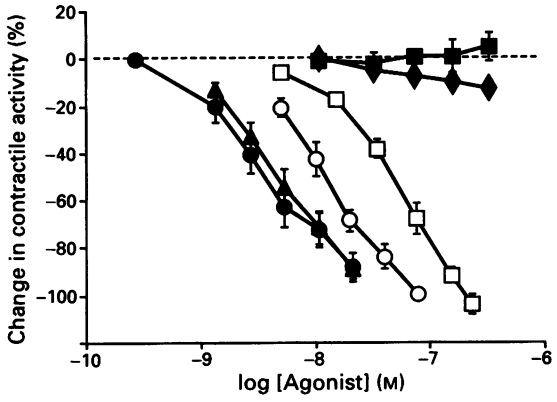

Figure 1 Log concentration-inhibition curves on rat isolated colon. Effects of cicaprost and isoprenaline on spontaneous activity (●, ○) and stable tone induced by 40 mM KCl (■, □), and cicaprost on contractile activity induced by 8.6 nM sulprostone (▲) and 40 mM KCl/8.6 nM sulprostone (◆) are shown. Values are means ± s.e.mean ($n = 6$).

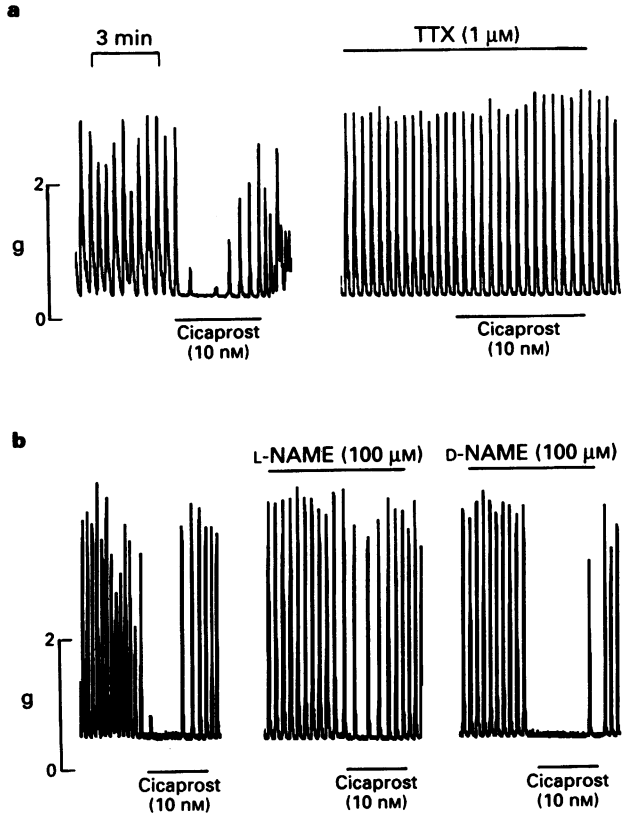

Figure 2 Rat isolated colon: experimental records showing the effect of treatment with (a) tetrodotoxin (TTX, 1 μM) and (b) N^{ω}-nitro-L-arginine methyl ester (L-NAME, 100 μM) and D-NAME (100 μM) on inhibitory responses to 10 nM cicaprost.

Effects of nitric oxide synthase inhibition

The nitric oxide synthase (NOS) inhibitor, L-NAME (10–500 μM), produced transient small contractions of the colon preparations. Cicaprost and nicotine responses were partially inhibited by L-NAME, whereas the actions of isoprenaline were unaffected (Figure 2b and 4a,d). The enantiomeric D-NAME, which is inactive as a NOS inhibitor, did not affect the action of cicaprost (control −77.6 ± 2.2%; 100 μM D-NAME treatment −78.7 ± 2.7%, $n = 6$). Sodium nitroprusside, a NO donor, inhibited the spontaneous activity of the colon preparation ($IC_{50} = 0.15$ μM; complete inhibition at 5 μM). Nitroprusside responses were unaffected by either TTX (1 μM) or L-NAME (100 μM).

Interference with postsynaptic purinergic systems

The effects of several treatments intended to inhibit postsynaptic purinergic systems were investigated on inhibitory responses to cicaprost, nicotine, ATP and adenosine.

Log concentration-response curves for ATP derived from two cumulative sequences of doses 80 min apart were identical (Figure 5a); the log concentration-response curve for 2-methylthio-ATP, a specific P_{2Y} agonist, is also shown. Desensitization to ATP was attempted by challenging with three doses of ATP (500 μM) added at 15 min intervals in between the first and second series of ATP doses. Examination of the second ATP curve shows that this procedure was most effective against 10 and 100 μM as opposed to 500 μM ATP (Figure 5a); cicaprost responses were unaffected by this treatment (Figure 5d).

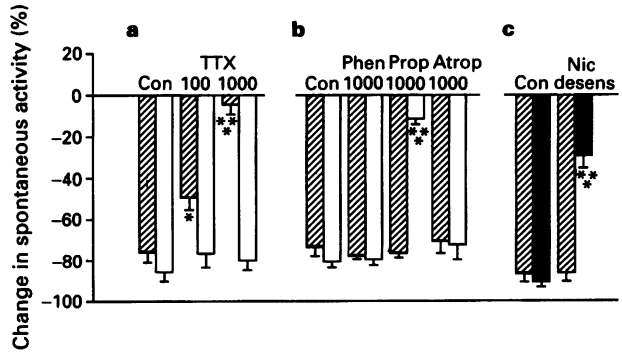

Figure 3 Spontaneous activity of rat isolated colon. Effects of treatment with (a) tetrodotoxin (TTX) and (b) phentolamine (Phen), propranolol (Prop) or atropine (Atrop) on inhibitory responses to cicaprost (10 nM, hatched columns) and isoprenaline (20 nM, open columns). Concentrations are nM. Means ± s.e.mean ($n = 6$). (c) Effects of desensitization with 3–4 applications of 10 μM nicotine (Nic desens) on inhibitory responses to cicaprost (10 nM, hatched columns) and nicotine (10 μM, solid columns) ($n = 4$). $^{*}P < 0.05$, $^{**}P < 0.01$, $^{***}P < 0.001$ as compared to appropriate control (Con).

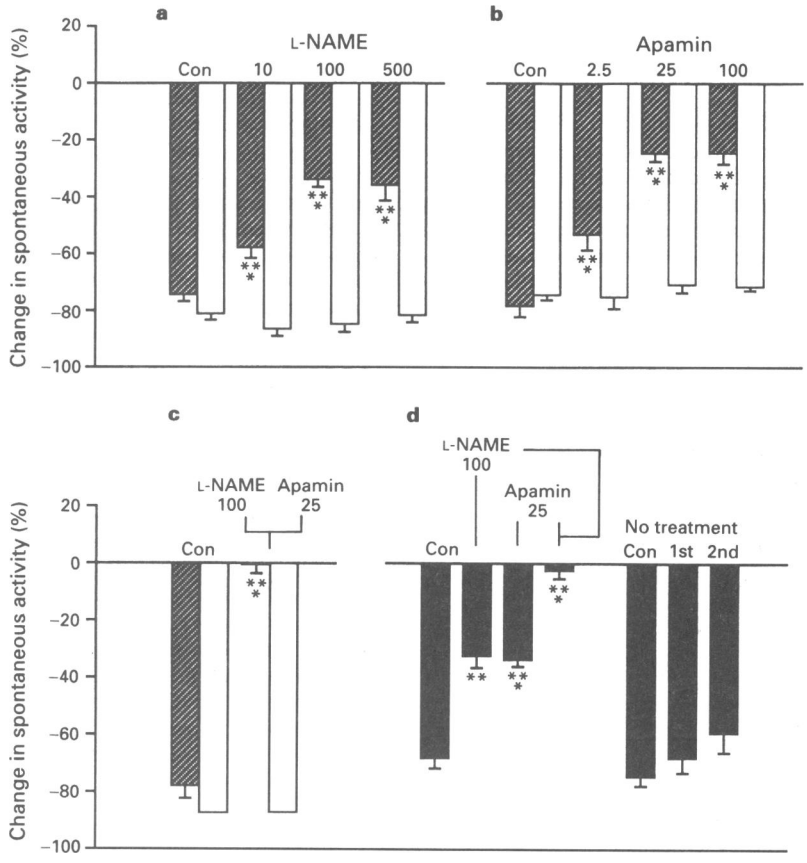

Figure 4 Spontaneous activity of rat isolated colon. Effects of treatment with (a) N^{ω}-nitro-L-arginine methyl ester (L-NAME, 10–500 μM), (b) apamin (2.5–100 nM) and (c) a combination of 100 μM L-NAME and 25 nM apamin on inhibitory responses to cicaprost (10 nM, hatched columns) and isoprenaline (20 nM, open columns). Means ± s.e.mean of 6 experiments, except for isoprenaline in (c), where $n = 2$. (d) Effects of 100 μM L-NAME alone and 25 nM apamin alone (both 1st treatment period, $n = 3$), and in combination (2nd treatment period, $n = 6$) on inhibitory responses to nicotine (3 μM, solid columns); the right hand part of the panel shows nicotine responses on non-treated preparations during control, 1st and 2nd treatment periods ($n = 6$). $^{*}P < 0.05$, $^{**}P < 0.01$, $^{***}P < 0.001$ as compared to appropriate control (Con).

At 300 μM, the P_{2X}/P_{2Y}-receptor antagonist, suramin, produced a rightward shift of the ATP curve for responses within the 0–50% inhibition range (dose ratio = 10–20) (Figure 5b). However, no inhibition was seen when the ATP concentration was raised to 500 μM. Suramin did not inhibit adenosine responses (Figure 5c). DPCPX, a potent antagonist at adenosine A_1-receptors, was used at high concentrations of 5 μM in an attempt to block adenosine A_2-receptors in the colon. The success of this strategy is indicated by marked inhibition of adenosine responses without significant inhibition of ATP responses (Figure 5b,c). Neither suramin (300 μM) nor DPCPX (5 μM) had any effect on cicaprost responses (Figure 5d).

Apamin (25 nM) markedly inhibited responses to ATP and adenosine (Figure 5b,c), and partially inhibited responses to both cicaprost and nicotine, while not affecting those to isoprenaline (Figure 4b,d). Cicaprost and nicotine induced no obvious change in spontaneous activity ($< \pm 5\%$ and $< \pm 10\%$ respectively) or basal tension in the presence of 100 μM L-NAME and 25 nM apamin; isoprenaline inhibition was unaffected by this combination (Figure 4c,d).

Interference with the action of vasoactive intestinal peptide

VIP inhibited the spontaneous activity of the colon with an IC_{50} value of about 50 nM. On five preparations, 100 nM VIP produced 92 ± 2% inhibition, which was reduced to 33 ± 4% in the presence of 1 μM TTX ($P < 0.01$).

Two VIP analogues, [Lys^1,$Pro^{2,5}$,$Arg^{3,4}$,Tyr^6]-VIP and [D-*p*-chloro-Phe^6,Leu^{17}]-VIP were examined as potential antagonists of VIP action. The former at 1 μM transiently contracted the colon; subsequent submaximal responses to either VIP (100 nM) or cicaprost were unaffected. The latter analogue at 1 and 5 μM also had no effect on VIP responses; it was not tested against cicaprost.

Prolonged exposure to VIP as a means of desensitization was attempted on three colon preparations (which turned out to be somewhat more sensitive to VIP than normal). VIP at 100 nM completely inhibited spontaneous activity of the colon, but after about 5 min contact, spontaneous activity resumed and had returned to the control level after 20 min. Although this appeared to indicate substantial desensitization, a second 100 nM VIP challenge (without washout of the first dose) resulted in total inhibition, which returned to control level slightly quicker than the first response. Similarly, a third 100 nM VIP challenge produced about 95% inhibition, followed by complete recovery; at this time, addition of cicaprost induced a response identical to the pre-VIP control.

Inhibitory responses to 100 nM VIP were almost abolished when α-chymotrypsin (2 u ml^{-1}) was present in the organ bath (control −74.7 ± 5.0%; treatment −1.7 ± 3.8%, $n = 5$). In contrast, cicaprost responses were not inhibited (control −66.5 ± 3.9%; treatment −76.5 ± 4.6%, $n = 5$).

Relaxation of KCl-induced tone

Addition of 40 mM KCl to the organ bath resulted in the generation of a stable level of tone, some 30 to 50% of that obtained with a near maximal KCl concentration of 120 mM; spontaneous activity was completely or almost completely

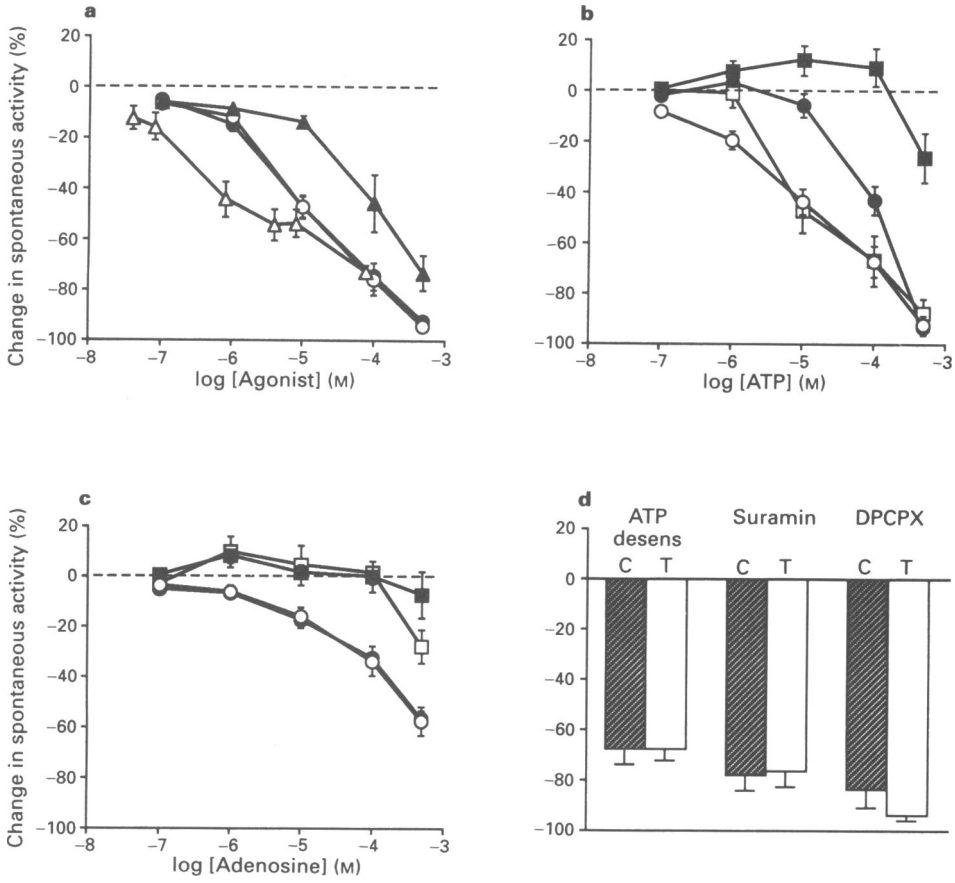

Figure 5 Inhibition of spontaneous activity of rat isolated colon; log concentration-response curves for second cumulative sequences (all $n = 4$). (a) ATP acting alone (○) and corresponding ATP first sequence (●); ATP after desensitization by 3 × 500 μM ATP (▲); 2-methylthio-ATP (△). (b) ATP acting alone (control curve for suramin) (○) and in the presence of suramin (300 μM, ●), 8-cyclopentyl-1,3-dipropylxanthine (DPCPX, 5 μM, □) and apamin (25 nM, ■). ATP control curves for DPCPX and apamin are not shown, but are similar to the suramin control curve. (c). Adenosine, same conditions as (b). (d) Effects of desensitization to ATP (as in a), suramin (300 μM) and DPCPX (5 μM) on inhibitory responses to cicaprost (10 nM); C = control, T = treatment ($n = 4$). Means ± s.e.mean.

lost. Subsequent addition of cicaprost (10-310 nM) was without effect, whereas isoprenaline could still elicit complete relaxation (IC_{50} = 50 nM) (Figures 1 and 6a,b). Both SNP (0.1–5 μM) and ATP (100 μM) also inhibited KCl tone (not shown).

The PGE analogue, sulprostone, at 8.6 nM induced contractions of the colon preparation equivalent to the 40 mM KCl response; there was some enhancement of spontaneous activity. The contractile responses, which were more pronounced in distal segments, were not blocked by pretreatment with phentolamine, propranolol, atropine or TTX (all at 1 μM). Cicaprost reduced both the tone and the rhythmic contractions in sulprostone-treated preparations; its EC_{50} value was 4.5 nM and 90% inhibition was achieved at 20 nM (Figure 1). TTX at 1 μM abolished these cicaprost responses. In the presence of 40 mM KCl, sulprostone (8.6 nM) elicited a further increase in tension but spontaneous activity remained absent; cicaprost (10–310 nM) produced only minimal relaxation (Figures 1 and 6c).

In the presence of tone elicited by 40 mM KCl, iloprost (10–500 nM) contracted the colon preparation (Figure 6d).

Discussion

There are a number of reports in the literature on the neuronal stimulant actions of IP-receptor agonists. For example, in relation to sensory events, prostacyclin activates 'cardiopulmonary receptors' in the large pulmonary vessels of the dog to elicit vagal bradycardia (Nganele & Hintze, 1987), and cicaprost potentiates sensory discharge from the arthritic ankle joint of the rat following depression with either acetylsalicylic acid or paracetamol (McQueen *et al.*, 1991). In a spinal cord/functionally-attached tail preparation from the neonate rat, cicaprost also enhanced responses of peripheral nociceptors to thermal and chemical stimuli (Rueff & Dray, 1993). In terms of motor actions, cicaprost elicits contraction of the longitudinal muscle of the guinea-pig ileum by releasing both acetylcholine (Gaion & Trento, 1983) and a substance P-like transmitter (Jones & Lawrence, 1993) from enteric nerves. In addition, preliminary experiments indicate that cicaprost increases the twitch response of the guinea-pig vas deferens to electrical field stimulation (EFS) by enhancing ATP release (Jones, 1993).

As a result of the present studies, activation of IP-receptors on enteric neurones in the rat colon to release inhibitory transmitters can now be added to the above list. Thus the neuronal Na^+ channel blockers, STX and TTX, abolish the inhibitory action of cicaprost on the spontaneous activity of the colon. Their selectivity at the concentrations used is evidenced by a lack of effect on the pacemaker function of the colon: anatomical and electrophysiological investigations of the contractility of rat and dog colon preparations have shown that three tissue components are involved: smooth muscle cells, a network of pacemaker cells (interstitial cells of Cajal, ICC) linked to each other and to smooth muscle cells by gap junctions, and a largely inhibitory innervation which is concentrated on the ICC (Huizinga *et al.*, 1990; Faussone-Pellegrini, 1992; references therein). The inhibitory action of nicotine on the colon is

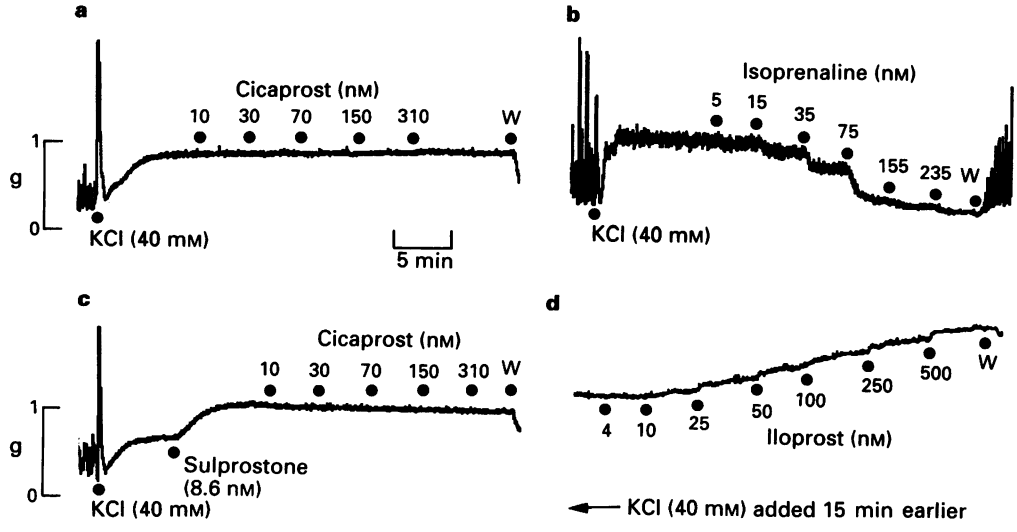

Figure 6 Rat isolated colon: experimental records showing the effects of (a) cicaprost, (b) isoprenaline and (d) iloprost in the presence of tone generated by 40 mM KCl, and (c) cicaprost on tone generated by a combination of 40 mM KCl and 8.6 nM sulprostone. Cumulative concentrations. W = wash.

also abolished by TTX. However, nicotine inhibition is more difficult to study because of its tendency to desensitization. Deliberate desensitization with nicotine did not affect cicaprost inhibition, implying that the action of cicaprost is not dependent on the integrity of nicotinic cholinergic synapses. In contrast to cicaprost and nicotine, the inhibitory action of isoprenaline is unaffected by TTX and appears to be non-neuronal in nature. Inhibitory β_3-adrenoceptors, with a low affinity for propranolol (pA_2 ~6.5), are present in the rat colon (Bianchetti & Manara, 1990; McLaughlin & MacDonald, 1990); this would explain the incomplete block of isoprenaline action by 1 μM propranolol in our studies. The inability of phentolamine, propranolol and atropine to inhibit the action of cicaprost suggests that this agent releases a non-adrenergic, non-cholinergic (NANC) inhibitory transmitter. NANC neurotransmission (Burnstock, 1986) to gut structures appears to be common and the main transmitter candidates are ATP (Burnstock *et al.*, 1970), VIP (Goyal & Rattan, 1980) and nitric oxide (Bult *et al.*, 1990). In general, two or more NANC transmitters may operate simultaneously to elicit a relaxant effect (Manzini *et al.*, 1986; Maggi & Giuliani, 1993), although one of them may play a dominant role in particular segments of the intestine of some species.

Involvement of NO generation in the action of cicaprost

There is good agreement that NO makes a major contribution to inhibition of colonic activity elicited by activation of enteric neurones. Hata *et al.* (1990) showed that relaxation of the circular muscle of the rat proximal colon due to local distension was abolished by N^G-nitro-L-arginine (L-NOARG), a NOS inhibitor; L-arginine, the precursor of NO (Palmer *et al.*, 1988a), but not D-arginine, largely reversed the effect of L-NOARG. Similarly in rat colon, relaxations of circular muscle to distension and longitudinal muscle to EFS were essentially abolished by L-NOARG (Suthamnatpong *et al.*, 1993; 1994). In the guinea-pig colon, L-NOARG almost abolished the relaxation induced by EFS (Zagorodnyuk & Maggi, 1994). In our experiments, inhibitory responses to both cicaprost and nicotine were partially (50–60%) blocked by L-NAME at appropriate concentrations (see Rees *et al.*, 1990). D-NAME however did not affect cicaprost action, compatible with stereospecific inhibition of NOS by arginine analogues (see Palmer *et al.*, 1988b). Thus it appears that cicaprost- and nicotine-induced inhibitions of spontaneous activity in the rat colon are mediated in part by NO. Constitutive NOS has been found in enteric nerves (Bredt *et al.*, 1990), but there has been some discussion in the literature (see Zagorodnyuk & Maggi, 1994) as to whether colonic relaxation is produced by NO generated within nerves or by another transmitter, for example VIP (Grider *et al.*, 1992), inducing NO generation in smooth muscle. Our experiments do not distinguish between these two possibilities.

The involvement of purinergic transmission in the action of cicaprost

Bailey & Hourani (1992) have shown that ATP and adenosine relax the carbachol-contracted rat colon (IC_{25} = 35 and 80 μM) through activation of P_{2Y}-purinoceptors and adenosine A_2-receptors respectively. From our experiments, these two receptors also appear to mediate inhibition of spontaneous activity, although both ATP and adenosine show somewhat greater potency (IC_{25} = 2.5 and 35 μM respectively). 2-Methylthio-ATP was more potent than ATP, consistent with the known properties of this specific P_{2Y} agonist (Gough *et al.*, 1973; O'Connor *et al.*, 1991).

Our studies provide no real evidence for a purinergic contribution to the inhibitory action of cicaprost. Firstly, desensitization to ATP had no effect on cicaprost responses. Secondly, suramin, a P_{2X}/P_{2Y}-receptor antagonist (Dunn & Blakely, 1988; Den Hertog *et al.*, 1989; Hoyle *et al.*, 1990; Leff *et al.*, 1990), did not affect cicaprost-induced inhibition. Although suramin is a weak antagonist (300 μM was used), it did act specifically, blocking the inhibitory action of ATP but not that of adenosine. Higher concentrations of suramin could not be used because of their depressant effect on spontaneous activity. Thirdly, the potent adenosine A_1-receptor antagonist, DPCPX (Collis *et al.*, 1989; Bruns, 1990), used at high concentration to block adenosine A_2-receptors, did not inhibit cicaprost responses.

The bee venom peptide apamin has been shown to block inhibitory responses to ATP in guinea-pig taenia coli (Den Hertog *et al.*, 1985), guinea-pig internal anal sphincter (Lim & Muir, 1986) and rat gastric fundus (LeFebvre *et al.*, 1991). In our experiments, apamin also markedly inhibited or abolished the inhibitory effects of ATP and adenosine. These observations indicate that ATP and adenosine probably inhibit spontaneous activity by opening low conductance calcium-activated K^+-channels in smooth muscle, since apamin is known to block these channels specifically (Banks *et al.*, 1979; Maas & Den Hertog, 1979). Apamin partially inhibited and in combination with L-NAME abolished the

inhibitory actions of both cicaprost and nicotine on the colon. This suggests that the second transmitter released from enteric nerves opens calcium-activated K^+-channels. Although the value of this observation in terms of transmitter identification is limited (α_1-adrenoceptor-mediated inhibition is also apamin-sensitive), it does provide further support against a β_3-adrenoceptor contribution, since isoprenaline inhibition was apamin-insensitive. Since cicaprost and nicotine produced no excitatory effects in the presence of the L-NAME/apamin combination, it would appear that their stimulant actions are limited to inhibitory enteric neurones (at least at the concentrations employed).

Involvement of VIP in the action of cicaprost

The inhibitory effects of VIP on the rat colon were partially blocked by TTX, suggesting that both prejunctional and postjunctional sites of action are involved. A prejunctional action of VIP has also been reported in the dog and cat trachea (Hakoda & Ito, 1990); however, in these tissues VIP inhibits the release of an excitatory transmitter.

In the studies of Suthamnatpong *et al.* (1993), the VIP antagonist, VIP 10–28, inhibited the EFS response of the distal rat colon to a maximum of 35%; it had no effect on EFS responses of the proximal and middle colon. In our experiments, two VIP antagonists, [Lys^1,Pro^{2,5},Arg^{3,4},Tyr^6]-VIP (Gozes *et al.*, 1989) and [D-*p*-chloro-Phe^6,Leu^{17}]-VIP (Pandol *et al.*, 1986), did not inhibit responses to either VIP or cicaprost. In this context, [D-*p*-chloro-Phe^6,Leu^{17}]-VIP and another antagonist, [Ac-Tyr^1,D-Phe^2]-GRF(1-29)-NH_2, were without effect on responses to exogenous VIP in the guinea-pig isolated trachea (Ellis & Farmer, 1989). However in the cat trachea, these two antagonists abolished the pre-juctional action of VIP to suppress the excitatory junction potential (Xie *et al.*, 1991). Clearly we are in the position of having useful antagonists for one subtype of VIP receptor and not for the other(s).

Information was then sought from VIP desensitization experiments. However, as in the studies of Suthamnatpong *et al.* (1993), it proved difficult to achieve significant desensitization to VIP. Although inhibitory responses to VIP faded with time, subsequent addition of VIP still elicited good inhibitory responses. The mechanism underlying this profile of action is not clear.

As a last resort, evidence of the involvement of VIP as a transmitter was sought from the use of α-chymotrypsin, an enzyme that cleaves peptide bonds adjacent to tyrosine, lysine and arginine residues; all three amino acids are present in VIP. In previous studies, evidence has been obtained both for (rat gastric fundus, De Beurme & Lefebvre, 1987) and against (guinea-pig taenia coli, Mackenzie & Burnstock, 1980; rat duodenum, Manzini *et al.*, 1986) a role for VIP in NANC relaxation. The finding that α-chymotrypsin treatment did not inhibit the relaxation induced by cicaprost appears to exclude a transmitter role for not only VIP but also other susceptible peptides such as calcitonin gene-related peptide (CGRP). We emphasise 'appears to exclude', since, as suggested by others, there is no evidence that VIP released from neurones within the tissue is subject to the same degree of inactivation as VIP in the bathing fluid.

Effects of agonists when tone is raised with K^+

Raising the external K^+ concentration to produce submaximal contraction of the colon preparation was accompanied by loss of spontaneous activity. Under these conditions, isoprenaline, sodium nitroprusside and ATP induced relaxation, whereas cicaprost was completely inactive. Use of the EP_1/EP_3-receptor agonist, sulprostone, to raise the tone of the preparation did not result in loss of spontaneous activity; in this case cicaprost still induced a TTX-sensitive relaxation. However if sulprostone was combined with high K^+, spontaneous activity was lost and cicaprost was again inactive. Two mechanisms may be relevant to the lack of effect of cicaprost in the presence of high K^+. Firstly, cicaprost may still release inhibitory transmitters, but they are ineffective since their action on the pacemaker is abrogated by high K^+. Secondly, the high K^+ may prevent the transmitter-releasing action of cicaprost. This is an interesting concept, since it raises the possibility that activation of IP-receptors on enteric neurones leads to closing of K^+ channels and membrane depolarization. This action may not proceed through the G_S-adenylate cyclase pathway typical of the inhibitory actions of prostacyclin on platelet function. An analogous situation is the presynaptic inhibitory actions of opioid agonists, where mediation through cyclic AMP is being abandoned in favour of direct G-protein links with K^+ and/or Ca^{2+} channels in the plasma membrane (see Di Chiara & North, 1992).

The loss of IP-receptor-mediated inhibition in the presence of high K^+ exposes the true contractile action of iloprost on the rat colon. Iloprost is known to be a potent agonist at EP_1-receptors (Dong *et al.*, 1986). However, the nature of the EP-receptor mediating contraction of the rat colon has not been reported; preliminary observations in our laboratory suggest that it is more likely to be an EP_3- than an EP_1-receptor.

In conclusion, the present study demonstrates that the inhibitory actions of IP-receptor agonists on the contractility of the rat colon are neuronally-mediated and that at least two NANC transmitter mechanisms appear to be involved. NO is likely to be one of the inhibitory transmitters, whereas some evidence has been obtained against a role for ATP, adenosine and VIP. Further studies are warranted to characterize the 'neuronal' IP-receptors involved, in terms of molecular structure, G-protein coupling and structure-activity relationships.

This work was supported by a grant from the UPGC of Hong Kong. Gifts of prostanoids from Schering AG (Berlin, Germany) are gratefully acknowledged. The authors thank Mr K.M. Chan for technical assistance.

References

BAILEY, S.J. & HOURANI, S.M.O. (1992). Effects of purines on the longitudinal muscle of the rat colon. *Br. J. Pharmacol.*, **105**, 885–892.

BANKS, B.E., BROWN, C., BURGESS, G.M., BURNSTOCK, G., CLARET, M., COCKS, T.M. & JENKINSON, D.H. (1979). Apamin blocks certain neurotransmitter-induced increases in potassium permeability. *Nature*, **282**, 415–417.

BIANCHETTI, A. & MANARA, L. (1990). *In vitro* inhibition of intestinal motility by phenylethanolaminotetralines: evidence of atypical β-adrenoceptors in rat colon. *Br. J. Pharmacol.*, **100**, 831–839.

BREDT, D.S., HWANG, P.M. & SNYDER, S.H. (1990). Localization of nitric oxide synthase indicating a neural role for nitric oxide. *Nature*, **347**, 768–770.

BRUNS, R.F. (1990). Adenosine receptors: role and pharmacology. *Ann. N.Y. Acad. Sci.*, **603**, 211–226.

BULT, H., BOECKXSTAENS, G.E., PELKMANS, P.A., JORDAENS, F.H., VAN MAERCHE, Y.M. & HERMAN, A.G. (1990). Nitric oxide as an inhibitory non-adrenergic, non-cholinergic neurotransmitter. *Nature*, **345**, 346–347.

BURNSTOCK, G. (1986). The non-adrenergic, non-cholinergic nervous system. *Arch. Int. Pharmacodyn. Ther.*, **280**, 1–15.

BURNSTOCK, G., CAMPBELL, G., SATCHELL, D. & SMYTHE, A. (1970). Evidence that adenosine triphosphate or a related nucleotide is the transmitter substance released by non-adrenergic inhibitory nerves in the gut. *Br. J. Pharmacol.*, **40**, 668–688.

COLLIS, M.G., STOGGALL, S.M. & MARTIN, F.M. (1989). Apparent affinity of 1,3-dipropyl-8-cyclopentylxanthine for adenosine A_1 and A_2 receptors in isolated tissues from guinea-pigs. *Br. J. Pharmacol.*, **97**, 1274–1278.

DE BEURME, F.A. & LEFEBVRE, R.A. (1987). Influence of α-chymotrypsin and trypsin on the non-adrenergic non-cholinergic relaxation in the gastric fundus. *Br. J. Pharmacol.*, **91**, 171–177.

DEN HERTOG, A., NELEMANS, A. & VAN DEN AKKER, J. (1989). The inhibitory action of suramin on the P_2-purinoceptor response in smooth muscle cells of guinea-pig taenia caeci. *Eur. J. Pharmacol.*, **166**, 531–534.

DEN HERTOG, A., PIELKENROOD, J. & VAN DEN AKKER, J. (1985). Effector mechanisms for α,β-methylene ATP derivatives in guinea-pig taenia caeci. *Eur. J. Pharmacol.*, **110**, 95–101.

DI CHIARA, G. & NORTH, R.A. (1992). Neurobiology of opiate abuse. *Trends Pharmacol. Sci.*, **13**, 185–193.

DONG, Y.J., JONES, R.L. & WILSON, N.H. (1986). Prostaglandin E receptor subtypes in smooth muscle: agonist activities of stable prostacyclin analogues. *Br. J. Pharmacol.*, **87**, 97–107.

DUNN, P.M. & BLAKELY, A.G.H. (1988). Suramin: a reversible P_2-purinoceptor antagonist in the mouse vas deferens. *Br. J. Pharmacol.*, **93**, 243–245.

ELLIS, J.L. & FARMER, S.G. (1989). The effects of vasoactive intestinal peptide (VIP) antagonists, and VIP and peptide histidine isoleucine antisera on non-adrenergic, non-cholinergic relaxations of tracheal smooth muscle. *Br. J. Pharmacol.*, **96**, 513–520.

FAUSSONE-PELLEGRINI, M.S. (1992). Histogenesis, structure and relationships of interstitial cells of Cajal (ICC): from morphology to functional interpretation. *Eur. J. Morphol.*, **30**, 137–148.

GAION, R.M. & TRENTO, M. (1983). The role of prostacyclin in modulating cholinergic neurotransmission in guinea-pig ileum. *Br. J. Pharmacol.*, **80**, 279–286.

GOUGH, G.R., MAGUIRE, M.H. & SATCHELL, D.G. (1973). Three new adenosine-triphosphate analogs. Synthesis and effects on isolated gut. *J. Med. Chem.*, **16**, 1188–1190.

GOYAL, R.K. & RATTAN, S. (1980). VIP as a possible neurotransmitter of non-cholinergic, non-adrenergic inhibitory neurones. *Nature*, **288**, 378–380.

GOZES, I., MELTZER, E., RUBINROUT, S., BRENNEMAN, D.E. & FRIDKIN, M. (1989). Vasoactive intestinal peptide potentiates sexual behavior: inhibition by novel antagonist. *Endocrinology*, **125**, 2945–2949.

GRIDER, J.R., MURTHY, K.S., JIN, J.G. & MAKHLOUF, G.M. (1992). Stimulation of nitric oxide from muscle cells by VIP: prejunctional enhancement of VIP release. *Am. J. Physiol.*, **262**, G774–G778.

GRYGLEWSKI, R.J., BUNTING, S., MONCADA, S., FLOWER, R.J. & VANE, J.R. (1976). Arterial walls are protected against deposition of platelet thrombi by a substance (prostaglandin X) which they make from prostaglandin endoperoxides. *Prostaglandins*, **12**, 685–713.

HAKODA, H. & ITO, Y. (1990). Modulation of cholinergic neurotransmission by the peptide VIP, VIP antiserum and VIP antagonists in dog and cat trachea. *J. Physiol.*, **428**, 133–154.

HATA, F., ISHII, T., KANADA, A., YAMANO, N., KATAOKA, T., TAKEUCHI, T. & YAGASAKI, O. (1990). Essential role of nitric oxide in descending inhibition in the rat proximal colon. *Biochem. Biophys. Res. Commun.*, **172**, 1400–1406.

HOYLE, C.H.V., KNIGHT, G.E. & BURNSTOCK, G. (1990). Suramin antagonizes responses to P_2-purinoceptor agonists and purinergic nerve stimulation in the guinea-pig urinary bladder and taenia coli. *Br. J. Pharmacol.*, **99**, 617–621.

HUIZINGA, J.D., BEREZIN, I., DANIEL, E.E. & CHOW, E. (1990). Inhibitory innervation of colonic smooth muscle cells and interstitial cells of Cajal. *Can. J. Physiol. Pharmacol.*, **68**, 447–454.

JONES, R.L. (1993). Prostacyclin analogues potentiate contraction of the guinea-pig vas deferens to electrical field stimulation. *Br. J. Pharmacol.*, **108**, 16P.

JONES, R.L. & LAWRENCE, R.A. (1993). The NK_1-receptor antagonist CP-96,345 partially inhibits cicaprost-induced contractions of the guinea-pig ileum. *Pharmacol. Commun.*, **3**, 147–155.

JONES, R.L., WILSON, N.H., MARR, C.G., MUIR, G. & ARMSTRONG, R.A. (1993). Diphenylmethylazine prostanoids with prostacyclin-like actions on human platelets. *J. Lipid Mediators*, **6**, 405–410.

LAWRENCE, R.A., JONES, R.L. & WILSON, N.H. (1992). Characterization of receptors involved in the direct and indirect actions of prostaglandins E and I on the guinea-pig ileum. *Br. J. Pharmacol.*, **105**, 271–278.

LEFEBVRE, R.A., DE BEURME, F.A. & SAS, S. (1991). Effect of apamin on the responses to VIP, ATP and NANC neurone stimulation in the rat and cat gastric fundus. *J. Auton. Pharmacol.*, **11**, 73–83.

LEFF, P., WOOD, B.E. & O'CONNOR, S.E. (1990). Suramin is a slowly-equilibrating but competitive antagonist at P_{2X}-receptors in the rabbit isolated ear artery. *Br. J. Pharmacol.*, **101**, 645–649.

LIM, S.P. & MUIR, T.C. (1986). Neuroeffector transmission in the guinea-pig internal anal sphincter: an electrical and mechanical study. *Eur. J. Pharmacol.*, **128**, 17–24.

MAAS, A.J.J. & DEN HERTOG, A. (1979). The effect of apamin on the smooth muscle cells of the guinea-pig taenia coli. *Eur. J. Pharmacol.*, **58**, 151–156.

MACKENZIE, I. & BURNSTOCK, G. (1980). Evidence against vasoactive intestinal polypeptide being the non-adrenergic, non-cholinergic inhibitory transmitter released from nerves supplying the smooth muscle of the guinea-pig taenia coli. *Eur. J. Pharmacol.*, **67**, 255–264.

MAGGI, C.A. & GIULANI, S. (1993). Multiple inhibitory mechanisms mediate non-adrenergic non-cholinergic relaxation in the circular muscle of the guinea-pig colon. *Naunyn-Schmied. Arch. Pharmacol.*, **347**, 630–634.

MANZINI, S., MAGGI, C.A. & MELI, A. (1986). Pharmacological evidence that at least two different non-adrenergic non-cholinergic inhibitory systems are present in the rat small intestine. *Eur. J. Pharmacol.*, **123**, 229–236.

MCLAUGHLIN, D.P. & MACDONALD, A. (1990). Evidence for the existence of 'atypical' β-adrenoceptors (β_3-adrenoceptors) mediating relaxation in the rat distal colon *in vitro*. *Br. J. Pharmacol.*, **101**, 569–574.

MCQUEEN, D.S., IGGO, A., BIRRELL, G.J. & GRUBB, B.D. (1991). Effects of paracetamol and aspirin on neural activity of joint mechanonociceptors in adjuvant arthritis. *Br. J. Pharmacol.*, **104**, 178–182.

MEANWELL, N.A., ROMINE, J.L & SEILER, S.M. (1994). Non-prostanoid prostacyclin mimetics. *Drugs Future*, **19**, 361–385.

NGANELE, D.M. & HINTZE, T.H. (1987). Prostacyclin reduces preload in conscious dogs via a vagal reflex mechanism. *Am. J. Physiol.*, **253**, H1477–H1483.

O'CONNOR, S.E., DAINTY, I.A. & LEFF, P. (1991). Further subclassification of ATP receptors based on agonist studies. *Trends Pharmacol. Sci.*, **12**, 137–141.

PALMER, R.M., ASHTON, D.S. & MONCADA, S. (1988a). Vascular endothelial cells synthesize nitric oxide from L-arginine. *Nature*, **333**, 664–666.

PALMER, R.M., REES, D.D., ASHTON, D.S. & MONCADA, S. (1988b). L-arginine is the physiological precursor for the formation of nitric oxide in endothelium-dependent relaxation. *Biochem. Biophys. Res. Commun.*, **153**, 1251–1256.

PANDOL, S.J., DHARMSATHAPHORN, K., SCHOEFFIELD, M.S., VALE, W. & RIVIER, J. (1986). Vasoactive intestinal peptide receptor antagonist [4Cl-D-Phe^6,Leu^{17}]VIP. *Am. J. Physiol.*, **250**, G553–G557.

REES, D.D., PALMER, R.M.J., SCHULZ, R., HODSON, H.F. & MONCADA, S. (1990). Characterization of three inhibitors of endothelial nitric oxide synthase *in vitro* and *in vivo*. *Br. J. Pharmacol.*, **101**, 746–752.

RUEFF, A. & DRAY, A. (1993). Pharmacological characterization of the effects of 5-hydroxytryptamine and different prostaglandins on peripheral sensory neurons *in vitro*. *Agents Actions*, **38**, C13–C15.

STURZEBECHER, S., HABEREY, M., MUELLER, B., SCHILLINGER, E., SCHRODER, G., SKUBALLA, W., STOCK, G., VORBRUGGEN, H. & WITT, W. (1986). Pharmacological profile of a novel carbacyclin derivative with high metabolic stability and oral activity in the rat. *Prostaglandins*, **31**, 95–109.

SUTHAMNATPONG, N., HATA, F., KANADA, A., TAKEUCHI, T. & YAGASAKI, O. (1993). Mediators of nonadrenergic, noncholinergic inhibition in the proximal, middle and distal regions of rat colon. *Br. J. Pharmacol.*, **108**, 348–355.

SUTHAMNATPONG, N., HOSOKAWA, M., TAKEUCHI, T., HATA, F. & TAKEWAKI, T. (1994). Nitric oxide-mediated inhibitory response of rat proximal colon: independence from changes in membrane potential. *Br. J. Pharmacol.*, **112**, 676–682.

WATSON, S. & GIRDLESTONE, D. (ed.). (1994). Prostanoid receptors. In *Receptor and Ion Channel Nomenclature Supplement. Trends Pharmacol. Sci.* pp. 36–37. Cambridge: Elsevier Trends Journals.

XIE, Z., HIROSE, T. & ITO, Y. (1991). Effects of vasointestinal polypeptide antagonists on cholinergic neurotransmission in dog and cat trachea. *Br. J. Pharmacol.*, **104**, 938–944.

ZAGORODNYUK, V. & MAGGI, C.A. (1994). Electrophysiological evidence for different release mechanism of ATP and NO as inhibitory NANC transmitters in guinea-pig colon. *Br. J. Pharmacol.*, **112**, 1077–1082.

(Received October 7, 1994
Revised January 3, 1995
Accepted January 17, 1995)

British Journal of Pharmacology (1995) 115, 172-176

Differences in response to 5-HT_4 receptor agonists and antagonists of the 5-HT_4-like receptor in human colon circular smooth muscle

[1]F.S-F. Tam, [2]K. Hillier, *K.T. Bunce & *C. Grossman

Clinical Pharmacology Group, Faculty of Medicine, University of Southampton, Southampton, SO16 7PX, UK and *Glaxo Group Research & Development Ware, Herts

1 In isolated circular smooth muscle strips of human colon 5-hydroxytryptamine (5-HT) produced a concentration-related inhibition of spontaneous motility.

2 The azabicycloalkyl benzimidazolones, BIMU 8 and BIMU 1, which have 5-HT_4 receptor stimulant properties, inhibited motility with EC_{50} values of 0.76 μM and 3.19 μM respectively and their E_{max} values were not significantly different from 5-HT (EC_{50}, 0.13 μM).

3 The 5-HT_4 receptor antagonist, DAU 6285 (1-10 μM), displaced the 5-HT concentration-response curve to the right in a parallel concentration-dependent manner without depressing the maximum. The Schild plot was linear and the slope did not differ significantly from unity giving a pA_2 value of 6.32.

4 The high affinity selective 5-HT_4 receptor antagonist, GR 113808, at a concentration of 3 nM displaced the 5-HT concentration-response curve in a parallel manner giving an apparent pK_B estimate of 8.9 $\pm$ 0.24. However, higher concentrations of 10-100 nM GR 113808 did not result in a further significant displacement of the 5-HT concentration-response curve and there was no suppression of E_{max}.

5 GR 113808 (10 nM) also caused a parallel displacement of the concentration-response curve to the 5-HT_4 receptor agonist, 5-methoxytryptamine (5-MeOT) giving apparent pK_B values ranging from 8.3-9.3.

6 GR 113808 (3-100 nM) failed to displace 5-HT or 5-MeOT concentration-response curves in tissue strips from 3 patients out of a total of 10 patients studied in whom the response to 5-HT and 5-MeOT was normal.

7 The 5-HT_4 receptor antagonist, SDZ 205-557 (0.3-10 μM), had no significant effect on 5-HT-induced inhibition of spontaneous motility.

8 The present results are discussed in the light of variability of response to GR 113808 and SDZ 205-557 in other tissues.

9 Overall, our data indicate that human colon circular smooth muscle can be regarded as a site in which 5-HT_4-like receptors are present but it is as yet unclear whether these results are also an indication of receptor variation.

Keywords: DAU 6285; GR 113808; 5-HT_4-like receptors; human colon; SDZ 205-557; benzimidazoles

Introduction

A range of different 5-hydroxytryptamine (5-HT) receptor subtypes have been identified in the gastrointestinal tract. Their stimulation or blockade can result in a variety of motor and secretory changes. The 5-HT_4 receptor subtype which is positively coupled to adenyl cyclase and originally identified by Dumuis *et al.* (1988a,b) has been found to be widely distributed in the gastrointestinal tract of a variety of species. In the guinea-pig ileum (Eglen *et al.*, 1990; Wardle & Sanger, 1993) and colon (Elswood *et al.*, 1991) activation of neuronally located 5-HT_4 receptors induces release of acetylcholine which results in contraction and/or an increase of electrically-evoked contraction. However, in the rat oesophagus (Reeves *et al.*, 1991; Baxter *et al.*, 1991) and ileum (Tuladhar *et al.*, 1991), stimulation of muscle cell located 5-HT_4 receptors results in direct relaxation.

We have previously cited data on the presence of muscle cell-located 5-HT_4-like receptors in the intertaenial circular muscle of human colon, stimulation of which results in relaxation (Tam *et al.*, 1994). Our evidence was based on the rank order of potencies of a range of indole derivatives. Additionally, substituted benzamides which block 5-HT_3 but stimulate 5-HT_4 receptors were agonists on the circular muscle. Tropisetron, a weak 5-HT_4 receptor antagonist but potent 5-HT_3 antagonist (literature pA_2 values approximately 5.8-6.7 and 7.8-10.6 respectively) antagonized the 5-HT and 5-methoxytryptamine (5-MeOT)-induced relaxant responses on the circular muscle with a pK_B value of 6. Ondansetron, methysergide and methiothepin were without effect on 5-HT-induced inhibition of motility. We have now further investigated the 5-HT receptor type on circular muscle of human colon using the azabicycloalkyl benzimidazolones which have improved selectivity of action at 5-HT_4 receptors and the high affinity and selective 5-HT_4 receptor antagonist GR 113808 (Gale *et al.*, 1994). A preliminary account of these studies has been published in abstract form (Hillier *et al.*, 1994).

Methods

Tissues preparation and concentration-response curves

Colon samples from 20 patients undergoing resections for carcinoma were prepared and studied under the conditions described by Tam *et al.* (1994). Twenty per cent of samples were from the ascending colon and the remainder were from

[1]Present address: Department of Pharmacology, The Chinese University of Hong Kong, Shatin, NT, Hong Kong.
[2]Author for correspondence.

the descending or sigmoid colon. The region from which we obtained our samples was confirmed histopathologically. Although responses of tissues from different colon regions did not appear to vary, the samples from the ascending colon were small in number. We have not, therefore, rigorously compared regional variations.

In a previous study (Tam *et al.*, 1994) we showed that a cumulative concentration-response curve to 5-HT or 5-MeOT (within the range 0.01–100 μM in final bath concentration) produced concentration-related inhibition of spontaneous activity of the circular muscle of the human colon. A second concentration-response curve repeated 30 min after the first was superimposable upon the first response curves if the spontaneous activity measured immediately before the second constructed response-curve was used as the control for the second curve; the spontaneous activity prior to the second response curve was 51.7 ± 10.7% less than before the first curve ($n = 4$).

Agonist studies

In studies with purported agonists a concentration-response curve to 5-HT was constructed. After washing out and leaving for 30 min a concentration-response curve to BIMU 8, BIMU 1 or DAU 6285 was constructed.

Antagonist studies

Following construction of a concentration-response curve to 5-HT, the 5-HT$_4$ receptor antagonists, DAU 6285 (1–10 μM), GR 113808 (3–100 nM) or SDZ 205-557 (0.3–10 μM) were added for 30 min prior to construction of a second response curve. The level of spontaneous activity after 30 min contact with these antagonists and prior to construction of the second response curve to 5-HT was not different from that observed prior to the second concentration-response curves of control experiments. Only one concentration of antagonist was used in any one strip.

In further studies concentration-response curves were constructed to the 5-HT$_4$ receptor stimulant 5-MeOT. GR 113808 was added at one concentration (10 nM) for 30 min and a second concentration-response curve constructed. *n* values quoted are the number of patients studied.

Data are expressed as mean ± s.e.mean. Statistical analyses were by Student's unpaired *t* test. Equipotent molar ratios (e.p.m.rs) relative to 5-HT were calculated in each tissue examined and expressed as geometric means with 95% confidence limits.

pK_B values for antagonists were calculated using the Schild equation $pK_B = \log_{10}(CR-1) - \log_{10}[B]$ where CR is the concentration ratio of the agonist used in the absence and presence of the antagonist [B] (Arunlakshana & Schild, 1959).

Drugs used

5-Hydroxytryptamine maleate, 5-methoxytryptamine hydrochloride and isoprenaline hydrochloride were purchased from Sigma Chemicals (UK). BIMU 1 ([endo-*N*-8-methyl-8-azabicyclo-(2, 3,1) oct-3-yl]-2,3-dihydro-3-ethyl-2-oxo-1*H*-benzimidazol-1-carboxamide), BIMU 8 ([endo-*N*-8-methyl-8-azabicyclo-2(3,2,1)oct-3-yl]-2,3-dihydro-3-isopropyl-2-oxo-1*H*-benzimidazol-1-carboxamide) and DAU 6285 ([endo-6-methoxy-8-methyl-8-azabicyclo-(3,2,1) oct-3-yl] 2, 3-dihydro-2-oxo-1*H*-benzimidazole-1-carboxylate) were gifts from Dr C.A. Rizzi, Boehringer Ingelheim (Italy). SDZ 205-557 (2-methoxy-4-amino-6-chlorobenzoic acid 2-(diethylamino)ethyl ester) was a gift from Pfizer (U.K.). GR 113808 ([1[2-methylsulphonyl) amino [ethyl] -4-piperidinyl] methyl-1-methyl-1*H*-indole-3-carboxylate) was a gift from Glaxo (UK).

All drugs were dissolved in water at a stock concentration of 10^{-2} M. They were further diluted to the required concentration in Krebs buffer.

Results

Agonist effects

Figure 1 shows that 5-HT, BIMU 8 and BIMU 1 (0.01–100 μM) produced concentration-related inhibitions of spontaneous contractions ($n = 6$). EC_{50} values and E_{max} values for each agonist are shown in Table 1. The rank order of potency was 5-HT > BIMU 8 > BIMU 1. The E_{max} of BIMU 1 and BIMU 8 at 100 μM were not significantly different from that of 5-HT. DAU 6285, another azabicycloalkyl benzimidazolone, however, was relatively inactive as an agonist

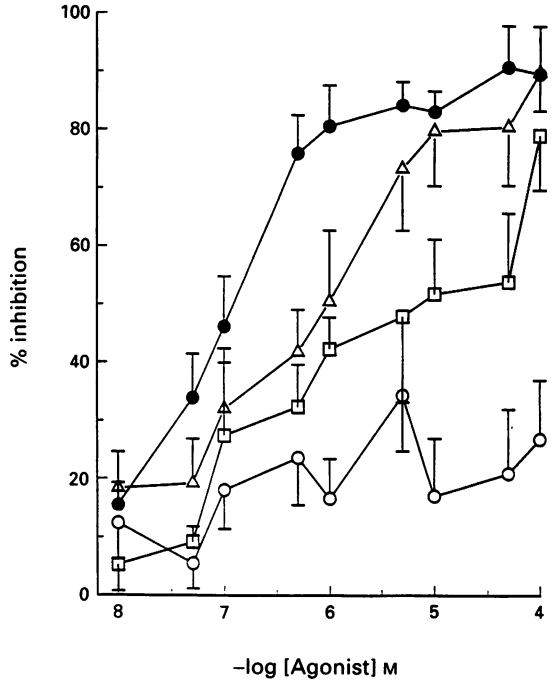

Figure 1 The effect of 5-hydroxytryptamine (5-HT) and some azabicycloalkyl benzimidazolones on the inhibition of spontaneous contractions in the circular muscle of human colon. A cumulative concentration-response curve to 5-HT (●) was constructed and after washing out the drug and leaving for 30 min, a concentration-response curve to BIMU 8 (△), BIMU 1 (□) and DAU 6285 (○) was constructed. Each point is the mean value with s.e.mean. Tissues from 6 patients were utilised in deriving these data. The effect of each benzimidazolone was examined on tissues from each patient.

Table 1 The effect of 5-hydroxytryptamine (5-HT) and azabicycloalkyl benzimidazolones on the spontaneous contractions of the intertaenial circular muscle of human colon

Compound	*EC_{50}* (95% CL)	*e.p.m.r.* (95% CL)	*% maximum inhibition of spontaneous contractions*	n
5-HT	0.13 (0.04–0.42)	1	9.10 ± 7.12	6
BIMU 8	0.76 (0.10–5.91)	4 (0.23–13.5)	90.1 ± 6.61	6
BIMU 1	3.19 (0.32–32.1)	29 (2.63–53.1)	79.2 ± 9.39	6
DAU 6285	–	–	–	6

The EC_{50} value (μM) of each drug is the mean of the EC_{50} values obtained from each patient. The equipotent molar ratios (e.p.m.rs) are the mean ratios calculated from each patient. Other values are mean ± s.e.mean. The number of muscle strips from each patient utilised for each agonist studied was between 1 and 3.
CL, confidence limits; *n*, number of patients.

with concentrations of 0.1–100 μM all causing only approximately 20% inhibition of spontaneous contractions.

Antagonist studies

The 5-HT$_4$ receptor antagonist, DAU 6285 (1, 3, 5 and 10 μM) caused concentration-related parallel displacements in the concentration-response curve to 5-HT while not significantly altering E_{max} (Figure 2a).

The pA_2 value of 6.32 was determined by Schild regression analysis and the slope was 0.84 which was not significantly different from unity (Figure 2b). SDZ 205-557 (0.3–10 μM) was tested as an antagonist in tissues obtained from 13 patients. Overall SDZ 205-557 caused no significant displacements of the concentration-response curves in concentrations up to 10 μM in tissues from 11 patients. The concentration-ratios (95% confidence limits) were 0.3 μM, 0.62 (0.27 – 1.42); 1 μM, 0.62 (0.13 – 2.85); 3 μM, 1.23 (0.51 – 2.96) 10 μM, 1.01 (0.49 – 2.08), $n = 11$. In the tissues from the remaining 2 patients, SDZ 205-557 produced antagonist effects of 5-HT-induced responses with pK_B value of 7.12–8.07, estimated from each concentration of SDZ 205-557. Figure 3 shows the results of the 5-HT$_4$ receptor antagonist, GR 113808 (3–100 nM). GR 113808 showed antagonist effects of 5-HT-induced response in the tissues obtained from 7 patients but was without effect at the same concentrations in 3 patients. In tissues where a response was obtained the antagonism was not, however, concentration-dependent (Figure 3). GR 113808 (3 nM) produced a rightward displacement of the concentration-response curve to 5-HT but at higher concentrations, GR 113808 resulted in little further displacement of the curve to the right. The pK_B values estimated at each concentration are shown in Table 2 and ranged from 7.8–8.9. In tissues from 3 of these 7 patients, the antagonist effect of 10 nM GR 113808 on the agonist 5-MeOT was also studied ($n = 3$). The pK_B values of GR

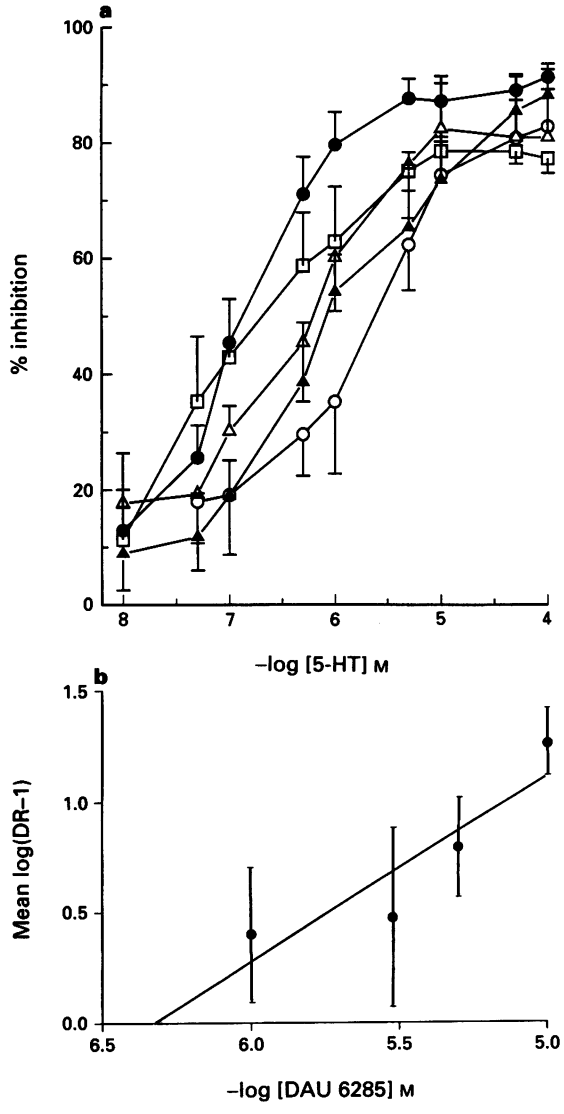

Figure 2 The effect of DAU 6285 on 5-hydroxytryptamine (5-HT)-induced inhibition of spontaneous contractions in the circular muscle of human colon. (a) Cumulative concentration-response curves to 5-HT (0.01–100 μM) were constructed (●). After washing out 5-HT, DAU 6285 at 1 (□), 3 (△), 5 (▲) or 10 (○) μM was added and incubated for 30 min before construction of the second concentration-response curve to 5-HT. The number of patients studied for each concentration of DAU 6285 was 4–6 and 2–3 muscle strips were used from each patient for each concentration-response curve. Other details as in Figure 1. (b) Schild plot of the antagonist effect of DAU 6285 on the 5-HT-induced inhibition of spontaneous contractions of the intertaenial circular muscle of human colon. The pA_2 value of DAU 6285 (6.32) with slope equal to 0.84 (not significantly different from unity). The number of patients studied was 4–6.

Table 2 The effect of GR 113808 on the 5-hydroxytryptamine (5-HT)-induced inhibition of spontaneous contractility in the intertaenial circular muscle of human colon

[GR 113808] (nM)	pK_B (±s.e.mean)	n
3	8.9 ± 0.24	7
10	8.6 ± 0.24	7
30	8.1 ± 0.15	7
100	7.8 ± 0.24	7

The values for each pK_B are derived from the data in Figure 3.

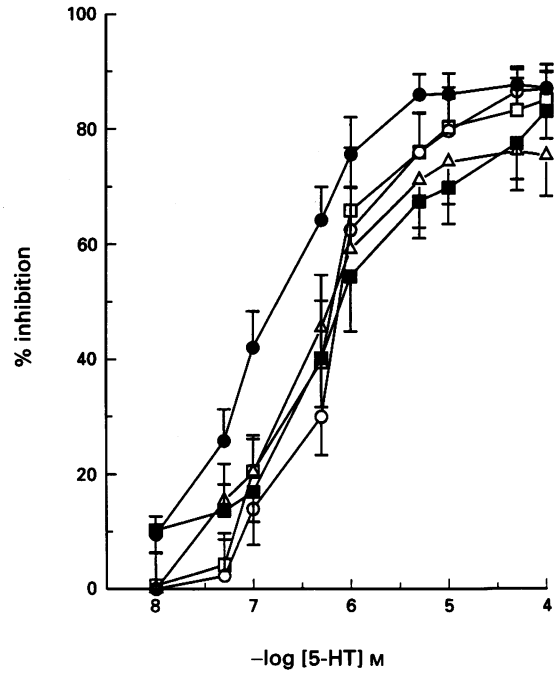

Figure 3 The effect of GR 113808 on 5-hydroxytryptamine (5-HT)-induced inhibition of spontaneous contractions in the intertaenial circular muscle of human colon. Concentration-response curves to 5-HT were constructed cumulatively (0.001–100 nM) with 2 min contact time for each concentration (●). After washing out the 5-HT, GR 113808 at 3 (□), 10 (△), 30 (○) or 100 (■) nM was added and incubated for 30 min before repeating the concentration-response curve to 5-HT. The pK_B values for GR 113808 at each concentration are shown in Table 2. Seven patients were studied and 2–3 muscle strips were utilised from each patient.

113808 (10 nM) against 5-MeOT were as follows with pK_B values against 5-HT in tissues from the same patients shown for comparison in parentheses: 9.3 (7.9); 7.9 (7.9); 8.3 (8.0).

In tissues from 3 of the 10 patients studied in which GR 113808 failed to affect 5-HT, it also failed to inhibit responses to 5-MeOT; the responses to the agonists in these tissues did not, however, differ from the normal response. DAU 6285 (10 μM), SDZ 205-557 (10 μM) and GR 113808 (100 nM) had no significant effect on the concentration-related isoprenaline-induced (0.01–100 μM) inhibition of the spontaneous contractions ($n = 4$, data not shown).

Discussion

Addition of 5-HT to circular muscle strips of human colon results in inhibition of spontaneous contractility. No desensitization to 5-HT was seen under the conditions used. With a range of indoles, substituted benzamides and tropisetron, we showed that the 5-HT receptor on circular muscle fulfilled the pharmacological criteria widely accepted as describing a 5-HT$_4$ subtype. Moreover, the receptors were predominantly located on the smooth muscle cells as tetrodotoxin produced only a small displacement to the right in the 5-HT response curve (Tam *et al.*, 1994); however, we cannot at this time unequivocally exclude the presence of an additional neuronally-located component to the 5-HT response. The response to 5-HT appears to be similar in different regions of the colon but the possibility of regional variation in response requires further appraisal as the majority of the tissues studied were from the descending and sigmoid colon.

In the present study the 5-HT$_4$ receptor-selective benzimidazolone agonists, BIMU 8 and BIMU 1, were found to inhibit spontaneous contractions. The rank orders of potency were similar to those obtained in studies in the mouse embryo colliculi neurones (Dumuis *et al.*, 1991), the rat oesophagus (Baxter & Clarke, 1992) and the guinea-pig ileum (Rizzi *et al.*, 1992; Tonini *et al.*, 1992). The concentration-response curves to BIMU 8 were largely parallel with those of 5-HT and E_{max} was similar. The less active BIMU 1 achieved a similar mean E_{max} but the responses to higher concentrations in this study were more variable. The benzimidazolone, DAU 6285, has been reported to have selective and competitive antagonist actions at 5-HT$_4$ receptors in the mouse embryo colliculi neurone (pK_B = 6.6–6.7, Dumuis *et al.*, 1992), the guinea-pig ileum (pK_B = 6.8–7.0, Waikar *et al.*, 1993) and the rat oesophagus (pK_B = 6.8–7.1, Baxter & Clarke, 1992; Waikar *et al.*, 1993) and the human right atrium (pK_B = 6.8, Schiavone *et al.*, 1991). DAU 6285 also has 5-HT$_3$ receptor antagonist properties (Turconi *et al.*, 1991) but we have shown that the 5-HT$_3$ antagonist, ondansetron, does not affect the 5-HT response curve in the preparation described for this study (Tam *et al.*, 1994). In our hands, DAU 6285 was a competitive inhibitor of the actions of 5-HT at the receptor site in the colon circular muscle causing parallel displacements in the concentration-response curves at concentrations between 1–10 μM. The pA_2 value was 6.3 and the slope of the Schild plot did not differ significantly from unity. In human colon DAU 6285 does appear to have a somewhat lower pK_B value than has been observed in animal studies. This slightly lower value was also found in studies of DAU 6285 on the secretory response in human small intestine (pA_2 = 6.17; Borman & Burleigh, 1993).

GR 113808 is a potent and selective competitive 5-HT$_4$ receptor antagonist in the guinea-pig colon (pK_B = 9.2), rat oesophagus (pK_B = 9.5, Grossman *et al.*, 1993), isolated human right atrium (pK_B 8.8, Kaumann, 1993) and isolated human detrusor muscle (pK_B 8.9, Tonini *et al.*, 1994). In this study 3 nM GR 113808 antagonized the response to 5-HT with an apparent pK_B of 8.9. However, higher concentrations of GR 113808 (up to 100 nM) were not simply competitive and failed to displace the 5-HT response curve significantly further to the right. The E_{max} was not significantly reduced with higher concentrations. The estimated pK_B values using each single concentration of GR 113808 (3–100 nM) ranged from 9.30 to 7.8. A possible explanation is that steady-state conditions may not have been reached in the presence of GR 113808 and 5-HT. However, Gale *et al.* (1994) show that incubation of guinea-pig colon with GR 113808 for periods of 15–60 min produced similar rightward displacements in the concentration-effect curves to 5-HT. GR 113808 was also not simply competitive when it was used to inhibit 5-HT-induced tachycardia in piglet right atrium, an action purported to be via the 5-HT$_4$ receptor. Medhurst & Kaumann (1993) found that 10 nM GR 113808 caused blockade of 5-HT-induced tachycardia but 100 nM caused little further displacement and also reduced the E_{max}. Another 5-HT$_4$ antagonist, SB 203186 (1-piperidinyl)ethyl 1*H*-indole 3 carboxylate) in concentrations of 0.02–10 μM did, however, produce concentration-related displacements in the 5-HT-response curve, with a pK_B of 8.3 and a linear Schild plot, the slope of which did not differ from unity. The authors suggested that GR 113808 may be having a non-specific effect on this system. The proposal that it may also be having a non-specific action on the human colon in inhibiting the response to 5-HT, therefore, requires consideration. This is unlikely, however, as GR 113808 (100 nM) had no significant effect upon isoprenaline-induced relaxation, nor did it suppress E_{max}. Further studies of GR 113808 using more selective 5-HT agonists will help to clarify matters. If with more selective 5-HT$_4$ agonist, GR 113808 does cause concentration-dependent displacements to the right, it would suggest the possibility of the presence of another co-existing receptor subtype contributing to the 5-HT-induced relaxation. We did find that GR 113808 antagonized responses to the 5-HT$_4$ receptor agonist 5-MeOT with pK_B values similar to those seen with 5-HT, but with 5-MeOT it was only possible to use one concentration of GR 113808 (10 nM). An unresolved observation at this time is that in tissues from 3 patients of 10 studied, GR 113808 at 3–100 nM produced no significant antagonism despite the fact that control responses to 5-HT were normal.

SDZ 205-557 has also been utilised as a 5-HT$_4$-selective receptor antagonist which has been shown to block competitively the 5-HT responses at the 5-HT$_4$ receptor in the guinea-pig hippocampus (Eglen *et al.*, 1993), the guinea-pig ileum, (Buchheit *et al.*, 1992), the rat oesophagus (Eglen *et al.*, 1993) and the piglet left atrium (Lorrain *et al.*, 1992) with pK_B's ranging from 7.3–7.5. SDZ 205-557 does seem, however, to vary in its ability to antagonize competitively 5-HT$_4$ receptors. In the piglet left atrium (Lorrain *et al.*, 1992) and in human right atrium (Zerkowski *et al.*, 1993) SDZ 205-557 competitively antagonized 5-HT-induced tachycardia with a pA_2 value of 7.3 and 7.7 respectively. However, in piglet right atrium the inhibitory effect of SDZ 205-557 against 5-HT-induced tachycardias was not simply competitive and the slope of the Schild plot was shallow, making estimates of pK_B values unreliable (Medhurst & Kaumann, 1993). In this study with concentrations of SDZ 205-557 of up to 10 μM we were unable to show any significant displacement of the 5-HT concentration-response curve. In tissues from only 2 patients of the 13 studied was antagonism of 5-HT responses seen with SDZ 205-557.

In conclusion, the 5-HT receptors identified in the intertaenial circular muscle of human colon can be defined as 5-HT$_4$-like receptor type in which azabicycloalkyl benzimidazolones, BIMU 8 and BIMU 1, mimicked the effect of 5-HT. The response to 5-HT can also be antagonized by the potent and selective 5-HT$_4$ receptor antagonists, DAU 6285 and GR 113808 although the effect of the latter is not simply competitive. Further study with other newly-developed selective 5-HT$_4$ antagonists is required to investigate the presence of species and/or tissue differences of this receptor type.

The pharmacologically defined 5-HT$_4$ receptor has now

been cloned and transiently expressed in COS-7 cells. Two splice variants 5-HT$_4$S and 5-HT$_4$L differing in the length and sequence of their carboxy termini have been isolated (Gerald *et al.*, 1994). Regional differences are apparent in that the 5-HT$_4$S transcript is restricted to the rat striatum whereas the 5-HT$_4$L transcript is expressed throughout the brain except in the cerebellum. It is, as yet, uncertain whether this major finding has biological implications for the differences being detected between receptors termed 5-HT$_4$ in human and laboratory animal tissues.

We thank Dr C.A. Rizzi, Boehringer Ingelheim for gifts of benzimidazolones, and the surgeons of Southampton General Hospital and Royal Hampshire County Hospital, Winchester for surgical samples.

References

ARUNLAKSHANA, O. & SCHILD, H.O. (1959). Some quantitative uses of drug antagonism. *Br. J. Pharmacol. Chemother.*, **14**, 48–58.

BAXTER, G.S., CRAIG, D.A. & CLARKE, D.E. (1991). 5-Hydroxytryptamine$_4$ receptors mediate relaxation of the rat oesophageal tunica muscularis mucosae. *Naunyn-Schmied. Arch. Pharmacol.*, **343**, 439–446.

BAXTER, G.S. & CLARKE, D.E. (1992). Benzimidazolone derivatives act as 5-HT$_4$ receptor ligands in rat oesophagus. *Eur. J. Pharmacol.*, **212**, 225–229.

BORMAN, R.A. & BURLEIGH, D.E. (1993). Evidence for the involvement of a 5-HT$_4$ receptor in the secretory response of human small intestine to 5-HT. *Br. J. Pharmacol.*, **110**, 927–928.

BUCHHEIT, K-H., GAMSE, R. & PFANNKUCHE, H.J. (1992). SDZ 205-557, a selective, surmountable antagonist for 5-HT$_4$ receptors in the isolated guinea pig ileum. *Naunyn-Schmied. Arch. Pharmacol.*, **345**, 387–393.

DUMUIS, A., BOUHELAL, R., SEBBEN, M. & BOCKAERT, J. (1988a). A 5-HT receptor in the central nervous system positively coupled with adenylate cyclase is antagonized by ICS 205-930. *Eur. J. Pharmacol.*, **146**, 187–188.

DUMUIS, A., BOUHELAL, R., SEBBEN, M., CORY, R. & BOCKAERT, J. (1988b). A non-classical 5-hydroxytryptamine receptor positively coupled with adenylate cyclase in the central nervous system. *Mol. Pharmacol.*, **34**, 880–887.

DUMUIS, A., GOZLAN, H., SEBBEN, M., ANGANAY, H., RIZZI, C.A., TURCONI, M., MONFERINI, E., GIRALDO, E., SCHIANTARELLI, P., LADINSKY, H. & BOCKAERT, J. (1992). Characterization of a novel serotonin (5-HT$_4$) receptor antagonist of the azabicycloalkyl benzimidazolone class: DAU 6285. *Naunyn-Schmied. Arch. Pharmacol.*, **345**, 264–269.

DUMUIS, A., SEBBEN, M., MONFERINI, E., NICHOLA, M., TURCONI, M., LADINSKY, H. & BOCKAERT, J. (1991). Azabicycloalkyl benzimidazolone derivatives as a novel class of potent agonists at the 5-HT$_4$ receptor positively coupled to adenylate cyclase in brain. *Naunyn-Schmied. Arch. Pharmacol.*, **343**, 245–251.

EGLEN, R.M., ALVAREZ, R., JOHNSON, L.G., LEUNG, E. & WONG, E.H.F. (1993). The action of SDZ 205,557 at 5-hydroxytryptamine (5-HT$_3$ and 5-HT$_4$) receptors. *Br. J. Pharmacol.*, **108**, 376–382.

EGLEN, R.M., SWANK, S.R., WALSH, L.K.M. & WHITING, R.L. (1990). Characterization of 5-HT$_3$ and 'atypical' 5-HT receptors mediating guinea-pig ileal contractions *in vitro*. *Br. J. Pharmacol.*, **101**, 513–520.

ELSWOOD, C.J., BUNCE, K.T. & HUMPHREY, P.P.A. (1991). Identification of putative 5-HT$_4$ receptors in guinea-pig ascending colon. *Eur. J. Pharmacol.*, **196**, 149–155.

GALE, J.D., GROSSMAN, C.J., WHITEHEAD, J.W.F., OXFORD, A.W., BUNCE, K.T. & HUMPHREY, P.P.A. (1994). GR 113808: a novel, selective antagonist with high affinity for the 5-HT$_4$ receptor. *Br. J. Pharmacol.*, **111**, 332–338.

GERALD, C., ADHAM, N., KAO, H.T., SCHECHTER, L.E., OLSEN, MA., BARD, J.A., LAZ, T.M., VAYSSE, P.J.J., BRANCHEK, T.A. & WEINSHANK, R.L. (1994). The 5-HT$_4$ receptor: molecular cloning of two splice variants. *3rd IUPHAR Satellite Meeting on Serotonin*. July 30–Aug 3, Chicago, Abst 54, page 82.

GROSSMAN, C.J., KILPATRICK, G.J. & BUNCE, K.T. (1993). Development of a radioligand binding assay for 5-HT$_4$ receptors in the guinea-pig and rat brain. *Br. J. Pharmacol.*, **198**, 618–624.

HILLIER, K., TAM, F.S-F., BUNCE, K.T. & GROSSMAN, C. (1994). Inhibition of motility induced by activation of 5-HT$_4$-like and 5-HT$_1$-like receptors in human colon smooth muscle. *Br. J. Pharmacol.*, **112**, 102P.

KAUMANN, A.J. (1993). Blockade of human atrial 5-HT$_4$ receptors by GR 113808. *Br. J. Pharmacol.*, **110**, 1172–1174.

LORRAIN, J., GROSSET, A. & O'CONNOR, S.E. (1992). 5-HT$_4$ receptors, present in piglet atria and sensitive to SDZ 205-557, are absent in papillary muscle. *Eur. J. Pharmacol.*, **229**, 105–108.

MEDHURST, A.D. & KAUMANN, A.J. (1993). Characterization of the 5-HT$_4$ receptor mediating tachycardia in piglet isolated right atrium. *Br. J. Pharmacol.*, **110**, 1023–1030.

REEVES, J., BUNCE, K.T., HUMPHREY, P.P.A. & GUNNING, S.J. (1989). Further characterisation of the 5-HT receptor mediating smooth muscle relaxation in the rat oesophagus. *Br. J. Pharmacol.*, **98**, 800P.

RIZZI, C.A., COCCINI, T., ONORI, L., MANZO, L. & TONINI, M. (1992). Benzimidazolone derivatives: a new class of 5-hydroxytryptamine$_4$ receptor agonists with prokinetic and acetylcholine releasing properties in the guinea pig ileum. *J. Pharmacol. Exp. Ther.*, **261**, 412–419.

SCHIAVONE, A., GIRALDO, E., GIUDICI, L. & TURCONI, M. (1991). DAU 6285: a novel 5-HT$_4$ receptor antagonist (abstract). *Serotonin 1991: 5-HT-CNS Receptors and Brain Function* (July 14–18, Birmingham) p81.

TAM, F.S-F., HILLIER, K. & BUNCE, K.T. (1994). Characterization of the 5-hydroxytryptamine receptor type involved in inhibition of spontaneous activity of isolated human colonic circular muscle. *Br. J. Pharmacol.*, **113**, 143–150.

TONINI, M., CANDURA, S.M., ONORI, L., COCCINI, T., MANZO, L. & RIZZI, C.A. (1992). 5-Hydroxytryptamine$_4$ receptor agonists facilitate cholinergic transmission in the circular muscle of guinea pig ileum: antagonism by tropisetron and DAU 6285. *Life Sci.*, **50**, PL173–PL-178.

TONINI, M., MESSORI, E., FRANCESCHETTI, G.P., RIZZI, C.A., CASTOLDI, A.F., COCCINI, C. & CANDURA, S.M. (1994). Characterization of the 5-HT receptor potentiating neuromuscular cholinergic transmission in strips of human isolated detrusor muscle. *Br. J. Pharmacol.*, **113**, 1–2.

TULADHAR, B.R., COSTALL, B. & NAYLOR, R.J. (1991). Investigation of the 5-HT$_4$ receptor mediating relaxation of the rat ileum. In *The 10th Iranian Congress of Physiology and Pharmacology*, Ahwaz, Iran. Abstract 89.

TURCONI, M., SCHIANTARELLI, P., BORSINI, F., RIZZI, C.A., LADINSKY, H. & DONETTI, A. (1991). Azabicycloalkyl benzimidazolones: interaction with serotonergic 5-HT$_3$ and 5-HT$_4$ receptors and potential therapeutic implications. *Drugs of the Future*, **16**, 1011–1026.

WAIKAR, M.V., HEDGE, S.S., FORD, A.P.D.W. & CLARKE, D.E. (1993). Pharmacological analysis of endo-6-methody-8-azabicyclo [3,2,1]oct-3-yl-2, 3-dihydro-2-oxo-1H-benzimidazolone-1-carboxylate hydrochloride (DAU 6285) at the 5-hydroxytryptamine$_4$ receptor in the tunica muscularis mucosal of rat esophagus and ileum of guinea pig: role of endogenous 5-hydroxytryptamine. *J. Pharmacol. Exp. Ther.*, **264**, 654–661.

WARDLE, K.A. & SANGER, G.J. (1993). The guinea-pig distal colon – a sensitive preparation for the investigation of 5-HT$_4$ receptor-mediated contractions. *Br. J. Pharmacol.*, **110**, 1593–1599.

ZERKOWSKI, H-R., BROEDE, A., KUNDE, K., HILLEMANN, S., SCHÄFER, E., VOGELSANG, M., MICHEL, M.C. & BRODDE, O-E. (1993). Comparison of the positive inotropic effects of serotonin, histamine, angiotensin II, endothelin and isoprenaline in the isolated human right atrium. *Naunyn-Schmied. Arch. Pharmacol.*, **347**, 347–352.

(Received September 20, 1994
Revised December 19, 1994
Accepted January 23, 1995)

British Journal of Pharmacology (1995) 115, 177–185

A study on P_{2X} purinoceptors mediating the electrophysiological and contractile effects of purine nucleotides in rat vas deferens

[1]Baljit Singh Khakh, *Annmarie Surprenant & Patrick P.A. Humphrey

Glaxo Institute for Applied Pharmacology, Department of Pharmacology, University of Cambridge, Cambridge and *Glaxo Institute for Molecular Biology, 14 chemin des Aulx, 1228 CH, Geneva, Switzerland

1 We have studied both the electrophysiological and contractile effects of the purine nucleotide, adenosine-5'-triphosphate (ATP), as well as a number of its structural analogues as agonists at P_{2X} purinoceptors in the rat vas deferens *in vitro*.

2 Electrophysiological effects were investigated by a whole cell voltage clamp technique (holding potential −70 mV) with fast flow concentration-clamp applications of agonists in single isolated smooth muscle cells. ATP, 2-methylthio adenosine-5'-triphosphate (2-MeSATP) and α,β methylene adenosine-5'-triphosphate (α,β-meATP) all evoked inward currents over a similar concentration range (0.3–10 μM), being approximately equipotent with similar concentrations for threshold effects (0.3 μM). ADP (10 μM) also evoked a rapid current of similar peak amplitude to that seen with ATP (10 μM).

3 α,β-meATP was the most potent agonist in producing contractions of the rat vas deferens whole tissue preparation, with a threshold concentration equal to that in the electrophysiological studies (0.3 μM). However, ATP and 2-MeSATP were at least ten times less potent in studies measuring contraction than in the electrophysiological studies. Furthermore, their concentration-effect curves were shallow with smaller maximal responses than could be achieved with α,β-meATP. ADP, AMP and adenosine were inactive at concentrations up to 1 mM. The rank order of agonist potencies observed for contraction was α,β-meATP>> ATP = 2-MeSATP.

4 Measurement of inorganic phosphate (iP), as a marker of purine nucleotide metabolism in the vas deferens whole tissue preparation, indicated that ATP and 2-MeSATP were rapidly metabolized, whereas α,β-meATP was stable for up to 2 h. Removal of divalent cations prevented breakdown of ATP and 2-MeSATP, suggesting that metabolism involved a Ca^{2+}/Mg^{2+}-dependent enzyme.

5 It appears that in isolated preparations of rat vas deferens, the low potency of ATP and 2-MeSATP can be explained by rapid agonist breakdown by ectonucleotidases. However, this is not the case in the single cell studies where the use of rapid concentration-clamp applications revealed the true potency of the agonists. Under such conditions the three agonists were all equal in potency indicating that the rank order of agonist potencies of α,β-meATP>> ATP = 2-MeSATP is not in fact characteristic of smooth muscle P_{2X}-purinoceptors as commonly believed.

Keywords: ATP; P_{2X}-purinoceptor; vas deferens; ectonucleotidase

Introduction

Adenosine-5'-triphosphate (ATP) is now widely recognized as a co-transmitter with noradrenaline in the sympathetic nervous system (see Burnstock, 1986; von Kügelgen & Starke, 1991). The most convincing evidence in favour of ATP/noradrenaline co-transmission comes from studies on vas deferens (Sneddon & Burnstock, 1984; Sneddon & Westphall, 1984; Stjarne & Astrand, 1984; see also review by von Kügelgen & Starke, 1991). In rat vas deferens, ATP appears to mediate the rapid twitch component of the contractile response to electrical field stimulation, whereas noradrenaline mediates the slower tonic component (French & Scott, 1983; Amobi & Smith, 1987a,b). Evidence is also emerging that ATP can function as a fast synaptic transmitter at neuro-neuronal synapses in autonomic neurones (Evans *et al.*, 1992) and in the central nervous system (Edwards *et al.*, 1992).

Specific cell surface receptors for ATP, termed P_2-purinoceptors (Burnstock, 1978) have been subdivided into P_{2X} and P_{2Y}-purinoceptor subtypes, largely on the basis of rank orders of agonist potencies (Burnstock & Kennedy, 1985). Since this time several other members of the P_2-purinoceptor family have been proposed (Gordon, 1986; see Abbrachio *et al.*, 1993). The original classification (Burnstock & Kennedy, 1985; Kennedy, 1990) classified the P_{2Y}-purinoceptor as a G-protein coupled receptor which could be identified using the potent and selective agonist 2-MeSATP. The recent cloning of the gene for the P_{2Y}-purinoceptor from chick brain has provided confirmation that the receptor is indeed a member of the G-protein superfamily (Webb *et al.*, 1993; see also Barnard *et al.*, 1994). In contrast the P_{2X}-purinoceptor was classified as a ligand gated cation channel, at which α,β-meATP is a potent and selective agonist (Burnstock & Kennedy, 1985; Kennedy, 1990). Since the original proposal P_{2X} and P_{2Y}-purinoceptors have been characterized in functional studies, largely on the basis of the relative potencies of 2-MeSATP and α,β-meATP (Burnstock, 1990; Kennedy, 1990; Abbrachio *et al.*, 1993; Abbrachio & Burnstock, 1994; Fredholm *et al.*, 1994).

However, we have suggested that the low potency of ATP and its shallow concentration-effect curve as a contractile agonist in rat isolated vas deferens, may be in part due to agonist breakdown or removal (Khakh *et al.*, 1994), thereby underestimating its true potency as an agonist at P_{2X}-purinoceptors. In the present study we have compared the electrophysiological actions of ATP and some of its structural analogues as agonists applied using fast flow concentration-clamp in single smooth muscle cells from rat vas deferens, in an attempt to circumvent the problem of agonist breakdown. The findings were compared with those in whole tissue experiments measuring contraction of rat bisected

[1] Author for correspondence at: Glaxo Institute for Applied Pharmacology, Department of Pharmacology, University of Cambridge, Tennis Court Road, Cambridge CB2 1QJ.

isolated vas deferens. In addition we have obtained a measure of agonist breakdown using inorganic phosphate (iP) production as a marker. The findings are discussed in relation to current criteria for characterization of smooth muscle P_2-purinoceptors, particularly of the P_{2X} type, in isolated tissues.

Some of these results have been presented briefly to the British Pharmacological Society (Khakh *et al.*, 1994).

Methods

Single cell studies

Smooth muscle cells were dissociated by a method based on that already described (Clapp & Gurney, 1991). Male Sprague-Dawley rats (50 g) were killed by carbon dioxide asphyxiation and decapitation. This method of euthanasia is approved by the Office Vetrinaire Cantonal of Geneva where the experiments were conducted. Vasa deferentia were rapidly removed and placed in Ca^{2+}/Mg^{2+} free Hanks buffer (HBSS; Gibco). Adherent connective tissue and mesentery were removed and the tissue chopped into pieces approximately 2 mm square. The pieces were immersed in 2 ml of HBSS with papain 41 iu ml^{-1} (Worthington Biochemicals) and then refrigerated for 18 h at 4°C. This solution was then heated to 37°C in a water incubator and after 10 min the tissue pieces were triturated 10–20 times, in the same solution with fire-polished glass pipettes at times 10, 12, 14, 16 and 18 min until smooth muscle cells could be seen (by inspection of 10 μl aliquots under a light microscope). The solution was then centrifuged at 80 *g* for 10 min, the supernatant discarded and the pellet resuspended in 0.8 ml of extracellular buffer (for composition see below). Aliquots of suspended cells (60 μl) were plated onto 12 mm diameter glass coverslips and left for 20 min at 37°C in a cell incubator. All myocytes were used within 3–3.5 h of plating.

Electrophysiological recordings

Recordings were carried by a whole cell voltage clamp technique using 5 MΩ patch pipettes with seal resistancs of between 20–50 GΩ. Extracellular HEPES buffer had the following composition (mM): NaCl 160, $MgCl_2$ 1.0, $CaCl_2$ 2.0, KCl 2.0, D-glucose 11.0, HEPES 10.0. The buffer was continually superfused at a rate of 1–3 ml min^{-1} through the microscope stage bath (vol 0.5 ml). Intracellular pipette solution contained (mM) K-aspartate 160, NaCl 5.0, HEPES 10.0 and BAPTA 11.0. The pH and osmolarity of internal and external solutions were maintained at 7.4 and 300–312 mosmol ml^{-1}, respectively. Currents were filtered (−3 db) with a 3-pole bessel filter, digitised at 0.5–2 kHz and analysed with a axograph software (Axon instruments).

Agonists were applied using the solenoid operated concentration clamp U-tube method of Fenwick *et al.* (1992). The time course of solution changes was estimated by measuring changes in junction potential as a result of U tube application of distilled water. The time to onset was between 20–300 ms and the rise time (10–90%) was invariably between 10–12 ms.

Each agonist was applied at only one concentration to one cell from any one coverslip. Concentration-effect curves are shown as peak amplitude current responses to a 2 s application of agonist recorded from between 4–12 cells as indicated in the text. Antagonist experiments were performed by exposing cells to 100 μM suramin for 2 min in the superfusion system immediately after attaining whole cell voltage clamp and then applying agonist for 2 s via the U tube in the continued presence of suramin. The fast flow agonist solution also contained 100 μM suramin. Subsequently, cells were superfused with suramin-free medium and then a second application of agonist was made to the same cell in the absence of suramin. All cells were voltage clamped at −70 mV, and all recordings made at room temperature (approx. 22–25°C). The waning of the response in the continued presence of agonist was quantified by fitting to a single exponential and expressed in terms of decay constants using Axograph software (Axon Instruments).

Measurement of contractile activity

Sprague-Dawley rats (200–350 g) were killed by stunning and decapitation. Vasa deferentia were rapidly removed and placed in a Petri dish containing gassed (95% O_2, 5% CO_2, pH 7.4) modified Krebs buffer of the following composition (mM): NaCl 118, $NaHCO_3$ 25, KCl 4.7, $MgSO_4.7H_2O$ 0.6, $K_2H_2PO_4$ 1.5, D-glucose 11.1, $CaCl_2$ 1.3 and indomethacin 6 μM. The tissues were freed of connective tissue and adhering fat, and bisected transversely such that each vasa gave two equal preparations, one prostatic and one epididymal, i.e. four preparations from each animal. The preparations were mounted with cotton thread in 4 ml organ baths under 0.5 g resting tension and immersed in gassed Krebs buffer at 37°C. Tension changes were recorded with a Dynamometer UF1 isometric force transducer and the recordings displayed on a lectromed multitrace 8 channel pen recorder. The preparations were equilibrated under 0.5 g resting tension for a period of 30 min with frequent washes during which time tension was maintained at 0.5 g.

Following equilibration, the preparations were exposed to 100 mM potassium chloride (KCl) three times on a 15 min dose interval. Subsequent contractions (increases in tension) to agonists were expressed as a percentage of the mean contraction to the three doses of potassium chloride. Control first concentration-effect curves were determined for α,β-meATP (10 nM–100 μM) using sequential dosing on a 15 min dose interval to all 4 preparations from each animal. The preparations were washed with Krebs buffer after a maximum response had been attained and then left unchallenged for 1 h. Subsequently in one of the four preparations a second concentration-effect curve was determined for α,β-meATP, and a different agonist was tested in each of the other three preparations. The four preparations obtained from each animal were studied in a Latin square design. All data shown are the mean ± s.e.mean from at least four animals.

Measurement of inorganic phosphate

A colourimetric assay was used to measure the production of iP as a reflection of purine nucleotide metabolism. The method is similar to that already described (Lanzetta *et al.*, 1979) which is based on the method of Hess & Derr (1975). Briefly the method uses a mixture of the dye, malachite green (0.045%), and ammonium molybdate (4.2% in 4 M HCl) that changes colour from yellow to green on complexing with iP. Colour changes were measured as absorbance changes at 660 nm in a spectrophotometer (Perkin Elmer). Absorbance values for the samples were converted to nmol of iP by using a standard curve (which was constructed daily with KH_2PO_4 used as the source of iP). Data are presented as changes in μM concentrations of iP.

Experiments were designed to mimic as far as possible the conditions in the whole tissue contraction studies. The only difference was that a HEPES based buffer (for composition see under single cell studies) was used instead of Krebs buffer to circumvent the problem of background phosphate in the bathing medium. All solutions and drugs used in the measurement of iP were made with ultra pure water (> 18.0 MΩ; Elga water purifier). Bisected vas deferens were placed in 4 ml of HEPES buffer oxygenated continually with 100% O_2 at 37°C, pH 7.35–7.4, and left to equilibrate for 30 min before proceeding further. The four preparations from each animal were arranged in a Latin square design such that the three preparations were incubated with either 100 μM ATP, 2-MeSATP or α,β-meATP and the fourth

preparation always served as a time-dependent control with no drug. Samples of buffer (50 μl) were taken 1 min before adding the drug, immediately after adding the drug (time 0), and then every 10 min for up to 2 h.

Drugs

α,β-Methylene adenosine-5'-triphosphate lithium salt (α,β-meATP), ATP, ADP, AMP, adenosine, HEPES and BAPTA were all purchased from Sigma. 2-Methylthio adenosine-5'-triphosphate tetra sodium salt (2-MeSATP) was obtained from Research Biochemicals Inc. All drugs were made freshly and diluted to the relevant concentration in Krebs solution for contraction experiments and in HEPES buffer for voltage clamp studies and iP measurements.

Results

Single cell studies

Initial observations Preliminary studies showed that a 2 s application of ATP (0.3–10 μM) via the U tube fast perfusion system evoked inward currents in all cells tested in a concentration-dependent manner. The ATP-evoked currents waned in amplitude during the application of agonist. A second application of ATP up to 6 min later showed marked diminution in peak current amplitude response compared to the first application, a property here referred to as tachyphylaxis (Figure 1). The waning of the response during the agonist application and the tachyphylaxis following first application was a property of all concentrations of ATP. Consequently only one concentration of agonist was added to a cell from any one coverslip, in an attempt to circumvent these effects.

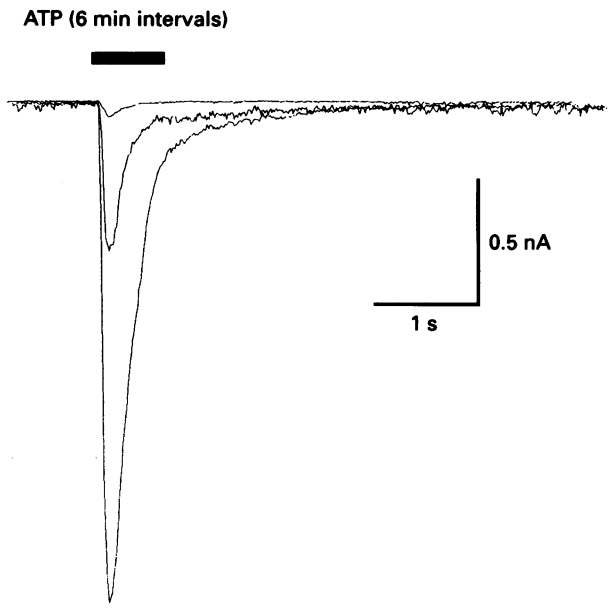

Figure 1 Three superimposed current recordings from a single smooth muscle cell of rat vas deferens in response to U tube concentration clamp application of 3 μM ATP for 0.5 s at 6 min intervals. The response to the second application of 3 μM ATP was markedly smaller, about 30% of initial, and a third application 6 min later produced a response which was only about 10% of the original for this cell. This phenomenon of tachyphylaxis was observed in all cells tested but was not quantified. In this and all further figures the agonist was applied for the time periods as indicated by the solid bar above current recordings.

Concentration-dependence and kinetics of agonist-evoked currents

ATP evoked inward currents over the concentration range 0.1–10 μM. The threshold concentration for responses evoked by ATP was 0.1 μM with a mean peak amplitude response of 65 ± 10 pA ($n = 5$) (see Figure 2). Increasing concentrations of ATP produced larger inward currents (Figures 2 and 3), with progressively shorter rise times, e.g. rise time (10–90% peak) at 0.1 μM was 164.8 ± 27.3 ms ($n = 5$) and at 10 μM 43.5 ± 4.2 ms ($n = 8$; see Figure 2). The decay time of the ATP evoked current could be fitted by a single exponential with time constant values (τ) that were unrelated to agonist concentration (174.3 ± 47 $n = 4$; 221.3 ± 35.6 $n = 11$; and 161.7 ± 14.7 ms $n = 8$ for 1, 3 and 10 μM ATP, respectively). Concentrations of ATP higher than 30 μM were not employed since the rise time at 30 μM ATP was approaching the rise time for the U tube application system. Thus higher concentrations of ATP would have exceeded the limits of adequate solution exchange and underestimated the peak current responses (data not shown). 2-MeSATP was tested over a similar concentration-range to ATP. The threshold for producing a response was between 0.1–1 μM, further the mean peak amplitude current responses were not significantly different from those to ATP at the same concentrations (Figure 3). The response to 2-MeSATP was also rapid (rise time 20.3 ± 3.6 ms at 10 μM; $n = 6$) and the current evoked waned during agonist application (τ = 150 ± 24.2 ms at 10 μM; $n = 6$).

α,β-meATP evoked inward currents with a threshold of between 0.1–0.3 μM. Mean peak amplitude current responses were not significantly different from responses to ATP or 2-MeSATP (Figure 3). However rise times for the α,β-meATP evoked currents were slower than for ATP or 2-MeSATP e.g. 58 ± 9.9 ms at 10 μM compared to 43.5 ± 4.6 and 20.3 ± 3.6 ms for ATP and 2-MeSATP, respectively. Thus it was possible to investigate the actions of α,β-meATP up to 30 μM before the limits of the U tube perfusion system were exceeded; rise time at 30 μM was 34.3 ± 15.8 ms ($n = 3$). The decay constant was slower than for ATP or 2-MeSATP, such that for α,β-meATP (10 μM) τ was 775.8 ± 294.2 ($n = 7$) compared to 161.7 ± 14.7 ($n = 8$) and 150 ± 24.2 ms ($n = 6$) for ATP and 2-MeSATP, respectively (see Figure 2).

ADP (10 μM) evoked an inward current with a similar rise time (58.5 ± 6.2 ms; $n = 4$) and a similar mean peak amplitude (1738 ± 728 pA) current response as that to ATP (1242 ± 364 pA) at the same concentration. However its decay constant of 642.7 ± 77.6 ms ($n = 4$) was significantly longer ($P < 0.05$; Student's t test). AMP and adenosine (both 30 μM) evoked little or no inward current, mean peak amplitudes were 20.3 ± 13.6 and 4.4 ± 4.4 pA, respectively (both $n = 4$); in the same cells ATP was applied to establish cell viability and evoked large inward currents.

Antagonism by suramin

Following a 2 min exposure of cells to 100 μM suramin ATP, 2-MeSATP and α,β-meATP (all at 3 μM) evoked small inward currents of mean peak current amplitude 22.8 ± 13.6, 14.0 ± 10.5 and 18.8 ± 18.8 pA, respectively (all $n = 4$). Replacement of bathing buffer with suramin-free buffer and re-applying agonists 2 min later evoked large inward currents in all cells, with mean peak amplitudes of 1477 ± 519, 1895 ± 661 and 1938 ± 889 pA ($n = 4$ for each), respectively (Figure 4). Likewise the effect of ADP (10 μM) was also abolished by 100 μM suramin ($n = 2$ see Figure 5).

Whole tissue studies

Concentration-dependence of agonists as contractile agents In preliminary studies the actions of ATP and α,β-meATP were studied in epididymal and prostatic preparations to investigate the possibility that differences in agonist potency may exist between the two halves (Sneddon & Machaly, 1992). In

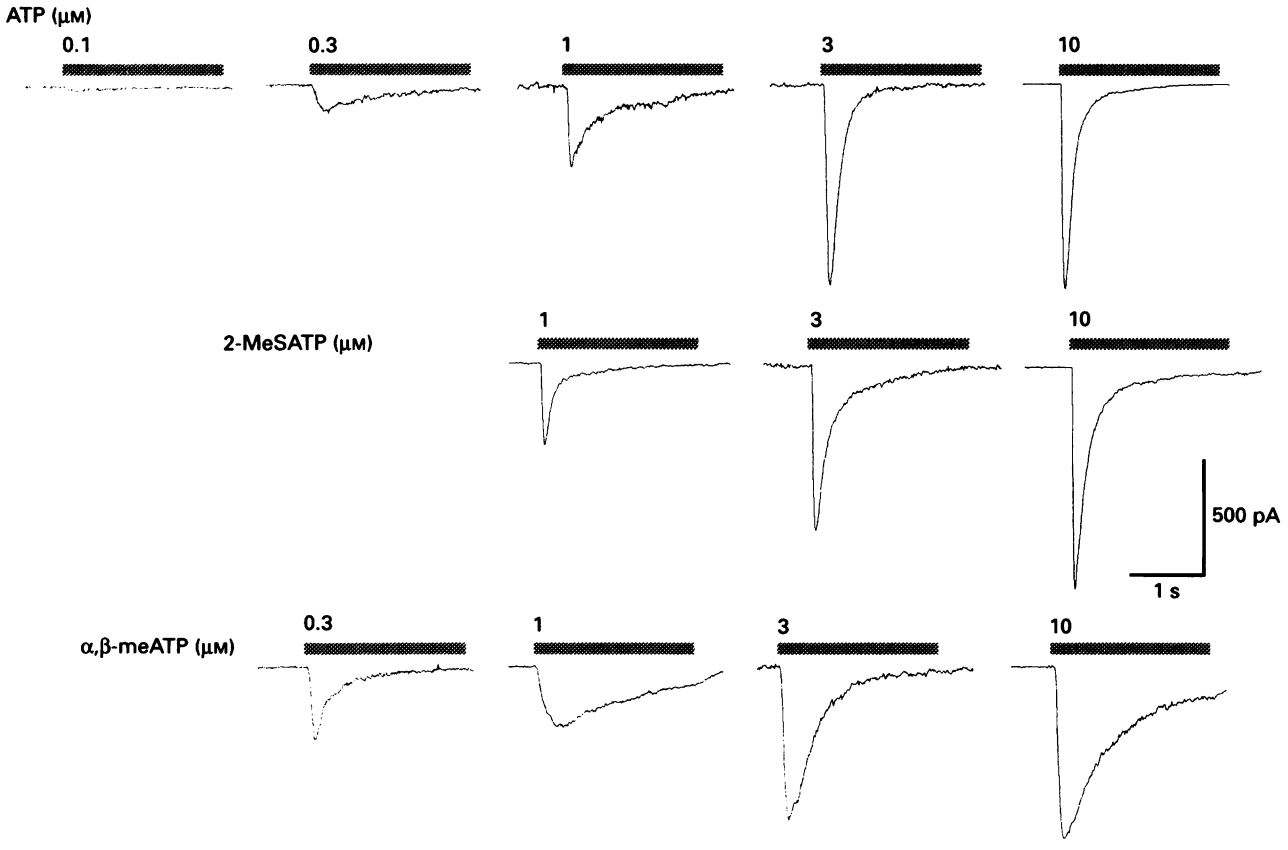

Figure 2 Recordings from single smooth muscle cells of rat vas deferens in response to application of agonists. Upper panels show application of ATP in increasing concentrations as indicated in Figure 1, note threshold is about 0.1 μM. The middle panels show 2-MeSATP evoked inward currents demonstrating concentration-dependency. The lower panels show that α,β-meATP also evoked inward currents in a concentration-dependent manner. Each current recording shown is from a different cell, but is representative of between 4–11 such recordings for each agonist concentration (see Figure 3 and text).

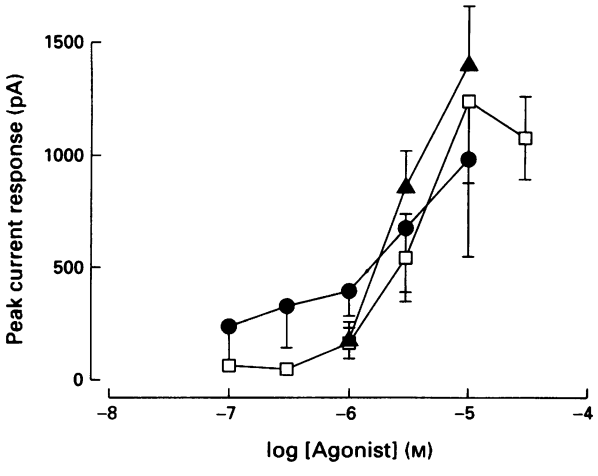

Figure 3 Concentration-effect curves to ATP (□), 2-MeSATP (▲) and α,β-meATP (●) from single smooth muscle cells. Each point on the concentration-effect curves is the mean ± s.e.mean peak inward current for each agonist concentration ($n = 4–11$). All three agonists are approximately equal in potency, ATP had an apparent EC_{50} of about 3 μM. In some cases undirectional error bars are shown for clarity.

such experiments epididymal and prostatic preparations were mounted for isometric tension recording as described in the Methods. Concentration-effect curves (10 nM–100 μM) were determined to α,β-meATP and ATP in both halves. In the case of α,β-meATP concentration-effect curves showed the same threshold concentration for responses (0.3 μM) and similar response amplitudes for both epididymal and prostatic preparations, such that the pEC_{50} for α,β-meATP was 5.34 ± 0.13 and 5.79 ± 0.34 (both $n = 4$; no significant difference at $P = 0.05$) for epididymal and prostatic preparations, respectively. In the case of ATP no EC_{50} value could be calculated since concentration-effect curves were shallow and flat, however mean response amplitudes were not markedly different at all concentrations of ATP examined, such that responses to 1, 10 and 100 μM ATP were 0.6 ± 0.6, 2.4 ± 0.9 and 5.6 ± 1.5 and 1.1 ± 0.9, 2.7 ± 1.5 and 6.0 ± 1.7% of the response to 100 mM KCl for epididymal and prostatic preparations, respectively. Consequently no account was taken of anatomical location other than to pool data from systematically randomized preparations from each animal (see Methods).

ATP induced contractions of rat vas deferens over the concentration range 10 μM–1 mM; threshold concentrations for contraction were about 10 μM. The concentration-effect curve to ATP was shallow (Figure 6) so that at the highest concentration of ATP tested (up to 1 mM) responses were only 17.3 ± 4.4% of the contraction to 100 mM KCl ($n = 4$). Similarly, 2-MeSATP (3–100 μM) displayed a shallow concentration-effect curve, with threshold concentrations for contraction being about 3 μM; the response to 100 μM 2-MeSATP was 17.7 ± 2.3% of the response of 100 mM KCl ($n = 4$). In contrast, α,β-meATP induced contractions of rat vas deferens over the range 0.3–100 μM, with threshold concentrations at 0.3 μM. The concentration-effect curve to α,β-meATP was steep and response amplitude was related to the concentration of α,β-meATP. At the highest concentration of α,β-meATP tested (100 μM) the contractile response was 79.1 ± 11.4% of the response to 100 mM KCl ($n = 4$). However, the concentration-effect curve to α,β-meATP did not appear to reach a well-defined maximal response. ADP,

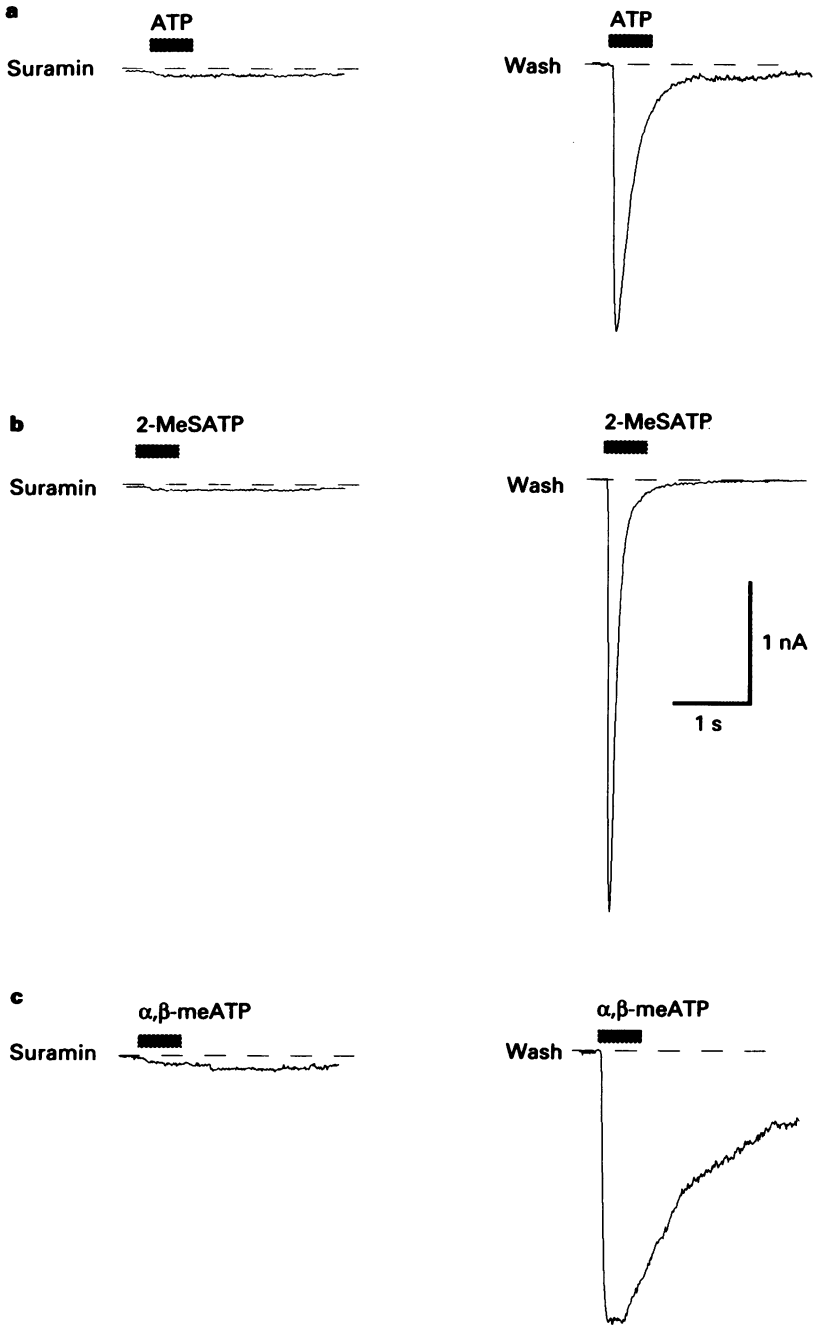

Figure 4 Suramin antagonism of agonist-induced currents in single vas deferens smooth muscle cells. The left hand recordings are in the presence of 100 μM suramin and the right hand traces (indicated as wash) are from the same cells after suramin washout. Large inward currents were recorded in response to application of (a) ATP, (b) 2-MeSATP and (c) α,β-meATP when suramin was absent. All agonist concentrations were 3 μM. Current recordings shown are representative of four such experiments.

AMP and adenosine produced little or no agonist effects at concentrations up to 100 μM.

Measurement of inorganic phosphate

When either ATP or 2-MeSATP (both at 100 μM) were incubated with bisected vasa deferentia and 50 μl samples taken every 10 min and analysed for iP, both compounds led to an increase in iP concentration in a time-dependent manner. After 120 min ATP and 2-MeSATP provided 205.7 ± 24.0 and 216.2 ± 26.9 μM of iP from 100 μM agonist (all $n = 8$). Incubation of either agonist alone (100 μM) with no tissue, resulted in no production of iP (data not shown). Further, time-dependent controls (Figure 7) showed that the tissue alone did not produce any iP over the course of the experiments. In contrast to the findings with ATP and 2-MeSATP, incubation of tissues with α,β-meATP led to little increase in iP in the 2 h period (Figure 7a).

However, in the absence of divalent cations and with the addition of 1 mM EDTA, there was little or no increase in iP with ATP or 2-MeSATP (both 100 μM) so that the levels of iP were not different from control preparations that had received no agonist ($n = 4$; Figure 7b).

Discussion

Cell surface receptors for ATP, termed P_2-purinoceptors have been subdivided into P_{2X} and P_{2Y} subtypes largely on the basis of rank orders of agonist potencies (Burnstock & Ken-

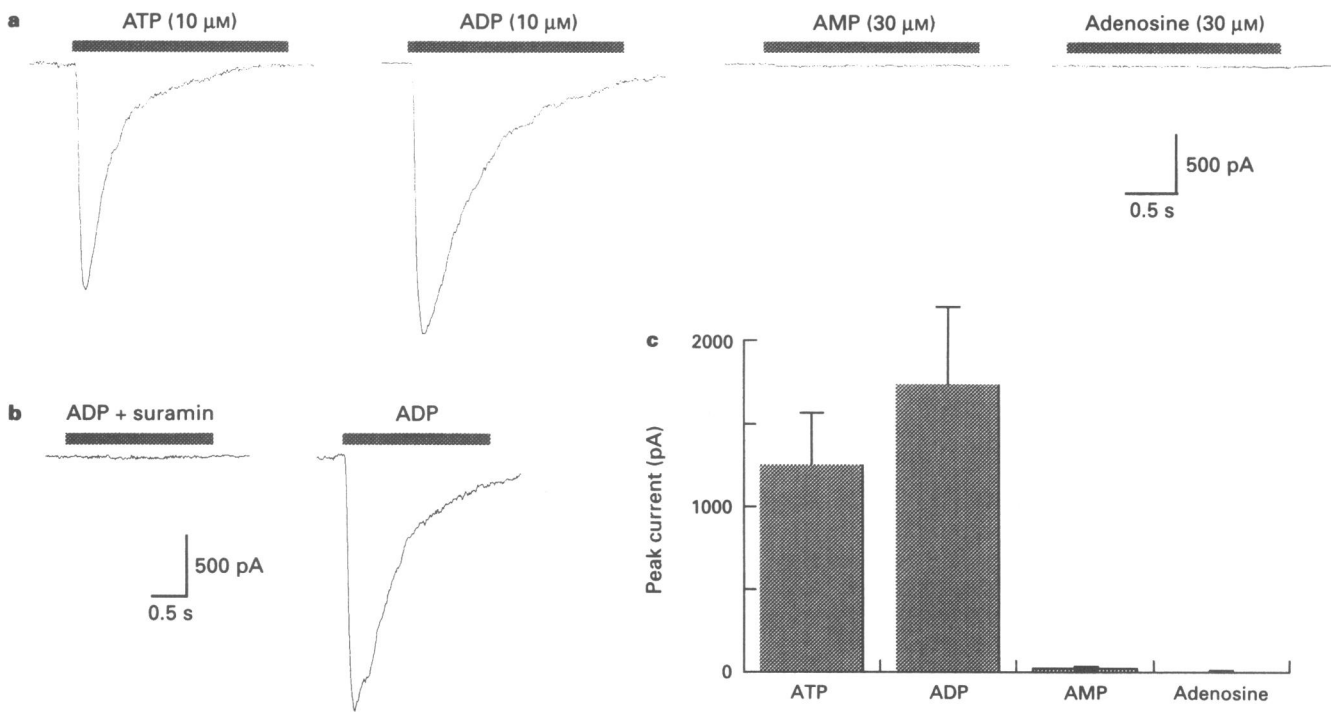

Figure 5 Actions of ADP, AMP and adenosine on single vas deferens smooth muscle cells. (a) Current recordings from different cells showing that ADP and ATP but not AMP and adenosine evoked inward currents. (b) Application of ADP (10 μM) in the presence of suramin (100 μM) evoked no inward current while subsequent application of ADP after suramine washout evoked a large inward current in the same cell (one of two such observations shown). (c) Summary of all experiments shown in (a) where values are mean ± s.e.mean of 4–5 cells.

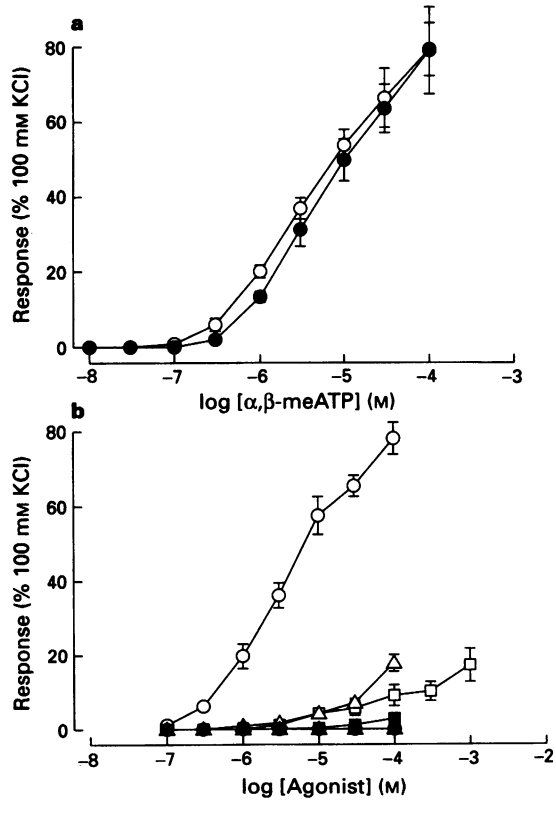

Figure 6 Contractile action of ATP and its structural analogues in rat isolated vas deferens. (a) Time-dependent controls, showing the first (○) and second control concentration-effect curves (●) to α,β-meATP determined with a 1 h washout between curves. Note curves to α,β-meATP were reproducible over the course of experimentation. (b) Second concentration-effect curves to ATP (□), 2-MeSATP (△), α,β-meATP (○), ADP (■), AMP (▲) and adenosine (●). Data shown are mean ± s.e.mean from at least four rats.

nedy, 1985). The structural analogue of ATP, α,β-meATP has been considered a potent and selective agonist at P_{2X}-purinoceptors and 2-MeSATP a potent agonist at P_{2Y}-purinoceptors (Burnstock & Kennedy, 1985). Much of the data supporting the original classification of the P_{2X}-purinoceptors derived from studies carried out in whole isolated preparations. The possible contribution of differential agonist breakdown to the rank orders of agonist potencies identified has been considered by a number of investigators. Nevertheless the caveat seems to have been largely disregarded and data with these agonists has been widely used in the characterization of P_2-purinoceptors using functional studies in a variety of tissues (Burnstock, 1990; Kennedy, 1990; Abbrachio & Burnstock, 1994; Abbrachio *et al.*, 1993; Fredholm *et al.*, 1994).

We have previously suggested that the low potency of ATP and 2-MeSATP in rat and guinea-pig vas deferens could be due to agonist breakdown or removal thus underestimating their true potency at P_{2X}-purinoceptors (Khakh *et al.*, 1994). We have now compared the agonist actions of ATP and a number of its structural analogues in single smooth muscle cells of rat vas deferens studied by single cell voltage clamp with those in isolated preparations of rat vas deferens measuring contraction. We have shown that, in the single cell studies, metabolically unstable analogues are equal in potency to the more stable ones, whereas in the isolated whole tissue preparations they are at least 10 to 30 times less potent. We suggest that the current approach to the characterization of P_{2X}-purinoceptors, based on relative agonist potencies, is inappropriate (Burnstock & Kennedy, 1985; Burnstock, 1990; Kennedy, 1990; Abbrachio *et al.*, 1993; Abbrachio & Burnstock, 1994; Fredholm *et al.*, 1994), since it relies on data where the potency of the metabolically unstable agonists is underestimated. We propose that ATP and 2-MeSATP must be considered as potent agonists at smooth muscle P_{2X}-purinoceptors, the archetypal and selective P_{2X}-purinoceptor agonist, α,β-meATP, being no more potent. Furthermore there is now evidence that P_{2X}-

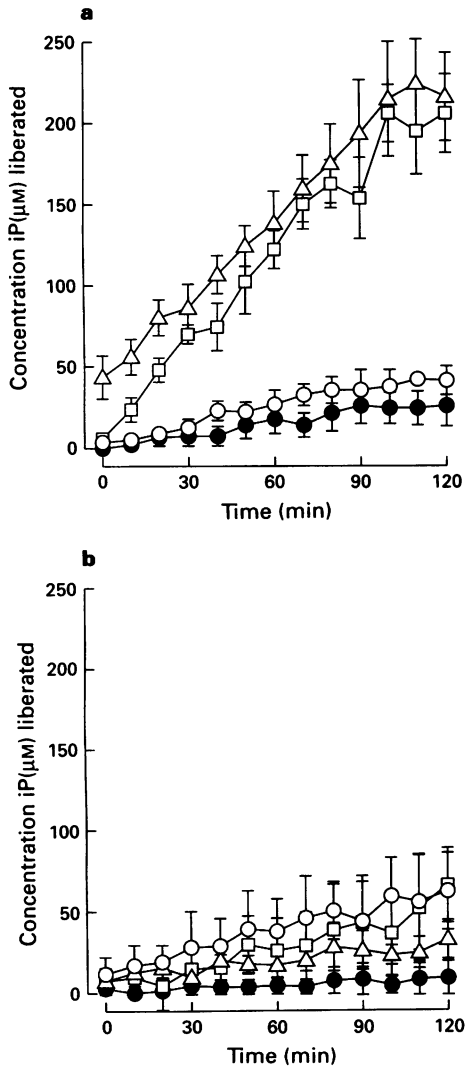

Figure 7 Inorganic phosphate production from purine nucleotides in isolated vas deferens. (a) Graph of increase in iP with time following incubation with 100 μM ATP (□), 2-MeSATP (△) and α,β-meATP (○) as compared to control (●) in bisected vas deferens. Note incubation with ATP or 2-MeSATP both resulted in significant increases in iP whereas α,β-meATP did not. (b) As in (a) but buffer contains 1 mM EDTA and no Ca^{2+} or Mg^{2+}. Note that little iP is produced following incubation with ATP, 2-MeSATP or α,β-meATP under these conditions. Data shown are mean ± s.e.mean from 4–8 rats.

purinoceptors in neurones are different from those in smooth muscle but similar problems concerning the use of purine nucleotide agonists in their characterization would seem to apply (see Trezise *et al.*, 1994b; 1995; Khakh *et al.*, 1995).

Single cell studies

Agonists were applied to the myocytes using the fast flow U tube method (Fenwick *et al.*, 1992). ATP, 2-MeSATP and α,β-meATP all evoked inward currents in every cell tested. The agonists evoked inward currents with rise times of less than 60 ms at 10 μM each agonist, which is consistent with a direct action at a ligand-gated ion channel (Inoue & Brading, 1990). Rapid rise times to peak effect followed by waning of the response during the continued presence of agonist were a feature of all agonists tested in this study, although α,β-meATP evoked inward currents with a slower rise time and decay constant than either ATP or 2-MeSATP. The slower rise time for the α,β-meATP-evoked current relative to ATP and 2-MeSATP is consistent with other studies on smooth muscle (Evans & Kennedy, 1994) and autonomic neurones (Khakh *et al.*, 1995). These differences in kinetics may reflect either a slower rate of association with the receptor or a lower intrinsic efficacy of α,β-meATP for P_{2X}-purinoceptors. A difference between decay constants for α,β-meATP, ATP and 2-MeSATP has also been reported in dissociated rat tail artery smooth muscle cells (Evans & Kennedy, 1994) and this may reflect differing affinities of the agonists for the open and desensitized states of the channel.

Responses mediated by neuronal P_{2X}-purinoceptors in autonomic ganglia exhibit little if any wane during agonist application for up to 20 s applications (Khakh *et al.*, 1995). This is in contrast to the profound wane seen in the present study for smooth muscle P_{2X}-purinoceptors (see Figures 1–3). In addition responses to each of the agonists were tachyphylactic when administered up to 6 min apart (Figure 1). This finding is consistent with that of Evans & Kennedy (1994) and Nakazawa & Matsuki (1987) but different from studies of Friel (1988) and Inoue & Brading (1990). However, the gene encoding for the P_{2X}-purinoceptor from rat vas deferens has recently been cloned and similar patterns of wane and tachyphylaxis were observed for the responses mediated by the recombinant P_{2X}-purinoceptors expressed and studied in oocytes and mammalian cells (Valera *et al.*, 1994). Thus, the tachyphylaxis associated with the smooth muscle P_{2X}-purinoceptors seen in our study probably results from the structure of the receptor-channel rather than the experimental procedure.

The most discordant observation of Friel (1988) was that α,β-meATP was not an agonist in smooth muscle cells, whereas we found that it was equal in potency to ATP and 2-MeSATP. However our findings are broadly consistent with published data in rat tail artery (Evans & Kennedy, 1994), bladder (Inoue & Brading, 1990) and for the recombinant P_{2X}-purinoceptor expressed in HEK cells (Valera *et al.*, 1994). In this study, full concentration-effect curves could not be obtained to agonists since at the highest concentrations tested, the rise times for the responses were approaching the rise times for adequate solution exchange, thus higher concentrations of agonist would have underestimated the peak amplitude. However, from comparison of threshold concentrations and peak amplitude responses it would appear that there was little or no difference in potencies between the three agonists.

Two pertinent questions arise from these findings. First, do all the agonists act at a common receptor on the smooth muscle cell? We consider that this is likely to be the case since all the agonists were antagonized by the P_2-purinoceptor antagonist, suramin (Dunn & Blakeley, 1988) and also the agonists cross-desensitized each other, indicative of a common site of action (unpublished observation; see also Evans & Kennedy, 1994). Secondly, is the ATP-evoked inward current responsible for smooth muscle depolarization and subsequent contraction in isolated whole tissue preparations? Although we have not investigated this in the present study we feel that this is a reasonable supposition, because in bladder muscle cells the depolarization induced by ATP resembles closely the profile of the e.j.p. measured from isolated tissues, supporting the contention that the mechanisms of the responses measured in single cells underlies that of the contraction of isolated preparations (Inoue & Brading, 1990).

Measurement of contractile activity

The finding that ATP is more potent that ADP, AMP or adenosine in contracting the bisected vas deferens preparation is consistent with previous findings (Taylor *et al.*, 1982) and suggests the involvement of a P_2-purinoceptor (Burnstock, 1978). Furthermore the high potency of α,β-meATP relative to ATP and 2-MeSATP suggests the involvement of a P_{2X}-purinoceptor (Abbrachio & Burnstock, 1994). Based on the experiments in this study on rat whole tissue vas deferens

a rank order of agonist potencies of α,β-meATP>>ATP = 2-MeSATP was found which is that expected of a P_{2X}-purinoceptor (Burnstock & Kennedy, 1985).

However, the original classification of P_{2X}-purinoceptors (Burnstock & Kennedy, 1985) does not addresss the shallow concentration-effect curve or low potency of ATP as an agonist in whole tissue preparations such as the rat vas deferens. One possible explanation for the low potency of ATP and 2-MeSATP is that in isolated tissue preparations they are metabolised rapidly thereby underestimating their true potency at P_{2X}-purinoceptors. In contrast, in single cells significant purine metabolism is unlikely to occur during rapid agonist applications, where currents are measured over milliseconds without diffusion gradients. In order to investigate this explanation further we have measured the production of iP, expected to result from the metabolism of purine nucleotides in whole tissue studies.

Measurement of inorganic phosphate

Incubation of rat isolated vas deferens in the presence of either 100 μM ATP or 2-MeSATP produced a large increase in iP over a 2 h period, which amounted to approximately 200 μM iP from 100 μM nucleotide agonist. In control preparations which received no agonist, no iP was detectable. It seems reasonable to assume that the measurement of iP production underestimates the true rate of metabolism of purine nucleotides in the vicinity of the receptor. Thus the quantity of purine nucleotide in the bathing medium is far in excess of physiological levels and the metabolising enzymes may be closely associated with the receptor in the synapse as is the case for acetylcholinesterase and the nicotinic receptor (Zimmerman *et al.*, 1994). Hence iP levels can only be used as a measure of relative stability of analogues and not as a measure of rate of metabolism in the immediate environment of the receptor. α,β-meATP, unlike ATP and 2-MeSATP, produced no increase in iP for up to 2 h, indicating that it is metabolically stable. These findings indicating that ATP and 2-MeSATP are both metabolically unstable and that α,β-meATP is in contrast stable to degradation are in good agreement with previous data (Welford *et al.*, 1986; 1987).

Complete removal of Ca^{2+} and Mg^{2+} and addition of 1 mM EDTA prevented the increase in iP from ATP and 2-MeSATP; we assume this reflects the Ca^{2+}- and Mg^{2+}-dependency of the enzyme responsible for metabolism. It has also been shown that the enyzmes responsible for the breakdown of ATP in oocytes are sensitive to complete removal of Ca^{2+} and Mg^{2+} (Ziganshin *et al.*, 1995). Further, in isolated vagus nerve evidence has been provided, using indirect methods, that metabolism of ATP is dependent on submicromolar concentrations of Ca^{2+} and Mg^{2+}, such that inhibition of metabolism can only be achieved by using 1 mM EDTA (Trezise *et al.*, 1994a,b). Thus our findings are in agreement with those of others (Ziganshin *et al.*, 1995; Trezise *et al.*, 1994a,b) which suggest that the enzyme(s) involved belongs to a family of Ca^{2+} and Mg^{2+}-dependent ectonucleotidases.

Summary

Caveats concerning the use of agonists in drug receptor classification are well known (Kenakin, 1993). In the present study we have demonstrated in rat vas deferens, one of the preparations in which the role of ATP as a co-transmitter was first established and purinoceptors first classified (see von Kügelgen & Starke, 1991; Burnstock & Kennedy, 1985), that an agonist-based classification of P_{2X}-purinoceptors is misleading because of problems associated with underestimating the potency of metabolisable analogues such as ATP and 2-MeSATP. We suggest, on the basis of our single cell studies, that ATP and 2-MeSATP must be considered as potent agonists for the P_{2X}-purinoceptors in smooth muscle, equal in potency to the archetypal agonist, α,β-meATP.

Unequivocal characterization of P_{2X}-purinoceptors in functional studies can only be achieved on the basis of affinity estimates with potent competitive antagonists. However it is reassuring to note that the agonist profile of the recombinant P_{2X}-purinoceptor from rat vas deferens (Valera *et al.*, 1994) is remarkably similar to that which we suggest as truly characteristic of P_{2X}-purinoceptors in vas deferens smooth muscle.

The authors appreciate the useful and informative discussions with Drs Richard Evans, Wasyl Fenuik, Ian Kennedy, Anton Michel, Alan North and Derek Trezise.

References

ABBRACHIO, M.P., CATTABENI, F., FREDHOLM, B.B. & WILLIAMS, M. (1993). Purinoceptor nomeclature: a status report. *Drug Dev. Res.*, **28**, 207–213.

ABBRACHIO, M.P. & BURNSTOCK, G. (1994). Purinoceptors: are there families of P2X and P2Y purinoceptors? *Pharmacol. Ther.*, **64**, 445–475.

AMOBI, N. & SMITH, H.S. (1987a). Effects of α,β-methylene ATP on biphasic responses of rat vas deferens. *Eur. J. Pharmacol.*, **133**, 75–82.

AMOBI, N. & SMITH, H.S. (1987b). Adrenergic and 'non-adrenergic' contributions to the two-component tetanus in the rat vas deferens. *Eur. J. Pharmacol.*, **135**, 173–182.

BARNARD, E.A., BURNSTOCK, G. & WEBB, T.E. (1994). G protein coupled receptors for ATP and other nucleotides: a new receptor family. *Trends Pharmacol. Sci.*, **15**, 67–71.

BURNSTOCK, G. (1978). A basis for distinguishing two types of purinergic receptors. In *Cell Membrane Receptors for Drugs and Hormones: A Multidisciplinary Approach.* ed. Staub, R.W. & Bolis, L. pp. 107–118. New York, NY: Raven Press.

BURNSTOCK, G. (1986). The changing face of autonomic neurotransmission. *Acta Physiol. Scand.*, **126**, 67–91.

BURNSTOCK, G. (1990). Purinergic mechanisms. *Ann. N.Y. Acad. Sci.*, **603**, 1–17.

BURNSTOCK, G. & KENNEDY, C. (1985). Is there a basis for distinguishing two types of P_2-purinoceptor? *Gen. Pharmacol.*, **16**, 433–440.

CLAPP, L.H. & GURNEY, A.M. (1991). Outward currents in rabbit pulmonary artery cells dissociated with a new technique. *Exp. Physiol.*, **76**, 677–693.

DUNN, P.M. & BLAKELEY, A.G.H. (1988). Suramin: a reversible P_2-purinoceptor antagonist in the mouse vas deferens. *Br. J. Pharmacol.*, **93**, 243–245.

EDWARDS, F.A., GIBB, A.J. & COLQUHOUN, D. (1992). ATP receptor mediated synaptic currents in the central nervous system. *Nature*, **359**, 144–147.

EVANS, R.J., DERKACH, V. & SURPRENANT, A. (1992). ATP mediates fast synaptic transmission in mammalian neurones. *Nature*, **357**, 503–505.

EVANS, R.J. & KENNEDY, C. (1994). Characterisation of P_2-purinoceptors in the smooth muscle of the rat tail artery: a comparison between contractile and electrophysiological responses. *Br. J. Pharmacol.*, **113**, 853–860.

FENWICK, E.M., MARTY, A. & NEHER, E. (1982). A patch clamp study of bovine chromaffin cells and their sensitivity to acetylcholine. *J. Physiol.*, **331**, 557–597.

FREDHOLM, B.B., ABBRACHIO, M.P., BURNSTOCK, G., DALY, J.W., HARDEN, T.K., JACOBSON, K.A., LEFF, P. & WILLIAMS, M. (1994). Nomenclature and classification of purinoceptors. *Pharmacol. Rev.*, **46**, 143–155.

FRENCH, A.M. & SCOTT, N.C. (1983). Evidence to support the hypothesis that ATP is a co-transmitter in the rat vas deferens. *Experientia*, **39**, 264–266.

FRIEL, D.D. (1988). An ATP-sensitive conductance in single smooth muscle cells from the rat vas deferens. *J. Physiol.*, **401**, 361–380.

GORDON, J.L. (1986). Extracellular ATP: effects, sources and fate. *Biochem. J.*, **233**, 309–319.

HESS, H.H. & DERR, J.E. (1975). Assay of inorganic and organic phosphorus in the 0.1–5 nanomole range. *Analyt. Biochem.*, **63**, 607–613.

INOUE, R. & BRADING, A.F. (1990). The properties of the ATP-induced depolarization and current in single cells isolated from the guinea-pig urinary bladder. *Br. J. Pharmacol.*, **100**, 619–625.

KENAKIN, T. (1993). *Pharmacological Analysis of Drug-Receptor Interaction*. ed. Kenakin, T. New York, N.Y.: Raven Press.

KENNEDY, C. (1990). P_1- and P_2-purinoceptor subtypes – an update. *Arch. Int. Pharmacodyn. Ther.*, **303**, 30–50.

KHAKH, B.S., HUMPHREY, P.P.A. & SURPRENANT, A. (1995). Electrophysiological properties of P_{2X} purinoceptors in rat superior cervical, nodose and guinea pig coeliac neurones. *J. Physiol.*, (in press).

KHAKH, B.S., KENNEDY, I. & HUMPHREY, P.P.A. (1994). Relative agonist potencies at P_2 purinoceptors in rat and guinea-pig vas deferens. *Br. J. Pharmacol.*, **122**, 406P.

VON KÜGELGEN, I.V. & STARKE, K. (1991). Noradrenaline-ATP co-transmission in the sympathetic nervous system. *Trends Pharmacol. Sci.*, **12**, 319–324.

LANZETTA, P.A., ALVAREZ, L.J., REINACH, P.S. & CANDIA, O.A. (1979). An improved assay for nanomole amounts of inorganic phosphate. *Analyt. Biochem.*, **100**, 95–97.

NAKAZAWA, K. & MATSUKI, N. (1987). Adenosine triphosphate-activated inward current in isolated smooth muscle cells from rat vas deferens. *Pflügers Arch.*, **409**, 644–666.

SNEDDON, P. & BURNSTOCK, G. (1984). Inhibition of excitatory junction potentials in guinea pig vas deferens by α,β-methylene ATP: further evidence for ATP and noradrenaline as cotransmitters. *Eur. J. Pharmacol.*, **100**, 85–90.

SNEDDON, P. & MACHALY, M.. (1992). Regional variation in purinergic and adrenergic responses in isolated vas deferens of rat, rabbit and guinea pig. *J. Auton. Pharmacol.*, **12**, 421–428.

SNEDDON, P. & WESTPHALL, D.P. (1984). Pharmacological evidence that adenosine triphosphate and noradrenaline are cotransmitters in the guinea pig vas deferens. *J. Physiol.*, **347**, 561–580.

STJARNE, L. & ASTRAND, P. (1984). Discrete events measure single quanta of ATP secreted from sympathetic nerves of guinea-pig and mouse vas deferens. *Neuroscience*, **13**, 21–28.

TAYLOR, D.A., WEISE, S., FAIZON, E.P. & YARBOROUGH, G.G. (1982). Pharmacological characterisation of purinergic receptors in the rat vas deferens. *J. Pharmacol. Exp. Ther.*, **224**, 40–45.

TREZISE, D.J., BELL, N.J. & HUMPHREY, P.P.A. (1994a). Inhibitory effects of micromolar concentrations of divalent cations on depolarisation responses to ATP of the rat isolated vagus nerve. *Br. J. Pharmacol.*, **113**, 57P.

TREZISE, D.J., BELL, N.J., KENNEDY, I. & HUMPHREY, P.P.A. (1994b). Effects of divalent cations on the potency of ATP and related agonists in the rat isolated vagus nerve: implications for P_2 purinoceptor classification. *Br. J. Pharmacol.*, **113**, 463–470.

TREZISE, D.J., MICHEL, A.D., GRAHAMES, C.B.A., KHAKH, B.S., SURPRENANT, A.-M. & HUMPHREY, P.P.A. (1995). The selective P_{2X} purinoceptor agonist β,γ-methylene-L-adenosine 5'-triphosphate discriminates between smooth muscle and neuronal P_{2X} purinoceptors. *Naunyn-Schmied. Arch. Pharmacol.*, (in press).

VALERA, S., HUSSY, N., EVANS, R.J., ADAMI, N., NORTH, A., SURPRENANT, A. & BUELL, G. (1994). Cloning and expression of the P_{2X} receptor for extracellular ATP reveals a new class of ligand gated ion channel. *Nature*, **371**, 516–519.

WEBB, T.E., SIMON, J., KRISHEK, B.J., BATESON, A.N., SMART, T.G., KING, B.F., BURNSTOCK, G. & BARNARD, E.A. (1993). Cloning and functional expression of a brain G-protein-coupled receptor. *FEBS Lett.*, **324**, 219–225.

WELFORD, L.A., CUSACK, N.J. & HOURANI, S.M.O. (1986). ATP analogues and the guinea-pig taenia coli: a comparison of the structure-activity relationships of ectonucleotidases with those of the P_2-purinoceptor. *Eur. J. Pharmacol.*, **129**, 217–224.

WELFORD, L.A., CUSACK, N.J. & HOURANI, S.M.O. (1987). The structure-activity relationships of ectonucleotidases and of excitatory P_2-purinoceptors: evidence that desphosphorylation of ATP analogues reduced pharmacological potency. *Eur. J. Pharmacol.*, **141**, 123–130.

ZIGANSHIN, A.U., ZIGANSHINA, L.E., KING, B.F. & BURNSTOCK, G. (1994). Characteristics of ecto-ATPase of Xenopus oocytes and the inhibitory actions of suramin on ATP breakdown. *Pflügers Arch. Eur. J. Physiol.*, **429**, 412–418.

ZIMMERMAN, H. (1994). Signalling via ATP in the nervous system. *Trends Neurosci.*, **17**, 420–426.

(Received November 3, 1994
Revised January 5, 1995
Accepted January 24, 1995)

British Journal of Pharmacology (1995) 115, 186–190

Inhibition by zinc protoporphyrin-IX of receptor-mediated relaxation of the rat aorta in a manner distinct from inhibition of haem oxygenase

Lars Ny, Karl-Erik Andersson & [1]Lars Grundemar

Department of Clinical Pharmacology, Lund University Hospital, S-221 85 Lund, Sweden

1 Carbon monoxide (CO), produced by haem oxygenase through degradation of haem, has been claimed to be a neuromessenger and a possible regulator of vascular tone. We examined whether the haem oxygenase inhibitor, zinc protoporphyrin-IX (ZnPP) and other porphyrins affect the relaxation evoked by various agents in the rat isolated aorta.

2 Pretreatment with ZnPP (0.1 mM) virtually abolished the relaxation evoked by vasoactive intestinal peptide (VIP) and atrial natriuretic peptide (ANP). ZnPP also evoked a rightward shift of the concentration-response curve for the relaxation induced by acetylcholine.

3 In contrast, ZnPP did not affect the relaxation evoked by forskolin and 3-morpholino-sydnonimine, agents which directly activate adenylate and guanylate cyclase, respectively.

4 Although, less effective than ZnPP, tin protoporphyrin-IX (SnPP; 0.1 mM) and protoporphyrin-IX (PP; 0.1 mM) also attenuated the VIP-evoked relaxation.

5 The elevation of cyclic AMP and cyclic GMP levels evoked by VIP and ANP, respectively, were abolished by pretreatment with ZnPP (0.1 mM).

6 ZnPP, SnPP and PP did not affect the contraction evoked by phenylephrine.

7 The results show that ZnPP inhibits relaxation induced by VIP, ANP and acetylcholine, probably by interfering with membrane receptor-coupled signal transduction pathways. This inhibition does not seem to be dependent upon inhibition of haem oxygenase. The lack of specificity of the haem oxygenase inhibiting metalloporphyrins makes them less suitable as pharmacological tools in the investigation of a messenger role for CO.

Keywords: Metalloporphyrins; carbon monoxide; blood vessel; relaxation; cyclic nucleotides; second messenger; vasoactive intestinal peptide; atrial natriuretic peptide; acetylcholine

Introduction

Substantial evidence has indicated that nitric oxide (NO) is an endogenous mediator of various physiological processes in the brain and periphery (e.g. Moncada *et al.*, 1991). It was recently suggested that another gas, carbon monoxide (CO), which is produced by microsomal haem oxygenase, also may be a neuronal messenger in the brain (Maines *et al.*, 1993; Verma *et al.*, 1993). Both NO and CO are known to increase guanosine 3′:5′-cyclic monophosphate (cyclic GMP) levels in various tissues (Brüne & Ullrich, 1987; Furchgott & Jothianandan, 1991). Haem oxygenase is the rate limiting step in the degradation of haem-containing compounds, resulting in the formation of CO and biliverdin (e.g. Maines *et al.*, 1993). Haem oxygenase exists in two isoforms haem oxygenase-1 and haem oxygenase-2 (Maines *et al.*, 1993). High levels of haem oxygenase or haem oxygenase-2 mRNA have been found in the rat liver, spleen and brain (Vreman & Stevenson, 1988; Verma *et al.*, 1993).

It has been speculated that CO, which shares many properties with NO, may be a regulator of vascular tone (Marks *et al.*, 1991; Schmidt, 1992). The evidence for such a view is, however, circumstantial. Like NO, exogenously applied CO has been shown to relax various isolated blood vessels and to increase cyclic GMP levels (Furchgott & Jothianandan, 1991; Moncada *et al.*, 1991; Lefer *et al.*, 1993; Zygmunt *et al.*, 1994). We have recently demonstrated haem oxygenase activity in various blood vessel homogenates, including rat aorta, by measurement of CO production using a gas chromatographic method (Grundemar *et al.*, 1995). Certain metalloporphyrins, like zinc protoporphyrin-IX (ZnPP) and tin protoporphyrin-IX (SnPP), are haem oxygenase inhibitors, of which primarily ZnPP has been used in studies suggesting a messenger role for CO in the brain and periphery (e.g. Verma *et al.*, 1993; Rattan & Chakder, 1993).

However, little is known about the specificity of these metalloporphyrins. The aim of the study was to examine whether ZnPP and other porphyrins affect relaxation evoked by agents with different modes of action in the rat isolated aorta.

Methods

Mechanical activity

Female Sprague-Dawley rats (250–300 g) were killed by CO_2 asphyxia and the thoracic aorta was dissected out. The aorta was placed in an ice-cold Krebs solution and cut into 2 mm long ring segments. The preparations were transferred to thermostatically controlled (37°C) 5 ml tissue baths containing Krebs solution bubbled with 5% CO_2 and 95% O_2, resulting in a pH of 7.4, and mounted between two L-formed hooks, one of which was attached to a force transducer (Grass FT03) for measurement of mechanical activity, and the other was connected to a sledge, which allowed adjustment of the passive tension of the vessel. The recordings were made on a Grass polygraph, 7D or 7E. The vessels were repeatedly stretched for 1 h until a stable resting tension of 8 mN was obtained. The contractile capacity was examined by adding an isotonic 60 mM potassium Krebs solution (for composition see below). In order to construct concentration-

[1] Author for correspondence.

response curves, drugs were added in a cumulative manner. Relaxation was studied in preparations precontracted by phenylephrine (0.1–3 μM), corresponding to 50-70% of the contraction obtained by potassium Krebs solution. The potassium-induced contraction amounted to 10.6 ± 0.2 mN ($n = 86$).

Measurement of cyclic GMP and adenosine 3':5'-cyclic monophosphate (cyclic AMP) concentrations

Cyclic nucleotide levels were analyzed in aortic segments after recording of mechanical activity. The preparations were separated into two groups, either incubated with ZnPP 0.1 mM or with vehicle only (control). The content of cyclic nucleotides in the aortic segments was measured (1) at the tension level obtained after phenylephrine-contraction, (2) after exposure to VIP 1 μM, and (3) after exposure to ANP 30 nM. When the vessels had reached a stable tension level, they were rapidly removed from the tissue bath and frozen in liquid nitrogen. The tissue was homogenized in 2 ml 10% trichloroacetic acid (TCA), with a glass-glass homogenizer, and centrifuged at 1500 *g* (4°C) for 10 min. The protein content in the pellets was determined by the method described by Bradford (1976), with bovine serum albumin used as standard. The supernatants were extracted 5 times with 5 ml of water-saturated diethyl ether. The aqueous phase was evaporated and the residue stored at −20°C. Residues were dissolved in 0.05 M sodium acetate, and the amounts of cyclic GMP and cyclic AMP were quantitated by using [^{125}I]-cyclic GMP and [^{125}I]-cyclic AMP RIA kits (RIANEN, Du Pont Company, Boston, MA, U.S.A.). [^{3}H]-cyclic AMP was added to the TCA tissue homogenate in order to determine the recovery of cyclic GMP and cyclic AMP during the ether extraction. The mean recovery was 80%.

Solutions

The normal Krebs solution used had the following composition (in mM): NaCl 119, KCl 4.6, $NaHCO_3$ 15, $CaCl_2$ 1.5, $MgCl_2$ 1.2, NaH_2PO_4 1.2 and glucose 11. High K^+-Krebs solution contained: KCl 60, NaCl 60, $NaHCO_3$ 15, $CaCl_2$ 1.5, $MgCl_2$ 1.2, NaH_2PO_4 1.2 and glucose 11.

Drugs

The chemicals were obtained from the following sources: acetylcholine (Aldrich, Steinheim, Germany), forskolin, protoporphyrin-IX, vasoactive intestinal peptide (VIP; Sigma Chemical Company, St Louis, MO, U.S.A.), atrial natriuretic peptide (ANP; rat; Peninsula Laboratories Inc, Belmont, CA, U.S.A.), 3-morpholino-sydnonimine, (SIN-1; Casella AG, Germany), ZnPP and SnPP (Porphyrin Products Inc, Logan, UT, U.S.A.). ZnPP and SnPP were dissolved in 0.2 M NaOH and PP in alcohol and 0.2 M HCl. All other drugs were dissolved in and diluted with saline. The preincubation time with ZnPP, SnPP and PP was 60 min. All experiments were performed in darkness by covering the tissue bath with a black plastic film.

Calculations and statistics

Results are expressed as mean ± s.e. mean. When the statistical difference between two means was determined, Student's unpaired two-tailed *t* test was used. $P < 0.05$ was regarded as significant. Outliers were checked for by Dixon's gap test. (*n*) refers to the number of vessels examined, each from a different animal. pIC_{50}, the negative logarithm of the concentration that evokes a 50% relaxation of the precontracted vessel, was determined by regression analysis using the values immediately above and below half maximum response.

Results

Effects of porphyrins on vascular tone

Pretreatment with ZnPP (0.1 mM) did not affect the basal tone of the rat isolated aorta. However, in phenylephrine-contracted vessels ZnPP (0.1 mM) virtually abolished the relaxation evoked by VIP and ANP (Table 1, Figure 1 a and b). In addition, ZnPP evoked a rightward shift of the concentration-response curve for the relaxation induced by acetylcholine (Table 1). In contrast, ZnPP did not affect the relaxation evoked by forskolin and SIN-1, agents which directly activate adenylate and guanylate cyclase, respectively (Table 1, Figure 2 a and b). Although, less effective than ZnPP, SnPP and PP (each 0.1 mM) also attenuated the VIP-evoked relaxation (Table 1). ZnPP, SnPP and PP had no effect on the initial contraction evoked by phenylephrine. This contraction amounted to 56 ± 2%, 54 ± 6%, 52 ± 3% and 58 ± 2% of the K^+-response in vessels treated with ZnPP, SnPP, PP, and in untreated vessels, respectively. The corresponding phenylephrine concentrations were 0.7 ± 0.2 μM, 0.7 ± 0.5 μM, 0.5 ± 0.1 μM and 0.6 ± 1.0 μM in ZnPP, SnPP, PP, and untreated vessels, respectively.

Effects of zinc protoporphyrin on cyclic AMP and cyclic GMP levels

The effects of ZnPP on cyclic nucleotide levels are shown in Figures 3 and 4. VIP, but not ANP increased the cyclic AMP level in the rat isolated aorta. Pretreatment with ZnPP (0.1 mM) abolished the VIP-evoked increase of cyclic AMP. ZnPP *per se* did not affect the basal cyclic AMP level. ANP, but not VIP increased the cyclic GMP level in the aorta. Pretreatment with ZnPP abolished the ANP-evoked increase of cyclic GMP. ZnPP *per se* did not appear to affect the basal cyclic GMP level.

Discussion

The original suggestion that endogenous CO may be a neuronal messenger was based upon the observation that haem oxygenase-2 or its mRNA was detected in certain neuronal structures in the brain and that it was associated with guanylate cyclase mRNA (e.g. Maines *et al.*, 1993;

Table 1 Inhibitory effects of porphyrins on relaxation evoked by various vasodilator agents in the rat isolated aorta

	pIC_{50} (M)	P	n
VIP	6.90 ± 0.31		
VIP + ZnPP (0.1 mM)	–	NA	6
VIP	*7.64 ± 0.22		
VIP + SnPP (0.1 mM)	*6.62 ± 0.23	<0.01	6
VIP	6.37 ± 0.16		
VIP + PP (0.1 mM)	7.10 ± 0.23	<0.05	6
ANP	8.95 ± 0.08		
ANP + ZnPP (0.1 mM)	–	NA	6
Acetylcholine	7.79 ± 0.20		
Acetylcholine + ZnPP (0.1 mM)	6.98 ± 0.21	<0.05	6
Forskolin	7.07 ± 0.11		
Forskolin + ZnPP (0.1 mM)	6.89 ± 0.12	NS	6
SIN-1	6.62 ± 0.13		
SIN-1 + ZnPP (0.1 mM)	6.61 ± 0.15	NS	7

For abbreviations, see text
*pIC_{25} value since no pIC_{50} value could be determined after SnPP pretreatment. NS not statistically significant. NA, not applicable. –, the maximum relaxation was less than 25%.

Verma *et al.*, 1993). A series of metalloporphyrins, such as ZnPP and SnPP have been used clinically for inhibition of haem oxygenase activity in efforts to prevent jaundice (Maines, 1988). ZnPP has also been used as a pharmacological tool in order to establish a messenger role for CO both in the central and peripheral nervous systems. ZnPP has for instance been shown to inhibit long-term potentiation in the rat hippocampus (Zhuo *et al.*, 1993; Stevens & Wang, 1993), to lower cyclic GMP activity in olfactory neurones (Verma *et al.*, 1993), to block glutamate-evoked effects in the rat nucleus tractus solitarii (Glaum & Miller, 1993), and to reduce depolarization-induced glutamate release in cortical synaptoneurosomes (Shinomura *et al.*, 1994). In the periphery, ZnPP has been shown to inhibit neurally mediated relaxation of the opossum anal sphincter (Rattan & Chakder, 1993), and potassium currents in human jejunal smooth muscle cells (Farrugia *et al.*, 1993). These results have been interpreted to mean that endogenous CO may be a messenger in the brain and gut.

However, concern has been raised about the specificity of metalloporphyrins (Morris & Collinridge, 1993). Some metalloporphyrins are light-sensitive and in the presence of light they are inactive on haem oxygenase (Greenbaum & Kappas, 1991). It has, however, been suggested that ZnPP is less light-sensitive than other metalloporphyrins (Vreman *et al.*, 1990). Nonetheless, we have recently shown that ZnPP (at a concentration 10 times lower than that used in the present study), when exposed to ordinary laboratory light conditions, but not in darkness, abolished acetylcholine-induced vasodilatation in a manner probably distinct from inhibition of haem oxygenase (Zygmunt *et al.*, 1994). In order to avoid unspecific effects of light-exposed ZnPP, the experiments in the present study were carried out in darkness.

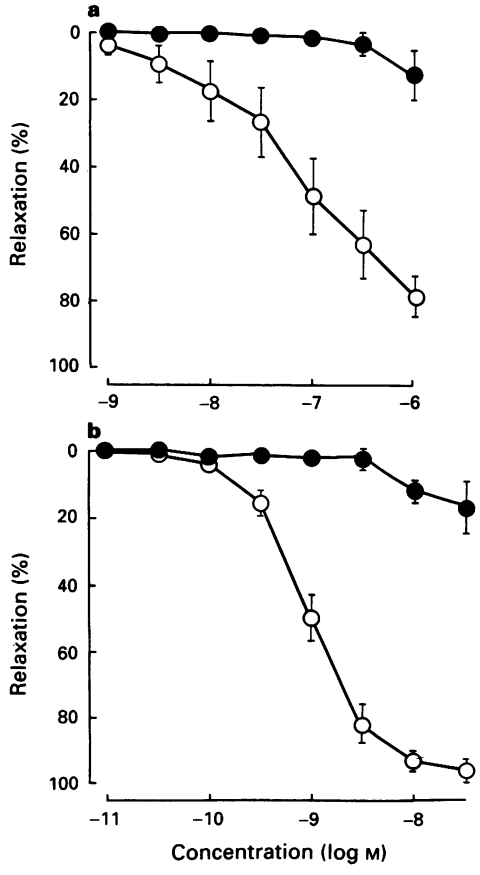

Figure 1 Effect of increasing concentrations of vasoactive intestinal peptide (VIP) (a) or atrial natriuretic peptide (ANP) (b) without pretreatment (○) and pretreated with ZnPP (0.1 mM) (●) on the rat isolated aorta precontracted with phenylephrine.

Recently, haem oxygenase activity in homogenates from the rat aorta has been demonstrated (Grundemar *et al.*, 1995). The results from the present study have shown that ZnPP virtually abolished VIP- and ANP-evoked relaxation in the rat isolated aorta. Also the acetylcholine-induced relaxation was attenuated by ZnPP. These compounds relax vessels

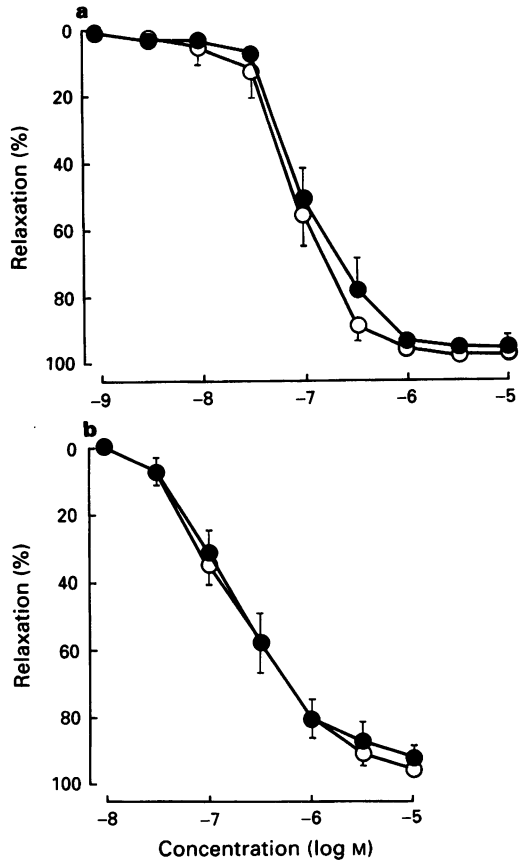

Figure 2 Effect of increasing concentrations of forskolin (a) or morpholino sydnonimine (SIN-1) (b) without pretreatment (○) and pretreated with ZnPP (0.1 mM) (●) on the rat isolated aorta precontracted with phenylephrine.

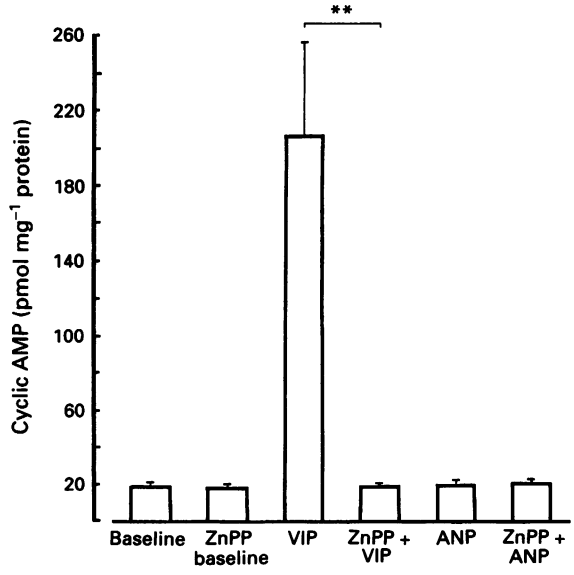

Figure 3 Concentrations of cyclic AMP (pmol mg^{-1} protein) in aortic segments after exposure to vasoactive intestinal peptide (VIP, 1 μM) or atrial natriuretic peptide (ANP, 30 nM), with or without pretreatment with ZnPP 0.1 mM. $^{**}P<0.01$, $n=6$.

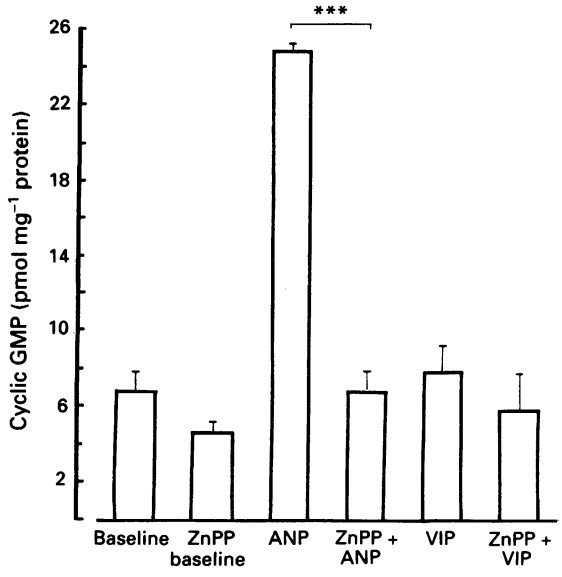

Figure 4 Concentrations of cyclic GMP (pmol mg^{-1} protein) in aortic segments after exposure to vasoactive intestinal peptide (VIP, 1 μM) or atrial natriuretic peptide (ANP, 30 nM), with or without pretreatment of ZnPP 0.1 mM. ***$P<0.001$, $n=6$.

via activation of different intracellular pathways. The VIP-induced relaxation in rat aorta is associated with activation of adenylate cyclase (Schoeffter & Stocklet, 1985), and ANP activates particulate guanylate cyclase in vascular smooth muscle cells (e.g. Winquist & Hintze, 1990). Acetylcholine releases NO from the endothelium. NO, in turn, activates soluble guanylate cyclase (Caulfield, 1993). Furthermore, we found that the VIP- and ANP-induced elevations of cyclic AMP and cyclic GMP levels, respectively, were inhibited by ZnPP. By contrast, the relaxation evoked by the stimulator of adenylate cyclase, forskolin, or the NO donator, SIN-1, was unaffected by ZnPP.

Thus, ZnPP was shown to inhibit relaxation and increases in cyclic AMP and cyclic GMP levels evoked by mediators, which act through activation of membrane-associated receptors, but not relaxation evoked by agents, which directly stimulate adenylate cyclase or guanylate cyclase. The effect was not specific for ZnPP, since SnPP and PP (the latter does not inhibit haem oxygenase) also attenuated the VIP-induced relaxation. Moreover, the phenylephrine-evoked contraction was unaffected by ZnPP, and the other porphyrins, suggesting that ZnPP did not affect the contractile capacity of the blood vessels. It seems that ZnPP interfered with relaxant but not contractile signal transduction pathways within the plasma membrane.

The concentration of ZnPP used in the present series of experiments (0.1 mM) was within the concentration-range used in studies suggesting a messenger role for CO (10 μM–2 mM ; Farrugia *et al.*, 1993; Rattan & Chakder, 1993; Verma *et al.*, 1993; Zhuo *et al.*, 1993). ZnPP and other synthetic metalloporphyrins have been shown to inhibit soluble guanylate cyclase in tissue homogenates (Ignarro *et al.*, 1984). Since ZnPP was unable to inhibit the relaxant effect of SIN-1, which activates soluble guanylate cyclase it is possible that ZnPP has a poor ability to reach this cytosol-located enzyme in the intact tissue. As there is no obvious common denominator between the receptors of VIP and ANP and the respective target protein (adenylate cyclase and particulate guanylate cyclase, respectively) and the mechanism by which acetylcholine releases NO from the endothelium, the effect of ZnPP seems to be unspecific.

Taken together, the present results suggest that ZnPP inhibits relaxation induced by VIP, ANP and acetylcholine, at least partly by interfering with receptor-coupled dilator signal transduction pathways in the plasma membrane. These effects of ZnPP seem to be distinct from inhibition of microsomal haem oxygenase. It appears that the lack of specificity of the haem oxygenase inhibiting metalloporphyrins makes them unsuitable as pharmacological tools in the investigation of a messenger role for CO.

This study was supported by the Swedish Medical Research Council (grant no 6837), the Medical Faculty, University of Lund, the Crafoord Foundation, the Royal Physiographic Society, Lund, and the Swedish Society for Medical Research, Sweden.

References

BRADFORD, M.M. (1976). A rapid and sensitive method for the quantitation of microgram quantities of protein utilizing the principle of protein-dye binding. *Analyt. Biochem.*, **72**, 248–254.

BRÜNE, B. & ULLRICH, V. (1987). Inhibition of platelet aggregation by carbon monoxide is mediated by activation of guanylate cyclase. *J. Pharmacol. Exp. Ther.*, **32**, 497–504.

CAULFIELD, M.P. (1993). Muscarinic receptor characterization, coupling and function. *Pharmacol. Ther.*, **58**, 319–379.

FARRUGIA, G., IRONS, W.A., RAE, J.L., SARR, M.G. & SZURSZEWSKI, J.H. (1993). Activation of whole cell currents in isolated human jejunal circular smooth muscle cells by carbon monoxide. *Am. J. Physiol.*, **264**, G1184–G1189.

FURCHGOTT, R.F. & JOTHIANANDAN, S. (1991). Endothelium-dependent and -independent vasodilation involving cyclic GMP: relaxation induced by nitric oxide, carbon monoxide and light. *Blood Vessels*, **28**, 52–61.

GLAUM, S.R. & MILLER, R.J. (1993). Zinc protoporphyrin-IX blocks the effects of metabolotropic glutamate receptor activation in the rat nucleus tractus solitarii. *Mol. Pharmacol.*, **43**, 965–969.

GREENBAUM, N.L. & KAPPAS, A. (1991). Comparative photoactivity of tin and zinc porphyrin inhibitors of heme oxygenase: pronounced photolability of the zinc compounds. *Photochem. Photobiol.*, **54**, 183–192.

GRUNDEMAR, L., JOHANSSON, M.-B., EKELUND, M. & HÖGESTÄTT, E.D. (1995). Heme oxygenase activity in blood vessel homogenates as measured by carbon monoxide production. *Acta Physiol. Scand.*, **153**, 203–204.

IGNARRO, L.J., BALLOT, B. & WOOD, K.S. (1984). Regulation of soluble guanylate cyclase activity by porphyrins and metalloporphyrins. *J. Biol. Chem.*, **259**, 6201–6207.

LEFER, D.J., MA, X.-I & LEFER, M. (1993). A comparison of vascular biological actions of carbon monoxide and nitric oxide. *Meth. Find. Clin. Pharmacol.*, **15**, 617–622.

MAINES, M.D. (1988). Heme oxygenase: function, multiplicity, regulatory mechanisms, and clinical applications. *FASEB J.*, **2**, 2557–2568.

MAINES, M.D., MARK, J.A. & EWING, J.F. (1993). Heme oxygenase, a likely regulator of cGMP production in the brain: Induction *in vivo* of HO-1 compensates for depression in NO synthase activity. *Mol. Cell. Neurosci.*, **4**, 398–405.

MARKS, G.S., BRIEN, J.F., NAKATSU, K. & McLAUGHLIN, B.E. (1991). Does carbon monoxide have a physiological function? *Trends Pharmacol. Sci.*, **12**, 185–188.

MONCADA, S., PALMER, M.J. & HIGGS, E.A. (1991). Nitric oxide; Physiology, pathophysiology and pharmacology. *Pharmacol. Rev.*, **43**, 109–142.

MORRIS, R. & COLLINRIDGE, G. (1993). Expanding the potential: news; (comment on: Nature, 1993, **364**, 147–149). *Nature*, **364**, 104–105.

RATTAN, S. & CHAKDER, S. (1993). Inhibitory effect of CO on internal anal sphincter: heme oxygenase inhibitor inhibits NANC relaxation. *Am. J. Physiol.*, **265**, G799–G804.

SCHMIDT, H.H.H.W. (1992). NO, CO and OH. Endogenous soluble guanylyl cyclase-activating factors. *FEBS Lett.*, **307**, 102–107.

SCHOEFFTER, P. & STOCKLET, J.-C. (1985). Effect of vasoactive intestinal polypeptide (VIP) in cyclic AMP level and relaxation in rat isolated aorta. *Eur. J. Pharmacol.*, **109**, 275–279.

SHINOMURA, T., NAKO, S.-I. & MORI, K. (1994). Reduction of depolarization-induced glutamate release by heme oxygenase inhibitor: possible role of carbon monoxide in synaptic transmission. *Neurosci. Lett.*, **166**, 131–134.

STEVENS, C.F. & WANG, Y. (1993). Reversal of long-term potentiation by inhibitors of haem oxygenase. *Nature*, **364**, 147–149.

VERMA, A., HIRSCH, D.J., GLATT, C.E., RONETT, G.V. & SNYDER, S.H. (1993). Carbon monoxide: a putative neuronal messenger. *Science*, **259**, 381–384.

VREMAN, H.J., GILLMAN, M.J., DOWNUM, K.R. & STEVENSSON, D.K. (1990). *In vitro* generation of carbon monoxide from organe molecules and synthetic metalloporphyrins mediated by light. *Dev. Pharmacol. Ther.*, **15**, 112–124.

VREMAN, H.J. & STEVENSON, D.K. (1988). Heme oxygenase activity as measured by carbon monoxide production. *Anal. Biochem.*, **168**, 31–38.

WINQUIST, R.J. & HINTZE, T.H. (1990). Mechanisms of atrial natriuretic factor-induced vasodilation. *Pharmacol. Ther.*, **48**, 417–426.

ZHUO, M., SMALL, S.A., KANDEL, E.R. & HAWKINS, R.D. (1993). Nitric oxide and carbon monoxide produce activity-dependent long-term synaptic enhancement in hippocampus. *Science*, **260**, 1946–1950.

ZYGMUNT, P.M., HÖGESTÄTT, E.D. & GRUNDEMAR, L. (1994). Light-dependent effects of zinc protoporphyrin IX on endothelium-dependent relaxation resistant to N^{ω}-nitro-L-arginine. *Acta Physiol. Scand.*, **152**, 137–143.

(Received September 5, 1994
Revised December 23, 1994
Accepted February 3, 1995)

British Journal of Pharmacology (1995) 115, 191-197

ET_A receptor-mediated constrictor responses to endothelin peptides in human blood vessels *in vitro*

[1]Janet J. Maguire & Anthony P. Davenport

Clinical Pharmacology Unit, University of Cambridge, Box 110, Addenbrooke's Hospital, Cambridge, CB2 2QQ

1 We have characterized the constrictor endothelin receptors present in human isolated blood vessels using ET_A and ET_B selective agonists and antagonists.

2 Monophasic dose-response curves were obtained for ET-1 with EC_{50} values of 6.8 nM in coronary artery, 3.9 nM in internal mammary artery, 17.4 nM in pulmonary artery, 14.5 nM in aorta and 3.2 nM in saphenous vein. In coronary artery, ET-2 was equipotent with ET-1 with an EC_{50} value of 5.7 nM. The non-selective peptide, sarafotoxin 6b, was 2-3 times less potent than ET-1 but the maximum responses to these two were comparable.

3 In each vessel ET-3 was much less active than ET-1. No response was obtained to ET-3 in aorta and pulmonary artery or in up to 50% of coronary artery, mammary artery and saphenous vein preparations. In those preparations that did respond, dose-response curves were incomplete at 300 nM. Variable contractions were also obtained with the ET_B-selective agonist, sarafotoxin 6c (S6c). Where responses were detected, although S6c was more potent than ET-1 (EC_{50} values of 0.6-1.2 nM), the maximum response produced was always less than 20% of that to ET-1.

4 The synthetic ET_B agonists, BQ3020 and [^{1,3,11,15}Ala]-ET-1, were without effect in any of the five blood vessels at concentrations up to 3 μM.

5 ET-1-induced vasoconstriction was blocked by the ET_A-selective antagonists, BQ123 and FR139317. Schild-derived pA_2 values were 7.0, 7.4 and 6.9 for BQ123 and 7.6, 7.9 and 7.3 for FR139317 in coronary artery, mammary artery and saphenous vein, respectively, consistent with antagonism of ET_A receptors. Slopes of the Schild regressions were not significantly different from one. Comparable values of pA_2 were estimated for 3 μM BQ123 in aorta (7.4 ± 0.5) and pulmonary artery (6.9) from the Gaddum-Schild equation.

6 In conclusion we have shown that in human isolated blood vessels, ET-1 is more potent than ET-3 suggesting the presence of vasoconstrictor ET_A receptors. This is supported by the lack of effect of the ET_B agonists, BQ3020 and [^{1,3,11,15}Ala]-ET-1 and the ability of the ET_A antagonists, BQ123 and FR139317 to block ET-1 responses. Some preparations did contract in response to low concentrations of the ET_B-selective sarafotoxin 6c but responses were variable and the maximum was always much less than that to ET-1 in the same preparations. Therefore although constrictor ET_B receptors were present on the smooth muscle of human blood vessels, vasoconstriction elicited by the endothelin peptides *in vitro* is via ET_A receptor activation.

Keywords: Endothelins; ET_A and ET_B receptors; vasoconstriction; human coronary artery; internal mammary artery; pulmonary artery; aorta; saphenous vein; BQ123; FR139317

Introduction

The three known endothelin (ET) peptides (Yanagisawa *et al.*, 1988; Inoue *et al.*, 1989) mediate their actions via two distinct receptor subtypes. ET-1 and ET-2 have equal affinity for the ET_A receptor with ET-3 much less potent, whereas all three are equipotent at the ET_B receptor (Arai *et al.*, 1990; Sakurai *et al.*, 1990). A high degree of sequence homology exists between the endothelins and the sarafotoxin peptides which are isolated from snake venom. Like ET-1 and ET-2, sarafotoxin 6b (S6b) does not distinguish ET_A and ET_B receptors whereas sarafotoxin 6c (S6c) is a highly selective ET_B agonist (Sokolovsky, 1994).

In animals it is now well established that whilst ET_A receptors are localized to smooth muscle cells and mediate vasoconstriction, ET_B receptors are found on both endothelial cells and on the underlying smooth muscle cells (Sakurai *et al.*, 1992). Thus ET_B receptors mediate both vasodilatation via the endothelial receptor, which causes the release of endothelium-derived relaxing factors, and vasoconstriction via the smooth muscle receptor (Gardiner *et al.*, 1992; Harrison *et al.*, 1992; Okamura *et al.*, 1992; Cristol *et al.*, 1993).

There is much interest in the precise role played by the endothelin peptides in the control of vascular tone in both physiological and pathophysiological states. In a number of cardiovascular diseases it has been observed that plasma ET concentrations are elevated from normal (see for example Tomita *et al.*, 1989; DeRay *et al.*, 1991; Cacoub *et al.*, 1993; Wei *et al.*, 1994). The implication is that endothelin antagonists may be therapeutic in some instances and evidence to support this has come from a number of animal models of vascular disease. For example, intracisternal administration of BQ123 prevents early vasospasm in a rat model of subarachnoid haemorrhage (Clozel & Watanabe, 1992) and similar results have been obtained against delayed cerebral vasospasm in the dog (Itoh *et al.*, 1993). ET_A antagonists are also effective in reducing infarct size in a dog model of coronary occlusion and reperfusion (Grover *et al.*, 1993) and in limiting tissue damage in rat models of cyclosporine nephrotoxicity (Fogo *et al.*, 1992) and chronic renal failure (Benigni *et al.*, 1993).

The relative contribution made by either ET_A or ET_B receptors to vasoconstriction appears to be dependent on both the species and vascular bed under investigation (Davenport & Maguire, 1994). Therefore, although it has been demonstrated that ET-1 powerfully constricts human

[1] Author for correspondence.

blood vessels both *in vivo* (Hughes *et al.*, 1989; Kiowski & Linder, 1992; Haynes & Webb, 1993; Sørensen *et al.*, 1994) and *in vitro* (Davenport *et al.*, 1989; Franco-Cereceda, 1989; Costello *et al.*, 1990; Dalman *et al.*, 1990; Lüscher *et al.*, 1990; Papadopoulus *et al.*, 1990; McKay *et al.*, 1991; Chester *et al.*, 1992; McNamara *et al.*, 1992; Maguire & Davenport, 1993; Maguire *et al.*, 1994b), before the pharmacological profile of a clinically useful endothelin antagonist can be established those endothelin receptor subtypes mediating contraction of human blood vessels need to be determined. As an initial step to achieve this we have carried out a systematic characterization of constrictor endothelin receptors in human coronary, internal mammary and pulmonary artery, aorta and saphenous vein. We have determined the relative potencies of ET-1 and ET-3 to give an initial classification of receptors as ET_A (ET-1 more potent) or ET_B (ET-1 and ET-3 equipotent) according to the currently accepted endothelin receptor nomenclature (Watson & Girdlestone, 1994). We have also compared ET-1 with the non-selective agonist, sarafotoxin 6b. The ET_A-selective antagonists, BQ123 (Ihara *et al.*, 1992) and FR139317 (Sogabe *et al.*, 1992) were tested for their ability to block ET-1-induced vasoconstriction and further characterization was made by use of the ET_B-selective agonists, sarafotoxin 6c, BQ3020 and [^{1,3,11,15}Ala]-ET-1 (Molenaar *et al.*, 1992) to identify constrictor ET_B receptors. A preliminary account of these data has been presented to the British Pharmacological Society (Maguire & Davenport, 1993).

Methods

Tissue preparation

Coronary arteries were obtained from the recipient hearts of 36 patients undergoing transplantation for ischaemic heart disease (16 males, 54 ± 2 years mean age ± s.d.), dilated cardiomyopathies (10 males, 3 females, 47 ± 4 years), heart-lung disease (1 male, 3 females, 34 ± 20 years), pulmonary hypertension (2 females, 31 ± 6 years) and congestive heart failure (1 male, 57 years). Sections of aorta ($n = 4$) and pulmonary artery ($n = 3$) were obtained from a small number of these patients. Arteries were dissected free of fat, transferred to oxygenated Krebs solution and used on the day of collection. Histologically normal saphenous veins and internal mammary arteries were obtained from 55 patients (43–76 years) receiving coronary artery bypass grafts.

Coronary and internal mammary arteries and saphenous vein were cut into 2 mm rings, aorta and pulmonary artery were cut into strips approximately 2 mm × 15 mm. The endothelium was gently removed (confirmed histologically) and preparations were transferred to 25 ml organ baths containing oxygenated Krebs-Henseleit solution, maintained at 37°C. Vessels were connected to isometric force transducers (Swema, Stockholm, Sweden), appropriate resting tension was applied to each preparation (50% of that required to elicit a maximum response to 50 mM KCl) and they were allowed to equilibrate for 90 min. Patency of preparations was determined by control responses to 50 mM KCl, contractile responses were recorded on a Graphtec chart recorder (Linton Instrumentation, Diss, Norfolk, UK).

Agonist responses

Cumulative dose-response curves were constructed to ET-1, ET-2, ET-3, sarafotoxin 6b (S6b), sarafotoxin 6c (S6c), BQ3020 and [^{1,3,11,15}Ala]-ET-1 (10^{-10}–10^{-6} M). One agonist only was tested per preparation and each response was allowed to reach a maximum (approximately 10–20 min) before the next was added. At the end of the dose-response curves, 50 mM KCl was added to the bathing medium to elicit the maximum possible response from each preparation. Agonists responses were subsequently determined as a percentage of this. Some preparations (particularly coronary and internal mammary arteries) exhibited spontaneous or agonist-induced rhythmic activity, which are thought to be due to Ca^{2+} fluxes (these were abolished by calcium antagonists). As this activity occasionally started part way through the dose-response curves, responses to agonists were always measured as the increase in baseline tension (upon which rhythmic activity may or may not be superimposed). From each experiment EC_{50} values (concentration of agonist producing 50% of the maximum response for that agonist) were determined from the graphs of agonist concentration ($\log_{10}$) plotted against agonist response as a percentage of that to 50 mM KCl. Individual EC_{50} values were then combined to give the geometric mean (± 95% confidence interval) for each agonist. EC_{50} values for ET-1 and S6b were compared by the Mann Whitney U test with a significance level of 0.05.

Antagonist experiments

In some experiments, cumulative dose-response curves were constructed to ET-1 in the absence (control) and presence of increasing concentrations of the cyclic pentapeptide, BQ123 (0.3–3 μM) or the linear tripeptide FR139317 (0.3–3 μM). The antagonists were added to the bathing medium 30 min prior to addition of ET-1. As before, the experiments were terminated with 50 mM KCl and ET-1 responses expressed as a percentage of this response. Values of pA_2 for each antagonist were determined by analysis of the Schild regressions (Arunlakshana & Schild, 1959). Limited amounts of aorta and pulmonary artery were available and therefore only the effect of 3 μM BQ123 was determined in these preparations. The pA_2 value was then estimated from the Gaddum-Schild equation, assuming slope of unity

$$pA_2 = \log_{10}[(\text{dose-ratio} - 1)/\text{antagonist concentration}]$$

Materials

ET-1, ET-2, ET-3, S6b, and S6c were purchased from Novabiochem (Nottingham, UK). Stock solutions (10^{-4} M) of these peptides were dissolved in 0.1% acetic acid and kept at −20°C. BQ123 (cyclo (D-Trp-D-Asp-L-Pro-D-Val-L-Leu)), BQ3020 ([^{11,15}Ala]Ac-ET-$1_{(6-21)}$) and [^{1,3,11,15}Ala]-ET-1 (Molenaar *et al.*, 1992) were synthesized by solid phase t-Boc chemistry. BQ3020 and [^{1,3,11,15}Ala]-ET-1 were dissolved in distilled water to give stock solutions of 10^{-3} M. BQ123 and FR139317 (N-[(hexahydro-1-azepinyl)carbonyl]L-Leu(1-Me) D-Trp-3(2-pyridyl)D-Ala) were dissolved in dimethylsulphoxide (DMSO). The concentration of peptides was determined by u.v. spectrophotometry. All other reagents were from Sigma Chemical Co. (Poole, Dorset, UK) or BDH (Lutterworth, Leics., UK) and were of analar grade or better. Krebs solution was of the following composition (mM): NaCl 90, KCl 5, $MgSO_4.7H_2O$ 0.5, Na_2HPO_4 1, $NaCO_3$ 45, $CaCl_2$ 2.25, glucose 10, glutamate 5, Na pyuvate 5, fumarate 5, EDTA 0.04.

Results

Endothelin and sarafotoxin peptide responses in human blood vessels

The contractile responses elicited by 50 mM KCl were greater in the artery preparations (coronary artery 2.0 ± 0.1, $n = 37$; internal mammary artery 1.4 ± 0.1, $n = 48$; pulmonary artery, 1.2 ± 0.4, $n = 7$; aorta, 1.4 ± 0.4 g tension, $n = 7$; mean ± s.e.mean) than in saphenous vein (0.71 ± 0.13 g tension, $n = 37$).

Monophasic dose-response curves (Figure 1) were obtained in response to increasing concentrations of ET-1 with EC_{50} values of 6.8 nM in coronary artery, 3.9 nM in internal mammary artery, 17.4 nM in pulmonary artery, 14.5 nM in aorta

and 3.2 nM in saphenous vein (Table 1). The maximum response to ET-1 in coronary and internal mammary arteries was approximately 60% of that to 50 mM KCl, 40% in aorta and pulmonary artery, but over 80% in saphenous vein. Saphenous vein preparations were not significantly more sensitive to ET-1 than the artery preparations, although veins and arteries from the same vascular bed have not been compared in this study. ET-2 was equipotent with ET-1 in coronary artery with an EC_{50} value of 5.7 nM ($n = 4$), with each peptide producing comparable maximum responses (Figure 2). Ninety percent of coronary arteries and saphenous vein preparations and 50% of internal mammary arteries did contract in response to high concentrations of ET-3. However, the ET-3 dose-response curves were displaced well to the right of those to ET-1 and were incomplete at 300 nM (Figures 2–4). At this concentration ET-3 was without effect in strips of aorta and pulmonary artery (Table 1).

S6b was always 2–3 times less potent than ET-1 (Table 1) but the maximum responses were the same (Figures 2–4).

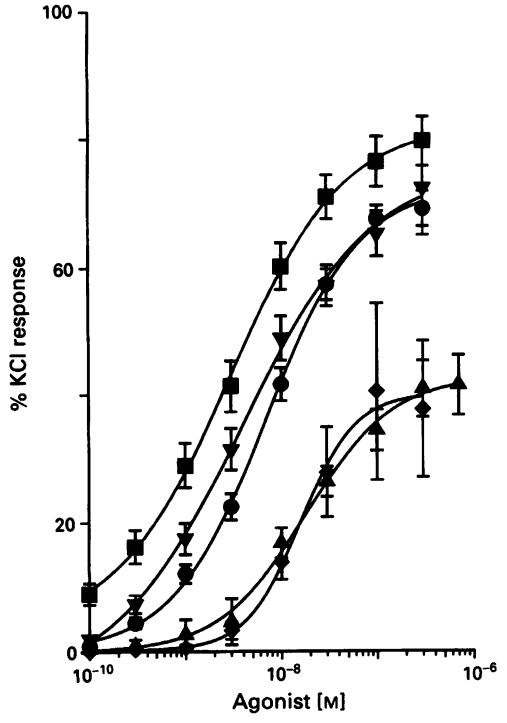

Figure 1 Cumulative dose-response curves to endothelin-1 (10^{-10}–7×10^{-7} M) in human coronary artery (●, $n = 36$), internal mammary artery (▼, $n = 41$), aorta (▲, $n = 4$), pulmonary artery (◆, $n = 3$) and saphenous vein (■, $n = 37$). Peptide responses are expressed as a percentage of the maximal contraction obtained with 50 mM KCl. Data points are the mean ± s.e.mean from n patients.

Table 1 EC_{50} values for endothelin and sarafotoxin peptides in human isolated blood vessels

	ET-1	*ET-3*	*S6b*	*S6c*	*BQ3020*
Coronary* artery	6.8† (5.3–8.8)	>100	19.5† (15–26)	1.2 (0.5–2.9)	Inactive
Aorta	14.5 (1.8–114)	Inactive	36.0	Inactive	Inactive
Pulmonary artery	17.4 (6.8–44)	Inactive	28.0 (23–35)	Inactive	ND
Mammary artery	3.9† (2.7–5.7)	>100	12.2† (5.7–26)	0.6 (0.3–1.1)	Inactive
Saphenous vein	3.2† (2.1–5.0)	>100	8.4† (5.4–13)	1.2 (0.2–9.4)	Inactive

*ET-2 in coronary artery $EC_{50} = 5.7$ nM (1.8–18.2 nM). Values are geometric mean (nM) with 95% confidence intervals in parentheses.
†EC_{50} values for ET-1 and S6b significantly different (Mann Whitney U test $P < 0.05$). For ET-3 and S6c data are from those blood vessels which responded.
ND: not determined. Inactive: no response at up to 300 nM for ET-3 and S6c and 3 μM for BQ3020. Responses for [^{1,3,11,15}Ala]-ET-1 were the same as BQ3020.

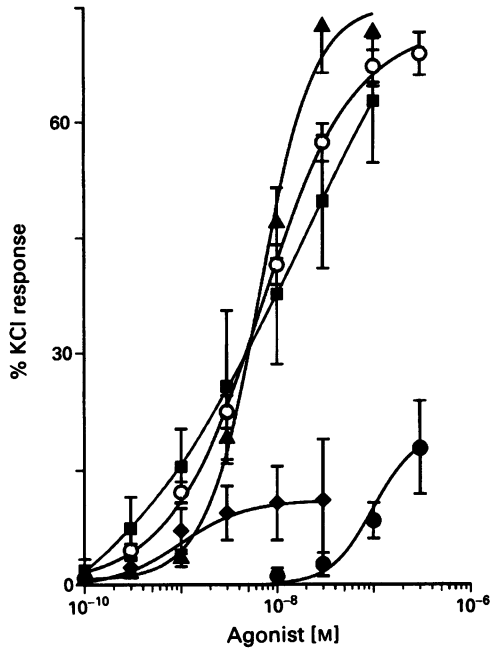

Figure 2 Cumulative dose-response curves to endothelin-1 (ET-1) (○) ($n = 36$), ET-2 (■) ($n = 4$), ET-3 (●) ($n = 10$), sarafotoxin 6b (S6b) (▲) ($n = 6$) and S6c ($n = 10$) (◆) in human isolated coronary artery. Peptide responses are expressed as a percentage of the maximal contraction obtained with 50 mM KCl. Data are the mean ± s.e.mean from n patients. All data for ET-3 and S6c (responders and non-responders) are included.

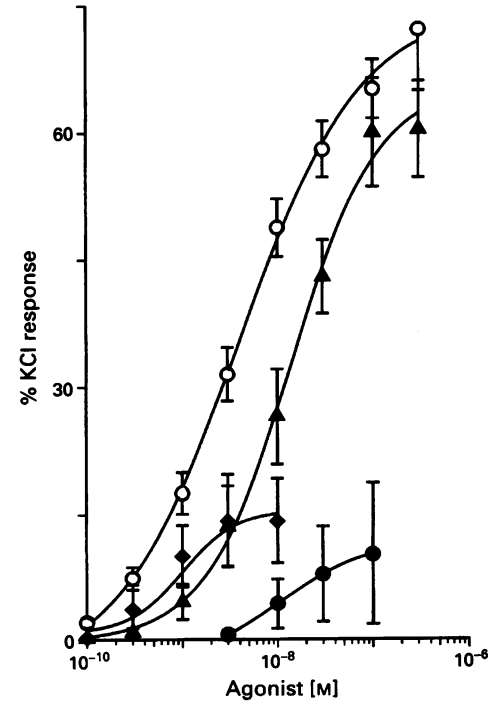

Figure 3 Cumulative dose-response curves to endothelin-1 (ET-1) (○) ($n = 41$), ET-3 (●) ($n = 6$), sarafotoxin 6b (S6b) (▲) ($n = 9$) and S6c (◆) ($n = 10$) in human internal mammary artery. Peptide responses are expressed as a percentage of the maximal contraction obtained with 50 mM KCl. Data are the mean ± s.e.mean from n patients. All data for ET-3 and S6c (responders and non-responders) are included.

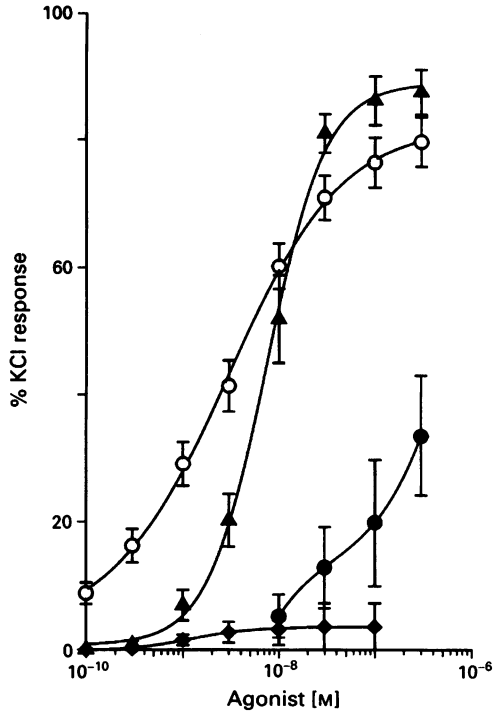

Figure 4 Cumulative dose-response curves to endothelin-1 (ET-1) (○) ($n = 37$), ET-3 (●) ($n = 7$), sarafotoxin 6b (S6b) (▲) ($n = 9$) and S6c (◆) ($n = 9$) in human saphenous vein. Peptide responses are expressed as a percentage of the maximal contraction obtained with 50 mM KCl. Data are the mean ± s.e.mean from n patients. All data for ET-3 and S6c (responders and non-responders) are included.

Interestingly in coronary artery (Figure 2) and saphenous vein (Figure 4) the dose-response curve to S6b appeared to be steeper than that to ET-1.

As with ET-3, responses to S6c were variable. Constriction occurred in 50% of preparations, and although potent (EC_{50} values 0.6–1.2 nM) the maximum responses obtained with S6c were only approximately 20% of that to ET-1 (Table 1, Figures 2–4). No responses, either agonist or antagonist, were obtained with the ET_B-selective compounds, BQ3020 and [$Ala^{1,3,11,15}$]-ET-1 (3 μM) in any of the blood vessels tested (Table 1).

Antagonist potencies

In the presence of BQ123 (0.3–3 μM) (Figure 5) and FR139317 (0.3–3 μM) (Figure 6) ET-1 dose response curves were shifted to the right in a parallel, dose-dependent manner without attenuation of the maximum response in coronary artery, internal mammary artery and saphenous vein. As previously observed (Davenport *et al.*, 1993) no portion of the ET-1 dose-response curve was resistant to antagonism by these ET_A-selective compounds. The slopes of the Schild regressions were not significantly different from one, suggesting these antagonists act in a competitive way. pA_2 values for both BQ123 (7.0, 7.4 and 6.9) and FR139317 (7.6, 7.9 and 7.3) (Table 2) in coronary artery, internal mammary artery and saphenous vein, respectively, were consistent with values published for antagonism of ET_A receptors in a number of animal systems. FR139317 was approximately three times more potent than BQ123. ET-1 responses were similarly antagonized by 3 μM BQ123 in aorta ($pA_2 = 7.4 \pm 0.5$, $n = 4$) and pulmonary artery ($pA_2 = 6.9$, $n = 1$).

Discussion

We have demonstrated that in human epicardial coronary artery, internal mammary artery, pulmonary artery, aorta and saphenous vein, *in vitro* vasoconstriction by the endothelin peptides is due to the activation of smooth muscle ET_A receptors. This is suggested by the relative potencies of ET-1 and ET-3, the lack of effect of the ET_B-selective agonists, BQ3020 and [^{1,3,11,15}Ala]-ET-1 and the ability of the ET_A-selective antagonists, BQ123 and FR139317 to block ET-1 responses with potencies comparable to those obtained in animal tissues (such as rat aorta) which express only ET_A

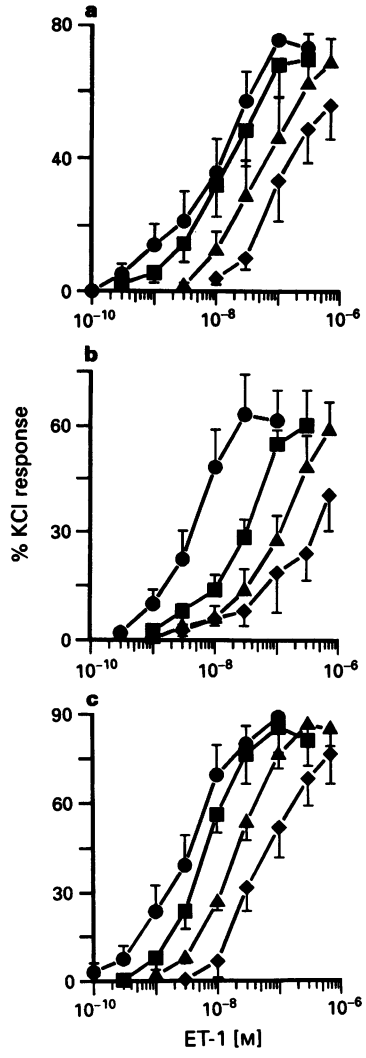

Figure 5 Antagonism of endothelin-1 (ET-1)-mediated vasoconstriction in coronary artery (a), internal mammary artery (b) and saphenous vein (c) by BQ123. ET-1 control (●); + 0.3 μM BQ123 (■); + 1 μM BQ123 (▲) and 3 μM BQ123 (◆). BQ123 was added to the bathing medium 30 min prior to the addition of ET-1. Data are the mean ± s.e.mean with data from at least six patients.

Table 2 Antagonism of endothelin-1 (ET-1)-mediated vasoconstriction in human isolated blood vessels by ET_A-selective antagonists, BQ123 and FR139317

	BQ123			*FR139317*		
Blood vessel	pA_2	Slope	K_B (nM)*	pA_2	Slope	K_B (nM)*
Coronary artery	7.0	1.05	91.2	7.6	0.73	126
Mammary artery	7.4	1.08	33.9	7.9	0.84	33.1
Saphenous vein	6.9	0.92	141.3	7.3	0.80	87.1

The slopes of the regression lines were not significantly different from one.
*K_B values calculated from Schild regressions with slopes constrained to unity.

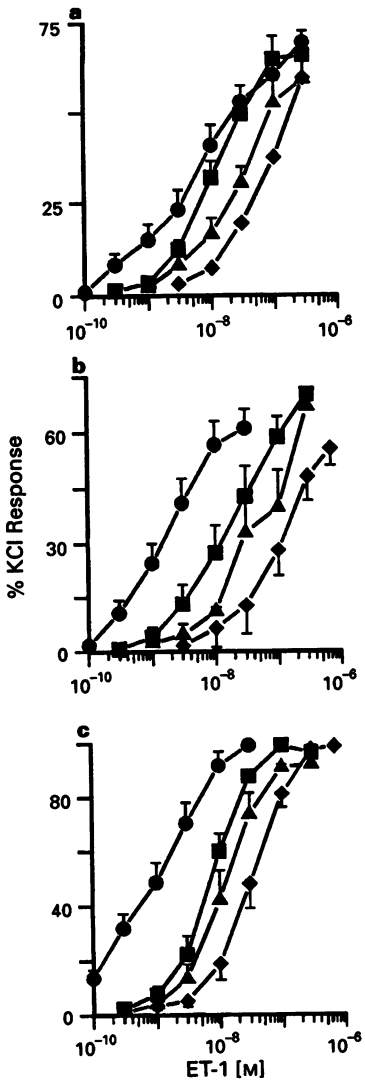

Figure 6 Antagonism of endothelin-1 (ET-1)-mediated vasoconstriction in coronary artery (a), internal mammary artery (b) and saphenous vein (c) by FR139317. ET-1 control (●); + 0.3 μM FR139317 (■); + 1 μM FR139317 (▲) and 3 μM FR139317 (◆). FR139317 was added to the bathing medium 30 min prior to the addition of ET-1. Data are the mean ± s.e.mean with data from at least six patients.

receptors. In contrast to porcine coronary artery, in which BQ123 blocks only part of the ET-1-induced contraction (Ihara *et al.*, 1992), no portion of the monophasic ET-1 dose-response curves was resistant to these antagonists in each of the five preparations (Figures 5 and 6). No attenuation of the maximum responses to ET-1 was observed in the presence of 0.3–3 μM BQ123 or FR139317 and slopes of the Schild regressions were not significantly different from one. Where responses were obtained to ET-3, threshold concentrations were 30–100 times those observed for ET-1. These results are in concordance with our own findings in human renal artery and vein (Maguire *et al.*, 1994b) and a number of smaller studies on human coronary artery (Opgaard *et al.*, 1994), pulmonary artery (Hemsén *et al.*, 1990; Hay *et al.*, 1993; Fukuroda *et al.*, 1994) and mammary artery (Liu *et al.*, 1994). Additionally we have demonstrated that established constrictor responses to ET-1 in coronary artery, internal mammary artery and saphenous vein can be completely reversed by addition of micromolar concentrations of either BQ123 or FR139317 (Maguire & Davenport, 1994). If ET_B receptors contributed significantly to ET-1-mediated vasoconstriction in these vessels, complete reversal with ET_A antagonists should not be possible.

We know from our experiments employing reverse transcriptase-polymerase chain reaction assays that the media of each of these blood vessels contains mRNA encoding both the ET_A and the ET_B receptor. However, ligand binding experiments clearly demonstrate that in each case, ET_A receptors comprise at least 85% of the total endothelin receptor population (Davenport *et al.*, 1995). The low density of ET_B receptors in these tissues may be sufficient to explain the apparent lack of involvement of this subtype in the overall constrictor responses of the endothelin peptides. Blood vessels from some patients do respond to the ET_B-selective agonist, S6c. The low concentrations of S6c at which vasoconstriction occurs suggests the involvement of ET_B receptors. This response is not mediated by ET_A receptors as an established S6c contraction is not reversed by BQ123 (not shown). It is not known why only S6c of the available ET_B-selective agonists is able to elicit contractile responses in these human blood vessels. One possible explanation is that S6c has higher efficacy for its receptor than the endothelins (or the endothelin analogues [^{1,3,11,15}Ala]-ET-1 and BQ3020) and is therefore sometimes able to elicit a contraction despite the low receptor number. Since the same variability in responsiveness to S6c was observed with coronary arteries from patients with both ischaemic and non-ischaemic heart disease and from the undiseased saphenous vein and mammary artery preparations, it is difficult at present to correlate the occurrence or degree of S6c contraction with any particular underlying condition of the patient. Therefore, whilst in common with other groups we are able to demonstrate that both constrictor ET_A and ET_B receptors are present in human vascular smooth muscle (Seo *et al.*, 1994; White *et al.*, 1994), our data imply that only the ET_A receptor is important for endothelin-mediated vasoconstriction, at least in those blood vessels investigated.

Our data are also comparable with the recent findings of Godfraind (1993), who demonstrated that constriction of human small diameter epicardial coronary arteries was due only to ET_A receptor activation (Schild slopes for BQ123 were one). However, in this study, responses in larger diameter coronaries appeared to be due to the activation of a heterogeneous endothelin receptor population (Schild slopes for BQ123 were less than one). The coronary arteries used in our experiments probably correspond to the larger diameter vessels used by Godfraind; however, we find that Schild slopes for both BQ123 and FR139317 were not significantly different from one. This is consistent with our previous finding that ET-1 vasoconstriction in coronary artery, internal mammary artery and saphenous vein can be competitively blocked by the non-peptide ET_A antagonist 50-235 (Maguire *et al.*, 1994a). The reason for this discrepancy is not entirely clear but the conclusion from both studies, that ET_A receptors at least predominate in human coronary arteries, is the same.

Recent reports describing 'atypical' endothelin receptors appear to be based on two main observations. Firstly, BQ123-insensitive ET-1 or S6c responses are not blocked by the putative ET_B antagonist, IRL1038 (Urade *et al.*, 1992) and therefore deemed non ET_A/non ET_B. Secondly, ET-1 responses which appear to be ET_A-mediated (ET-1 > ET-3) are not antagonized by low concentrations ($\leq$ 1 μM) of BQ123. Observations such as these in human blood vessels have been made by two groups. In a detailed study by Riezebos *et al.* (1994) although constriction of human small arteries was found to be mediated by ET_A receptors, responses in small veins were due to activation of two receptors. Not only were the Schild slopes for BQ123 against ET-1 less than one but ET-3 gave a biphasic curve, the lower concentrations of which were insensitive to BQ123 and IRL1038. The authors suggested the presence of an additional non ET_A/non ET_B receptor in these vessels. In the light of the recent retraction by Urade *et al.* (1994) and our own findings that in human left ventricle IRL1038 exhibits low selectivity and low potency for the ET_B receptor (Peter & Davenport,

1994), the lack of effect of IRL 1038 is not convincing evidence for the absence of ET_B receptors. We would therefore suggest that these observations are consistent with the presence of a small population of constrictor ET_B receptors.

Similarly, Bax and colleagues (1993) using human saphenous vein, concluded that two receptors were present, neither of which was the classical ET_A receptor. One was sensitive to ET-1 and low concentrations of S6b but insensitive to BQ123; the other sensitive to S6b and BQ123 but not ET-1. This is in contrast to our own findings that mRNA for both ET_A and ET_B receptors are present in human saphenous vein and, using the subtype selective ligands BQ123, FR139317 and BQ3020, that [^{125}I]-ET-1 binds to both ET_A and ET_B receptors in saphenous vein homogenates with ET_A receptors comprising about 90% of total (Davenport *et al.*, 1995). We have observed that higher concentrations of antagonists are required to block ET-1 responses in functional assays than predicted by their nanomolar affinity in binding assays. To complicate matters further, S6b and ET-3 are more sensitive to these compounds *in vitro*. It has been suggested that this is due to receptor heterogeneity (Bax *et al.*, 1994). However, as nanomolar concentrations of BQ123 compete for [^{125}I]-ET-1 binding (Davenport *et al.*, 1995) and [^{125}I]-S6b binding (unpublished data) in human blood vessels this suggests that the discrepancy occurs at the functional level and may be due to a difference in the way ET-1 binds to or activates the ET_A receptor compared to S6b or ET-3. This is an area which requires further investigation as ultimately we need to design antagonists which potently block the *in vivo* effects of ET-1, not those of S6b.

In conclusion we have evidence for ET_A and ET_B mRNA and receptors in the media of large diameter human blood vessels (Davenport *et al.*, 1995), but our data suggest that the endothelin peptides mediate their constrictor effects in these blood vessels via activation of the ET_A receptor. A selective ET_A receptor antagonist may therefore be clinically effective in those conditions in which ET levels are raised, with the additional benefit of leaving unaffected the beneficial vasodilator ET_B receptors and non-vascular ET_B receptors. Evidence suggesting that ET_A receptors also predominate in the small diameter resistance arterioles which are responsible for the maintenance of, and changes in, vascular tone comes from microautoradiographical data from human kidney. Using BQ123 and BQ3020 in competition with [^{125}I]-ET-1, ET_A but not ET_B receptors appear to localize to intrarenal arterioles (Karet *et al.*, 1993). However, it remains to be determined whether this is the case in all human vascular beds.

We are grateful to the consultant and theatre staff of Papworth Hospital, Cambridge, for permission to collect vascular tissue and to Dr A.M. Doherty for the synthesis of FR139317. Supported by grants from the British Heart Foundation, Royal Society, BBSRC and Isaac Newton Trust.

References

ARAI, H., HORI, S., ARAMORI, I., OHKUBO, H. & NAKANISHI, S. (1990). Cloning and expression of a cDNA encoding an endothelin receptor. *Nature*, **348**, 730–732.

ARUNLAKSHANA, O. & SCHILD, H.O. (1959). Some quantitative uses of drug antagonists. *Br. J. Pharmacol. Chemother.*, **14**, 48–58.

BAX, W.A., AGHAI, Z., VAN TRICHT, C.L.J., WASSENAAR, C. & SAXENA, P. (1994). Different endothelin receptors involved in endothelin-1- and sarafotoxin S6B-induced contractions of the human isolated coronary artery. *Br. J. Pharmacol.*, **113**, 1471–1479.

BAX, W.A., BOS, E. & SAXENA, P.R. (1993). Heterogeneity of endothelin/sarafotoxin receptors mediating contraction of the human isolated saphenous vein. *Eur. J. Pharmacol.*, **239**, 267–268.

BENIGNI, A., ZOJA, C., CORNA, D., ORISIO, S., LONGARETTI, L., BERTANI, T. & REMUZZI, G. (1993). A specific endothelin subtype A receptor antagonist protects against injury in renal disease progression. *Kidney Int.*, **44**, 440–445.

CACOUB, P., DORENT, R., MAISTRE, G., NATAF, P., CARAYON, A., PIETTE, J.P., GODEAU, P., CABROL, C. & GANDJBAKHCH, I. (1993). Endothelin-1 in primary pulmonary hypertension and the Eisenmenger syndrome. *Am. J. Cardiology*, **71**, 448–450.

CHESTER, A.H., O'NEIL, G.S., ALLEN, S.P., LUU, T.N., TADJKARIMI, S. & YACOUB, M.H. (1992). Effect of endothelin on normal and diseased human coronary arteries. *Eur. J. Clin. Invest.*, **22**, 210–213.

CLOZEL, M. & WATANABE, H. (1992). BQ123, a peptidic endothelin ET(A) receptor antagonist, prevents the early cerebral vasospasm following subarachnoid haemorrhage after intracisternal but not intravenous injection. *Life Sci.*, **52**, 825–834.

COSTELLO, K.B., STEWART, D.J. & BAFFOUR, R. (1990). Endothelin is a potent constrictor of human vessels used in coronary revascularization surgery. *Eur. J. Pharmacol.*, **186**, 311–314.

CRISTOL, J.-P., WARNER, T.D., THIEMERMANN, C. & VANE, J.R. (1993). Mediation via different receptors of the vasoconstrictor effects of endothelins and sarafotoxins in the systemic circulation and renal vasculature of the anaesthetised rat. *Br. J. Pharmacol.*, **108**, 776–779.

DALMAN, R.L., HARKER, C.T., TAYLOR, L.M. & PORTER, J.M. (1990). Contractile responses of human vascular tissue to endothelin. *Surgical Forum*, **41**, 332–334.

DAVENPORT, A.P. & MAGUIRE, J.J. (1994). Is endothelin-induced vasoconstriction mediated only by ET_A receptors in humans? *Trends Pharmacol. Sci.*, **15**, 9–11.

DAVENPORT, A.P., NUNEZ, D.J., HALL, J.A., KAUMANN, A.J. & BROWN, M.J. (1989). Autoradiographical localisation of binding sites for [^{125}I] endothelin-1 in humans, pigs and rats: functional relevance in man. *J. Cardiovasc. Pharmacol.*, **13** (Suppl. 5), S166–S170.

DAVENPORT, A.P., O'REILLY, G. & KUC, R.E. (1995). Endothelin ET_A and ET_B mRNA and receptors are expressed by smooth muscle in the human vasculature: majority of the ET_A subtype. *Br. J. Pharmacol.*, **114**, 1110–1116.

DAVENPORT, A.P., O'REILLY, G., MOLENAAR, P., MAGUIRE, J.J., KUC, R.E., SHARKEY, A., BACON, C.R. & FERRO, A. (1993). Human endothelin receptors characterised using reverse transcriptase-polymerase chain reaction, *in situ* hybridisation and subtype selective ligands BQ123 and BQ3020: evidence for expression of ET_B receptors in human vascular smooth muscle. *J. Cardiovasc. Pharmacol.*, **22**, 22–25.

DERAY, G., CARAYON, A. & LEHOANG, P. (1991). Increased endothelin level after cyclosporine therapy. *Ann. Intern. Med.*, **114**, 809.

FOTO, A., HELLINGS, S.E., INAGAMI, T. & KON, V. (1992). Endothelin receptor antagonism is protective in rats with cyclosporine A-induced nephrotoxicity. *Kidney Int.*, **42**, 770–774.

FRANCO-CERECEDA, A. (1989). Endothelin- and neuropeptide Y-induced vasoconstriction of human epicardial coronary arteries *in vitro*. *Br. J. Pharmacol.*, **97**, 968–972.

FUKURODA, T., KOBAYASHI, M., OZAKI, S., YANO, M., MIYAUCHI, T., ONIZUKA, M., SUGISHITA, Y., GOTO, K. & NISHIKIBE, M. (1994). Endothelin receptor subtypes in human versus rabbit pulmonary arteries. *J. Appl. Physiol.*, **76**, 1976–1982.

GARDINER, S.M., KEMP, P.A., BENNETT, T. & DAVENPORT, A.P. (1992). Regional haemodynamic response to [Ala^{1,3,11,15}] endothelin-1 in conscious rats. *Br. J. Pharmacol.*, **107**, 415P.

GODFRAIND, T. (1993). Evidence for receptor heterogeneity of endothelin receptor distribution in human coronary artery. *Br. J. Pharmacol.*, **110**, 1201–1205.

GROVER, G.J., DZWONCZYK, S. & PARHAM, C.S. (1993). The endothelin-1 receptor antagonist BQ123 reduces infarct size in a canine model of coronary occlusion and reperfusion. *Cardiovasc. Res.*, **27**, 1613–1618.

HARRISON, V.J., RANDRIANTSOA, A. & SCHOEFFTER, P. (1992). Heterogeneity of endothelin-sarafotoxin receptors mediating contraction of pig coronary artery. *Br. J. Pharmacol.*, **105**, 511–513.

HAY, D.W.P., LUTTMANN, M.A., HUBBARD, W.C. & UNDEM, B.J. (1993). Endothelin receptor subtypes in human and guinea-pig pulmonary tissues. *Br. J. Pharmacol.*, **110**, 1175–1183.

HAYNES, W.G. & WEBB, D.J. (1993). Endothelium-dependent modulation of responses to endothelin-1 in human veins. *Clin. Sci.*, **84**, 427–433.

HEMSÉN, A., FRANCO-CERECEDA, A., NATRAN, R., RUDEHILL, A. & LUNDBERG, J.M. (1990). Occurrence, specific binding sites and functional effects of endothelin in human cardiopulmonary tissue. *Eur. J. Pharmacol.*, **191**, 319–328.

HUGHES, A.D., THOM, S.A., WOODALL, N., SCHACHTER, M., HAIR, W.M., MARTIN, G.N. & SEVER, P.S. (1989). Human vascular response to endothelin-1: observations in vivo and in vitro. *J. Cardiovasc. Pharmacol.*, **13** (Suppl. 5), S225–S228.

IHARA, M., ISHIKAWA, K., FUKURODA, T., SAEKI, T., FUNABASHI, K., FUKAMI, T., SUDA, H. & YANO, M. (1992). In vitro biological profile of a highly potent novel endothelin (ET) antagonist BQ123 selective for the ET_A receptor. *J. Cardiovasc. Pharmacol.*, **20** (Suppl. 12), S11–S14.

INOUE, A., YANAGISAWA, M., KIMURA, S., KASUYA, Y., MIYAUCHI, T., GOTO, K. & MASAKI, T. (1989). The human endothelin family: three structurally and pharmacologically distinct isopeptides predicted by three separate genes. *Proc. Natl. Acad. Sci. U.S.A.*, **86**, 2863–2867.

ITOH, S., SASAKI, T., IDE, K., ISHIKAWA, K., NISHIKIBE, M. & YANO, M. (1993). A novel endothelin ET_A receptor antagonist, BQ-485, and its preventitive effect on experimental cerebral vasospasm in dogs. *Biochem. Biophys. Res. Commun.*, **195**, 969–975.

KARET, F., KUC, R.E. & DAVENPORT, A.P. (1993). Novel ligands BQ123 and BQ3020 characterize endothelin receptor subtypes ET_A and ET_B in human kidney. *Kidney Int.*, **44**, 36–42.

KIOWSKI, W. & LINDER, L. (1992). Reversal of endothelin-1-induced vasoconstriction by nifedipine in human resistance vessels in vivo in healthy subjects. *Am. J. Cardiology*, **69**, 1063–1066.

LIU, J.J., CASLEY, D., WOJTA, J., GALLICCHIO, M., DAUER, R. & JOHNSTON, C.I. (1994). Effects of calcium- and ET(A)-receptor antagonists on endothelin-induced vasoconstriction and levels of endothelin in the human internal mammary artery. *Clin. Exp. Pharmacol. Physiol.*, **21**, 49–57.

LÜSCHER, T.F., YANG, Z., TSCHUDI, M., VON SEGESSER, L., STULZ, P., BOULANGER, C., SIEBENMANN, R., TURINA, M. & BÜHLER, F.R. (1990). Interaction between endothelin-1 and endothelium-derived relaxing factors in human arteries and veins. *Circ. Res.*, **66**, 1088–1094.

MCKAY, K.O., BLACK, J.L., DIMENT, L.M. & ARMOUR, C.L. (1991). Functional and autoradiographic studies of endothelin-1 and endothelin-2 in human bronchi, pulmonary arteries and airway parasympathetic ganglia. *J. Cardiovasc. Pharmacol.*, **17** (Suppl. 7), S206–S209.

MCNAMARA, D.B., LIGHT, J.T., MINKES, R.K., SAROYAN, R.M., KVAMME, P., ROWE, N., WEBB, W.R., FOX, L., KERSTEIN, M.D., MILLS, N.L. & KADOWITZ, P.J. (1992). Comparative effects of endothelin (ET-1) and U46619 on human saphenous vein and gastroepiploic artery, sources of human autologous grafts. *Mol. Cell. Biochem.*, **117**, 81–85.

MAGUIRE, J.J., BACON, C.R., FUJIMOTO, M. & DAVENPORT, A.P. (1994a). Myricerone caffeoyl ester (50-235) is a non-peptide antagonist selective for human ET_A receptors. *J. Hypertension*, **12**, 675–680.

MAGUIRE, J.J. & DAVENPORT, A.P. (1993). Endothelin-induced vasoconstriction in human isolated vasculature is mediated predominantly via activation of ET_A receptors. *Br. J. Pharmacol.*, **110**, 47P.

MAGUIRE, J.J. & DAVENPORT, A.P. (1994). Pre- or post administration of BQ123 and FR139317 antagonizes endothelin-1 (ET-1)-induced contraction of human blood vessels *in vitro*. *Br. J. Pharmacol.*, **111**, 149P.

MAGUIRE, J.J., KUC, R.E., O'REILLY, G. & DAVENPORT, A.P. (1994b). Vasoconstrictor endothelin receptors characterized in human renal artery and vein *in vitro*. *Br. J. Pharmacol.*, **113**, 49–54.

MOLENAAR, P., KUC, R.E. & DAVENPORT, A.P. (1992). Characterization of two new ET_B selective radioligands, [^{125}I]-BQ3020 and [^{125}I]-[Ala^{1,3,11,15}]ET-1 in human heart. *Br. J. Pharmacol.*, **107**, 637–639.

OKAMURA, T., MATSUMOTO, T., IKEMOTO, F. & TODA, N. (1992). Mechanisms of the biphasic responses to endothelin-3 in dog coronary arteries. *Br. J. Pharmacol.*, **107**, 1037–1041.

OPGAARD, O.S., ADNER, M., GULBENKIAN, S. & EDVINSSON, L. (1994). Localization of endothelin immunoreactivity and demonstration of constrictory endothelin-A receptors in human coronary arteries and veins. *J. Cardiovasc. Pharmacol.*, **23**, 576–583.

PAPADOPOULOUS, S.M., GILBERT, L.L., WEBB, R.C. & D'AMATO, C.J. (1990). Characterization of contractile responses to endothelin in human cerebral arteries: implications for cerebral vasospasm. *Neurosurgery*, **26**, 810–815.

PETER, M.G. & DAVENPORT, A.P. (1994). Characterisation of the endothelin ET_A antagonists BQ123 and FR139317 in human, rat and porcine hearts, and the ET_B selective antagonist IRL 1038 in human tissue. *Br. J. Pharmacol.*, **112**, 122P.

RIEZEBOS, J., WATTS, I.S. & VALLANCE, P.J.T. (1994). Endothelin receptors mediating functional responses in human small arteries and veins. *Br. J. Pharmacol.*, **111**, 609–615.

SAKURAI, T., YANAGISAWA, M. & MASAKI, T. (1992). Molecular characterization of endothelin receptors. *Trends Pharmacol. Sci.*, **13**, 103–108.

SAKURAI, T., YANAGISAWA, M., TAKUWA, Y., MIYAZAKI, H., KIMURA, S., GOTO, K. & MASAKI, T. (1990). Cloning of a cDNA encoding a non-isopeptide-selective subtype of the endothelin receptor. *Nature*, **348**, 732–735.

SEO, B., OEMAR, B.S., SIEBENMANN, R., VON SEGESSER, L. & LÜSCHER, T.F. (1994). Both ET_A and ET_B receptors mediate contraction to endothelin-1 in human blood vessels. *Circulation*, **89**, 1203–1208.

SOGABE, K., NIREI, H., SHOUBO, M., NOMOTO, A., HENMI, K., NOTSU, Y. & ONO, T. (1992). A novel endothelin receptor antagonist: studies with FR 139317. *Jpn. J. Pharmacol.*, **58**, 105P.

SOKOLOVSKY, M. (1994). Endothelins and sarafotoxins: receptor heterogeneity. *Int. J. Biochem.*, **26**, 335–340.

SØRENSEN, S.S., MADSEN, J.K. & PEDERSEN, E.B. (1994). Systemic and renal effect of intravenous infusion of endothelin-1 in healthy human volunteers. *Am. J. Physiol.*, **266**, F411–F418.

TOMITA, K., UJJIE, K., NAKANISHI, T., TOMITA, S., MATSUDA, O., ANDO, K., SHICHIRI, M., HIRATA, Y. & MARUMO, F. (1989). Plasma endothelin levels in patients with acute renal failure. *New Engl. J. Med.*, **324**, 1127.

URADE, Y., FUITANI, Y., ODA, K., WATAKABE, T., UMEMURA, I. & TAKAI, M. (1992). An endothelin B receptor-selective antagonist: IRL1038, (Cys^{11}-Cys^{15})-endothelin-1(11-21). *FEBS Lett.*, **311**, 12–16.

URADE, Y., FUJITANI, Y., ODA, K., WATAKABE, T., UMEMURA, I., TAKAI, M., OKADA, T., SAKATA, K. & KARAKAI, H. (1994). Retraction: an endothelin B receptor-selective antagonist: IRL-1038, (Cys^{11}-Cys^{15})-endothelin-1(11-21)(FEBS Lett. 311 (1992) 12–16. *FEBS Lett.*, **342**, 103.

WATSON, S. & GIRDLESTONE, D. (1994). Receptor and ion channel nomenclature supplement. *Trends Pharmacol. Sci.*, Fifth Edition, 18.

WEI, C.-M., LERMAN, A., RODEHEFFER, R.J., MCGREGOR, C.G.A., BRANDT, R.R., WRIGHT, S., HEUBLEIN, D.M., KAO, P.C., EDWARDS, W.D. & BURNETT, J.C. (1994). Endothelin in human congestive heart failure. *Circulation*, **89**, 1580–1586.

WHITE, D.G., GARRATT, H., MUNDIN, J.W., SUMNER, M.J., VALLANCE, P.J. & WATTS, I.S. (1994). Human saphenous vein contains both endothelin ET_A and ET_B contractile receptors. *Eur. J. Pharmacol.*, **257**, 307–310.

YANAGISAWA, M., KURIHARA, H., KIMURA, S., TOMOBE, Y., KOBAYASHI, M., MITSUI, Y., YAZAKI, Y., GOTO, K. & MASAKI, T. (1988). A novel potent vasoconstrictor peptide produced by vascular endothelial cells. *Nature*, **332**, 411–415.

(Received August 3, 1994
Revised December 13, 1994
Accepted January 17, 1995)

British Journal of Pharmacology (1995) 115, 198–202

Inhibitory action of betaxolol, a β_1-selective adrenoceptor antagonist, on voltage-dependent calcium channels in guinea-pig artery and vein

Motoko Setoguchi, [1]Yusuke Ohya, Isao Abe & Masatoshi Fujishima

Second Department of Internal Medicine, Kyushu University, Faculty of Medicine, Maidashi 3-1-1, Higashi-ku, Fukuoka, Japan

1 The effects of betaxolol, (±)-1-[4-[2-(cyclopropylmethoxy) ethyl] phenoxy]-3-(isopropylamino)-2-propanol hydrochloride, a β_1-selective adrenoceptor antagonist, on voltage-dependent Ca^{2+} channels were investigated in single smooth muscle cells from guinea-pig mesenteric artery and portal vein using a whole-cell variant of the patch-clamp technique. Ca^{2+} channel currents were recorded with bath solutions contained 10 mM Ba^{2+} for arterial cells and 2 mM Ca^{2+} for venous cells.

2 Betaxolol inhibited Ca^{2+} channel currents dose-dependently in both mesenteric artery cells and portal vein cells. The two isomers, (+)-betaxolol and (−)-betaxolol (relative β-antagonistic efficacies of 0.1 and 1, respectively), had similar potencies for inhibiting Ca^{2+} channel currents in portal vein cells. Propranolol did not inhibit the currents. Thus the inhibitory action of betaxolol on Ca^{2+} channel currents was independent of the β-adrenoceptor.

3 The inhibitory action of betaxolol on Ca^{2+} channel currents was compared with that of diltiazem and of nifedipine in mesenteric artery cells. The current inhibition depended on the stimulation frequency with all drugs (use-dependent block). All drugs also accelerated the current decay and shifted the voltage-dependent inactivation curve in a negative direction.

4 In conclusion, betaxolol inhibited Ca^{2+} channel currents in vascular smooth muscle cells. The mode of inhibitory action was similar to that of diltiazem and nifedipine. Our results suggest that betaxolol is a unique β-adrenoceptor antagonist that has a direct inhibitory action on voltage-dependent Ca^{2+} channels in vascular smooth muscle cells.

Keywords: Betaxolol; calcium channel; voltage clamp; vascular muscle; mesenteric artery; portal vein

Introduction

β-Adrenoceptor antagonists are widely used as first-line antihypertensive agents. It is known that non-selective β-adrenoceptor antagonists without intrinsic sympathomimetic activity initially increase peripheral resistance, mainly by inhibiting β_2-adrenoceptors on the vascular smooth muscle membrane. Betaxolol, ((±)-1-[4-[2-(cyclopropylmethoxy) ethyl] phenoxy] -3-(isopropylamino)-2-propanol hydrochloride) is a β_1-selective adrenoceptor antagonist without intrinsic sympathomimetic activity (Beresford & Heel, 1986). Intravenous injection of this drug *in vivo* decreased peripheral resistance in anaesthetized dogs (Satoh *et al.*, 1990). It has also been reported that betaxolol relaxed the high-K^+-induced contraction of rat aortic strips dose-dependently *in vitro* (Bessho *et al.*, 1991), suggesting that betaxolol might possess a direct vasodilator action, probably due to the inhibition of Ca^{2+} influx across the cell membrane. However, the effects of betaxolol on Ca^{2+} channels in vascular smooth muscle cells have not yet been examined. The present study was designed to investigate the effects of betaxolol on Ca^{2+} channels directly in single vascular smooth muscle cells using the patch-clamp technique.

Methods

Single-cell dispersion

Female guinea-pigs (body weight 250 to 300 g) were stunned by a blow to the head and then decapitated. Single smooth muscle cells were obtained by collagenase treatment (collagenase; Wako Chemical Co, Tokyo, Japan) from a mesenteric arterial branch (diameter <300 μm) and the portal vein by methods described previously (for mesenteric artery: Ohya *et al.*, 1993, for portal vein: Ohya & Sperelakis, 1989).

Electrical recordings

A whole-cell voltage clamp was performed with a patch pipette through a voltage clamp amplifier (Axopatch 1-D, Axon Instruments Inc., Foster City, CA, U.S.A.) by the method of Hamill *et al.* (1981). The conditions and procedures were basically the same as those previously published (Ohya & Sperelakis, 1989; Ohya *et al.*, 1993). Recording electrodes were made from Pyrex glass capillary tubing. The arterial cell was held at −80 mV and command potentials were applied every 30 s. In venous cells, the holding potential was −60 mV and the stimulating interval was 10 s. Data were obtained after the current amplitude had been stabilized (usually 3 to 4 min after the whole-cell configuration was obtained). The Ca^{2+} channel current apparently did not run down over the next 15 min under these conditions (after 15 min, relative amplitude was 0.97 ± 0.02 ($n = 4$) of the stabilized amplitude). Membrane currents were low-pass-filtered at 2 kHz, digitized with a sampling frequency of 5 to 10 kHz, and stored in a personal computer system for subsequent analysis. The leak and residual capacitive currents were subtracted using the P/4 protocol. The liquid junction potential of 10 mV was corrected. Current recording was carried out at room temperature (22 to 24°C).

Solutions and chemicals

To isolate the inward Ca^{2+} channel currents, the pipette was filled with a high Cs^+ solution of the following composition

[1] Author for correspondence.

(mM): Cs aspartate 130, CsCl 20, $ATPNa_2$ 3, $MgCl_2$ 3, EGTA 10, HEPES 10, pH 7.3 titrated with CsOH. The bath solution contained (mM): $BaCl_2$ 10, NaCl 150, KCl 6, glucose 5.4, HEPES 5, pH 7.3 titrated with NaOH (for mesenteric artery), or $CaCl_2$ 2, $MgCl_2$ 1, TrisCl 150, KCl 6, glucose 5.4, HEPES 5, pH 7.3 titrated with NaOH (for portal vein).

The drugs used were: (±)-betaxolol, (−)-betaxolol and (+)-betaxolol (gifts from Yoshitomi Pharm. Co., Ltd., Osaka, Japan); propranolol hydrochloride (Sigma, St. Louis, MO, U.S.A.); diltiazem (Calbiochem, San Diego, CA, U.S.A.); and nifedipine (a gift from Bayer Pharm. Co., Ltd., Osaka, Japan). The drugs were dissolved directly in deionized water, except nifedipine, which was dissolved in 100% ethanol and diluted at least 1000 times. This concentration of ethanol (below 0.1%) did not alter the currents. Final drug concentrations are stated in the text.

Curve fitting and statistics

Fitting of the data to each equation was performed by the nonlinear least-squares method. The data were expressed as mean ± s.e. Statistical significance was determined by Student's *t* test (unpaired) or one-way analysis of variance. A *P* value of less than 0.05 was considered statistically significant.

Results

Figure 1 shows the effects of betaxolol on Ca^{2+} channel currents in mesenteric artery cells. Inward currents were evoked by command potentials of −30 mV or more depolarized potential from a holding potential of −80 mV. The complete current-voltage curves before and after application of 10 μM betaxolol are shown in Figures 1a and b. The same experiments were done on 7 cells, and average inhibitions of the current amplitude at given command potentials are shown in Figure 1c. The greater inhibition was observed at the more depolarized command potential.

Figure 2 shows the relationship between the relative amplitude of the inward current and the concentration of betaxolol. The current was evoked by command potential of 10 mV with stimulating interval of 30 s. The IC_{50} value for betaxolol obtained was 46 μM in arterial cells.

Betaxolol inhibited Ca^{2+} channel currents in portal vein cells. At 10 μM, betaxolol inhibited the current by 19 ± 4% ($n = 8$) (Figure 3). The IC_{50} was 45 μM in portal vein cells in experiments using various concentrations of betaxolol (values not shown). The inhibitory actions of betaxolol on the Ca^{2+} channel current were compared with those of the racemates, (+)-betaxolol and (−)-betaxolol (Figure 3). At 10 μM, (+)-betaxolol and (−)-betaxolol inhibited the calcium current by 17 ± 3% ($n = 6$) and 15 ± 2% ($n = 5$), respectively. In contrast, 10 μM propranolol did not inhibit the current.

The inhibitory action of betaxolol on Ca^{2+} channel currents was compared with those of two types of Ca^{2+} antagonists, a benzothiazepine derivative, diltiazem (10 μM) and a dihydropyridine derivative, nifedipine (0.1 μM) in arterial cells. Diltiazem and nifedipine inhibited the inward current by 24 ± 5% ($n = 8$) and 39 ± 5% ($n = 5$), respectively. Figure 4 shows the potentiation of the current inhibition by repetitive membrane depolarization (use-dependent block), induced by betaxolol, diltiazem, and nifedipine. Figure 4a depicts typical results with betaxolol at three different frequencies of 0.3, 1, and 2 Hz. Before application of the drug (control), the train pulses at frequencies of 0.3, 1, and 2 Hz did not reduce the amplitude of Ca^{2+} channel current (Figure 4a(i)). With 10 μM betaxolol, the current inhibition showed an accumulation during the repetitive stimulations at all frequencies (Figure 4a(ii)). The higher frequency caused the greater inhibition. The use-dependent block was evaluated with the current amplitude evoked by the 15th stimulation (Figure 4b). The amplitude of the 15th stimulation was significantly smaller than that of the 1st

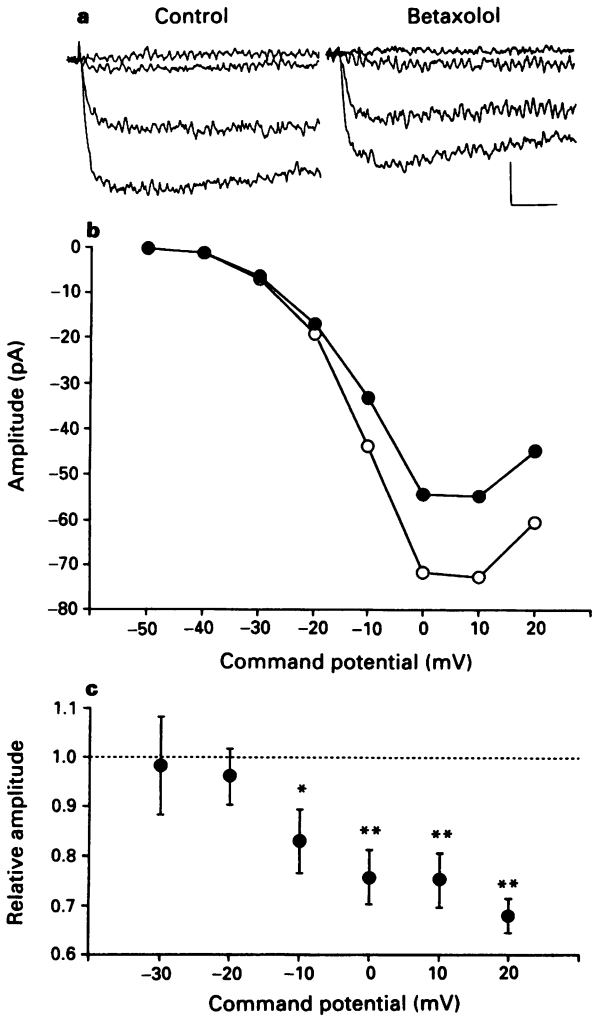

Figure 1 Inhibitory action of betaxolol on the Ca^{2+} channel current recorded from single mesenteric artery cells. (a) Current traces obtained at command potentials of −50 mV to 10 mV in 20-mV steps from a holding potential of −80 mV. The scales are 40 pA (vertical) and 10 ms (horizontal). (b) Peak amplitudes of the currents, recorded in the absence (control, ○) and presence of 10 μM betaxolol (●), are plotted against the command potentials. (c) Relationship between the command potential and the current inhibition. The amplitudes at any given command potential in the absence of betaxolol were normalized as 1.0. and those observed at the same potential in the presence of 10 μM betaxolol were expressed in a relative manner. Each value is expressed as mean ± s.e. from 7 cells. Overall analysis of variance *F* ratio was 4.82 ($P < 0.001$). $^*P < 0.05$ and $^{**}P < 0.01$ compared with 1.0.

stimulation at all frequencies with all drugs. This use-dependent block was significantly more profound at 1 Hz and 2 Hz with diltiazem than with betaxolol or nifedipine.

The effects of betaxolol, diltiazem, and nifedipine on the current decay are compared in Figure 5. To emphasize difference in the current decay, the control and drug traces are superimposed with the drug trace magnified so that peak amplitudes of the two traces match (Figure 5a). Without drug, the decay of Ba^{2+} current was minimal. All drugs significantly accelerated the decay; the rate of decay over 100 ms was 5 ± 2% ($n = 5$) without drug, 22 ± 5% ($n = 5$) with betaxolol, 27 ± 4% ($n = 5$) with diltiazem and 30 ± 4% ($n = 5$) with nifedipine (Figure 5b).

The effects of betaxolol on voltage-dependent inactivation of the Ca^{2+} channels were investigated. The steady-state inactivation curve was obtained using the double-pulse protocol. After various levels of the conditioning potential were applied for 10 s, a test pulse to 0 mV evoked the current. The

conditioning and test pulses were separated by a short (10 ms) return to the holding potential to assign the channels to either the closed or inactivated state. Three drugs significantly shifted the steady-state inactivation curve in a negative direction (shift in V_h: betaxolol, −11 mV; diltiazem, −24 mV; nifedipine, −38 mV) (Figure 6). Dissociation constants for the resting channels (K_R) and inactivated channels (K_I) were obtained according to the modulated-receptor hypothesis (Bean, 1984), i.e. the change in V_h with the drug (ΔV_h) was as follows: $\Delta V_h = k$ In $\{(1+[drug]/K_I)/(1+[drug]/K_R)\}$, where k was a Boltzman coefficient and [drug] was the drug concentration. K_R values of betaxolol, diltiazem, and nifedipine were 46 μM, 50 μM, and 0.17 μM, respectively, and K_I values were 5.1 μM, 1.2 μM, and 0.002 μM, respectively.

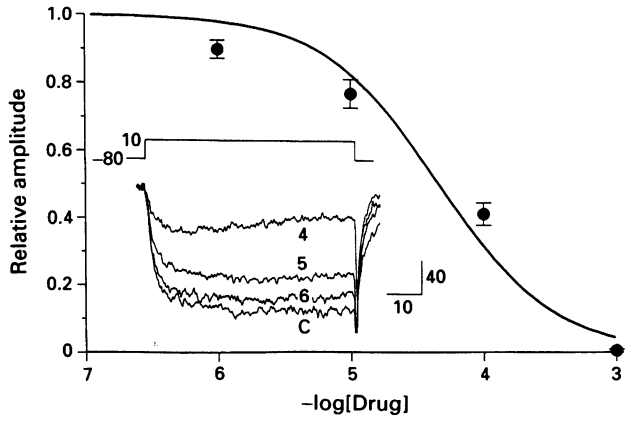

Figure 2 Dose-response relationship of action of betaxolol on the Ca^{2+} channel current in mesenteric artery cells. Relative amplitudes of the Ca^{2+} channel current evoked by a command potential of 10 mV (from a holding potential of −80 mV) are plotted against the betaxolol concentration. A control amplitude (before application of betaxolol) was normalized as 1.0. A continuous curve was obtained by fitting data to the Michaelis-Menten equation: $I_{drug}/I_{control} = 1/(1+[drug]/K_d)$, where I_{drug} is the current amplitude recorded with a certain concentration of drug. $I_{control}$ is the current amplitude recorded before application of the drug, and K_d is a dissociation constant (46 μM). Each point represents the mean ± s.e. of 6 to 9 values. Inset, currents recorded before (c) and after application of 1 μM (6), 10 μM (5), and 100 μM (4) betaxolol are superimposed. Currents were evoked by a command potential of 10 mV from a holding potential of −80 mV. The scales are 40 pA (vertical) and 10 ms (horizontal).

Discussion

The main finding of the present study was that betaxolol inhibited Ca^{2+} channel currents recorded in single smooth muscle cells from guinea-pig mesenteric artery and portal vein. The mode of inhibitory action of betaxolol was similar to that of Ca^{2+} antagonists such as diltiazem and nifedipine.

Betaxolol has two racemic forms. As a β-adrenoceptor antagonist, (+)-betaxolol has one-tenth the effect of (−)-betaxolol or (±)-betaxolol (Bessho H., personal communication). In contrast, the two isomers had the same potency in inhibiting Ca^{2+} channels in the present study. In addition, propranolol had no effect on Ca^{2+} channel currents. These results suggested that the inhibition of Ca^{2+} channel currents by betaxolol was due to a direct effect on Ca^{2+} channels and was independent of the β-adrenoceptor.

In the present study, diltiazem and nifedipine (1) inhibited Ca^{2+} channel currents in a frequency-dependent fashion (use-dependent block); (2) shifted the steady-state inactivation curve in a negative direction; and (3) accelerated the decay of the Ba^{2+} current. These characteristics were similar to those reported in cardiac and smooth muscle cells using the whole-cell clamp method (Lee & Tsien, 1983; Sanguinetti & Kass, 1984; Bean, 1984; Terada *et al.*, 1987).

Betaxolol showed a use-dependent block of Ca^{2+} channels similar to diltiazem and nifedipine, i.e. the repetitive depolarization with high frequency potentiated the current inhibition. Betaxolol shifted the steady-state inactivation curve in a negative direction; thus, the inhibition was more potent at a more depolarized holding potential. This result can be understood by postulating that betaxolol binds with a high affinity to the inactivated channels and with a low affinity to the resting channels, as suggested for Ca^{2+} antagonists and local anaesthetic drugs (Bean, 1984). In addition,

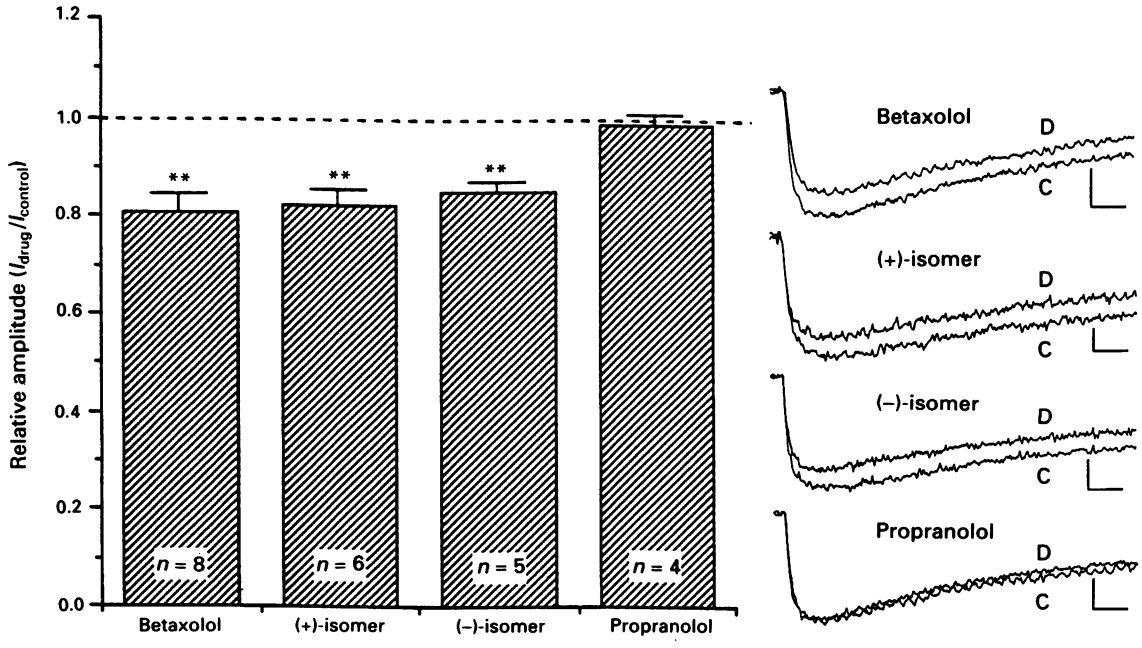

Figure 3 Inhibition of the Ca^{2+} channel current by betaxolol, its two racemates and propranolol in portal vein cells. Columns show relative amplitudes in the presence of 10 μM drugs (mean ± s.e.). Amplitude before application of the drug was normalized as 1.0. $^{**}P<0.01$ compared with 1.0. Insets, current traces before (C; control) and after (D; drug) application of 10 μM drug, which were evoked by voltage step-up from −60 mV to 0 mV. The scales are 40 pA (vertical) and 10 ms (horizontal).

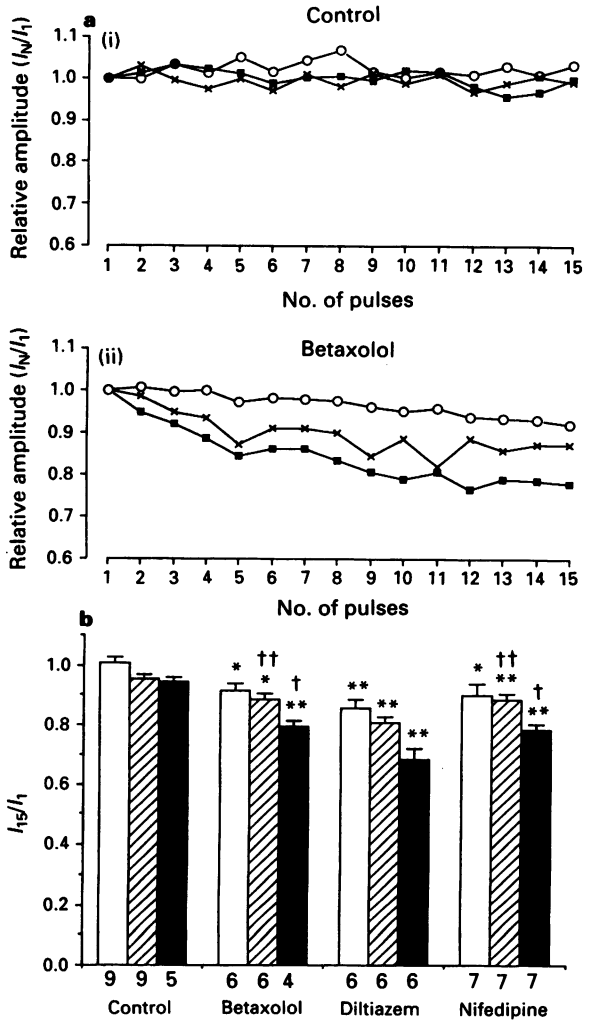

Figure 4 Effect of repetitive depolarizations on the amplitude of the currents. (a) The graphs plot the relative amplitude of Ca^{2+} channel current during a series of step pulses at the frequency of 0.3 Hz (○), 1 Hz (×), and 2 Hz (■). (i) Control; (ii) 10 μM betaxolol. The amplitude of current evoked by the first pulse was normalized as 1.0. The Ca^{2+} channel current was elicited by 70 ms command pulses to 10 mV from a holding potential of −80 mV. (b) Columns show mean ± s.e. of 4 to 9 experiments for relative amplitude of current evoked by the 15th pulse of repetitive depolarizations at 0.3 Hz (open column), 1 Hz (hatched column), and 2 Hz (solid column). $*P<0.05$, $**P<0.01$ compared with control, $\dagger P<0.05$, $\dagger\dagger P<0.01$ compared with diltiazem.

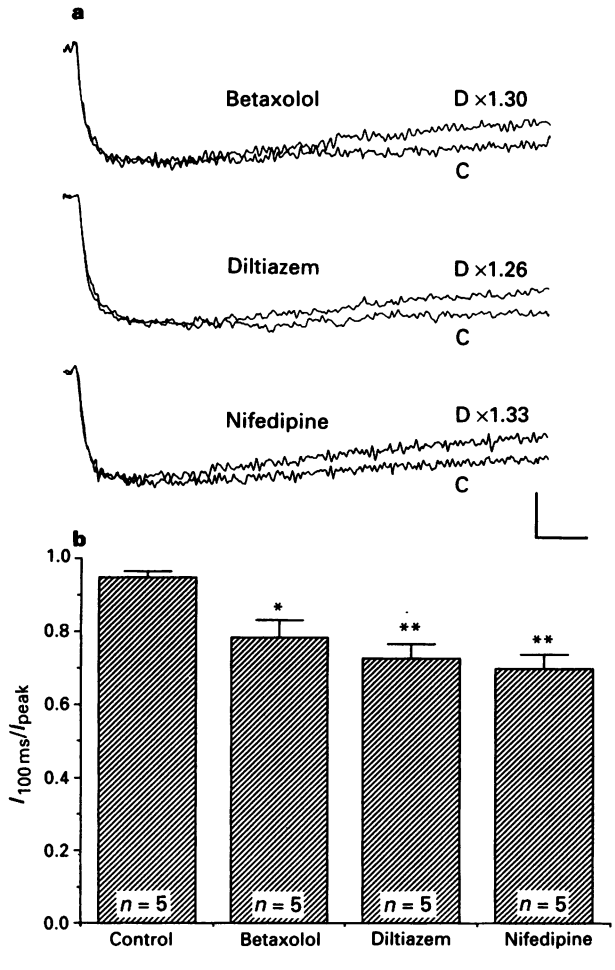

Figure 5 (a) Comparison of the current decay over 100 ms with the absence (C; control) and the presence of drugs (D; drug) in mesenteric artery cells. The drug trace is magnified so that the peak amplitudes of the traces before and after drug are matched. Magnification of the traces with betaxolol, diltiazem and nifedipine are 1.30, 1.26, and 1.33, respectively. Horizontal scale indicates 10 ms. Vertical scale for control currents is 40 pA. (b) Columns show relative amplitudes after 100 ms ($I_{100\,ms}/I_{peak}$) (mean ± s.e.). Currents were evoked by a command potential of 10 mV from a holding potential of −80 mV. Bath solution contained 10 mM Ba^{2+}. $*P<0.05$ and $**P<0.01$ compared with control.

betaxolol accelerated the decay of the Ba^{2+} current. This result suggests that betaxolol may also have a high affinity for the open state of Ca^{2+} channels. The above observations suggest that betaxolol shares several fundamental characteristics with Ca^{2+} antagonists such as diltiazem and nifedipine and with other Ca^{2+} antagonists reported previously (Terada *et al.*, 1987, Kuga *et al.*, 1990). To clarify which kinetic properties of the Ca^{2+} channels are modified by betaxolol, further studies such as the single channel-recording are required.

The inhibition of Ca^{2+} channel currents by betaxolol was larger at the higher command potentials. This observation may suggest that betaxolol acted on Ca^{2+} channels voltage-dependently. This command-potential dependency of the current inhibition may also be understood by the presence of T-type current which is resistant to Ca^{2+} antagonists (Ohya & Sperelakis, 1989; Kuga *et al.*, 1990). If the T-type current was also resistant to betaxolol, the current inhibition was decreased at negative command potentials where the T-type current was evoked.

Acute application of β-adrenoceptor antagonists without intrinsic sympathomimetic activity initially increases peripheral resistance, while chronic administration decreases it. It has been reported that intravenous injection of betaxolol decreased the peripheral resistance in anaesthetized dogs (Satoh *et al.*, 1990) and hypertensive rats (Bessho *et al.*, 1990). Since injection of other β-adrenoceptor antagonists such as propranolol or atenolol did not decrease the peripheral resistance, betaxolol may directly affect the peripheral vascular bed via a mechanism independent of β-adrenoceptor inhibition.

The antihypertensive effect of betaxolol in clinical use has been observed at plasma concentrations of 0.03 μM to 0.15 μM in the literature (Warrington & Turner, 1980; Beresford & Heel, 1986). In the present study, betaxolol inhibited Ca^{2+} channels in the resting state and inactivated state with a K_d of about 50 μM and about 5 μM, respectively. Since betaxolol is lipophilic (Beresford & Heel, 1986), betaxolol may accumulate in the cell membrane when chronically administered, as do other lipophilic drugs. Mason *et al.* (1991) showed that the intrinsic affinities of some lipophilic drugs for their receptor sites were over 3 orders of magnitude greater than that predicted from an aqueous equilibrium

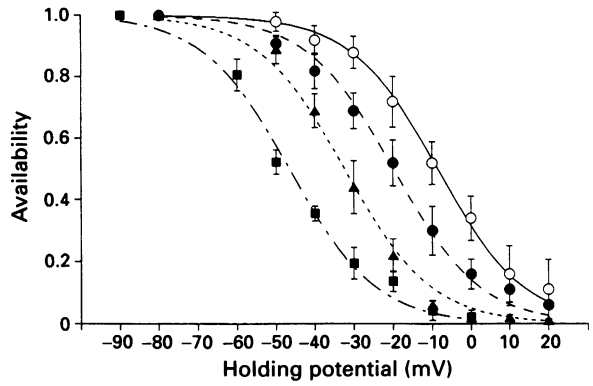

Figure 6 Steady-state inactivation curves obtained in the absence (○) and presence of 10 μM betaxolol (●), 10 μM diltiazem (▲) and 0.1 μM nifedipine (■). Conditioning pulse for 10 s at various amplitudes was applied before a test pulse to 0 mV. Amplitude of the current evoked by the test pulse was normalized by that evoked without the conditioning potential. Normalized amplitude (availability) is plotted against the conditioning potential. Each point represents the mean ± s.e. of 3 to 8 values. Four curves were obtained by fitting data to the Boltzman distribution: $P = 1/[1+\exp\{(V-V_h)/k\}]$, where P is the availability, V is the conditioning potential, V_h is the potential required for half-inhibition of the current, and k is the Boltzman coefficient. The V_h of control, betaxolol, diltiazem and nifedipine were -8 ± 4 mV ($n = 6$), -20 ± 4 mV ($n = 6$), -32 ± 3 mV ($n = 6$), and -47 ± 1 mV ($n = 8$), respectively, and the k value was 11 mV in all groups. The shifts of the steady-state inactivation curve by the drugs were significantly different from one another ($P<0.05$).

constant. If the concentration of betaxolol around Ca^{2+} channels in the cell membrane was higher than that in plasma, betaxolol at the thereapeutic dose may inhibit Ca^{2+} channels in the vascular tissues as well as blocking β-adrenoceptors.

In conclusion, betaxolol exhibited the profile of a Ca^{2+} antagonist in the voltage-clamp study using single vascular smooth muscle cells. This property was independent of the β-adrenoceptor inhibition. Whether this Ca^{2+} antagonistic action of betaxolol could be involved in its therapeutic action should be further tested.

We thank Yoshitomi Pharm. Co., Ltd., Osaka, Japan, and Mitsubishi Kasei Co. Ltd., Tokyo, Japan, for providing betaxolol hydrochloride and its two isomers, and Bayer Pharm. Co., Ltd., Osaka, Japan, for providing nifedipine. This work was partly supported by grants from the Ministry of Education, Science, and Culture, Japan.

References

BEAN, B.P. (1984). Nitrendipine block of cardiac calcium channels: High-affinity binding to the inactivated state. *Proc. Natl. Acad. Sci. U.S.A.*, **81**, 6388–6392.

BERESFORD, R. & HEEL, R.C. (1986). Betaxolol, a review of its pharmacodynamic and pharmacokinetic properties and therapeutic efficacy in hypertension. *Drugs*, **31**, 6–28.

BESSHO, H., SUZUKI, J., NARIMATSU, A. & TOBE, A. (1990). Antihypertensive effect of betaxolol, a cardioselective β-adrenoceptor antagonist, in experimental hypertensive rats. (in Japanese, abstract in English) *Nippon Yakurigaku Zasshi*, **95**, 347–354.

BESSHO, H., SUZUKI, J. & TOBE, A. (1991). Vascular effects of betaxolol, a cardioselective β-adrenoceptor antagonist, in isolated rat arteries. *Jpn. J. Pharmacol.*, **55**, 351–358.

HAMILL, O.P., MARTY, A., NEHER, E., SAKMANN, B. & SIGWORTH, F.J. (1981). Improved patch-clamp techniques for high-resolution current recordings from cell and cell-membrane patches. *Pflügers Arch.*, **391**, 85–100.

KUGA, T., SADOSHIMA, J., TOMOIKE, H., KANAIDE, H., AKAIKE, N. & NAKAMURA, M. (1990). Action of Ca^{2+} antagonists on two types of Ca^{2+} channels in rat aorta smooth muscle cells in primary culture. *Circ. Res.*, **67**, 469–480.

LEE, K.S. & TSIEN, R.W. (1983). Mechanism of calcium channel blockade by verapamil, D600, diltiazem and nitrendipine in single dialysed heart cells. *Nature*, **302**, 790–794.

MASON, R.P., RHODES, D.G. & HERBETTE, L.G. (1991). Reevaluating equilibrium and kinetic binding parameters for lipophilic drugs based on a structural model for drug interaction with biological membranes. *J. Med. Chem.*, **34**, 869–877.

OHYA, Y., ABE, I., FUJII, K., TAKATA, Y. & FUJISHIMA, M. (1993). Voltage-dependent Ca^{2+} channels in resistance arteries from spontaneously hypertensive rats. *Circ. Res.*, **73**, 1090–1099.

OHYA, Y. & SPERELAKIS, N. (1989). ATP regulation of the slow calcium channels in vascular smooth muscle cells of guinea pig mesenteric artery. *Circ. Res.*, **64**, 145–154.

SANGUINETTI, M.C. & KASS, R.S. (1984). Voltage-dependent block of calcium channel current in the calf cardiac Purkinje fiber by dihydropyridine calcium channel antagonists. *Circ. Res.*, **55**, 336–348.

SATOH, N., SUZUKI, J., BESSHO, H., KITADA, Y., NARIMATSU, A. & TOBE, A. (1990). Effects of betaxolol on cardiohemodynamics and coronary circulation in anesthetized dogs: Comparison with atenolol and propranolol. *Jpn. J. Pharmacol.*, **54**, 113–119.

TERADA, K., NAKAO, K., OKABE, K., KITAMURA, K. & KURIYAMA, H. (1987). Action of the 1,4-dihydropyridine derivative, KW-3049, on the smooth muscle membrane of the rabbit mesenteric artery. *Br. J. Pharmacol.*, **92**, 615–625.

WARRINGTON, S.J. & TURNER, P. (1980). Blood concentrations and pharmacodynamic effects of betaxolol (SL 75212), a new β-adrenoceptor antagonist, after oral and intravenous administration. *Br. J. Clin. Pharmacol.*, **10**, 449–452.

(Received June 6, 1994
Revised December 28, 1994
Accepted January 23, 1995)

British Journal of Pharmacology (1995) 115, 203-209

Drug-induced defaecation in rats: role of central 5-HT_{1A} receptors

[1]Tiziano Croci, Marco Landi, [2]Alberto Bianchetti & Luciano Manara

SANOFI-MIDY S.p.A. Research Center, Via G.B. Piranesi 38, 20137 Milan, Italy

1 We investigated the acute effects of 5-hydroxytryptamine (5-HT), and of the 5-HT_{1A} receptor agonists, 8-hydroxy-2-(di-n-propylamino)tetralin (8-OH-DPAT), buspirone and SR 57746A, on rat faecal pellet output and water content.

2 5-HT, 8-OH-DPAT, buspirone and SR 57746A, a new selective 5-HT_{1A} receptor agonist, displaced [^{3}H]-8-OH-DPAT from specific binding sites in rat hippocampus membranes (K_i, nM: 1.8, 1.2, 15, 3.1 respectively) and stimulated rat defaecation dose-dependently. SR 57746A and buspirone induced 1 g dry weight of faeces at 1.3 and 6.1 mg kg^{-1}, p.o. (AD_1) respectively. 8-OH-DPAT and 5-HT stimulated defaecation after s.c. injection (AD_1, 0.07 and 7.5 mg kg^{-1}, respectively). All these agents increased faecal water content.

3 The putative 5-HT_{1A} receptor antagonist, pindolol, injected s.c. or i.c.v., significantly reduced the defaecation induced by systemically administered 8-OH-DPAT, buspirone or SR 57746A, but not 5-HT.

4 Pretreatment with *p*-chlorophenylalanine (i.p.) or 5,7-dihydroxytryptamine (i.c.v.), according to protocols designed to cause either generalized or CNS-limited 5-HT depletion respectively, also reduced the defaecation induced by buspirone or SR 57746A.

5 No specific 5-HT_{1A} binding sites could be labelled by incubating rat colon membranes with [^{3}H]-8-OH-DPAT, and *in vitro* preparations of rat colon segments showed no response to 8-OH-DPAT or SR 57746A up to 5 μM.

6 After eight days' repeated daily treatment, complete tolerance developed to the stimulant effects of SR 57746A and buspirone on faecal water content, but not on faecal pellet output. This suggests that faecal mass excretion and water exchange through the gut wall are affected by independent mechanisms.

7 The present findings support the involvement of central 5-HT_{1A} receptors in intestinal propulsion and regulation of luminal fluid content, presumably accounting for the drug-induced defaecation in rats.

Keywords: Defaecation; 5-HT_{1A} receptor; faecal water content; buspirone; 8-OH-DPAT; SR 57746A; 5-HT

Introduction

The role of 5-hydroxytryptamine (5-HT) in the regulation of intestinal motor activity and endoluminal fluid content has long been recognized (Costa & Furness, 1979; Costa *et al.*, 1982). However, the underlying mechanisms are still largely unknown. In the gut 5-HT may affect motility either directly by stimulating smooth muscle receptors (Buchheit *et al.*, 1985) or indirectly through enteric 5-hydroxytryptaminergic interneurones, which modulate the intestinal peristaltic reflex by releasing other neurotransmitters (Costa *et al.*, 1982; Buchheit *et al.*, 1985; De Ponti *et al.*, 1991). 5-HT itself is highly concentrated in enterochromaffin cells and can be released by appropriate stimuli into the portal circulation or gut lumen (Racke & Schworer, 1991), thus influencing fluid balance and intestinal motility.

Gut motility is under the influence of the central nervous system (CNS) which may affect the intrinsic automaticity of the enteric nervous system through efferent pathways. Although different gut-located 5-HT receptor subtypes are certainly involved in the modulation of intestinal motility and secretion (Costall & Naylor, 1990), the role of CNS 5-HT in enteric functions is virtually unknown.

In a preliminary study, we found that putative 5-HT_{1A} receptor agonists, reportedly active as central antidepressant and anxiolytic drugs (Goa & Ward, 1986; Traber & Glaser, 1987; Robinson *et al.*, 1989; Jenkins *et al.*, 1990; Cervo *et al.*, 1994) stimulated faecal excretion by rats (Croci *et al.*, 1990a,b; Bianchetti *et al.*, 1990; 1991). The present work was aimed at clarifying the importance of central 5-HT_{1A} receptors in the effects on faecal output and water content of 8-hydroxy-2-(di-n-propylamino)tetralin (8-OH-DPAT), buspirone and the potent, selective new 5-HT_{1A} receptor agonist SR 57746A (4-(3-trifluoromethylphenyl)-*N*-[2-(naphth-2-yl)-ethyl]-1,2,3,6-tetrahydropyridine HCl) (Bachy *et al.*, 1993).

Methods

Male Crl:CD BR (Charles River Italia) rats weighing 220 ± 20 g were used, handled according to internationally accepted principles for the care and use of laboratory animals (E.E.C. Council directive 86/609, OJ L358, 1, Dec. 12, 1987). Rats were humanely killed by cervical dislocation.

Faecal excretion

Faecal excretion was assessed according to the method described by Croci & Bianchetti (1992). On the day of the experiment, the rats were placed individually in grid-floor cages, with food and water *ad libitum*, and randomly allocated to different treatments. The food was withdrawn at 08 h 00 min and 3 h later the animals were given one of the following drugs in 2 ml kg^{-1} of the appropriate vehicle: 5-HT or 8-OH-DPAT dissolved in saline, SR 57746A or buspirone suspended in 0.5% carboxymethylcellulose (CMC). Drug-free control rats received only the vehicles (each animal was given s.c. saline and p.o. CMC).

Immediately after treatment, gentle thumb pressure was applied to the perianal region to expel faecal pellets from the rectum. The pellets discharged during the next 90 min (s.c.

[1] Author for correspondence.
[2] Present address: PHARMACIA, Farmitalia Carlo Erba; Preclinical Research, Via Giovanni XXIII 23, 20014 Nerviano, Italy.

treatment) or 210 min (oral treatment) were collected and weighed immediately (wet weight) and after drying (10 h at 50°C) to constant weight (dry weight). The doses inducing 1 g (dry weight) faecal excretion (AD_1) were extrapolated from log-dose response-curves (Finney, 1964). Action on secretion and/or reabsorption of fluids was assessed from the ratio of wet to dry faecal weight. For drug-free controls this was obtained from the weights of the faeces excreted by all rats in the 2–3 h before treatment, since control rats generally did not defaecate during the 90 or 210 min observation period.

Antagonism of faecal excretion stimulated by 5-hydroxytryptamine receptor agonists was assessed after either s.c. (2 ml kg^{-1}) or i.c.v. (10 µl/rat) pindolol, according to the protocols described in the Tables.

To deplete brain 5-HT, rats were treated with i.c.v. 5,7-dihydroxytryptamine (5,7-DHT) following the procedure described by Carli *et al.* (1989), or i.p. *p*-chlorophenylalanine (*p*CPA) according to Hutson *et al.* (1987).

Rats anaesthetized with ethyl-ether were immobilized in a Kopf stereotaxic instrument. 5,7-DHT dissolved in 0.1% ascorbic acid was infused (20 s) i.c.v. in a volume of 20 µl into the right lateral ventricle. The control animals received ascorbic acid only. To protect noradrenaline-containing neurones from the action of 5,7-DHT, the rats received desmethylimipramine, 25 mg kg^{-1}, i.p. 30 min before 5,7-DHT. These animals were used for faecal excretion experiments on the third day after 5,7-DHT. *p*CPA was injected daily for three consecutive days and rats were used for faecal excretion experiments 24 h after the last injection.

To assess whether the acute effects on faecal output and water content changed after repeated treatment with 5-HT$_{1A}$ receptor agonists, rats were treated daily at 11 h 00 min with buspirone, SR 57746A or CMC for eight consecutive days. Faecal excretion (wet and dry weight of faeces) was assessed daily as described above.

Statistical analysis was based on ANOVA plus Duncan's test (Kramer, 1956).

Binding assays

Radioligand binding assays with [^{3}H]-8-OH-DPAT were carried out either on rat hippocampus previously frozen and stored at −20°C or on fresh rat distal colon segments (5–6 cm) taken 10 cm from the ileo-caecal junction. Membranes from rat hippocampus or colon were prepared according to Bennett & Snyder (1976) or Landi *et al.* (1992) respectively.

The membrane preparation, containing about 2 mg protein ml^{-1}, was used immediately for binding experiments. Protein was assayed according to Lowry *et al.* (1951) with bovine serum albumin as standard.

In both preparations (colon and hippocampus), the binding assay for [^{3}H]-8-OH-DPAT (180–264 Ci mmol^{-1}, radiochemical purity > 98%) was run in triplicate at 25°C for 30 min incubation. Samples contained 500 µl membrane suspension and 1 nM [^{3}H]-8-OH-DPAT in a total volume of 1 ml. The compounds tested for competition with the binding of the radiolabelled ligand were dissolved in distilled water or ethanol; the ethanol concentration in the assay (10 µl ml^{-1}) did not affect binding.

Incubation of samples was started by the addition of membranes and stopped by rapid vacuum filtration through Whatman GF/B filters, followed by two consecutive 5-ml cold Tris-HCl (50 mM, pH 7.4) washes on a Brandel Cell Harvester. The [^{3}H]-8-OH-DPAT bound was measured by liquid scintillation spectrometry in a Beckman LS 6000IC beta counter. Non-specific binding was determined in the presence of 10 µM 5-HT. In the hippocampus, specific binding was calculated as the difference between total and non-specific binding, and accounted for 85–90% of the total.

Data were plotted and analysed according to published procedures (Scatchard, 1949). Saturation curves were fitted to a one-site model, using a non-linear regression computer programme, Accufit Saturation (Beckman, London Software). The inhibitory constant (K_i) was calculated according to Cheng & Prusoff (1973) while the IC_{50} was obtained by converting the binding data to logits and plotting them against the log of the inhibitor concentration to obtain linear regression (Finney, 1964).

Isolated distal colon preparation

Rat distal colon segments (about 5 cm, 2 cm from the rectum) were carefully dissected and mounted in a 20 ml organ bath containing warm (32°C) aerated (100% O_2) Tyrode solution of the following composition, mM: NaCl 136.9, KCl 2.68, $MgCl_2$ 1.05, $CaCl_2$ 1.82, NaH_2PO_4 0.417, $NaHCO_3$ 11.9, glucose 5.5. The tissue was stretched with a weight of 0.5 g and tonic contractions elicited by 5-HT were recorded isotonically and scored as the percentage of maximal effect. After 60 min equilibration, 5-HT or the 5-HT$_{1A}$ receptor agonists were added, the concentrations being increased stepwise. Only one cumulative curve was obtained for each preparation (contact time for each concentration 3 to 5 min). The concentration of 5-HT (EC_{50}) raising tonus by 50% over the basal value was extrapolated from the regression lines obtained by plotting log-concentration against response.

Chemicals

The following drugs were purchased from commercial sources: Sigma-Aldrich Corp., St-Louis, Missouri, U.S.A., buspirone HCl, (±)-pindolol, *p*CPA, 5,7-DHT, carbachol, 5-HT creatinine sulphate, pargyline; RBI, Natick, Ma, U.S.A., 8-OH-DPAT HBr, ketanserin; Amersham, Buckinghamshire, England, [^{3}H]-8-OH-DPAT. Mesulergine was kindly provided by Sandoz Pharma, Switzerland and desmethylimipramine HCl by Ciba-Geigy, Varese, Italy.

SR 57746A was synthesized in the Chemistry Section of the SANOFI-MIDY S.p.A. Research Centre, Milan, Italy.

Results

Binding of drugs acting at 5-HT receptors

In hippocampal membranes [^{3}H]-8-OH-DPAT bound saturably with an affinity constant (K_d) of 0.9 ± 0.2 nM and a B_{max} of 185 ± 22 fmol mg^{-1} protein (mean ± s.e.mean of three experiments), as revealed by saturation analysis with eight concentrations of [^{3}H]-8-OH-DPAT ranging from 0.125 to 16 nM. Binding was rapid, reversible and stable for at least 60 min. [^{3}H]-8-OH-DPAT specific binding to hippocampal membranes was competitively inhibited by the 5-HT receptor agonists, 5-HT, 8-OH-DPAT, SR 57746A and buspirone; the K_i (nM, 95% confidence limits) were 1.8 (1.7–1.9), 1.2 (1–1.5), 3.1 (2.9–3.4) and 15 (13–16), in that order. The putative 5-HT$_{1A}$ receptor antagonist, pindolol also competed for [^{3}H]-8-OH-DPAT binding sites with high affinity, K_i 36 (31–41) nM. The slope of the Hill plot was never significantly different from unity.

No specific binding could be detected in rat distal colon membranes incubated with [^{3}H]-8-OH-DPAT (1 nM).

Stimulation of faecal excretion by 5-HT$_{1A}$ receptor agonists

Table 1 shows the dose-related effects of 5-HT$_{1A}$ receptor agonists and 5-HT on rat faecal excretion. After s.c. injection, 8-OH-DPAT was about 100 times more potent than 5-HT in inducing defaecation (AD_1 0.07 and 7.5 mg kg^{-1} respectively) and increasing the faecal water content, as indicated by the higher than control ratios of wet to dry weights. However, 8-OH-DPAT (1 mg kg^{-1}) and 5-HT (12 mg kg^{-1}) were completely inactive when given orally (faecal dry weights, g ± s.e.mean, 0.08 ± 0.03 and 0.02 ± 0.02

Table 1 Effects of 5-HT, 8-OH-DPAT, buspirone and SR 57746A on rat defaecation

		Dose (mg kg^{-1})	*Faecal dry weight* (g)	*AD$_1$*[a] (mg kg^{-1})	*Wet/dry weight of faeces*
Control		–	0.01 ± 0.01		1.98 ± 0.05[b]
5-HT	s.c.	4	0.80 ± 0.04**		3.43 ± 0.13**
		12	1.17 ± 0.05**	7.5	3.16 ± 0.11**
		36	1.36 ± 0.05**	(5.9–9.8)	3.60 ± 0.13**
8-OH-DPAT	s.c.	0.0125	0.46 ± 0.16*		2.44 ± 0.15**
		0.05	0.76 ± 0.15**	0.07	2.37 ± 0.11**
		0.2	1.59 ± 0.10**	(0.04–0.12)	2.63 ± 0.12**
Buspirone	p.o.	1	0.18 ± 0.08		NE[c]
		4	0.75 ± 0.09**	6.1	2.41 ± 0.17*
		16	1.54 ± 0.12**	(4.7–7.7)	2.69 ± 0.11**
SR 57746A	p.o.	0.25	0.41 ± 0.09*		NE[c]
		1	0.64 ± 0.12**	1.3	2.30 ± 0.12*
		4	1.56 ± 0.15**	(0.5–3.1)	2.73 ± 0.05**

[a]AD$_1$: dose inducing excretion of 1 g (dry weight) of faeces during 90 min (s.c.) or 210 min (p.o.) after drugs.
[b]Faeces collected 2–3 h before treatment.
[c]Not evaluable.
Data are mean ± s.e.mean from 8 rats. In parentheses 95% confidence limits. Control (drug-free) rats received only vehicles (saline and CMC). See Methods for details. *$P<0.05$, **$P<0.01$ vs control (Duncan's test).

respectively). SR 57746A and buspirone were both effective orally, the former being about five times more potent (Table 1). 8-OH-DPAT (1 μg/rat, i.c.v.) caused the excretion of 0.8 ± 0.1 g of faeces during the 30-min collection time. All agents significantly increased the wet/dry weight ratio of faeces.

Prevention of 5-HT$_{1A}$ receptor agonist-induced faecal excretion by pindolol

As shown in Table 2, pindolol (1 or 5 mg kg^{-1}, s.c.) significantly prevented defaecation and the increase of the wet/dry weight ratio of faeces induced by 8-OH-DPAT (0.2 mg kg^{-1}, s.c.), SR 57746A (4 mg kg^{-1}, p.o.), or buspirone (12 mg kg^{-1}, p.o.), but not by 5-HT (12 mg kg^{-1}, s.c.). In rats chronically implanted with cannulae, given pindolol i.c.v. (1 or 2.5 μg/rat), faecal excretion (dry weight) induced by SR 57746A or 8-OH-DPAT, but not by 5-HT, was likewise prevented (Table 3). Unlike its effect when given s.c., the i.c.v. administration of pindolol (a) slightly but significantly increased faecal output and (b) did not prevent the increase in faecal water content induced by the 5-HT$_{1A}$ receptor agonists (Table 3).

Effect of 5,7-DHT and p*CPA on drug-induced faecal excretion*

As shown in Tables 4 and 5, in rats pretreated with *p*CPA (160 mg kg^{-1} per day i.p. for three days) or 5,7-DHT (150 μg/rat i.c.v.), SR 57746A and buspirone were less effective in promoting the excretion of faeces (dry weight), although the wet/dry weight ratio was still as high as in non-pretreated animals. However, pretreatment with either *p*CPA or 5,7-DHT by themselves significantly raised the wet:dry weight ratio (Tables 4, 5). Rats given *p*CPA or 5,7-DHT also had lower body weight than untreated controls (about 25 g). In the same experiments, in additional groups of rats pretreated with *p*CPA or 5,7-DHT the scores for which are not presented in the Tables, the cholinomimetic carbachol (0.2 mg kg^{-1}, s.c.) was as effective in promoting defaecation as in non-pretreated animals (dry weight of faeces, g ± s.e.mean: carbachol, 1.14 ± 0.16; *p*CPA + carbachol, 0.89 ± 0.18; 5,7-DHT + carbachol, 1.0 ± 0.2). Carbachol also increased the wet/dry weight ratio of faeces but this was not affected by *p*CPA pretreatment.

Table 2 Antagonism of 5-HT, 8-OH-DPAT, buspirone and SR 57746A-induced rat defaecation by s.c. pindolol

	Pindolol dose (mg kg^{-1})	*Faecal dry weight* (g)	*Wet/dry weight of faeces*
Control	–	0.03 ± 0.03	1.88 ± 0.07[a]
–	1	0.06 ± 0.05	NE[b]
–	5	0.02 ± 0.02	NE[b]
5-HT	–	1.31 ± 0.15**	3.05 ± 0.06**
	1	1.05 ± 0.10**	2.92 ± 0.10**
8-OH-DPAT	–	1.60 ± 0.11**	2.65 ± 0.09**
	1	0.34 ± 0.13*^{OO}	2.01 ± 0.10^{OO}
	5	0.16 ± 0.06^{OO}	NE[b]
Buspirone	–	1.73 ± 0.09**	2.79 ± 0.07**
	1	1.23 ± 0.09**^{OO}	2.66 ± 0.07**
	5	0.20 ± 0.08*^{OO}	2.06 ± 0.06^{OO}
SR 57746A	–	1.75 ± 0.06**	2.60 ± 0.08**
	1	1.24 ± 0.08**^{OO}	2.60 ± 0.07**
	5	0.17 ± 0.07^{OO}	1.85 ± 0.09^{OO}

[a]Faeces collected 2–3 h before treatment. [b]Not evaluable.
Data are mean ± s.e.mean from 8 rats. 5-HT (12 mg kg^{-1}, s.c.) and 8-OH-DPAT (0.2 mg kg^{-1}, s.c.) were given 30 min after pindolol and buspirone (12 mg kg^{-1}, p.o.) and SR 57746A (4 mg kg^{-1}, p.o.) immediately after. Control (drug-free) rats received only vehicles (saline and CMC). See Methods for details.
*$P<0.05$, **$P<0.01$ vs control; $^{OO}P<0.01$ vs 8-OH-DPAT, buspirone or SR 57746A alone (Duncan's test).

Effect of repeated treatment with 5-HT$_{1A}$ receptor agonists on faecal excretion

Throughout repeated oral treatment (8 days) with either buspirone (4 or 16 mg kg^{-1}) or SR 57746A (1 or 4 mg kg^{-1}), stimulation of faeces excretion was dose-related with no real difference between the results on any given day in terms of faecal dry weight (Figure 1) and faecal pellet number (data not shown). During the first four days of treatment with either compound, some rats (10 to 30%) presented loose stools, especially at the higher doses. This was no longer apparent as treatment continued. The ratio of wet to dry weight of faeces after the first dose was always considerably higher than in drug-free controls, but tolerance developed

within a few days (days 5 to 6 for buspirone and 2 to 5 for SR 57746A depending on the dose) and the wet/dry weight of faeces returned to drug-free ratios. The body weight increase of rats on the 8th day was not significantly different from controls in the buspirone or SR 57746A groups (Δ g ± s.e.mean: buspirone 4 and 16 mg kg^{-1}, 40 ± 3 and 39 ± 2; SR 57746A 1 and 4 mg kg^{-1}, 40 ± 2 and 38 ± 3; controls, 41 ± 3).

Table 3 Antagonism of 5-HT, 8-OH-DPAT, buspirone and SR 57746A-induced rat defaecation by i.c.v. pindolol

	Pindolol dose (μg/rat)	*Faecal dry weight* (g)	*Wet/dry weight of faeces*
Control	–	0.02 ± 0.02	1.86 ± 0.10[a]
–	1	0.20 ± 0.07*	NE[b]
–	2.5	0.41 ± 0.12**	2.90 ± 0.06
5-HT	–	1.48 ± 0.13**	2.85 ± 0.08**
	1	1.24 ± 0.10**	2.92 ± 0.10**
	–	1.83 ± 0.06**	2.75 ± 0.08**
8-OH-DPAT	1	0.42 ± 0.03**^{OO}	2.91 ± 0.10**
	2.5	0.42 ± 0.09**^{OO}	3.00 ± 0.13**
	–	1.82 ± 0.15**	2.76 ± 0.07**
SR 57746A	1	0.70 ± 0.14**^{OO}	2.78 ± 0.09**
	2.5	1.11 ± 0.10**^{O}	2.85 ± 0.11**

[a]Faeces collected 2–3 h before treatment. [b]Not evaluable. Average faecal excretion (g ± s.e.mean) from at least 12 rats. Pindolol in a volume of 10 μl/rat was given i.c.v. concurrently with 5-HT (12 mg kg^{-1}, s.c.) and 8-OH-DPAT (0.2 mg kg^{-1}, s.c.) or 45 min after SR 57746A (4 mg kg^{-1}, p.o.). Control (drug-free) rats received only vehicles (saline and CMC). See Methods for details.
*$P<0.05$, **$P<0.01$ vs control; $^{O}P<0.05$, $^{OO}P<0.01$ vs SR 57746A or 8-OH-DPAT alone (Duncan's test).

Effect of 5-HT receptor agonists on isolated distal colon

The isolated colon preparation presented a low degree of spontaneous contractions. 5-HT induced a concentration-dependent increase of the basal tonus: EC_{50} = 130 (100–160) nM, that was partially prevented by the 5-HT$_2$ receptor antagonist, ketanserin and the 5-HT$_{1C}$ receptor antagonist, mesulergine, but not by pindolol. 8-OH-DPAT and SR 57746A up to 5 μM did not induce any contraction, or affect the tonus of the colon.

Discussion

Defaecation by rats is environmentally influenced and drugs can either increase or reduce it depending on experimental conditions (Sanberg *et al.*, 1989; Croci *et al.*, 1994). Our model is suitable for the evaluation of defaecation induced acutely by different agents, since control animals do not defaecate throughout the standard observation period (Croci & Bianchetti, 1992).

We investigated the effects of the 5-HT$_{1A}$ receptor agonists, 8-OH-DPAT, buspirone and SR 57746A, either *in vitro* on 5-HT$_{1A}$ binding and rat isolated colon contractility or *in vivo* on rat faecal pellet output and water content. SR 57746A bound to [^{3}H]-8-OH-DPAT-labelled rat hippocampal membranes at nanomolar concentrations and induced faecal excretion as did 8-OH-DPAT and buspirone, suggesting that 5-HT$_{1A}$ receptors are involved in their intestinal effects. Moreover 8-OH-DPAT and buspirone promoted defaecation at doses within the range of those reportedly effective in several behavioural and other *in vivo* functional tests (Kennet *et al.*, 1987; Cervo & Samanin, 1987; Moser *et al.*, 1990; Martin *et al.*, 1991). Activation of 5-HT$_{1A}$ receptors is further supported as a common mechanism for increasing faecal pellet output and water content, since both were prevented by pindolol at doses previously found to antagonize 5-HT$_{1A}$-mediated responses (Hjorth & Carlsson, 1986; Sharp *et al.*,

Table 4 Effect of *p*CPA on faecal excretion stimulated by buspirone or SR 57746A

	Dose (mg kg^{-1}, p.o.)	p*CPA*	*Faecal dry weight* (g)	*Wet/dry weight of faeces*
Control	–	–	0 ± 0	1.87 ± 0.03[a]
	–	+	0.04 ± 0.04	2.43 ± 0.12**[a]
Buspirone	12	–	1.84 ± 0.08**$^{\square\square}$	3.26 ± 0.11**$^{\square}$
	12	+	0.75 ± 0.19**$^{\square\square OO}$	2.69 ± 0.11**
SR 57746A	4	–	2.36 ± 0.12**$^{\square\square}$	3.03 ± 0.12**$^{\square}$
	4	+	0.40 ± 0.13*^{OO}	2.53 ± 0.24*

[a]Faeces collected 2–3 h before treatment.
Data are mean ± s.e.mean from at least 8 rats. *p*CPA (160 mg kg^{-1} per day) was injected i.p. daily for three consecutive days. Drugs were administered 24 h after the last *p*CPA injection. Control (drug-free) rats received only vehicles (saline and CMC). See Methods for details. *$P<0.05$, **$P<0.01$ vs control; $^{\square}P<0.05$, $^{\square\square}P<0.01$ vs *p*CPA alone; $^{O}P<0.05$, $^{OO}P<0.01$ vs SR 57746A or buspirone alone (Duncan's test)

Table 5 Effect of i.c.v. 5,7-DHT on faecal excretion stimulated by buspirone or SR 57746A

	Dose (mg kg^{-1}, p.o.)	*5,7-DHT*	*Faecal dry weight* (g)	*Wet/dry weight of faeces*
Control	–	–	0.02 ± 0.02	2.00 ± 0.09[a]
	–	+	0.04 ± 0.03	2.74 ± 0.10**[a]
Buspirone	12	–	2.01 ± 0.17**$^{\square\square}$	3.04 ± 0.11**
	12	+	1.30 ± 0.09**$^{\square\square OO}$	3.29 ± 0.18**
SR 57746A	4	–	2.22 ± 0.10**$^{\square\square}$	2.93 ± 0.10**
	4	+	1.21 ± 0.08**$^{\square\square OO}$	2.67 ± 0.12**

[a]Faeces collected 2–3 h before buspirone or SR 57746A.
Data are mean ± s.e.mean from at least 8 rats. Rats were injected concurrently with i.c.v. 5,7-DHT (150 μg/rat) and i.p. DMI (25 mg kg^{-1}) three days before drugs. Control (drug-free) rats received only vehicles (saline and CMC). See Methods for details. Faeces were collected for 210 min after buspirone or SR 57746A.
**$P<0.01$ vs control; $^{\square\square}P<0.01$ vs 5,7-DHT alone; $^{OO}P<0.01$ vs SR 57746A or buspirone alone (Duncan's test).

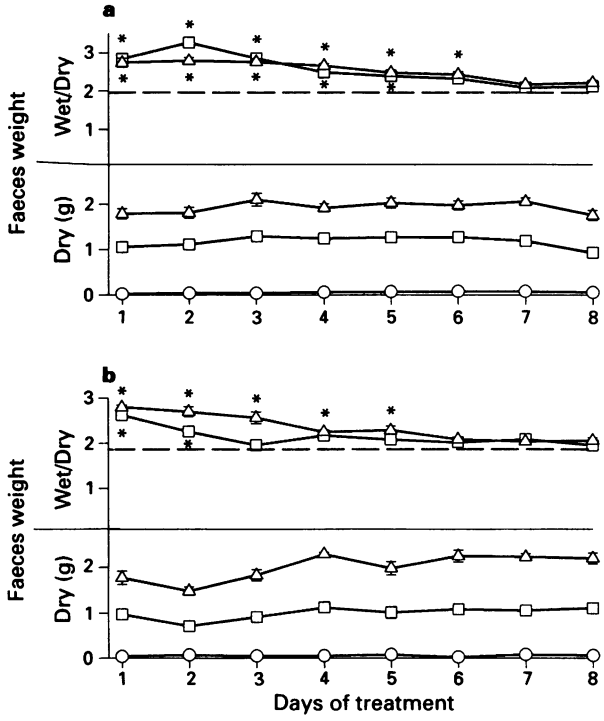

Figure 1 Effect of repeated daily oral doses of (a) buspirone (□, 4 mg kg^{-1}; △, 16 mg kg^{-1}) and (b) SR 57746A (□, 1 mg kg^{-1}; △, 4 mg kg^{-1}) on rat faecal pellet output (dry weight of faeces; ○, control) and water content (wet/dry weight of faeces). Data are mean ± s.e.mean from 10 rats in each experimental group. The mean ± s.e.mean of wet/dry weight of faeces in control rats (dotted line) was 1.96 ± 0.06 and 1.92 ± 0.05 for buspirone and SR 57746A respectively. *$P<0.01$ vs control (Duncan's test).

1993). It is worth noting that 5-HT acts peripherally on different 5-HT receptor subtypes (Croci *et al.*, 1990b) and indeed, in spite of its high affinity for 5-HT$_{1A}$ binding sites, it promotes faecal excretion at s.c. doses 100 times higher than 8-OH-DPAT.

The overall evidence produced by the present study certainly upholds the view that in rats, 5-HT$_{1A}$ receptor agonists promote defaecation by stimulating receptors in the CNS rather than peripherally in intestinal smooth muscle and/or myenteric plexus. Thus the representative 5-HT$_{1A}$ receptor agonist, 8-OH-DPAT, injected i.c.v., induced defaecation. We found no intestinal 5-HT$_{1A}$ sites, since there was no specific [^{3}H]-8-OH-DPAT binding in rat distal colon membranes and neither 8-OH-DPAT nor SR 57746A had any effect on the tonus of the isolated distal colon. This, however, was dose-dependently contracted by 5-HT, an effect partially prevented by the 5-HT$_{1C}$ and 5-HT$_2$ receptor antagonists mesulergine and ketanserin, but not by the putative 5-HT$_{1A}$ receptor antagonists, pindolol.

Pindolol i.c.v. significantly reduced the defaecation promoting effects of SR 57746A and 8-OH-DPAT, but not of 5-HT. This is unlikely to be a result of pindolol diffusing into the periphery because: (a) in an additional experiment (results not shown), the same dose of pindolol given i.v. was unable to prevent faecal excretion induced by 5-HT$_{1A}$ receptor agonists; (b) pindolol, i.c.v. or s.c., did not prevent the presumed peripheral action of 5-HT on defaecation. In addition, it is worth pointing out that the incomplete prevention of the defaecation promoting action of 5-HT$_{1A}$ receptor agonists by i.c.v. pindolol is inherent to its dose-dependent intrinsic agonist activity under these conditions, which is consistent with its otherwise mixed agonist-antagonist properties at central 5-HT$_{1A}$ receptors (Hjorth & Carlsson, 1986).

In rat brain, 5-HT$_{1A}$ receptors are located both pre- and postsynaptically where they subserve different functions (Tricklebank *et al.*, 1984; Goodwin *et al.*, 1985; 1986; Dourish *et al.*, 1986; Gilbert *et al.*, 1988). In the present study, the fact that pretreatment with i.c.v. 5,7-DHT or i.p. *p*CPA (both known to deplete 5-HT stores in the CNS) prevented buspirone- or SR 57746A-induced faecal excretion in rats suggests that presynaptic 5-HT$_{1A}$ receptors on central 5-hydroxytryptaminergic neurones are involved in the intestinal effects of these agonists. The fact that only the increase in dry weight of faeces, not in water content, was prevented to a greater extent in rats pretreated with 5,7-DHT or *p*CPA is accounted for by their ability to increase faecal water content on their own. Carbachol-induced faecal excretion was not prevented by pretreating rats with 5,7-DHT or *p*CPA, indicating the 5-HT specificity of their inhibition of drug-induced defaecation.

Buspirone or SR 57746A-induced faecal excretion was prevented more by *p*CPA than by 5,7-DHT. Although we did not measure the actual CNS and intestinal 5-HT depletion by these agents, with the protocols adopted 5,7-DHT (i.c.v.) should have depleted rat brain 5-hydroxytryptaminergic neurones by about 70% (Cervo & Samanin, 1987) while *p*CPA (i.p.) should deplete brain 5-HT by about 90% and 5-HT in the colon by about 50% (Weber, 1970). Thus greater central and/or peripheral 5-HT depletion could explain the more substantial prevention by *p*CPA of 5-HT$_{1A}$ receptor agonist-induced defaecation in our experiments. In addition SR 57746A was somewhat more susceptible than buspirone to both the 5-HT depleting agents. Since buspirone in rats is actively biotransformed into the α_2-adrenoceptor antagonist, 1-(2-pyrymidinyl) piperazine (Caccia *et al.*, 1986), which is also a potent inducer of rat defaecation, through a different, non-5-hydroxytryptaminergic mechanism (Croci & Bianchetti, 1992), this could partly explain the difference from SR 57746A.

Repeated daily doses of the 5-HT$_{1A}$ receptor agonists led to progressive loss of their overall effectiveness on faecal excretion. After eight days of treatment, complete tolerance developed to the effects of SR 57746A or buspirone on faecal water content, but not on faecal dry weight. These results suggest that the drug mechanisms stimulating faecal pellet output and affecting water exchange through the gut wall are independent. Tolerance to the faecal water content increasing effect seemed to arise sooner with SR 57746A than with buspirone. Unlike SR 57746A, which appears to be a full 5-HT$_{1A}$ receptor agonist (Bachy *et al.*, 1993), buspirone has partial agonist properties (Millan *et al.*, 1991), possibly accounting for the slower tolerance.

In conclusion the present findings support a role of 5-HT$_{1A}$-5-hydroxytryptaminergic mechanisms in the CNS in drug-induced defaecation in rats. Our *in vitro* radioligand binding or functional assays, provided no evidence of 5-HT receptor subtypes accounting for such mechanisms in the rat distal colon, although 5-HT$_{1A}$ receptors are present in the guinea-pig ileum, as shown by electrophysiologically (Galligan *et al.*, 1988) and mechanically monitored (Fozard & Kilbinger, 1985) responses to appropriate agonists and antagonists in isolated preparations. Yet acceleration of postprandial colonic transit by 5-HT$_{1A}$ receptor agonists in an *in vivo* rat model, has been recently attributed to a local rather than central receptor subtype-specific 5-HT mechanism (Gué *et al.*, 1994). We assume that the experimental condition we adopted involves the stimulation of central 5-HT$_{1A}$ receptors presumably activating efferent cholinergic pathways (Croci *et al.*, 1990b), leading to propulsive contraction of gut smooth muscle (Croci *et al.*, 1994).

The relevance of these findings for other species is unknown but, should they apply to man, 5-HT$_{1A}$ receptor agonists might have clinical potential for treating hypomotility disorders of the lower intestinal tract, such as idiopathic constipation.

We would like to thank Mr Mario Cassisi and Mr Giulio Aureggi for their excellent technical assistance.

References

BACHY, A., STEINBERG, R., SANTUCCI, V., FOURNIER, M., LANDI, M., HAMON, M., MANARA, L., KEANE, P.E., SOUBRIE, P. & LE FUR, G. (1993). Biochemical and electrophysiological properties of SR 57746A a new potent 5-HT$_{1A}$ receptor agonist. *Fundam. Clin. Pharmacol.*, **7**, 487–497.

BENNETT, J.P. & SNYDER, S.H. (1976). Serotonin and lysergic acid diethylamide binding in rat brain membranes: relationship to postsynaptic serotonin receptors. *Mol. Pharmacol.*, **12**, 373–389.

BIANCHETTI, A., BASSANI, A., CROCI, T., BASILISCO, G. & MANARA, L. (1991). 5-HT$_{1A}$-receptors agonists that promote fecal excretion induce colonic contractions in fed rats. *J. Gastroint. Motil.*, **3**, 172P.

BIANCHETTI, A., CROCI, T. & MANARA, L. (1990). The new serotoninergic compound SR 57746A promotes fecal excretion in rats by stimulation of central 5-HT$_{1A}$ receptors. *Pharmacol. Res.*, **22**, 53P.

BUCHHEIT, K.H., ENGEL, G., MULSCHLER, E. & RICHARDSON, B. (1985). Study of the contractile effect of 5-hydroxytryptamine (5-HT) in the isolated longitudinal muscle strip from guinea-pig ileum: evidence for two distinct release mechanisms. *Naunyn-Schmied. Arch. Pharmacol.*, **329**, 36–41.

CACCIA, S., CONTI, I., VIGANO, G. & GARATTINI, S. (1986). 1-(2-pyrimidinyl)-piperazine as active metabolite of buspirone in man and rat. *Pharmacology (Basel)*, **33**, 46–51.

CARLI, M., PRONTERA, C. & SAMANIN, R. (1989). Evidence that central 5-hydroxytryptaminergic neurones are involved in the anxiolytic activity of buspirone. *Br. J. Pharmacol.*, **96**, 829–836.

CERVO, L., BENDOTTI, C., TARIZZO, G., CAGNOTTO, A., SKORUPSKA, M., MENNINI, T. & SAMANIN, R. (1994). Potential antidepressant properties of SR 57746A, a novel compound with selectivity and high affinity for 5-HT$_{1A}$ receptors. *Eur. J. Pharmacol.*, **253**, 139–147.

CERVO, L. & SAMANIN, R. (1987). Potential antidepressant properties of 8-hydroxy-2-(di-n-propylamino)tetralin, a selective serotonin$_{1A}$ receptor agonist. *Eur. J. Pharmacol.*, **144**, 223–229.

CHENG, Y.C. & PRUSOFF, W.H. (1973). Relationship between the inhibition constant (Ki) and the concentration of inhibitor which causes 50 per cent inhibition (IC_{50}) of an enzymatic reaction. *Biochem. Pharmacol.*, **22**, 3099–3105.

COSTA, M. & FURNESS, J.B. (1979). The sites of action of 5-hydroxytryptamine in nerve-muscle preparations from guinea-pig small intestine and colon. *Br. J. Pharmacol.*, **65**, 237–248.

COSTA, M., FURNESS, J.B., CUELLO, A.C., VERHOFSTAD, A.A.J., STEINBUSH, H.W.J. & ELDE, R.P. (1982). Neurons with 5-hydroxytryptamine-like immunoreactivity in the enteric nervous system: their visualization and reactions to drug treatment. *Neuroscience*, **7**, 351–363.

COSTALL, B. & NAYLOR, R.J. (1990). 5-hydroxytryptamine: new receptors and novel drugs for gastrointestinal motor disorders. *Scand. J. Gastroenterol.*, **25**, 769–787.

CROCI, T., BASILISCO, G., BASSANI, A. & MANARA, L. (1994). Manometric patterns of rat colonic motor activity and defecation. Effect of selective 5-HT$_{1A}$ agonist 8-OH-DPAT. *Dig. Dis. Sci.*, **39**, 1968–1973.

CROCI, T. & BIANCHETTI, A. (1992). Stimulation of faecal excretion in rats by α_2-adrenergic antagonists. *J. Pharm. Pharmacol.*, **44**, 358–360.

CROCI, T., BIANCHETTI, A. & MANARA, L. (1990a). 8-OH-DPAT and buspirone promote fecal excretion in rats by stimulation of central serotonin 5-HT$_{1A}$ receptors. *Eur. J. Pharmacol.*, **183**, 2203P.

CROCI, T., BIANCHETTI, A. & MANARA, L. (1990b). Serotonin and 8-OH-DPAT promote fecal excretion in rats by different serotoninergic mechanisms. *Pharmacol. Res.*, **22**, 137P.

CROCI, T., EMONDS-ALT, X. & MANARA, L. (1994). SR 48968 selectively prevents faecal excretion following activation of tachykinin NK$_2$-receptors in rats. *J. Pharm. Pharmacol.*, **46**, 383–385.

DE PONTI, F., COSENTINO, M., LECCHINI, S., FRIGO, G.M. & CREMA, A. (1991). Physiopharmacology of the peristaltic reflex: an update. *Ital. J. Gastroenterol.*, **23**, 264–269.

DOURISH, C.T., HUTSON, P.H. & CURZON, G. (1986). Para-chlorophenylalanine prevents feeding induced by the serotonin agonist 8-hydroxy-2-(di-n-propylamino) tetralin (8-OH-DPAT). *Psychopharmacology*, **89**, 467–471.

FINNEY, D.J. (1964). *Statistical Methods in Biological Assays*. 2nd edn. London: Griffin.

FOZARD, J.R. & KILBINGER, H. (1985). 8-OH-DPAT inhibits transmitter release from guinea-pig enteric cholinergic neurones by activating 5-HT$_{1A}$ receptors. *Br. J. Pharmacol.*, **86**, 601P.

GALLIGAN, J.J., SURPRENANT, A., TONINI, M. & NORTH, R.A. (1988). Differential localization of 5HT$_1$ receptors on myenteric and submucosal neurons. *Am. J. Physiol.*, **18**, G603–G611.

GILBERT, F., BRAZELL, C., TRICKLEBANK, M.D. & STAHL, S.M. (1988). Activation of the 5-HT$_{1A}$ receptor subtype increases rat plasma ACTH concentration. *Eur. J. Pharmacol.*, **147**, 431–439.

GOA, K.L. & WARD, A. (1986). Buspirone. A preliminary review of its pharmacological properties and therapeutic efficacy as an anxiolytic. *Drugs*, **32**, 114–129.

GOODWIN, G.M., DE SOUZA, R.J. & GREEN, A.R. (1985). The pharmacology of the hypothermic response in mice to 8-hydroxy-2-(di-n-propylamino) tetralin (8-OH-DPAT): a model of presynaptic 5-HT$_1$ function. *Neuropharmacology*, **24**, 1187–1194.

GOODWIN, G.M., DE SOUZA, R.J. & GREEN, A.R. (1986). The effects of a 5-HT$_1$ receptor ligand ipsapirone (TVXQ 7821) on 5-HT synthesis and the behavioural effects of 5-HT agonists in mice and rats. *Psychopharmacology*, **89**, 382–387.

GUÉ, M., DEL RIO-LACHEZE, C., JUNIEN, J.L. & BUÉNO, L. (1994). Central CCK-8s receptors trigger the sigma ligand- and 5-HT$_{1A}$ agonists-induced acceleration of post-prandial colonic transit in rats. *Neurogastroenterol. Mot.*, **6**, 29–35.

HJORTH, S. & CARLSSON, A. (1986). Is pindolol a mixed agonist-antagonist at central serotonin (5-HT) receptors? *Eur. J. Pharmacol.*, **129**, 131–138.

HUTSON, P.H., DONOHOE, T.P. & CURZON, G. (1987). Hypothermia induced by the putative 5-HT$_{1A}$ agonist LY165163 and 8-OH-DPAT is not prevented by 5-HT-depletion. *Eur. J. Pharmacol.*, **143**, 221–228.

JENKINS, S.W., ROBINSON, D.S., FABRE, L.F., ANDARY, J.J., MESSINA, M.E. & REICH, L.A. (1990). Gepirone in the treatment of major depression. *J. Clin. Psychopharmacol.*, **10**, 77S–85S.

KENNET, G.A., MARCOU, M., DOURISH, C.T. & CURZON, G. (1987). Single administration of 5-HT$_{1A}$ agonists decreases 5-HT$_{1A}$ presynaptic but not postsynaptic receptor-mediated responses: relationship to antidepressant-like action. *Eur. J. Pharmacol.*, **138**, 53–60.

KRAMER, C.Y. (1956). Extension of multiple range test to groups with unequal numbers of replications. *Biometrics*, **12**, 307–310.

LANDI, M., BIANCHETTI, A., CROCI, T. & MANARA, L. (1992). Phenylethanolaminotetralines compete with [^{3}H]-dihydroalprenolol binding to rat colon membranes without evidencing atypical β-adrenergic sites. *Biochem. Pharmacol.*, **44**, 665–672.

LOWRY, O.H., ROSEBROUGH, N.J., FARR, A.L. & RANDALL, R.J. (1951). Protein measurement with the Folin phenol reagent. *J. Biol. Chem.*, **193**, 265–275.

MARTIN, P., TISSIER, M.-H., ADRIEN, J. & PUECH, A.J. (1991). Antidepressant-like effects of buspirone mediated by the 5-HT$_{1A}$ post-synaptic receptors in the learned helplessness paradigm. *Life Sci.*, **48**, 2505–2511.

MILLAN, M.J., CANTON, H., RIVET, J.M., LEJEUNE, F., LAUBIE, M. & LAVIELLE, G. (1991). S 14671: a novel napththylpiperazine 5-HT$_{1A}$ agonist of high efficacy and exceptional in vivo potency. *Eur. J. Pharmacol.*, **203**, 319–322.

MOSER, P.C., TRICKLEBANK, M.D., MIDDLEMISS, D.N., MIR, A.K., HIBERT, M.F. & FOZARD, J.R. (1990). Characterization of MDL 73005EF as a 5-HT$_{1A}$ selective ligand and its effects in animal models of anxiety: comparison with buspirone, 8-OH-DPAT and diazepam. *Br. J. Pharmacol.*, **99**, 343–349.

RACKE, K. & SCHWORER, H. (1991). Regulation of serotonin release from the intestinal mucosa. *Pharmacol. Res.*, **23**, 13–25.

ROBINSON, D.S., ALMS, D.R., SHROTRIYA, R.C., MESSINA, M. & WICKRAMARATNE, P. (1989). Serotoninergic anxiolytics and treatment of depression. *Psychopathol.*, **22**, 27–36.

SANBERG, P.R., RUSSELL, H.R., HAGENMEYER-HOUSER, S.H., GIORDANO, N., ZUBRYCKI, E.M. & GARVER, D.L. (1989). Neuroleptic-induced emotional defecation: effects of scopolamine and haloperidol. *Psychopharmacol.*, **99**, 60–63.

SCATCHARD, G. (1949). The attraction of proteins for small molecules and ions. *Ann. N.Y. Acad. Sci.*, **51**, 660–672.

SHARP, T., MCQUADE, R., BRAMWELL, S. & HJORTH, S. (1993). Effect of acute and repeated administration of 5-HT$_{1A}$ receptor agonists on 5-HT release in rat brain in vivo. *Naunyn-Schmied. Arch. Pharmacol.*, **348**, 339–346.

TRABER, J. & GLASER, T. (1987). 5-HT$_{1A}$ receptor-related anxiolytics. *Trends Pharmacol. Sci.*, **8**, 432–437.

TRICKLEBANK, M.D., FORLER, C. & FOZARD, J.R. (1984). The involvement of subtypes of the 5-HT$_1$ receptor and catecholaminergic systems in the behavioural response to 8-hydroxy-2-(di-n-propylamino) tetralin in the rat. *Eur. J. Pharmacol.*, **106**, 271–282.

WEBER, L.J. (1970). P-chlorophenylalanine depletion of gastrointestinal 5-hydroxytryptamine. *Biochem. Pharmacol.*, **19**, 2169–2172.

(Received July 19, 1994
Revised January 11, 1995
Accepted January 18, 1995)

British Journal of Pharmacology (1995) 115, 210-216

Intrinsic activity of the non-prostanoid thromboxane A_2 receptor antagonist, daltroban (BM 13,505), in human platelets *in vitro* and in the rat vasculature *in vivo*

Frédéric Bertolino, Jean-Pierre Valentin, Myriam Maffre, *Françoise Grelac, Anne-Marie Bessac, *Jacques Maclouf, André Delhon, *Sylviane Lévy-Toledano, Jean-François Patoiseau, Francis C. Colpaert & [1]Gareth W. John

Centre de Recherche Pierre Fabre, 81106 Castres and *INSERM Unité 348, Hôpital Lariboisière, 75010 Paris, France

1 We evaluated the effects of daltroban on (i) human platelet shape change and aggregation *in vitro*, and (ii) mean systemic and pulmonary arterial pressures (MAP and MPAP, respectively) as well as haematocrit, in anaesthetized, open-chest Sprague-Dawley rats, compared with those of a chemically distinct prostanoid thromboxane A_2 (TxA_2) receptor antagonist, SQ 29,548, and agonist, U-46619.

2 In human platelets *in vitro*, daltroban (10 nM–100 μM; $n = 6$ per group) concentration-dependently induced shape change, attaining at 50 μM, a maximum amplitude of 0.83 ± 0.09 mV representing $46.4 \pm 4.8\%$ of that evoked by U-46619 (1.78 ± 0.20 mV at 0.2 μM; $n = 9$); and inhibited U-46619-induced platelet aggregation with an IC_{50} of 77 (41–161)nM. SQ 29,548 (10 nM–100 μM; $n = 6$ per group) failed to evoke any platelet shape change, but potently inhibited U-46619-induced platelet aggregation with an $IC_{50} < 10$ nM.

3 In anaesthetized rats *in vivo*, daltroban (10–2500 μg kg^{-1}, i.v. infused over 2 min; $n = 4$–8 per group) produced a bell-shaped dose-response curve for MPAP and haematocrit, and evoked maximal increases of 12.7 ± 2.1 mmHg and $5.8 \pm 1.5\%$ at 80 μg kg^{-1} ($n = 6$) and 630 μg kg^{-1} ($n = 8$), respectively (both $P < 0.05$) with ED_{50}s of 20 (16–29) and 217 (129–331) μg kg^{-1}, respectively. By comparison, U-46619 (0.16–20 μg kg^{-1}, i.v.), induced dose-dependent increases in MPAP and haematocrit (25.4 ± 1.0 mmHg and $16.1 \pm 2.9\%$ at the highest dose; $n = 12$, both $P < 0.01$), with ED_{50}s of 1.8 (1.3–2.5) and 3.9 (3.5–5.4) μg kg^{-1}, respectively. Daltroban dose-dependently increased MAP with a maximum amplitude of 42.2 ± 4.4 mmHg at a dose of 80 μg kg^{-1} [$ED_{50} = 94$ (64–125) μg kg^{-1}], similar to that induced by U-46619 (41.3 ± 9.6 mmHg) at a dose of 0.63 μg kg^{-1} [$ED_{50} = 0.22$ (0.13–0.24) μg kg^{-1}]. SQ 29,548 (10–2500 μg kg^{-1}, i.v.; $n = 4$ per group) failed to modify significantly any of these parameters.

4 Our results clearly demonstrate that daltroban, in a similar manner to the TxA_2 analogue, U-46619, but unlike the TxA_2 receptor antagonist, SQ 29,548, exhibits significant intrinsic activity in human platelets *in vitro* and in the rat vasculature *in vivo*, possibly through TxA_2 receptor activation.

Keywords: Arterial pressure; daltroban; human platelet aggregation; shape change; pulmonary hypertension; thromboxane A_2; TxA_2/PGH_2 receptors

Introduction

Thromboxane A_2 (TxA_2) is a labile arachidonic acid metabolite which has been implicated in the pathogenesis of human and experimental cardiovascular diseases (Misra, 1994). Consequently, a large number of prostanoid and non-prostanoid TxA_2 receptor antagonists have been developed and are currently undergoing clinical investigation. This class of agent was, in general, found to be safe, well tolerated, although clear evidence of efficacy in large studies remains to be established, particularly with respect to aspirin (Misra, 1994). Prostanoid analogues of TxA_2 induce platelet aggregation, vascular smooth muscle cell contraction *in vivo*, pulmonary hypertension *in vivo* as well as haemoconcentration (reviewed by Hall, 1991; Halushka & Mais, 1989; Misra, 1994; Bertolino *et al.*, 1994; 1995). Intrinsic activity at TxA_2/PGH_2 or other receptors could limit the therapeutic use of certain TxA_2 receptor antagonists (Terres *et al.*, 1987). Based on biochemical and pharmacological *in vitro* studies, intrinsic activities have been suspected for several, if not most of the non-prostanoid TxA_2/PGH_2 receptor antagonists described to date (Janssens *et al.*, 1985; Lumley *et al.*, 1988; Kakushi *et al.*, 1991; Miki *et al.*, 1992). In contrast, a number of prostanoid compounds seem to be devoid of intrinsic activity (Ogletree *et al.*, 1985; Darius *et al.*, 1995). Recently, high concentrations (100 μM) of daltroban (BM 13,505; {4-[2-(4-chlorobenzenesulphonylamino)-ethyl] benzene-acetic acid}), a well characterized non-prostanoid TxA_2 receptor antagonist (Lefer, 1988), was found to increase intracellular calcium in vascular smooth muscle cells (Miki *et al.*, 1992). At the present time, the intrinsic activity of this compound has not been characterized *in vitro* or demonstrated *in vivo*.

The aim of the present study was to determine whether daltroban exerted significant intrinsic activity compared with those of a chemically distinct prostanoid TXA_2 receptor antagonist, SQ 29,548 ({[1S-[1α,2α(5z),3α,4α]]-7-[3-[[2-[(phenylamino)-carbonyl]hydrazino]methyl]-7-oxabicyclo[2.2.1]hept-2-yl]-5-heptenoic acid}; Ogletree *et al.*, 1985), and agonist, U-46619 ((15S)-hydroxy-11α,9α-(epoxymethano)prosta-5Z, 13E-dienoic acid) on (i) human platelet shape change and aggregation *in vitro*, and (ii) mean systemic and pulmonary arterial pressures and haematocrit, in anaesthetized, open-chest Sprague-Dawley rats, a model we have previously shown to be particularly sensitive to TxA_2/PGH_2 receptor agonists (Bertolino *et al.*, 1994; 1995).

Methods

All experiments were carried out in accordance with French law and local ethical committee guidelines for human and animal research.

[1] Author for correspondence at: Centre de Recherche Pierre Fabre, Division of Cardiovascular Diseases II, 17, Avenue Jean Moulin, 81106 Castres cédex, France

Effect of U-46619, daltroban, and SQ 29,548 on human platelet shape change and aggregation

Human whole blood, obtained by ante-cubital venous puncture from 27 healthy adult volunteers who had not received any medication for at least 8 days, was collected into plastic tubes containing acid-citrate-dextrose (ACD-C; 9:1, v/v) anticoagulant, containing 1 mM aspirin (final concentration) and centrifuged for 20 min at 120 *g* at room temperature in order to obtain platelet-rich plasma (PRP). Platelets were then filtered twice on a metrizamide gradient, as previously described (Lévy-Toledano *et al.*, 1976), washed and resuspended in buffer, pH 7.4 (composition, mM: HEPES 10, NaCl 140, KCl 3, $MgCl_2$ 0.5 and $NaHCO_3$ 5). Platelet suspensions were standardized at a platelet count of $250-300 \times 10^9\ l^{-1}$.

The platelet shape change and aggregation responses to U-46619 (Cayman Chemical Company, Ann Arbor, MI, U.S.A.; 0.2 μM, $n=9$ blood samples from separate volunteers) were measured relative to buffer, after preincubation at 37°C for 1 min with increasing concentrations of either daltroban (BM 13,505, Division of Medicinal Chemistry, Pierre Fabre Research Center, France; 10 nM–10 μM, $n=6$ blood samples from separate volunteers), SQ 29,548 (Bristol-Myers Squibb Research Laboratories, Princeton, NJ, U.S.A.; 10 nM–10 μM, $n=6$ blood samples from separate volunteers) or vehicle (dimethylsylphoxide, DMSO, final concentration: 0.2%, $n=6$ blood samples from separate volunteers), with a dual channel platelet aggregometer (Chronolog, ChronoLog Corporation, Havertown, PA, U.S.A.) and recorded on a chart recorder set at 25 mV sensitivity. Peak shape change responses were measured as the maximal decrease in light transmission after U-46619, daltroban and SQ 29,548 additions. Aggregation, measured 2 min after U-46619 addition, was expressed as percentage intensity relative to the percentage transmittance of buffer (i.e., 100% transmittance). Concentration-response relationships for daltroban and SQ 29,548-induced platelet shape change and inhibition of U-46619-induced aggregation were constructed and average EC_{50} values were determined for each group.

Effect of U-46619, daltroban, and SQ 29,548 on systemic and pulmonary arterial pressures, and haematocrit

Male Sprague-Dawley rats (OFA, Iffa-Credo, France) were housed in climate-controlled conditions and provided standard rat chow and water *ad libitum*. On the day of the experiment, rats were anaesthetized by i.p. injection of sodium pentobarbitone (60 mg kg^{-1}; Sanofi Laboratories, France), placed on a heated table to maintain rectal temperature at 37 ± 0.5°C then prepared for acute experimentation as previously described (Bertolino *et al.*, 1994; 1995). Briefly, animals underwent tracheotomy and were mechanically ventilated (Harvard Apparatus, South Natick, MA, U.S.A.). Catheters were inserted into the penile vein and the right carotid artery, respectively for infusing fluids and drugs, sampling blood, and continuous measurement of arterial pressure via a Statham P10EZ pressure transducer (Viggo-Spectramed, Oxnard, CA, U.S.A.) connected to a Gould Model 8188 polygraph (Gould Instruments, France). A left thoracotomy was performed through the third intercostal space to expose the pulmonary artery. A curved 19-gauge needle, connected to a silastic tube (Dow Corning Corporation, Midland, MI, U.S.A.), was inserted near the bifurcation of the artery from the right ventricle. Prompt return of arterial blood through the silastic tubing attached to the needle confirmed successful placement. The silastic catheter was secured to the exposed muscle layer of the animal, then the thorax was closed. Pulmonary arterial pressure was recorded via a Statham pressure transducer connected to a Gould polygraph. Experiments were started 15–30 min after completion of surgical procedures and stabilisation of arterial pressures. Then, rats received an injection of the vehicle (Na_2CO_3, 2 mM; $n=8$), the TxA_2 analogue, U-46619, at one of the following doses (0.16, 0.63, 1.25, 2.5, 10 or 20 μg kg^{-1}; $n=4$, 4, 8, 4, 6 and 12 rats per group, respectively), daltroban, at one of the following doses (10, 40, 80, 160, 630, 940 or 2500 μg kg^{-1}; $n=4$, 6, 6, 6, 8, 6 and 6 rats per group, respectively) or SQ 29,548 at one of the following doses (10, 160 or 2500 μg kg^{-1}; $n=4$ rats per group, respectively). Vehicle or drugs were injected over 2 min as 1 ml kg^{-1} solution. Blood samples (50 μl) were withdrawn from the right carotid artery at −5, 3, and 15 min for determination of haematocrit by spinning blood at 12,000 r.p.m. in a microfuge (Clay Adams, Parsippany, NJ, U.S.A.) for 3 min.

Analytical techniques, calculations, logistic curve fitting and statistical analysis

Estimated changes in plasma volume were calculated according to the following formula: $dV = \{(100/100\text{-Hi}) \times [100 \times (\text{Hi-Hf})/\text{Hf}]\}$, where dV is the percentage change in plasma volume, Hi and Hf the initial and final haematocrit, respectively (Davies *et al.*, 1976). Data are expressed as means ± s.e.mean. One way analysis of variance with repeated

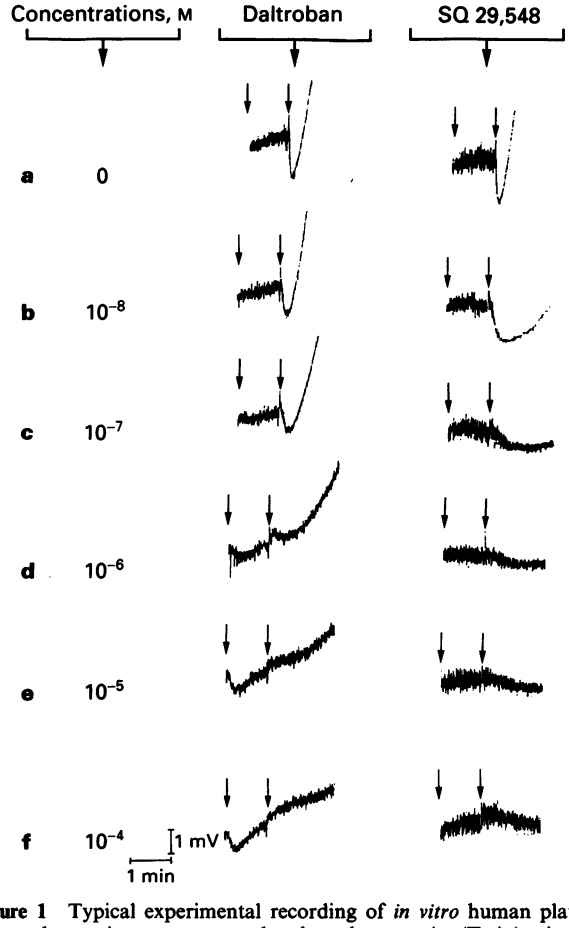

Figure 1 Typical experimental recording of *in vitro* human platelet shape change in response to the thromboxane A_2 (TxA_2)-mimetic, U-46619 (0.2 μM) after administration of either the vehicle (dimethylsulphoxide, a) or increasing concentrations of daltroban (left panel) or SQ 29,548 (right panel). Incubation of daltroban or SQ 29,548 with the platelets (first arrow) started 1 min before addition of U-46619 (second arrow). Daltroban, but not SQ 29,548, concentration-dependently induced a shape change (from 10^{-7} M, c); in addition, both compounds concentration-dependently antagonized U-46619-induced aggregation (from 10^{-8} M for SQ 29,548, b; from 10^{-7} M for daltroban, c).

measures and two way analysis of variance with the Fisher and Student's t tests as *post hoc* tests were used to assess significance between and among groups, respectively (StatView, Abacus Concepts, Inc., Berkeley, CA, U.S.A.). Geometric mean values for relative changes in platelet aggregation, shape change, mean systemic and pulmonary arterial pressures as well as haematocrit were calculated using the UltraFit programme (Biosoft, Ferguson, MO, U.S.A.). Dose-response curves were fitted using an operational sigmoid model (Marquardt algorithm; Marquardt, 1963); EC_{50} and ED_{50} refer to the mean agonist concentration or dose, respectively, (with 95% confidence intervals in parentheses) inducing 50% of its maximal effect; IC_{50} refers to the mean antagonist concentration (with 95% confidence intervals in parentheses) inhibiting an agonist-induced response by 50%.

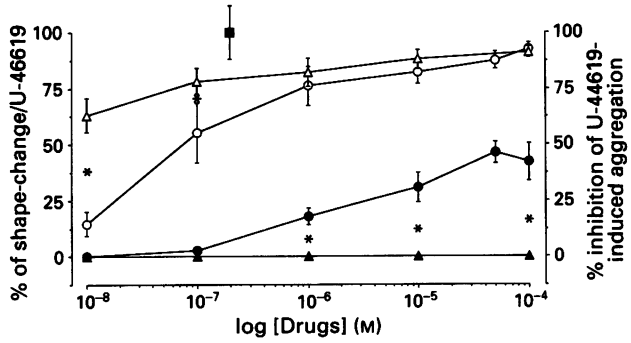

Figure 2 Concentration-response curves for daltroban (10 nM–100 μM; ○, ●), and SQ 29,548 (10 nM–100 μM; △, ▲) on relative changes of human platelet shape change (filled symbols) compared to U-46619 (0.2 μM; ■) and on relative inhibition of U-46619-induced aggregation (open symbols). Data are presented as mean ± s.e.mean of six experiments. *$P<0.05$ between daltroban and SQ 29,548 by factorial analysis of variance (Fisher test).

$P = 0.05$ was considered the minimum level of significance. For bell-shaped dose-response relationships, the apparent ED_{50} ($ED_{50\ app}$) was calculated from the rising part of the curve, assuming the peak of the bell-shaped curve to represent the maximum response.

Results

Effect of U-46619, daltroban, and SQ 29,548 on human platelet shape change and aggregation

In human platelets, *in vitro*, daltroban concentration-dependently induced a shape change (Figures 1 and 2), attaining, at 50 μM, a maximum amplitude of 0.83 ± 0.09 mV representing 46.4 ± 4.8% of that evoked by U-46619 (1.78 ± 0.20 mV at 0.2 μM); and inhibited U-46619-induced platelet aggregation with an IC_{50} of 77 nM (Table 1; Figure 2). SQ 29,548 failed to evoke any platelet shape change, but potently inhibited U-46619 induced platelet aggregation with an IC_{50} lower than 10 nM (Figures 1 and 2).

Effect of U-46619, daltroban and SQ 29,548 on systemic and pulmonary arterial pressures, and haematocrit

Injection of the vehicle (Na_2CO_3, 2 mM) was devoid of any significant effect on MAP and MPAP (Figures 3–6).

MPAP increased promptly, within 2–3 min, after intravenous injection of U-46619, then progressively returned to preinjection values (Figures 3b and 4a). The rise in MPAP was dose-dependent, with an ED_{50} of 1.8 μg kg^{-1} and a maximum of 25.4 ± 1.0 mmHg reached at the highest dose (Table 1; Figure 6a). Like U-46619, daltroban induced a rapid (within 2–3 min) and short lasting (<10 min) rise in MPAP (Figures 3c and 4b). Daltroban increased MPAP in a bell-shaped manner; the maximal increase (12.7 ± 2.1 mmHg; $P<0.05$; Figure 6a) being reached at a dose of 80 μg kg^{-1} with an $ED_{50\ app}$ about 10 fold higher than that of the full

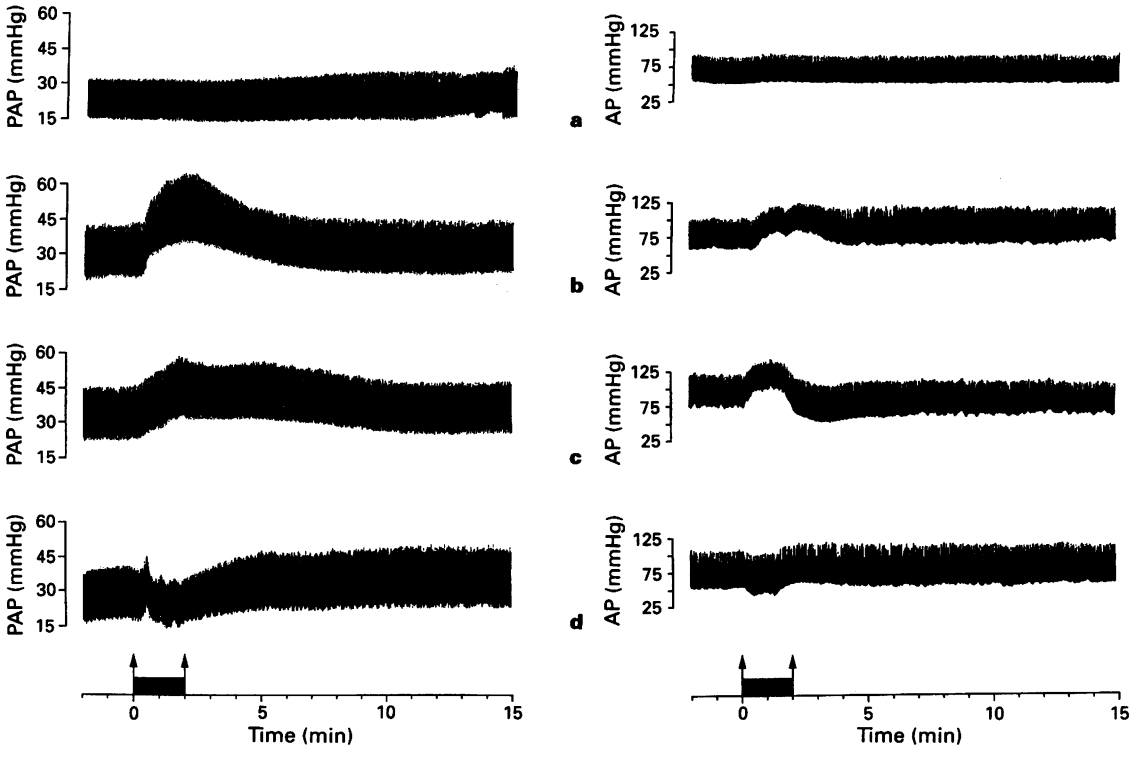

Figure 3 Typical experimental recording of systemic (AP; right panels) and pulmonary (PAP; left panels) arterial pressures in open-chest anaesthetized rats during administration of either the vehicle (Na_2CO_3, 2 mM; a), U-46619 (1.25 μg kg^{-1}; b), daltroban (80 μg kg^{-1}; c) or SQ 29,548 (2500 μg kg^{-1}; d). Vehicle or drugs were injected intravenously as a 1 ml kg^{-1} solution over 2 min as indicated by the arrows.

agonist, U-46619 (20 vs 1.8 $\mu g\,kg^{-1}$; Table 1). The maximal amplitude of the pulmonary pressor activity of daltroban was 53.2 ± 7.0% of that evoked by U-46619 (Table 1).

MAP rose transiently only at low doses of U-46619 (i.e., $\leq 2.5\,\mu g\,kg^{-1}$; Figures 3b, 5a and 6b) with an ED_{50} of $0.22\,\mu g\,kg^{-1}$ (Table 1) whereas no change or no hypertension occurred at higher doses. Similarly to U-46619, daltroban dose-dependently increased MAP with an ED_{50} of $94\,\mu g\,kg^{-1}$ attaining a plateau at doses higher than $160\,\mu g\,kg^{-1}$ (Figures 5b and 6b). The amplitude of the systemic pressor activity of daltroban was almost identical to that of U-46619 (42.2 ± 4.4 *versus* 41.3 ± 9.6 mmHg; Table 1; Figure 6b). Over the same range of doses used for daltroban, SQ 29,548 was devoid of any significant effects on either MAP or MPAP (Figures 3–6).

Within 3 min, the haematocrit increased dose-dependently by 4.6 ± 1.5, 10 ± 2.3 and 16.1 ± 2.9% after injection of 1.25, 10 and $20\,\mu g\,kg^{-1}$ of U-46619, respectively (all $P<0.05$, Figure 6c) with an ED_{50} of $3.9\,\mu g\,kg^{-1}$ (Table 1). The decrease in plasma volume calculated from the change in haematocrit amounted to 8.3 ± 2.5, 17.2 ± 3.9 and 26.2 ± 3.9% at 1.25, 10 and $20\,\mu g\,kg^{-1}$, respectively. A slight but not significant tendency for the haematocrit to decrease was detected following injection of the vehicle (−1.5 ± 0.7%,

Table 1 Intrinsic activities of U-46619 and daltroban on human platelet shape change, mean systemic and pulmonary arterial pressures and hæmatocrit

	Human platelet shape change		*Mean pulmonary arterial pressure*		*Mean systemic arterial pressure*		*Hæmatocrit*	
Agonist	EC_{50} (μM)	ΔE_{max} (mV)	ED_{50} ($\mu g\,kg^{-1}$)	ΔE_{max} (mmHg)	ED_{50} ($\mu g\,kg^{-1}$)	ΔE_{max} (mmHg)	ED_{50} ($\mu g\,kg^{-1}$)	ΔE_{max} (%)
U-46619	0.2*	1.78 ± 0.20	1.8 (1.3–2.5)	25.4 ± 1.0	0.22 (0.13–0.24)	41.3 ± 9.6	3.91 (3.5–5.4)	16.1 ± 2.9
Daltroban	2.49 (1.7–3.8)	0.83 ± 0.09	20** (16–29)	12.65 ± 2.1	94 (64–125)	42.2 ± 4.4	217** (129–331)	5.8 ± 1.5
Ratio Daltroban/U-46619	12.5	0.5	11.1	0.5	428.3	1.0	55.4	0.4

ΔE_{max} refers to the maximal amplitude of the response (± s.e.mean); EC_{50} and ED_{50} refer to the mean agonist concentration and dose respectively, inducing 50% of its maximal effect (with 95% confidence intervals in parentheses). Ratio Daltroban/U-46619 represents the ratio of daltroban/U-46619 EC_{50} values. *refers to the concentration of full agonist, U-46619, which produced a maximal response. **ED_{50app} (see Methods for details).

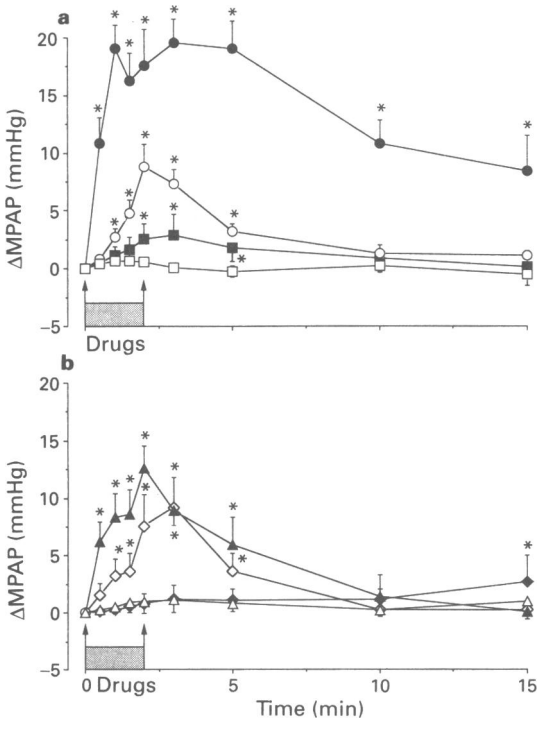

Figure 4 Time course of absolute changes in mean pulmonary arterial pressure (MPAP) in open chest anaesthetized rats during administration of (a) either U-46619 at doses of $0.16\,\mu g\,kg^{-1}$ (■, $n=4$), $1.25\,\mu g\,kg^{-1}$ (○, $n=8$), and $20\,\mu g\,kg^{-1}$ (●, $n=10$) or the vehicle (Na_2CO_3, 2 mM, □, $n=8$), and of (b) either daltroban at doses of $10\,\mu g\,kg^{-1}$ (◆, $n=4$), $40\,\mu g\,kg^{-1}$ (◇, $n=6$), and $80\,\mu g\,kg^{-1}$ (▲, $n=6$) or SQ 29,548 ($2500\,\mu g\,kg^{-1}$; △, $n=4$). Vehicle or drugs were injected intravenously as a $1\,ml\,kg^{-1}$ solution over 2 min as indicated by the arrows. Data are presented as mean ± s.e.mean. $*P<0.05$ *versus* baseline by repeated measures analysis of variance.

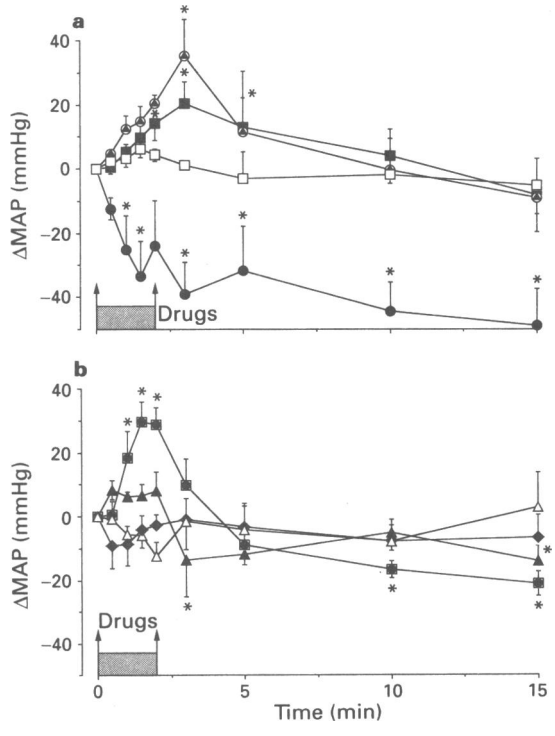

Figure 5 Time course of absolute changes in mean systemic arterial pressure (MAP) in open-chest anaesthetized rats during administration of (a) either U-46619 at doses of $0.16\,\mu g\,kg^{-1}$ (■, $n=4$), $0.63\,\mu g\,kg^{-1}$ (◭, $n=4$), and $20\,\mu g\,kg^{-1}$ (●, $n=10$) or the vehicle (Na_2CO_3, 2 mM, □, $n=8$), and of (b) either daltroban at doses of $10\,\mu g\,kg^{-1}$ (◆, $n=4$), $80\,\mu g\,kg^{-1}$ (▲, $n=6$), and $2500\,\mu g\,kg^{-1}$ (◙, $n=6$) or SQ 29,548 ($2500\,\mu g\,kg^{-1}$; △; $n=4$). Vehicle or drugs were injected intravenously as a $1\,ml\,kg^{-1}$ solution over 2 min as indicated by the arrows. Data are presented as mean ± s.e.mean. $*P<0.05$ *versus* baseline by repeated measures analysis of variance.

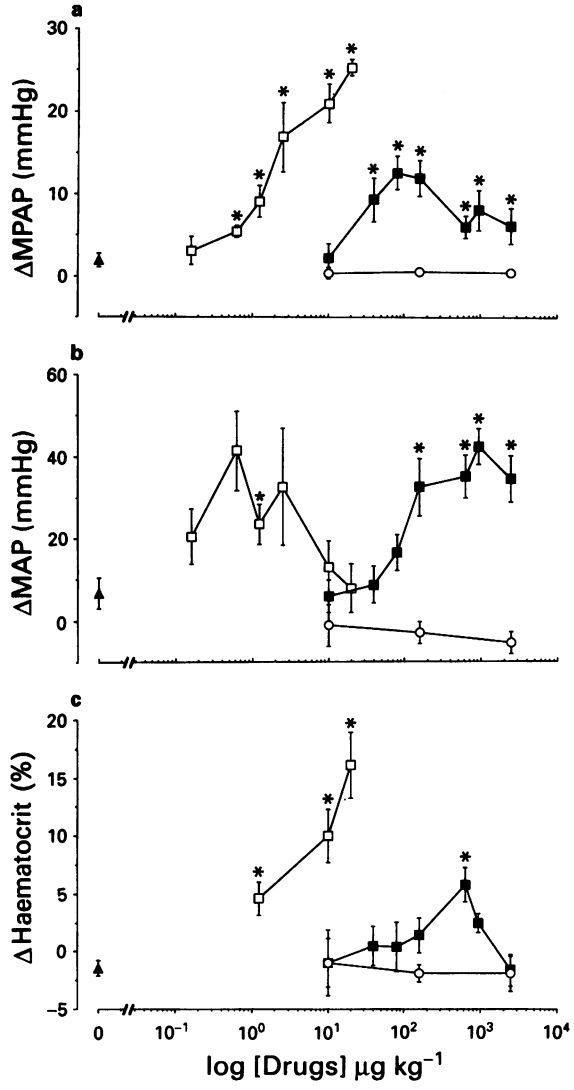

Figure 6 Dose-response curves of U-46619 (0.16–20 μg kg^{-1}; □), daltroban (10–2500 μg kg^{-1}; ■), and SQ 29,548 (10–2500 μg kg^{-1}; ○) on maximal absolute peak changes in mean pulmonary (MPAP; a) and systemic (MAP; b) arterial pressures, as well as haematocrit (c), in anaesthetized open-chest rats. The vehicle group is presented by (▲). Data are presented as mean ± s.e.mean. Each group of animals was of 4–12 rats. *$P<0.05$ *versus* baseline by factorial analysis of variance (Fisher test).

NS). As described for U-46619, daltroban similarly dose-dependently increased the haematocrit (Figure 6c) reaching a maximal effect of 5.8 ± 1.5% at 630 μg kg^{-1} with an $ED_{50\ app}$ of 217 μg kg^{-1} (Table 1). Such an increase in haematocrit corresponded to a calculated decrease in plasma volume of 10.3 ± 2.4%. The change in haematocrit was less marked at the dose of 940 μg kg^{-1} and did not differ from the vehicle at the highest dose. The maximal haemoconcentrating activity of daltroban represented 41.2 ± 8.6% of that evoked by U-46619 (Table 1). SQ 29,548 did not significantly affect the haematocrit (Figure 6c).

Discussion

The present study demonstrated that daltroban, like the full agonist, U-46619, but unlike the TxA_2/PGH_2 receptor antagonist SQ 29,548 (i) induced human platelet shape change *in vitro* and (ii) increased systemic and pulmonary arterial pressures as well as haematocrit *in vivo*. These results indicate unequivocally that daltroban, but not SQ 29,548, exerts significant intrinsic activity both *in vitro* and *in vivo*, possibly *via* TxA_2/PGH_2 receptor activation.

The stable TxA_2 analogue, U-46619, induced human platelet shape change, as previously reported (Ogletree *et al.*, 1985), via activation of TxA_2/PGH_2 receptors since it was concentration-dependently antagonized by SQ 29,548. The concentration of U-46619 used in the present study was previously shown to induce a maximal shape change response (Ogletree *et al.*, 1985; 1992). SQ 29,548 failed to evoke any platelet shape change, but potently inhibited U-46619-induced platelet aggregation with an IC_{50} lower than that of daltroban (<10 nM *versus* 77 nM). The inhibition was surmountable for both compounds. Like U-46619, daltroban concentration-dependently induced platelet shape change with a maximal response representing about half of that evoked by the full agonist. The prostanoid TxA_2/PGH_2 receptor antagonist S-1452 transiently altered platelet shape change, whereas other prostanoid TxA_2/PGH_2 receptor antagonists such as GR 32191 (vapiprost), BMS 180,291 (ifetroban sodium Misra *et al.*, 1994) and AH 23848 were devoid of any effect (Brittain *et al.*, 1985; Humphrey *et al.*, 1990; Kakushi *et al.*, 1991; Ogletree *et al.*, 1992). No conclusion can be drawn from these observations regarding an eventual structure (i.e., prostanoid *versus* non-prostanoid)-intrinsic activity relationship of these compounds on platelet shape change.

The TxA_2 analogue, U-46619, dose-dependently induced pulmonary hypertension, as reported previously (Yoshimura *et al.*, 1989; Nossaman *et al.*, 1992; Bertolino *et al.*, 1994; 1995) via activation of TxA_2/PGH_2 receptors (Bertolino *et al.*, 1994; 1995). Similarly to U-46619, daltroban increased pulmonary arterial pressure, but with a maximum representing approximately half of that induced by the full agonist, and with an $ED_{50\ app}$ that was about 10 fold higher than that of the full agonist, U-46619 (20 *versus* 1.8 μg kg^{-1}). Previous results on the systemic cardiovascular effects of U-46619 are conflicting (reviewed by Hall, 1991; Halushka & Mais, 1989); hyper (Stegmeier *et al.*, 1986)- or hypotension (Hui & Ogle, 1991) or both have been reported, depending on the dose (Bertolino *et al.*, 1994; 1995). Indeed, at the highest doses (i.e. >2.5 μg kg^{-1}), pulmonary hypertension developed and may consequently reduce cardiac output, thus explaining the decrease in systemic arterial pressure observed at such doses. Daltroban dose-dependently increased systemic arterial pressure, producing a maximal response of similar amplitude to that of the full agonist, U-46619. In contrast to the bell-shaped dose-response curve obtained in the pulmonary vascular bed, that produced by daltroban in the systemic vasculature was sigmoidal. This difference is not readily explainable; however, a bell-shaped dose-response curve could be produced by an agonist acting at separate receptors that mediate opposite effects (Barlow, 1994; Pliska, 1994). Interestingly, studies with distinct pharmacological ligands suggested the existence of two different binding sites for TxA_2 on platelets (Dorn, 1989; Takahara *et al.*, 1990; Dorn & DeJesus, 1991; Ogletree *et al.*, 1992) and that the 'shape change' receptor shared biochemical and pharmacological characteristics with the form of the receptor which transduced TxA_2-dependent vasoconstriction (Furci *et al.*, 1991). However, it is not known whether daltroban interacts with both recognition sites. Another possibility that cannot be excluded at present, however, is that daltroban causes desensitization and internalization of TxA_2/PGH_2 receptors, as has been described for the agonist, U-46619 (Liel *et al.*, 1988; Murray & FitzGerald, 1989), which could partly explain the bell-shaped dose-response relationship in MPAP and haematocrit. A reduction in systemic arterial pressure without any change in pulmonary arterial pressure has been reported shortly after intravenous injection of a single dose of TxA_2/PGH_2 receptor antagonist BMS 180,291 in anaesthetized monkeys (Schumacher *et al.*, 1992). Since SQ 29,548 was devoid of any effect on systemic and/or pulmonary arterial pressures, TxA_2 does not appear to play a major role

in the maintenance of basal arterial pressure. In this regard, TxA_2 receptor antagonism and TxA_2 synthase inhibition had no effect on systemic arterial pressure in hypertensive patients (Ritter *et al.*, 1993; Lyons *et al.*, 1993) or in anaesthetized dogs (Noguchi *et al.*, 1992).

The TxA_2 analogue, U-46619, caused a dose-dependent increase in haematocrit. We recently demonstrated that the rise in haematocrit (i) resulted from a transfer of plasma fluid from the vascular toward the interstitial compartment (Bertolino *et al.*, 1995), and (ii) was mediated through activation of TxA_2/PGH_2 receptors (Bertolino *et al.*, 1995). Like U-46619, daltroban increased haematocrit with a maximum representing approximately half of that induced by the full agonist, and with an ED_{50} that was about 55 fold higher than that of the full agonist, U-46619 (217 *versus* 3.9 $\mu g\,kg^{-1}$). However, the haemoconcentration dose-response curve produced by daltroban also showed a bell-shaped relationship.

Intrinsic activities have been suspected for TxA_2/PGH_2 receptor antagonists in several experimental models. Intrinsic activity of sulotroban (BM 13,177), one of the first non-prostanoid antagonists to be developed, has been reported *in vitro*; it induced small contractions of canine coronary artery (Lumley *et al.*, 1988) and rabbit femoral vein (Janssens *et al.*, 1985). However, in contrast to these reports, sulotroban was shown to have no intrinsic activity on rabbit aorta, canine or human coronary artery at concentrations up to 1 mM (Kopia *et al.*, 1989). Miki *et al.* (1992) showed that sulotroban induced a weak but detectable increase in intracellular calcium in cultured vascular smooth muscle cells at high concentrations. Agonist efficacy *in vitro* is well known to vary, depending upon the tissue studied, the density of receptors in question, and receptor-effector coupling (Kenakin, 1993). Thus is might be argued that sulotroban possessed insufficient efficacy to evoke any response in the latter blood vessels or smooth muscle cells. The prostanoid compound S-1452, transiently induced platelet shape change, as previously mentioned, evoked smooth muscle contraction *in vitro* (Hanasaki *et al.*, 1989; Nakajima & Ueda, 1989; Otani *et al.*, 1989; Kakushi *et al.*, 1991) and caused a transient increase in airway resistance in guinea-pigs *in vivo* (Asanuma *et al.*, 1993). In cat cerebral arteries, the intrinsic activity of S145 represented about one third of that of the high efficacy agonist (Nakajima & Ueda, 1989).

Agonist-like activity has been described *in vitro* for daltroban, a structurally similar analogue of sulotroban. Daltroban has been reported to be a more potent TxA_2 antagonist than sulotroban in inhibiting U-46619-induced contraction of the human pulmonary artery (Misra, 1994). In the present study, we showed that, like the full agonist (i.e. U-46619), daltroban induced (i) human platelet shape change, (ii) pulmonary hypertension and (iii) haemoconcentration in the rat; in each case, the maximal response represented about half of that induced by U-46619. Daltroban concentration-dependently contracted bovine isolated coronary arteries (Ogletree *et al.*, 1992) and increased intracellular calcium concentration in vascular smooth muscle cells (Miki *et al.*, 1992), with a maximum response representing, respectively, one-fifth and one-third of the value induced by the full agonist, U-46619. Both daltroban and U-46619 induced an increase in intracellular calcium concentration by an influx of extracellular calcium. Interestingly, TxA_2 receptor-mediated pulmonary vasoconstriction has been reported to depend upon an increase in cytosolic calcium concentration (Farrukh *et al.*, 1985).

The present study demonstrates the existence of intrinsic activity for daltroban, but not for SQ 29,548, as shown by the induction of human platelet shape change *in vitro*, and increases in systemic and pulmonary arterial pressures as well as haematocrit *in vivo*. Whether these changes are mediated through TxA_2/PGH_2 receptor activation and are therefore related to partial agonist properties of the drug, is currently being investigated.

References

ASANUMA, F., JYOYAMA, H. & KUROSAWA, A. (1993). Transient agonist-like action of the thromboxane A_2 antagonist S-1452 (d-S-145 Ca) and its reduction by gradual injection or oral administration. *Drug Dev. Res.*, **30**, 78–82.

BARLOW, R.B. (1994). Problems associated with the partiality of a partial agonist. *Trends Pharmacol. Sci.*, **15**, 320.

BERTOLINO, F., VALENTIN, J.P., MAFFRE, M., BESSAC, A.M. & JOHN, G.W. (1995). TxA_2 receptor activation elicits organ specific increases in microvascular permeability in the rat. *Am. J. Physiol.*, **268**, (*Regulatory Integrative Comp. Physiol.*, **37**), R366–R374.

BERTOLINO, F., VALENTIN, J.P., MAFFRE, M., JOVER, B., BESSAC, A.M. & JOHN, G.W. (1994). Prevention of thromboxane A_2 receptor-mediated pulmonary hypertension by a nonpeptide angiotensin II type 1 receptor antagonist. *J. Pharmacol. Exp. Ther.*, **268**, 747–752.

BRITTAIN, R.T., BOUTAL, L., CARTER, M.C., COLEMAN, R.A., COLLINGTON, E.W., GEISOW, H.P., HALLETT, P., HORNBY, E.J., HUMPHREY, P.P.A., JACK, D., KENNEDY, I., LUMLEY, P., MCCABE, P.J., SKIDMORE, I.F., PHIL, D., THOMAS, M. & WALLIS, C.J. (1985). AH23848: a thromboxane receptor-blocking drug that can clarify the pathophysiological role of thromboxane A_2. *Circulation*, **72**, 1208–1218.

DARIUS, H., SMITH, J.B. & LEFER, A.M. (1985). Beneficial effects of a new potent and specific thromboxane receptor antagonist (SQ 29,548) *in vitro* and *in vivo*. *J. Pharmacol. Exp. Ther.*, **235**, 274–281.

DAVIES, R.D., SLATER, H., FORSLING, M.L. & PAYNE, N. (1976). The response to arginine vasopressin and plasma renin to postural change in normal man, with observations on syncope. *Clin. Sci.*, **51**, 267–274.

DORN, G.W. (1989). Distinct platelet thromboxane A_2/prostaglandin H_2 receptor subtypes. A radioligand binding study of human platelets. *J. Clin. Invest.*, **84**, 1883–1891.

DORN, G.W. & DEJESUS, A. (1991). Human platelet aggregation and shape change are coupled to separate thromboxane A_2-prostaglandin H_2 receptors. *Am. J. Physiol.*, **260**, H327–H334.

FARRUKH, I.S., MICHAEL, J.R., SUMMER, W.R., ADKINSON, Jr, N.F. & GURTNER, G.H. (1985). Thromboxane-induced pulmonary vasoconstriction: involvement of calcium. *J. Appl. Physiol.*, **58**, 34–44.

FURCI, L., FITZGERALD, D.J. & FITZGERALD, G.A. (1991). Heterogeneity of prostaglandin H_2/thromboxane A_2 receptors: distinct subtypes mediate vascular smooth muscle contraction and platelet aggregation. *J. Pharmacol. Exp. Ther.*, **258**, 74–81.

HALL, S.E. (1991). Thromboxane A_2 receptor antagonist. *Med. Res. Rev.*, **11**, 503–579.

HALUSHKA, P.V. & MAIS, D.E. (1989). Basic and clinical pharmacology of thromboxane A_2. *Drugs Today*, **25**, 383–393.

HANASAKI, K., NAGASAKI, T. & ARITA, H. (1989). Characterization of platelet thromboxane A_2/prostaglandin H_2 receptor by a novel thromboxane receptor antagonist, [^{3}H] S-145. *Biochem. Pharmacol.*, **38**, 2007–2017.

HUI, S.C.G. & OGLE, C.W. (1991). Thromboxane-mimetic U-46619 causes depressor responses in anaesthetized rats. *J. Pharm. Pharmacol.*, **43**, 592–593.

HUMPHREY, P.P.A., HALLET, P., HORNBY, E.J., WALLIS, C.J., COLLINGTON, E.W. & LUMLEY, P. (1990). Pathophysiological actions of thromboxane A_2 and their pharmacological antagonism by thromboxane receptor blockade with GR 32191. *Circulation*, **81**, (suppl I), I42–I52.

JANSSENS, W.J., DECKMYN, H., GRESELE, P. & VERMYLEN, J. (1985). BM13.177 selectively inhibits endoperoxide analogue induced vascular contractions. *Arch. Int. Pharmacodyn.*, **276**, 28–34.

KAKUSHI, H., SHIKE, T., ARITA, H. & UCHIDA, K. (1991). Effect of (+)-S-1452 calcium salt dihydrate, an orally active antagonist of the thromboxane A_2/prostaglandin H_2 endoperoxide receptor, on platelet aggregation. *Folia Pharmacol. Jpn.*, **98**, 113–120.

KENAKIN, T. (1993). Efficacy. In *Pharmacologic Analysis of Drug-Receptor Interaction*. pp. 249–277. New York, NY: Raven Press.

KOPIA, G.A., SULPIZIO, A., SMITH, E.F. III, OHLSTEIN, E.H. HIEBLE, J.P., NICHOLS, A.J. & RUFFOLO, Jr, R.R. (1989). The thromboxane receptor antagonist BM13.177 (sulotroban) is not a partial agonist. *J. Mol. Cell. Cardiol.*, **21**, S195.

LEFER, A.M. (1988). Daltroban (BM-13.505) -a highly specific, potent thromboxane receptor antagonist. *Drugs Future*, **13**, 999–1005.

LÉVY-TOLEDANO, S., BREDOUX, R., RENDU, F., JEANNEAU, C., SAVARIAU, E. & DASSIN, E. (1976). Isolement et fonction des plaquettes. I) À partir du plasma riche en plaquettes. Comparaison de deux méthodes: filtration sur gel et centrifugation sur sur gradient d'albumine. II) Nouvelle méthode à partir du sang total: centrifugation sur gradients de métrizamide. *Nouv. Rev. Fr. Hématol.*, **16**, 367–380.

LIEL, N., MAIS, D.E. & HALUSHKA, P.V. (1988). Desensitization of platelet thromboxane A_2/prostaglandin H_2 receptors by the mimetic U-46619. *J. Pharmacol. Exp. Ther.*, **247**, 1133–1138.

LUMLEY, P., SEAGER, K. & WHITE, B. (1988). The TP-receptor blocking drugs GR32191 and BM13.177 have a differential profile of action on vascular smooth muscle. *Br. J. Pharmacol.*, **95**, 685P.

LYONS, D., FOWLER, G., PETRIE, J.C. & WEBSTER, J. (1993). The haemodynamic effects of GR 32191, a thromboxane A_2 receptor antagonist, in patients with renal artery stenosis and hypertension. *Br. J. Clin. Pharmacol.*, **36**, 271–273.

MARQUARDT, D.W. (1963). An algorithm for least squares estimation of non-linear parameters. *J. Soc. Indust. Appl. Math.*, **11**, 431.

MIKI, I., KASE, H. & ISHII, A. (1992). Difference in activities of thromboxane A_2 receptor antagonists in smooth muscle cells. *Eur. J. Pharmacol.*, **227**, 199–204.

MISRA, R.N. (1994). Recent progress in the clinical development of thromboxane A_2 receptor antagonists. *Exp. Opin. Invest. Drugs.*, **3**, 469–480.

MISRA, R.N., WHITE, R.E. & OGLETREE, M.L. (1994). Ifetroban sodium. *Drugs Future.*, **19**, 107–110.

MURRAY, R. & FITZGERALD, G.A. (1989). Regulation of thromboxane receptor activation in human platelets. *Proc. Natl. Acad. Sci. U.S.A.*, **86**, 124–128.

NAKAJIMA, M. & UEDA, M. (1989). Actions of a novel thromboxane A_2-receptor antagonist, S-145, on isolated monkey and cat arteries. *J. Cardiovasc. Pharmacol.*, **14**, 502–509.

NOGUCHI, K., OJIRI, Y., CHIBANA, T., MATSUZAKI, T. & SAKANASHI, M. (1992). Regional vascular responses to thromboxane A_2 analogue and their blockade with vapiprost, a selective thromboxane receptor blocking drug, in anaesthetized dogs. *Jpn. J. Pharmacol.*, **60**, 341–348.

NOSSAMAN, B.D., McMAHON, T.J., RAGHEB, M.S., IBRAHIM, I.N., BABYCOS, C.R., HOOD, J.S. & KADOWITZ, P.J. (1992). Blockade of thromboxane/endoperoxide receptor-mediated responses in the pulmonary vascular bed of the cat by sulotroban. *Eur. J Pharmacol.*, **213**, 1–7.

OGLETREE, M.L., HARRIS, D.N., GREENBERG, R., HASLANGER, M.F. & NAKANE, M. (1985). Pharmacological actions of SQ 29,548, a novel selective thromboxane antagonist. *J. Pharmacol. Exp. Ther.*, **234**, 435–441.

OGLETREE, M.L., HARRIS, D.N., SCHUMACHER, W.A., WEBB, M.L. & MISRA, R.N. (1992). Pharmacological profile of BMS 180,291: a potent, long-acting, orally active thromboxane A_2/prostaglandin endoperoxide receptor antagonist. *J. Pharmacol. Exp. Ther.*, **264**, 570–578.

OTANI, K., SHIMA, N. & DOTEUCHI, M. (1989). Pharmacological actions of S-145, a novel thromboxane A_2 receptor antagonist, in various smooth muscles. *Folia Pharmacol. Jpn.*, **94**, 319–328.

PLISKA, V. (1994). Models to explain dose-response relationships that exhibit a downturn phase. *Trends Pharmacol. Sci.*, **15**, 178–181.

RITTER, J.M., BARROW, S.E., DOKTOR, H.S., STRATTON, P.D., EDWARDS, J.S., HENRY, J.A. & GOULD, S. (1993). Thromboxane A_2 receptor antagonism and synthase inhibition in essential hypertension. *Hypertension*, **22**, 197–203.

SCHUMACHER, W.A., STEINBACHER, T.E., YOUSSEF, S. & OGLETREE, M.L. (1992). Antiplatelet activity of the long-acting thromboxane receptor antagonist BMS 180, 291 in monkeys. *Prostaglandins*, **44**, 389–397.

STEGMEIER, K., PILL, J. & PATSCHEKE, H. (1986). BM 13.505, a selective and potent TxA_2 receptor antagonist. *Naunyn-Schmied. Arch. Pharmacol.*, **332**, (Suppl.), R36 (Abstract).

TAKAHARA, K., MURRAY, R., FITZGERALD, G.A. & FITZGERALD, D.J. (1990). The response to thromboxane A_2 analogues in human platelets. Discrimination of two binding sites linked to distinct effector systems. *J. Biol. Chem.*, **265**, 6836–6844.

TERRES, W., KUPPER, W., HAMM, C.W. & BLEIFELD, W. (1987). Resting myocardial ischemia after intravenous infusion of BM 13.177 (sulotroban), a thromboxane receptor antagonist. *Thromb. Res.*, **48**, 577–583.

YOSHIMURA, K., TOD, M.L., PIER, K.G. & RUBIN, L.J. (1989). Role of venoconstriction in thromboxane hypertension and edema in lambs. *J. Appl. Physiol.*, **66**, 929–935.

(Received November 25, 1994
Revised January 24, 1995
Accepted January 31, 1995)

British Journal of Pharmacology

VOLUME 115 (1) MAY 1995

STOCKTON

BRITISH JOURNAL OF PHARMACOLOGY

The *British Journal of Pharmacology* welcomes contributions in all fields of experimental pharmacology including neuroscience, biochemical, cellular and molecular pharmacology. The Board of Editors represents a wide range of expertise and ensures that well-presented work is published as promptly as possible, consistent with maintaining the overall quality of the journal.

Edited for the British Pharmacological Society by

A.T. Birmingham
(Chairman)

R.W. Horton **W.A. Large**
(Secretaries)

Submission of manuscripts: Manuscripts (two copies) should be sent to The Editorial Office, British Journal of Pharmacology, St. George's Hospital Medical School, Cranmer Terrace, London SW17 0RE.

Authors should consult the Instructions to Authors and the Nomenclature Guidelines for Authors in Vol. **114,** 245–255. These Instructions and Guidelines also appear with the journal Index for Volumes **111–113,** 1994. A checklist of the essential requirements is summarised in each issue of the journal, or as the last page of the issue.

The *British Journal of Pharmacology* is published by Stockton Press, a division of Macmillan Press Ltd. It is the official publication of the British Pharmacological Society.

Scope The *British Journal of Pharmacology* is published twice a month. It welcomes contribution in all field of experimental pharmacology including neuroscience, biochemical, cellular and molecular pharmacology. The Board of Editors represents a wide range of expertise and ensures that well-presented work is published as promptly as possible, consistent with maintaining the overall quality of the journal

This journal is covered by Current Contents, Excerpta Medica, BIOSIS and Index Medicus.

Editorial Manuscripts (plus two copies) and all editorial correspondence should be sent to: The Editorial Office, British Journal of Pharmacology, St George's Hospital Medical School, Cranmer Terrace, London SW17 0RE, UK. Tel: +44 (0)181 767 6765; Fax: +44 (0)181 767 5645.

Advertisements Enquiries concerning advertisements should be addressed to: Michael Rowley, Hasler House, High Street, Great Dunmow, Essex CM6 1AP, UK. Tel: +44 (0)1371 874613; Fax: +44 (0)1371 872273.

Publisher All business correspondence, supplement enquiries and reprint requests should be addressed to British Journal of Pharmacology, Stockton Press, Houndmills, Basingstoke, Hampshire RG21 2XS, UK. Tel: +44 (0)1256 29242; Fax: +44 (0)1256 810526. Publisher: Marija Vukovojac. Editorial Assistant: Alice Ellingham. Production Controller: Karen Stuart.

Subscriptions – EU/Rest of World Subscription price per annum (3 volumes, 24 issues) £620, rest of world £820 (Airmail), £685 (Surface mail) or equivalent in any other currency. Orders must be accompanied by remittance. Cheques should be made payable to Macmillan Magazines and sent to: The Subscription Department, Macmillan Press Ltd, Houndmills, Basingstoke, Hampshire RG21 2XS, UK. Where appropriate, subscribers may make payments into UK Post Office Giro Account No. 519 2455. Full details must accompany the payment. Subscribers from EU territories should add sales tax at the local rate.

Subscriptions – USA USA subscribers call toll free 1-800-221-2123 or send check/money order/credit card details to: Stockton Press, 49, West 24th Street, New York, NY 10010; Tel: 212 627 5757, Fax: 212 627 9256. USA annual subscription rates: $1230 Airmail; $1030 Surface (Institutional/Corporate); $225 (Individual making personal payment).

British Journal of Pharmacology (ISSN 0007–1188) is published twice a month by Macmillan Press Ltd, c/o Mercury Airfreight International Ltd, 2323 Randolph Avenue, Avenel, NJ 07001, USA. Subscription price for institutions is $1030 per annum (surface). 2nd class postage is paid at Rahway NJ. Postmaster: send address corrections to Macmillan Press Ltd, c/o Mercury Airfreight International Ltd, 2323 Randolph Avenue, Avenel NJ 07001.

Reprints of any article in this journal are available from Stockton Press, Houndmills, Basingstoke, Hampshire RG21 2XS, UK. Tel: +44 (0)1256 29242; Fax: +44 (0)1256 810526.

ISSN 0007–1188

PREPARATION OF MANUSCRIPTS

Authors are strongly recommended to read the full *Instructions to Authors* and *Nomenclature Guidelines for Authors* (*Br. J. Pharmacol.* 1995, **114,** 245–255) before submitting a manuscript for publication in the *British Journal of Pharmacology*. The manuscript and cover letter should be checked against the following list before mailing.

The original and one copy of the manuscript must be supplied. Manuscripts must be typed in double-line spacing on one side of A4 paper, in type not smaller than 12 characters per inch or 10 point. Both copies to include Tables and a set of labelled Figures. One set of Figures without numbers or letters is also to be included. The text to be arranged in the following subsections:

1. **Title**—To have no more than 150 characters on a separate page, which should also include a Short Title (50 characters maximum) and the name and address of the author for correspondence.
2. **Summary**—To be arranged in numbered paragraphs (Full Papers) or a single paragraph (Special Reports).
   —to include aims, principal results and conclusions.
   —to include Key words (10 maximum) at end of summary.
3. **Introduction**—To contain concise statements of the problem and the aims of the investigation.
4. **Methods**—To have brief but adequate account of the procedures; *full names of drugs (including those referred to by manufacturer's code)*, sources of drugs and statistical tests to be stated.
5. **Results**—To have no repetition of data in Figures, Tables and text.
6. **Discussion**—Findings and conclusions to be placed in context of other relevant work.
   NB Simple repetition of results and unwarranted speculation are not acceptable.
7. **Acknowledgements**—Sources of support. Sources of drugs not widely available commercially.
8. **References**—All references in the text to be included in the Reference List and *vice versa*. References in alphabetical order with complete citations; Journals publishing 'in press' papers identified.
   References to manuscripts submitted to other journals but not yet accepted are not allowed.
9. **Tables**—Each on a separate page and prepared in accordance with current requirements of the Journal.
10. **Figures**—Both labelled and non-labelled Figures to be prepared in accordance with current requirements of the Journal (see *Instructions to Authors*, 1995, **114,** 245–251) and provided with Figure Number and Authors' names on back (*in pencil*).
    —each legend to be typed on a separate page and carrying keys to symbols.
    —keys to symbols and histograms must not appear on the figures themselves, but in the respective legends.
    —'box style' figures are not in keeping with the Journal style; line drawings etc must have only left-hand and bottom axes.
11. **Manuscripts**—To be accompanied by a declaration signed by each author that
    (a) results are original
    (b) approval of all persons concerned has been given to submit manuscripts for consideration (see also 12b)
    (c) the same material is neither 'in press' (i.e. is in proof or has definitely been accepted for publication) nor under consideration elsewhere. Furthermore it will not be submitted or published elsewhere before a decision has been reached by the Editorial Board of the *British Journal of Pharmacology* and will not be submitted elsewhere if accepted by the *British Journal of Pharmacology*.
    (d) Copyright assignment is included.
12. **Cover letter**—To state clearly
    (a) Corresponding author's full postal address, telephone, telex or Fax number
    (b) where appropriate, that *either* ethical approval has been given for investigation *or* Company or Institutional permission to publish work has been received.
13. **Reminder**—Packaging to be sufficiently robust to protect Figures and to withstand mailing.

Failure to comply with *Instructions to Authors* may lead to substantial delays in processing, review and publication and may even jeopardize acceptance of the manuscript.

NOMENCLATURE

Authors are reminded that accepted receptor and associated terminology is laid out in *Nomenclature Guidelines for Authors*, as published in the *British Journal of Pharmacology, Br. J. Pharmacol.*, 1995, **114,** 253–255.

SPECIAL REPORTS

The purpose of *Special Reports* is to provide rapid publication for **new** and **important** results which the Editorial Board considers are likely to be of special pharmacological significance. *Special Reports* will have publication priority over all other material and so authors are asked to consider carefully the status of their work before submission.

In order to speed publication there is normally no revision allowed beyond very minor typographical or grammatical corrections. If significant revision is required, the Board may either invite rapid re-submission or, more probably, propose that it be re-written as a Full Paper and be re-submitted for consideration. In order to reduce delays, proofs of *Special Reports* will be sent to authors but **essential corrections must reach the Production Office within 48 hours of receipt.** Authors should ensure that their submitted material conforms exactly to the following requirements.

Special Reports should normally occupy no more than two printed pages of the Journal; two illustrations (Figures or Tables, with legends) are permitted. As a guideline, with type face of 12 pitch and double-line spacing, a page of A4 paper could contain about 400 words. The absolute maximum length of the *Special Report* is 1700 words. For each Figure or Table, please deduct 200 words. The manuscript should comprise a Title page with key words (maximum of 10), a Summary consisting of a single short paragraph, followed by Introduction, Methods, Results, Discussion and References (maximum of 10). In all other respects, the requirements are the same as for Full Papers (see current 'Instructions to Authors').

BRITISH JOURNAL OF PHARMACOLOGY VOLUME 115 (1) 1995

SPECIAL REPORT

PAPERS

STOCKTON

Typeset by Elite Typesetting Techniques, Eastleigh, Hants
and printed in Great Britain by Unwin Brothers Ltd., The Gresham Press, Old Woking, Surrey